CORROSION RESISTANCE OF DUPLEX STAINLESS STEELS AND MMFX MICROCOMPOSITE STEEL FOR REINFORCED CONCRETE BRIDGE DECKS

By

Jianxin Ji

David Darwin

JoAnn P. Browning

A Report on Research Sponsored by

GERDAU AMERISTEEL CORPORATION

KANSAS DEPARTMENT OF TRANSPORTATION
Contract Nos. C1131 and C1281

SOUTH DAKOTA DEPARTMENT OF TRANSPORTATION
Project No. SD 2001-05

THE NATIONAL SCIENCE FOUNDATION
Research Grant No. CMS - 9812716

Structural Engineering and Engineering Materials

SM Report No. 80

THE UNIVERSITY OF KANSAS CENTER FOR RESEARCH, INC.

LAWRENCE, KANSAS

December 2005

ABSTRACT

Chloride-induced corrosion of reinforcing steel in concrete is one of the major durability concerns in reinforced concrete structures. In Northern America, the cost of maintenance and replacement for highway bridges due to corrosion damage is measured in billions of dollars. Of corrosion protection systems, reinforcing steels with inherently good corrosion resistance have received increased attention.

In this study, the corrosion performance of duplex stainless steels, including 2101 and 2205 duplex steels in both "as-rolled" and pickled conditions, and MMFX microcomposite steel were compared with the corrosion performance of conventional and epoxy-coated steel using laboratory tests. These tests include rapid macrocell tests, corrosion potential tests, bench-scale tests (the Southern Exposure and cracked beam tests), and two modified versions of the Southern Exposure test to determine the critical chloride threshold. The rapid macrocell tests were modified by replacing the simulated concrete pore solutions at the anode and cathode every five weeks to limit the effects of changes in the pH of the solutions. The corrosion resistance of the steels was evaluated based on the corrosion rates, corrosion potentials, mat-to-mat resistances, and critical chloride thresholds measured in these tests. Based on laboratory results, along with data from bridge deck surveys and field experience, the service lives of the steels for bridges decks were estimated and the cost effectiveness was compared based on a life-cycle cost analysis.

Results show that, in all rapid macrocell tests, replacing the test solution helps maintain the pH and reduces the corrosion rate and loss of steel. It is recommended that the test solution be replaced every five weeks. Statistically, effective chloride thresholds for reinforcing steel can be determined based on chloride samples from modified Southern Exposure and beam specimens.

Results show that conventional steel has the lowest corrosion resistance, with chloride thresholds ranging from 0.91 to 1.22 kg/m^3 (1.53 to 2.05 lb/yd^3) on a water-soluble basis. Epoxy-coated steel [with four 3.2-mm (0.125-in.) diameter holes in the coating in each test bar to simulate defects of 0.2 to 1% of the bar area] has good corrosion resistance, with corrosion losses ranging from 0.4 to 6% of the values for conventional steel. MMFX microcomposite steel exhibits higher corrosion resistance than conventional steel, with corrosion losses between 16% and 66% and chloride thresholds, 3.70 to 4.07 kg/m^3 (4.72 to 6.86 lb/yd^3), equal to three to four times the value of conventional steel. Bridge decks containing MMFX steel will be less cost effective than decks containing epoxy-coated steel.

Pickled 2101 steel and nonpickled and pickled 2205 steel exhibit significantly better corrosion resistance than conventional steel, with corrosion losses, respectively, ranging from 0.4% to 2%, 0.4% to 5%, and 0.2% to 0.5% of the value of conventional steel. Conservatively, the chloride thresholds of the steels are more than 10 times the value of conventional steel. Overall, 2205 steel has better corrosion resistance than 2101 steel, and pickled bars are more corrosion resistant than nonpickled bars. Pickled 2205 steel exhibits the best corrosion resistance of all the steels tested, while nonpickled 2101 steel has similar corrosion resistance to MMFX steel. The life cycle cost analyses show that in most cases bridge decks containing duplex stainless steels provide lower total life-cycle costs than bridge decks containing conventional, epoxy-coated, or MMFX steel. Pickled 2101 steel represents the lowest cost option.

Keywords: chlorides, concrete, corrosion, diffusion, duplex stainless steel, epoxy-coated steel, macrocell, MMFX steel, reinforcement, service life, threshold

ACKNOWLEDGEMENTS

This report is based on a thesis submitted by Jianxin Ji in partial fulfillment of the requirements of the Ph.D. degree. Major funding and material support for this research was provided by Gerdau AmeriSteel Corporation, the Kansas Department of Transportation under Contract Nos. C1131 and C1281, with technical oversight by Dan Scherschligt and Don Whisler, the National Science Foundation under NSF Grant No. CMS – 9812716, the South Dakota Department of Transportation under projects SD 2001-05 and SD 2002-16, with supervision by Technical Panel Chair, Dan Johnston, and the United States Department of Transportation Federal Highway Administration. Additional support for this project was provided by DuPont Corporation, 3M Corporation, Degussa, and LRM Industries.

TABLE OF CONTENTS

LIST OF TABLES

Page

LIST OF FIGURES

Page

CHAPTER 1

INTRODUCTION

1.1 GENERAL

Chloride-induced corrosion of reinforcing steel in concrete is a primary factor in the premature deterioration of highway bridges. Chlorides in deicing salts penetrate bridge decks and initiate the corrosion of reinforcing steel. The resulting corrosion products occupy a greater volume than the original steel and exert expansive forces on the surrounding concrete, causing cracking and spalling of the concrete. Structural deficiencies may occur because of "the loss of bond between the reinforcing steel and concrete due to cracking and spalling or as a result of the reduced steel cross-sectional area" (ACI Committee 222 2001). Besides highway bridges exposed to deicing salts, many structures in marine environments are likewise attacked by the chlorides in seawater.

In the United States, as the result of extensive use of deicing salts for snow and ice removal beginning in the early 1960s, the deterioration of highway bridge structures has resulted in significant costs for maintenance and replacement. In "snow belt" regions, many conventional reinforced concrete bridges have required maintenance after as little as 5 to 10 years of service, compared to a planned design life of 50 years or more. According to Koch et al. (2001), it was estimated that the annual direct cost of corrosion in highway bridges was $8.3 billion, with indirect costs to the user due to traffic delays and lost productivity at more than 10 times as much. Although alternative deicers, such as calcium magnesium acetate (CMA), have been investigated, the use of other deicers as a general replacement for salt is unlikely because of their high price and lower efficiency (Committee on the Comparative

Costs of Rock Salt and Calcium Magnesium Acetate for Highway Deicing 1991). In fact, the quantity of deicing salt used on highways has remained steady at about 15 million tons per year in recent years (Salt Institute website 2005). As a result, techniques that can significantly reduce or halt chloride-induced corrosion have been aggressively pursued.

Since the middle 1970s, the principal corrosion protection methods for bridge decks have involved the use of increased concrete cover, low permeability concrete, and epoxy-coated reinforcing steel. The increased cover and low permeability concrete increase the time required for chlorides to reach the reinforcing steel and lower the rate at which oxygen and moisture are available to participate in the corrosion process. The epoxy coating, which acts as a barrier, limits access of chlorides, oxygen, and moisture to the surface of the reinforcing steel.

The combination of these methods has greatly lengthened the life of bridge decks, but does not represent a perfect solution. The effectiveness of the increased cover and low permeability concrete is limited because of concrete cracking. Moreover, the increased cover, which is not required for structural purposes, increases the bridge dead load and the cost of construction. The main problems with epoxy-coated reinforcing steel are defects in the coating, damage to the coating during shipping and handling on the jobsite, and adhesion loss between the reinforcing steel and the coating over time, which can result in crevice corrosion involving hydrochloric acid attack of the steel. Due to these shortcomings, the long-term effectiveness of epoxy-coated reinforcing steel has been questioned (Clear 1992, Clear et al. 1995, Weyers et al. 1997, Pyc et al. 2000, Brown, Weyers, and Via 2003). Based on current construction practice, it is typically estimated that bridge decks with epoxy-coated reinforcing steel have a service life of only about 40 years (Koch et al.

2001) - even shorter in harsh environments. On the other hand, due to increasing construction and maintenance costs, many state transportation agencies have adopted a design life without major repairs of 75 to 100 years for concrete bridges (Clemeña and Virmani 2002). Obviously, there is concern that current practice, which relies primarily on epoxy-coated reinforcing steel, can achieve that objective. Accordingly, a number of other corrosion protection measures have been developed or are under development. These include the use of corrosion inhibitors, reinforcing bars with multiple coatings, metallic-clad reinforcing bars, and solid corrosion resistant alloys such as 304 and 316LN stainless steels, duplex stainless steels, and microcomposite MMFX steel. Among these, the stainless steels appear to be most promising (McDonald, Pfeifer, and Sherman 1998).

Each protective system has advantages and disadvantages. A prerequisite for selection is the requirement that the material must not only provide a significant improvement in corrosion resistance but also improve the cost effectiveness of the structure. The selection is, actually, a challenge because of the limited application history of most corrosion protection systems, which requires using accelerated laboratory tests to accurately predict the life expectancy of real structures and identify the most cost-effective method based on life cycle cost analysis.

The service life of bridge decks can be estimated by determining the time it takes for the chloride to reach the reinforcing steel and initiate corrosion and the time between the corrosion initiation and significant concrete damage. The time to corrosion initiation depends on the cover depth, the chloride penetration rate in cracked as well as uncracked concrete, and the chloride concentration necessary to depassivate the reinforcing steel (chloride threshold). The time from corrosion initiation to concrete damage depends on the corrosion rate of the reinforcing steel

and other factors, such as the volume of corrosion products expected to cause concrete cracking. The penetration rate of chlorides, the chloride threshold, and the corrosion rate of reinforcing steel are key parameters used to estimate the service life and compare the performance of corrosion protection systems.

In the current study, the chloride diffusion through concrete, the critical chloride threshold and the corrosion rate of reinforcing steel will be studied using laboratory test techniques. These tests include bench-scale tests (Southern Exposure and cracked beam tests), the rapid macrocell test, the corrosion potential test, and two modified versions of the Southern Exposure test to determine the critical chloride threshold. The tests will be used to compare the corrosion performance of several metallic reinforcing steels, MMFX microcomposite steel and two duplex stainless steels, with conventional and epoxy-coated reinforcing steel on the basis of the life cycle cost of bridge decks.

1.2 CHLORIDE-INDUCED CORROSION IN CONRETE

The corrosion of reinforcing steel is a spontaneous electrochemical process. Due to differences in the surface of the steel (such as different impurity levels in the iron, different values of residual stress) or differences in the local environment (such as different concentrations of oxygen or electrolyte in contact with the metal), two half-cell reactions can occur, respectively, at an anode and a cathode on the steel surface. The potential difference between the two half cells drives the corrosion. At the anode, iron is oxidized, producing a ferrous ion and two electrons.

$$Fe \rightleftharpoons Fe^{2+} + 2e^{-} \qquad (1.1)$$

When moisture and oxygen are available, water is reduced by oxygen, combining with electrons from the anode to form hydroxyl ions at the cathode.

$$H_2O + \tfrac{1}{2} O_2 + 2e^- \rightleftharpoons 2OH^- \quad (1.2)$$

The ferrous ion at the anode then combines with the hydroxyl ions to produce ferrous hydroxide.

$$Fe^{2+} + 2OH^- \rightarrow Fe(OH)_2 \quad (1.3)$$

The ferrous hydroxide can react to form ferric hydroxide $Fe(OH)_3$ [Eq. (1.4)] and hydrated ferric oxide or rust [Eq. (1.5)].

$$4Fe(OH)_2 + O_2 + 2H_2O \rightarrow 4Fe(OH)_3 \quad (1.4)$$

$$2Fe(OH)_3 \rightarrow Fe_2O_3 \cdot H_2O + 2H_2O \quad (1.5)$$

Reinforcing steel in concrete, however, is normally in a passive or non-corrosive condition due to the high pH (13 to 13.5) of the concrete pore solution. In the highly alkaline environment, the $Fe(OH)_2$ that forms at the anode is oxidized to γ-ferric hydroxide.

$$2Fe(OH)_2 + \tfrac{1}{2} O_2 \rightarrow 2\gamma\text{-}FeOOH + H_2O \quad (1.6)$$

"γ-FeOOH provides a tightly adhering passive oxide film on the surface of the steel that limits access of oxygen and moisture to the metal and prevents corrosion" (Mindess, Young, and Darwin 2003). The passive film can be destroyed by carbonation of the concrete and/or the presence of chloride ions.

The passive iron oxide film becomes unstable if the pH of the concrete pore solution drops below 11.5 (Jones 1996), which can be induced by the carbonation due to penetration of CO_2 into the concrete. Carbonation, however, occurs usually very slowly and is not of particular concern in quality concrete (Mindess, Young, and Darwin 2003).

The mechanism of depassivation by chlorides is not well understood. It is believed that chloride ions can penetrate the passive film or adsorb on its surface to react with the ferrous ions to form a soluble iron-chloride complex that can combine

with both hydroxyl ions and oxygen to form loose porous rust on the steel. The chlorides are released in the process. Chlorides act as catalysts in the corrosion process and are not consumed once they enter the concrete. The reactions are as follows:

$$Fe^{2+} + Cl^- \rightarrow (FeCl\,complex)^+ \quad (1.7)$$

$$(FeCl\,complex)^+ + 2OH^- \rightarrow Fe(OH)_2 + Cl^- \quad (1.8)$$

The chloride content of concrete can be expressed on either a water-soluble (chloride concentration in the pore solution) or acid-soluble (total chloride content in the concrete) basis depending on the analysis method. “Not all the chlorides present in the concrete can contribute to the corrosion of the steel” (ACI Committee 222 2001). Some of the chlorides will be removed from the pore solution by the chloride binding. It is generally believed that only the water-soluble chlorides promote corrosion. To initiate corrosion of reinforcing steel, a “threshold” level of chlorides needs to be present. The minimum concentration of chlorides required to initiate corrosion, on either a water-soluble or acid-soluble basis, is referred to as the critical chloride threshold. Considerable scatter is present in the value of the chloride threshold. A wide range in the value, from 0.1% to 1.0% chloride ion by weight of cement [approximately 0.35 to 3.5 kg/m^3 (0.6 to 6.0 lb/yd^3) of concrete], has been reported for conventional steel (Taylor, Nagi, and Whiting 1999). The acid-soluble chloride threshold is typically between 0.6 and 0.9 kg/m^3 (1.0 and 1.5 lb/yd^3) of concrete (ACI Committee 222 2001).

The chloride threshold depends mainly on the pH of the solution in contact with the steel. In fact, it has been suggested that because of the role that hydroxyl ions play in protecting steel from corrosion, it is more appropriate to express the corrosion threshold in terms of the ratio of chloride to hydroxyl ion content, $[Cl^-]/[OH^-]$. The

minimum value of $[Cl^-]/[OH^-]$ that can cause the breakdown of the passive film has been shown to be between 0.3 (Diamond 1986, Hansson and Sorensen 1990) and 0.6 (Hausmann 1967). The chloride threshold will be discussed in great detail in Section 1.6.

Chlorides may be introduced into concrete during mixing from several sources, including concrete admixtures, such as $CaCl_2$, contaminated aggregates, or mix water. They can also penetrate into mature concrete from the external environment due to exposure to deicing salts or seawater. Deicing salt is the main source of chlorides causing corrosion of steel in bridge decks.

For uncracked concrete, the penetration of chlorides into concrete often occurs by diffusion. The diffusion is usually modeled using Fick's second law, which is represented by

$$\frac{\partial C(x,t)}{\partial t} = D_c \frac{\partial^2 C(x,t)}{\partial x^2} \tag{1.9}$$

where

$C(x, t)$ = chloride concentration at depth x and time t;

D_c = diffusion coefficient.

Based on the assumptions that the chloride concentration at the surface and the diffusion coefficient are constant over time, the solution to Eq. (1.9) for a semi-infinite slab is

$$C(x,t) = C_i + (C_s - C_i)\left[1 - erf\left(\frac{x}{2\sqrt{D_c t}}\right)\right] \tag{1.10}$$

where

C_i = initial chloride concentration in concrete;

C_s = chloride concentration at the surface;

erf = error function [Eq. (1.11)]:

$$erf(z) = \frac{2}{\sqrt{\pi}} \int_0^z e^{-t^2} dt \tag{1.11}$$

The surface concentration and diffusion coefficient in Eq. (1.10) can be determined by fitting the equation to chloride profiles measured from laboratory specimens or structures in the field by a nonlinear regression analysis using the method of least squares. Once the surface concentration and diffusion coefficient are known, the chloride concentration in concrete can be predicted based on Eq. (1.10). It can be assumed that the surface concentration is a function of the exposure conditions and the diffusion coefficient depends on material properties. The higher the diffusion coefficient, the higher the rate of chloride penetration. The penetration of chlorides into bridge decks, however, is often more complicated than the ideal diffusion process. It depends on the soundness of the concrete, the properties of the concrete, and the environment. Chloride penetration in concrete will be further discussed in Section 1.5.

Once enough chlorides reach reinforcing steel in concrete, corrosion of the steel initiates. Depending on the distance between the anode and the cathode, the corrosion can develop as either microcell corrosion, if the anode and the cathode are very close to each other, or macrocell corrosion, if they are separated. In reinforced concrete bridge decks, macrocell, as well as microcell, corrosion is common because the upper mat of steel is generally exposed to significantly higher chloride and moisture contents than the bottom mat and has a more negative corrosion potential, which causes the entire top mat of steel to become anodic. This type of macrocell corrosion results in a marked increase in the corrosion rate.

It is noteworthy that depassivation, due to chlorides or carbonation, “is necessary but not sufficient” for the corrosion of steel in concrete (ACI Committee 222 2001). After corrosion initiation, the loss of steel depends on the corrosion rate, which depends on the nature of the steel, the availability of oxygen and moisture, the electrical resistivity of concrete, the pH, and the temperature.

Since the specific volume of the corrosion products, usually a mixture of the oxides $Fe(OH)_2$, $Fe(OH)_3$ and $Fe_2O_3 \cdot nH_2O$, is three to six times larger than that of iron (ACI Committee 222 2001), the corrosion of reinforcing steel can lead to tensile stress in the surrounding concrete, causing cracking and spalling. The total corrosion loss of steel expected to result in concrete cracking and spalling is an important parameter that determines the time from corrosion initiation to concrete damage, and thus, the service life of a structure. This value has been reported to be between 3 to 74 μm (0.0001 to 0.003 in.) depending primarily on the concrete cover, reinforcing bar diameter, and concrete properties if the corrosion products form uniformly on the steel surface (Torres-Acosta and Sagues 2004).

1.3 CORROSION EVALUATION TECHNIQUES

The performance of corrosion protection systems can be evaluated by monitoring the corrosion of reinforcing steel in synthetic aqueous solutions or cementitious environments using visual inspection, electrochemical techniques and nondestructive tests. In this section, two electrochemical parameters (corrosion potential and corrosion rate) and laboratory test methods for corrosion evaluation of reinforcing steel will be reviewed.

1.3.1 Corrosion potential

Corrosion potential is a thermodynamic parameter that indicates whether a metal in a given environment will have a tendency to corrode. It is a mixed potential of two or several half-cell reactions that are polarized from their equilibrium potential values to the mixed one. Corrosion potentials of reinforcing steel can be measured with a high-impedance voltmeter as a potential difference (voltage) with respect to a reference electrode. The two most common reference electrodes used in corrosion studies of steel are the copper-saturated copper sulfate electrode (CSE) and the saturated calomel electrode (SCE). The copper-saturated copper sulfate electrode is often used for field measurements and has a 0.316 V half-cell potential at 25^{o}C (77^{o}F) versus the standard hydrogen electrode (SHE) which is used as the defacto reference electrode with a defined potential of 0.0 V. The saturated calomel electrode is common for laboratory use and has a 0.241 V potential at 25^{o}C (77^{o}F) versus the SHE. “Corrosion potential measurements provide an indication of the state of corrosion and not the rate of corrosion” (ACI Committee 222 2001). Usually, the more negative the potential, the higher the tendency to corrode. ASTM C 876 provides a standard method for measuring corrosion potentials of uncoated reinforcing steel in concrete. According to ASTM C 876, the probability of active corrosion of reinforcing steel in concrete is given in Table 1.1.

Table 1.1 - Criteria for corrosion of steel in concrete based on potential results

Potential reading (V) versus CSE	Probability of steel corrosion in concrete
More positive than –0.200	Greater than 90% that no corrosion is occurring
–0.200 to –0.350	Corrosion activity is uncertain
More negative than –0.350	Greater than 90% that corrosion is occurring

Corrosion potentials for reinforcing steel in concrete are taken with the reference electrode in contact with the concrete surface. These readings are influenced by the concrete cover, the resistivity of the concrete, the availability of oxygen, the temperature, and the pH. For example, a higher moisture content in concrete over the reinforcing steel can shift the potential readings to more negative values (Elstner et al. 2003). Since the effect of these factors on corrosion potentials is sometimes significant, especially for field measurements, the interpretations of corrosion potentials recommended in the ASTM C 876 "should not be used as absolute criteria to determine the condition of steel in concrete" (Elsener et al. 2003). It is suggested that differences in corrosion potentials across a structure or specimen, rather than the absolute potential values, are better indicators of the corrosion state (ACI Committee 222 2001). In some cases, accurate interpretations of corrosion potential measurements require a combination of analyses of concrete resistivity, carbonation, and chloride content.

Corrosion potential measurement is usually not suitable to epoxy-coated steels due to the electrical insulation provided by the epoxy. The corrosion potential of galvanized steel and stainless steel can be measured in the same way as for conventional steel, but different criteria for interpreting the value may apply.

1.3.2 Corrosion rate

The corrosion rate of reinforcing steel indicates how fast reinforcing steel is being oxidized. It is usually expressed as a current density, $\mu A/cm^2$, by measuring the rate of electron flow from anodes to cathodes. Based on Faraday's law, current density can be converted to another expression for corrosion rate, a rate of loss of metal from the surface of the steel, μm/year (Jones 1996).

$$R = k\frac{ia}{nF\rho} = 11.6i \tag{1.12}$$

where

R = corrosion rate, given in rate of metal loss, μm/year;

i = corrosion rate, given in current density, μA/cm^2;

k = conversion factor = 31.5·10^4 amp·μm ·sec/μA·cm·year;

a = atomic weight of the metal = 55.8 g/mol for iron;

n = number of electrons transferred = 2 for iron;

F = Faraday's constant = 96500 Coulombs/mol;

ρ = density of the metal, g/cm^3 = 7.87 g/cm^3 for iron.

As explained in Section 1.2, corrosion can involve a macrocell, a microcell or a combination of the two. For concrete bridges decks, the measurement of the macrocell corrosion rate is generally not possible because the top and bottom mats of reinforcing steel are usually connected by steel wire ties and bar supports in the concrete slab. In laboratory tests that simulate the corrosion of steel in bridge decks such as ASTM G 109 test, however, ties and bar supports are not used and the macrocell corrosion rate can be determined by measuring the voltage drop across a resistor that electrically connects the anode and the cathode through an external circuit.

$$i = \frac{V}{RA} \tag{1.13}$$

where

i = corrosion rate, given in current density, μA/cm^2;

V = voltage drop across the resistor, mV;

R = resistance of the resistor, kΩ;

A = area of exposed metal at the anode bar, cm^2.

The measured macrocell corrosion rate can be affected significantly by the test methods (Balma et al. 2005) and the details of the test configuration, such as the anode to cathode area ratio and the size of the resistor connecting the anode and the cathode (McDonald, Pfeifer, and Sherman 1998). The measured macrocell corrosion rate should be used only to compare the relative performance of corrosion protection systems under same test conditions. When it is used to estimate the service life of bridge decks, a relationship between the corrosion rates of steel in bridge decks and the rates measured in specific laboratory tests must be established.

Microcell corrosion rates can be measured using Tafel extrapolation, linear polarization resistance (LPR), AC impedance, also called electrochemical impedance spectroscopy (EIS), and electrochemical noise techniques. Linear polarization resistance is generally the most suitable method for reinforcing steel in concrete due to its reliability and simplicity (Broomfield 1997). LPR techniques for reinforced concrete structures were evaluated and developed under the Strategic Highway Research Program (SHRP) (Fils et al. 1992) and in other research (Escalante, Cohen, and Kahn 1984, Clear 1989). A standard procedure has not yet been established for LPR measurements, but a recommendation by RILEM was published in 2004 (Andrade et al. 2004).

The LPR method is based on the observation that a portion of the polarization curve is linear, usually over a range of around ±10 mV versus the equilibrium corrosion potential of a metal. The slope of the linear region is referred to as the polarization resistance R_p and is inversely proportional to the corrosion current density, and thus, the corrosion rate of the metal. A LPR device usually includes a working electrode (the reinforcing steel tested), a noncorroding counter electrode, a

reference electrode, and a potentiostat. The polarization curve can be established by imposing a range of potentials on the reinforcing steel via the counter electrode and measuring the corresponding corrosion currents using the potentiostat.

The corrosion current density is obtained in terms of the polarization resistance using the Stern-Geary relationship (Jones 1996).

$$i = \frac{B}{R_p} \tag{1.14}$$

where

i = corrosion current density, μA/cm^2;

R_p = polarization resistance, kΩ·cm^2;

B = Stern-Geary constant = $\frac{\beta_a \beta_c}{2.303(\beta_a + \beta_c)}$, mV;

β_a = anodic Tafel constant, mV/decade;

β_c = cathodic Tafel constant, mV/decade.

To use Eq. (1.14), the anodic and cathodic Tafel constants (β_a and β_c) or the Stern-Geary constant (B) must be known. Although different values of β_a and β_c are often used, Eq. (1.14) is relatively insensitive to these values. A value of 150 mV/decade for β_a and a value of 250 mV/decade for β_c (Clear 1989) or, alternatively, a value of 120 mV/decade for both β_a and β_c (McDonald et al. 1998), resulting in B = 41 mV or 26 mV, respectively, have been suggested for reinforced concrete.

Interpretations of corrosion rates of reinforcing steel in concrete based on LPR tests have been suggested (Cady and Gannon 1992, Broomfield et al. 1993) and are summarized in Table 1.2. A value of 0.1 μA/cm^2 is equivalent to 1.16 μm/yr, according to Eq. (1.12).

The LPR method is often used in both lab and field tests. A difficulty in LPR measurements in a field test is to determine the area of steel tested. A guard ring usually helps and can increase the accuracy (ACI Committee 222 2001).

Table 1.2 - Criteria for corrosion of steel in concrete based on LRP results

Corrosion current density ($\mu A/cm^2$)	Corrosion conditions of steel in concrete
< 0.1	Passive state
0.1 to 0.5	Low to moderate corrosion
0.5 to 1	Moderate to high corrosion
> 1	High corrosion

1.3.3 Laboratory test methods

A number of laboratory test methods have been developed to provide a realistic model for the corrosion of reinforcing steel in concrete. Long-term bench-scale tests, such as the Southern Exposure, cracked beam, and ASTM G 109 tests, are used most often. The Southern Exposure and cracked beam tests and a rapid macrocell test will be used in this study. All of the tests involve macrocells and simulate the corrosion that occurs in a reinforced concrete bridge deck exposed to deicing salts. Usually, corrosion potential and corrosion rate are measured during the tests. In this section, previous work related to the tests is reviewed. The determination of the chloride threshold of reinforcing steel is discussed in the Section 1.6.

The *rapid macrocell test* was originally developed at the University of Kansas in 1990 under the SHRP program (Martinez et al. 1990, Chappelow et al. 1992) and has undergone development since then. The goal of the technique is to obtain a realistic measure of the performance of corrosion protection systems in a short period

of time (usually 15 weeks). A short time-to-corrosion is achieved in the test by exposing reinforcing bars with a very thin mortar cover to a harsh chloride environment.

Martinez et al. (1990) initially used the macrocell test to evaluate the effects of three deicing chemicals, calcium chloride, sodium chloride, and calcium magnesium acetate, on the corrosion of reinforcing steel. The test specimen consisted of a 127 mm (5 in.) long No. 13 (No. 4) reinforcing bar, symmetrically embedded 76 mm (3 in.) into a 102 mm (4 in.) long and 30 mm (1.2 in.) diameter mortar cylinder. A 15 mm (0.6 in.) wide epoxy band was applied around the bar at the interface between the exposed steel and the surrounding mortar to prevent crevice corrosion. Because of its shape, this type of specimen is often referred to as a “lollipop” specimen. After curing in lime-saturated water for 14 days to reach a passive condition, one test specimen, which served as the anode was placed in a 5-liter plastic container with simulated concrete pore solution containing a preselected concentration of a deicing chemical. The other test specimen, which served as the cathode, was placed in a second container with simulated pore solution. Crushed mortar fill was added to both of the containers to more closely simulate the concrete environment. The two specimens were electrically connected across a 100,000-ohm resistor and a salt bridge was used to connect the solutions in the two containers of the corrosion cell. The containers were sealed for the duration of the test to prevent carbon dioxide from neutralizing the pore solution and to prevent evaporation of the liquid. The corrosion current and the rate of corrosion were determined by measuring the voltage drop across the resistor at regular intervals. In the study, the macrocell test was also modified to determine the corrosion potential by replacing the container with the cathode specimen by a container with a standard calomel reference electrode in

saturated potassium chloride solution. The researchers found that the rapid macrocell test provided less consistent results than the corrosion potential test. They concluded that the relatively poor results were due to the very high resistance used in the macrocell test, which greatly limited the corrosion current. A lower resistance was recommended for use in future studies.

The rapid macrocell test was updated under the NCHRP-IDEA program (Smith, Darwin, and Locke 1995, Senecal, Darwin, and Locke 1995, Schwensen Darwin, and Locke 1995) to evaluate the corrosion performance of corrosion resistant steels. Several modifications were made to improve the consistency and repeatability of the test. First, a No. 16 (No. 5) bar was used instead of a No. 13 (No. 4) bar. This reduced the mortar cover over the reinforcing steel by 2 mm and further shortened the time to corrosion initiation. Second, air, scrubbed to remove CO_2, was bubbled into the pore solution surrounding the cathode to insure an adequate supply of oxygen. Third, one or two test specimens were used as the anode and twice as many as specimens were used as the cathode. The latter two modifications were made to assure that the cathodic reaction was not controlling the corrosion rate of the macrocell. Lastly, the 100,000-ohm resistor was replaced by a 10-ohm resistor to obtain a greater and more stable macrocell corrosion current. The researchers also showed that the potentials of both the anode and cathode could be taken after breaking the macrocell circuit for two hours, and the readings gave the same information as the corrosion potentials tests. They pointed out that this negated the reason for a separate corrosion potential test.

The rapid macrocell test continued to be developed in subsequent studies at the University of Kansas (Darwin et al. 1999, Kahrs et al. 2001, Darwin et al. 2002, Gong et al. 2002, Ge et al. 2004, Balma et al. 2005). It was found that rust often

formed on the exposed surface of the reinforcing bars (the portion not immersed in solution) in most anode “lollipop” specimens. This happened because that portion of the bar was exposed to a high humidity environment in the sealed container and was also easily contaminated by chlorides. Due to this shortcoming, the test failed to provide useful information of the effect of water-cement ratio on the corrosion of conventional reinforcing steel embedded in mortar (Ge et al. 2004). As a result, the lollipop specimen was replaced by the “mortar-wrapped” specimen in which the bar was totally imbedded in the mortar, and the lid was lowered (placed just above the level of the solution in the container), with the upper portion of the specimen exposed to the air. These modifications greatly improved the consistency and repeatability of the test. Results from the test have been shown to correlate well with those in longer-term tests, such as the Southern Exposure and cracked beam tests (Balma et al. 2005).

Specimens in *bench-scale tests* consist of small concrete slabs containing two mats of steel that simulate a portion of a concrete bridge deck. These tests typically require one to two years for completion. Of the different configurations used, the Southern Exposure and cracked beam tests have proven to give the most useful data. Rapid chloride ion transport is facilitated by a thin concrete cover or a crack over reinforcing steel and a severe “weathering” regime. The same testing regime is usually used for the Southern Exposure and cracked beam tests. The tests differ in that the cracked beam specimen has an artificial crack over the reinforcing steel on the top surface, while the Southern Exposure specimen does not.

The *Southern Exposure test* was originally used as an accelerated weathering method by Pfeifer and Scali (1981) to study the effectiveness of different chemical surface sealers for concrete bridge decks subjected to different environmental conditions. In the study, a weekly ponding and drying cycle was applied to small

concrete slabs. For the first 100 hours of each week, the surface of test specimens was ponded with a 15 percent NaCl solution at room temperature. After this period, the specimens were exposed to ultraviolet light and infrared heat in a chamber at 100 ^{o}F for 68 hours. The weekly cycle was repeated 24 times. This procedure simulated the alternate wet and dry environment found in southern climates (thus the term southern exposure) and accelerated the penetration of chlorides through the concrete.

The test was later modified by Pfeifer, Landgren, and Zoob (1987) to evaluate several corrosion protection systems, including increased cover thickness, decreased water-cement ratio, the addition of calcium nitrite to serve as a corrosion inhibitor, and the use of epoxy-coated and galvanized reinforcing steels for reinforced and prestressed concrete. The test slabs were 305 mm (12 in.) square and most were 178 mm (7 in.) thick. Two mats of steels were included in the test specimens. The top mat had two No. 13 (No. 4) bars and the bottom mat had four No. 13 (No. 4) bars. All bars in most of the slabs had a clear cover of 25.4 mm (1 in.) to the nearest surface. The bars extended out from the sides of the concrete and were connected electrically across a 10-ohm resistor. The sides of the concrete were coated with epoxy to minimize lateral movement of moisture and chlorides during the accelerated weathering tests. After an initial 3 days moist curing followed by a 25 days air curing, the specimens were subjected to the weekly Southern Exposure ponding and drying cycle for 48 weeks. The corrosion current between the top and bottom mats, instant-off potential, mat-to-mat resistance, and open circuit potentials were measured intermittently. Pfeifer et al. defined the instant-off potential as the voltage difference between the two mats of steel measured immediately after the circuit is opened. The instant-off potential reading increased as the corrosion current increased. Based on

their test results, Pfeifer et al. established a relationship between the measured corrosion current and the open circuit potential using a linear regression analysis:

$$I = -774.2P - 184.2 \quad (1.15)$$

where I = corrosion current in mA;

P = open circuit corrosion potential vs. CSE in volts.

They also found that the observed corrosion of conventional reinforcing steel could occur at corrosion potentials more negative than –0.230 V.

Lorentz, French, and Leon (1992) used similar procedures to evaluate the corrosion resistance of undamaged and damaged coated reinforcing steels, and corrosion performance as affected by concretes with different water-cement ratios, entrained air contents, and quantities of condensed silica fume. Their results supported the empirical relationship between the corrosion potential and the macrocorrosion current shown in Eq. (1.15). Based on a visual examination of reinforcing steel taken from specimens, they suggested that a macrocell current of more than 50 μA, equal to 0.2 $\mu A/cm^2$ (2.32 μm/yr) based on the area of the anode bars, was generally indicative of significant corrosion activity, corresponding a –0.300 V corrosion potential vs. CSE based on Eq. (1.15). They also observed that macrocells could form between bars in the same layer due to the uneven distribution of oxygen, moisture, and chlorides. They suggested that this observation be considered in future research.

Kenneth C. Clear Inc. (1992) investigated the corrosion performance of bent epoxy-coated reinforcing bars using the Southern Exposure test. Specimens had one bent and two straight epoxy-coated bars in the top mat and 4 uncoated conventional bars in the bottom mat, connected to form two separate macrocells. The specimens were subjected to the Southern Exposure cycling for 70 weeks and then were ponded

continuously with tap water for 42 weeks. It was found that corrosion of the specimens containing epoxy-coated reinforcing bars was negligible, while uncoated top mat steel in control specimens was heavily corroded by the end of the cycles. When ponded with tap water, however, most of the epoxy-coated bars exhibited some signs of corrosion: the mat-to-mat resistance decreased and the macrocell corrosion current increased significantly. The reason was later discussed by Clear et al. (1995). He suspected that the specimens had dried out somewhat during the cycles; therefore, there was not enough moisture to initiate corrosion on the epoxy-coated bars even though the chloride level in the concrete was high. Once the tap water ponding began, the moisture content increased and promoted the corrosion process.

The Southern Exposure and cracked beam tests were used at the University of Kansas to evaluate of the corrosion resistance of microalloyed reinforcing steel (Senecal, Darwin, and Locke 1995). The Southern Exposure specimens were 305 mm (12 in.) wide, 305 mm (12 in.) long, and 178 mm (7 in.) thick. The cracked beam specimens were half the width of the SE specimen and had one bar in the top mat and two bars in the bottom. Transverse cracks with a width of 0.25 mm to 0.38 mm (10 to 15 mils) were induced in the cracked beam specimens using three-point bending. No. 16 (No. 5) bars were used. Recommendations that were made in the study and adopted in the subsequent research at the University of Kansas include (1) extending the testing period for the bench-scale tests from 48 to 96 weeks to better evaluate the corrosion behavior of reinforcing steels, (2) using removable shims to establish grooves of known width to serve as cracks in the cracked beam specimens, (3) using longitudinal cracks along the length of the bar in the cracked beam specimens, and (4) casting a concrete dam monolithically with the specimens to prevent leakage of ponding solution, a problem that may occur with dams that are installed after casting.

McDonald, Pfeifer, and Sherman (1998) evaluated the corrosion performance of conventional, epoxy-coated, metallic-clad, and solid metallic reinforcing bars in concrete using the Southern Exposure and cracked beam test. In the study, the cracked beam specimens had the same size as the Southern Exposure specimen. Longitudinal cracks were formed directly above the bars in the specimens "using a 12-mil (0.3-mm) stainless steel shim, cast into the concrete down to the bar level and removed 1 day after the concrete was cast" (McDonald et al. 1998). The accelerating weathering procedure was modified. The specimens were ponded continuously for 12 weeks following the first 12 weekly ponding and drying cycles. The cycle was then repeated for a 96-week testing period. The addition of the continuous ponding period seemed to avoid the excess drying of the specimens that concerned Clear et al. (1995). McDonald et al. showed the effect of resistor size was significant when measuring the macrocell current, justifying the use of a 10-ohm resistor. Based on a measured corrosion rate at 37 μm/yr (1.5 mil/yr) for conventional bars and the observation that all specimens containing conventional bars were cracked within 48 weeks of testing, they pointed out that time-to-cracking could be calculated using macrocell corrosion rates based on the assumption that corrosion losses of 25 μm (1 mil) will cause concrete to crack. It was concluded that, in bench-scale tests, the macrocell current was a sufficient indicator of the corrosion of the reinforcing steels; results obtained from the more complex, time consuming polarization resistance and EIS tests generally provided the same information; and the coating performance of epoxy-coated reinforcing steel could also be evaluated based on the mat-to-mat resistance. High values of resistance resulted in low total corrosion. Southern Exposure specimens containing epoxy-coated bars exhibited low corrosion rates

when the mat-to-mat resistance exceeded 10,000 ohms (about 25 times the resistance exhibited by conventional steel specimens).

ASTM G 109 was developed to evaluate the effect of chemical admixtures on the corrosion of metals in concrete. The test has also been used to evaluate other kinds of corrosion protection systems (Balma et al. 2002, Trejo 2002). The G 109 specimen is somewhat smaller than the cracked beam specimen [305 × 152 × 178 mm (12 × 6 × 7 in.)] and has no cracks. A 3% sodium chloride solution and a 100-ohm resistor to connect top and bottom bars are used. The ponding and drying periods are two weeks each and the temperature is maintained at about 23 ± 3°C (73 ± 5°F). Because the evaluation period of the test is much longer than that of the SE and CB test due to its less severe exposure regime, the G 109 test is not used to evaluate the corrosion resistance of reinforcing steels in the current study.

1.4 CORROSION PROTECTION SYSTEMS

This section reviews most current corrosion protection methods, with emphasis on stainless steels and MMFX microcomposite steel.

1.4.1 Current practices

At present, methods that are used to reduce the corrosion of reinforcing steel in concrete can be placed in four categories: (1) electrochemical methods, (2) barrier methods, (3) corrosion inhibitors, and (4) alternative reinforcements.

Electrochemical methods, electrochemical chloride extraction and cathodic protection, are usually used to rehabilitate existing salt-contaminated concrete structures (cathodic protection is also used for new construction) and are not addressed further in this report.

Barrier methods involve increased concrete cover, low permeability concretes, concrete overlays, waterproof membranes, etc. These methods “prevent or delay the ingress of chloride, oxygen, and moisture through the concrete cover to the reinforcing steel” (Smith and Virmani 2000), thereby extending the time to corrosion initiation and/or reducing the corrosion rate.

Since 1974, the American Association of State Highway and Transportation Officials (AASHTO) Standard Specifications for Highway Bridges have required a minimum of 65 mm (2.5 in.) of concrete cover over the top mat of reinforcing steel with no positive corrosion protection in bridge deck slabs that are frequently exposed to deicing salts.

Low permeability concrete can be obtained by using a lower water-cement ratio and adding mineral admixtures to the concrete mix. “As the *w*/*c* ratio decreases, the porosity of the paste decreases and the concrete becomes more impermeable” (Mindess, Young, and Darwin 2003). For protecting reinforcing steel from corrosion in bridge decks, the AASHTO Specifications limited the *w*/*c* ratio to a maximum of 0.44 from 1974 to 1995 and to 0.45 after 1995 for air-entrained Class A concrete. Mineral admixtures such as silica fume and fly ash can react with calcium hydroxide to form calcium silicate hydrate (C-S-H). The increased fraction of C-S-H leads to a more homogenous microstructure in concrete, with a finer pore size and lower overall porosity (Mindess et al. 2003). Silica fume is the most effective mineral admixture for many applications because of its high activity and super-fine particle size.

Concrete overlay systems involve two-stage construction. The first-stage (the sub-deck) consists of conventional concrete and contains the main load-carrying reinforcing steel. The second-stage (the overlay) consists of improved concrete and creates a low permeability protective layer over the sub-deck. The most common

types of overlay are low-slump, high-density conventional concrete, silica fume concrete, and latex modified concrete. In principal, “with this system, the rigid overlay can be replaced when it begins to deteriorate and debonded from the sub-deck and before chloride ions can begin to penetrate into the sub-deck” (Smith and Virmani 2000). In practice, however, cracks in the overlay allow chlorides to reach the level of the reinforcing steel in the subdeck within the first year of service (Miller and Darwin 2000, Lindquist, Darwin, and Browning 2005).

Waterproofing membranes include preformed sheet membranes and liquid membranes. The field performance of waterproofing membranes is highly dependent on the quality of installation. The average service life applied to new decks is 15 to 20 years (Kepler, Darwin, and Locke 2000). One of the greatest problems in applying waterproofing membranes is blistering, which is “caused by the expansion of entrapped gases, solvents, or moisture in the concrete after application of the membrane” (ACI Committee 222 2001).

Since cracking of concrete bridge decks appears to be unavoidable (Schmitt and Darwin 1995, Miller and Darwin 2000), increased concrete cover, low permeability concretes, and concrete overlays are often used in conjunction with other corrosion protection systems, such as epoxy-coated reinforcing steel and corrosion inhibitors.

Corrosion inhibitors are chemical admixtures that can slow down or prevent the corrosion of reinforcing steel in concrete. Both inorganic and organic compounds are used. Currently, the most commonly used inorganic compound is calcium nitrite, $Ca(NO_2)_2$. It can form a γ-ferric oxide layer on the surface of the steel, as shown in Eq. (1.16). In this reaction, calcium nitrite competes with chloride ions reacting with

the steel and increases the chloride concentration needed to depassivate the reinforcing steel in the concrete.

$$Fe^{++} + OH^{-} + NO_2^{-} \rightarrow NO\uparrow + \gamma\text{-}FeOOH \quad (1.16)$$

The effectiveness of calcium nitrite is dependent on the ratio of chloride to nitrite ions. It is recommended that the $[Cl^-]/[NO^-]$ ratio be kept below 1.0 at the level of steel throughout the life of a structure (Virmani 1990).

Rheocrete 222^+, a water-based combination of amines and esters, is a widely used organic inhibitor, which protects reinforcing steel by reducing the permeability of the concrete and by forming a corrosion-resistance organic film on the reinforcing steel. Research in University of Kansas (Balma et al. 2005) has shown that, similar to rigid barriers, corrosion inhibitors provide good corrosion protection for uncoated reinforcing steel in sound concrete, but provide little advantage if concrete cracks.

Alternative reinforcements include epoxy-coated reinforcing steel, metallic-clad reinforcing steel, solid stainless steels, and other corrosion resistance alloys.

Beginning in the 1970s, epoxy-coated reinforcing steel, along with increased concrete cover and low permeability concrete has become the most common corrosion protection system. The epoxy coating is formed by electrostatically spraying dry epoxy powders over cleaned, preheated reinforcing bars. The coating functions in two ways, first by acting as a barrier, keeping oxygen, water, and chloride ions from reaching the surface of the steel, and second, by increasing the electrical resistance between adjacent steel locations. Following some early successful applications in bridge decks, poor corrosion performance of epoxy-coated reinforcing steel in the Florida Keys Bridges (Sagues, Powers, and Kessler 1994, Manning 1996) has lead to numerous laboratory studies and field evaluations. Many of these studies have demonstrated that epoxy-coated reinforcing steel provides a

viable option for corrosion protection for bridges decks (Smith and Virmani 1996, McDonald, Pfeifer, and Sherman 1998, Lee and Krauss 2004), while other studies have shown that the effectiveness of epoxy-coated reinforcing steel is questionable (Clear et al. 1995, Weyers et al. 1997, Pyc et al. 2000, Brown, Weyers, and Via 2003). Despite the controversy on the effectiveness of epoxy-coated reinforcing steel, one point is undisputed, the corrosion resistance of epoxy-coated reinforcing steel is closely related to the integrity of the coating, which can be impaired by defects in the coating and damage to the coating during shipment and handling on the jobsite. Small breaks in the coating can cause disbondment between the steel and the coating, especially under aggressive exposure conditions, and result in crevice corrosion underneath the coating, an environment that is low in oxygen and high in chlorides. Recommendations have been made to minimize the problems (Virmani and Clemena 1998). Since “it is impractical to detect and repair all defects” in the coating (Manning 1996), however, the concern about the long-term effectiveness of epoxy-coated reinforcing steel has continued.

Several reports have included reviews of laboratory studies and field applications of epoxy-coated reinforcing steel (Manning 1996, Smith and Virmani 2000, Kepler et al. 2000). The conclusions from the report by Kepler et al. include:

“1) The performance of epoxy-coated reinforcing steel is enhanced by quality concrete and adequate cover.

“2) Epoxy coatings lose their adhesion to reinforcing steel when exposed to moisture (whether this adhesion loss is a direct cause of corrosion damage is under debate).

"3) Performance of epoxy-coated reinforcement is related to the number of defects (holidays) in the coating. These defects directly affect the electrical resistivity of the reinforcement.

"4) Most problems that have been reported with epoxy-coated reinforcement have occurred in environments where the concrete is continuously wet, yet oxygen is still available (splash zones on piers or areas of high humidity). Often these environments have high average temperatures.

"5) There is little doubt that the time-to-corrosion induced cracking is increased in many concrete structures containing epoxy-coated reinforcement over the time to corrosion-induced cracking in bridge decks with no protective measures. However, the question remains open as to whether epoxy-coated steel provides adequate long-term protection to reinforced concrete highway structures that are exposed to moisture and chlorides."

Considering the shortcomings of the aforementioned corrosion protection systems, reinforcing steels with inherently good corrosion resistance that can potentially provide a 75 to 100 year corrosion free life for bridge decks have received increased attention. Two systems, stainless steel and MMFX microcomposite steel, will be reviewed in the balance of this section.

1.4.2 Stainless steels

Stainless steels are iron alloys containing a minimum of 12% chromium (Cr). This concentration of chromium can prevent the formation of rust by producing "a self-forming passive film of a mixed iron-chromium oxide on the metal surface" (Nurnberger 1996). The corrosion resistance of stainless steels increases as their chromium content increases and may be further improved by additions of other

elements, such as nickel (Ni), nitrogen (N), and molybdenum (Mo), which can also enhance strength, formability and toughness of the steels (Sedriks 1996). The corrosion resistance of stainless steels is adversely affected by the presence of a mill scale on their surface. The mill scale usually can be removed by pickling and sandblasting. Pickling has the better result (Bertolini et al. 2004). Stainless steels are usually divided into four categories according to their metallurgical structure: ferritic, austenitic, martensitic, and austenitic-ferritic. The last type, containing roughly equal amounts of austenite and ferrite, is also referred to as duplex stainless steel (Sedriks 1996). “Austenitic and austenitic-ferritic steels can be produced as ribbed bars within the normal range of strength and deformability requirements” (Nurnberger 1996). However, the strength of the austenitic steel bars “as rolled” is usually not sufficient. These bars need to be strengthened by subsequent treatment, such as cold or warm working (Nurnberger 1996). In the United States, stainless steel bars for concrete reinforcement are produced under ASTM A 955.

The stainless steels that have been used most often in concrete are 304, 316, and 316LN. They are specific types of austenitic steel with 18-20% chromium and 8-10% nickel (Nurnberger 1996). Duplex stainless steel 2205, which contains about 22% chromium and 5% nickel, has received increased attention for highway bridge structures because of both its higher corrosion resistance and excellent mechanical properties in the as-rolled condition (Smith and Tullman 1999).

The most common form of corrosion for stainless steels in concrete is pitting, a localized corrosion, which can be triggered by chromium depletion around sulfide impurities on the surface (Freemantle 2002). Once pitting has initiated, a localized, deaerated anode can form inside the pits with a large cathode on the surrounding

surface. At the anode, the ferrous ion hydrolyzes to produce acid chloride, combining with the chloride ions and moisture.

$$Fe^{2+} + 2Cl^{-1} + 2H_2O \rightarrow Fe(OH)_2 + 2HCl \quad (1.17)$$

The low pH microenvironment in the pits further accelerates the pitting corrosion process, which increases auto-catalytically as more chlorides, being negatively charged ions, are attracted to the anode, "promoting further hydrolysis and consequent acidity" (Jones 1996).

The corrosion resistance of 304 and 316 stainless steels was evaluated in synthetic aqueous solutions in accelerated screening tests by McDonald, Pfeifer, and Blake (1996). These tests involved 6-hour cycles consisting of dipping the bars in solutions for 1.25 hours and then removing the specimens to allow air-drying for 4.75 hours. Tests lasted for 90 days or 360 cycles in a pH 7, 3% NaCl solution that simulated conditions in cracked concrete. Companion tests were conducted in a solution with 0.3 N KOH, 0.05 N NaOH, and 3% NaCl for 56 days, followed by with a solution with 0.3 N KOH, 0.05 N NaOH, and 9% NaCl for the second 56 days, and then in a solution with 0.3 N KOH, 0.05 N NaOH, and 15% NaCl for the last 56 days. It was found that the microcorrosion rates of the stainless steels in both the pH 7 and pH 13 solutions were 1/300 to 1/1500 of the values measured for conventional steels, indicating that a significant corrosion free life could be obtained.

In a subsequent study, McDonald, Pfeifer, and Sherman (1998) investigated the corrosion performance of 304 and 316 stainless steels in concrete using Southern Exposure and cracked beam tests. Type 304 stainless steel, when used in both mats, had a corrosion rate that was about 1/1500 of the value of conventional steel in both cracked and uncracked concrete. For 304 bars coupled with the conventional steel in the bottom mat, however, half exhibited moderate to high corrosion rates, ranging

from 1/3 to 1/100 of the value of conventional steel. In contrast, Type 316 stainless steel bars had a corrosion rate that was about 1/800 of the value of conventional bars, irrespective of whether or not the stainless steel was connected to a conventional steel bottom mat. The average corrosion thresholds of 304 and 316 stainless steel (used in both mats) were, respectively, about 15 and 24 times higher than that of the conventional steel, ranging from 11 to 18 kg/m^3 (18.5 to 30.3 lb/yd^3). It was concluded that "Type 316 stainless reinforcing steel should be considered at design stage as a potential method for obtaining a 75 to 100 year design life" for bridge decks (McDonald et al. 1998).

Clemeña and Virmani (2002) compared the corrosion behavior of three types of stainless steel reinforcing bars, pickled 304 and 316LN and nonpickled 2205, with conventional ASTM A 615 steel in outdoor concrete blocks in a Virginia Transportation Research Council (VTRC) study. The test specimen was similar to that used in the Southern Exposure test. No. 16 (No. 5) stainless bars were embedded in the concrete blocks in three combinations: straight stainless steels in both mats, straight stainless steels on the top with conventional steel on the bottom, and bent stainless steel on the top with conventional steel on the bottom. Control specimens had bent or straight conventional reinforcing bars on the top with straight bars on the bottom. The specimens were subjected to three days of ponding with a saturated NaCl solution followed by four days of natural drying at the outdoor. The weekly cycle was repeated for about two years. Measurements included the macrocell current between the top and bottom mat, open-circuit potentials, microcell corrosion rates from polarization resistance tests, and chloride contents of selected concrete samples. After almost 2 years, it was found that none of the stainless steels showed any indication of corrosion. The mean macrocell current densities in the first 100 weeks for all stainless

steels when used at both mats "ranged from only - 0.0002 to 0.0004 μA/cm^2, which are virtually negligible considering that the error of measurements was ± 0.0007 μA/cm^2" (Clemeña and Virmani 2002). In comparison, the values for the straight and bent conventional steels were 0.414 and 0.857 μA/cm^2 (4.80 and 9.94 μm/yr), respectively, at least 1000 times larger. For specimens with stainless steel in the top mat and conventional steel in the bottom mat, moderate negative macrocell currents were observed, which meant that the bottom conventional steel was corroding. Polarization resistance tests showed that conventional steel had a mean microcorrosion rate of 2.41 μA/cm^2 (27.9 μm/yr), while the 304 and 316LN stainless steels had values that ranged from 0.03 to 0.12 μA/cm^2 (0.35 to 1.39 μm/yr), with a value of 0.07 μA/cm^2 (0.81 μm/yr) for the 2205. Based on the criteria shown in Table 1.2 in Section 1.3.2, these rates suggest that the stainless steels remained passivated. The average corrosion potentials at about 100 weeks for the 304, 316LN, and 2205 stainless steels were –0.212, –0.249, and –0.247 V vs. a CSE, respectively. Chloride content analysis showed that the stainless steels had chloride thresholds above 12.3 kg/m^3 (20.7 lb/yd^3), in agreement with the results reported by McDonald et al. (1998).

Later, several other reinforcing steels including one new duplex stainless steel with approximately 21% chromium and 1% nickel, called 2101 LDX (nonpickled), were added to the VTRC study (Clemeña 2003). All specimens investigated had bent bars in the top mat and straight bars in the bottom. It was found that the 2101 LDX steel became depassivated at 21 weeks and had mean macrocorrosion and microcorrosion rates of 0.50 and 0.85 μA/cm^2 (5.8 and 9.9 μm/yr), respectively, for the first 65 weeks, while the conventional steel started to corrode at 13 weeks with mean macrocorrosion and microcorrosion rates at 1.28 and 0.67 μA/cm^2 (14.8 and

7.77 μm/yr), respectively. Based on the chlorides content tests, the chloride corrosion threshold of the 2101 steel was estimated to be 3 times that of conventional steel.

Clemeña and Virmani concluded that pickled 304 and 316LN and nonpickled 2205 stainless steel provide good corrosion performance and have a chloride threshold 16 times higher than conventional steel, while the corrosion resistance of nonpickled 2101LDX is only a slight better than that of conventional steel.

The application of stainless steels in concrete structures has been limited due to their high initial price. However, if life cycle cost is taken into account, the use of stainless steels may be justified, a point that will be addressed in the current study. The impact of the high initial cost can also be greatly reduced since stainless steels are usually used only in the more vulnerable parts of structures, such as in bridge decks. There is likely to be some contact between stainless steel in the decks and conventional steel in other parts of the structure. McDonald et al. (1998) reported that the 304 stainless steel was susceptible to moderate corrosion when coupled with the conventional steel. Nevertheless, this result has not been reproduced by any other similar tests. The current research will also study the use of stainless steel in conjunction with conventional steel.

To reduce the cost, stainless steel clad reinforcing bars have been developed. The core consists of conventional steel which is encapsulated in a thin layer of stainless steel to resist corrosion. However, part of the savings resulting from the use of the lower cost core may be offset by the difficulties in the cladding process. Furthermore, crevice corrosion caused by pinholes in the cladding is a concern (Nurnberger 1996). Stainless steel clad reinforcement is currently under test at the University of Kansas, but will not be addressed further in this report.

1.4.2 Microcomposite Steel

A so-called microcomposite steel, brand name MMFX II, was introduced in Northern America by MMFX Steel Corporation of America. The steel contains approximately 9% chromium and is less expensive than stainless steel. The manufacturers claim that MMFX steel provides an economical combination of a high corrosion resistance along with high strength because of its ferritic-martensitic microstructure. They also claim that the microstructure resulting from the MMFX's patented and proprietary chemical composition and production process minimizes the formation of microgalvanic cells that are usually induced by the ferrite and pearlite (iron-carbide) phases in conventional steel (Trejo et al. 2000).

The prototype of the MMFX steel, a dual-phase ferritic martensitic (DFM) steel with a low amount (about 0.1%) of chromium, was developed at the University of California at Berkeley. The steel was "produced by heat-treatment in the ferrite-austenite phase field followed by quenching so as to transform the austenite to dislocated martensite," which improves corrosion resistance and achieves high strength (Trejo et al. 1994). The lack of facilities to heat treat and quench reinforcing steel on a production basis led the developers to formulate a microcomposite MMFX steel that could be manufactured without the quenching operation. The initial tests on the corrosion resistance of MMFX steel were limited to measurements of microcell corrosion initiation and microcell corrosion rate, using linear polarization resistance and Tafel extrapolation for the steel in various solutions. Based on an anodic polarization test (MMFX Steel Corporation of America 2002), MMFX steel appeared to have significantly improved corrosion resistance. Since macrocell corrosion usually predominates in reinforced concrete bridge decks, however, tests involving

the corrosion of reinforcing steel in cementitious materials where a macrocell has formed are necessary.

Trejo (2002) proposed a test program to determine the critical chloride threshold and the macrocorrosion rate for MMFX steel along with several other steels, including ASTM A 615 conventional steel, ASTM A 706 low-alloy steel, and 304 and 316LN stainless steel. The critical chloride threshold was determined using an accelerated chloride threshold (ACT) test that involved electrically accelerating the migration of chloride ions toward the steel in a mortar cylinder and conducting the polarization resistance measurements to monitor the corrosion initiation. The ASTM G 109 test was performed to obtain the macrocorrosion rates of the steels. It was planned to use the information from the tests to assess the service life of reinforced concrete bridge decks.

Preliminary results from the ACT test gave an average critical chloride threshold of 5.2 kg/m^3 (8.8 lb/yd^3) for the MMFX steel, compared to 0.6 kg/m^3 (1.0 lb/yd^3) for the ASTM A 615 steel and 5.5 kg/m^3 (9.2 lb/yd^3) for the 304 stainless steel. After 40 weeks, specimens in the ASTM G 109 test had not started to corrode.

Clemeña (2003) also evaluated the corrosion resistance of MMFX steel in the second series of the VTRC study. The MMFX bars started to corrode after approximately 35 weeks, with the corrosion potential dropping abruptly from about –0.200 V to a value more negative than –0.400 V. The corrosion threshold was estimated to be 4 to 5 times higher than that of conventional steel. For the first 65 weeks, the MMFX steel had a mean microcorrosion rate of 0.34 $\mu A/cm^2$ (3.94 μm/yr) and a mean macrocorrosion rate of 0.56 $\mu A/cm^2$ (6.50 μm/yr), equal to ¼ and ¾ respectively of the values for conventional steel. Similar to 2101 steel, MMFX steel appeared to have only slightly more corrosion resistance than conventional steel.

The mechanical and corrosion properties of MMFX steel were investigated at the University of Kansas (Darwin et al. 2002) to determine if the steel is a viable substitute of the epoxy-coated reinforcing steel in reinforced concrete bridge decks. In the study, the corrosion resistance of MMFX microcomposite, conventional, and epoxy-coated reinforcing steel was evaluated using rapid macrocell tests and the initial results (Gong et al. 2002, Balma et al. 2005) from the longer-term Southern Exposure and cracked beam tests. By incorporating the results of the corrosion evaluation in an economic analysis (Kepler et al. 2000), the life expectancy and cost effectiveness of MMFX steel were analyzed in comparison to those of conventional and epoxy-coated reinforcing steel. It was concluded that:

(1) The corrosion threshold chloride content for MMFX microcomposite steel was approximately four times higher than the corrosion threshold for conventional reinforcement. The corrosion rate for MMFX microcomposite steel was between one-third and two-thirds that of conventional reinforcing steel. In all evaluations, epoxy-coated steel meeting the requirements of ASTM A 775 provided superior corrosion performance to MMFX microcomposite steel.

(2) The corrosion products deposited on the surfaces of MMFX microcomposite steel and conventional reinforcing steel were similar.

(3) Bridge decks containing MMFX microcomposite reinforcing steel will require repair due to corrosion-induced concrete cracking approximately 30 years after construction, compared to conventional bridge decks, which require repair in 10 to 25 years, depending on exposure conditions. Bridge decks containing epoxy-coated reinforcement will require repair 30 to 40 years after construction.

(4) Bridge decks containing MMFX microcomposite steel does not appear to be cost effective when compared to bridge decks containing epoxy-coated reinforcement.

Updated results on the corrosion resistance of MMFX steel, including additional chloride threshold data will be presented in the current study. The corrosion performance and the cost effectiveness of the MMFX steel will be reevaluated based on these updated results.

1.5 CHLORIDE PENETRATION IN CONCRETE

Although the penetration of chlorides into concrete is a complicated chemical and physical process that involves chloride binding and many transport mechanisms such as diffusion, capillary suction, and convection, it is generally accepted that the dominant mechanism is diffusion, which is governed by the Fick's second law, as shown in Section 1.2. The solution to the second-order, partial differential equation, Eq. (1.9), depends on the boundary conditions. Besides Eq. (1.10), other solutions to the Eq. (1.9) with a time-dependent diffusion coefficient or surface concentration have been suggested, since concrete generally becomes more impermeable as hydration proceeds and as chlorides built up at the concrete surface in the case of concrete exposed to deicing salt (Uji, Matsuoka, and Maruya 1990, Berke and Hicks 1994, Weyers et al. 1994).

Many researchers (Mangat and Molloy 1994, Thomas and Bamforth 1999, Bamforth 1999) have shown that the relationship between the diffusion coefficient D_c and time can be expressed in the form:

$$D_c = D_i t^{-m} \tag{1.18}$$

where D_i is the diffusion coefficient factor, and m is an empirical coefficient that is a function of concrete properties. Mangat and Molloy (1994) suggested that m is strongly influenced by the water-cement ratio (w/c) and can be expressed as 2.5(w/c) – 0.6. Other studies (Bamforth 1999) have found that m is also dependant on mineral admixtures in concrete. The following solution was obtained by incorporation of the time dependence of the diffusion coefficient [Eq. (1.18)] into the Fick's second law [Eq. (1.9)] if the initial chloride content in the concrete is zero (Mangat and Molloy 1994):

$$C(x,t) = C_s\left[1 - erf\left(\frac{x}{2\sqrt{\frac{D_i}{1-m}t^{(1-m)}}}\right)\right] \tag{1.19}$$

Berke and Hicks (1994) suggested that the chloride concentration at the surface of bridge decks increases linearly with time at the rate about 0.7 kg/m^3 (1.2 lb/yd^3) per year and becomes constant at around 14.8 kg/m^3 (25 lb/yd^3). Another proposal was to assume that the surface chloride increases linearly with the square root of time (Uji, Matsuoka, and Maruya 1990). Solutions to Fick's second law for a linear and a square root buildup of chloride on the concrete surface with a constant diffusion coefficient are respectively:

$$C(x,t) = kt\left[\left(1 + \frac{x^2}{2D_c t}\right)erfc\left(\frac{x}{2\sqrt{D_c t}}\right) - \left(\frac{x}{\sqrt{\pi D_c t}}\right)e^{-x^2/4Dt}\right] \tag{1.20}$$

and

$$C(x,t) = k\sqrt{t}\left[\frac{-x\sqrt{\pi}}{2\sqrt{D_c t}}erfc\left(\frac{x}{2\sqrt{D_c t}}\right) + e^{-x^2/4Dt}\right] \tag{1.21}$$

where k and D_c are constants, and *erfc* is the complementary error function: 1- *erf* (Amey et al. 1998).

While solutions with variable C_s or D_c are available, Eq. (1.10) is used most often. Many researchers agree that Fick's second law, assuming constant diffusion coefficient and surface concentration, provides an effective and realistic tool to model chloride penetration in concrete. Values of C_s and D_c that are calculated by fitting Eq. (1.10) to a measured chloride profile represent average or "apparent" values over the period during which the profile developed. For concrete with same age, D_c can be used to compare the resistance of concretes to chlorides ingress. The current study will adopt this approach because (1) specimens studied in the laboratory are ponded periodically with a certain concentrated salt solution, and (2) with a test period of just two years, the diffusion properties of concrete will be considered to be approximately constant.

In laboratories, there are several standard methods to determine chloride diffusivity in concrete. These include two longer-term tests: the AASHTO T 259 90-day salt ponding test and the ASTM C 1556 bulk diffusion test and one electrically accelerated tests: ASTM C 1202 and AASHTO T 277, "Test Method of Electrical Indication of Concrete's Ability to Resist Chloride Ion Penetration." These methods are often used to compare the resistance of concretes to chloride ingress or determine the effects of variations in the properties of concrete on chloride diffusivity in terms of D_c or other parameters. In the current study, for the purpose of determining the chloride threshold, emphasis will be placed on chloride diffusion (C_s and D_c) in concrete specimens in the Southern Exposure test, since the test is the major laboratory technique for corrosion evaluation of reinforcing steel.

McDonald, Pfeifer, and Sherman (1998) studied chloride ingress in SE specimens without embedded reinforcing bars. The concrete specimens had a water-cement ratio of 0.47. Concretes cores were removed from test specimens about every

6 weeks; 9.5 mm (0.375 in.) slices centered at 13, 32, 51, and 64 mm (0.5, 1.25, 2, and 2.5 in.) depths from the ponded concrete surface were cut from the cores. Total chloride contents were determined using ASTM C 1152. By fitting the chloride profiles to Eq. (1.10), McDonald et al. calculated a surface concentration of 1.047 percent by weight of concrete and a diffusion coefficient of 2.6×10^{-5} mm^2/s. To find the time dependence of the diffusion coefficient and the surface concentration, they also determined the apparent diffusion coefficients and the surface concentrations for each of 13 time periods during the 96-week test (every 6 or 12 weeks). Contrary to expectations, the diffusion coefficient ranged from 1.56×10^{-5} to 4.5×10^{-5} mm^2/s and surface concentration varied from 0.75 to 1.37 percent chloride by weight of concrete without any trend. The data obtained in the study were also compared with data from an earlier study (Sherman, McDonald, and Pfeifer 1996). In the earlier study, the concrete specimens had the same raw materials and similar mix design, but were subjected to continuous ponding with 3% NaCl solution according to the AASHTO T 259 instead of the Southern Exposure ponding and drying cycle. The continuously ponded specimens exhibited a diffusion coefficient of 0.9×10^{-5} mm^2/s, while the ponding and drying cycle specimens had a diffusion coefficient of 2.5×10^{-5} mm^2/s, which showed that the Southern Exposure wet-dry cycles accelerate the penetration of chlorides into concrete.

Usually, field surveys are conducted to investigate the penetration of chlorides in bridge decks. Weyers et al. (1994) studied bridge deck chloride data submitted by 16 state departments of transportation. The data consisted of measurements taken from powdered concrete samples at over 2700 locations from 321 bridge decks. At every location, the concrete samples were taken at 13 mm (0.5 in.) increments to a depth of 51 mm (2.0 in.) or more from the uncracked surface of decks. The chloride

profile over a period of about 15 years surveyed on a biennial schedule was available for 15 of the 321 bridges. By analyzing the chloride profile of the 15 bridges, they found that the chloride content in the near surface [6.4 to 13 mm (0.25 to 0.5 inch)] increased rapidly and reached a constant value in about 5 years. They concluded that the constant surface concentration was a reasonable assumption and that it could be represented by the near surface chloride content at a depth from 13 to 19 mm (0.5 to 0.75 in.) considering "the chloride penetration of the surface concrete, 0 to 0.25 in. (0 to 13 mm), may not be strictly diffusion, but may be highly influenced by surface cracking as drying shrinkage cracking and/or capillary suction" (Weyers 1998). Using Eq. (1.10) and the measured near surface chloride content as the surface concentration, they calculated the apparent diffusion coefficients for every bridge. The means of the apparent diffusion coefficients and measured surface concentrations of some states are summarized in Table 1.3.

Table 1.3 - Means of the apparent diffusion coefficients D_c and measured surface concentrations C_s and coefficients of variation (*C.V.*) by state (Weyers et al. 1994)

State	Mean D_c, 10^{-6} mm^2/s ($in.^2$/year)	*C.V.*	Mean C_s, kg/m^3 (lb/yd^3)	*C.V.*
Delaware	1.01 (0.05)	0.00	5.2 (8.7)	0.05
Minnesota	1.01 (0.05)	1.19	3.9 (6.5)	0.52
Iowa	1.01 (0.05)	0.63	4.8 (8.1)	0.30
West Virginia	1.43 (0.07)	0.62	5.1 (8.5)	0.29
Indiana	1.84 (0.09)	0.40	5.4 (9.0)	0.43
Wisconsin	2.25 (0.11)	0.59	6.1 (10.1)	0.54
Kansas	2.44 (0.12)	1.22	2.2 (3.6)	0.78
New York	2.66 (0.13)	0.03	8.8 (14.6)	0.24
California	5.11 (0.25)	1.42	1.9 (3.2)	1.48
Florida	6.75 (0.33)	1.62	3.6 (6.0)	1.06

In the study, D_c values varied from 1.0×10^{-6} to 6.8×10^{-6} mm^2/s (0.05 to 0.33 $in.^2$/year) and the surface concentrations ranged from 2 to 9 kg/m^3 (3.2 to 14.6 lb/yd^3). The D_c values in colder northern states were lower than those in warmer coastal states. For northern states, Weyers stated that "the surface chloride concentrations reflect both the winter maintenance policy of the state and the amount annual snowfall" (Weyers 1998). The corrosion environments in the United States were categorized as "low, moderate, high, and severe with corresponding surface chloride content ranges of 0 to 4, 4 to 8, 8 to 10, 10 to 15 lb/yd^3." Weyers et al. (1994) also explained that the variation in the diffusion coefficients was induced by differences in the environmental temperatures and material properties, such as water-cement ratio.

The penetration of chlorides into bridge decks is often more complicated than assumed based on the ideal diffusion process due to concrete cracking. The effect of cracks on the corrosion of reinforcing steel in bridge decks "is a function of their origin, width, depth, spacing, and orientation" (ACI Committee 2004). No model is available that considers all of these factors. Miller and Darwin (2000) and Lindquist, Darwin, and Browning (2005) surveyed 59 reinforced concrete bridge decks for crack density and chloride concentration in both cracked and uncracked concrete in Kansas over the past several years. The decks included three types: silica fume overlay, conventional overlay, and monolithic concrete. Ages ranged from several months to 20 years. For each concrete placement on the 59 decks, concrete samples were taken at 19 mm (0.75 in.) increments to a depth of 95 mm (3.75 in.) at three cracks (on cracks) and at three uncracked locations (off cracks). The water-soluble chloride concentrations were reported and used to determine effective diffusion coefficients, surface concentrations, and the time to reach the chloride threshold. They found that the chloride concentrations on cracks increased nearly linearly with age and

decreased steadily as the sample depth increased. Linear tread lines of chloride content versus age at each depth were obtained using "on crack" chloride data, as shown in Figure 1.1.

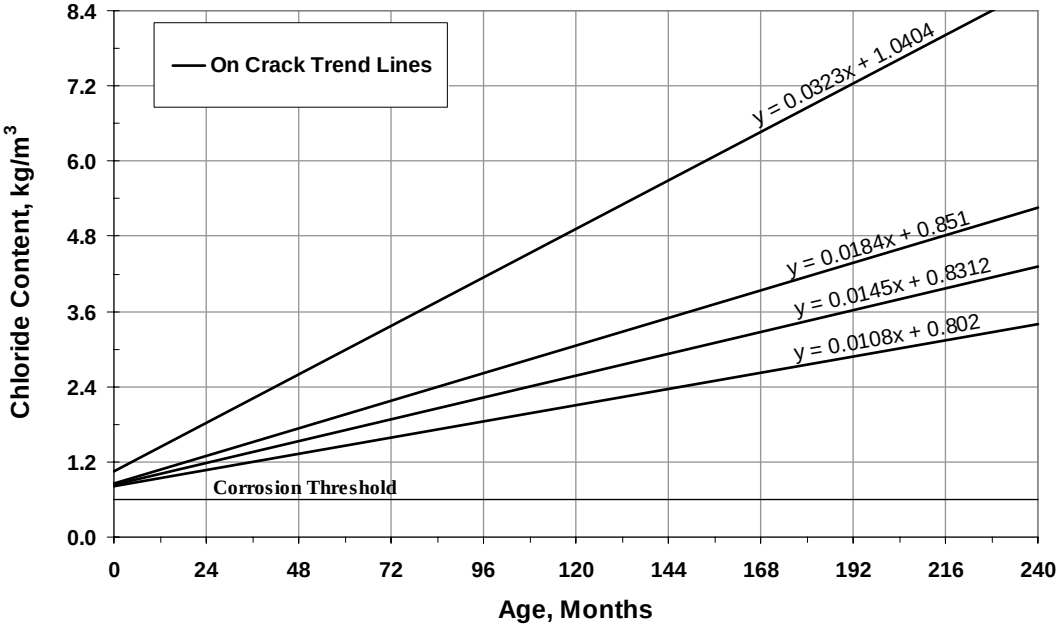

Figure 1.1 - Linear trend lines for interpolated chloride data taken on cracks at four depths. The depths are 25.4 mm (1.0 in.), 50.8 mm (2.0 in.), 63.5 mm (2.5 in.), and 76.2 mm (3.0 in.) and progress from top to bottom (Lindquist et al. 2005).

Based on the samples taken from uncracked concrete, an effective diffusion coefficient and apparent chloride surface concentrations were calculated for each deck placement using Fick's second law [Eq. (10)]. Overall, the effective diffusion coefficients were found to decrease with time, but the decrease was not monotonic. For three deck age categories: 0 to 48 months, 48 to 96 months, greater than 96 months, the mean effective diffusion coefficients were respectively, 1.04×10^{-6}, 1.97×10^{-6}, 1.85×10^{-6} mm^2/s for monolithic concrete decks, 1.74×10^{-6}, 0.93×10^{-6}, 0.93×10^{-6} mm^2/s for conventional overlay decks, and 1.50×10^{-6}, 0.81×10^{-6}, 1.27×10^{-6} mm^2/s for 5% silica fume overlay decks. Lindquist et al. also observed that the

apparent surface concentrations increased with age, shown in Fig.1.2. The mean surface concentrations for all deck types were 6.0 kg/m^3 (10.1 lb/yd^3) and 10.0 kg/m^3 (16.1 lb/yd^3) respectively, for the 0 to 48 months and 48 to 96 months.

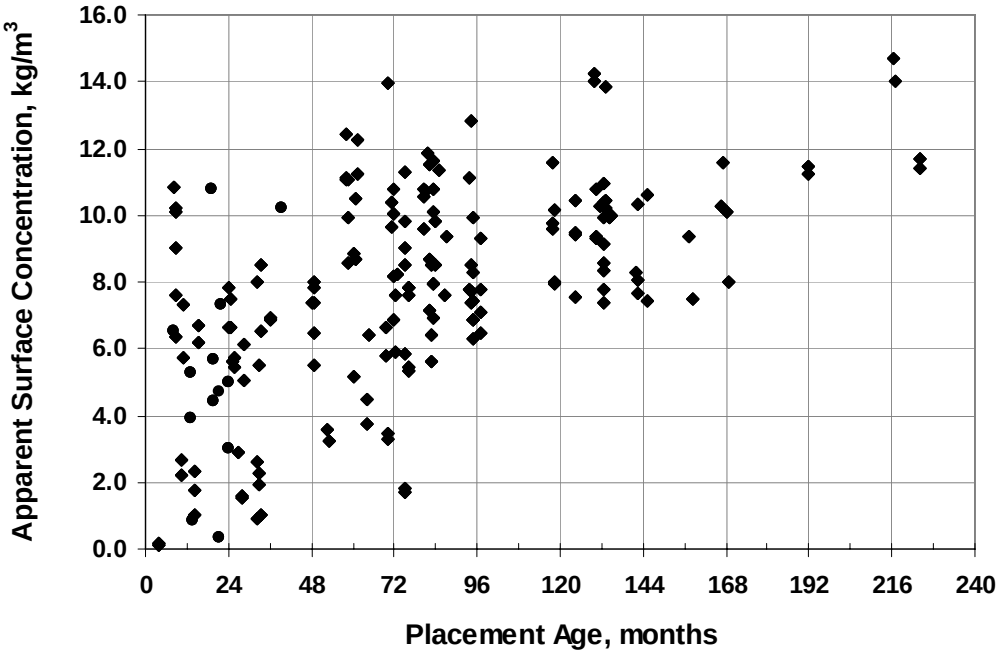

Figure 1.2-Average apparent surface concentration calculated from Fick's second law versus bridge deck placement age at the time of sampling (Lindquist et al. 2005).

The surface concentrations C_s obtained by Lindquist et al. (2005) are much higher than those obtained by Weyers et al. (1994) (average 2.2 kg/m^3) because they were calculated using a best fit of Fick's second law rather than being based on average values for near-surface samples, which were used by Weyers et al. (1994). Based on the survey data obtained by Lindquist et al. (2005), the average measured chloride content at a depth of 19 mm (0.75 in.) for all deck types was 3.2 kg/m^3 (5.4 lb/yd^3) for 48 to 96 moths, which is similar to the result obtained by Weyers et al.

These field surveys provide important information for service life predictions of reinforced concrete bridge decks.

1.6 CRITICAL CHLORIDE THRESHOLD

Numerous studies have been conducted to determine the critical chloride threshold, i.e., the minimum chloride concentration required to initiate corrosion of reinforcing steel in concrete. A range of results has been reported. The literature indicates that there may not be one universal threshold value because of the large number of variables that influence on the chloride concentration needed for depassivation and the lack of agreement on test methodologies.

In addition to the inherent properties of the steel, the chloride threshold is also dependent on the conditions in the surrounding environment, such as the availability of oxygen and moisture, the presence of voids at the steel-concrete interface, and especially the pH of the concrete (the concentration of hydroxyl ions in the pore solution) (Bertolini et al. 2004). Many factors such as the alkali content of cement, presence of mineral admixtures, degree of carbonation, and temperature can affect the pH of the concrete, and thus, the chloride threshold.

The higher the hydroxyl ion concentration, the higher the chloride concentration needed to initiate corrosion. Many studies have suggested that it is better to express the chloride threshold as a ratio of chloride to hydroxyl ion concentration. Based on early studies of steel immersed in synthetic concrete pore solution with chlorides (Hausmann 1967, Gouda 1970, Diamond 1986, Goni and Andrade 1990), threshold Cl^-/OH^- ratios of 0.3, 0.6, and 0.25 to 0.8 for conventional reinforcing steel have been proposed in different studies. More recent work has shown that the threshold Cl^-/OH^- ratio for steel embedded in mortar or concrete is generally higher than that found in the solution tests. For instance, Lambert, Page, and Vassie (1991), Hussain, Al-Gahtani, and Rasheeduzzafar (1996), and Alonso et al. (2000) reported threshold Cl^-/OH^- ratios of 3, 1.28 to 2.0, 1.17 to 3.98,

respectively. While the Cl^-/OH^- ratio is an important parameter to control corrosion initiation, due to difficulties in measuring the OH^{-1} concentration in mortar or concrete, many researchers favor expressing the chloride threshold as a chloride content by weight of cement or concrete, which is also a more meaningful number for service life prediction or other purposes in practice (Thomas 2002).

It is important to distinguish between acid-soluble and water-soluble chloride concentrations when describing the chloride content of concrete. The acid-soluble chloride concentration is often equal to total chloride in concrete, while the water-soluble chloride represents free chloride dissolved in concrete pore solution. They can be determined by methods including ASTM C 1152 for acid-soluble, ASTM C 1218 for water-soluble, ASSHTO T 260 (including test produces for both acid and water soluble chlorides), and a Soxhlet procedure recommended by ACI Committee 222 (2001) for water soluble chloride, which can exclude the chloride contained in aggregates. It is well known that not all chlorides in the concrete will promote the corrosion of the steel. Some of the chlorides will be removed from the pore solution by the chloride binding, the major form of which is the reaction between chlorides and tricalcium aluminate (C_3A) to form calcium chloroaluminate ($3CaO{\cdot}Al_2O_3{\cdot}CaCl_2{\cdot}10H_2O$). As a result, the higher the C_3A content of the cement, the more chlorides will be bound. The binding of the chlorides in concrete is also a function of many other factors, including the tetracalcium aluminoferrite (C_4AF) content, pH, water-cement ratio, mineral admixtures, and whether the chloride was introduced into concrete at the time of mixing or penetrated into the mature concrete from the external environment (ACI Committee 222 2001). While it appears to be more reasonable to express the chloride threshold as the water-soluble chloride content in concrete, the acid-soluble value is often used. One of the reasons involves

the belief that bound chloride can be released when the pH of the concrete drops and, thus, presents a corrosion risk "due to its contribution to the reservoir of available chloride at the steel concrete interface" (Glass and Buenfeld 1997).

There are currently no standard tests available for determining the chloride threshold of reinforcing steel in concrete. Different parameters have been used to indicate corrosion initiation, including mass loss (Thomas 1996), corrosion potential (Hausmann 1967, Gouda 1970, Hussain, Al-Gahtani, and Rasheeduzzafar 1996, Oh, Jang, and Shin 2003), microcorrosion rate (Goni and Andrade 1990, Lambert, Page, and Vassie 1991, Alonso et al. 2000, Trejo 2002), macrocorrosion rate (Schiessl 1996), or a combination of indications (Hope and Ip 1987). The criteria used most often include a corrosion potential shift to a value more negative than –0.350 V (vs. CSE) and a microcorrosion rate by the linear polarization resistance test that jumps to more than 0.1 $\mu A/cm^2$ (1.16 μm/yr). In ASTM G 109, a macrocell current of 10 μA or greater between the two mats of steel, equivalent to a current density of 0.072 $\mu A/cm^2$ and a corrosion rate of 0.83 μm/yr for a No. 16 [No. 5] bar, is considered to be the condition to terminate the test and might be considered as an indication of depassivation.

Reinforcing steel has been evaluated under different exposure conditions in different tests, such as immersing a bare bar in a solution of controlled composition and embedding the bar in mortar or concrete with chlorides added to the mixture or penetrating the hardened concrete from external sources. Although a "solution test" is rapid and also facilitates examining the effect of the Cl^-/OH^- ratio, these tests disregard the resistivity of the concrete, the conditions of the steel concrete interface, and the availability of oxygen and moisture (Thomas 2002). Therefore, the critical chloride threshold test in a cementitious environment is in all likelihood necessary as

it is for the evaluation of other corrosion resistance parameters. The balance of this section will review tests in concrete.

In concrete tests, to accelerate corrosion initiation of reinforcing steel, chlorides often are added in the concrete mix (Hope and Ip 1987, Oh, Jang, and Shin 2003). This method will not be adopted in the current study because a significant number of trial batches are required to obtain the correct minimum amount of the chlorides, especially when an estimate of the corrosion threshold is not available. Moreover, a higher percentage of chlorides will be bound when they are introduced at the time of mixing, rather than when hardened concrete is exposed to external chlorides. For example, Oh et al. (2003) reported that the acid soluble chloride threshold for conventional steel ranged from 0.45 to 0.91% by weight of cement, while the water soluble chloride threshold had a value of only about 0.1% in their tests.

As an accelerated test method, the Southern Exposure test can be used to determine the chloride threshold. During the test, once the depassivation of reinforcing steel has been identified, concrete samples close to the steel can be taken for the chloride content analysis. In the study by Pfeifer, Landgren, and Zoob (1987), powder samples were obtained by drilling three ¼ -in. holes into two sides of the SE test slabs in the plane of the top surface of the top bars when the corrosion current indicated the start of macrocell corrosion. The depth of the holes was 2 in. and the samples from the first inch were discarded. The holes were then filled with a sanded epoxy to allow the tests to continue. It was reported that the acid-soluble chloride content at time-to-corrosion for conventional steel ranged from 0.018% to 0.049% by weight of concrete [0.4 to 1.1 kg/m^3 (0.69 to 1.9 lb/yd^3)], with an average value of 0.032% [0.72 kg/m^3 (1.2 lb/yd^3)]. The concern with this technique is how

representative the results are if the concrete samples are taken from a just few locations.

Another way to determine the chloride threshold using the SE test is to obtain a chloride profile from test specimens, with or without bars. Based on the chloride profile, the threshold value can be determined using Fick's second law [Eq. (1.10)]. For example, Eq. (1.10) has four degrees of freedom, depth d, time t, surface concentration C_s, and diffusion coefficient D_c; if a chloride profile in the specimen is known, the surface concentration C_s, and diffusion coefficient D_c can be obtained using nonlinear regression analysis, as mentioned in Section 1.2. Once C_s and D_c are known, the chloride threshold of reinforcing steel can be determined at the time of corrosion initiation for the depth of steel. In the VTRC research (Clemeña 2003), chloride profiles were obtained from 16 randomly selected test specimens in which concrete samples were taken at depths ranging from 13 to 51 mm (0.50 to 2.0 in.), in 13 mm (0.5 in.) intervals, with exposure times ranging from 16 weeks to 94 weeks. Based on corrosion initiation times of 13, 21, and 35 weeks, and a depth of 33 mm (1.25 in.) from the concrete surface to the bar center [rather than a cover thickness of 25.4 mm (1.0 in.)], average acid chloride thresholds of 0.035, 0.169, and 0.169% by weight of concrete [0.80, 3.8, and 3.8 kg/m^3 (1.3, 6.4, and 6.4 lb/yd^3)] were reported for conventional, 2101 LDX, and MMFX-2 reinforcing steel, respectively. McDonald et al. (1998) investigated the chloride profile in dummy SE specimens, as described in Section 1.5. Instead of using the C_s and D_c (although both were calculated), they estimated the chloride concentrations at a depth of 25 mm (1 in.) by linear interpolation using data at depths of 12.7 mm (0.5 in.) and 31.7 mm (1.25 in.), obtaining average corrosion thresholds ranging from 11 to 18 kg/m^3 (18.5 to 30.3 lb/yd^3) for 304 and 316 stainless steel.

It is usually time-consuming to determine the chloride threshold because the penetration of chlorides into concrete is slow, even under severe test regimes such as the Southern Exposure cycling. In response, methods have been proposed to accelerate the migration of chlorides towards the reinforcing steel under the influence of an electrical field so that the test time can be reduced (Trejo 2002, Castellote, Andrade, and Alonso 2002). In these methods, mortar specimens with embedded reinforcing steel is ponded with NaCl solution; a noble metal mesh connected to the negative pole of a DC power source is placed in the salt solution acting as a cathode; another metal mesh or plate is placed outside or embedded inside the specimen to serve as an anode. By applying an initial voltage difference between the electrodes, negative ions (Cl^-, OH^-) are drawn into the concrete towards the bar and positive ions (Ca^{2+}, Na^+) are attracted to the cathode in the solution. After depassivation of the steel, mortar samples adjacent to the steel are evaluated for chloride ion concentration. In his accelerated chloride threshold (ACT) test, Trejo (2004) chose a 20 V potential difference, applied periodically, while the microcorrosion rate of the embedded steel was monitored using the linear polarization resistance test. Corrosion initiation was defined for the steel when the corrosion rate exceeded 10 $\mu A/cm^2$ (116 $\mu m/yr$). From the ACT test, average chloride thresholds of 0.5 kg/m^3 (0.9 lb/yd^3) for ASTM A 615 steel, 4.6 kg/m^3 (7.7 lbs/yd^3) for MMFX microcomposite steel, 5.0 kg/m^3 (8.5 lb/yd^3) for 304 stainless steel, and 10.8 kg/m^3 (18.1 lb/yd^3) for 316LN stainless steel were reported (Trejo and Pillai 2003, 2004). Castellote et al. (2002) developed an electrically accelerated method with the ability to simultaneously determine the chloride threshold of reinforcing steel and the diffusion coefficient of concrete. Microcorrosion rates of more than 0.10 $\mu A/cm^2$ (1.16 $\mu m/yr$) were considered to be indicate depassivation. Results from the test gave a chloride

threshold of 0.152% by weight of mortar and a critical Cl^-/OH^- of 2.0 for conventional steel, compared to the values of 0.277% and 1.5 from controlling tests without applying electrical field.

Further study of these methods is needed. For example, it is not clear how the accuracy of the tests is affected by the influence of applied electrical field on the OH^- concentration of the pore solution at the steel mortar interface (Trejo and Pillai 2003).

In this report, the critical chloride threshold will be studied for reinforcing steel embedded in concrete specimens using chlorides penetrating from the external environment, which simulates the type of exposure that occurs for bridge decks.

1.7 SERVICE LIFE PREDICTION MODELS OF REINFORCED CONCRETE BRIDGED DECKS

The accurate prediction of the service life of bridge decks is of great importance in the selection of corrosion protection systems (in this report “service life” means the time to first repair). Service life prediction methods involve empirical estimation, accelerated testing, mathematical modeling in terms of the processes of the chemical and physical deterioration, and applications of reliability and stochastic concepts. A combination of these methods is usually used (ACI Committee 365).

At present, most service life models for bridge decks follow the approach first proposed by Tuutti (1982), that is, dividing the service life (T_s) of bridge decks into two time periods.

1) The initiation period (T_i) - the time it takes for chlorides to penetrate the concrete cover and reach the threshold concentration at the depth of the embedded steel, causing corrosion to initiate.

2) The propagation period (T_p) - the time it takes after corrosion initiation for corrosion products to cause cracking, spalling, or a significant damage to the concrete.

The initiation period (T_i) - The time to corrosion initiation (T_i) is dependent on the concrete depth, the properties of the concrete, the environment, such as the amount of deicing salt applied and temperature, the chloride threshold of the reinforcing steel, and the soundness of concrete. Many methods have been developed to estimate the initiation time. Most of them simply use Fick's second law to model the penetration of chlorides without accounting for other mechanisms or the soundness of the concrete. Based on Eq. (1.10) with constant C_s and D_c, T_i can be expressed as

$$T_i = \frac{d^2}{4D_c}\left(erf^{-1}\frac{C_s - C_{cr}}{C_s - C_i}\right)^{-2} \tag{1.22}$$

where

d = concrete cover;

C_{cr} = critical chloride threshold of reinforcing steel;

C_s = surface concentration;

D_c = diffusion coefficient.

Field surveys are a major source of information on chloride diffusion coefficients and surface concentrations for bridge decks.

As shown in Table 1.3 in Section 1.5, Weyers et al. (1994) presented the apparent diffusion coefficients and the measured near surface chloride concentrations for bridges in different states. The time to corrosion initiation can be calculated based on the values in the table. For instance, the average near surface chloride concentration and chloride diffusion coefficient in Kansas were 2.2 kg/m^3 (3.71

lb/yd^3) and 2.44 × 10^{-6} mm^2/s, respectively. Based on Fick's second law [Eq. (1.22)], the time to reach a chloride concentration of 0.6 kg/m^3 (1.0 lb/yd^3) at a depth of 76.2 mm (3.0 in.) is 17.5 years.

As reported by Lindquist, Darwin, and Browning (2005), the average diffusion coefficient and mean surface concentration for monolithic concrete decks ranging in ages from 48 to 96 months in Kansas were 1.97×10^{-6} mm^2/s (0.096 in.^{2}/year) and 10.0 kg/m^3 (16.0 lb/yd^3), respectively. Using these values, the time for the chloride concentration to reach the corrosion thresholds of 0.6 kg/m^3 (1.0 lb/yd^3) at a depth of 76.2 mm (3.0 in.) is 13.6 years.

The apparent diffusion coefficient D_c can also by estimated from bulk diffusion tests such as ASTM C 1556. A computer based service life model, Life-365 (Concrete Corrosion Inhibitors Association 2001), which is based primarily on a model developed at the University of Toronto (Boddy et al. 1999), uses a relationship between the diffusion coefficient of plain portland cement concrete at 28 days age D_{28} and the water-cement ratio *w/c*,

$$D_{28} = 1\times10^{(-12.06 + 2.4\, w/c)}\ \text{m}^2/\text{s} \tag{1.23}$$

which is based on a large database of laboratory bulk diffusion tests. A time and temperature dependent diffusion coefficient $D(t, T)$ was expressed as follows, based on the D_{28}.

$$D(t,T) = D_{28}\left(\frac{28}{t}\right)^m \exp\left[\frac{U}{R}\left(\frac{1}{T_{ref}} - \frac{1}{T}\right)\right] \tag{1.24}$$

where

$D(t,T)$ = diffusion coefficient at time t (days) and absolute temperature T.

m = constant, same as m in Eq. (1.17) and (1.18).

U = activation energy of the diffusion process (35000 J/mol).

R = gas constant, 8.314 J/(mol·K)

T_{ref} = room temperature, 293 K.

The diffusion coefficient calculated using Eq. (1.23) and Eq. (1.24), for example, D = 2.5×10^{-6} mm^2/s for a portland cement concrete with w/c = 0.4 at 10 years at 10°C, is in agreement with the range of results reported by Weyers (1998) from field surveys (Bentz and Thomas 2001).

The Life-365 model estimates the initiation time using a finite difference implementation of Fick's second law [Eq. (1.9)] with a modified $D(t, T)$ using Eq. (1.24) at every time step (Bentz and Thomas 2001). The time to corrosion initiation for a 0.6 kg/m^3 (1.0 lb/yd^3) chloride threshold at a depth of 76.2 mm (3.0 in.) is 16.8 years, based on the model.

The methods using Fick's second law to predict the initiation time do not consider concrete cracking. However, reinforced concrete bridge decks do crack, and the cracks can definitely accelerate the onset of the corrosion processes. The penetration of chloride in cracked concrete was investigated by Miller and Darwin (2000) and Lindquist et al. (2005), as mentioned in Section 1.5. Based the results from the study by Miller and Darwin (2002), Darwin et al. (2002) estimated times to corrosion initiation at a depth of 76.2 mm (3 in.) of approximately 15 months for conventional steel and 71 months for MMFX microcomposite steel based on chloride thresholds of 0.94 lb/yd^3 for conventional steel and 3.32 lb/yd^3 for MMFX steel and an average background chloride concentration of 0.3 lb/yd^3. Updated results for chloride ingress in cracked concrete decks are shown in Fig. 1.1. Based on the trend lines for chloride content versus age at each depth, regardless of bridge deck type, even at 76.2 mm (3 in.) depth, chloride concentrations were found to exceed 0.9 kg/m^3 (1.5 lb/yd^3) by the end of the first winter season after construction.

The propagation period (T_p) – The length of this period depends on the corrosion rate of reinforcing steel, the amount of corrosion (the quantities of corrosion products or the thickness loss of steel) expected to result in concrete cracking, and the definition of "significant damage" (Bentz and Thomas 2001).

The corrosion rate of reinforcing steel can be measured using laboratory techniques. For real structures, however, it varies significantly with the concrete properties and the environmental conditions. The amount of corrosion needed to crack concrete involves the mechanical properties of concrete, the depth of concrete cover, the size of the reinforcing steel, the microstructure of steel/concrete interface, and the nature of the corrosion (uniform or localized) (Liu and Weyers 1998, Torres-Acosta and Sagues 2004). The definition of significant damage is dependent on the importance of the structure and the requirements of the owner.

Due to these uncertain factors, a simplified approach is used by some. Fixed values of 6 years and 20 years are assigned to uncoated and epoxy-coated reinforcing steel, respectively, in the Life-365 model.

Several refined methods, involving mathematical modeling and/or accelerated tests have been developed to determine the propagation period. These models usually define concrete cracking as the end of the service life of bridge decks and calculate or assume the amount of corrosion needed. The length of the propagation period can be obtained in terms of the amount of corrosion and the corrosion rate.

For uniform corrosion, a thickness loss of reinforcing steel resulting in a volume of corrosion products that will crack concrete has been reported ranging from 3 to 74 μm (0.0001 to 0.003 in.) (Torres-Acosta and Sagues 2004). Based on bench-scale tests, a value of 25 μm (0.001 in.) is often assumed (McDonald, Pfeifer, and Sherman 1998, Pfeifer 2000, Darwin et al. 2002). Using the value of 25 μm, along

with one-half of corrosion rates measured at 23 weeks in cracked beam tests, Darwin et al. (2002) estimated lengths of the corrosion propagation period of 11.6 years and 20.8 years for conventional and MMFX reinforcing steel, respectively.

Liu and Weyers (1998) developed a mathematical model to calculate the weight of corrosion products (W_{crit}) needed to crack concrete. The critical weight (W_{crit}) included three portions: (1) the quantities of corrosion products to fill the space of the original steel (W_o), (2) the quantities of corrosion products to fill the porous space around the steel concrete interface (W_p), and (3) the quantities of corrosion products to cause tensile stresses in the surrounding concrete that are high enough to cause cracking after the porous zone is filled (W_s). Assuming that the corrosion products form uniformly on the steel surface, for a unit length of reinforcing bar, the value of W_{crit} is expressed as follows:

$$W_{crit} = \rho_{rust}\pi\left(d_{\mathrm{o}} + d_{\mathrm{p}} + d_{\mathrm{s}}\right)\phi \tag{1.25}$$

where

ρ_{rust} = density of the corrosion products, assumed to be 3600 kg/m^3;

d_{o} = thickness of loss of reinforcing steel, $d_{\mathrm{o}} = \frac{w_{steel}}{\pi D \rho_{steel}}$, in which

W_{steel} is the amount of steel corroded and equals to 0.57 W_{crit} (0.57 is the ratio of molecular weight of iron to the average molecular weight of corrosion products, $Fe(OH)_2$ and $Fe(OH)_3$), ρ_{steel}, the density of the steel, is 7800 kg/m^3;

d_{p} = thickness of porous zone around the steel concrete interface, assumed to be 12.5 μm;

d_{s} = thickness of corrosion products to generate critical tensile stresses after the porous zone is filled. It is a function of concrete cover

depth, reinforcing bar size and concrete mechanical properties and can be obtained by the finite element method:

$d_s = \frac{Cf_t'}{E_{ef}}\left(\frac{a^2+b^2}{b^2-a^2} + \nu_c\right)$, in which $a = (\phi + 2d_p)/2$, $b = C + (\phi + 2d_p)/2$ and d_s = 12.1 μm and 33.5 μm assuming concrete tensile strength f_t' = 3.3 MPa (472 psi), effective elastic modulus E_{ef} = 9 GPa (1,3000,000 psi), and Poisson's ratio ν_c = 0.18 for No. 16 (No. 5) reinforcing steel with a concrete cover (C) of 25.4 mm (1 in.) and 76.2 mm (3 in.), respectively;

ϕ = diameter of reinforcing steel.

Based on this model [Eq. (1.25)], thickness losses of reinforcing steel resulting in a volume of corrosion products that will crack concrete (d_o), are equal to 8.8 μm (0.0004 in.) and 16.4 μm (0.0007 in.) for No. 16 (No. 5) reinforcing steel with a concrete cover of 25.4 mm (1 in.) and 76.2 mm (3 in.), respectively. These values are at the lower bound of the range of the values from laboratory tests (Torres-Acosta and Sagues 2004).

The corrosion of reinforcing steel may be localized in concrete bridge decks. Torres-Acosta and Sagues (2004) experimentally estimated the thickness loss of reinforcing steel (x_{crit}) required to crack concrete cover when only a fraction of the reinforcing bar corrodes. Carbon steel bars with different concrete cover to bar diameter and concrete cover to anode length ratios were embedded in cylindrical and prismatic concrete specimens and subjected to accelerated corrosion. By measuring mass losses and actual anodic lengths of the bars, they found that the value of x_{crit} ranged from 30 to 272 μm (0.0012 to 0.011 in.), compared to 3 to 74 μm (0.0001 to 0.003 in.) for uniform corrosion. Based on their results, as well as the results of others, they proposed an empirical equation for the x_{crit}, which is expressed as a

function of specimen dimensions, such as concrete cover *C*, reinforcing bar diameter ϕ, and anodic length *L*, as follows:

$$x_{crit} = 11\left(\frac{C}{\phi}\right)\left(\frac{C}{L}+1\right)^2 \text{ μm} \quad (1.26)$$

Based on Eq. (1.26), x_{crit} is equal to 26 μm (0.001 in.) for a Southern Exposure specimen using a 25 mm (1 in.) concrete cover (*C*), 16 mm (0.5 in.) bar diameter (ϕ), and 305 mm (12 in.) anodic bar length (*L*), which is consistent with the often assumed value of 25 μm (0.001 in.). For an epoxy-coated bar with four 3.2-mm (0.125 in.) diameter drilled holes on the top mat of the SE specimen, assuming that the tensile stress caused by the volume of the corrosion products from one hole on one side of the epoxy-coated bar is half of the stress caused by the corrosion products over a ring shaped region with length L same as the diameter of the hole, a thickness loss of the bar required to crack concrete cover (x_{crit}) is estimated to be 2852 μm, twice the corrosion loss given by Eq. 1.26 over the ring shaped region (Gong et al., 2005).

Once the service life of a bridge deck is estimated, a life cycle cost analysis can be conducted using economic analysis techniques, similar to that described by Kepler, Darwin, and Locke (2000).

1.8 OBJECTIVE AND SCOPE

The objective of this study is to evaluate the corrosion resistance and the cost effectiveness of duplex stainless and MMFX microcomposite steels compared to epoxy-coated and conventional reinforcing steel for bridges decks using laboratory tests.

The reinforcing steels evaluated include: (1) Four heats of conventional steel, N, N2, N3, N4, and epoxy-coated reinforcing steel used as control specimens; (2) two

duplex stainless steels, 2101 and 2205 with and without picking; and (3) MMFX microcomposite steel.

The objective will be achieved by:

(1) Evaluating the corrosion rate and corrosion potential of the reinforcing steels using the rapid macrocell test (with and without mortar cover on the steel) and two bench-scale tests, the Southern Exposure and cracked beam tests.

(2) Investigating the chloride profile of concrete specimens in the Southern Exposure test. Based on the chloride profile and Fick's second law, determining the equation of the chloride diffusion in the test specimens by means of a nonlinear regression analysis using the method of least squares.

(3) Determining the critical chloride threshold of the reinforcing steels using two approaches: First, using the chloride diffusion equation and time-to-corrosion of the steels in the Southern Exposure test. Second, by analyzing chloride contents adjacent to the steels in concrete specimens under Southern Exposure cycling at the time that corrosion initiates.

(4) Estimating the service life of bridge decks containing the reinforcing steels based on the laboratory results for the critical chloride threshold and corrosion rate, along with field survey data. Based on the service life, performing a life cycle cost analysis to compare the cost effectiveness of these steels for bridge decks over a 75-year economic life.

CHAPTER 2

EXPERIMENTAL WORK

2.1 GENERAL

In this study, the rapid macrocell, Southern Exposure (SE), and cracked beam (CB) tests are used to measure the corrosion rate and corrosion potential of reinforcing steel. Because these tests are not standardized, a full description of the test methods is presented. To determine the critical chloride threshold for each reinforcing steel, the chloride profiles of concrete specimens in the Southern Exposure test are investigated and powdered concrete samples are taken directly from bench-scale specimens for chloride ion analysis when corrosion initiates.

An additional set of corrosion potential tests are performed to compare conventional and MMFX steels in simulated concrete pore solutions with various NaCl concentrations. The test method and results are presented in Appendix D.

2.2 TESTED REINFORCING STEELS

The reinforcing steels evaluated in this study include:

1) Four heats of conventional ASTM A 615 reinforcing steel: N, N2, N3, and N4; 2) Epoxy-coated N3 reinforcing steel: ECR; 3) Microcomposite MMFX II steel: MMFX; 4) Two heats of 2101 duplex stainless steel “as rolled”: 2101, 2101(2), and pickled to remove the mill scale: 2101p and 2101(2)p; 5) 2205 duplex stainless steel “as rolled”: 2205, and pickled: 2205p.

The epoxy-coated reinforcing bars meet the requirements of ASTM A 775. MMFX steel contains about 9% chromium. Type 2101 steel contains about 21% chromium and 1% nickel, while 2205 steel contains about 25% chromium and 5%

nickel. The bars in the first heat of 2101 steel, 2101 and 2101p, were slightly deformed and had small cracks on the surface due to a lack of boron. The second heat, 2101(2) and 2101(2)p, was provided to allow a fair evaluation of the steel. For the pickled bars, 2101p, 2101(2)p, and 2205p, the pickling procedure involved blasting the bars to a near white finish with stainless steel grit and then placing them in a solution of 25% nitric acid and 3% to 6% hydrofluoric acid at 110 to 130º F for 40 to 50 minutes (Larsen 2004).

No. 16 [No. 5] bars were used for all tests. The chemical compositions and the mechanical properties of the reinforcing steels are presented in Tables 2.1 and 2.2, respectively.

Table 2.1- Chemical compositions of reinforcing steel as reported by producing mills

Designation	Heat No.	C	Mn	P	S	Si	Cr	Cu	Ni	Sn
N	K0-5152	0.400	1.010	0.022	0.032	0.220	0.200	0.300	0.200	0.010
N2	K0-C696	0.420	0.960	0.014	0.040	0.200	0.140	0.300	0.100	0.009
N3(1)	S44407	0.430	1.150	0.013	0.020	0.240	0.100	0.380	0.080	0.015
N3(2)	S44420	0.450	1.150	0.012	0.024	0.260	0.120	0.380	0.120	0.017
N4	231159	0.430	0.950	0.014	0.046	0.210	0.200	0.490	0.170	0.014
MMFX	810737	0.060	0.460	0.010	0.011	0.230	9.130	0.100	0.080	-
2101	-	0.032	4.990	0.023	0.001	0.490	21.33	0.350	1.530	-
2101(2)	-	0.030	4.900	0.019	0.001	0.770	21.42	0.350	1.520	-
2205	-	0.020	1.370	0.023	0.001	0.420	22.20	0.300	4.880	-

Designation	Heat No.	Mo	V	Nb	N	Al	Cb	Ca	B	Ti
N	K0-5152	0.040	0.003	-	-	-	-	-	-	-
N2	K0-C696	0.019	0.002	-	-	0.001	-	-	-	-
N3(1)	S44407	0.020	0.001	-	-	-	0.002	12 ppm	-	-
N3(2)	S44420	0.030	0.001	-	-	-	0.002	14 ppm	-	-
N4	231159	0.038	0.001	-	-	-	-	-	0.0005	0.001
MMFX	810737	0.020	0.018	0.007	118 ppm	-	-	-	-	-
2101	-	0.130	-	-	0.222	-	-	-	-	-
2101(2)	-	0.330	-	-	0.237	-	-	-	-	-
2205	-	3.260	-	-	0.192	-	-	-	-	-

Table 2.2- Mechanical properties of reinforcing steel

Designation	Heat No.	Yield strength		Tensile strength		Elongation % in 203 mm (8 in.)	Bending
		(MPa)	(ksi)	(MPa)	(ksi)		
N	K0-5152	466.6	67.7	774.0	112.3	13.0	OK
N2	K0-C696	467.1	67.7	745.1	108.1	15.0	OK
N3(1)	S44407	469.5	68.1	734.3	106.5	15.0	OK
N3(2)	S44420	469.5	68.1	740.5	107.4	12.5	OK
N4	231159	442.7	64.2	713.6	103.5	15.0	OK
MMFX	810737	-	-	1131.5	164.1	6.0	-
2101	-	460.1	66.7	722.1	104.7	36.0	-
2101(2)	-	519.2	75.3	760.9	110.3	35.6	-
2205	-	490.2	71.1	742.6	107.7	32.2	-

2.3 RAPID MACROCELL TEST

In the rapid macrocell test, reinforcing bars are evaluated with and without a mortar cover in simulated concrete pore solution with two different sodium chloride (NaCl) molal ion concentrations (1.6 m and 6.04 m). The test specimen, test procedure, apparatus and materials, and test program are described in this section.

2.3.1 Test specimens

The specimens in the rapid macrocell test consist of a 127 mm (5 in.) long, No. 16 [No. 5] reinforcing bars, either bare or embedded in mortar, as illustrated in Figure 2.1. The fabrication of the specimens is described as follows:

1) Preparation of reinforcing bars: One end of the bar is drilled and tapped 13 mm (0.5 in.) to accommodate a No. 10-24 machine screw. The sharp edges on the bar ends are removed by grinding. Uncoated bars are cleaned with acetone to remove grease and dirt from the surface. For epoxy-coated reinforcing steel, the bars are cleaned with soap and water. Then, the epoxy coating is penetrated by four 3.2 mm

(0.125 in.) diameter holes to simulate defects in the coating. The holes are made to a depth of 0.5 mm (0.020 in.) using a 3.2-mm (0.125-in.) diameter four-flute end mill. Two of the holes are placed at the midlength of the bars and the other two are placed about 32 mm (1.25 in.) from the untapped end, which will be submerged in the solution. This submerged end is protected using a plastic cap filled with Herberts O'Brien epoxy. The four holes represent about 1% damage to the evaluated area of the epoxy-coated bars.

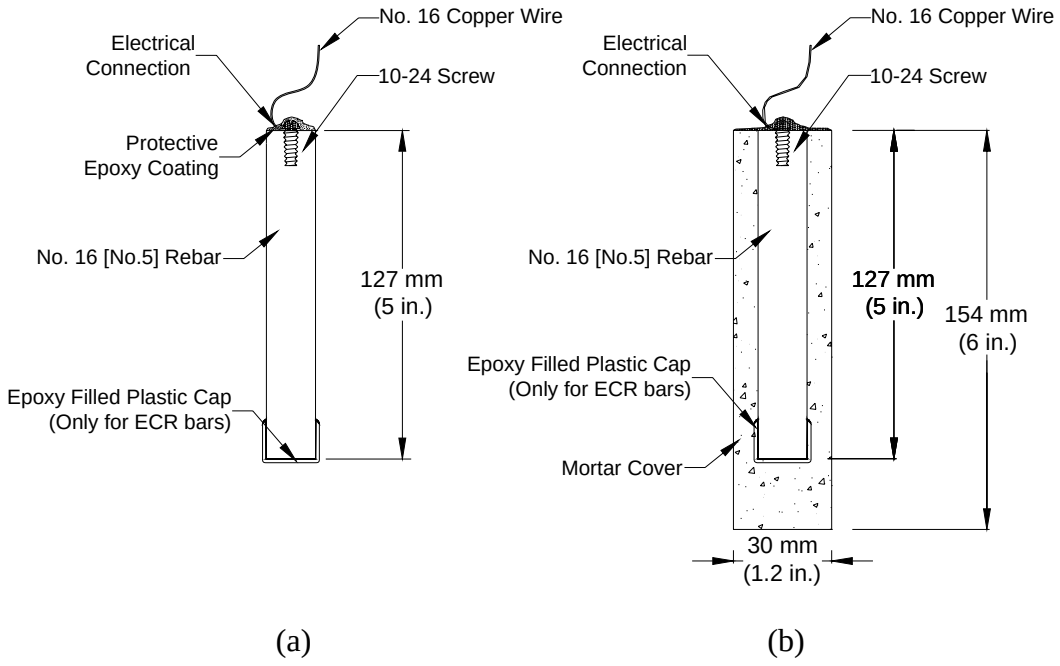

Figure 2.1 – Rapid macrocell specimens: (a) Bare bar and (b) Mortar-wrapped specimen

When the mortar-wrapped specimen is used, the prepared bare bar is symmetrically embedded in a 154 mm (6 in.) long mortar cylinder. The mortar cylinder has a 30 mm (1.2 in.) diameter and provides a 7 mm (0.28 in.) mortar cover

over the reinforcing bar. Mortar-wrapped bars are cast in a mold consisting of PVC pipes and fittings, as will be described in Section 2.3.3.

2) Casting: The mortar in this study is fabricated using Type I/II Portland cement, distilled water, and ASTM C 778 graded Ottawa sand with a water-cement ratio of 0.5 and sand-cement ratio of 2.0 by weight. The mix proportions represent the mortar constituent of concrete. The mortar is mixed following the procedures outlined in ASTM C 305. Mortar is placed in the cylindrical PVC mold in four layers. Each layer is rodded 25 times using a 2-mm (0.08-in.) diameter rod, followed by vibration for 30 seconds on a vibration table with an amplitude of 0.15 mm (0.006 in.) and a frequency of 60 Hz.

3) Curing: Specimens are cured in the molds for one day at room temperature and then removed from the molds and cured in saturated lime water (pH ≈ 12.4) for 13 days to reach a passive condition. After this period, the specimens are surface-dried with compressed air and then vacuum dried for one day.

4) Wiring and coating: For both bare and mortar-wrapped bars, a 16-gauge copper electrical wire is attached to the tapped end of each specimen with a 10-24×1/2 (13 mm [0.5 in.] long) screw. The electrical connection is then coated with two layers of Herberts O'Brien epoxy for bare bars and two layers of Ceilgard 615 epoxy for mortar-wrapped specimens.

2.3.2 Test procedure

After the specimens are prepared (15 days after casting for mortar-wrapped specimens), the macrocell test is set up, as shown in Figures 2.2 and 2.3.

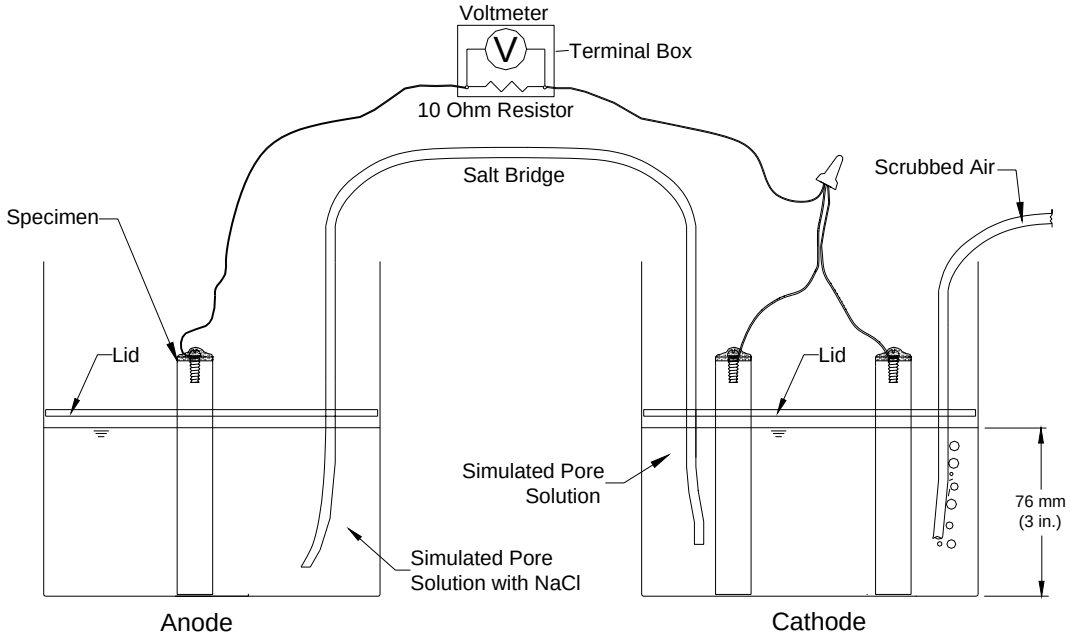

Figure 2.2 – Macrocell test setup with bare bars

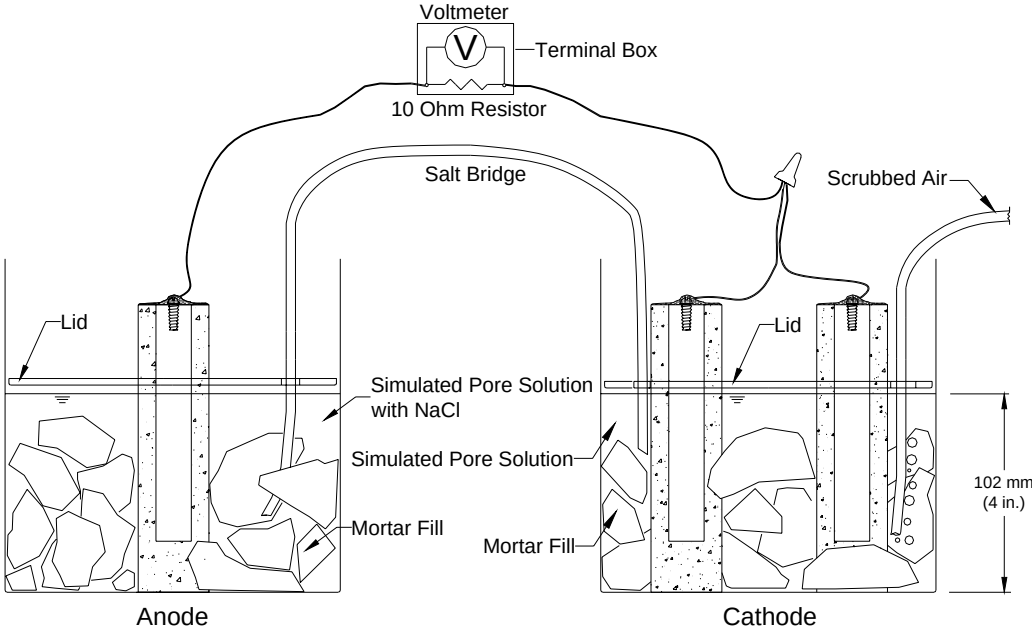

Figure 2.3 – Macrocell test setup with mortar-wrapped specimens

The test specimen, either a bare bar or a mortar-wrapped specimen, is placed in a 3.8-L (four-quart) cylindrical plastic container, along with simulated concrete pore solution containing a 1.6 m or 6.04 m ion concentration of sodium chloride (NaCl). This specimen acts as the anode. In the other container, two specimens, which act as the cathode, are immersed in pore solution without chlorides. For mortar-wrapped specimens, crushed mortar fill is added to the containers to more closely simulate the concrete environment. The solution depth exposes 76 mm (3 in.) of a bar below the level of the solution. Plastic lids are placed just above the surface of the solution to hold the specimens in place and reduce the evaporation of the solution. Holes are cut in the lids to introduce the specimens, a salt bridge, and tubing to supply air. The salt bridge connecting the solutions in the two containers provides an ionic path. Air, scrubbed to remove CO_2, is bubbled into the solution surrounding the cathode to ensure an adequate supply of oxygen for the catholic reaction. The anode and cathode are electrically connected through a 10-ohm resistor. The resistors are mounted between binding posts in a terminal box to consolidate the specimen wires.

The preparation of the simulated concrete pore solution, the mortar fill, the salt bridge, the air scrubber, and the terminal box is described in Section 2.3.3.

During the study, the macrocell test was modified to limit the effects of changes in the pH of the simulated pore solution due to carbonation. This was accomplished by replacing the solutions at the anode and the cathode every five weeks.

During the rapid macrocell test, the voltage drop across the resistor and the open circuit potentials of the anode and the cathode are measured daily for the first week and weekly thereafter. The whole test period is a minimum of 15 weeks. The

voltage drop is measured by connecting the two terminals of a high-impedance voltmeter to the two binding posts in the terminal box where the resistor is mounted. After the voltage drop is measured, the electrical circuit is opened by disconnecting the specimen wires from the binding posts for at least two hours; the potential readings are then taken with the voltmeter with respect to a saturated calomel electrode, which is immersed in the solution around tested specimen. After the corrosion potentials are taken, the circuit is closed.

As described in the Section 1.3.2, the corrosion rate in μm/yr can be determined from the voltage drop across the resistor: first, the current density is obtained using Eq. (1.13), based on the assumption that uniform corrosion occurs on the portion of the bar immersed in the solution (64 mm [2.5 in.] for specimens containing ECR bars with end caps and 76 mm [3 in.] for other specimens, with or without mortar), and then the current density is converted to a corrosion rate in μm/yr based on Faraday's law [Eq. (1.12)]. The calculation is expressed as follows:

$$\text{Corrosion rate in } \mu\text{m/yr} = 11.6\, i = 11.6\,\frac{V}{RA} \qquad (2.1)$$

where

i = current density, $\mu A/cm^2$;

V = voltage drop across the resistor, mV;

R = resistance of the resistor, kΩ; R = 10 Ω = 0.01 kΩ;

A = area of the anode bar immersed in the solution, cm^2;

A = 40 cm^2 for uncoated bars;

A = 32 cm^2 for total area of epoxy-coated bars;

A = 0.32 cm^2 for exposed area of epoxy-coated bars (area of four holes);

The minimum reading of the voltmeter is 1 μV. Therefore, the minimum measurable corrosion rate for uncoated bars in the test can be obtained by:

Voltage drop across 10-ohm resistor: 1 μV;

Macrocell current: = 1 μV/10 ohms = 0.1 μA;

Macro-current density: i = Macrocell current/area = 0.1 μA/40 cm^2 = 0.0025 μA/cm^2;

Corrosion rate = 11.6 i = 11.6 × 0.0025 = 0.029 μm/yr.

Likewise, the minimum measurable corrosion rate is 0.036 μm/yr and 3.6 μm/yr for epoxy-coated bars based on total area and exposed area, respectively.

2.3.3 Apparatus and materials

2.3.3.1 Apparatus

1) Containers: 3.8-L (four-quart) high-density polyethylene containers with lids are used for holding solutions and test specimens. The containers have a 178 mm (7 in.) diameter and a 191 mm (7.5 in.) height.

2) Terminal Box: The terminal box is used to make an electrical connection between an anode and a cathode across a 10-ohm resistor and group the connections for a number of test specimens. It consists of a project box mounted with binding posts. Each pair of binding posts connects a 10-ohm resistor and two wires from the anode and the cathode.

3) Air scrubber: To minimize the carbonation of the simulated concrete pore solution, an air scrubber is used to remove carbon dioxide from the compressed air that is bubbled into the solution surrounding the cathode. The air scrubber consists of a 19-L (5-gallon) container partially filled with a 1M sodium hydroxide solution. The container is sealed. Compressed air is channeled into the solution by plastic tubing

through a barbed fitting mounted at the top of the container. The portion of the tube immersed in the solution is about 1.5 m (5 ft) long and most of it is coiled and held down by small rocks at the bottom of the container. The coiled tube is punched with hundreds of small holes along its wall to allow the air to form small bubbles. The scrubbed air is channeled out of the container thought another barbed fitting and distributed to each cathode solution using plastic tubing and polypropylene T-shaped connectors. Screw clamps are placed on tubing branches to adjust the airflow. The NaOH solution is refreshed, if necessary, to maintain the pH above 12.5.

4) Voltmeter: Hewlett Packard 3456A digital voltmeter. The voltmeter is used to measure the voltage drop across the resistor and the corrosion potential of the bars and is capable of reading 0.001 mV.

5) Saturated Calomel Electrode (SCE): Accumet standard prefilled calomel reference electrode with porous ceramic junction.

6) Molds for mortar-wrapped specimens: The mold illustrated in Figure 2.4 is used to cast mortar-wrapped specimens, and consists of the following commercially available parts (Parts A to F):

Part A: a 154 mm (6 in.) long 1 in. PVC SDR 21 pipe (ASTM D 2241) with 30 mm (1.2 in.) internal diameter. The pipe is sliced longitudinally to facilitate demolding. The slice is covered with one layer of masking tape to avoid leakage during casting.

Part B: 1 in. PVC Schedule 40 fitting (ASTM D 2466). At one end of the fitting, the internal diameter is machined to 33 mm (1.2 in.) to fit the PVC pipe.

Part C: One laboratory grade No. 6 ½ rubber stopper with a centered 5 mm (0.19 in.) diameter hole.

Part D: One 10-24×1 (25mm [1.0 in.] long) machine screw.

Part E: Two pieces of 2×8 lumber. The wooden boards are 380 mm (15 in.) long. There are eight holes and recesses made in two rows (four holes each row) on each board to accommodate eight assembled molds and allow for mortar placement.

Part F: Six threaded rods and wing nuts. The rods are about 250 mm (10 in.) long and 6.4 mm (0.25 in.) diameter.

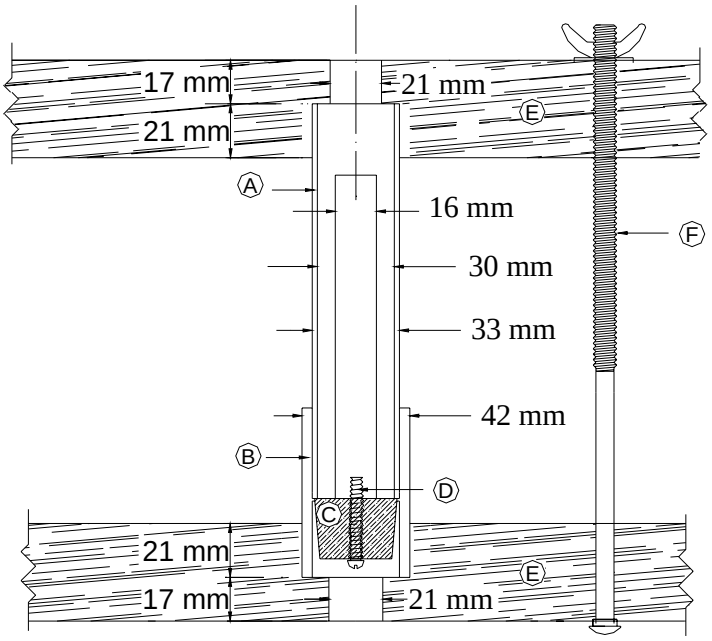

Figure 2.4 – Mold assembly for mortar-wrapped specimens

The PVC pipe serves as the side of the mold. The rubber stopper serves as the bottom of the mold. The PVC fitting is used to hold the PVC pipe and the rubber stopper in place. The 10-24 machine screw is used to mount and center the reinforcing bar in the mold. The wooden boards, the threaded rods, and the wing nuts

are used to fasten individual molds together and can allow several specimens to be cast at one time.

The assembly procedure for the molds is described as follows:

(a) Insert the rubber stopper, C, beginning from its narrow end, into the machined end of the PVC fitting, B, until the wide end of the rubber stopper is in tight contact with the shoulder on the internal surface of the fitting (the stopper is in the unmachined end of the fitting now).

(b) Insert the 10-24×1 machine screw, D, through the hole of the rubber stopper from the narrow end of the stopper and mount the prepared bare bar against the stopper by the screw.

(c) Cover the longitudinal slice along the side of the PVC pipe, A, with masking tape. Then insert the pipe into the machine end of the PVC fitting. The inserted end of the pipe should be against the surface of the rubber stopper. The assembly for an individual mold is finished.

(d) Six threaded rods, F, are inserted into the bottom wooden board. The assembled molds are placed into the recesses in the bottom wooden board, E. The top wooden board is then placed on the free end of the PVC pipes with the threaded rods inserted. The free ends of the PVC pipes are fitted into the recesses in the top wooden board and the nuts on the rods are tightened to fasten the molds together.

2.3.3.2 Materials

1) Concrete Pore Solution: Simulated concrete pore solution is used at the cathode. One liter of the solution contains 974.8 g of distilled water, 18.81 g of

potassium hydroxide (KOH), and 17.87 g of sodium hydroxide (NaOH), based on pore solution analysis by Farzammehr (1985).

2) Concrete Pore Solution with Sodium Chloride: The solution is used at the anode and is prepared by adding 45.6 or 172.1 g of NaCl to one liter of the simulated concrete pore solution to obtain a 1.6 or 6.04 molal ion concentration solution, equal to a 0.8 or 3.02 molal NaCl solution, respectively.

3) Salt bridges: A salt bridge provides an ionic path between the cathode and the anode. It consists of a 0.45 m (1.5 ft) long plastic tube filled with a conductive gel. To prepare salt bridge, 4.5 g of agar, 30 g of potassium chloride (KCl), and 100 g of distilled water are mixed and then heated over a hotplate until the solution starts to thicken. The heated mixture, enough to produce four salt bridges, is poured into plastic tubes using a funnel. The tubes are then placed in boiling water for one hour to firm the gel, keeping the ends of the tubes above the surface of the water. The gel in the salt bridges must be continuous without interruption by air bubbles.

4) Mortar: The mortar has a water-cement ratio of 0.5 and sand-cement ratio of 2.0 by weight, and is made with Type I/II portland cement (ASTM C 150), distilled water, and ASTM C 778 graded Ottawa sand. The mix proportions represent the mortar constituent of concrete. The mortar is mixed in accordance with the procedures outlined in ASTM C 305.

5) Mortar fill: Mortar fill is used to surround mortar-wrapped specimens. It consists of the same mixture as used in the test specimens. The fill is cast in a metal baking sheet to a depth of about 25 mm (1 in.). The mortar in the sheet is air-cured at room temperature for 15 days and is broken into 25 to 50 mm (1 to 2 in.) pieces prior to use.

6) Epoxy coating: Two component epoxies are used to coat the electrical connections between the wire and the bar. Herberts-O'Brien Rebar Patch Kit is used for bare bars, and Ceilgard 615 epoxy is used for mortar-wrapped specimens.

7) Plastic tubing: Clear vinyl tubing is used to channel the scrubbed air to the cathode and to make salt bridges. It has a 6.4 mm (0.25 in.) inner diameter and a 1.6 mm (0.0625 in.) wall thickness.

8) Wire: 16-gage insulated copper electrical wires are used to make the electrical connections to the bars.

9) Machine screws: 10-24×1/2 (13 mm [0.5 in.] long) screws are used to connect the wire to the bars.

10) Resistors: 0.5 or 0.25 watt 10-ohm resistors with a tolerance of 5% (resistances actually within 10 ± 0.3 ohms).

2.3.4 Test programs

The rapid macrocell test program is summarized in Tables 2.3 and 2.4. The tests included both bare and mortar-wrapped specimens. Bare anodes were subjected to a simulated pore solution with both a 1.6 m and 6.04 m ion NaCl, while mortar-wrapped anodes were subjected to a 1.6 m ion NaCl solution. The test specimens consisted of conventional steels (N2, N3, N4), epoxy-coated steel (ECR), MMFX micorcomposite steel (MMFX), and duplex stainless steels (2101, 2101p, 2101(2), 2101(2)p, 2205, and 2205p). Three to six replicates (five or six in most cases) were used for each test. Later in the study, some specimens were also tested by replacing the solutions every five weeks. These are marked with the "-r" in the tables. The results of the tests are presented in Chapter 3.

Table 2.3 – Test program for macrocell test with bare bars

Specimen Designation*	NaCl ion concentration	Steel type	Number of tests
Bare bars in 1.6 m NaCl ion concentration			
M-N2-r	1.6 m	Conventional	6
M-N3	1.6 m	Conventional	6
M-N4-r	1.6 m	Conventional	6
M-ECR-r	1.6 m	ECR at both anode and cathode	6
M-MMFX	1.6 m	MMFX	6
M-MMFX-r	1.6 m	MMFX	6
M-2101	1.6 m	2101	5
M-2101p	1.6 m	2101 pickled	5
M-2101(2)	1.6 m	2101(2)	6
M-2101(2)p	1.6 m	2101(2) pickled	6
M-2205	1.6 m	2205	5
M-2205p	1.6 m	2205 pickled	5
M-N4/2101(2)p-r	1.6 m	N4 at anode, 2101(2)p at cathode	3
M-2101(2)p/N4-r	1.6 m	2101(2)p at anode, N4 at cathode	3
Bare bars in 6.04 m NaCl ion concentration			
M-N2h	6.04 m	Conventional	5
M-N2h-r	6.04 m	Conventional	6
M-MMFXh-r	6.04 m	MMFX	6
M-2101h	6.04 m	2101	5
M-2101ph	6.04 m	2101	5
M-2101(2)h	6.04 m	2101(2)	6
M-2101(2)ph	6.04 m	2101(2) pickled	6
M-2101(2)ph-r	6.04 m	2101(2) pickled	6
M-2205h	6.04 m	2205	6
M-2205h-r	6.04 m	2205	6
M-2205ph	6.04 m	2205 pickled	5
M-2205ph-r	6.04 m	2205 pickled	6

*** A – B – C**

A: test method: M = macrocell test.

B: steel type and test condition → N, N2, N3, and N4: conventional steel; MMFX: MMFX II microcomposite steel; ECR: epoxy-coated steel; 2101 and 2101(2): Duplex stainless steel (21% chromium, 1% nickel), 2205: Duplex stainless steel (25% chromium, 5% nickel), p: pickled, h: 6.04 m ion concentration

C: r: the test solutions are replaced every five weeks.

Table 2.4 – Test program for Macrocell test with mortar-wrapped specimens

Specimen Designation*	NaCl ion concentration	Steel type	Number of tests
M-N2m	1.6 m	Conventional	5
M-N2m-r	1.6 m	Conventional	6
M-N3m	1.6 m	Conventional	6
M-MMFXm	1.6 m	MMFX	6
M-MMFXm-r	1.6 m	MMFX	6
M-N3/MMFXm	1.6 m	N3 at anode and MMFX at cathode	3
M-MMFX/N3m	1.6 m	MMFX at anode and N3 at cathode	3
M-ECR/N3m	1.6 m	ECR at anode and N3 at cathode	6
M-ECRm-r	1.6 m	ECR at both anode and cathode	6
M-2101m	1.6 m	2101	4
M-2101pm	1.6 m	2101 pickled	4
M-2101(2)m	1.6 m	2101(2)	6
M-2101(2)pm	1.6 m	2101(2) pickled	6
M-2205m	1.6 m	2205	6
M-2205pm	1.6 m	2205 pickled	6

*** A – B – C**
A: test method: M = macrocell test.
B: steel type and test condition → N, N2, N3, and N4: conventional steel; MMFX: MMFX II microcomposite steel; ECR: epoxy-coated steel; 2101 and 2101(2): Duplex stainless steel (21% chromium, 1% nickel), 2205: Duplex stainless steel (25% chromium, 5% nickel), p: pickled, m: mortar-wrapped specimens
C: r: the test solutions are replaced every five weeks.

2.4 BENCH-SCALE TESTS

Two bench-scale tests, the Southern Exposure (SE) and the cracked beam (CB) tests, are used to evaluate the corrosion performance of reinforcing steel in the current study. In this section, the test specimen, test procedure, apparatus and materials, and test program are described.

2.4.1 Test specimens

The specimen used for the Southern Exposure test is shown in Figure 2.5. It consists of a 305 mm (12 in.) wide, 305 mm (12 in.) long, 178 mm (7 in.) high concrete slab containing two mats of reinforcing steel. The top mat of steel has two

bars and the bottom mat has four bars. All bars have a clear concrete cover of 25.4 mm (1 in.) to the nearest surface. A dam is cast integrally with the slab to retain solution on the top surface.

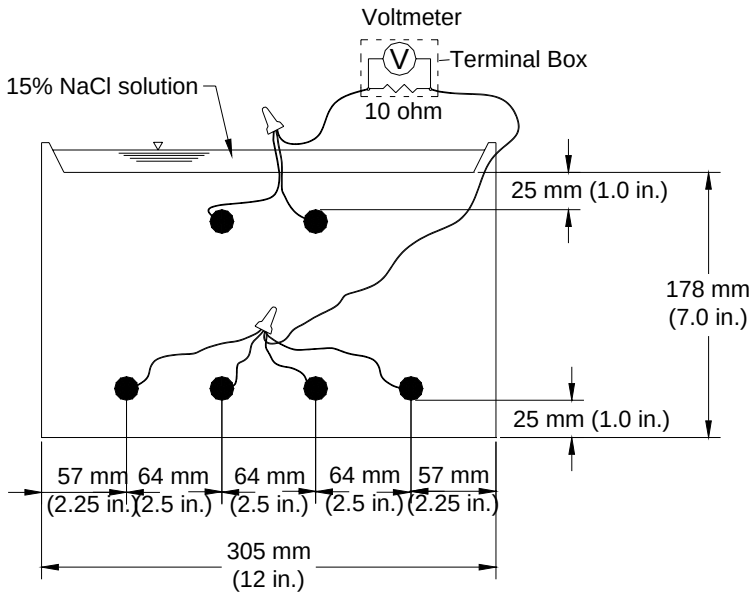

Figure 2.5 - Southern Exposure specimen

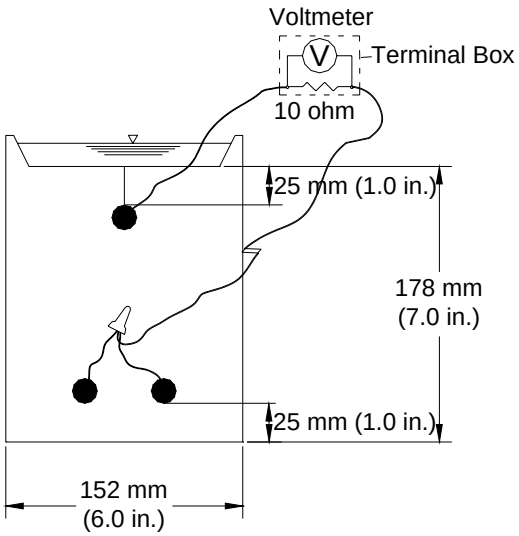

Figure 2.6 – Cracked beam specimen

The specimen for the cracked beam test is similar to the SE specimen, as shown in Figure 2.6. They differ in that the CB specimen is half the width of the SE specimen with one bar on top and two bars on the bottom, and a 0.3 mm (0.012 in.) wide, 152 mm (6 in.) long simulated crack is placed in the concrete parallel to and above the top reinforcing bar.

Fabrication of the SE and CB specimens is described as follows:

1) Preparation of reinforcing bar: Each reinforcing bar is cut to a length of 305 mm (12 in.). Both ends of the bar are drilled and tapped 13 mm (0.5 in.) to accommodate a No. 10-24 machine screw. The sharp edges on the bar ends are removed with a grinder. Uncoated bars are cleaned with acetone to remove grease and dirt from the surface. Epoxy-coated reinforcing bars are cleaned with soap and water. The epoxy coating is then penetrated by four 3.2 mm (0.125 in.) diameter holes to simulate defects in the coating. The holes are made to a depth of 0.5 mm (0.020 in.) using a 3.2-mm (0.125-in.) diameter four-flute end mill. Two of the holes are placed about 102 mm (4 in.) from one end of the bar, opposite each other, and the other two are placed about 102 mm (4 in.) from the other end of the bar. The four holes represent about 0.2% damage on the evaluated area of the epoxy-coated bar.

2) Mold Assembly: The mold is made to cast the specimen in an inverted position. It consists of several pieces of 19 mm (0.75 in.) thick plywood, including 4 sides and a bottom. Inside the mold, a smaller beveled wooden piece is bolted to the bottom to create the integral concrete dam after casting. For the cracked beam molds, a 152 mm (6 in.) long, 0.3 mm (0.012 in.) wide longitudinal slot is made in the center of the beveled wood to accommodate a 0.3 mm (0.012 in.) thick stainless steel shim. The shim projects 25 mm (1 in.) from the slot and just touches the tested bar. After demolding, the shim is removed from the concrete to form the crack. All parts of the

mold are fastened with angles and clamps. The inside corners are sealed with clay. The bars are supported by 10-24×1 (25 mm [1.0 in.] long) screws through 4.8 mm (0.19 in.) diameter holes in two side molds. When epoxy-coated bars are tested, two of the holes in the coating face up and the other two face down.

3) Casting: Concrete is mixed in accordance with the requirements in ASTM C 192 for mechanical mixing. The concrete mix proportions are given in Table 2.5 (Section 2.4.3.2). The concrete has a water-cement ratio of 0.45 and an air content of 6%. The specimens are cast in two layers. Each layer is vibrated for 30 seconds on a vibrating table with amplitude of 0.15 mm (0.006 in.) and a frequency of 60 Hz. The concrete surface is finished with a wooden float.

4) Curing: The specimens are cured in the mold for 24 hours at room temperature, except the CB specimens, which usually require earlier demolding (8-12 hours) to facilitate the removal of the shim. After removed from the mold, specimens are cured at room temperature in a plastic bag with water until 72 hours after casting. The specimens are then removed from the bag and air-cured for 25 days. Testing starts 28 days after casting.

5) Wiring and coating: Two days before testing begins, 16-gage copper electrical wire is attached to one end of each bar embedded in the specimens with 10-24×1/2 (13 mm [0.5 in.] long) screw. The other end of the bars is sealed with the same kind of screw. All four sides of the specimens, including the electrical connections, are then coated with two layers of Ceilgard 615 epoxy. The epoxy is mixed and applied according to manufacturer's recommendations.

2.4.2 Test procedure

The same procedure is used for the Southern Exposure and cracked beam tests. On the first day of the tests, the specimens are placed on two pieces of 2×2 lumber to allow for air movement under the specimens. Two wires, one each from the top and bottom mats of the steel are connected across a 10-ohm resistor mounted in a terminal box. Typically, the terminal box contains 6 resistors for 6 specimens. The specimens are subjected to a 96-week "Southern Exposure" cycle. The voltage drop across the resistor, the mat-to-mat resistance, and the corrosion potential of both mats of steel are measured weekly. The detailed procedure is described as follows: [This description is adapted from Balma et al. (2005)].

1) The specimens are ponded with a 15% NaCl (6.04 m ion concentration) solution at room temperature, 20 to 26^{o} C (68 to 78^{o} F). This solution is left on the specimen for four days. The specimens are covered with a plastic sheet to reduce evaporation.

2) On the fourth day, the voltage drop across the 10-ohm resistor connecting the two mats of steel is recorded for each specimen. The circuit is then disconnected, and the mat-to-mat resistance is recorded. Two hours after disconnecting the specimens, the solution on top of the specimens is removed with a vacuum, and the corrosion potentials with respect to a copper-copper sulfate electrode (CSE) of the top and bottom mats of steel are recorded.

3) After the readings have been obtained, the circuit is reconnected. A heat tent is placed over the specimens, which maintains a temperature of 38 ± 2^{o} C (100 ± 3^{o} F). The specimens remain under the tent for three days.

4) After three days, the tent is removed and the specimens are again ponded with a 15% NaCl solution, and the weekly cycle starts again.

5) This weekly ponding and drying cycle is repeated for 12 weeks. The specimens are then subjected to 12 weeks of continuous ponding. During this period the solution is not removed and the specimens are not placed under the heat tents. Since the specimens are ponded, the corrosion potential during this period is taken with respect to a saturated calomel reference electrode (SCE) instead of a copper-copper sulfate electrode (CSE), since the SCE is more convenient when the electrode has to be immersed in solution.

6) After 12 weeks of the ponding and drying cycle and 12 weeks of continuous ponding, the ponding and drying cycle begins again. This 24-week cycle is repeated to complete a 96-week test period.

Based on Eq. (2.1), the corrosion rate in μm/yr can be obtained from the measured voltage drop. In this case, the anode areas, *A*, are 152 and 304 cm^2 for cracked beam and Southern Exposure specimens, respectively. For the CB and SE specimens with epoxy-coated bars containing four holes, the exposed areas at the holes are 0.32 cm^2 and 0.64 cm^2, respectively.

Since the minimum reading of the voltmeter is 1 μV, the minimum measurable corrosion rate for uncoated bars (or epoxy-coated bars based on total area) can be obtained by:

Voltage drop across 10-ohm resistor: 1 μV;

Macrocell current: = 1 μV/10 ohms = 0.1 μA;

Current density: i = Macrocell current/ area = 0.1 μA/152 cm^2 and 0.1 μA/304 cm^2 = 0.00066 μA/cm^2 and 0.00033 μA/cm^2 for CB and SE specimens, respectively;

Corrosion rate = 11.6 i = 0.0076 and 0.0038 μm/yr for CB and SE specimens, respectively.

Likewise, the minimum measurable corrosion rate is 3.6 μm/yr and 1.8 μm/yr based on the exposed areas for CB and SE specimens with epoxy-coated bars, respectively.

2.4.3 Apparatus and materials

2.4.3.1 Apparatus

1) Heating tent [This description is adapted from Senecal et al. (1995)]: The heating tent is designed to be mobile and can hold 6 SE and 6 CB specimens at once. The tent is an oblong structure, 1.2 m (3.5 feet) high, 1.33 m (4 feet) wide, and 2.67 m (8 feet) long. The roof and ends are made of 19 mm (0.75 in.) thick plywood and are connected together by six 2.67 m (8 feet) studs. The sides of the tent are covered in two layers of plastic, separated by a 25 mm (1 in.) dead space. Three 250 watt heating lamps are evenly spaced along the roof of the tent. When the tent is placed over the specimens, the lamps are 4450 mm (18 in.) above the specimens. A thermostat with a temperature probe senses the temperature within the tent and maintains a temperature range of 38 ± 1.5° C (100 ± 3° F).

2) Terminal Box: Similar to the terminal box used for the rapid macrocell test, the terminal box consists of a project box containing several sets of three binding posts, as shown in Figure 2.7. A 10-ohm resistor is placed between the inner post and the outer post that connects the wire from the top mat of the steel. A 152 mm (6 in.) long 16-gage electrical wire is placed between the inner post and the other outside post that connects the wire from the bottom mat to facilitate closing or breaking the circuit.

3) Voltmeter: Hewlett Packard 3456A digital voltmeter. The voltmeter is used to measure the voltage drop across the resistor and the corrosion potential of the bars and is capable of reading 0.001 mV.

4) AC Ohmmeter: Hewlett Packard 4338A digital AC milliohmmeter. The meter is used to measure the resistance between the top and bottom mats of reinforcing steel.

5) Copper-copper sulfate electrode (CSE): Miller Co. Electrode Model RE-5. The copper-copper sulfate electrode is used to take potential readings during ponding and drying cycles.

6) Saturated Calomel Electrode (SCE): Accumet standard prefilled calomel reference electrode with porous ceramic junction. The saturated calomel electrode is used to take potential readings during the continuous ponding cycle.

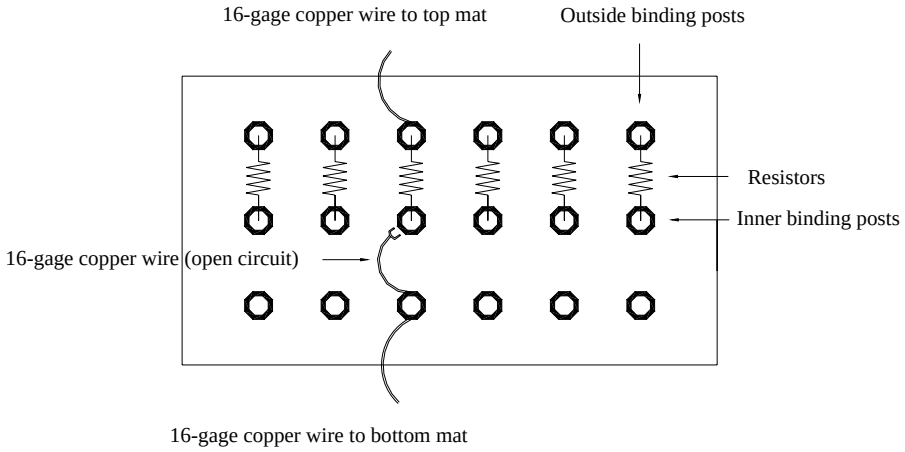

Figure 2.7 – Terminal box for bench-scale tests

2.4.3.2 Materials

1) Concrete: The concrete mix proportions are given in Table 2.5.

Table 2.5 – Concrete Mix design

***w/c* ratio**	**Water (kg/m^3)**	**Cement (kg/m^3)**	**Fine Aggregate (kg/m^3)**	**Coarse Aggregate (kg/m^3)**	**Air-Entraining admixture (mL/m^3)**
0.45	*160*	*355*	*852*	*874*	*90*

The properties of the materials are as follows: Type I/II portland cement; Coarse aggregate: crushed limestone with maximum size = 19 mm (0.75 in.), bulk specific gravity (SSD) = 2.58, absorption (dry) = 2.27%, unit weight = 1536 kg/m^3 (95.9 lb/ft^3); fine aggregate: Kansas River sand with bulk specific gravity (SSD) = 2.62, absorption (dry) = 0.78%, fineness modulus = 3.18; Air-entraining admixture: Daravair 1400 from W.R. Grace.

2) Epoxy coating: Two-component Ceilgard 615 epoxy is used to coat the four sides of the specimens, including the electrical connections.

3) Salt solution: 15% NaCl solution (6.04 molal ion concentration). A 600 ml of the solution is used to pond one SE specimen and 300 ml is used to pond one CB specimen.

4) Wire: 16-gage copper electrical wires are used to make the electrical connections to the bars.

5) Machine screws: 10-24×1 (25 mm [1.0 in.] long) screws are used to mount the bars in the wooden mold. 10-24×1/2 (13 mm [0.5 in.] long) screws are used to connect the wire to the bars.

6) Resistors: 0.5 or 0.25 watt 10-ohm resistors with 5% tolerance.

7) Wood: 2×2 lumber is used to support the specimens to allow for air movement under the specimens.

8) Plastic sheeting: 3.5-mil clear plastic sheeting is used to cover the specimens during ponding to reduce evaporation.

2.4.4 Test programs

The bench scale test program is summarized in Table 2.6. The reinforcing steels tested include conventional steels (N, N3), epoxy-coated steel (ECR), MMFX microcomposite steel (MMFX), and duplex stainless steels (2101, 2101p, 2101(2), 2101(2)p, 2205, and 2205p). The epoxy-coated steel was tested with four holes in each bar and with conventional steel in the bottom mat. In both the Southern Exposure and cracked beam tests, six replicates were used for conventional steel, epoxy-coated steel, and MMFX steel, and five for the duplex stainless steels, except for the first heat 2101 and 2101p bars for which three replicates were used. In addition, three SE specimens were used to test combinations of N2 and 2205 steel, and N3 and MMFX steel to evaluate possible galvanic effects and three SE specimens were used to evaluate bent MMFX bars. The results of the tests are presented in Chapter 3.

Table 2.6 - Test program for bench scale tests

Specimen Designation*	**Steel type**	***w/c* ratio**	**Number of tests**
Southern Exposure test			
SE-N	Conventional	0.45	6
SE-N3	Conventional	0.45	6
SE-MMFX	MMFX	0.45	6
SE-MMFXb	MMFX	0.45	3
SE-ECR/N3	ECR at top, N3 at bottom	0.45	6
SE-2101	2101	0.45	3
SE-2101p	2101 pickled	0.45	3
SE-2101(2)	2101(2)	0.45	5
SE-2101(2)p	2101(2) pickled	0.45	5
SE-2205	2205	0.45	5
SE-2205p	2205 pickled	0.45	5
SE-N4/MMFX	N3 at top, MMFX at bottom	0.45	3
SE-MMFX/N4	MMFX at top, N3 at bottom	0.45	3
SE-N/2205	N at top, 2205 at bottom	0.45	3
SE-2205/N	2205 at top, N at bottom	0.45	3
Cracked Beam test			
CB-N	Conventional	0.45	6
CB-N3	Conventional	0.45	6
CB-MMFX	MMFX	0.45	6
CB-ECR/N3	ECR at top, N3 at bottom	0.45	6
CB-2101	2101	0.45	5
CB-2101p	2101 pickled	0.45	5
CB-2101(2)	2101(2)	0.45	5
CB-2101(2)p	2101(2) pickled	0.45	5
CB-2205	2205	0.45	5
CB-2205p	2205 pickled	0.45	5

*** A - B**

A: test method: SE = Southern Exposure test; CB = cracked beam test.

B: steel type and test condition → N, N2, N3, and N4: conventional steel; MMFX: MMFX II microcomposite steel; ECR: epoxy-coated steel; 2101 and 2101(2): Duplex stainless steel (21% chromium, 1% nickel), 2205: Duplex stainless steel (25% chromium, 5% nickel), p: pickled, b: bent bars on the top mat.

2.5 CRITICAL CHLORIDE THRESHOLD TESTS

In this study, two procedures are used to determine the critical chloride threshold of reinforcing steel. One involves the investigation of the chloride profile within a concrete specimen in the Southern Exposure test to obtain the parameter in a general equation for chloride diffusion. The chloride threshold can then be determined based on the equation and the time of corrosion initiation in the test. The other involves the direct analysis of the chloride content in the concrete adjacent to the reinforcing steel when corrosion starts in SE or beam specimens (CB specimens without the crack). In this section, the methods of sampling and testing for chloride ion concentration in concrete and the test procedure and program for determining the chloride profile and the critical chloride threshold are presented.

2.5.1 Sampling and testing for chloride ion concentration in concrete

Pulverized concrete samples are obtained by drilling 6.4 mm (0.25 in.) diameter holes using a rotary impact drill into the side of bench scale specimens. The sampling procedure is as follows:

1) Place specimens on two pieces of 2×2 lumber on the floor and let the side to be drilled face up. Carefully clean the concrete surface twice, first using tap water and then distilled water. Dry the surface using paper towels.
2) Measure and mark locations to be drilled.
3) Using a Dewalt DW515 heavy-duty hammer drill with a 152 mm (6 in.) long, 6.4 mm (0.25 in.) diameter drill bit, drill perpendicular to the concrete surface (parallel to the ponded surface of the specimen) to a depth of 12.7 mm (0.5 in.). Discard the powdered concrete by cleaning the drilled hole and surrounding area using a vacuum.

4) Continue drilling the concrete to a depth of 89 mm (3.5 in.) [63.5 mm (2.5 in.) for beam specimens], collect the powdered sample on a piece of printing paper using a 2-inch pure bristle brush, and then transfer the sample into a zip lock plastic bag.
5) Clean the drill bit with the brush and then distilled water, dry it with paper towels prior to the next sampling operation. While sampling, prevent the sample and all sampling tools from contacting any source of contamination.
6) After sampling, the holes are then filled with modeling clay to allow the tests to continue, if appropriate.

Each hole produces a sample yield of about six grams (four grams if the depth of the hole is 64 mm [2.5 in.] for beam specimens).

Three analysis methods are used to determine the water-soluble or acid-soluble (or both) chloride content in the concrete sample. The methods are included in Procedure A (the potentiometric titration test) in AASHTO T260-97 “Standard Method of Test for Sampling and Testing for Chloride Ion in Concrete and Concrete Raw Materials” and Procedure C (the probe test) in AASHTO T260-94. Procedure A in AASHTO T260-97 involves using a nitric acid (HNO_3) solution and boiled distilled water to digest the powdered concrete sample for total and water-soluble chlorides, respectively, and titrating the chlorides with a silver nitrate solution. Millivolt readings are taken for the sample solution using an ion selective electrode and a voltmeter during the titration. The endpoint of the titration is indicated by the largest difference in two consecutive voltmeter readings. Procedure A serves as a laboratory test method. Procedure C in AASHTO T260-94 involves digesting the powdered concrete sample using a 20 mL mild acid solution, which is a combination

of acetic acid, isopropyl alcohol, and distilled water, and then stabilizing the sample solution by the addition of 80 mL of a stabilizing solution. A millivolt reading is taken for the 100 mL sample solution using a chloride ion specific electrode with a voltmeter. The reading can be converted to a total chloride concentration in the concrete sample based on a calibration equation for the apparatus and a comparison between the potentiometric titration and this probe method. Procedure C is rapid and usually serves as a field test method.

In the study, an Orion Model 94-17B chloride selective electrode, an Orion Model 90-02 double junction reference electrode, and a Fluke 83 digital multimeter are used in all of the methods.

The detailed analysis procedure and calculation of the three methods are outlined in:

Method 1: Section 5.1, 5.2 and 5.4.1 in AASHTO T260-97 for determination of total chloride ion content (Procedure A).

Method 2: Section 5.1, 5.3 and 5.4.1 in AASHTO T260-97 for determination of water-soluble chloride ion content (Procedure A).

Method 3: Section 20, 21, and 22 in AASHTO T260-94 for determination of total chloride ion content (procedure C).

When *Method 3* is used, two well-known errors in Procedure C in AASHTO T260-94 (Khan 1997, Peterson et al. 1998) are corrected. They are: (1) a factor of 0.00333 should be used in Eq. 2 instead of 0.0333; (2) a factor of 0.00333 should be used in Eq. 5 instead of 0.003. In addition, the values of A and B in Eq. 3 are established by running both *Method 1* and *Method 3* for 45 chloride samples. The factors C and D in Eq. 4 are obtained by the calibration described in the procedure every time before testing.

To get the values of A and B and evaluate the accuracy of the chloride analysis in the study, 45 powdered concrete samples, each of which contains about 18 grams, are taken from three dummy SE specimens (Southern Exposure specimens without reinforcing bars) at five depths at three times (the sampling method is same as that described in Section 2.5.2 for chloride profile except that three holes, instead of one hole, are drilled at each depth to produce yield of about 18 grams for each sample). For 30 of the 45 samples, each sample is divided into four parts. Three of them are analyzed for the chloride content using the three aforementioned methods, respectively, in the lab and one part is sent to Kansas Department of Transportation (KDOT) to be tested for water-soluble chlorides using Procedure A in AASHTO T260-97. For the other 15 samples, each sample is divided into three parts and tested in the lab using the three methods. The results are shown and compared in Chapter 4.

In this study, the chloride content, in percent of weight of concrete, is converted to kg/m^3 (lb/yd^3) of concrete by multiplying by the unit weight of concrete, taken as 2243 kg/m^3 (3780 lb/yd^3).

2.5.2 Chloride profile

To obtain the chloride profile for the Southern Exposure specimens, dummy SE specimens (SE specimens without reinforcing bars) are fabricated. The specimens are subjected to the same Southern Exposure cycling as normal SE specimens. Pulverized concrete samples at five different depths are obtained periodically using the sampling method described in Section 2.5.1. The depths of the samples (that is, the distances of the center of the drilled holes from the ponded surface of the specimens) are 12.7 mm (0.5 in.), 25.4 mm (1 in.), 38.1 mm (1.5 in.), 76.2 mm (3 in.), and 139.7 mm (5.5 in.). Tests performed are as follows:

In the first study, three dummy SE specimens are made to take samples at the five depths every six weeks. The locations of the drilled holes are shown in the Figure 2.8. On each side of the specimen, four columns of holes are drilled to complete a 96-week test period (16 sampling dates in total). The samples are analyzed for the total chloride content using *Method 3* (Section 2.5.1).

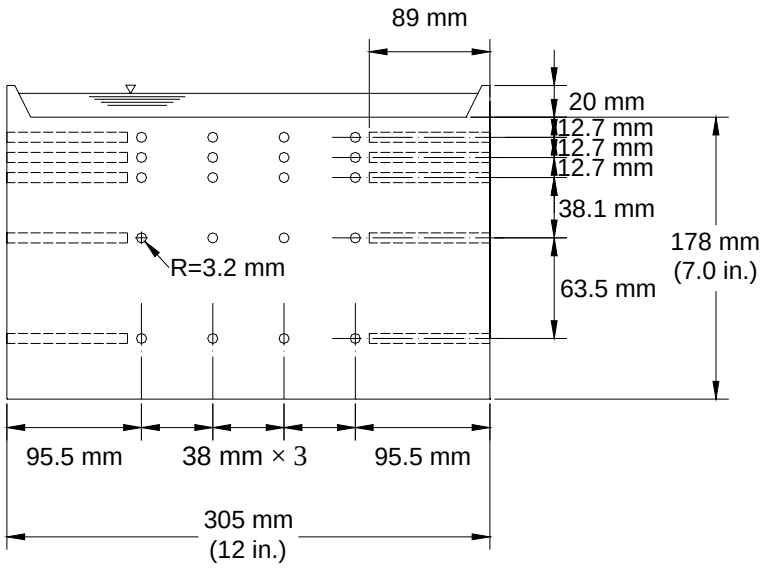

Figure 2.8 – sampling locations for dummy SE specimens

Another six dummy SE specimens are fabricated to take samples at 2, 4, 6, 12 weeks, and then every 12 weeks during the 96-week test period in the second study. For these specimens, before the test starts (at 0 weeks), samples are taken at the depths of 25.4 and 139.7 mm (1 and 5.5 in.) The chloride contents in these samples at 0 weeks are considered to be the initial chloride content in the specimens. For these six dummy specimens, all concrete samples are analyzed for both water-soluble chloride and total chloride content using *Method 2* and *Method 3*, respectively.

The test programs for chloride profiles using the SE specimens are summarized in the Table 2.7.

Table 2.7 - Test programs for chloride profiles of SE specimens

Specimen Designation*	*w/c* ratio	Number of tests	Time intervals of sampling	Chlorides tested	Methods of testing**
SE-D1	0.45	3	Every 6 weeks	Total	**Method 3**
SE-D2	0.45	6	0, 2, 4, 6, 12, then every 12 weeks	Water-soluble and total	*Method 2* and *method 3*

* **A-B**: A: test method, SE = Southern Exposure test.
B: D1 and D2 = dummy specimens in the first and second study, respectively.
** The test methods are described in Section 2.5.1.

2.5.3 Direct determination of chloride threshold

To obtain the chloride threshold directly, concrete samples at the level of reinforcing steel in SE and beam specimens are taken immediately after the reinforcing steel begins to corrode. For each sample, holes are centered so that the top of the holes and the top surface of the bar are in a same plane. Since the concrete cover for each bar is not exactly 25.4 mm (1 in.), the actual value is measured to determine the depth of the sample.

Corrosion initiation for these specimens is considered to have occurred when either the macrocorrosion rate first reaches a value greater than or equal to 0.3 μm/year or the corrosion potential of the top mat of steel first shifts to a value more negative than –0.350 V with respect to a copper-saturated copper sulfate electrode (CSE).

Samples to determine the critical chloride threshold are obtained in threes ways: First, chloride samples are taken from the normal SE specimens summarized in Table 2.6. Since it was observed that the two bars in the top mat of the SE specimen could begin to corrode at the different times due to uneven diffusion of chlorides, the corroded bar is identified by disconnecting the two bars and measuring the corrosion potential of each when the corrosion rate or corrosion potential of the specimen

reaches the critical value. In this case, chloride samples are obtained by drilling 2 holes parallel to the bar into the front side of the specimen. The powered samples from each hole are mixed together and analyzed for water-soluble chlorides using *Method 2*. The sampling locations are shown in the Figure 2.9. Using this procedure, a total 15 samples were obtained, four for MMFX steel, three for 2101 pickled steel, five for 2101(2) steel, one for 2101(2) pickled steel, and two for 2205 steel.

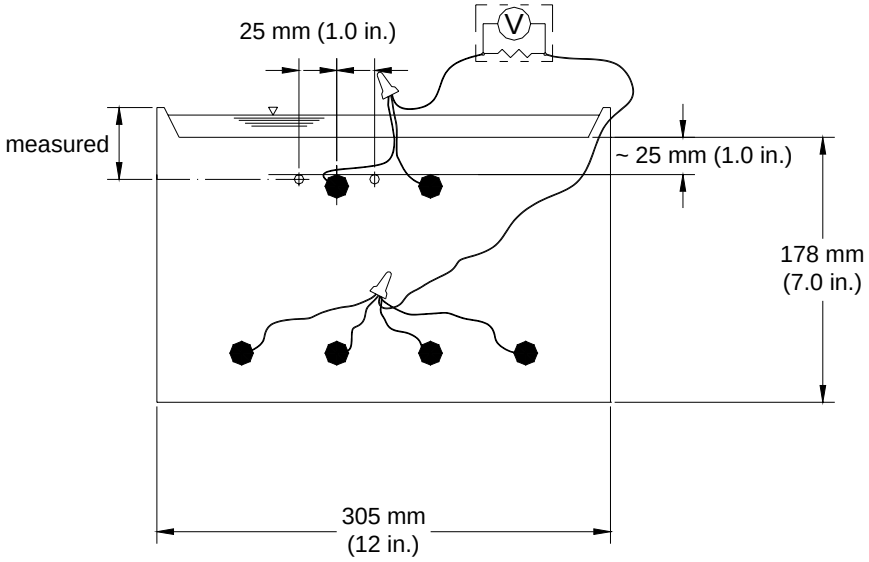

Figure 2.9 - sampling locations in SE specimens (front view)

Second, chloride samples are taken from modified SE specimens where each top mat bar is connected to two bottom mat bars across a 10-ohm resistor. When corrosion begins for the top bar, ten powdered samples are obtained by drilling ten holes perpendicular to the bar into the side of the SE specimen. The holes are at the side closest to the corroding bar. The sampling locations are shown in the Figures 2.10a and 2.10b.

The holes are then filled with modeling clay to allow the tests to continue until the other bar corrodes.

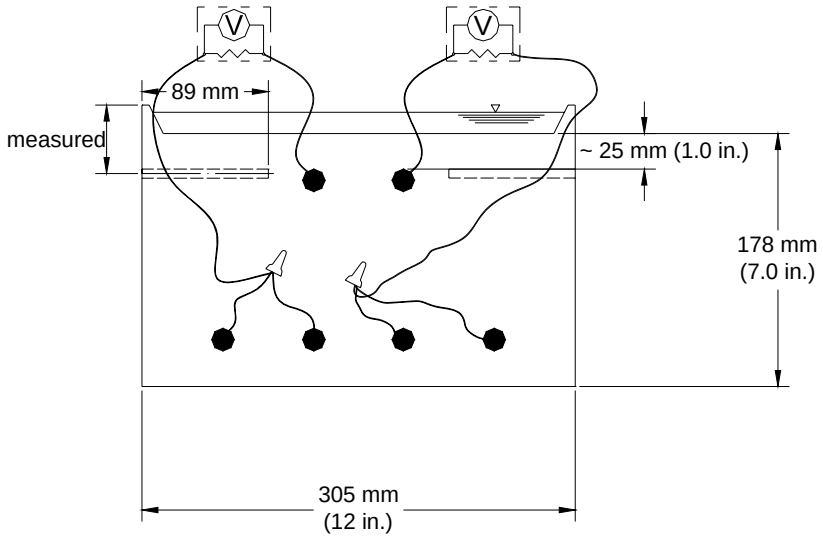

Figure 2.10a - Sampling locations in modified SE specimens (front view)

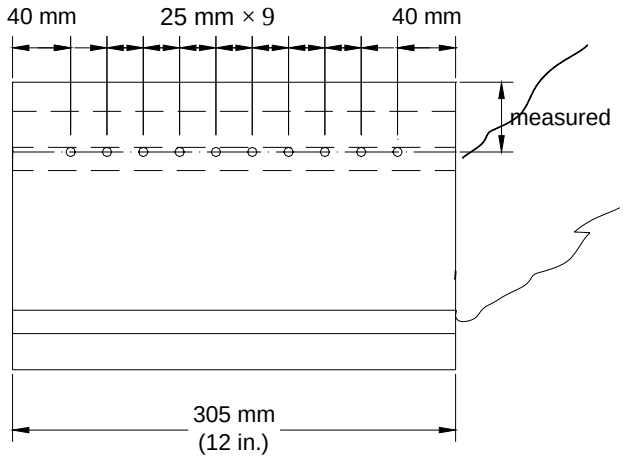

Figure 2.10b - Sampling locations in modified SE specimens (side view)

Third, chloride samples are taken from beam specimens that are fabricated using the mold for the CB specimen with the slot to form the crack sealed with a layer of masking tape. The purpose of the beam test is to obtain a high number chloride samples for a single bar. The sampling method is same as that used for the modified SE specimen, expect that sampling is performed from both sides of the specimen (20 samples for one specimen), as illustrated in Fig. 2.11.

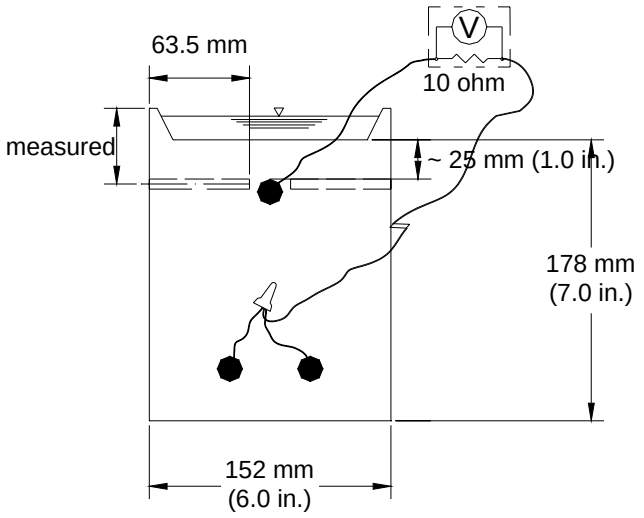

Figure 2.11 - Sampling locations in beam specimens (front view)

Six modified SE specimens and three beam specimens are fabricated to determine the chloride threshold of conventional and MMFX reinforcing steel. The concrete samples are analyzed for water-soluble chlorides using *Method 2*. The test program is summarized in the Table 2.8.

Results of the critical chloride threshold tests are presented in Chapter 4.

Table 2.8 -Test programs for determining chloride thresholds directly

Test specimens*	Type of steel	Number of specimens	Samples of each specimen	Chlorides tested	Methods of testing**
MSN-N2	N2	6	10	water-soluble	*Method 2*
MSN-MMFX	MMFX	6	10	water-soluble	*Method 2*
B-N2	N2	3	20	water-soluble	*Method 2*
B-MMFX	MMFX	3	20	water-soluble	*Method 2*

*** A-B**:
A: test method, MSE =modified Southern Exposure test; B = beam test.
B: steel type, N2 = conventional N2 steel; MMFX = Microcomposite MMFX II steel.
** The test method is described in Section 2.5.1.

CHAPTER 3

CORROSION EVALUATION OF REINFORCING STEELS

This chapter presents the results obtained from the rapid macrocell, Southern Exposure, and cracked beam tests of conventional, epoxy-coated, MMFX microcomposite, and duplex stainless reinforcing steels described in Section 2.1. The results include the corrosion rate, total corrosion loss, and corrosion potential of the anode and cathode for the rapid macrocell test and the corrosion rate, total corrosion loss, corrosion potential of the top and bottom mats of steel, and mat-to-mat resistance for the bench-scale tests. Since the corrosion rate is an instantaneous value and often fluctuates, the total corrosion loss, an integral of the corrosion rate over time, is also reported. Most of tested bars are also visually inspected at the end of the test.

In this chapter, the average values of the results are plotted versus time (the individual results as a function of time are presented in Appendices A and B), and the individual corrosion rates and losses and their averages at the end of tests are summarized. In many cases, the difference between the average corrosion rates and losses for different reinforcement systems is small. The Student's t-test is used to determine whether the difference in the averages at the end of the test period is statistically significant. A brief description and the results of the Student's t-test are presented in Appendix C (Tables C.1 to C.14).

During this study, a modification to the rapid macrocell test was made by replacing the test solutions every five weeks, as described in Section 2.3.2. The average corrosion rates and corrosion losses of steels in the tests with and without the test solution replaced are summarized and compared in Section 3.5.

The critical chloride corrosion threshold results are reported in Chapter 4.

3.1 CONVENTIONAL REINFORCING STEEL

Conventional reinforcing steels were evaluated as "control samples" in parallel with other forms of reinforcing steel. This section summarizes the results for all conventional steels (the conventional steels will be compared with the other steels in Sections 3.2 through 3.4). The results for conventional steels N2, N3, and N4 (in most cases for six specimens each) in the macrocell test are presented in Tables 3.1 and 3.2 and Figures 3.1 through 3.9. The results for conventional steels N and N3 (six specimens each) in the bench-scale tests are presented in Tables 3.3 and 3.4 and Figures 3.10 through 3.14. The results for the Student's t-test are shown in Tables C.1 and C.2. Compared to the other steels in this study, the conventional steels exhibited the lowest corrosion resistance in all tests. Overall, there is no statistically significant difference between the conventional steels.

3.1.1 Rapid macrocell tests

Bare bar specimens in 1.6 m ion NaCl solution – Bare conventional steels N2, N3, and N4 were evaluated in simulated pore solution with 1.6 m ion NaCl. For N3 steel, the test solutions were not replaced, while for the N2 and N4 steels, the test solutions were replaced every five weeks, as indicated by "r" in the specimen designation.

The average corrosion rates are plotted versus time in Figure 3.1 and the values at 15 weeks are tabulated in Table 3.1. The results show that the three conventional steels exhibited similar corrosion performance, with N3 steel showing higher corrosion rates than N2 and N4 steel. The N2, N3, and N4 steels had average

corrosion rates primarily between 30 to 40 μm/yr within the first week and corroded at a rate of 21, 36, and 28 μm/yr at 15 weeks, respectively.

The average total corrosion losses versus time are shown in Figure 3.2. The average total corrosion losses at 15 weeks are summarized in Table 3.2. The N2, N3, and N4 steels had average total corrosion losses of 6.6, 9.0, and 6.1 μm, respectively, at the end of the test.

Tables C.1 and C.2 show that there is no significant difference in the average corrosion rates or losses at 15 weeks between the N2 and N4 steels (both tested with the test solutions replaced) at any level of significance (α).

In this study, the corrosion potentials in all rapid macrocell tests are measured with respect to a saturated calomel electrode (SCE), which gives readings about 0.075 V more positive than measured with a copper-copper sulfate electrode (CSE). With the SCE, corrosion potentials more negative than –0.275 V indicate active corrosion. The average corrosion potentials of the anode and cathode as a function of time are shown in Figures 3.3a and 3.3b, respectively, for the bare conventional steels in 1.6 m ion NaCl solution. The anode potentials for the steels ranged from –0.350 to –0.550 V during the tests, indicating that active corrosion started at the beginning of the test, while the cathode potentials remained around –0.200 V, indicating a passive condition.

Bare bar specimens in 6.04 m ion NaCl solution – Bare N2 reinforcing bars were tested in 6.04 m ion NaCl and simulated concrete pore solution without and with replacing the solutions every five weeks.

The average corrosion rates and total corrosion losses are showed in Figures 3.4 and 3.5, respectively, and the values at 15 weeks are summarized in Tables 3.1 and 3.2. As expected, the steel exhibited greater corrosion in the high chloride

concentration solution than in 1.6 m ion NaCl solution, with an initial corrosion rate of about 40 μm/yr. The corrosion rate dropped with time. At 15 weeks, the average corrosion rate and corrosion loss were 26 μm/yr and 9.8 μm when the solution was not replaced and 30 μm/yr and 8.9 μm when the solution was replaced every five weeks, compared to a values of 21 μm/yr and 6.6 μm in the 1.6 m ion NaCl solution. The results of the Student's t-test for comparing the N2 steel in the tests with and without the test solution replaced are presented in Section 3.5.

The average corrosion potentials of the anode and cathode are shown in Figure 3.6a and Figure 3.6b, respectively. During most of the test period, the anode potentials remained more negative than –0.500 V and the cathode potentials remained more positive that –0.275 V, whether or not the solutions were replaced.

*Mortar-wrapped specimen*s – Mortar-wrapped specimens with N2 and N3 steels were evaluated in simulated pore solution with 1.6 m ion NaCl, without replacing the test solutions. For N2 steel, the tests were also performed with the solution replaced every five weeks.

The average corrosion rates and corrosion losses versus time are shown in Figures 3.7 and 3.8, respectively, and the values at 15 weeks are summarized in Tables 3.1 and 3.2. The results of the Student's t-test for comparing N2 and N3 steels in the tests without the solutions replaced are presented in Tables C.1 and C.2. The results of the Student's t-test for comparing the N2 steel in the tests with and without the solutions replaced are presented in Section 3.5.

Because the bars were initially in a passive condition and not in contact with chlorides, the mortar-wrapped specimens initially corroded at a low rate. As chlorides diffused through the mortar cover, however, corrosion rates increased rapidly within the first few weeks. For N3 steel without replacing the test solutions (N3m), the

corrosion rate reached a maximum of 24 μm/yr at 4 weeks. For N2 steel without replacing the solutions (N2m), the corrosion rate was 7.1 μm/yr at 4 weeks, peaking at 23 μm/yr at 8 weeks. For N2 steel when replacing the test solutions every 5 weeks (N2m-r), the corrosion rate reached 9.3 μm/yr at 4 weeks, and then increased slowly. The average corrosion rate in all cases was about 17 μm/yr at the end of the test. At this point, total corrosion losses equaled 3.8 μm for N2 steel, 5.3 μm for N3 steel, and 3.5 μm for N2 steel when replacing the solutions. Table C.2 shows that difference in the corrosion losses between N2 and N3 steels is significant at $\alpha = 0.10$.

As shown in Figure 3.9, the average corrosion potentials of the anodes had initial values close to –0.200 V with respect to a saturated calomel electrode, but had dropped to values below –0.275 V within the first week for two of the steels (N3m and N2m-r), taking four weeks for N2 steel (N2m). At the end of the test, the average anode corrosion potentials ranged from –0.550 to –0.600 V.

Visual Inspection – After the end of the tests, the conventional steels were visually inspected (the mortar cover was removed from the mortar-wrapped specimens). Figures 3.43 and 3.46, showing the corrosion products on the anode bars, are presented in conjunction with the figures for MMFX steel in Section 3.3.1.

Table 3.1 - Average corrosion rates at 15 weeks for specimens with conventional steels in macrocell test

Specimen designation*	Steel type	Specimen corrosion rates (μm/yr)						Average (μm/yr)	Standard deviation
		1	2	3	4	5	6		
Bare bars in 1.6 m NaCl									
M-N3	N3	52.60	0.26	67.77	40.17	32.43	22.08	35.88	23.61
M-N2-r	N2	15.17	20.63	19.68	5.35	31.99	32.25	20.85	10.28
M-N4-r	N4	31.23	22.16	16.68	40.66	26.74	31.12	28.10	8.30
Bare bars in 6.04 m NaCl									
M-N2h	N2	33.87	37.80	12.17	24.51	18.96		25.46	10.52
M-N2h-r	N2	42.11	29.51	32.28	24.83	22.66	26.56	29.66	6.98
Mortar-wrapped specimens in 1.6 m NaCl									
M-N2m	N2	17.43	19.02	24.83	5.49	14.65		16.28	7.09
M-N3m	N3	11.21	9.16	26.07	19.31	21.15	19.31	17.70	6.36
M-N2m-r	N2	17.28	22.89	18.96	11.96	14.51		17.12	4.19

*** A-B-C**

A: test method; M = macrocell test.

B: steel type and test condition; N2, N3, and N4 = conventional steel; h = 6.04 m ion concentration; m = mortar-wrapped specimens.

C: r = the test solutions are replaced every five weeks.

Table 3.2 - Average total corrosion losses for specimens with conventional steels in macrocell test

Specimen designation*	Steel type	Specimen total corrosion losses (μm)						Average (μm)	Standard deviation
		1	2	3	4	5	6		
Bare bars in 1.6 m NaCl									
M-N3	N3	12.33	4.15	13.49	11.17	7.08	5.50	8.95	3.88
M-N2-r	N2	6.26	8.15	6.89	4.13	7.17	6.94	6.59	1.35
M-N4-r	N4	7.02	5.25	4.93	7.61	6.53	5.24	6.10	1.11
Bare bars in 6.04 m NaCl									
M-N2h	N2	12.32	11.64	6.93	9.28	8.63		9.76	2.21
M-N2h-r	N2	10.53	10.26	8.59	8.41	7.99	7.48	8.88	1.24
Mortar-wrapped specimens in 1.6 m NaCl									
M-N2m	N2	4.04	2.96	2.22	3.75	6.09		3.81	1.46
M-N3m	N3	5.13	4.75	6.55	5.21	4.79	5.12	5.26	0.66
M-N2m-r	N2	3.09	4.72	2.41	3.35	3.75		3.47	0.86

*** A-B-C**

A: test method; M = macrocell test.

B: steel type and test condition; N2, N3, and N4 = conventional steel; h = 6.04 m ion concentration; m = mortar-wrapped specimens.

C: r = the test solutions are replaced every five weeks.

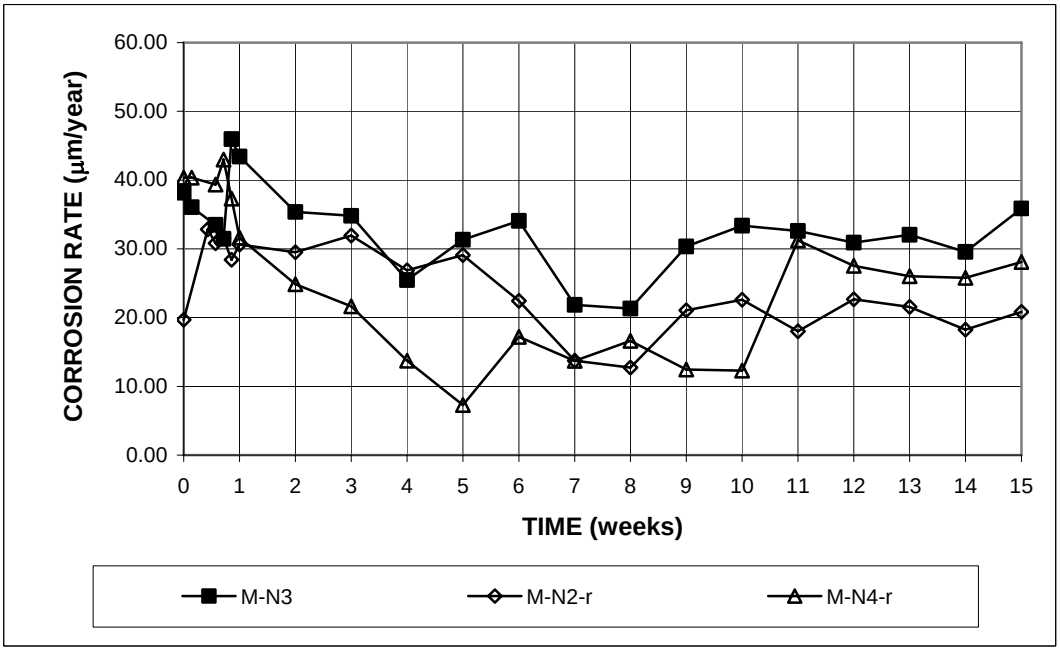

Figure 3.1 - Macrocell test. Average corrosion rates, bare conventional steels in simulated concrete pore solution with 1.6 molal ion NaCl.

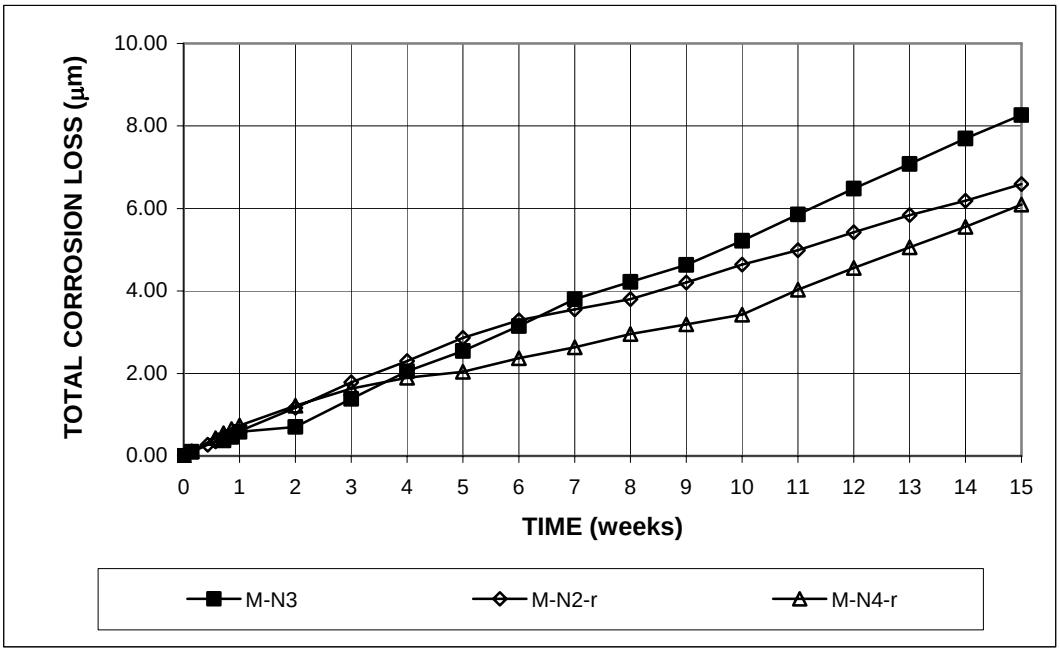

Figure 3.2 - Macrocell test. Average total corrosion losses, bare conventional steels in simulated concrete pore solution with 1.6 molal ion NaCl.

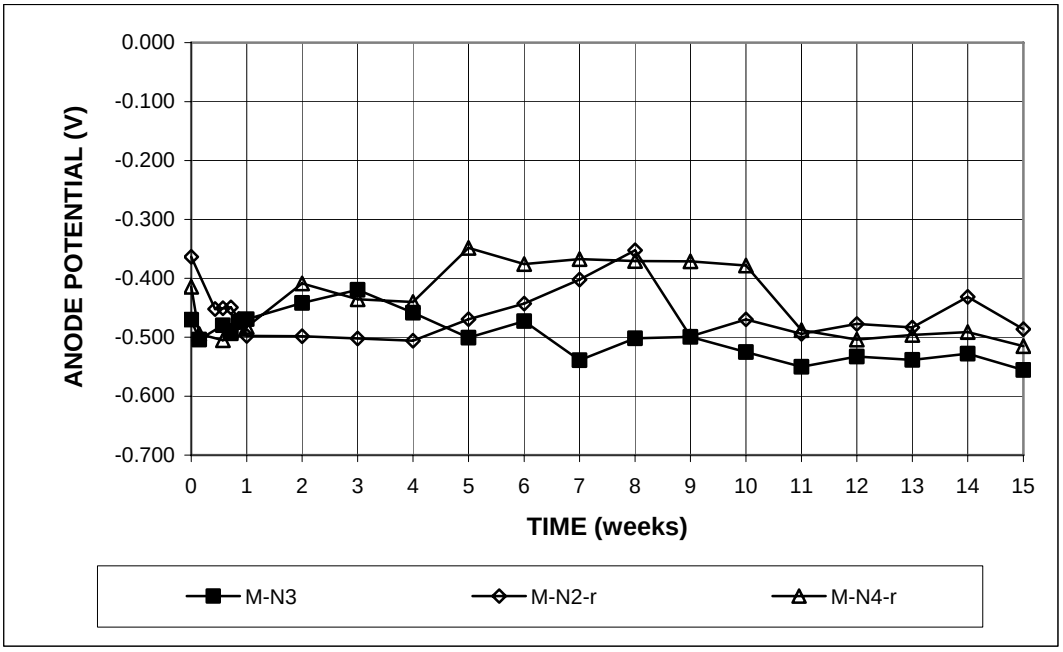

Figure 3.3a - Macrocell test. Average anode corrosion potentials with respect to saturated calomel electrode, bare conventional steels in simulated concrete pore solution with 1.6 molal ion NaCl.

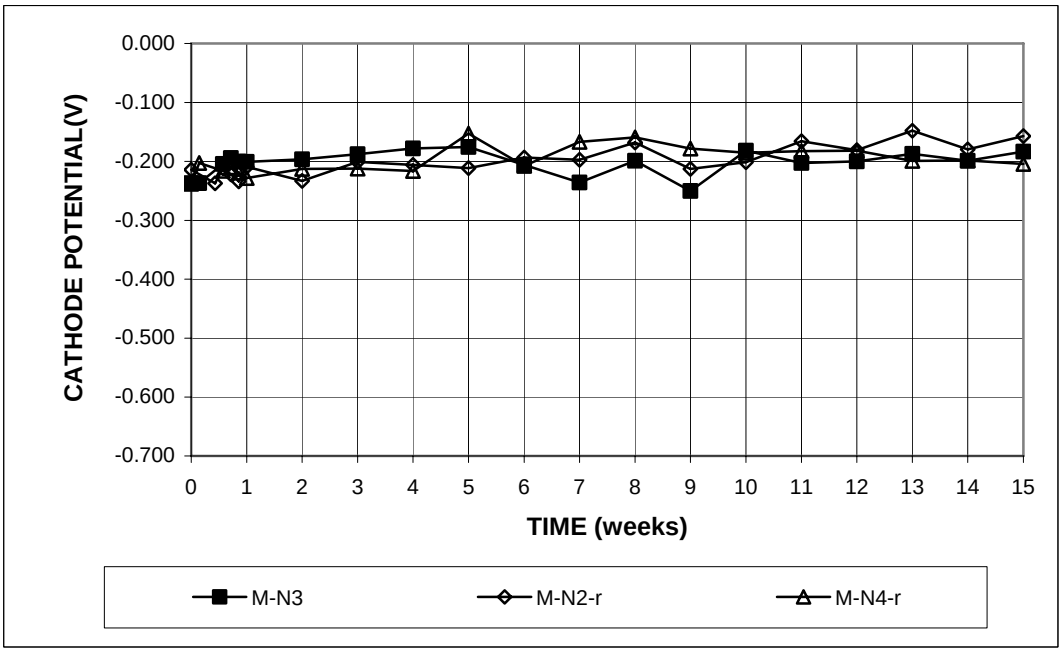

Figure 3.3b - Macrocell test. Average cathode corrosion potentials with respect to saturated calomel electrode, bare conventional steels in simulated concrete pore solution with 1.6 molal ion NaCl.

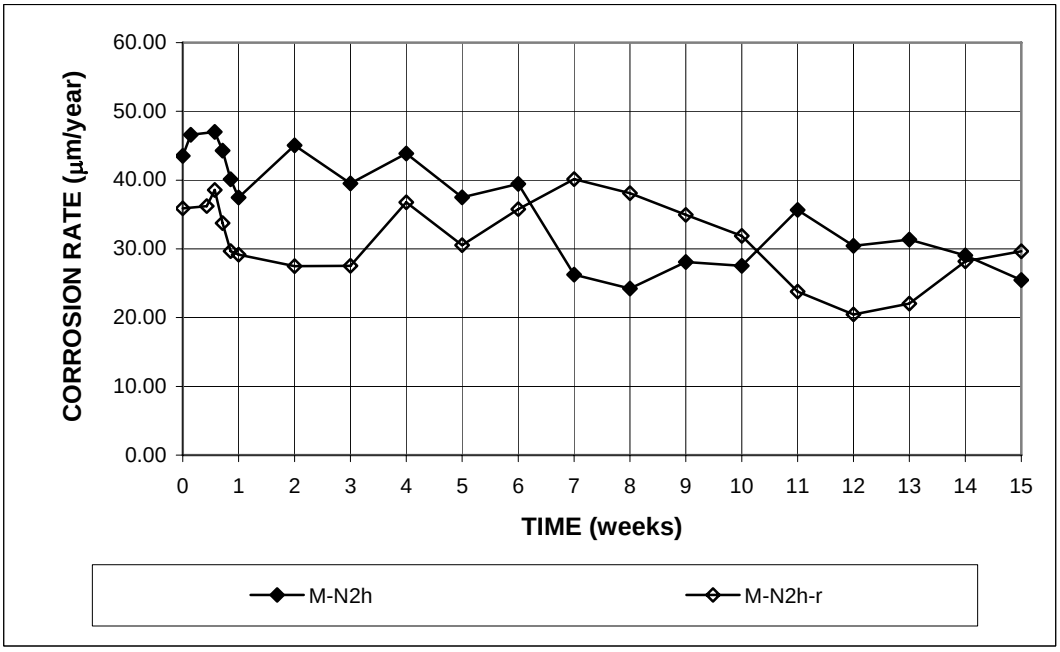

Figure 3.4 - Macrocell test. Average corrosion rates, bare conventional steels in simulated concrete pore solution with 6.04 molal ion NaCl.

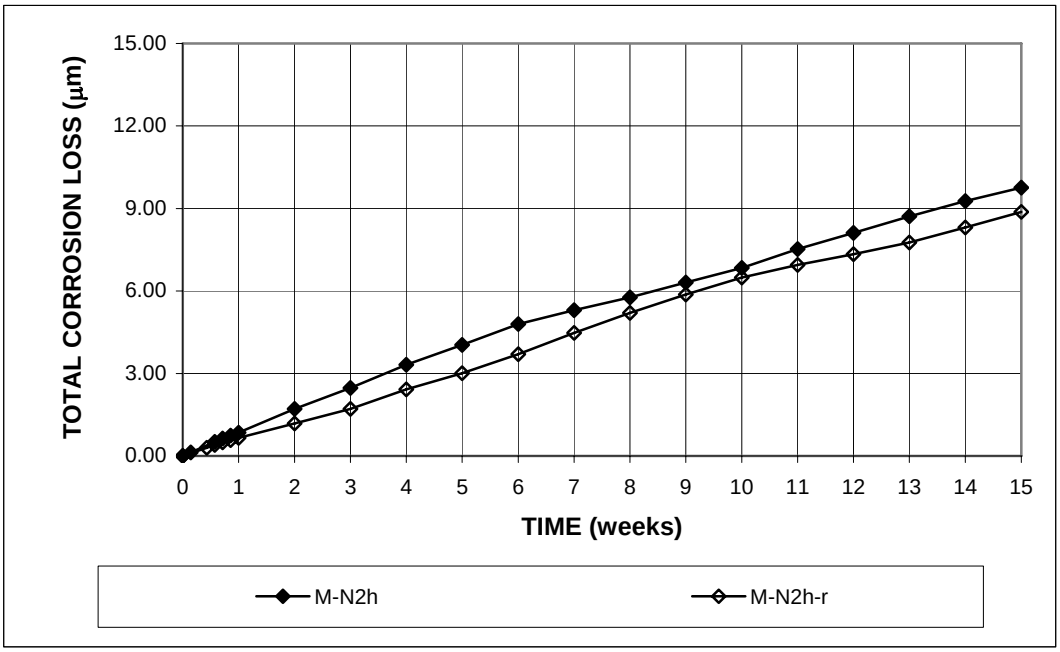

Figure 3.5 - Macrocell test. Average total corrosion losses, bare conventional steels in simulated concrete pore solution with 6.04 molal ion NaCl.

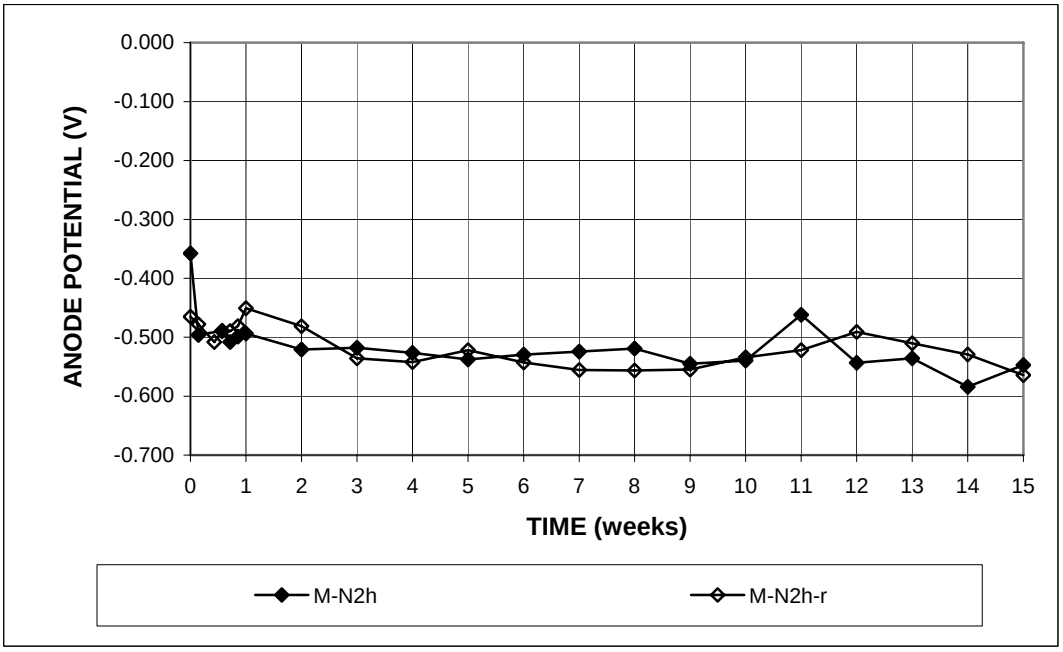

Figure 3.6a - Macrocell test. Average anode corrosion potentials with respect to saturated calomel electrode, bare conventional steels in simulated concrete pore solution with 6.04 molal ion NaCl.

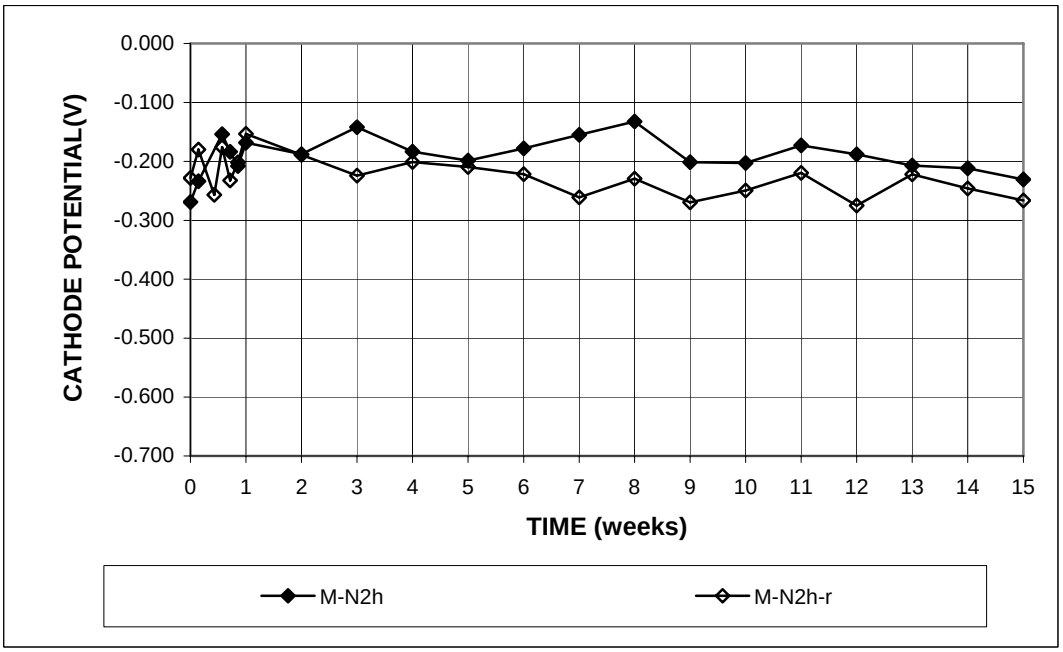

Figure 3.6b - Macrocell test. Average cathode corrosion potentials with respect to saturated calomel electrode, bare conventional steels in simulated concrete pore solution with 6.04 molal ion NaCl.

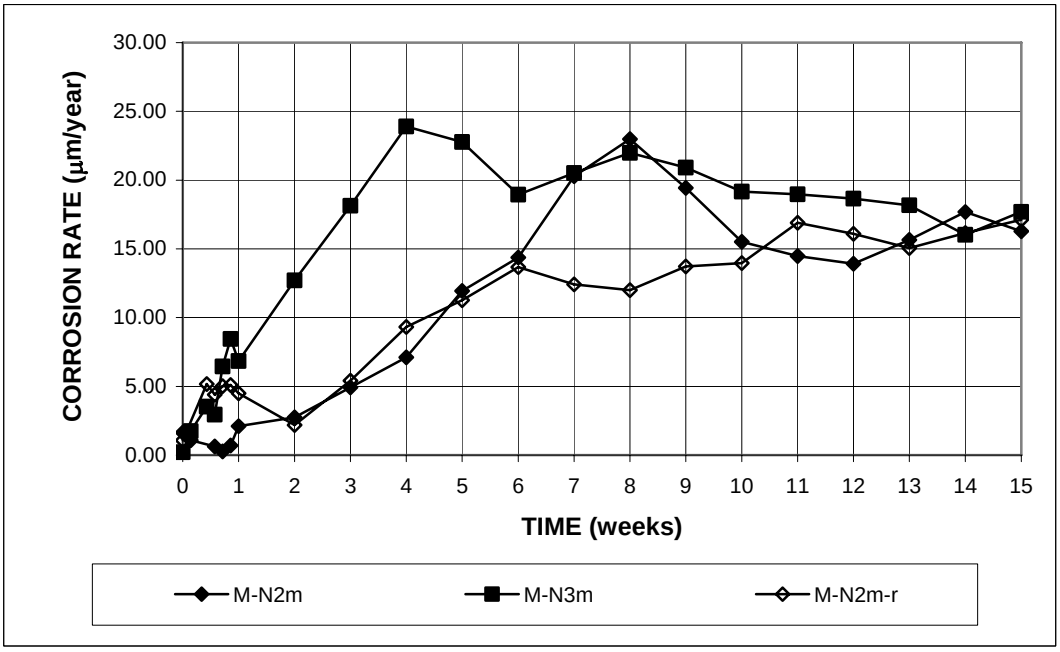

Figure 3.7 - Macrocell test. Average corrosion rates, mortar-wrapped conventional steels in simulated concrete pore solution with 1.6 molal ion NaCl.

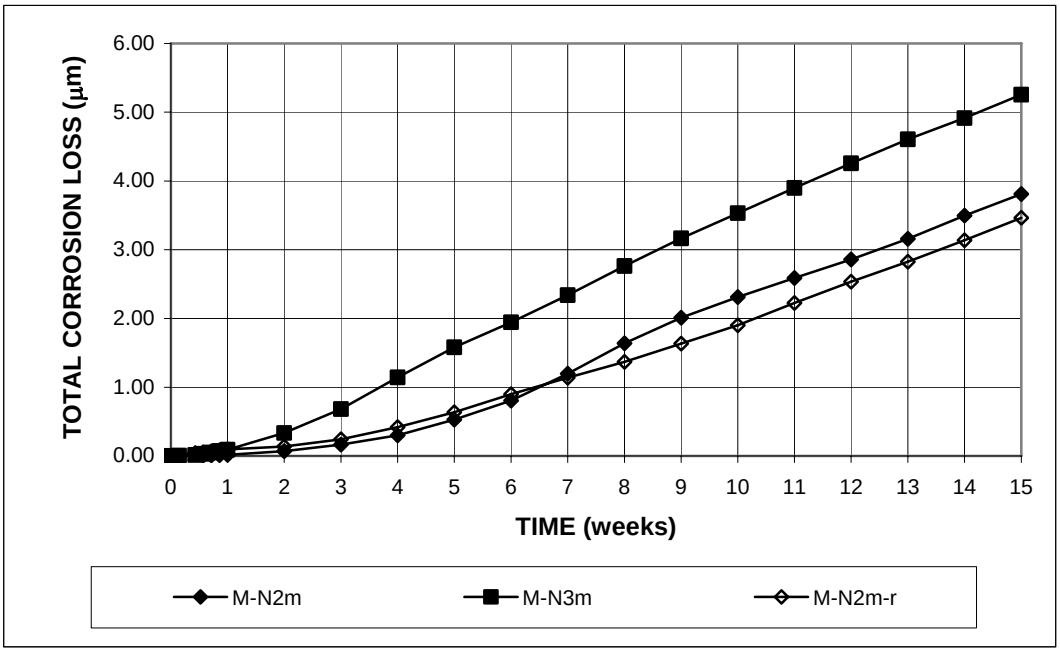

Figure 3.8 - Macrocell test. Average total corrosion losses, mortar-wrapped conventional steels in simulated concrete pore solution with 1.6 molal ion NaCl.

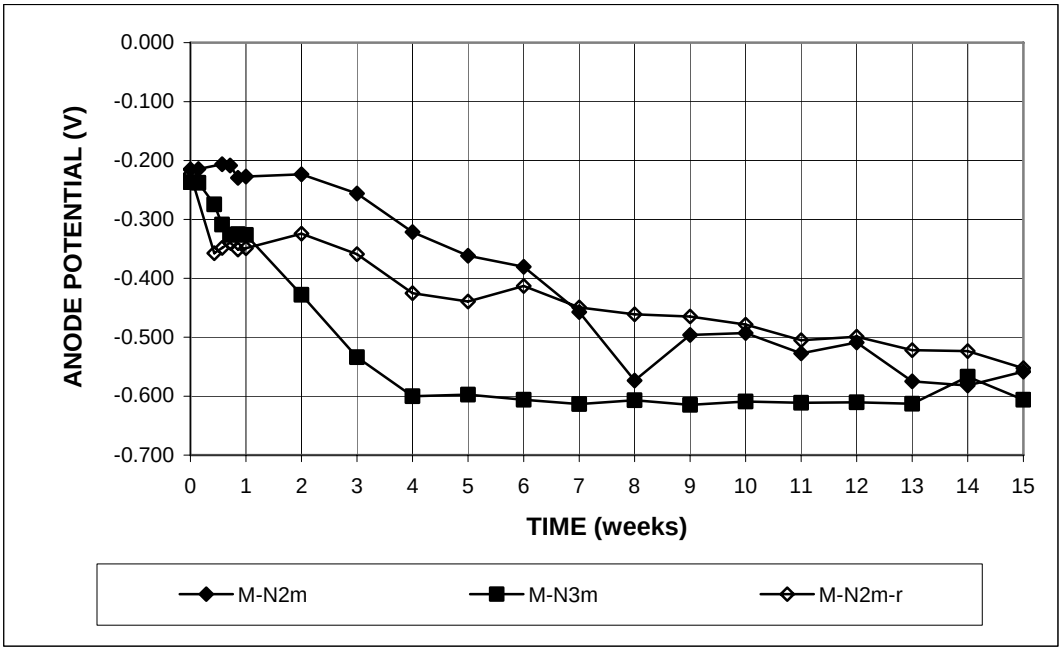

Figure 3.9a - Macrocell test. Average anode corrosion potentials with respect to saturated calomel electrode, mortar-wrapped conventional steels in simulated concrete pore solution with 1.6 molal ion NaCl.

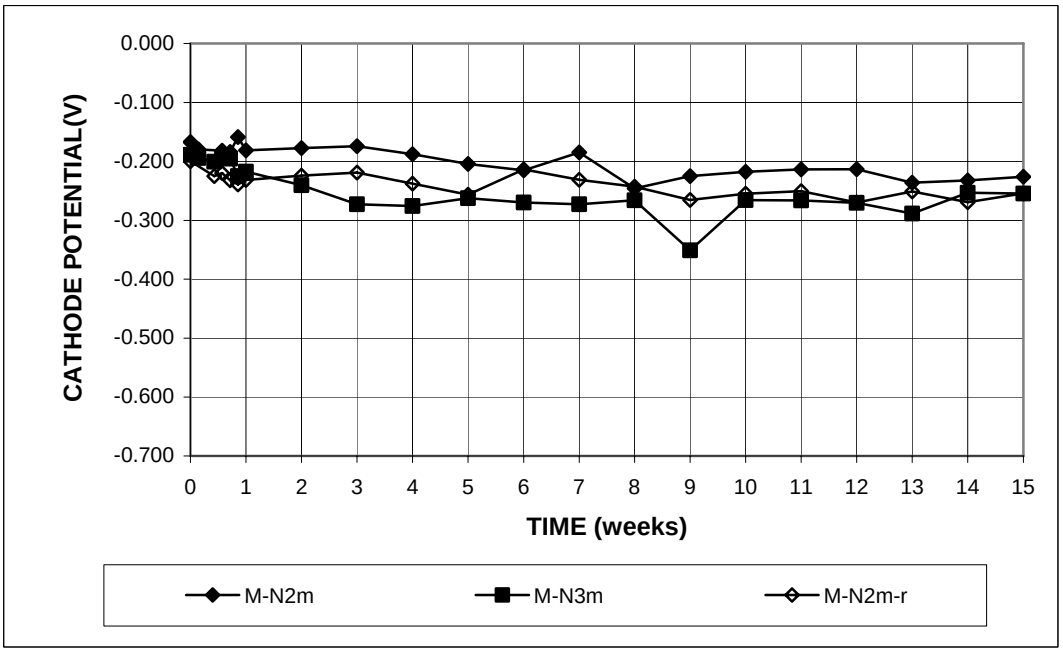

Figure 3.9b - Macrocell test. Average cathode corrosion potentials with respect to saturated calomel electrode, mortar-wrapped conventional steels in simulated concrete pore solution with 1.6 molal ion NaCl.

3.1.2 Bench-scale tests

The results for the bench-scale tests of conventional steels N and N3 are summarized in Tables 3.3 and 3.4 and Figures 3.10 through 3.15. The results of the Student's t-test are shown in Tables C.1 and C.2.

Southern Exposure – Figures 3.10 and 3.11 show the average corrosion rates and total corrosion losses, respectively, for the Southern Exposure test of N and N3 steels. The values at 96 weeks, the end of the test, are summarized in Tables 3.3 and 3.4. During the first 44 weeks, both of the steels corroded at a similar rate, reaching about 7.5 μm/yr. After 44 weeks, the corrosion rate of N3 steel fluctuated around 9 μm/yr, while the corrosion rate of N steel decreased slowly to a value of about 3 μm/yr at 96 weeks. The total average corrosion loss at the end of the test was 7.6 μm for N steel and 12.0 μm for N3 steel. Tables C.1 and C.2 show that the differences in either the corrosion rates or losses at 96 weeks, between N and N3 steels, are not significant at any level of significance (α).

The average corrosion potentials with respect to a copper-copper sulfate electrode (comparison for the bench-scale tests will be with respect to the CSE) for the top and bottom mats of steel are plotted versus time in Figures 3.12a and 3.12b, respectively. For the CSE, a high probability of corrosion is indicated by corrosion potentials more negative than –0.350 V, as shown in Table 1.1. The results show that the average potential of the top mat dropped below –0.350 V after 6 weeks for N steel and 10 weeks for N3 steel. The corrosion potential at 96 weeks was about –0.600 V for both steels. Surprisingly, the average corrosion potentials of the bottom mat for both the steels dropped below –0.350 V before 20 weeks, and then fluctuated between –0.300 and –0.400 V until about 80 weeks, indicating that some chlorides had reached the bottom mat. During the last several weeks of the tests, the potentials of

the bottom mats became more negative than –0.500 V, within about 0.050 V of the top mat. The decrease in the potential difference between the top and bottom bars caused a decrease in the corrosion rate. Some individual specimens exhibited a corrosion rate of zero at 96 weeks, as shown in Table 3.3. In these cases, the total corrosion losses reflect the overall corrosion performance more accurately than the corrosion rate at the end of the test.

The mat-to-mat resistances for the Southern Exposure test of the steels, in conjunction with the values of the other steels in this study, are presented in Figures 3.27, 3.52, and 3.89 in Sections 3.2 through 3.4.

Cracked beam – For cracked beam tests of conventional N and N3 steels, the average corrosion rates and total corrosion losses are shown in Figures 3.13 and 3.14, respectively. The values at 96 weeks are summarized in Tables 3.3 and 3.4. Both of the steels corroded similarly during most of the test period. Corrosion initiated at a relatively high rate, ranging from about 15 to 20 μm/yr and then decreased gradually. During the second half of the test, the corrosion rate of the steels had a few peaks, as high as 30 μm/yr for the N3 steel and 9 μm/yr for the N steel. At 96 weeks, the average corrosion rates were 2.2 and 1.4 μm/yr and the total corrosion losses were 10 μm and 14 μm for N and N3 steel, respectively. The high initial corrosion rates indicate that the chlorides had rapid access to the steel due to the crack in the specimen. The drop in the corrosion rate is likely due to the deposition of corrosion products on the surface of the bars which, first, limits the access of oxygen and chlorides to the steel, and secondly, reduces the anodic area. The jumps in corrosion rates during the second half of the test period may be due to the concrete cracking, caused by the higher volume of the corrosion products compared to the original metal, which exposed the bars to additional chlorides.

Tables C.1 and C.2 show that the differences in either the corrosion rates or losses at 96 weeks between N and N3 steels are not significant at any level of significance (α).

As shown in Figures 3.15a and 3.15b, the corrosion potential of the top mats of the steels dropped below –0.500 V by the end of the first week and remained between –0.500 and –0.600 V thereafter, demonstrating the effect of quick access of chlorides to the steel along the crack. As in the SE test, the corrosion potential of the bottom mats dropped below –0.500 V as the test progressed; because the difference between the top and bottom mat corrosion potentials decreased, some cracked beam specimens also exhibited a corrosion rate of zero at 96 weeks.

The mat-to-mat resistances for the crack beam test of the steels are compared with the values of the other steels in Figures 3.31, 3.56, and 3.97 in Sections 3.2 through 3.4.

Visual Inspection – After the end of the tests, the bars were removed from the concrete. For both the Southern Exposure and cracked beam tests, the conventional bars at the top mat exhibited corrosion products, as shown in Figures 3.59 and 3.60, which are presented in conjunction with the figures for MMFX steel in Section 3.3.2.

Table 3.3 - Average corrosion rates at 96 weeks for specimens with conventional steels in bench-scale tests

Specimen designation*	Steel type	Specimen corrosion rates (μm/yr)						Average (μm/yr)	Standard deviation
		1	2	3	4	5	6		
Southern Exposure test									
SE-N	N	5.11	0.00	0.00	1.67	5.35	4.52	2.77	2.52
SE-N3	N3	0.00	25.09	0.00	0.00	11.46	7.96	7.42	9.94
Cracked beam test									
CB-N	N	0.03	0.02	2.39	4.21	6.40	0.00	2.17	2.68
CB-N3	N3	0.00	0.00	0.00	0.00	8.56	0.00	1.43	3.50

*** A-B**

A: test method; SE = Southern Exposure test, CB = Cracked beam test.

B: steel type and test condition; N and N3 = conventional steel.

Table 3.4 - Average total corrosion losses for specimens with conventional steels in bench-scale tests

Specimen designation*	Steel type	Specimen total corrosion losses (μm)						Average (μm)	Standard deviation
		1	2	3	4	5	6		
Southern Exposure test									
SE-N	N	10.36	9.57	8.04	4.35	6.42	7.10	7.64	2.18
SE-N3	N3	11.59	27.81	3.23	8.39	14.24	6.63	11.98	8.65
Cracked beam test									
CB-N	N	12.63	10.09	6.48	10.91	13.68	6.25	10.01	3.09
CB-N3	N3	27.54	16.45	12.47	6.91	10.28	9.87	13.92	7.38

*** A-B**

A: test method; SE = Southern Exposure test, CB = Cracked beam test.

B: steel type and test condition; N and N3 = conventional steel.

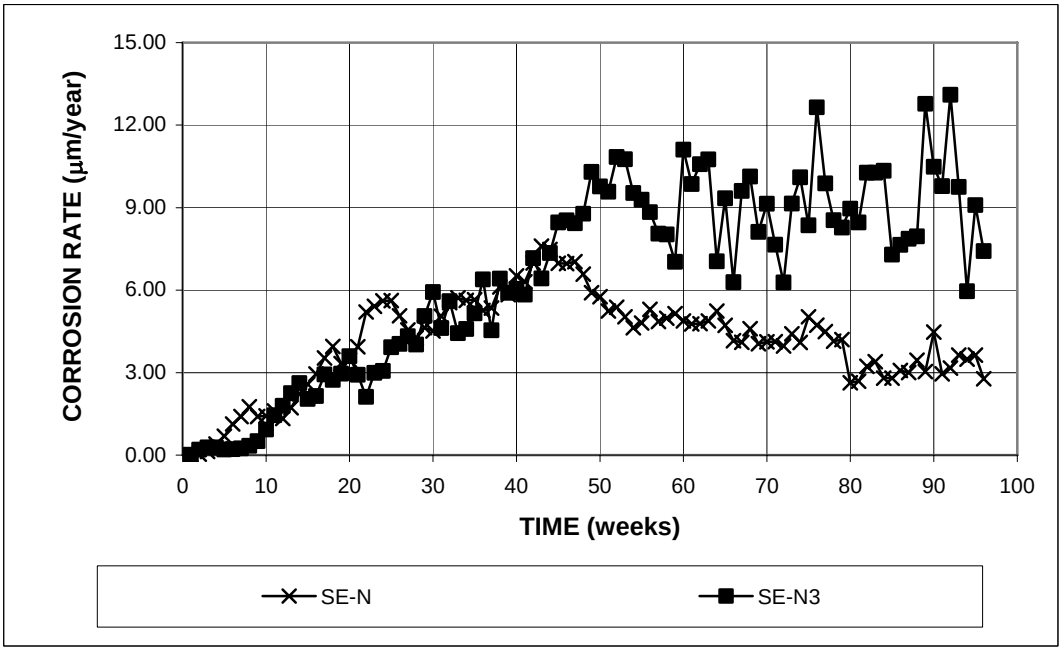

Figure 3.10 - Southern Exposure test. Average corrosion rates of conventional steels, specimens w/c = 0.45, ponded with 15% NaCl solution.

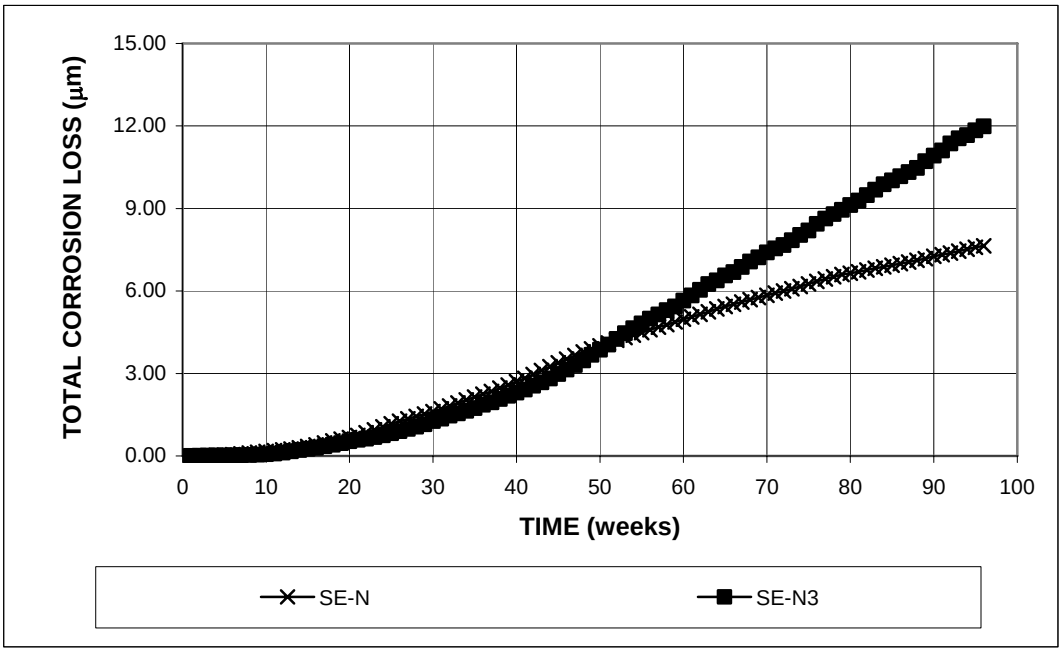

Figure 3.11 - Southern Exposure test. Average total corrosion losses of conventional steels, specimens w/c = 0.45, ponded with 15% NaCl solution.

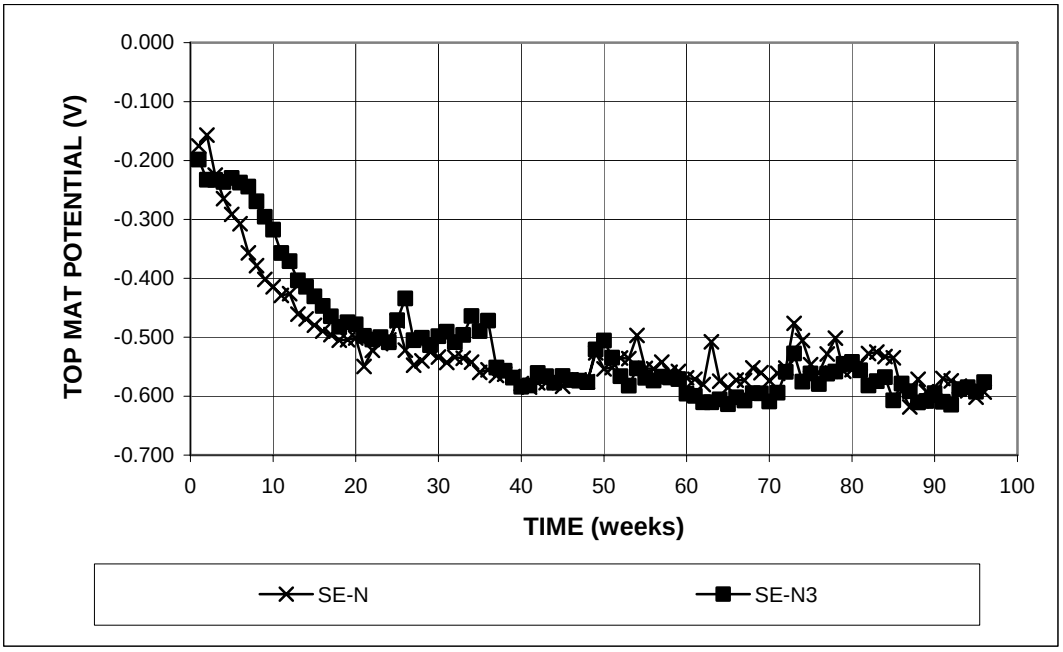

Figure 3.12a - Southern Exposure test. Average top mat corrosion potentials with respect to copper-copper sulfate electrode for conventional steels, specimens w/c = 0.45, ponded with 15% NaCl solution.

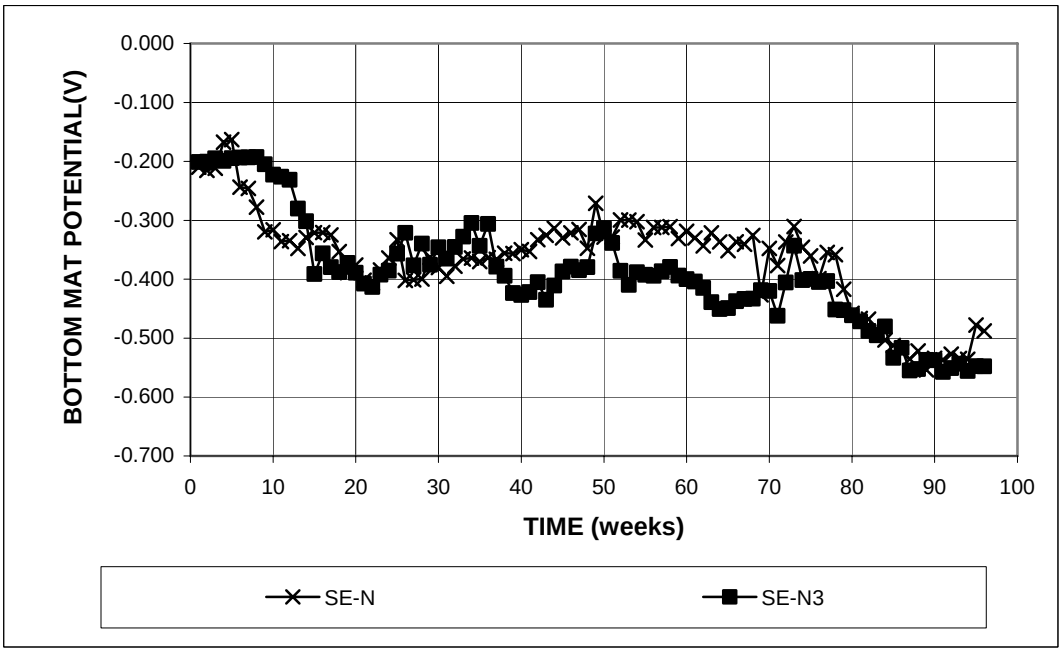

Figure 3.12b - Southern Exposure test. Average bottom mat corrosion potentials with respect to copper-copper sulfate electrode for conventional steels, specimens w/c = 0.45, ponded with 15% NaCl solution.

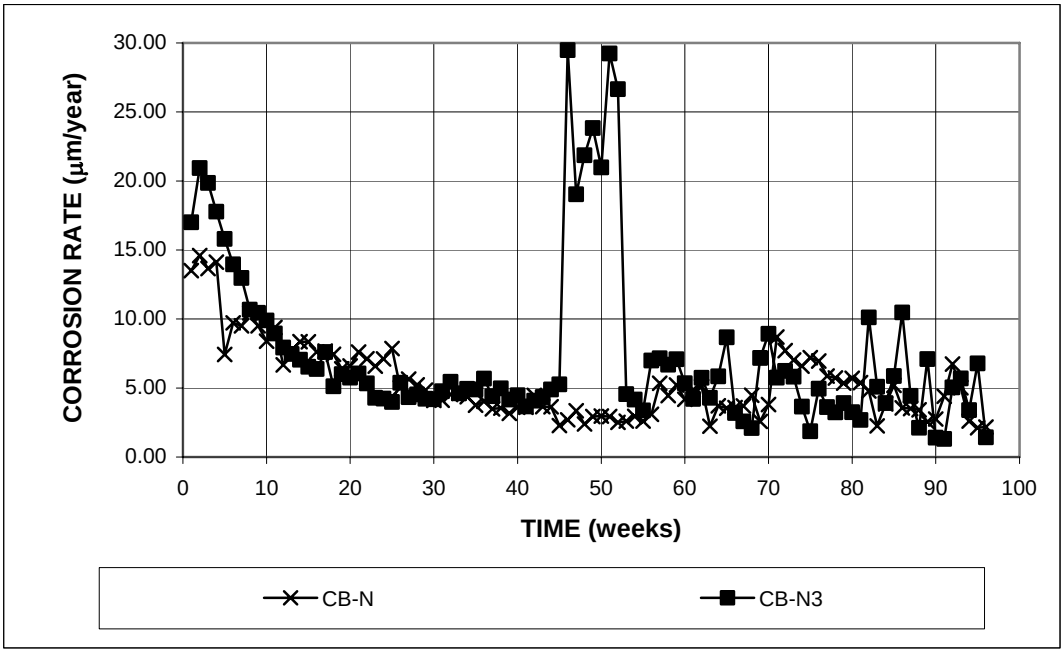

Figure 3.13 - Cracked beam test. Average corrosion rates of conventional steels, specimens w/c = 0.45, ponded with 15% NaCl solution.

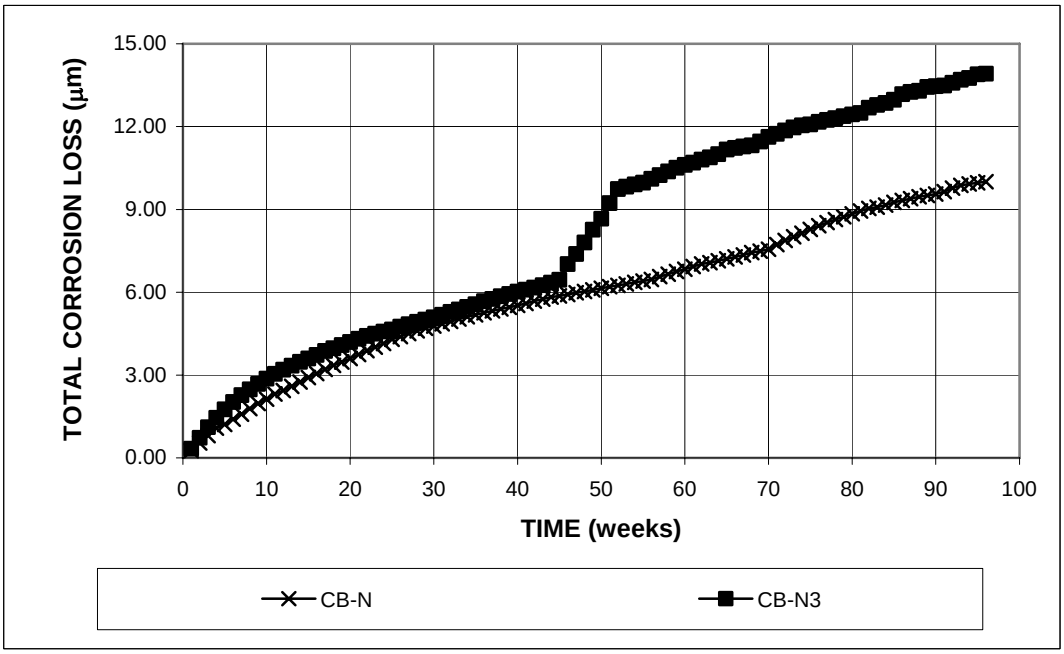

Figure 3.14 - Cracked beam test. Average total corrosion losses of conventional steels, specimens w/c = 0.45, ponded with 15% NaCl solution.

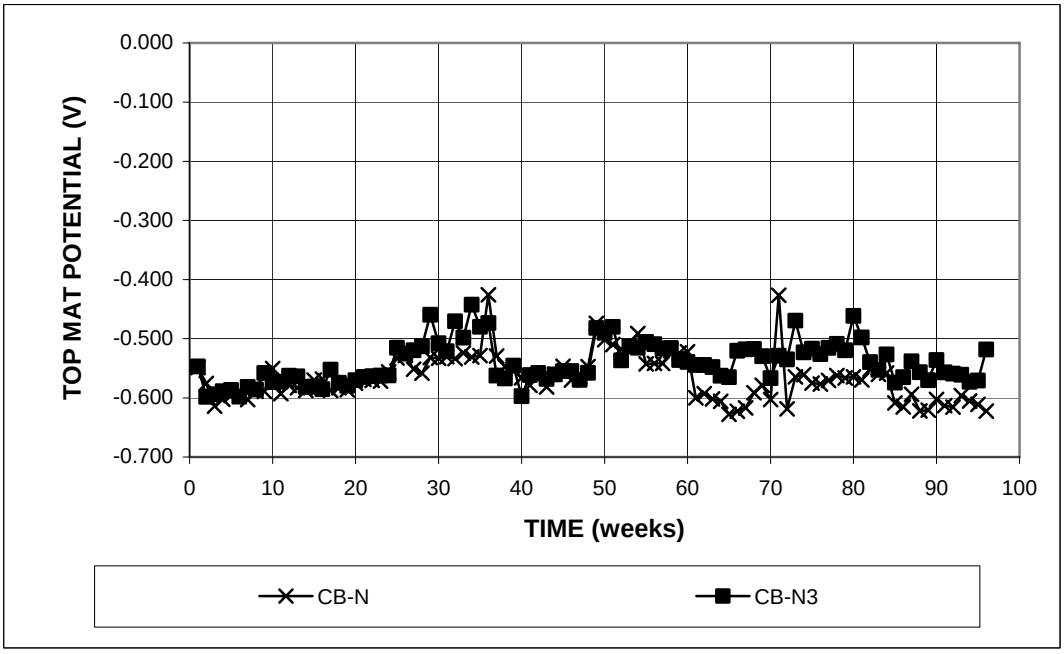

Figure 3.15a - Cracked beam test. Average top mat corrosion potentials with respect to copper-copper sulfate electrode for conventional steels, specimens w/c = 0.45, ponded with 15% NaCl solution.

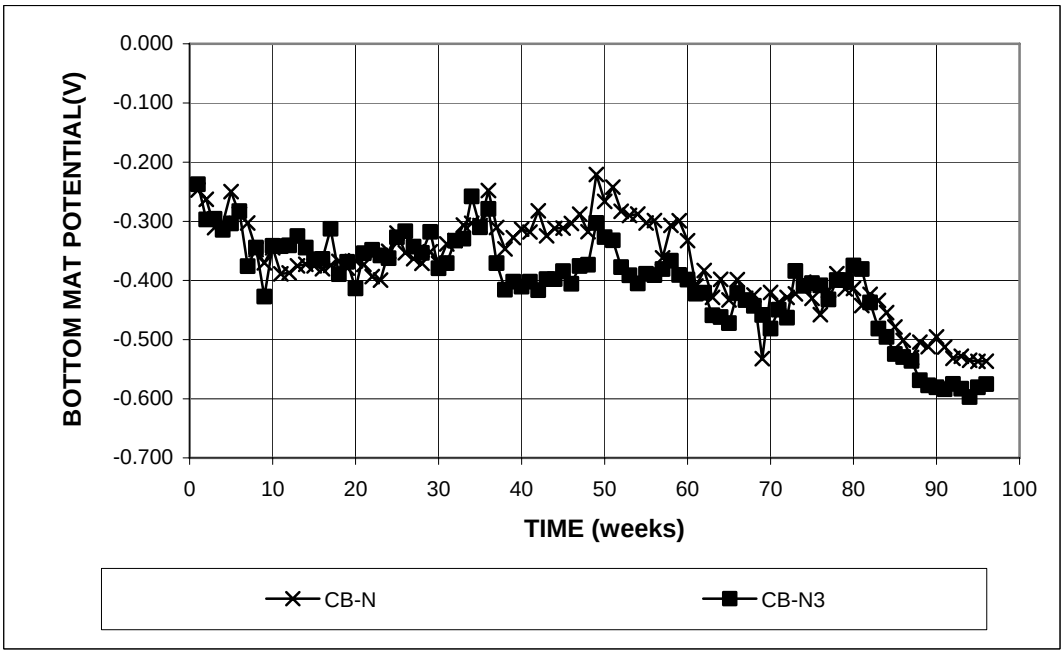

Figure 3.15b - Cracked beam test. Average bottom mat corrosion potentials with respect to copper-copper sulfate electrode for conventional steels, specimens w/c = 0.45, ponded with 15% NaCl solution.

3.2 EPOXY-COATED REINFORCING STEEL

The results for epoxy-coated N3 reinforcing steel in the macrocell test are presented in Tables 3.5 and 3.6 and Figures 3.16 through 3.21. The results for epoxy-coated N3 reinforcing steel in the bench-scale tests are presented in Tables 3.7 and 3.8 and Figures 3.22 through 3.29. For comparison, the results for N3 conventional steel are also presented again in the figures and tables. The results for the Student's t-test are shown in Tables C.3 and C.4. As discussed in Sections 2.3 and 2.4, the epoxy coating on all bars was penetrated by four 3.2 mm (0.125 in.) diameter holes. The corrosion rate and total corrosion loss are calculated based on both the total anodic area and the exposed area of the holes. The results show that epoxy-coated steel exhibits much lower corrosion rates based on the total area and higher corrosion rates based on the exposed area than conventional steel; whether epoxy-coated or uncoated bars are used as the cathode has a great effect on the corrosion rate of epoxy-coated reinforcing steel, as demonstrated by the test results.

3.2.1 Rapid macrocell tests

Bare bar specimens – Bare epoxy-coated bars, used at both the anode and the cathode, were evaluated in simulated concrete pore solution with 1.6 m ion NaCl (M-ECR-r). The solutions were replaced every five weeks. Epoxy-coated steel was not tested in 6.04 m ion NaCl solution.

Figures 3.16a and 3.16b differ only in the scale of the vertical axis. They show the average corrosion rates as a function of time. Table 3.5 summarizes the values at 15 weeks. At the beginning of the test, the epoxy-coated steel corroded at a rate of 0.5 μm/yr based on the total area (M-ECR-r^T), compared to conventional N3 steel with a rate of about 40 μm/yr. The corrosion rate increased rapidly to 1.5 μm/yr by the end

of the second week and then increased slowly, reaching 2.1 μm/yr at 15 weeks, about 6% of the rate exhibited by conventional steel. The corrosion rates based on the exposed area (M-ECR-r^E) were 100 times those based on the total area.

The average total corrosion losses versus time are shown in Figures 3.17a, and Figure 3.17b. Figure 3.17b expands the vertical axis in Figure 3.17a. The corrosion losses at 15 weeks are summarized in Table 3.6. At 15 weeks, the corrosion loss for the epoxy-coated steel was about 0.5 μm based on the total area and 50 μm based on the exposed area, compared to 6 to 9.0 μm for the three conventional steels described in Section 3.1.

The average corrosion potentials of the anode and the cathode are shown in Figures 3.18a and 3.18b, respectively. After the first week, the corrosion potential of the anode for the epoxy-coated steel remained around –0.600 V, about 0.100 V more negative than those shown by conventional steel for most of the test period. The corrosion potential of the cathode for the epoxy-coated steel, about 0.050 V more negative than for conventional steel, was around –0.250 V throughout the test period, indicating a passive condition.

Mortar-wrapped specimens – Mortar-wrapped epoxy-coated reinforcing steel was evaluated in two ways: (1) with uncoated conventional steel as the cathode (M-ECR/N3m) and (2) with epoxy-coated bars with four drilled holes as the cathode (M-ECRm-r). The test solutions were replaced every five weeks when epoxy-coated steel was used in the cathode (Note, these tests were performed later in the study, after the newer test procedures had been adopted).

The average corrosion rates are plotted versus time in Figures 3.19a and 3.19b. Table 3.5 summarizes the corrosion rates at 15 weeks. Figure 3.19a shows that when uncoated steel was used as the cathode, the corrosion rate of epoxy-coated steel

was very high based on the exposed area (M-ECR/N3m^{E}), reaching a value of 192 μm/yr at four weeks (when the effects of replacing the solutions do not apply) and 533 μm/yr at 15 weeks. Figure 3.19b expands the vertical axis in Figure 3.19a and shows that the corrosion rate of epoxy-coated steel based on the total area (M-ECR/N3m^{T}) was 5.3 μm/yr at 15 weeks, equal to about 30% of that exhibited by conventional steel (N3), 17.7 μm/yr (Table C.3 shows that the difference is significant at $\alpha = 0.02$). When epoxy-coated steel was used as the cathode, however, the epoxy-coated bars corroded at a much lower rate. Even based on the exposed area of steel, the average corrosion rate for the epoxy-coated steel (M-ECRm-r^{E}) was lower than that exhibited by the conventional steel during most of the test period; the corrosion rate had a maximum value of 26 μm/yr at 3 weeks and remained below 5 μm/yr for the second half of the test period. At 15 weeks, the epoxy-coated steel corroded at 1.2 μm/yr based on exposed area, less than 7% of that shown by the conventional steel (Table C.3 shows that the difference is significant at $\alpha = 0.02$), while based on the total area, the average corrosion rate was 1% of the value based on exposed area. The results demonstrate that the cathode area has great effect on the corrosion rate of the epoxy-coated steel and that it is important to use all epoxy-coated reinforcing steel on bridge decks, rather than just the top mat of steel.

The average corrosion losses are shown in Figures 3.20a and 3.20b, and the values at 15 weeks are summarized at Table 3.6. At 15 weeks, compared to a value of 5.3 μm for the conventional N3 steel, the average total corrosion losses based on the exposed area for the epoxy-coated steel were 39 μm when uncoated steel was used as the cathode and 2.3 μm when epoxy-coated steel was used as the cathode, while the values based on the total area equal to 1% of the values based on the exposed area. Table C.4 shows that the differences in the corrosion losses between the N3 steel

specimens and either the ECR/N3m^{T} or the ECRm-r^{E} specimens are significant at α = 0.02.

The average corrosion potentials of the anode and the cathode are shown in Figures 3.21a and 3.21b, respectively. The corrosion potential at the anode for N3 steel dropped rapidly in the first few weeks, becoming more negative than –0.275 V by the end of the first week and –0.600 V at four weeks. The anode corrosion potential of the epoxy-coated steel with conventional steel as the cathode remained near –0.300 V until 13 weeks and dropped to a value close to –0.500 V at the end of the test. When epoxy-coated steel was used as the cathode, the anode potential remained around –0.275 V for the first 6 weeks and then dropped, reaching a value of –0.400 V at 15 weeks. For epoxy-coated reinforcing steel, whether coated or uncoated steel was used as the cathode, the corrosion potentials of the cathode remained close to –0.200 V, indicating a passive condition and that the high corrosion rate exhibited by epoxy-coated steel with uncoated steel as the cathode was caused by the increase of the cathode area, rather than any difference in the corrosion potentials of the anode and cathode.

Table 3.5 - Average corrosion rates at 15 weeks for specimens with epoxy-coated steel in macrocell test

Specimen designation*	Steel type	Specimen corrosion rates (μm/yr)						Average (μm/yr)	Standard deviation
		1	2	3	4	5	6		
Bare bars in 1.6 m NaCl									
M-N3	N3	52.60	0.26	67.77	40.17	32.43	22.08	35.88	23.61
M-ECR-r^{T}	ECR3	0.18	2.49	2.75	3.33	1.50	2.53	2.13	1.12
M-ECR-r^{E}	ECR3	18.30	248.9	274.5	333.1	150.1	252.5	212.9	112.2
Mortar-wrapped specimens in 1.6 m NaCl									
M-N3m	N3	11.21	9.16	26.07	19.31	21.15	19.31	17.70	6.36
M-ECR/N3m^{T}	ECR3/N3	0.04	18.45	0.77	6.48	6.22	0.00	5.33	7.09
M-ECR/N3m^{E}	ECR3/N3	3.66	1845	76.86	647.8	622.2	0.00	532.5	709.1
M-ECRm-r^{T}	ECR3	0.00	0.00	0.00	0.00	0.00	0.07	0.01	0.03
M-ECRm-r^{E}	ECR3	0.00	0.00	0.00	0.00	0.00	7.32	1.22	2.99

*** A-B-C**

A: test method, M = macrocell test. **B:** steel type and test condition, N3 = conventional steel; ECR = epoxy--coated steel; ECR/N3 = epoxy-coated steel as the anode, conventional steel as the cathode; m = mortar-wrapped specimens. **C:** r = the test solutions are replaced every five weeks.

^{T}: Based on total area of bar exposed to solution.

^{E}: Based on exposed area of four 3.2 mm (0.125 in.) diameter holes in the coating

Table 3.6 - Average total corrosion losses for specimens with epoxy-coated steel in macrocell test

Specimen designation*	Steel type	Specimen total corrosion losses (μm)						Average (μm)	Standard deviation
		1	2	3	4	5	6		
Bare bars in 1.6 m NaCl									
M-N3	N3	12.33	4.15	13.49	11.17	7.08	5.50	8.95	3.88
M-ECR-r^{T}	ECR3	0.26	0.61	0.62	0.61	0.30	0.68	0.51	0.18
M-ECR-r^{E}	ECR3	26.3	60.9	62.0	60.7	30.0	67.6	51.26	18.08
Mortar-wrapped specimens in 1.6 m NaCl									
M-N3m	N3	5.13	4.75	6.55	5.21	4.79	5.12	5.26	0.66
M-ECR/N3m^{T}	ECR3/N3	0.01	1.30	0.09	0.64	0.28	0.02	0.39	0.50
M-ECR/N3m^{E}	ECR3/N3	1.28	129.6	9.19	63.6	28.4	2.07	39.02	50.22
M-ECRm-r^{T}	ECR3	0.03	0.02	0.02	0.02	0.01	0.03	0.02	0.01
M-ECRm-r^{E}	ECR3	2.88	2.42	2.38	1.72	1.31	2.82	2.25	0.62

*** A-B-C**

A: test method, M = macrocell test. **B:** steel type and test condition, N3 = conventional steel; ECR = epoxy--coated steel; ECR/N3 = epoxy-coated steel as the anode, conventional steel as the cathode; m = mortar-wrapped specimens. **C:** r = the test solutions are replaced every five weeks.

^{T}: Based on total area of bar exposed to solution.

^{E}: Based on exposed area of four 3.2 mm (0.125 in.) diameter holes in the coating.

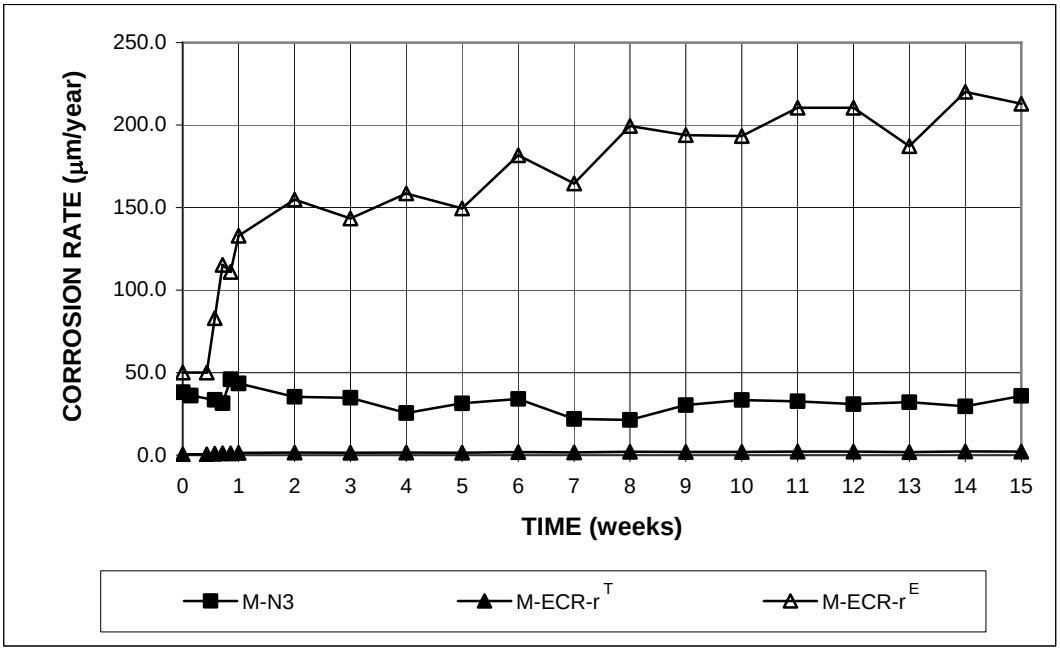

(a)

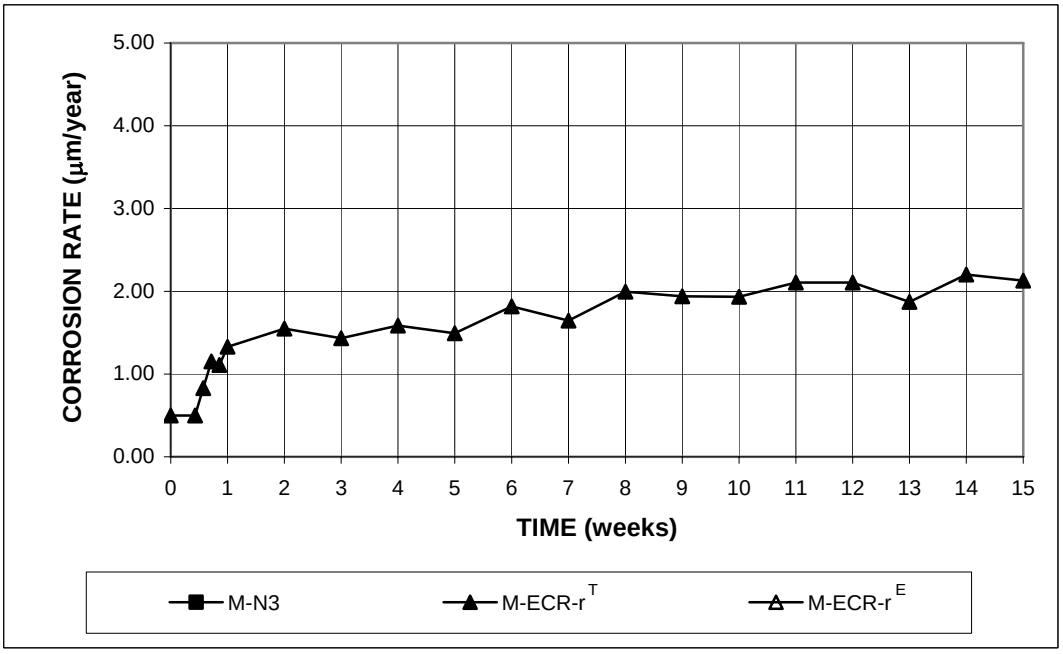

(b)

T: Based on total area of bar exposed to solution.
E: Based on exposed area of four 3.2 mm (0.125 in.) diameter holes in the coating

Figure 3.16 - Macrocell test. Average corrosion rates, bare epoxy-coated steels in simulated concrete pore solution with 1.6 molal ion NaCl.

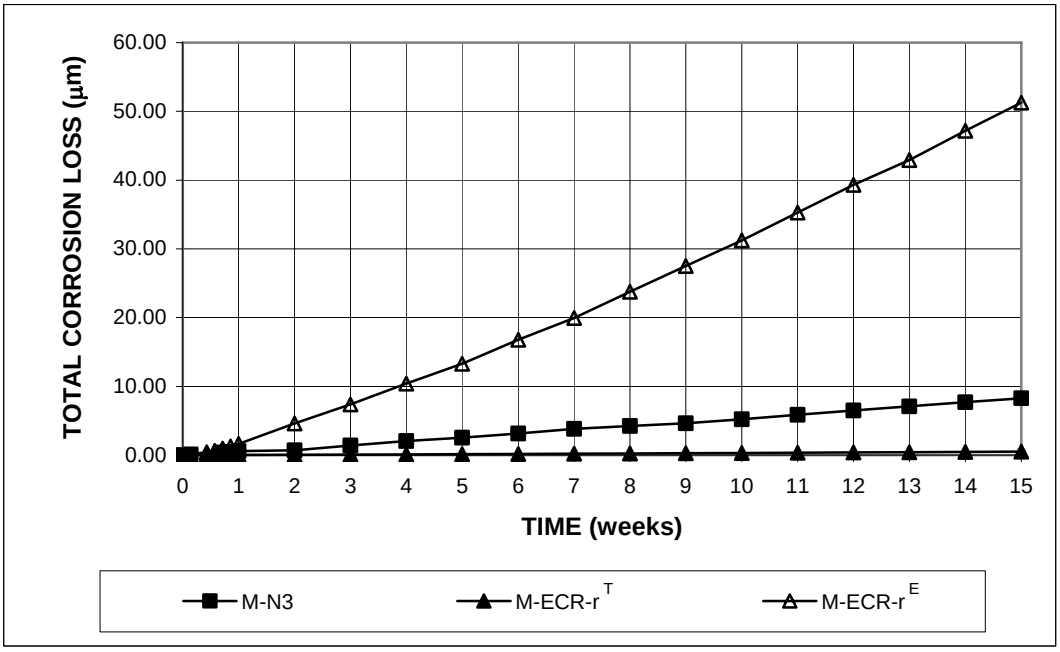

(a)

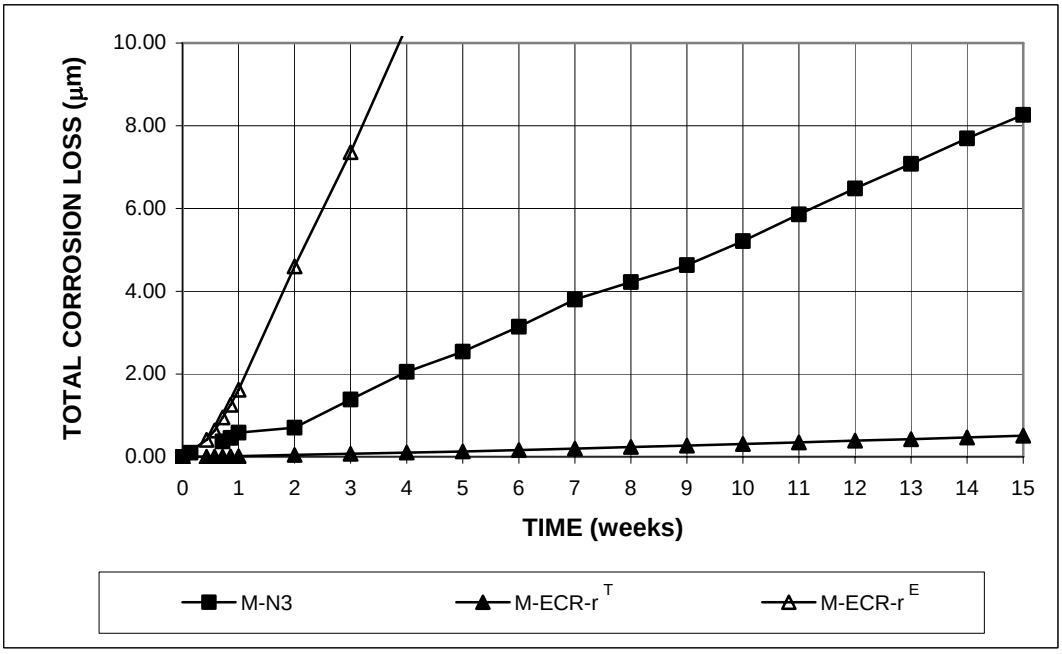

(b)

T: Based on total area of bar exposed to solution.
E: Based on exposed area of four 3.2 mm (0.125 in.) diameter holes in the coating

Figure 3.17 - Macrocell test. Average total corrosion losses, bare epoxy-coated steel in simulated concrete pore solution with 1.6 molal ion NaCl.

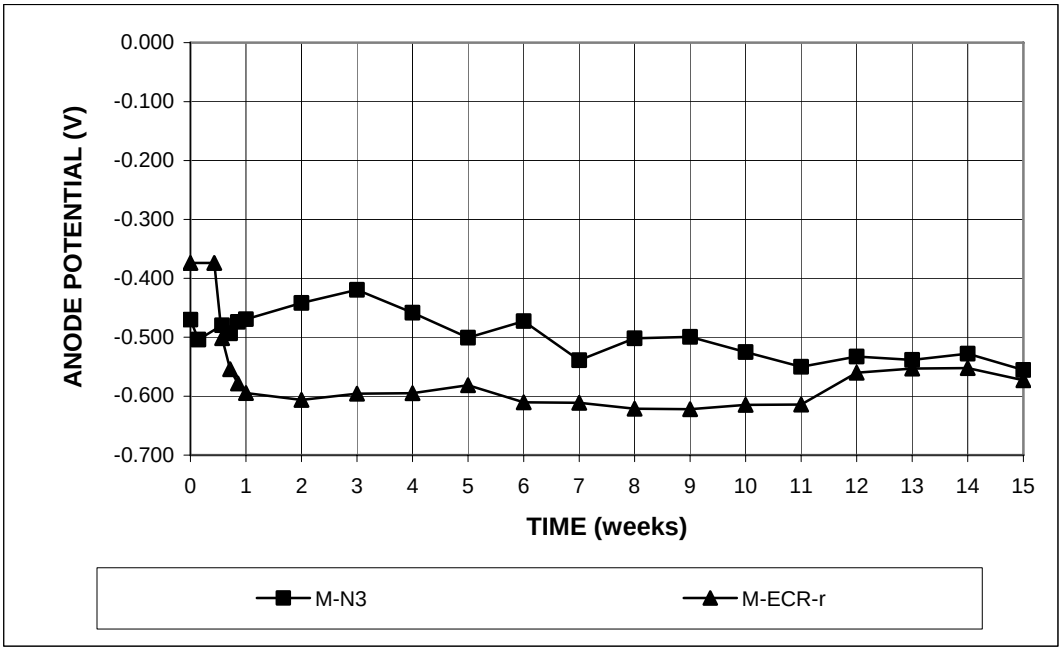

Figure 3.18a - Macrocell test. Average anode corrosion potentials with respect to saturated calomel electrode, bare epoxy-coated steel in simulated concrete pore solution with 1.6 molal ion NaCl.

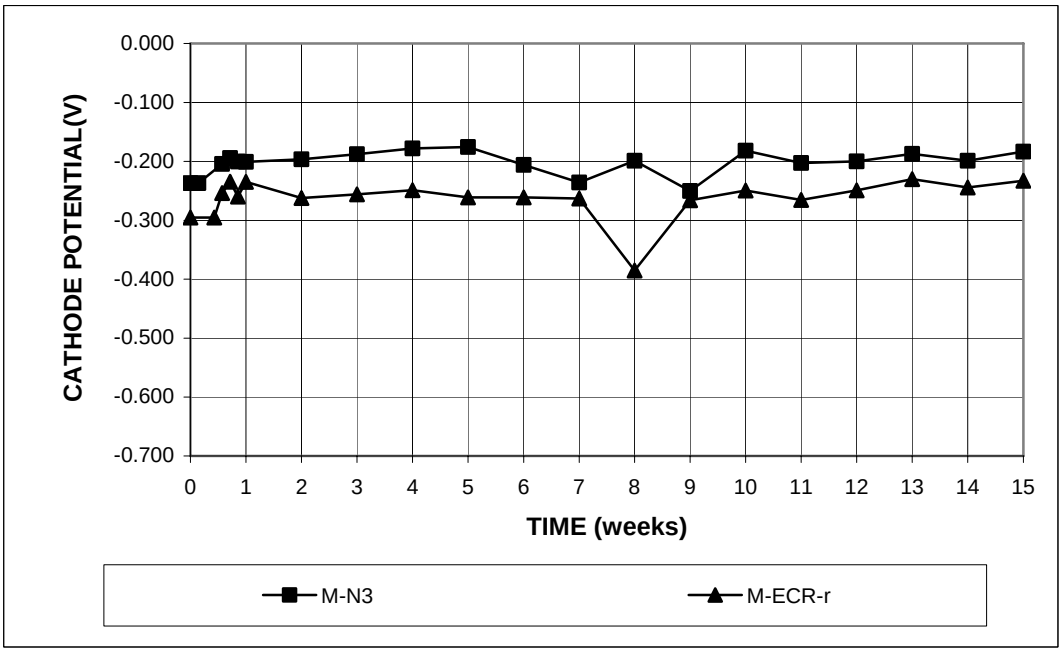

Figure 3.18b - Macrocell test. Average cathode corrosion potentials with respect to saturated calomel electrode, bare epoxy-coated steel in simulated concrete pore solution with 1.6 molal ion NaCl.

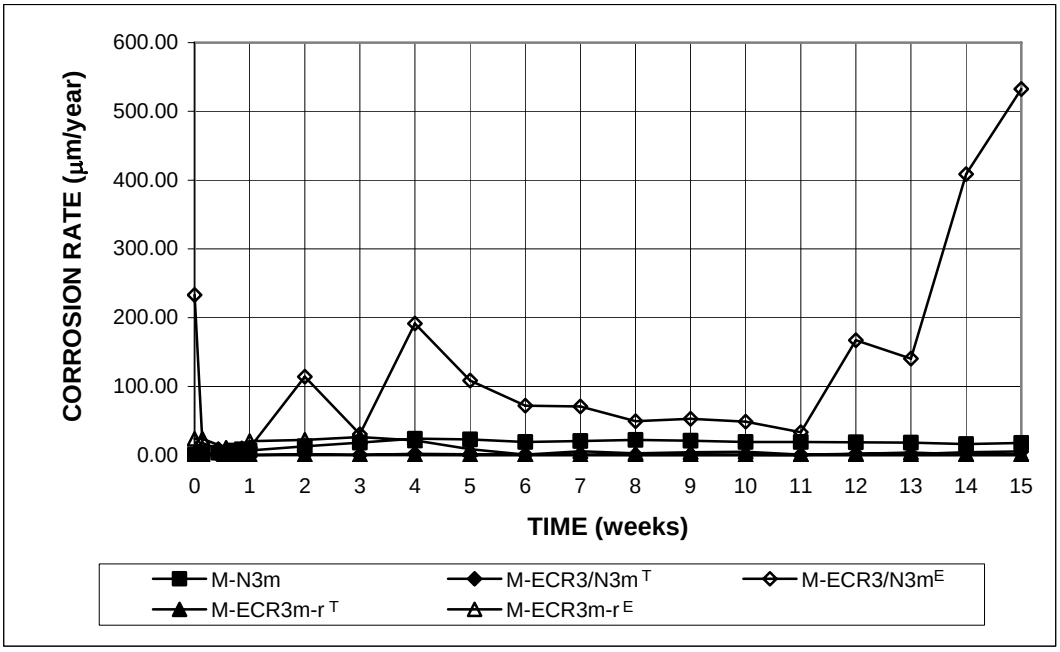

(a)

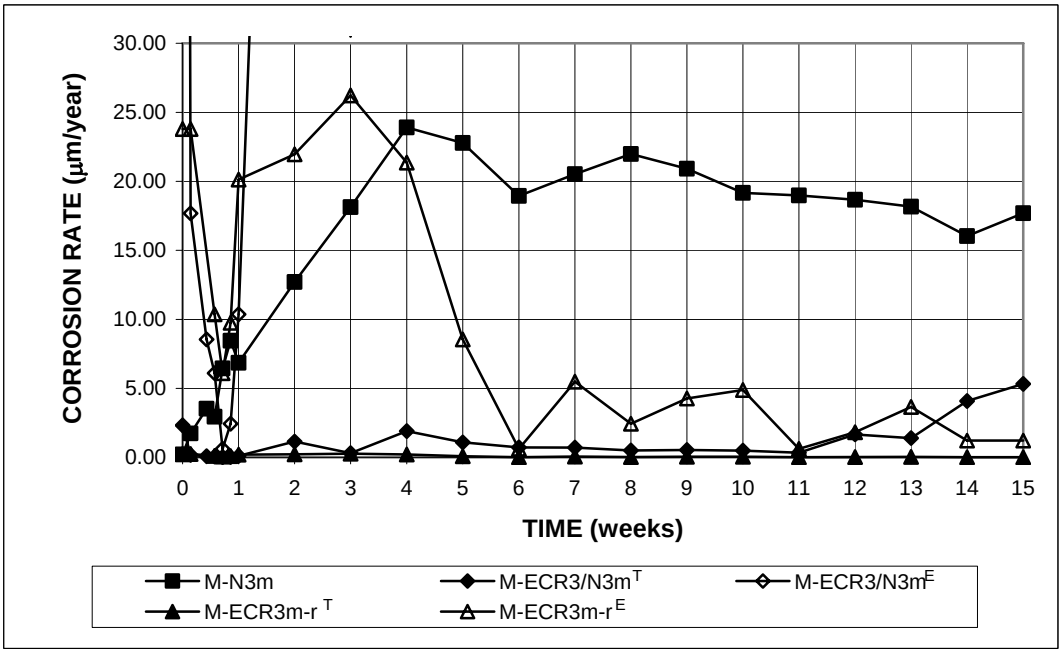

(b)

T: Based on total area of bar exposed to solution.
E: Based on exposed area of four 3.2 mm (0.125 in.) diameter holes in the coating.

Figure 3.19 - Macrocell test. Average corrosion rates, mortar-wrapped epoxy-coated steel in simulated concrete pore solution with 1.6 molal ion NaCl.

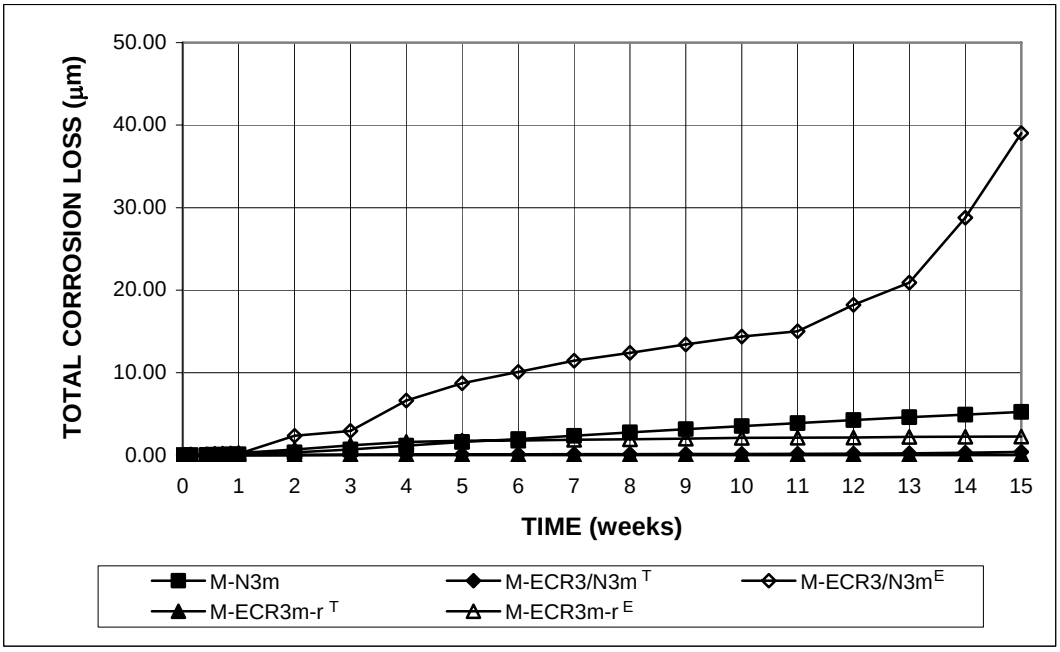

(a)

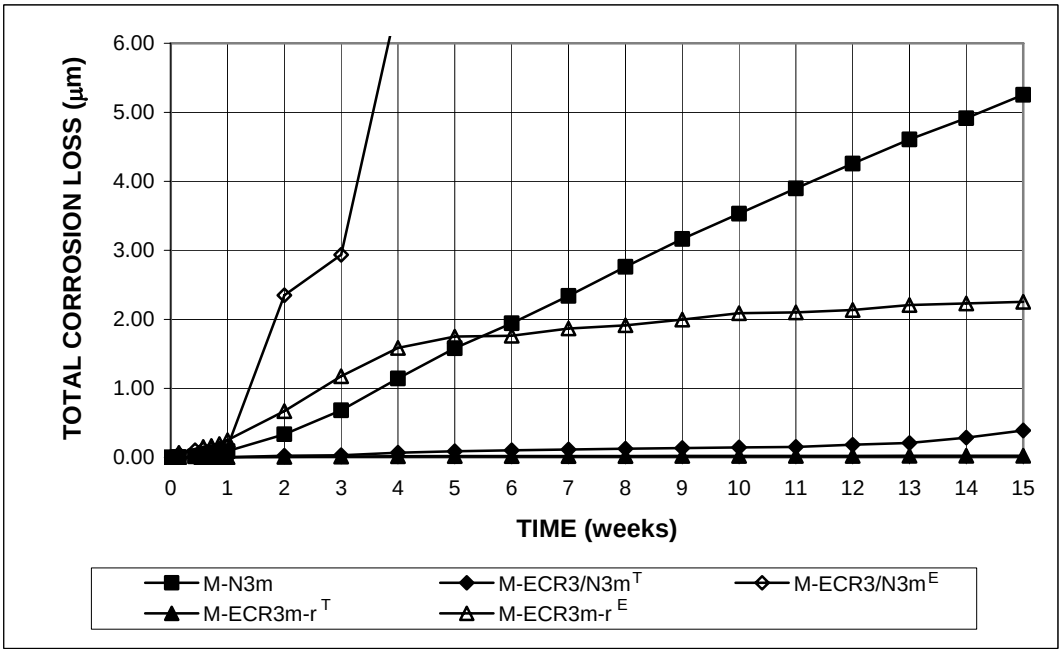

(b)

T: Based on total area of bar exposed to solution.
E: Based on exposed area of four 3.2 mm (0.125 in.) diameter holes in the coating.

Figure 3.20 - Macrocell test. Average total corrosion losses, mortar-wrapped epoxy-coated steel in simulated concrete pore solution with 1.6 molal ion NaCl.

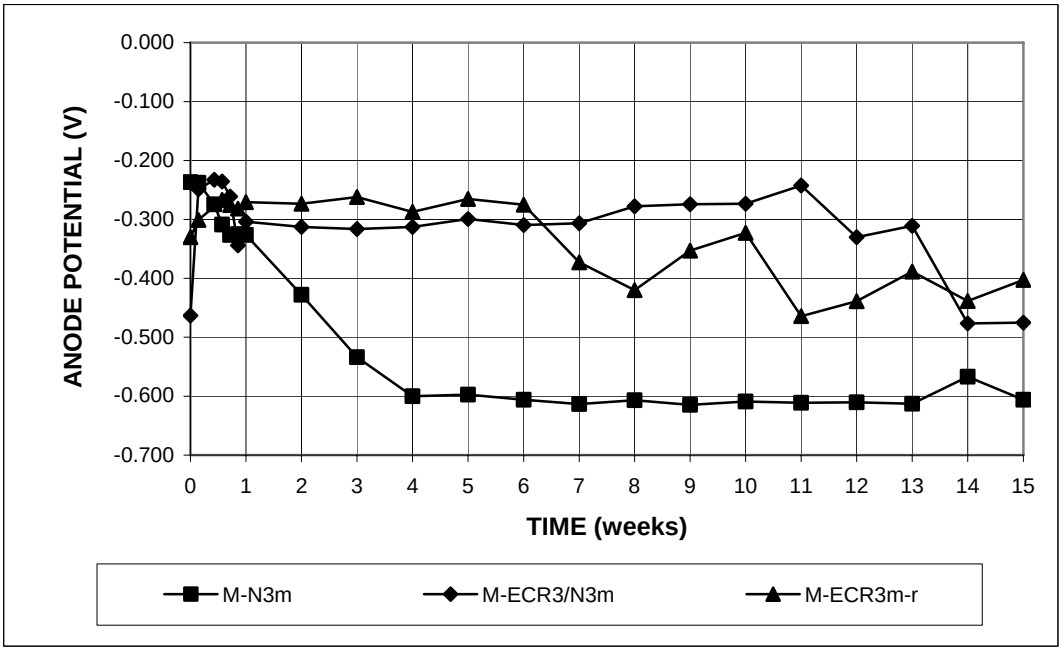

Figure 3.21a - Macrocell test. Average anode corrosion potentials with respect to saturated calomel electrode, mortar-wrapped epoxy-coated steel in simulated concrete pore solution with 1.6 molal ion NaCl.

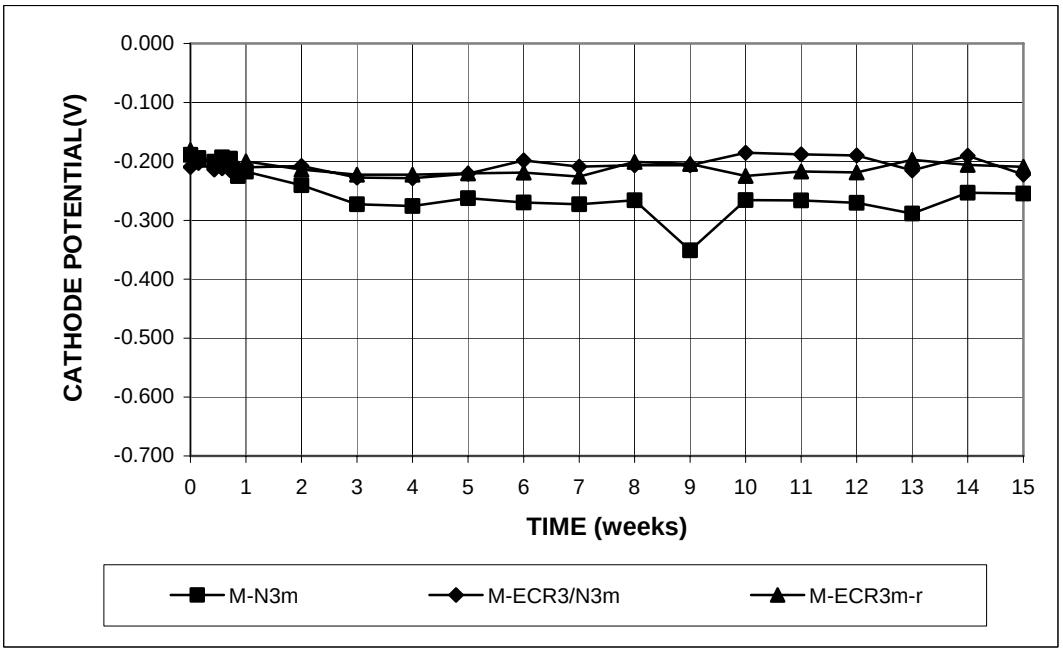

Figure 3.21b - Macrocell test. Average anode corrosion potentials with respect to saturated calomel electrode, mortar-wrapped epoxy-coated steel in simulated concrete pore solution with 1.6 molal ion NaCl.

Visual Inspection – At the end of the tests, the anode epoxy-coated bars were visually inspected. For bare bars, corrosion products were found at the drilled holes in the epoxy, as shown in Figure 3.22. For mortar-wrapped specimens, the mortar cover was removed; corrosion products were observed at the drilled holes for the bars with uncoated steel as the cathode, as shown in Figure 3.23, while no corrosion products were observed for the bars with epoxy-coated steel as the cathode.

Figure 3.22 - Bare epoxy-coated anode bar (M-ECR-r-5) in 1.6 m ion NaCl solution at 15 weeks, showing corrosion products at the drilled holes (the test solutions are replaced every five weeks).

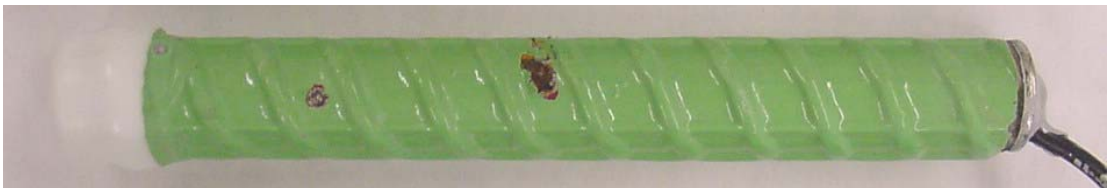

Figure 3.23 – Epoxy-coated anode bar (M-ECR/N3m-2) after removal of mortar cover at 15 weeks, showing corrosion products at the drilled holes (the test solutions are not replaced).

3.2.2 Bench-scale tests

In both the Southern Exposure and cracked beam tests, epoxy-coated reinforcing steel was in the top mat and conventional steel was used in the bottom

mat. Follow-on tests at the University of Kansas are underway with epoxy-coated steel in both mats. Results for those specimens will appear in a later report.

Southern Exposure – The average corrosion rates and total corrosion losses of the epoxy-coated steel are compared with those of conventional steel in Figures 3.24 and 3.25, respectively. Figure 3.24b expands the vertical axis in Figure 3.24a and Figure 3.25b expands the vertical axis in Figure 3.25a. The corrosion rates and corrosion losses at 96 weeks are tabulated in Tables 3.7 and 3.8, respectively. The results show that the corrosion rate of epoxy-coated steel in Southern Exposure specimens increased with time. At 96 weeks, the average corrosion rate and corrosion loss based on the exposed area equaled 1269 μm/yr and 684 μm, respectively, while the corrosion rate and corrosion loss based on the total area, were 2.64 μm/yr and 1.42 μm, respectively, equal to 1/480 of the values based on the exposed area and 36% of the corrosion rate and 12% of the total corrosion loss of conventional steel. It is expected that the corrosion rate of the epoxy-coated steel would have been much lower if epoxy-coated steel had been used in the bottom mat, as shown in the rapid macrocell test.

The results of the Student's t-test are shown in Tables C.3 and C.4. There is no significant difference in the average corrosion rates based on the total area at 96 weeks between conventional steel and epoxy-coated steel [as discussed in Section 3.1.2, the reason is that some conventional specimens exhibited a corrosion rate of zero at 96 weeks due to the corrosion of the bottom mat of steel. If based on the rates at 70 weeks, the difference is significant at $\alpha = 0.02$ (Balma et al. 2005)], while the difference in the corrosion losses is significant at $\alpha = 0.02$ at 70 weeks and at $\alpha = 0.05$ at 96 weeks.

The average corrosion potentials of the top and bottom mats of steel are shown in Figures 3.26a and 3.26b, respectively. The average potentials of the top mat for both conventional and epoxy-coated steels had initial values of about –0.200 V and remained more positive than –0.350 V for the first 10 weeks, indicating a passive condition. After 10 weeks, the top mat potential for the epoxy-coated steel fluctuated between about –0.300 and –0.400 V until 40 weeks and then dropped gradually to a value close to –0.550 V at the end of the test, compared to the top mat potential for conventional steel, which dropped rapidly, from –0.300 V at 10 weeks to –0.500 V at 20 weeks, and then, remained between –0.500 and –0.600 V. The average bottom mat potential of specimens with epoxy-coated steel also dropped, from about –0.200 V at 10 weeks to –0.300 V at 15 weeks, and then fluctuated around –0.300 V for the rest of the test period, compared to the bottom mat potentials for all-conventional steel specimens, which became more negative than –0.350 V at 15 weeks, and then remained around –0.400 V until 78 weeks and dropped to a value of –0.550 V at the end of the test.

The average mat-to-mat resistances of conventional steel and epoxy-coated steel as a function of time are shown in Figure 3.27. The mat-to-mat resistance for conventional steel N3 remained below 500 ohms for the duration of the test, while the value for the epoxy-coated steel fluctuated around 1500 ohms during most of the test period. The electrical insulation provided by the epoxy increased the mat-to-mat resistance. As mentioned in Section 1.3, the performance of epoxy-coated reinforcing steel could also be evaluated based on the mat-to-mat resistance. High values of resistance result in low total corrosion. A follow-on study at the University of Kansas shows that some Southern Exposure specimens with epoxy-coated steel in both mats

have the mat-to-mat resistance up to 10,000 ohms and exhibit very little corrosion (Gong et al. 2005).

Cracked beam – The average corrosion rate and corrosion losses for conventional and epoxy-coated steels are shown in Figures 3.28 and 3.29, respectively. Again, Figure 3.28b expands the vertical axis in Figure 3.28a and Figure 3.29b expands the vertical axis in Figure 3.29a. The average corrosion rate and corrosion losses at 96 weeks are summarized in Tables 3.7 and 3.8, respectively. Based on the total area, the epoxy-coated steel exhibited an average corrosion rate of 3.3 μm/yr at the first week, equal to about 20% of the value for conventional steel; then, the corrosion rate dropped slightly and remained a value close to 1.5 μm/yr between 10 and 80 weeks and then increased gradually to a rate of 3.8 μm/yr at 96 weeks. At the end of the test for epoxy-coated steel, the average corrosion loss based on the total area was 3.4 μm, equal to about 24% of that exhibited by conventional steel, 14 μm. The corrosion rate and total corrosion loss based on the exposed area are 480 times those based on the total area (Figures 3.28a and 3.29a).

Tables C.3 and C.4 show that the difference in the corrosion rates at 96 weeks between conventional and epoxy-coated steels is not statistically significant. [If based on the values at 70 weeks, the difference is significant at $\alpha = 0.20$ (Balma et al. 2005)]. The difference in the corrosion loss, however, is significant at $\alpha = 0.02$.

The average corrosion potentials of the top and bottom mats of steel are shown in Figures 3.30a and 3.30b, respectively. The epoxy-coated and conventional steels exhibited similar top mat corrosion potentials throughout the test period, with values ranging from –0.500 to –0.600 V, indicating a high tendency to corrode. The average corrosion potential of the bottom mat for epoxy-coated steel specimens primarily remained between –0.250 V and –0.400 V throughout the test. The

conventional steel specimens exhibited similar bottom mat potential, until after 80 weeks, when it dropped to a value close to –0.600 V for the last few weeks of the test.

The average mat-to-mat resistances are shown in Figure 3.31. For conventional steel, except for a few high values during the first few weeks of the test, the average mat-to-mat resistance increased from an initial value of around 300 ohms, to a value close to 1500 ohms at 81 weeks, and then exhibited a rapid drop, with values below 250 ohms from 84 to 96 weeks. The drop in the mat-to-mat is likely attributed to specimen cracking caused by the high volume of the corrosion products. For the epoxy-coated steel, the mat-to-mat resistance started at about 1000 ohms during the first few weeks, increased to values as high as 5400 ohms by 84 weeks, and then dropped rapidly to a value of 3000 ohms at 96 weeks. The reason of the drop for the epoxy-coated steel is unknown. At 96 weeks, the average local corrosion loss of the epoxy-coated steel, 1634 μm, is less than the value needed to crack a concrete cover of 25 mm (1.0 in.), which is 2852 μm based on the empirical equation [Eq. (1.26)] presented by Torres-Acosta and Sagues (2004).

Table 3.7 - Average corrosion rates at 96 weeks for specimens with epoxy-caoted steel in bench-scale test

Specimen designation*	Steel type	Specimen corrosion rates (μm/yr)						Average (μm/yr)	Standard deviation
		1	2	3	4	5	6		
Southern Exposure test									
SE-N3	N3	0.00	25.09	0.00	0.00	11.46	7.96	7.42	9.94
SE-ECR/N3^{T}	ECR/N3	3.20	5.72	2.18	1.75	0.94	2.05	2.64	1.68
SE-ECR/N3^{E}	ECR/N3	1537	2749	1047	840	454	985	1268	805
Cracked beam test									
CB-N3	N3	0.00	0.00	0.00	0.00	8.56	0.00	1.43	3.50
CB-ECR/N3^{T}	ECR/N3	10.76	2.97	3.37	2.99	1.84	0.56	3.75	3.58
CB-ECR/N3^{E}	ECR/N3	5168	1427	1618	1438	886	271	1801	1722

*** A-B**

A: test method, SE = Southern Exposure test and CB = cracked beam test.

B: steel type and test condition, N3 = conventional steel; ECR = epoxy-coated steel; ECR/N3 = epoxy-coated steel as the anode, conventional steel as the cathode.

^{T}: Based on total area of bar exposed to solution.

^{E}: Based on exposed area of four 3.2 mm (0.125 in.) diameter holes in the coating.

Table 3.8 - Average total corrosion losses for specimens with epoxy-coated steel in bench-scale test

Specimen designation*	Steel type	Specimen total corrosion losses (μm)						Average (μm)	Standard deviation
		1	2	3	4	5	6		
Southern Exposure test									
SE-N3	N3	11.59	27.81	3.23	8.39	14.24	6.63	11.98	8.65
SE-ECR/N3^{T}	ECR/N3	1.97	3.15	1.16	1.23	0.35	0.69	1.42	1.01
SE-ECR/N3^{E}	ECR/N3	945	1512	557	592	170	331	684	483
Cracked beam test									
CB-N3	N3	27.54	16.45	12.47	6.91	10.28	9.87	13.92	7.38
CB-ECR/N3^{T}	ECR/N3	8.10	2.34	3.74	4.56	0.71	0.96	3.40	2.75
CB-ECR/N3^{E}	ECR/N3	3888	1126	1797	2191	341	462	1634	1321

*** A-B**

A: test method, SE = Southern Exposure test and CB = cracked beam test.

B: steel type and test condition, N3 = conventional steel; ECR = epoxy-coated steel; ECR/N3 = epoxy-coated steel as the anode, conventional steel as the cathode.

^{T}: Based on total area of bar exposed to solution.

^{E}: Based on exposed area of four 3.2 mm (0.125 in.) diameter holes in the coating.

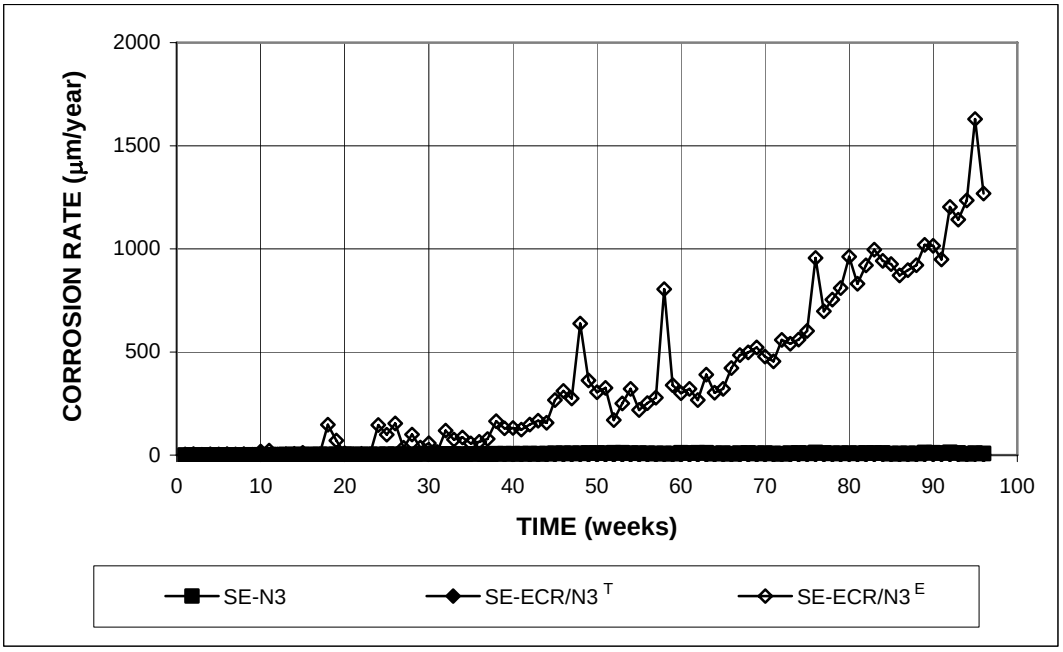

(a)

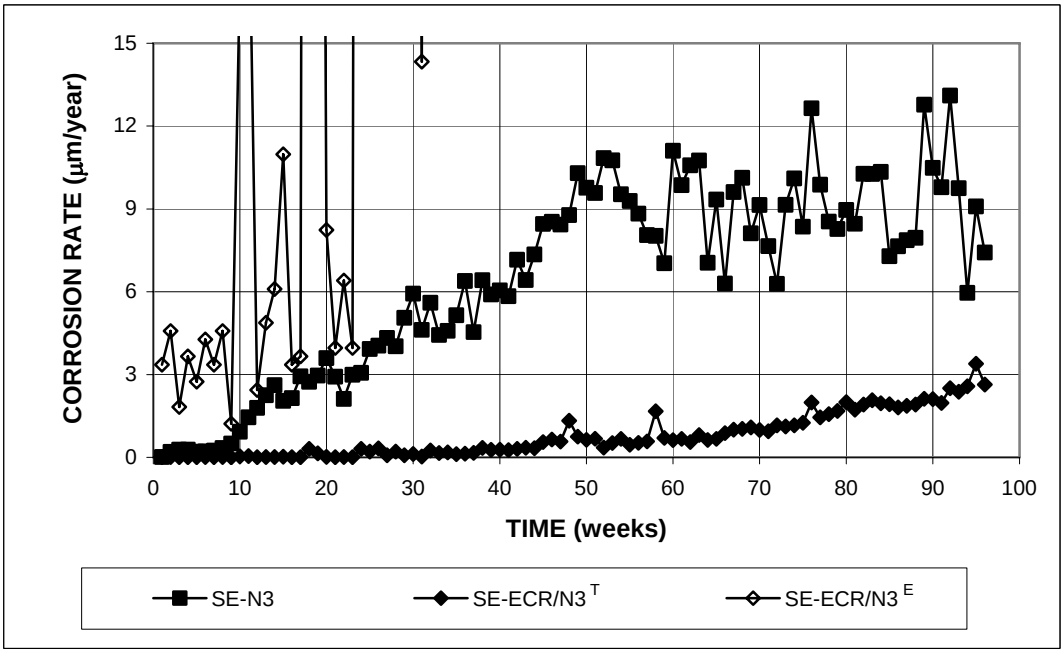

(b)

T: Based on total area of bar exposed to solution.
E: Based on exposed area of four 3.2 mm (0.125 in.) diameter holes in the coating.

Figure 3.24 - Southern Exposure test. Average corrosion rates of epoxy-coated steel, specimens w/c = 0.45, ponded with 15% NaCl solution.

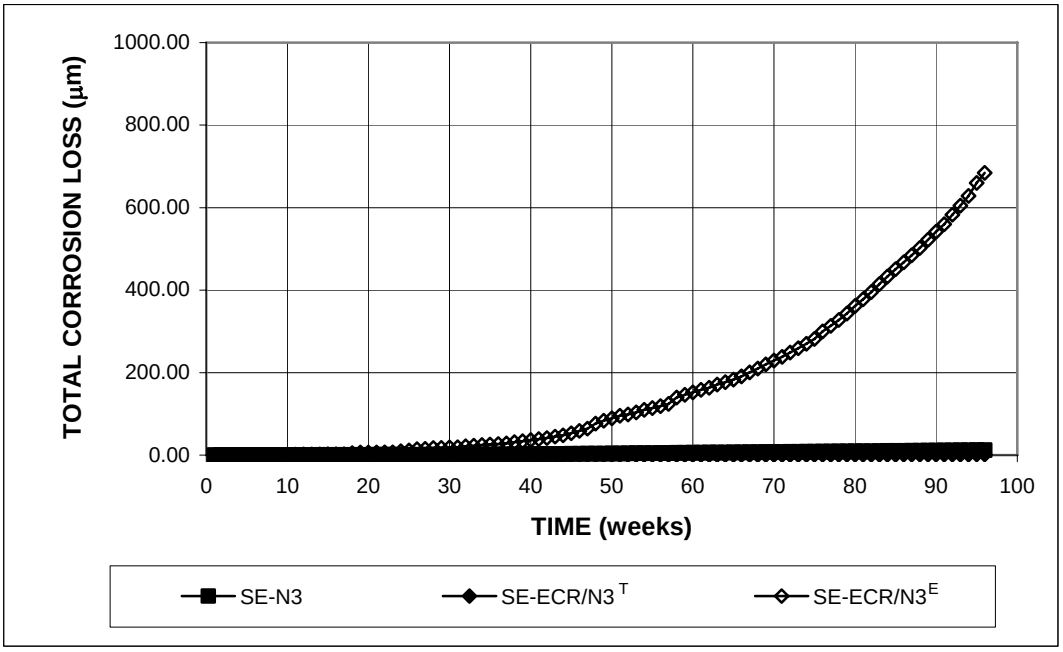

(a)

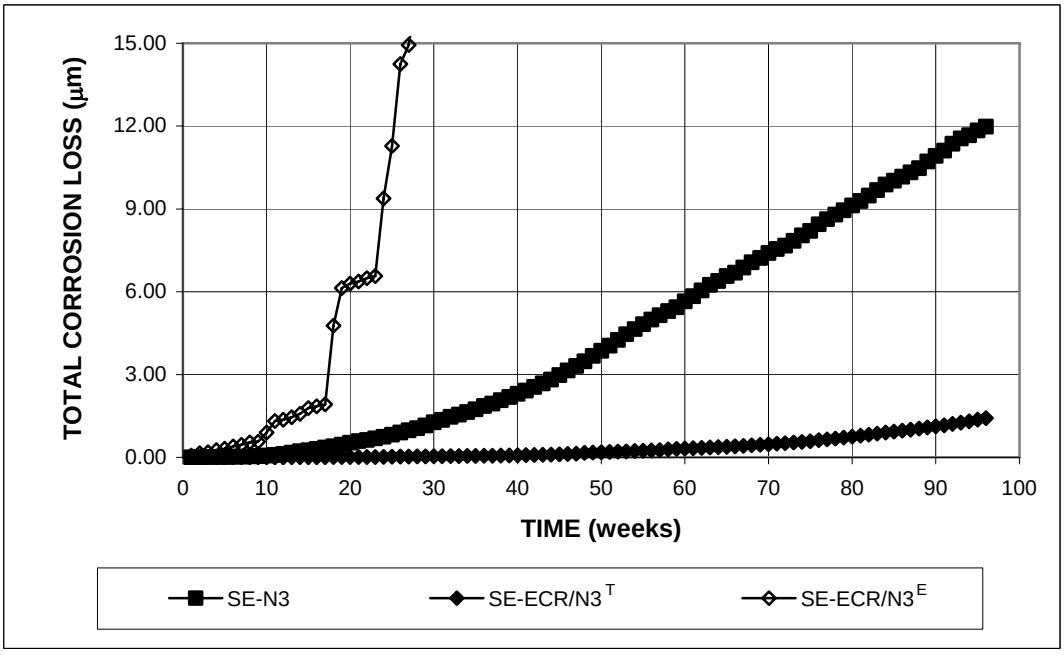

(b)

T: Based on total area of bar exposed to solution.
E: Based on exposed area of four 3.2 mm (0.125 in.) diameter holes in the coating.

Figure 3.25 - Southern Exposure test. Average total corrosion losses of epoxy-coated steel, specimens w/c = 0.45, ponded with 15% NaCl solution.

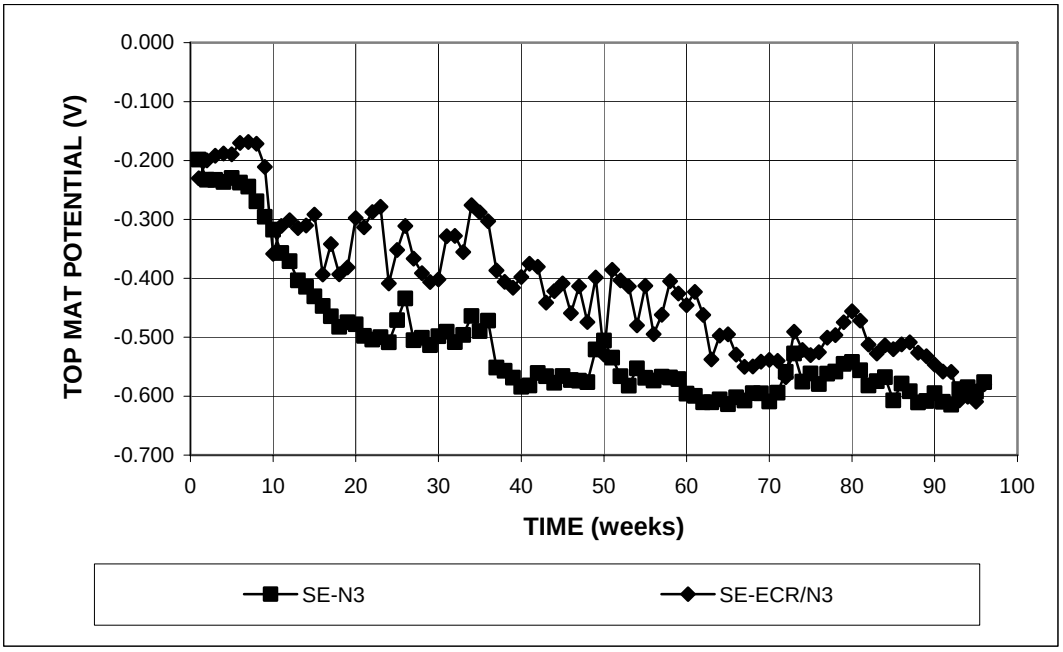

Figure 3.26a - Southern Exposure test. Average top mat corrosion potentials with respect to copper-copper sulfate electrode for epoxy-coated steels, specimens w/c = 0.45, ponded with 15% NaCl solution.

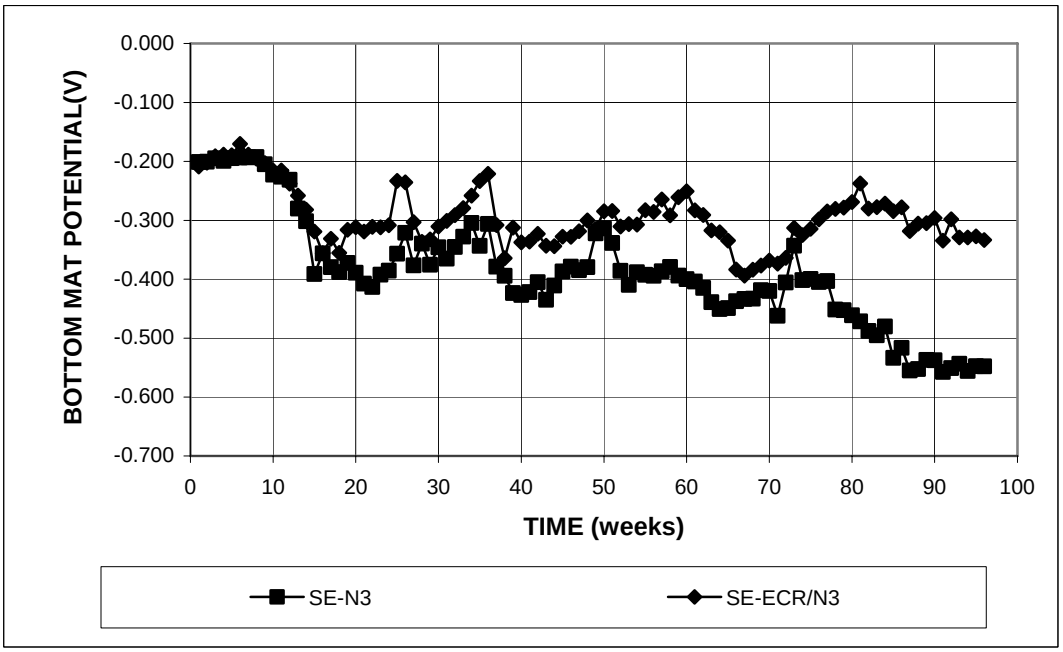

Figure 3.26b - Southern Exposure test. Average bottom mat corrosion potentials with respect to copper-copper sulfate electrode for epoxy-coated steels, specimens w/c = 0.45, ponded with 15% NaCl solution.

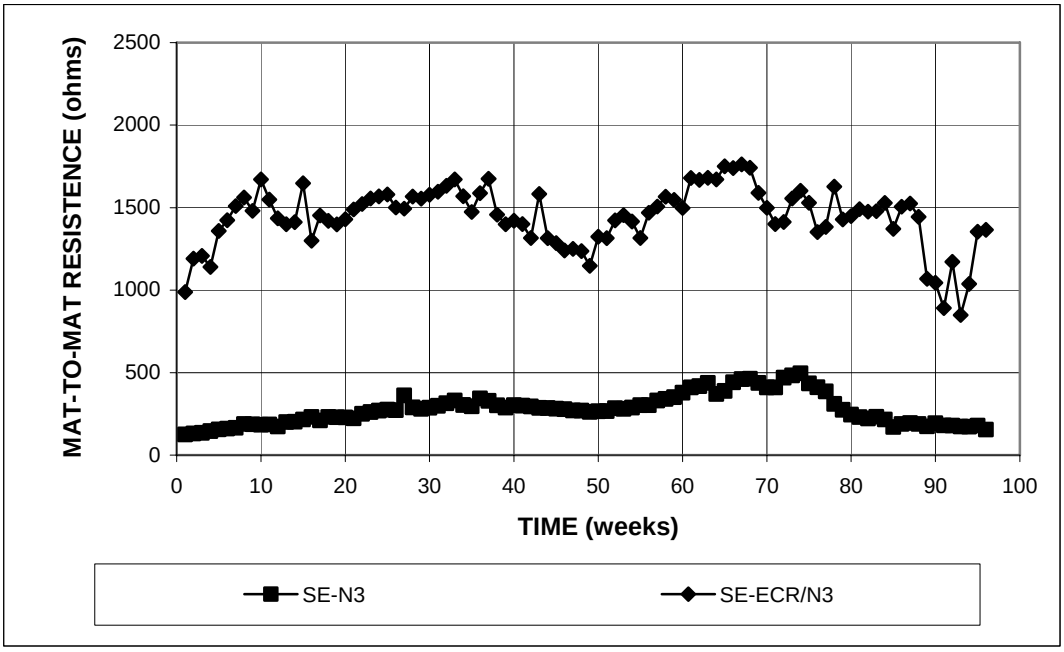

Figure 3.27 - Southern Exposure test. Average mat-to-mat resistances for specimens with epoxy-coated steel, specimens w/c = 0.45, ponded with 15% NaCl solution.

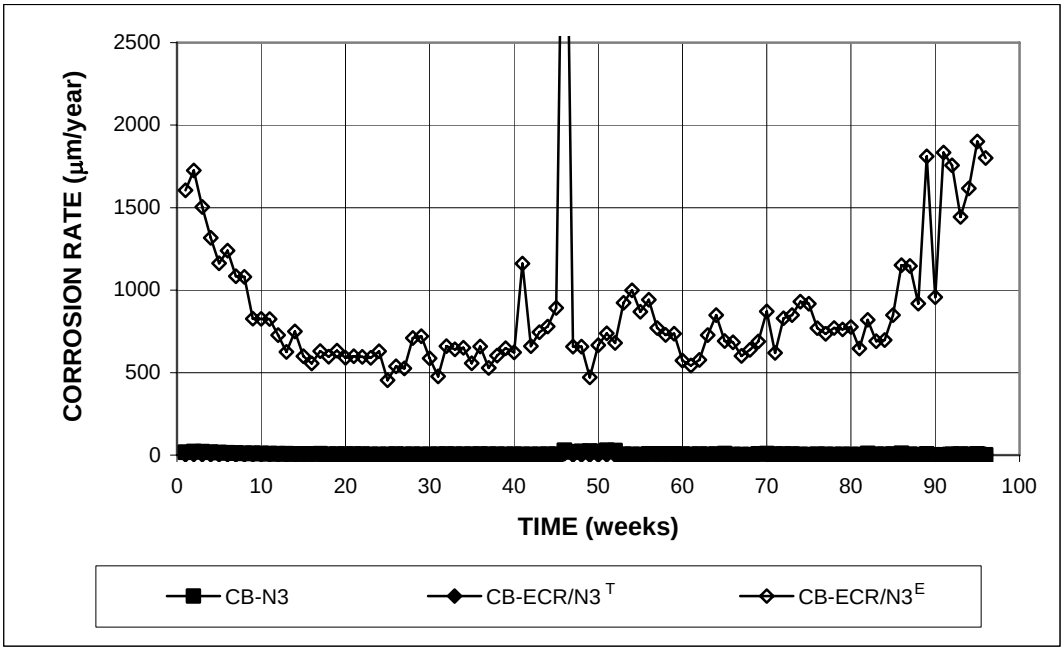

(a)

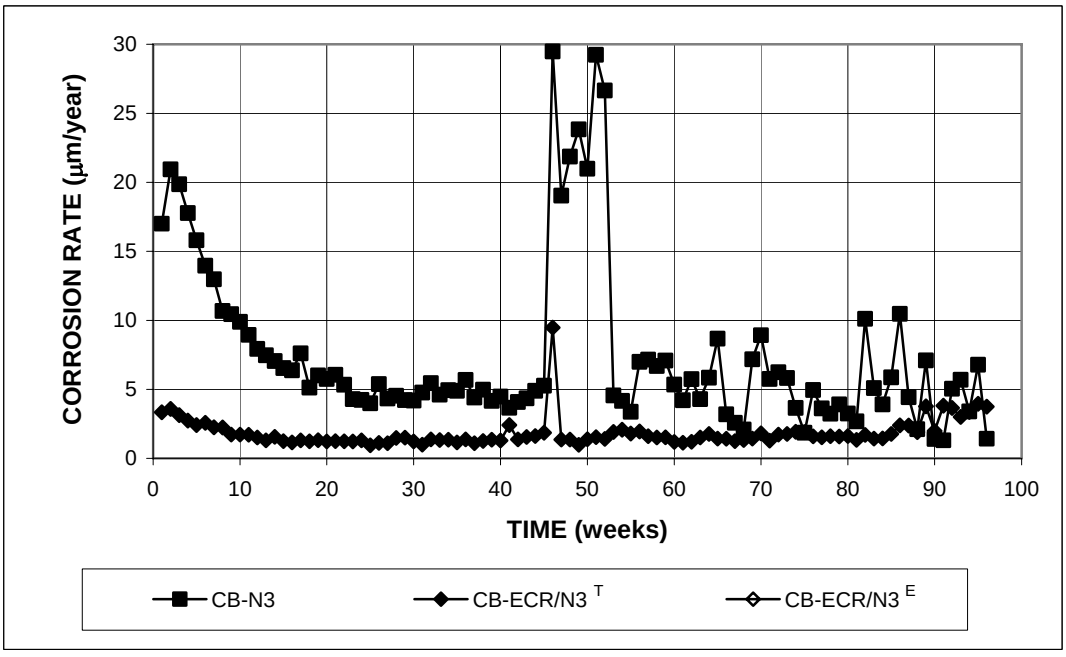

(b)

T: Based on total area of bar exposed to solution.
E: Based on exposed area of four 3.2 mm (0.125 in.) diameter holes in the coating

Figure 3.28 - Cracked beam test. Average corrosion rates of epoxy-coated steel, specimens w/c = 0.45, ponded with 15% NaCl solution.

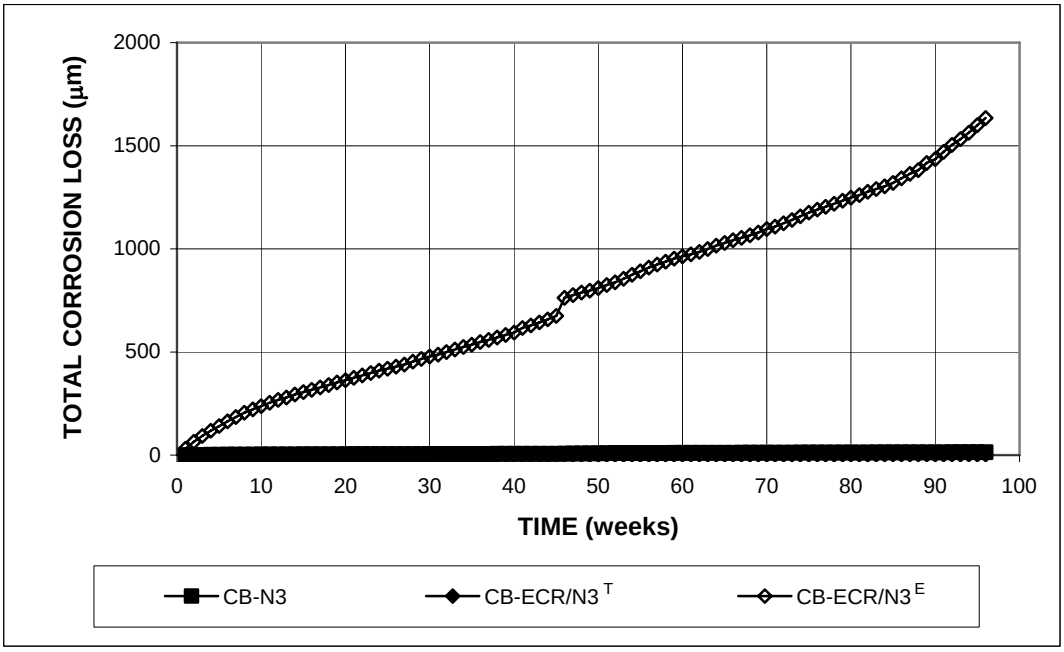

(a)

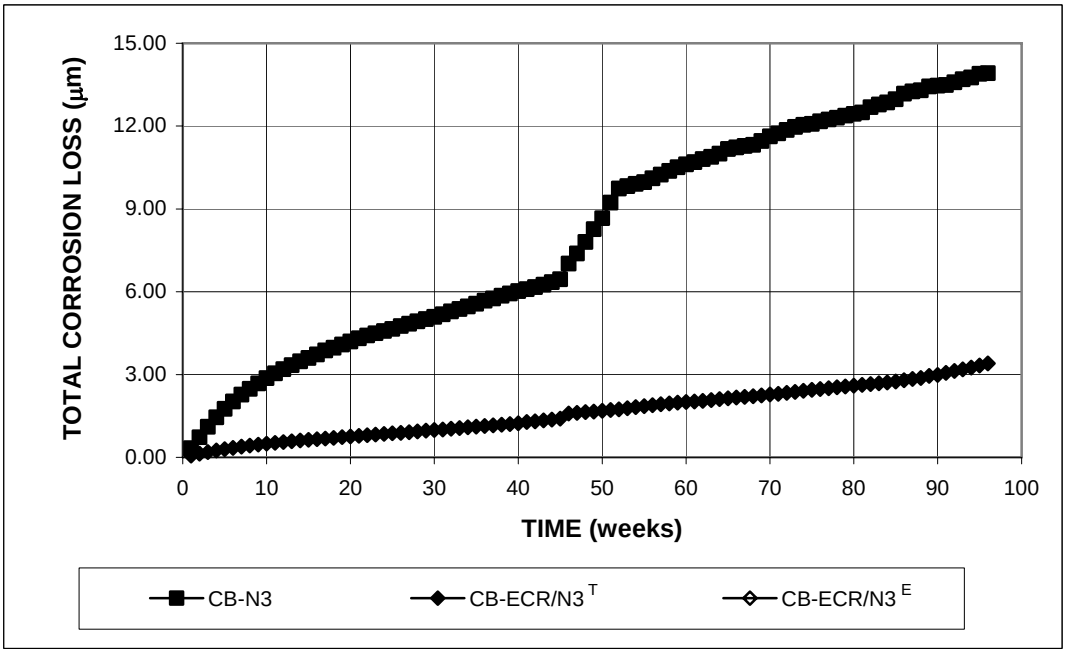

(b)

T: Based on total area of bar exposed to solution.
E: Based on exposed area of four 3.2 mm (0.125 in.) diameter holes in the coating.

Figure 3.29 - Cracked beam test. Average total corrosion losses of epoxy-coated steel, specimens w/c = 0.45, ponded with 15% NaCl solution.

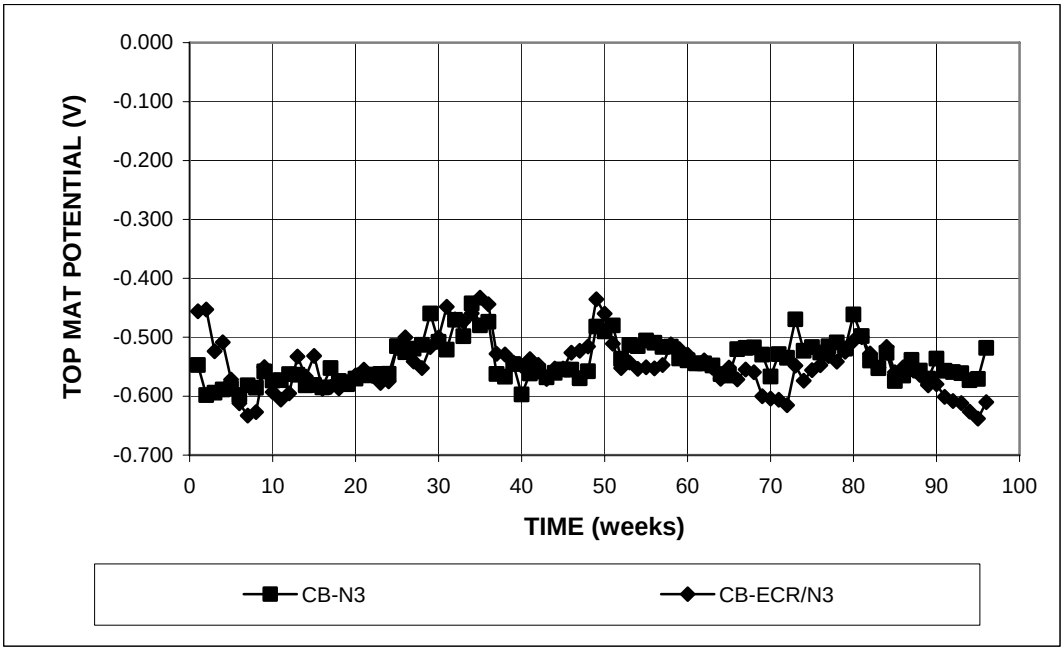

Figure 3.30a - Cracked beam test. Average top mat corrosion potentials with respect to copper-copper sulfate electrode for epoxy-coated steel, specimens w/c = 0.45, ponded with 15% NaCl solution.

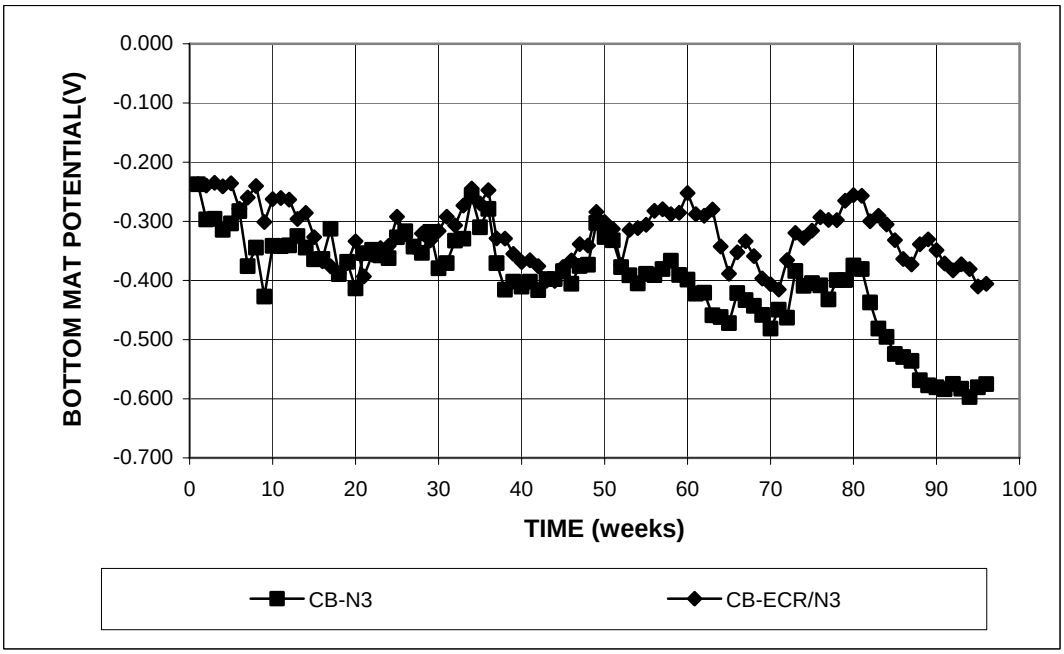

Figure 3.30b - Cracked beam test. Average bottom mat corrosion potentials with respect to copper-copper sulfate electrode for epoxy-coated steel, specimens w/c = 0.45, ponded with 15% NaCl solution.

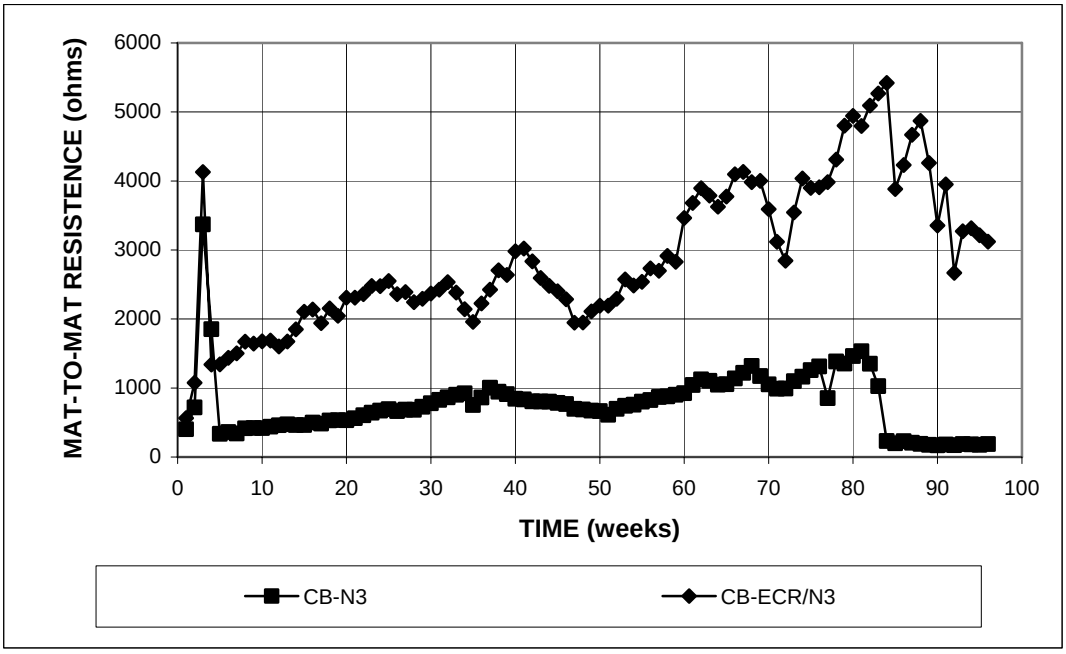

Figure 3.31 - Crack beam test. Average mat-to-mat resistances for specimens with epoxy-coated steel, specimens w/c = 0.45, ponded with 15% NaCl solution.

Visual Inspection – After the end of the tests, the bars were removed from the concrete. For both the Southern Exposure and cracked beam specimens, the epoxy-coated bars in the top mat exhibited corrosion products, as shown in Figures 3.32 and 3.33.

Figure 3.32 – Epoxy-coated bar from the top mat of an SE specimen (SE-ECR/N3-2) at 96 weeks, showing corrosion products at the drilled holes in the coating.

Figure 3.33 – Epoxy-coated bar from the top mat of a CB specimen (CB-ECR/N3-2) at 96 weeks, showing corrosion products at the drilled holes in the coating.

3.3 MMFX MICROCOMPOSITE STEEL

MMFX Microcomposite steel was tested in the "as delivered" condition. The results for the macrocell tests are presented in Tables 3.9 and 3.10 and Figures 3.34 through 3.42. The results for the bench-scale tests are presented in Tables 3.11 and 3.12 and Figures 3.43 through 3.48. For comparison, these figures and tables also include relative results for N2 and N3 conventional steels. The results of the Student's t-test are shown in Tables C.5 and C.6. In all evaluations, microcomposite MMFX steel exhibited higher corrosion resistance than conventional steel, with corrosion rates at the end of the test between 8% and 80% and total corrosion losses between 16% and 66% of the value for conventional reinforcing steel.

3.3.1 Rapid macrocell tests

Bare bar specimens in 1.6 m NaCl solution – Bare MMFX reinforcing bars were tested in simulated concrete pore solution containing a 1.6 m ion concentration of NaCl, with and without replacing the solutions every five weeks. The results are compared with those for the N2 and N3 steels, which were tested with and without replacing the solutions, respectively. The effects of replacing the solutions are discussed in Section 3.5.

The average corrosion rates for MMFX and the conventional steels are shown in Figure 3.34, and the values at 15 weeks are tabulated in Table 3.9. The results of the Student's t-test are shown in Table C.5. MMFX steel exhibited corrosion rates between 4 and 20 μm/yr throughout the test period. By the end of the first week, the corrosion rate for the MMFX steel was about 10 μm/yr. At 15 weeks, without replacing the test solutions every 5 weeks, MMFX steel (MMFX) was corroding at a rate of 19.8 μm/yr, corresponding to 55% of the corrosion rate of the N3 conventional

steel (N3), 36 μm/yr (the difference is significant at $\alpha = 0.20$); when replacing the test solutions every 5 weeks, MMFX steel (MMFX-r) was corroding at a rate of 16.8 μm/yr, corresponding to 80% of the corrosion rate of the N2 conventional steel (N2-r), 21 μm/yr (the difference is not statistically significant).

The average total corrosion losses for MMFX and the conventional steels are shown in Figure 3.35, and the values at 15 weeks are summarized in Table 3.10. The results of the Student's t-test are presented in Table C.6. At 15 weeks, without replacing the test solutions every 5 weeks, the total corrosion loss of MMFX steel was 2.52 μm, equal to 28% of that of N3 conventional steel; when the test solutions were replaced every 5 weeks, the total corrosion loss of the MMFX steel was 2.81 μm, equal to 43% of that of N2 conventional steel. Both of the differences between MMFX steel and the conventional steels are significant at $\alpha = 0.02$.

As shown in Figure 3.36a, all anode MMFX and conventional reinforcing bars were undergoing active corrosion throughout the test period, with the conventional steel showing more negative corrosion potentials than MMFX steel. Initially, MMFX steel had an anode corrosion potential around –0.300 V. By the end of the first week, the corrosion potential dropped to about –0.400 V. At 15 weeks, without and with replacing the test solutions, the average anode corrosion potentials were –0.490 and –0.445 V for MMFX steel and –0.556 and –0.490 V for conventional steel, respectively. Figure 3.36b shows that the average corrosion potentials for all the cathode bars remained around –0.200 V, indicating a passive condition.

Bare bar specimens in 6.04 m NaCl solution – Bare MMFX reinforcing bars were tested in simulated concrete pore solution containing 6.04 m ion NaCl, replacing the solution every five weeks.

The average corrosion rate and total corrosion loss for MMFX steel and conventional N2 steel in the high chloride concentration are presented in Figures 3.37 and 3.38, respectively. Tables 3.9 and 3.10 summarize the corrosion rates and total corrosion losses at 15 weeks, respectively. The results of the Student's t-test are shown in Tables C.5 and C.6. Initially, MMFX steel (MMFXh-r) exhibited a corrosion rate of 15.3 μm/yr, about half of the rate of the conventional steel (N2h-r). The corrosion rate for the MMFX steel fluctuated within a narrow range throughout the test period. At 15 weeks, MMFX steel was corroding at 20 μm/yr, with a total corrosion loss of 5.8 μm, while the conventional steel had a corrosion rate of 30 μm/yr and a total corrosion loss of 8.9 μm. The difference in the corrosion rates is significant at $\alpha = 0.05$ and the difference in the corrosion losses is significant at $\alpha = 0.02$. Earlier studies (Darwin et al. 2002, Gong et al. 2002, Balma et al. 2005) showed that sandblasted MMFX and conventional steel corroded at approximately the same rate in the high chloride concentration test. In this study, both the average corrosion rate and total corrosion loss exhibited by MMFX steel are two thirds of the values for conventional steel at the end of the test.

The average corrosion potentials of the anode and cathode are shown in Figures 3.39a and 3.39b, respectively. The values for MMFX steel and conventional steel were similar, with MMFX steel showing a slightly more positive corrosion potential than the conventional steel at both the anode and the cathode. During the test, the MMFX steel exhibited corrosion potentials between –0.400 and –0.500 V at the anode, indicating a high tendency to corrode, while the cathode corrosion potentials for MMFX remained around –0.200 V, indicating a passive condition. For both MMFX and conventional steels, the average corrosion potentials of the anode in the high NaCl concentration solution were about 0.050 V more negative than the

values in the 1.6 m ion NaCl solution, while the cathode corrosion potentials for the high NaCl concentration solution tests were similar to the values in the low NaCl concentration solution.

Mortar-wrapped specimens – Mortar-wrapped MMFX reinforcing bars were tested in simulated concrete pore solution containing 1.6 m ion NaCl, replacing the solution (compared with N2 steel) and without replacing the solution every five weeks (compared with N3 steel). In addition, the effect of the combining MMFX and conventional steels was evaluated by using (1) MMFX steel as the anode and N3 steel as the cathode (MMFX/N3m) and (2) N3 steel as the anode and MMFX steel as the cathode (N3/MMFXm). In these tests, the test solutions were not replaced every five weeks.

The average corrosion rates are shown in Figure 3.40, and the values at 15 weeks are summarized in Table 3.9. The results of the Student's t-test are presented in Table C.5. The two conventional steels (N2m-r and N3m) had the highest corrosion rates, with values of 5 to 7 μm/yr by the end of the first week and 17 to 18 μm/yr at 15 weeks. MMFX steel exhibited slower corrosion initiation and lower corrosion rates than conventional steel. Without replacing the test solutions, the corrosion rate for MMFX steel (MMFXm) remained negligible (values < 0.25 μm/yr) for the first 2 weeks and then increased slowly with time, peaking at 10.6 μm/yr at 15 weeks, equal to 60% of the corrosion rate of the conventional steel (N3m). When replacing the test solutions, the MMFX steel (MMFXm-r) began to exhibit significant corrosion at 5 weeks, reached a maximum corrosion rate of 4.4 μm/yr at 9 weeks, and completed the 15-week test with a corrosion rate of 1.4 μm/yr, equal to 8% of the value of the conventional steel (N2m-r).

Table C.5 shows that the difference in the average corrosion rates at 15 weeks between the N3m and MMFXm specimens is statistically significant at $\alpha = 0.05$ and the difference between the N2m-r and MMFXm-r specimens is significant at $\alpha = 0.02$. A comparison for MMFXm and MMFXm-r specimens is presented in Section 3.5.

For the macrocells containing mixed MMFX and conventional steel, at 15 weeks, specimens with conventional steel at the anode and MMFX steel at the cathode (N3/MMFXm) had a corrosion rate of 12.1 μm/yr, lower than that exhibited by conventional steel specimens (N3m) (the difference is significant at $\alpha = 0.20$); specimens with MMFX steel at the anode and conventional steel at the cathode (MMFX/N3m) had a corrosion rate of 13.0 μm/yr, higher than that exhibited by MMFX steel specimens (MMFXm) (the difference is not statistically significant), and even the N3/MMFXm specimen. Overall, the specimens with MMFX steel at the cathode showed a lower corrosion rate.

The average total corrosion losses are shown in Figure 3.41, and the values at 15 weeks are summarized in Table 3.10. The results of the Student's t-test are presented in Table C.6. At 15 weeks, the average corrosion loss for MMFX steel was 1.4 μm without replacing the test solutions and 0.55 μm when replacing the test solutions, equal to 26% of the value for conventional N3 steel (5.26 μm) and 16% of the value for conventional N2 steel (3.47 μm), respectively. The N3/MMFXm specimens had a corrosion loss of 2.63 μm, while the MMFX/N3m specimens had a corrosion loss of 1.82 μm. The differences in the corrosion losses between the MMFXm and N3m specimens, and between the MMFXm-r and N2m-r specimens are significant at $\alpha = 0.02$. The difference between the N3m and N3/MMFXm specimens

is significant at $\alpha = 0.02$, while the difference between the MMFXm and MMFX/N3m is significant at $\alpha = 0.20$.

The average corrosion potentials of the anode are shown in Figure 3.42a. The anode corrosion potentials for conventional steel (N3) and conventional steel with MMFX steel as the cathode (N3/MMFXm) dropped to values below –0.275 V (indicating active corrosion) at the third day and 3 weeks, respectively, ending at –0.600 V at 15 weeks, while the anode corrosion potentials for MMFX steel (without replacing the test solutions, MMFXm) and MMFX steel with conventional steel as cathode (MMFX/N3m) dropped below –0.275 V at 4 and 7 weeks, respectively, ending with values around –0.500 V. For MMFX steel with the test solutions replaced (MMFXm-r), the average anode corrosion potentials dropped to values below –0.275 V at 11 weeks and then rose slightly, ending at –0.256 V. Figure A.76a in Appendix A shows that the anode corrosion potentials for three of six MMFX specimens remained more positive than –0.275 V throughout the test period, while the values for the other three specimens became more negative than –0.275 V after 4 weeks, 4 weeks, and 10 weeks, respectively, ranging from –0.300 V to –0.500 V.

Figure 3.42b shows that the corrosion potentials of the cathodes for the all-MMFX macrocells (MMFXm and MMFXm-r) remained more positive than –0.200 V for the duration of the test, indicating a passive condition. For the remaining macrocells, the cathode potentials were primarily between –0.200 to –0.300 V, indicating a slight tendency to corrode.

Table 3.9 - Average corrosion rates at 15 weeks for specimens with conventional and MMFX steels in macrocell test

Specimen designation*	Steel type	Specimen corrosion rates (μm/yr)						Average (μm/yr)	Standard deviation
		1	2	3	4	5	6		
Bare bars in 1.6 m NaCl									
M-N3	N3	52.60	0.26	67.77	40.17	32.43	22.08	35.88	23.61
M-N2-r	N2	15.17	20.63	19.68	5.35	31.99	32.25	20.85	10.28
M-MMFX	MMFX	12.34	8.03	23.06	18.21	32.25	25.03	19.82	8.83
M-MMFX-r	MMFX	15.43	27.92	14.88	16.18	12.54	14.02	16.83	5.57
Bare bars in 6.04 m NaCl									
M-N2h-r	N2	42.11	29.51	32.28	24.83	22.66	26.56	29.66	6.98
M-MMFXh-r	MMFX	18.67	22.98	14.59	30.58	24.25	9.80	20.14	7.40
Mortar-wrapped specimens in 1.6 m NaCl									
M-N2m-r	N2	17.28	22.89	18.96	11.96	14.51		17.12	4.19
M-N3m	N3	11.21	9.16	26.07	19.31	21.15	19.31	17.70	6.36
M-MMFXm	MMFX	8.87	17.37	10.12	9.54	11.68	5.98	10.59	3.81
M-MMFXm-r	MMFX	0.09	0.06	5.40	0.12	0.72	1.88	1.38	2.09
M-N3/MMFXm	N3/MMFX	15.03	10.58	10.55				12.05	2.58
M-MMFX/N3m	MMFX/N3	15.20	11.44	12.28				12.98	1.97

*** A-B-C**

A: test method; M = macrocell test.

B: steel type and test condition; N2 and N3 = conventional steel; MMFX = mircrocomposite MMFX steel; MMFX/N3 = MMFX steel as the anode, N3 steel as the cathode; N3/MMFX = N3 steel as the anode, MMFX steel as the cathode; h = 6.04 m ion concentration; m = mortar-wrapped specimens.

C: r = the test solutions are replaced every five weeks.

Table 3.10 - Average total corrosion losses for specimens with conventional and MMFX steels in macrocell test

Specimen designation*	Steel type	Specimen total corrosion losses (μm)						Average (μm)	Standard deviation
		1	2	3	4	5	6		
Bare bars in 1.6 m NaCl									
M-N3	N3	12.33	4.15	13.49	11.17	7.08	5.50	8.95	3.88
M-N2-r	N2	6.26	8.15	6.89	4.13	7.17	6.94	6.59	1.35
M-MMFX	MMFX	3.12	2.15	3.19	1.19	1.78	3.68	2.52	0.96
M-MMFX-r	MMFX	2.16	3.73	1.53	3.58	2.01	3.86	2.81	1.02
Bare bars in 6.04 m NaCl									
M-N2h-r	N2	10.53	10.26	8.59	8.41	7.99	7.48	8.88	1.24
M-MMFXh-r	MMFX	6.24	5.05	6.30	6.50	5.65	5.23	5.83	0.61
Mortar-wrapped specimens in 1.6 m NaCl									
M-N2m-r	N2	3.09	4.72	2.41	3.35	3.75		3.47	0.86
M-N3m	N3	5.13	4.75	6.55	5.21	4.79	5.12	5.26	0.66
M-MMFXm	MMFX	2.18	0.56	1.88	0.99	1.68	0.93	1.37	0.63
M-MMFXm-r	MMFX	0.02	0.02	1.77	0.02	0.36	1.15	0.55	0.74
M-N3/MMFXm	N3/MMFX	3.33	2.21	2.35				2.63	0.61
M-MMFX/N3m	MMFX/N3	1.60	1.75	2.11				1.82	0.26

*** A-B-C**

A: test method; M = macrocell test.

B: steel type and test condition; N2 and N3 = conventional steel; MMFX = mircrocomposite MMFX steel; MMFX/N3 = MMFX steel as the anode, N3 steel as the cathode; N3/MMFX = N3 steel as the anode, MMFX steel as the cathode; h = 6.04 m ion concentration; m = mortar-wrapped specimens.

C: r = the test solutions are replaced every five weeks.

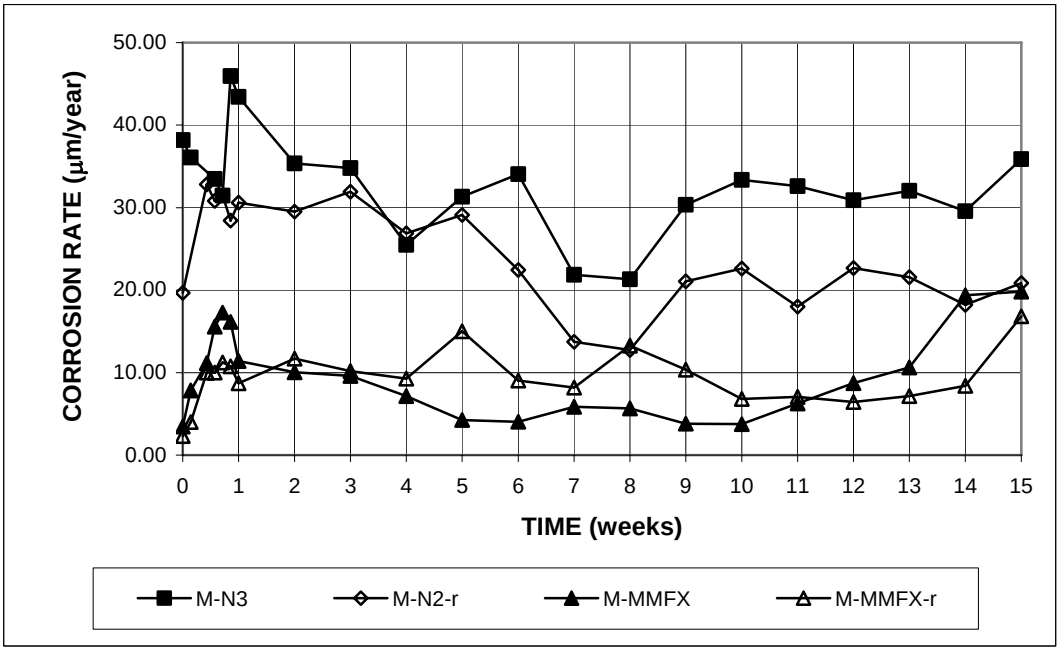

Figure 3.34 - Macrocell test. Average corrosion rates, bare conventional and MMFX steels in simulated concrete pore solution with 1.6 molal ion NaCl.

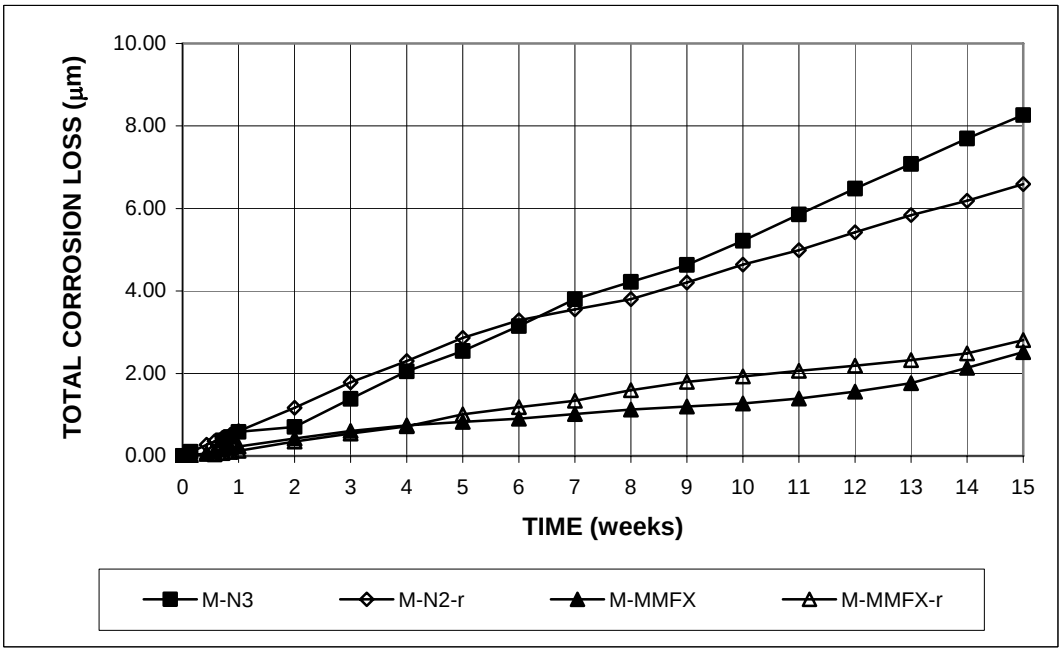

Figure 3.35 - Macrocell test. Average total corrosion losses, bare conventional and MMFX steels in simulated concrete pore solution with 1.6 molal ion NaCl.

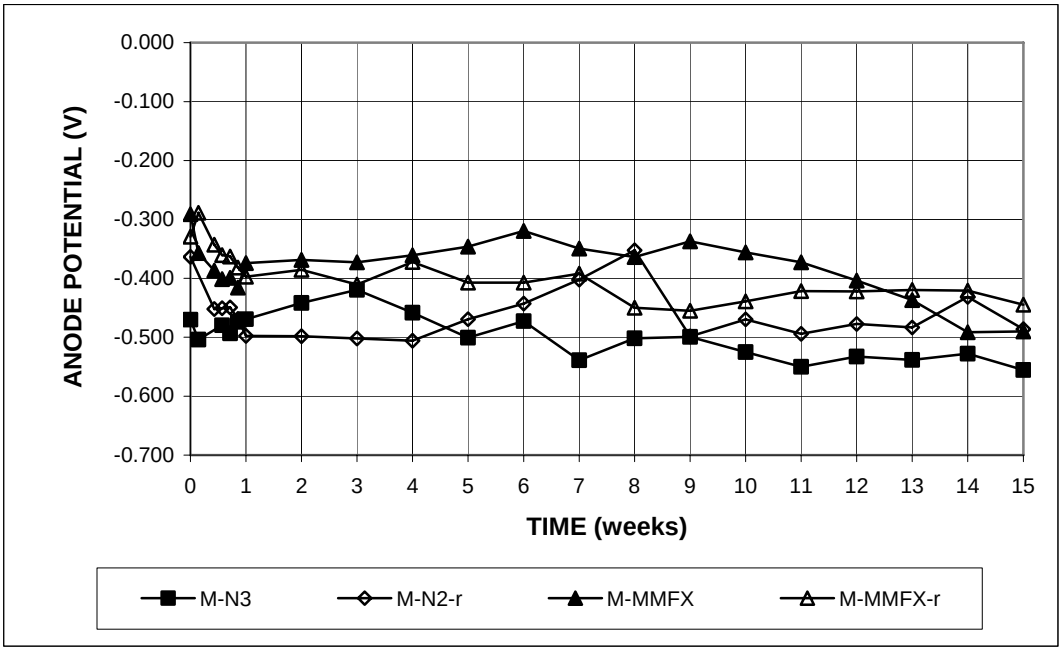

Figure 3.36a - Macrocell test. Average anode corrosion potentials with respect to saturated calomel electrode, bare conventional and MMFX steels in simulated concrete pore solution with 1.6 molal ion NaCl.

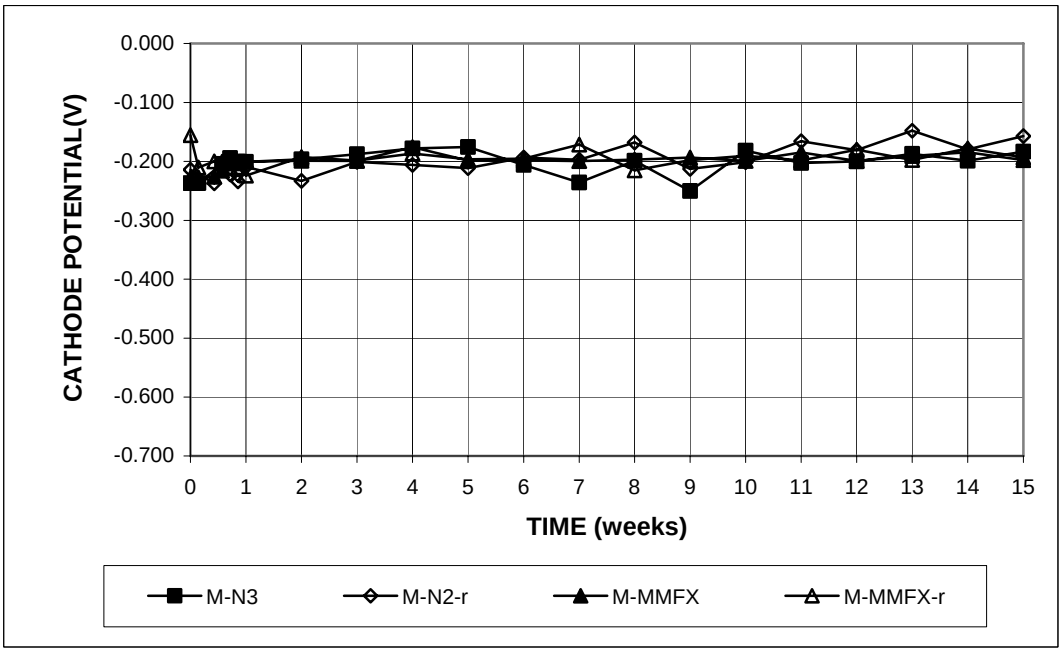

Figure 3.36b - Macrocell test. Average cathode corrosion potentials with respect to saturated calomel electrode, bare conventional and MMFX steels in simulated concrete pore solution with 1.6 molal ion NaCl.

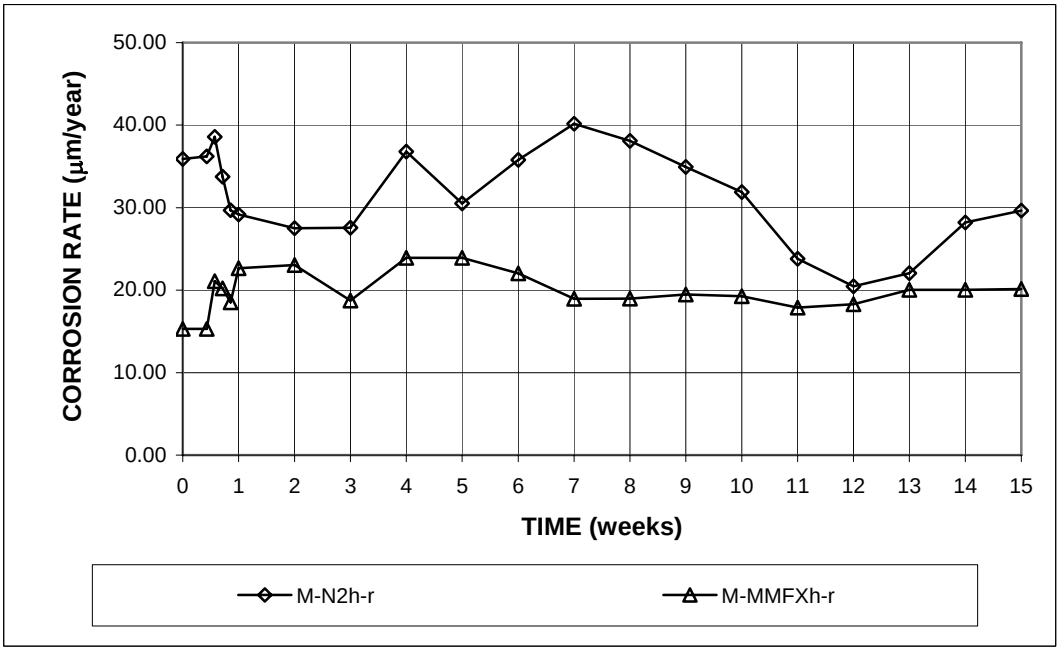

Figure 3.37 - Macrocell test. Average corrosion rates, bare conventional and MMFX steels in simulated concrete pore solution with 6.04 molal ion NaCl.

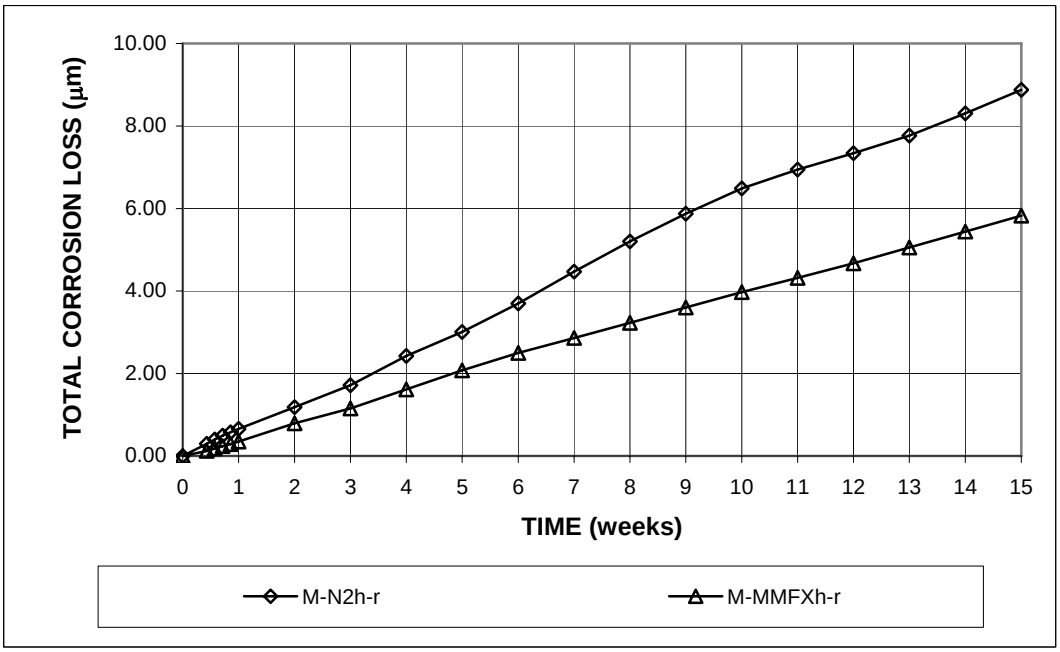

Figure 3.38 - Macrocell test. Average total corrosion losses, bare conventional and MMFX steels in simulated concrete pore solution with 6.04 molal ion NaCl.

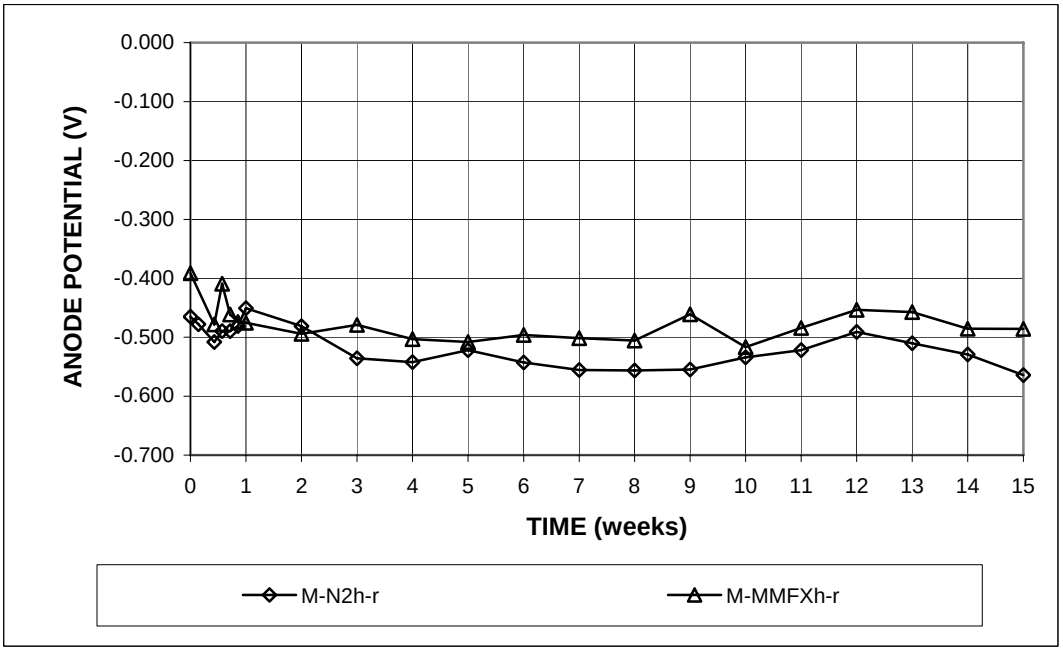

Figure 3.39a - Macrocell test. Average anode corrosion potentials with respect to saturated calomel electrode, bare conventional and MMFX steels in simulated concrete pore solution with 6.04 molal ion NaCl.

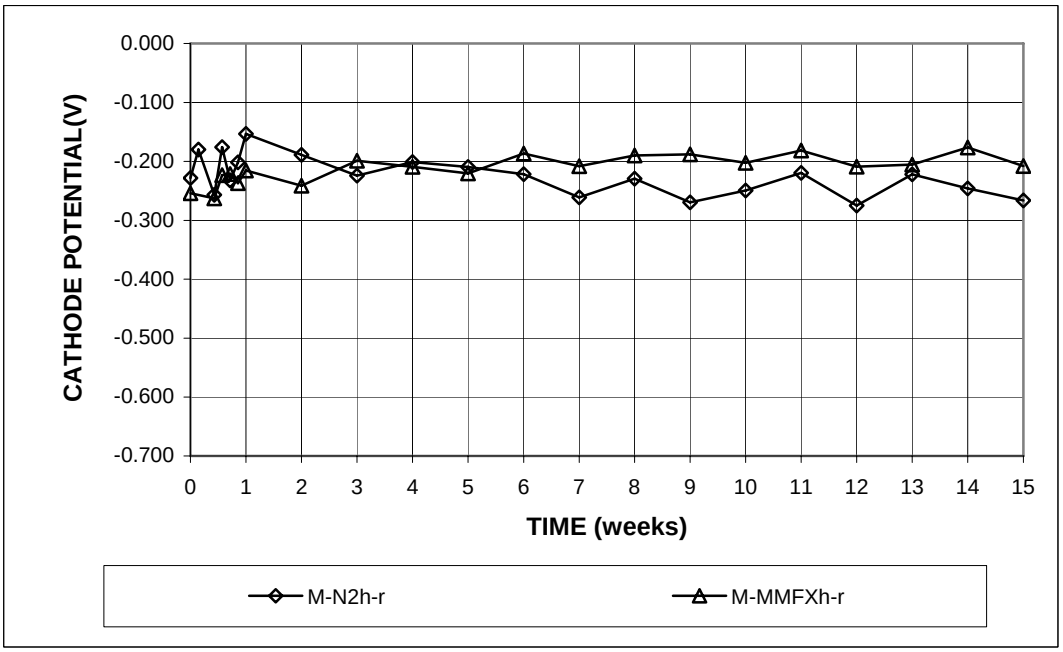

Figure 3.39b - Macrocell test. Average cathode corrosion potentials with respect to saturated calomel electrode, bare conventional and MMFX steels in simulated concrete pore solution with 6.04 molal ion NaCl.

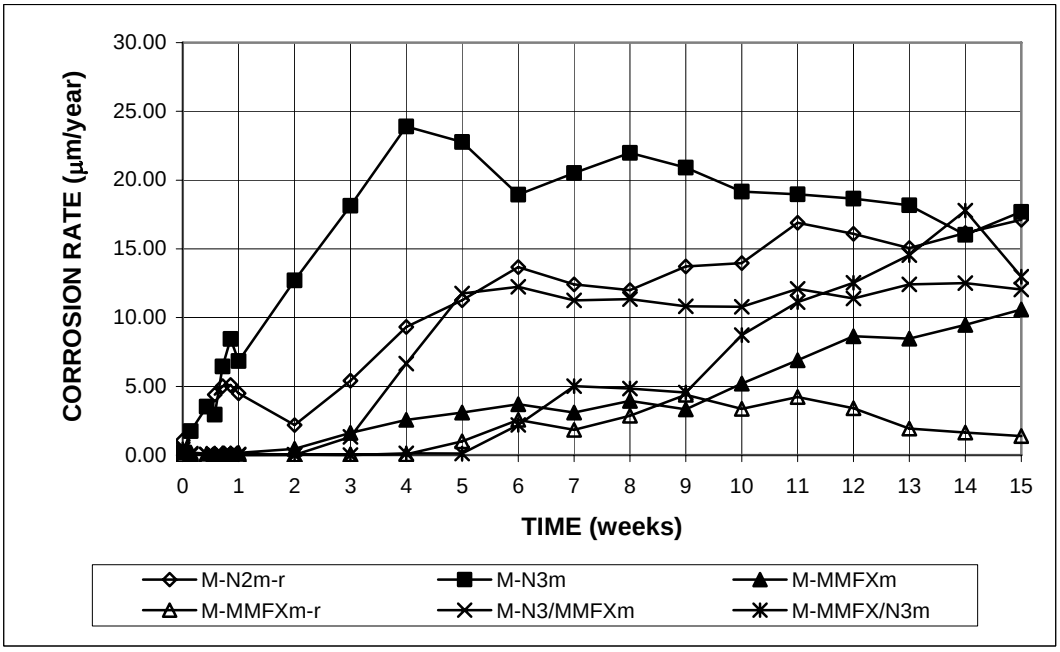

Figure 3.40 - Macrocell test. Average corrosion rates, mortar-wrapped conventional and MMFX steels in simulated concrete pore solution with 1.6 molal ion NaCl.

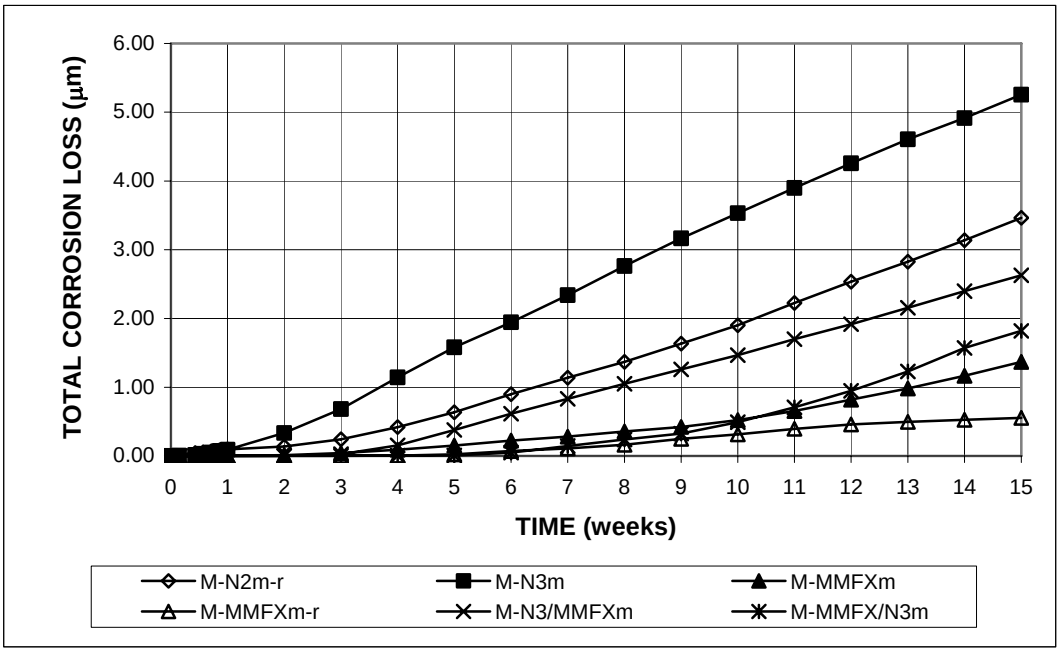

Figure 3.41 - Macrocell test. Average total corrosion losses, mortar-wrapped conventional and MMFX steels in simulated concrete pore solution with 1.6 molal ion NaCl.

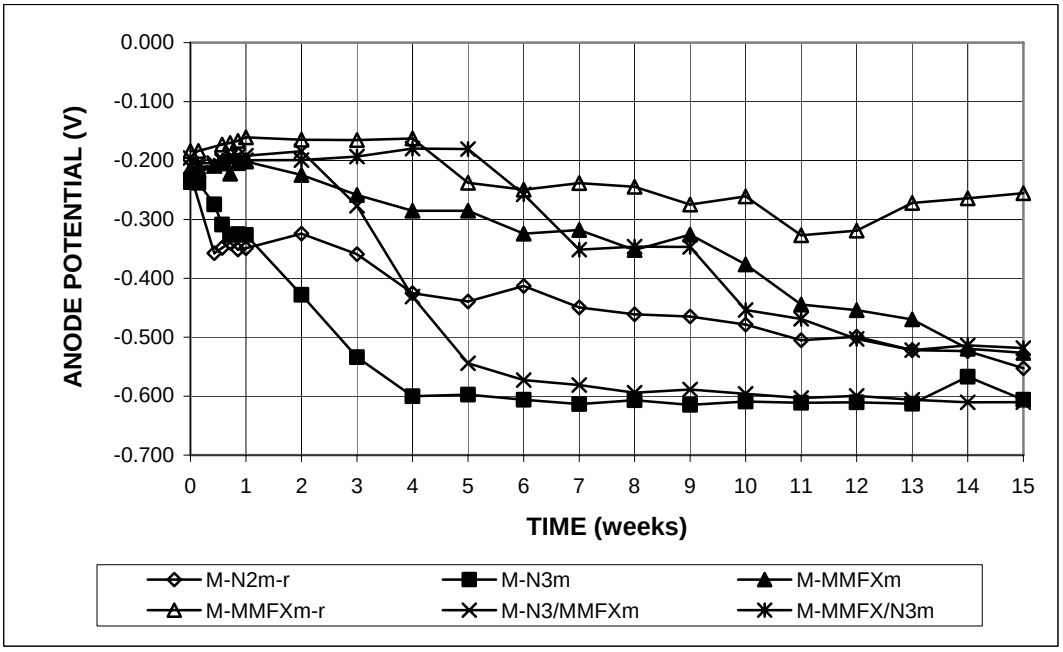

Figure 3.42a - Macrocell test. Average anode corrosion potentials with respect to saturated calomel electrode, mortar-wrapped conventional and MMFX steels in simulated concrete pore solution with 1.6 molal ion NaCl.

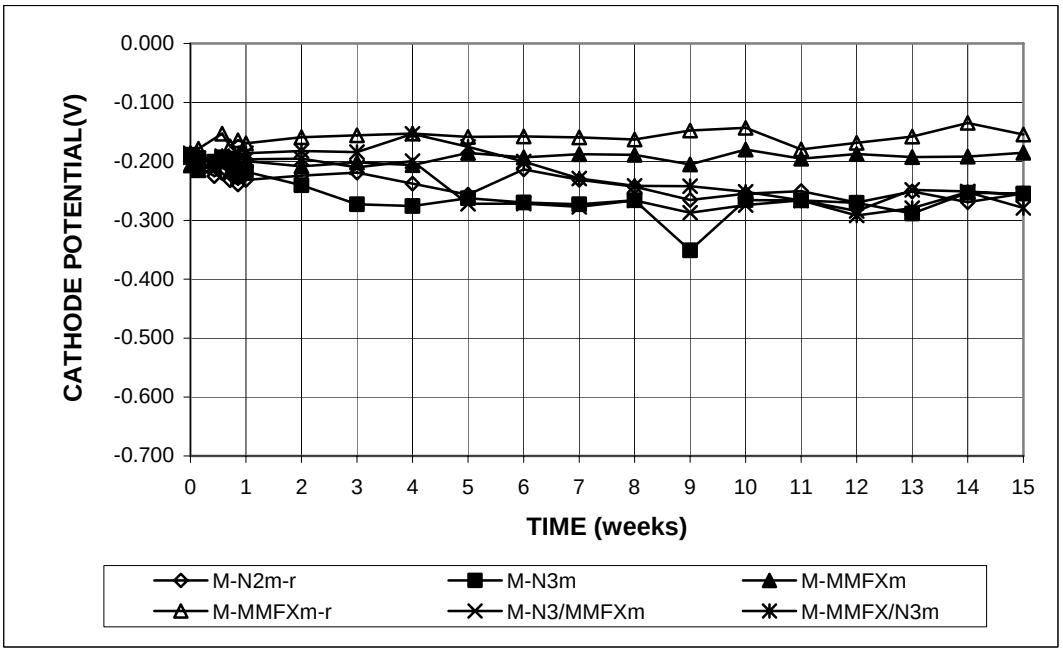

Figure 3.42b - Macrocell test. Average cathode corrosion potentials with respect to saturated calomel electrode, mortar-wrapped conventional and MMFX steels in simulated concrete pore solution with 1.6 molal ion NaCl.

Visual Inspection – At the end of the tests, the conventional and MMFX bars were visually inspected (the mortar cover was removed from the mortar-wrapped specimens). As shown in Figures 3.43 through 3.48, corrosion products were observed on the anode bars for both conventional steel and MMFX steel, except for three of the six mortar-wrapped MMFX bars in the test when the solutions were replaced every five weeks.

Figure 3.43 – Corrosion products on bare conventional steel anode bar (M-N3-3) in 1.6 m ion NaCl solution at 15 weeks (the test solutions not replaced).

Figure 3.44 – Corrosion products on bare MMFX steel anode bar (M-MMFX-3) in 1.6 m ion NaCl solution at 15 weeks (the test solutions not replaced).

Figure 3.45 – Corrosion products on bare MMFX steel anode bar (M-MMFX-r-3) in 1.6 m ion NaCl solution at 15 weeks (the test solutions replaced every five weeks).

Figure 3.46 – Corrosion products on conventional steel anode bar (M-N3m-3) after removal of mortar cover at 15 weeks (the test solutions not replaced).

Figure 3.47 – Corrosion products on MMFX steel anode bar (M-MMFXm-3) after removal of mortar cover at 15 weeks (the test solutions not replaced).

Figure 3.48 – Corrosion products on MMFX steel anode bar (M-MMFX-r-2) after removal of mortar cover at 15 weeks (the test solutions replaced every 5 weeks).

As will be shown in Appendix D, an additional set of corrosion potential tests were performed to compare conventional N2 with MMFX steel in simulated concrete pore solution at NaCl molal ion concentrations of 0.2, 0.4, 0.5, 0.6, 0.7, 1.0, 1.6, and 6.04 m. Three bare bars were tested for each concentration. The solutions were changed every five weeks to maintain the pH. The corrosion potentials were taken with respect to a saturated calomel electrode (SCE).

The results show that the average corrosion potentials for the two steels become progressively more negative, indicating a higher tendency to corrode, as the

NaCl concentration increases. At the 0.2 and 0.4 m ion NaCl concentrations, during most of the test period, conventional and MMFX steels exhibited corrosion potentials more positive than –0.275 V, indicating a passive condition, with MMFX steel showing slightly more negative values than conventional steel. Both conventional and MMFX steels exhibited active corrosion (corrosion potentials more negative than –0.275 V with respect to SCE) at molal ion concentrations of 0.5 m and above, corresponding to a critical Cl^-/OH^- ratio of 0.31. At the higher concentrations (1.6 and 6.04 m), conventional steel exhibited average corrosion potentials about 0.050 to 0.100 V more negative than MMFX steel, with values between –0.400 and –0.500 V at the 1.6 m concentration and values around –0.500 V at the 6.04 m concentration. The average corrosion potentials for both steels in the corrosion potential test are similar to the anode corrosion potentials exhibited by the steels in the corresponding macrocell tests, as shown in Figures 3.36a and 3.39a.

Overall, the corrosion potentials for conventional and MMFX steels are nearly identical, indicating that both steels have a similar tendency to corrode. The corrosion tendency, however, does not provide an indication of the corrosion rate, which is a function of the full electrochemical behavior of the steel.

3.3.2 Bench-scale tests

Southern Exposure and cracked beam specimens with MMFX steel in both the top and bottom mats were evaluated. In addition, Southern Exposure specimens with two combinations of MMFX and conventional N3 steel, (1) MMFX steel at the top mat (MMFX/N3) and (2) N3 steel at the top mat (N3/MMFX), and Southern Exposure specimens with bent MMFX steel (MMFXb) at the top mat were also

tested. The corrosion rates and total corrosion losses at the end of the 96-week test period are presented in Tables 3.12 and 3.12, respectively.

Southern Exposure test – The average corrosion rates are shown in Figure 3.49, and the values at 96 weeks are summarized in Table 3.11. The results of the Student's t-test are presented in Table C.5. The average corrosion rate for specimens with straight MMFX steel began to increase from a negligible value at 10 weeks to 2.8 μm/yr at 49 weeks. It then fluctuated narrowly around 2.5 μm/yr, ending with a value of 3.5 μm/yr, equal to 46 % of the corrosion rate of conventional N3 steel at 96 weeks. Specimens with MMFX steel in the top mat and conventional steel at bottom mat (MMFX/N3) began to exhibit significant corrosion at 26 weeks and reached a maximum corrosion rate of 5.5 μm/yr at 47 weeks; thereafter, the corrosion rate dropped, with a rate of 2.2 μm/yr at the end of the test. The N3/MMFX specimens had corrosion rates similar to those of the N3 specimens during the first 40 weeks; after 40 weeks, the corrosion rate dropped from about 6 μm/yr to a value of 1.78 μm/yr at 96 weeks. During early stages of the test, bent MMFX (MMFXb) specimens exhibited the highest corrosion rate, as high as 6.8 μm/yr at 10 weeks. The corrosion rate dropped with time, reaching a value of 0.98 μm/yr at the end of the test.

Table C.5 shows that there is no significant difference in the corrosion rates at 96 weeks between the N3 and either the MMFX or N3/MMFX specimens [both of the differences are significant at $\alpha = 0.05$ at 70 weeks (Balma et al. 2005)]; at 96 weeks, the difference between the MMFX and MMFX/N3 specimens is significant at $\alpha = 0.2$ and the difference between the MMFX and MMFXb specimens is significant at $\alpha = 0.02$.

The average total corrosion losses are shown in Figure 3.50, and the values at 96 weeks are summarized in Table 3.12. The results for the Student's t-test are

presented in Table C.6. At 96 weeks, the average corrosion loss for MMFX steel was 3.1 μm, equal to 26% of the value for conventional steel (12 μm), while the average corrosion loss was 3.2 μm for the MMFX/N3 specimens, 5.91 μm for the N3/MMFX specimens, and 5.05 μm for the bent MMFX specimens. As demonstrated by the results in the mortar-wrapped macrocell test (the total corrosion losses at 15 weeks were 5.3 μm for the N3 specimens, 1.37 μm for the MMFX specimens, 2.62 μm for the N3/MMFX specimens, and 1.82 μm for the MMFX/N3 specimens), the average total corrosion losses indicate that the anode bars with MMFX steel as the cathode produced comparatively better corrosion resistance than those with conventional steel as the cathode.

Table C.6 shows that the difference in the corrosion losses between the N3 and MMFX specimens is significant at $\alpha = 0.10$; the difference between the N3 and N3/MMFX specimens is significant at $\alpha = 0.20$; the difference between the MMFX and MMFX/N3 specimens is not statistically significant; and the difference between the MMFX and MMFXb specimens is significant at $\alpha = 0.10$. It is not clear, however, that bending MMFX steel in fact causes additional corrosion because only three MMFXb specimens were evaluated and the average corrosion rate of the specimens changed over time, from the highest during the first 12 weeks to the lowest in the second half of the test period compared to the values for N3 and MMFX specimens.

The average corrosion potentials of the top mat of steel with respect to a copper-copper sulfate electrode are present in Figure 3.51a. The top mat potentials for the all-MMFX steel specimens (MMFX) and the MMFX/N3 specimens dropped below –0.350 V, indicating active corrosion, at 24 weeks and 18 weeks, respectively, while the top mat potentials for the all conventional steel specimens (N3) and the N3/MMFX specimens became more negative than –0.350 V at 11 weeks and 8

weeks, respectively. The bent MMFX bars exhibited active corrosion by the end of the first week. At the end of the test, the top mat potentials for all specimens were more negative than –0.500 V. Figure 3.51b shows that MMFX steel at the bottom mat exhibited active corrosion (corrosion potentials more negative than –0.350 V) at an average of 30 weeks for the all-MMFX specimens and 31 weeks for the N3/MMFX specimens.

The average mat-to-mat resistances for the Southern Exposure specimens are shown in Figure 3.52. For all specimens, the mat-to-mat resistances had an initial value of about 150 ohms and then increased at a similar rate to about 400 ohms at 35 weeks; thereafter, the mat-to-mat resistances exhibited a large scatter. For specimens with all conventional bars, the average mat-to-mat resistance increased to about 500 ohms at 74 weeks and then dropped, reaching 155 ohms at 96 weeks, while the resistances for other specimens kept increasing with time, but at different rates, with values ranging from 750 ohms for the MMFX specimens to 2600 ohms for the MMFXb specimens at the end of the test. The scatter in the mat-to-mat resistances may be attributed to the deposition of corrosion products on the bars, corrosion-induced cracking of the concrete, and changes in the moisture content of the specimens.

Cracked beam test – The average corrosion rates and total corrosion losses for cracked beam specimens with MMFX steel are presented in Figures 3.53 and 3.54, respectively. The values at 96 weeks are summarized in Tables 3.11 and 3.12. The results of the Student's t-test are presented in Tables C.5 and C.6. In the first few weeks, MMFX steel exhibited a higher average corrosion rate than during the balance of the test, with a value as high as 5.3 μm/yr at 4 weeks. Then the corrosion rate dropped slowly, ending with a value of 1.0 μm/yr at 96 weeks, equal to 72% of that

of conventional steel [this difference is not statistically significant, while the difference is significant at $\alpha = 0.20$ at 70 weeks (Balma et al. 2005)]. At 96 weeks, the average total corrosion loss for conventional N3 steel was 13.9 μm, while the corrosion loss for MMFX steel was 5.1 μm, corresponding to 37% of the value exhibited by conventional steel. The difference is significant at $\alpha = 0.05$.

The average corrosion potentials of the top and bottom mats of steel are presented in Figures 3.55a and 3.55b, respectively. The results show that the top mats of MMFX steel and conventional steel had similar corrosion potentials during most of the test period, with the MMFX steel showing about 0.100 V more positive values during the first few weeks. The top mat of MMFX steel exhibited active corrosion by the end of the first week, with a corrosion potential of –0.424 V, compared to –0.547 V for the conventional steel. The corrosion potential then fluctuated between –0.400 and –0.600 V, ending with a value of –0.557 V at 96 weeks.

The average corrosion potential for the bottom mat of the MMFX specimens remained more positive than –0.350 V before 27 weeks, indicating a passive condition, and then remained between –0.300 and –0.400 V until 87 weeks. After 87 weeks, the average corrosion potential was below –0.400 V for the MMFX specimens.

The average mat-to-mat resistances are shown in Figure 3.56. Similar to conventional steel, the cracked beam specimens with MMFX steel also exhibited increased mat-to-mat resistance, with a value of about 400 ohms at the first week and 2000 ohms at the end of the test. Up to 48 weeks, MMFX steel and conventional steel had the similar mat-to-mat resistances. After 48 weeks, the mat-to-mat resistance of the MMFX steel was higher than the value of the conventional steel. Unlike the conventional steel, MMFX steel did not undergo a sharp drop at the end of the test.

Table 3.11 - Average corrosion rates at 96 weeks for specimens with conventional and MMFX steels in bench-scale test

Specimen designation*	Steel type	Specimen corrosion rates (μm/yr)						Average (μm/yr)	Standard deviation
		1	2	3	4	5	6		
Southern Exposure test									
SE-N3	N3	0.00	25.09	0.00	0.00	11.46	7.96	7.42	9.94
SE-MMFX	MMFX	3.10	2.80	6.42	1.62	2.57	3.65	3.36	1.64
SE-MMFXb	MMFX	0.42	0.99	1.53				0.98	0.56
SE-N3/MMFX	N3/MMFX	1.18	2.43	1.71				1.78	0.63
SE-MMFX/N3	MMFX/N3	1.71	2.05	2.75				2.17	0.53
Cracked beam test									
CB-N3	N3	0.00	0.00	0.00	0.00	8.56	0.00	1.43	3.50
CB-MMFX	MMFX	0.00	0.00	1.33	2.44	1.79	0.64	1.03	0.99

*** A-B**

A: test method; SE = Southern Exposure test; CB = cracked beam test.

B: steel type and test condition; N2 and N3 = conventional steel; MMFX = mircrocomposite MMFX steel; MMFX/N3 = MMFX steel as the anode, N3 steel as the cathode; N3/MMFX = N3 steel as the anode, MMFX steel as the cathode. b = bent bars at the anode.

Table 3.12 - Average total corrosion losses for specimens with conventional and MMFX steels in bench-scale test

Specimen designation*	Steel type	Specimen total corrosion losses (μm)						Average (μm)	Standard deviation
		1	2	3	4	5	6		
Southern Exposure test									
SE-N3	N3	11.59	27.81	3.23	8.39	14.24	6.63	11.98	8.65
SE-MMFX	MMFX	4.72	2.09	4.17	2.24	2.93	2.20	3.06	1.13
SE-MMFXb	MMFX	5.35	3.65	6.16				5.05	1.28
SE-N3/MMFX	N3/MMFX	3.30	6.29	8.13				5.91	2.44
SE-MMFX/N3	MMFX/N3	2.65	3.43	3.56				3.21	0.49
Cracked beam test									
CB-N3	N3	27.54	16.45	12.47	6.91	10.28	9.87	13.92	7.38
CB-MMFX	MMFX	6.17	4.72	4.44	6.50	5.52	3.36	5.12	1.17

*** A-B**

A: test method; SE = Southern Exposure test; CB = cracked beam test.

B: steel type and test condition; N2 and N3 = conventional steel; MMFX = mircrocomposite MMFX steel; MMFX/N3 = MMFX steel as the anode, N3 steel as the cathode; N3/MMFX = N3 steel as the anode, MMFX steel as the cathode. b = bent bars at the anode.

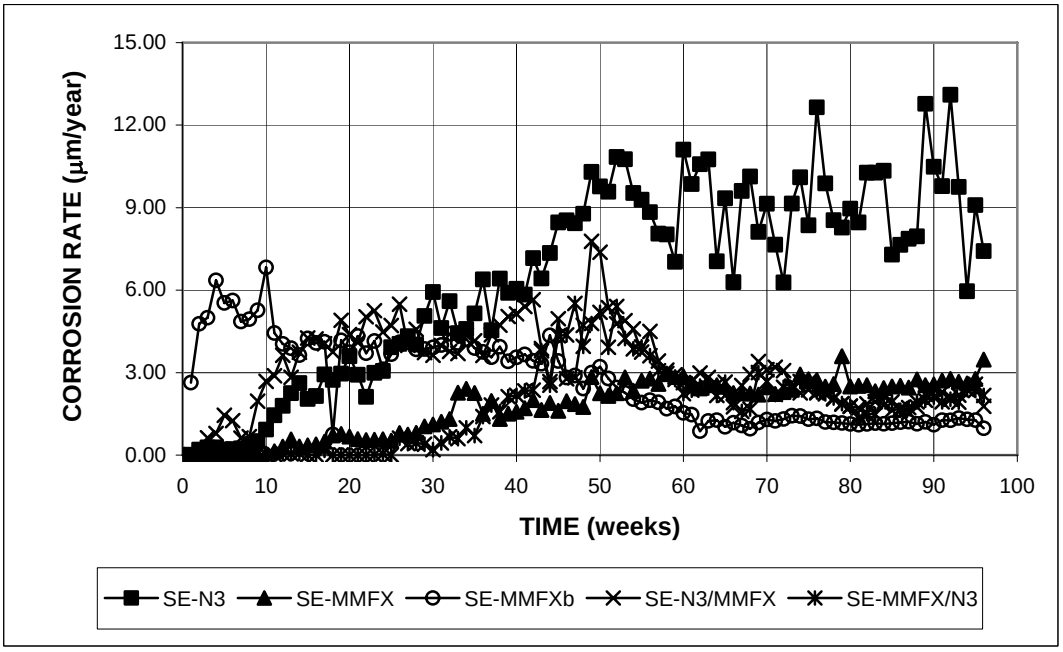

Figure 3.49 - Southern Exposure test. Average corrosion rates of conventional and MMFX steels, specimens w/c = 0.45, ponded with 15% NaCl solution.

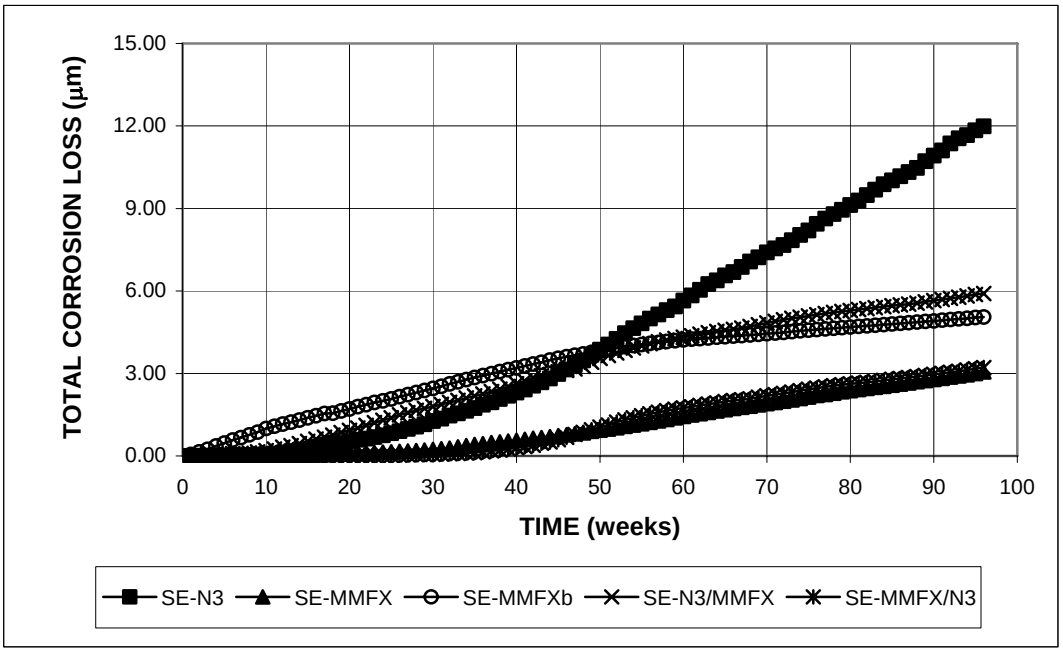

Figure 3.50 - Southern Exposure test. Average total corrosion losses of conventional and MMFX steels, specimens w/c = 0.45, ponded with 15% NaCl solution.

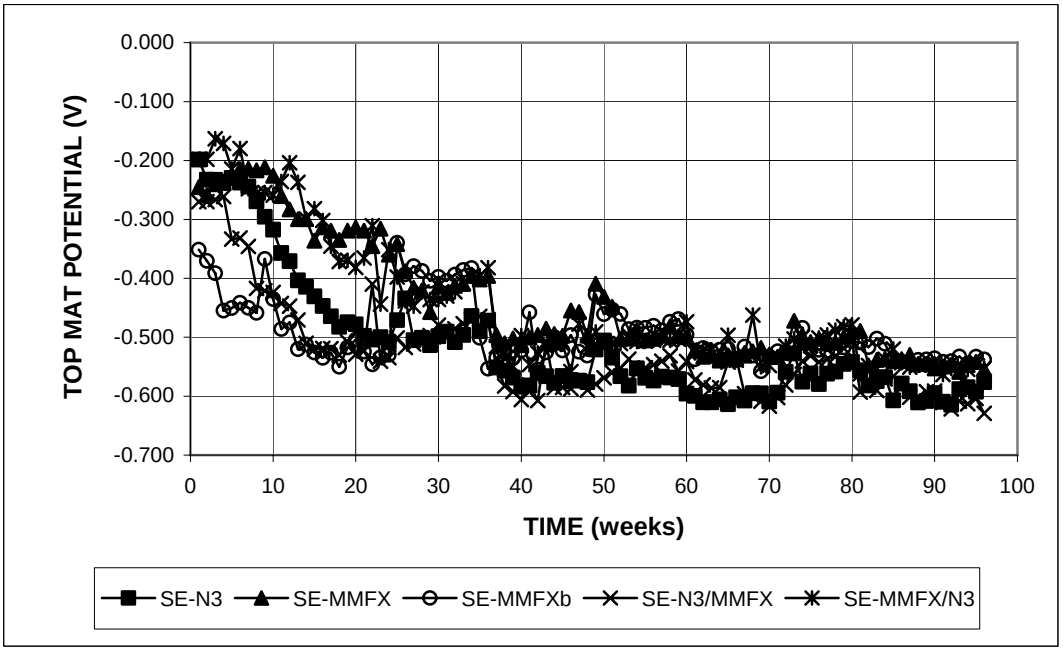

Figure 3.51a - Southern Exposure test. Average top mat corrosion potentials with respect to copper-copper sulfate electrode for conventional and MMFX steels, specimens w/c = 0.45, ponded with 15% NaCl solution.

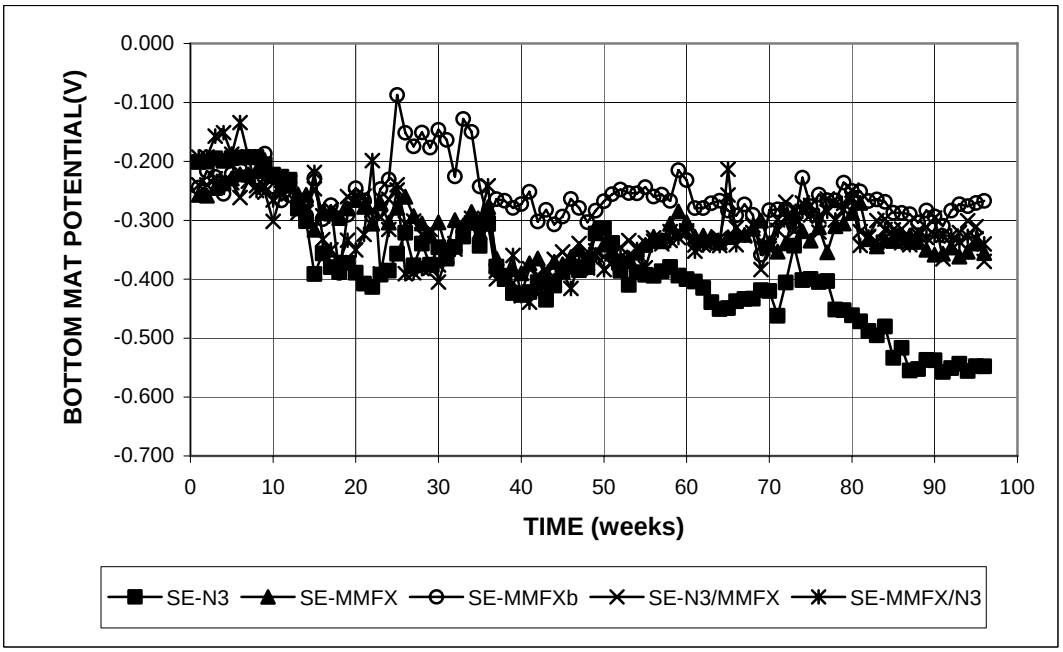

Figure 3.51b -Southern Exposure test. Average bottom mat corrosion potentials with respect to copper-copper sulfate electrode for conventional and MMFX steels, specimens w/c = 0.45, ponded with 15% NaCl solution.

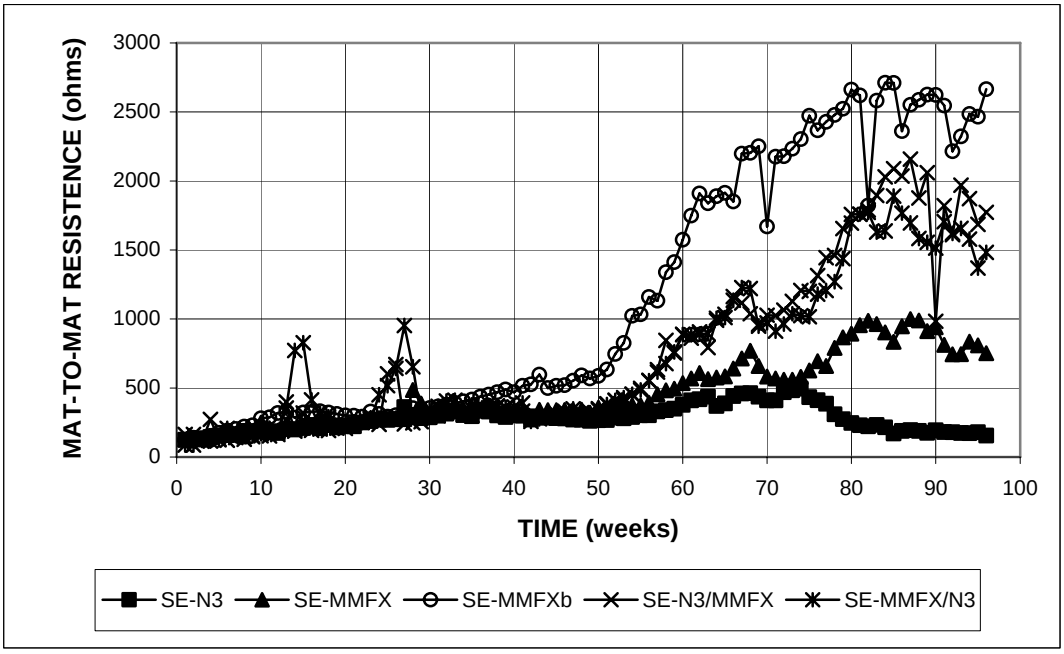

Figure 3.52 - Southern Exposure test. Average mat-to-mat resistances for specimens with conventional and MMFX steels, specimens w/c = 0.45, ponded with 15% NaCl solution.

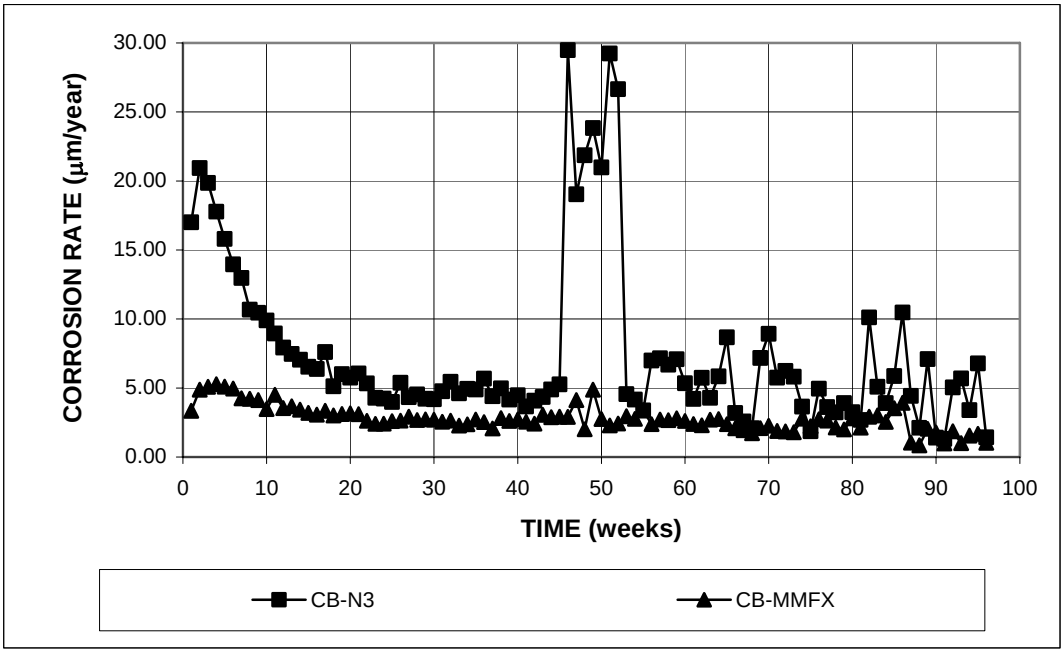

Figure 3.53 - Cracked beam test. Average corrosion rates of conventional and MMFX steels, specimens w/c = 0.45, ponded with 15% NaCl solution.

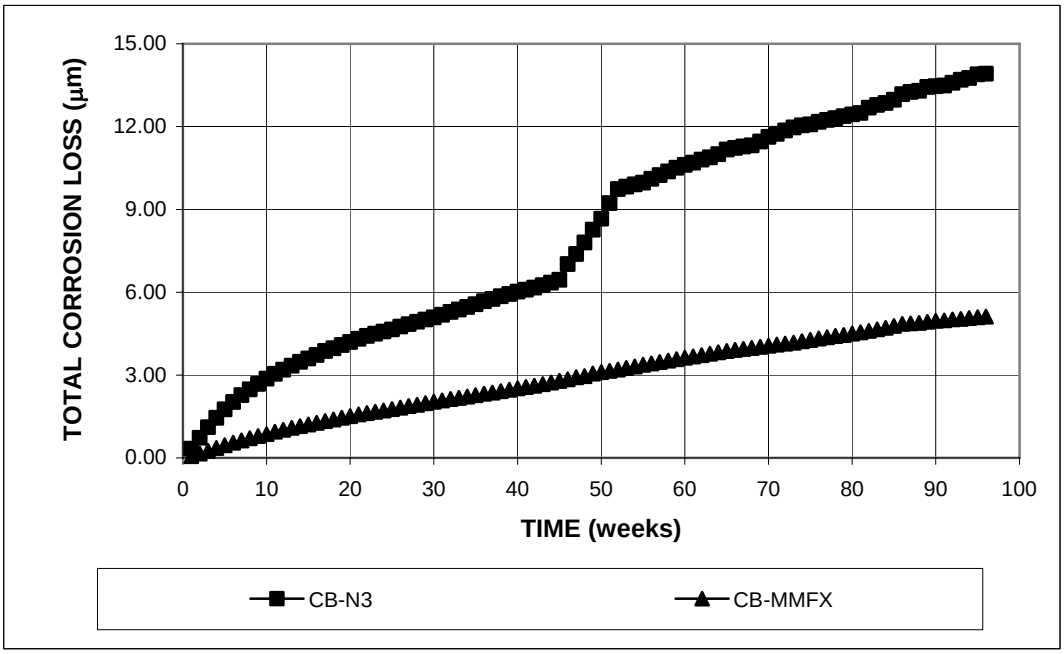

Figure 3.54 - Cracked beam test. Average total corrosion losses of conventional steel and MMFX steels, specimens w/c = 0.45, ponded with 15% NaCl solution.

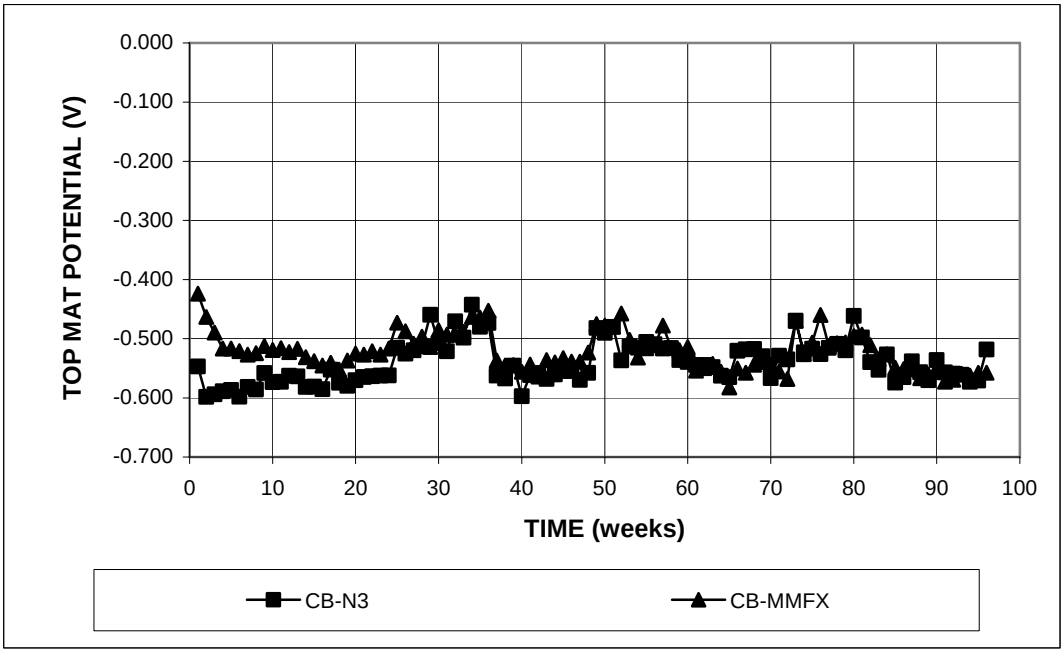

Figure 3.55a - Cracked beam test. Average top mat corrosion potentials with respect to copper-copper sulfate electrode for conventional and MMFX steels, specimens w/c = 0.45, ponded with 15% NaCl solution.

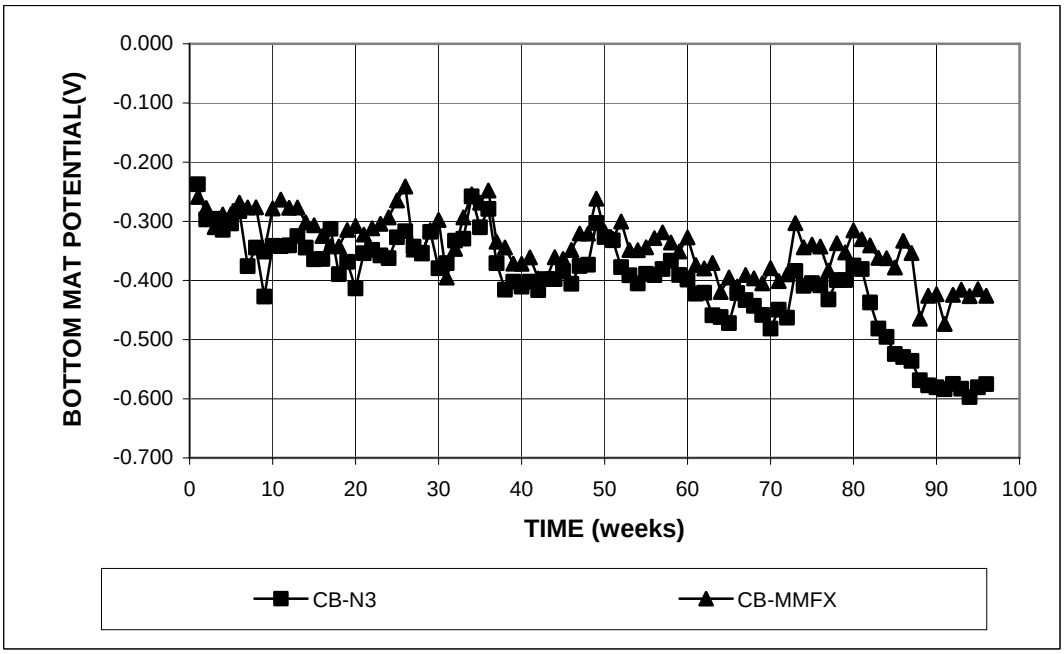

Figure 3.55b - Cracked beam test. Average top mat corrosion potentials with respect to copper-copper sulfate electrode for conventional and MMFX steels, specimens w/c = 0.45, ponded with 15% NaCl solution.

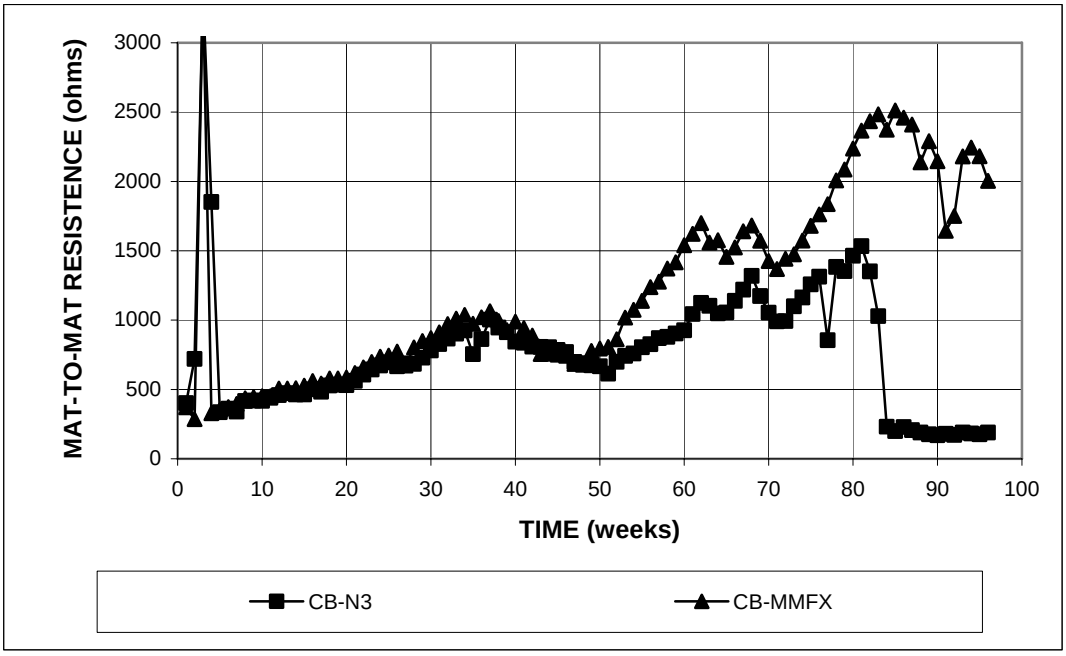

Figure 3.56 - Crack beam test. Average mat-to-mat resistances for specimens with MMFX and conventional steels, specimens w/c = 0.45, ponded with 15% NaCl solution.

Visual Inspection – At the end of the tests, the bars were removed from the concrete. For both the Southern Exposure and cracked beam specimens, the MMFX bars in the top mat exhibited corrosion products, as shown in Figures 3.57 and 3.58. For comparison, the corrosion products on the conventional steel bars are shown in Figures 3.59 and 3.60.

Figure 3.57 – MMFX reinforcing bar from the top mat of an SE specimen (SE-MMFX-1) at 96 weeks, showing corrosion products.

Figure 3.58 – MMFX reinforcing bar from the top mat of a CB specimen (CB-MMFX-1) at 96 weeks, showing corrosion products.

Figure 3.59 – Conventional steel bar from the top mat of an SE specimen (SE-N3-2) at 96 weeks, showing corrosion products.

Figure 3.60 – Conventional steel bar from the top mat of a CB specimen (CB-N3-4) at 96 weeks, showing corrosion products.

3.4 DUPLEX STAINLESS STEELS

The duplex stainless steels evaluated in this study include two heats of 2101 steel and one heat of 2205 steel in both the "as-rolled" and pickled conditions, 2101, 2101p, 2101(2), 2101(2)p, 2205, and 2205p. The bars in the first heat of 2101 steel were slightly deformed and had small cracks on the surface due to a lack of boron. The second heat was provided to allow a fair evaluation of the steel. The results for the macrocell tests are presented in Tables 3.13 through 3.20 and Figures 3.61 through 3.75. The results for the bench-scale tests are presented in Tables 3.21 through 3.24 and Figures 3.86 through 3.97. For comparison, these figures and tables include corresponding results for N, N2, N3, and N4 conventional steels. The results of the Student's t-test are shown in Tables C.7 through C.12. The results demonstrate that pickled 2101 steel and nonpickled and pickled 2205 steel exhibit significantly better corrosion resistance than conventional steel, while the nonpickled 2101 steel has similar corrosion resistance to MMFX steel. Overall, 2205 steel has better corrosion resistance than 2101 steel when evaluated in the same condition and pickled bars have higher corrosion resistance than nonpickled bars.

3.4.1 Rapid macrocell tests

Bare bar specimens in 1.6 m ion NaCl – Bare duplex stainless reinforcing bars were tested in simulated concrete pore solution containing 1.6 m ion NaCl (without replacing the solution every 5 weeks). In addition, the effect of the combination of duplex stainless steel and conventional steel was evaluated by using (1) 2101(2)p as the anode and N4 steel as the cathode [2101(2)p/N4], and (2) N4 steel as the anode and 2101(2)p steel as the cathode [N4/2101(2)p]. For the combinations, the test solutions were replaced every five weeks.

Figures 3.61a and 3.61b show the average corrosion rates of bare conventional and duplex stainless reinforcing bars subjected to a 1.6 m ion concentration of NaCl. The average corrosion rates at 15 weeks are summarized in Table 3.13.

The highest corrosion rate was exhibited by conventional steel (N3), peaking at 46 μm/yr during the first week and then fluctuating primarily between 30 and 40 μm/yr over the balance of the 15-week test period. The corrosion rates of the duplex stainless steels depended on the chromium (Cr) and nickel (Ni) contents, and whether the bars were pickled or nonpickled. Nonpickled 2101 steels, 2101 and 2101(2), exhibited corrosion rates up to 11 and 6.3 μm/yr during the first week, respectively. At 15 weeks, the corrosion rates were, respectively, 2.4 μm/yr and 3.1 μm/yr. The values at the end of the test correspond to 6.7% and 8.5% of the value for conventional steel (36 μm/yr). Table C.7 shows that the differences between conventional steel and either 2101 or 2101(2) steel are significant at $\alpha = 0.02$.

The results show that pickling significantly increased the corrosion performance of 2101 steel. The average corrosion rate for 2101p steel reached its highest value, 2.5 μm/yr, during the first week and then dropped, remaining below 0.25 μm/yr after 5 weeks until the end of the test, while the corrosion rate for 2101(2)p steel remained below 0.25 μm/yr, except for an jump to about 0.5 μm/yr between 12 and 14 weeks, caused by one of the specimens corroding at 1.5 to 2.5 μm/yr at that time. At 15 weeks, the 2101p and 2101(2)p steels were corroding at 0.17 and 0.04 μm/yr, respectively, equal to 0.5% and 0.1% of the value for conventional steel. Type 2205 steel provided significant corrosion resistance, whether in the pickled or nonpickled form, with pickled 2205 showing better corrosion performance than nonpickled 2205. Throughout the test, the average corrosion rates for nonpickled 2205 steel remained below 0.25 μm/yr, with the exception of the value

at 9 weeks, 0.43 μm/yr, while the corrosion rate for pickled 2205 remained below 0.25 μm/yr.

The results of the Student's t-test for comparing the corrosion rates at 15 weeks between pickled and nonpickled steels are shown in Table C.9. The difference between 2101 and 2101p steels is significant at $\alpha = 0.02$; the difference between 2101(2) and 2101(2)p steels is significant at $\alpha = 0.05$; and the difference between 2205 and 2205p steels is not statistically significant.

The results of the Student's t-test comparing the corrosion rates at 15 weeks between 2101(2)p steel and either 2205 or 2205p steels are shown in Table C.11. The difference between 2101(2)p and 2205 steels is significant at $\alpha = 0.20$, while the difference between 2101(2)p and 2205p steels is significant at $\alpha = 0.05$.

The average total corrosion losses are shown in Figures 3.62a and 3.62b, and the values at 15 weeks are listed in Table 3.14. At 15 weeks, conventional N3 steel exhibited the highest corrosion loss, 9.0 μm, followed by the nonpickled 2101 steels, 2101 and 2101(2), at about 1.0 and 1.4 μm, respectively (Table C.8 shows that the differences between conventional steel and either 2101 or 2101(2) steel are significant at $\alpha = 0.02$). At this point, the picked 2101 steels, 2101p and 2101(2)p, had corrosion losses of 0.09 and 0.04 μm, respectively. 2205 steel exhibited the same total corrosion loss as the 2101(2)p steel, 0.04 mm, equal to 0.4% of the loss for conventional steel, while pickled 2205 steel (2205p) had the lowest total corrosion loss, 0.02 μm, corresponding to 0.2% of the value for conventional steel.

The results of the Student's t-test comparing the average corrosion losses at 15 weeks between pickled and nonpickled steels are shown in Table C.10. The difference between 2101 and 2101p steels is significant at $\alpha = 0.2$; the difference

between 2101(2) and 2101(2)p steels is significant at $\alpha = 0.02$; and the difference between 2205 and 2205p steel is significant at $\alpha = 0.2$.

The results of the Student's t-test for comparing the corrosion losses between 2101(2)p steel and either 2205 or 2205p steel are shown in Table C.12. The differences between 2101(2)p steel and either 2205 or 2205(2)p steel are not statistically significant.

The average corrosion potentials of the anode and cathode with respect to a SCE are shown in Figures 3.63a and 3.63b, respectively. Conventional N3 steel had the most negative corrosion potential at the anode, with values of –0.450 V to –0.500 V during the first week and –0.560 V after 15 weeks, indicating a high tendency to corrode. Of the duplex steels, the two heats of nonpickled 2101 steel exhibited average anode corrosion potentials between –0.200 and –0.300 V. The corrosion potential at the anode for the remaining steels remained more positive than –0.200 V, indicating a low tendency to corrode. The average corrosion potentials at the cathode for all duplex stainless steels remained more positive than –0.200 V and became more positive with time.

The average corrosion rates and total corrosion losses for the combinations of the 2101(2)p steel and conventional N4 steel are shown in Figures 3.64 and 3.65, respectively. Tables 3.13 and 3.14 summarize the average corrosion rates and total corrosion losses at 15 weeks. The results for the Student's t-test are presented in Tables C.7 and C.8. 2101(2)p steel with conventional steel as the cathode exhibited good corrosion resistance, similar to that of 2101(2)p steel at both the anode and the cathode. After 15 weeks, the 2101(2)p/N4 specimens had an average corrosion rate of 0.24 μm/yr, with a total corrosion loss of 0.02 μm, compared to 0.04 μm/yr and 0.04 μm for the 2101(2)p specimens. The differences in both the corrosion rates and losses

are not statistically significant. Conventional steel with the 2101(2) steel as the cathode had an initial corrosion rate of 32 μm/yr, ending with a rate of 13 μm/yr, and a corrosion loss of 4.4 μm, lower than exhibited by the macrocell with conventional N4 steel at both the anode and the cathode, which had a corrosion rate of 28 μm/yr and a corrosion loss of 6.1 μm at 15 weeks. The differences in both the corrosion rates and losses are significant at $\alpha = 0.20$.

The average corrosion potentials of the anode and cathode for the combination of the 2101(2)p steel and conventional N4 steel are shown in Figures 3.66a and 3.66b, respectively. The anode corrosion potentials of the 2101(2)p/N2 macrocell were similar to those of the all 2101(2)p macrocell, remaining more positive than –0.200 V throughout the test period, indicating a low tendency to corrode, while conventional steel with 2101(2)p steel as the cathode had similar anode corrosion potentials (primarily between –0.400 and –0.500 V) to those of the conventional steel macrocells used alone. The cathode corrosion potential of the all-conventional steel macrocell was around –0.200 V, while the cathode corrosion potentials of the remaining macrocells were more positive than –0.200 V.

Table 3.13 - Average corrosion rates at 15 weeks for bare conventional and duplex stainless steels in concrete pore solution with 1.6 m ion NaCl in macrocell test

Specimen designation*	Steel type	Specimen corrosion rates (μm/yr)						Average (μm/yr)	Standard deviation
		1	2	3	4	5	6		
Bare bars in 1.6 m NaCl									
M-N3	N3	52.60	0.26	67.77	40.17	32.43	22.08	35.88	23.61
M-N4-r	N4	31.23	22.16	16.68	40.66	26.74	31.12	28.10	8.30
M-2101	2101	3.12	1.73	1.42	2.17	3.53		2.39	0.90
M-2101p	2101p	0.43	0.00	0.00	0.23	0.20		0.17	0.18
M-2101(2)	2101(2)	0.06	6.79	1.68	3.44	4.02	2.31	3.05	2.30
M-2101(2)p	2101(2)p	0.06	0.03	0.00	0.00	0.06	0.09	0.04	0.03
M-2205	2205	0.12	0.29	0.09	0.03	0.12		0.13	0.10
M-2205p	2205p	0.09	0.06	0.14	0.09	0.09		0.09	0.03
M-N4/2101(2)p-r	N4/2101(2)p	1.91	11.65	25.63				13.06	11.93
M-2101(2)p/N4-r	2101(2)p/N4	0.49	0.06	0.17				0.24	0.22

*** A-B-C**

A: test method; M = macrocell test.

B: steel type and test condition; N3 and N4 = conventional steel; 2101 and 2101(2) = two heats of 2101 duplex stainless steel (21% chromium, 1% nickel), 2205 = 2205 duplex stainless steel (22% chromium, 5% nickle), N4/2101(2) = N4 steel as the anode, 2101(2) steel as the cathode; 2101(2)/N4 = 2101(2) steel as the andoe, N4 steel as the cathode; p = pickled.

C: r = the test solutions are replaced every five weeks.

Table 3.14 - Average total corrosion losses at 15 weeks for bare conventional and stainless steels in concrete pore solution with 1.6 m ion NaCl in macrocell test

Specimen designation*	Steel type	Specimen total corrosion losses (μm)						Average (μm)	Standard deviation
		1	2	3	4	5	6		
Bare bars in 1.6 m NaCl									
M-N3	N3	12.33	4.15	13.49	11.17	7.08	5.50	8.95	3.88
M-N4-r	N4	7.02	5.25	4.93	7.61	6.53	5.24	6.10	1.11
M-2101	2101	0.63	0.72	0.32	0.54	2.92		1.03	1.07
M-2101p	2101p	0.13	0.06	0.01	0.10	0.13		0.09	0.05
M-2101(2)	2101(2)	1.44	1.57	1.19	0.81	1.54	1.97	1.42	0.39
M-2101(2)p	2101(2)p	0.04	0.01	0.02	0.03	0.03	0.13	0.04	0.04
M-2205	2205	0.03	0.03	0.03	0.06	0.03		0.04	0.01
M-2205p	2205p	0.03	0.02	0.03	0.02	0.02		0.02	0.00
M-N4/2101(2)p-r	N4/2101(2)p	5.69	3.50	3.99				4.39	1.15
M-2101(2)p/N4-r	2101(2)p/N4	0.04	0.01	0.02				0.02	0.01

*** A-B-C**

A: test method; M = macrocell test.

B: steel type and test condition; N3 and N4 = conventional steel; 2101 and 2101(2) = two heats of 2101 duplex stainless steel (21% chromium, 1% nickel), 2205 = 2205 duplex stainless steel (22% chromium, 5% nickle), N4/2101(2) = N4 steel as the anode, 2101(2) steel as the cathode; 2101(2)/N4 = 2101(2) steel as the andoe, N4 steel as the cathode; p = pickled.

C: r = the test solutions are replaced every five weeks.

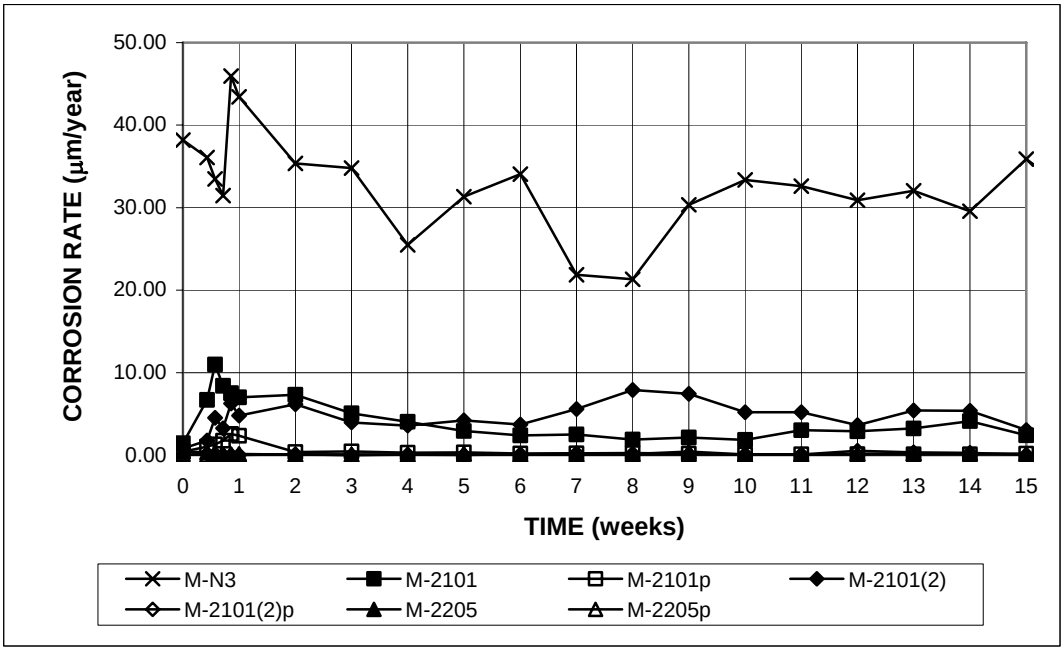

(a)

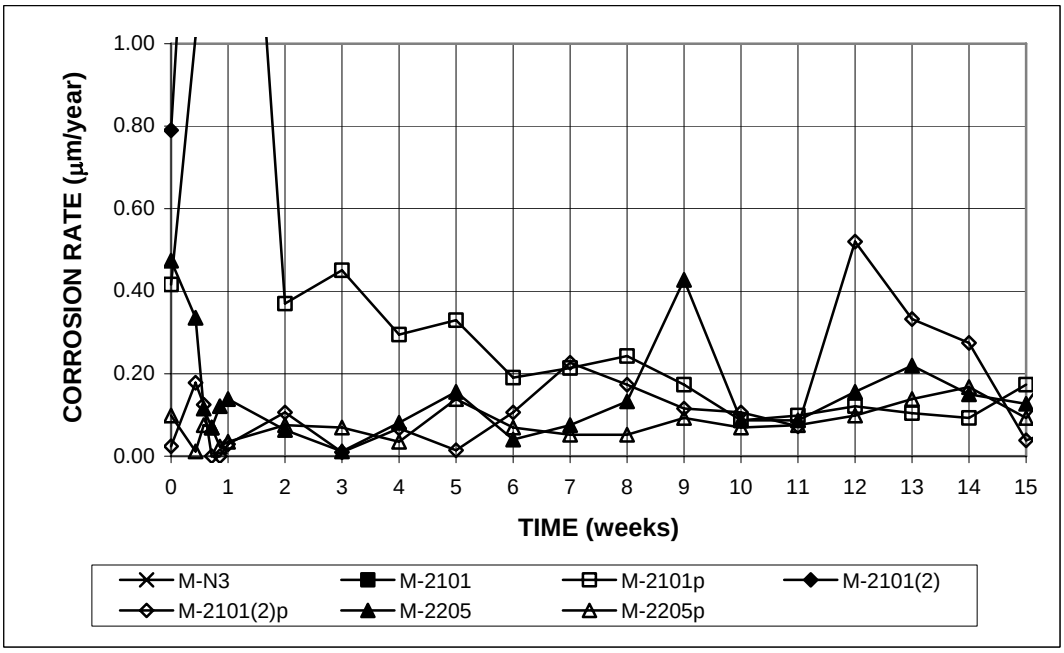

(b)

Figure 3.61 - Macrocell test. Average corrosion rates for bare conventional and duplex stainless steels in simulated concrete pore solution with 1.6 molal ion NaCl.

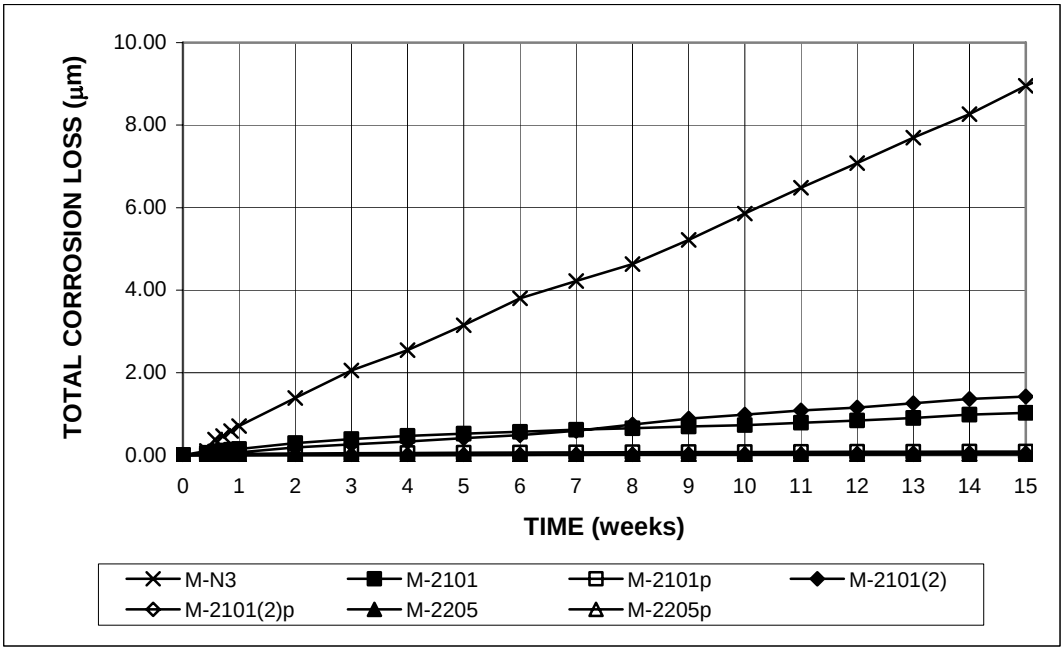

(a)

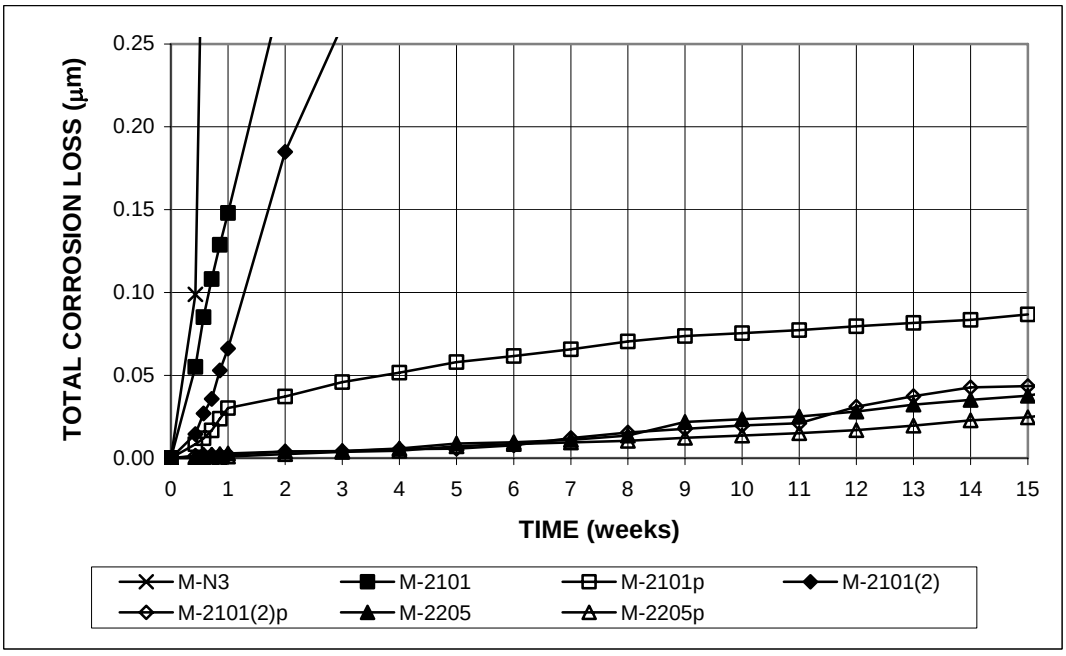

(b)

Figure 3.62 - Macrocell test. Average total corrosion losses for bare conventional and duplex stainless steels in simulated concrete pore solution with 1.6 molal ion NaCl.

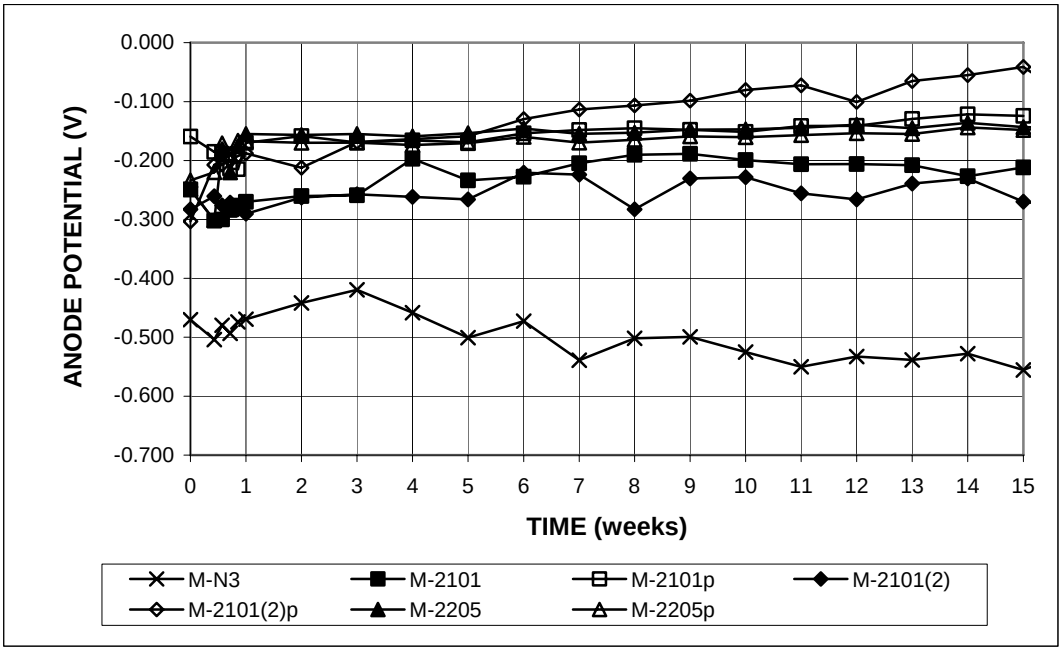

Figure 3.63a - Macrocell test. Average anode corrosion potentials with respect to saturated calomel electrode for bare conventional and duplex stainless steels in simulated concrete pore solution with 1.6 molal ion NaCl.

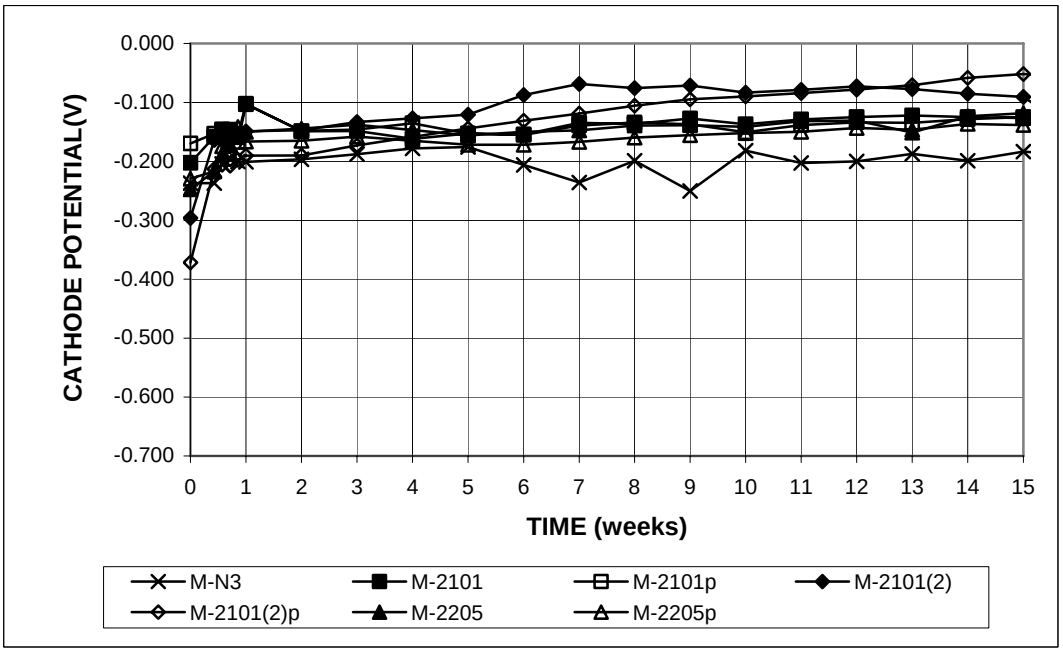

Figure 3.63b - Macrocell test. Average cathode corrosion potentials with respect to saturated calomel electrode for bare conventional and duplex stainless steels in simulated concrete pore solution with 1.6 molal ion NaCl.

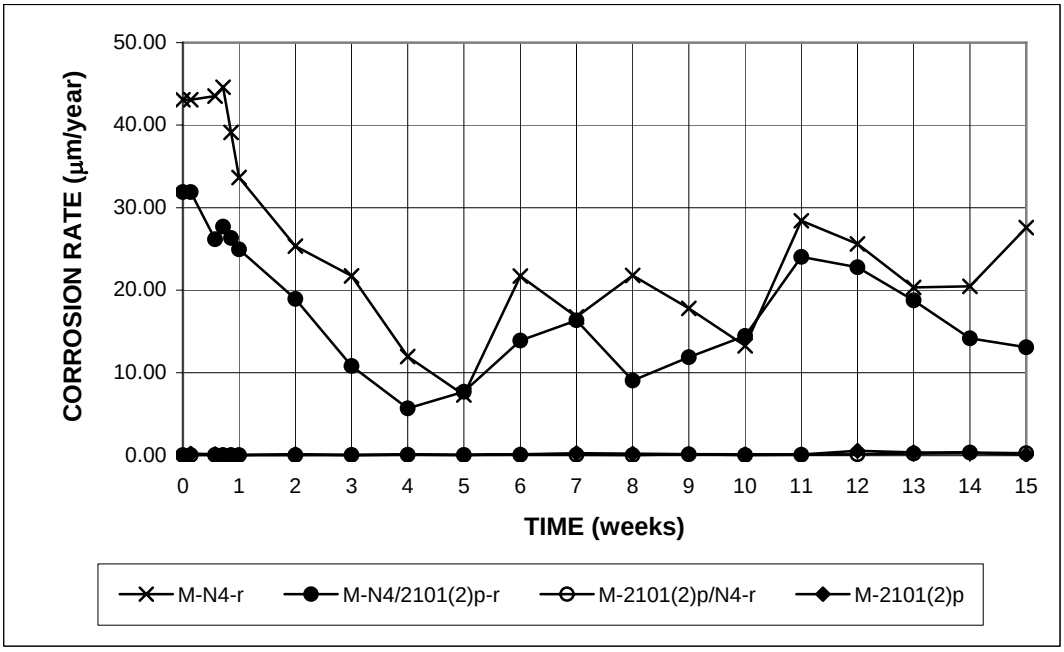

(a)

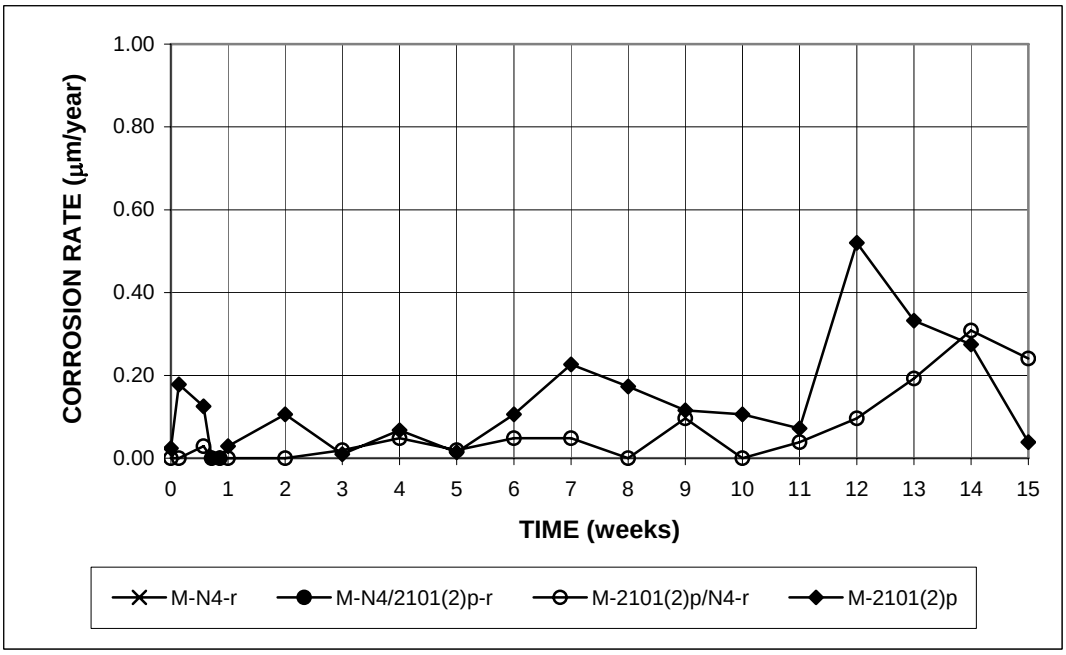

(b)

Figure 3.64 - Macrocell test. Average corrosion rates for bare conventional steel, duplex stainless steel, and combinations of the steels in simulated concrete pore solution with 1.6 molal ion NaCl.

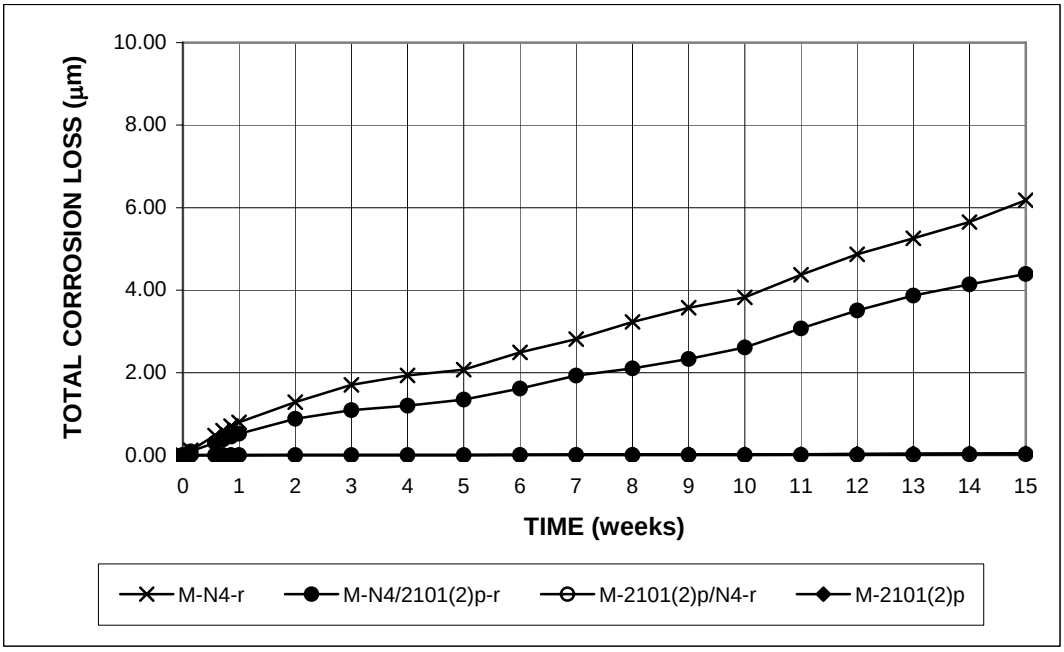

(a)

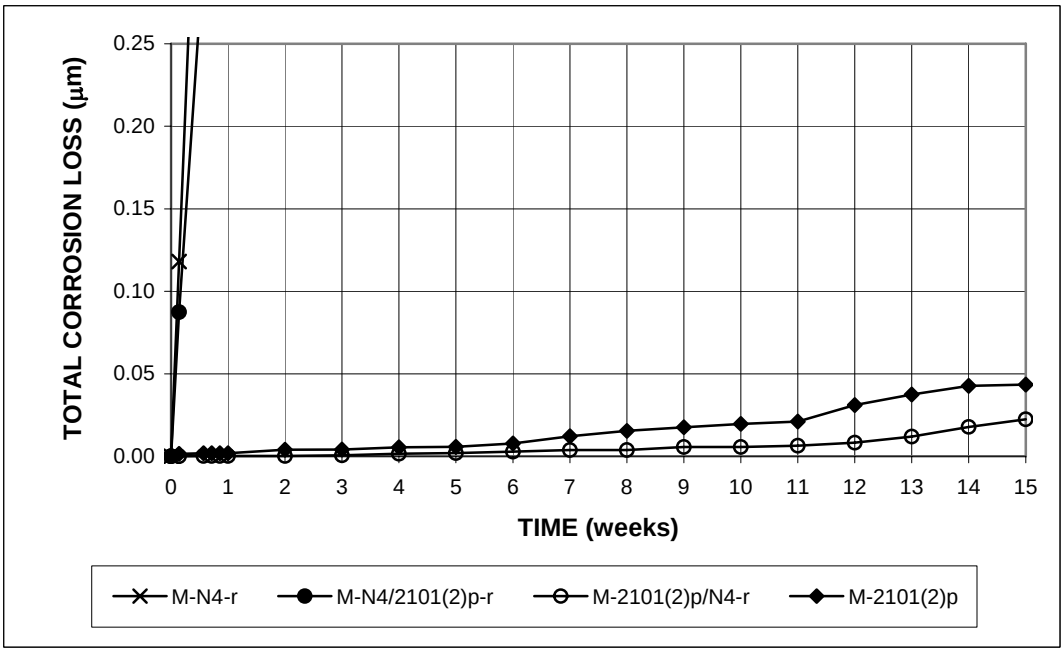

(b)

Figure 3.65 - Macrocell test. Average total corrosion losses for bare conventional steel, duplex stainless steel, and combinations of the steels in simulated concrete pore solution with 1.6 molal ion NaCl.

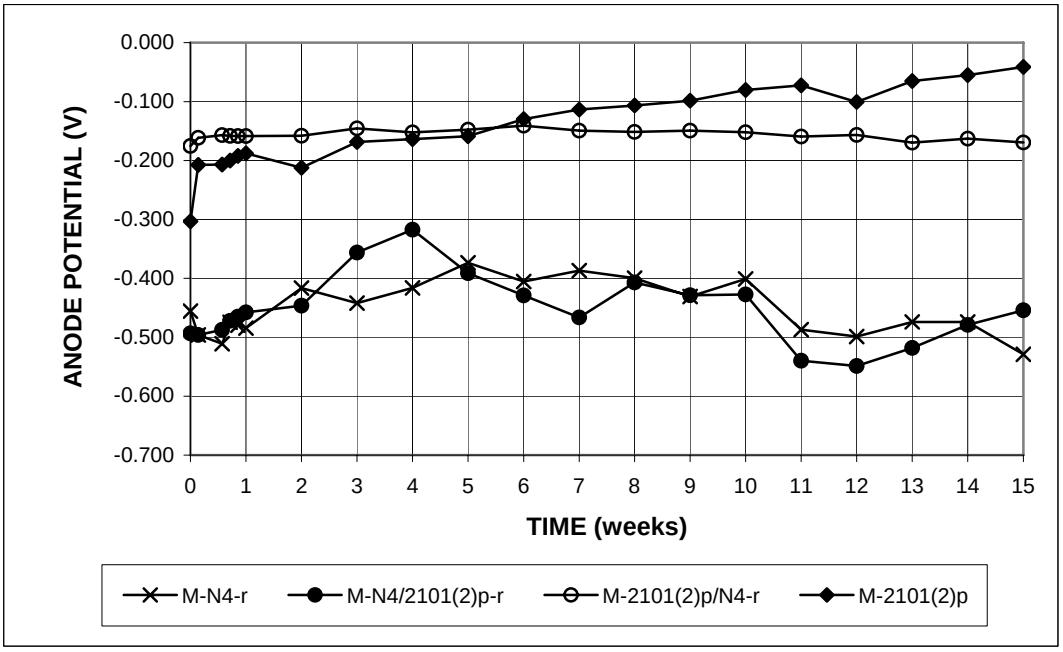

Figure 3.66a - Macrocell test. Average anode corrosion potentials with respect to saturated calomel electrode for bare conventional steel, duplex steel, and combinations of the steels in simulated concrete pore solution with 1.6 molal ion NaCl.

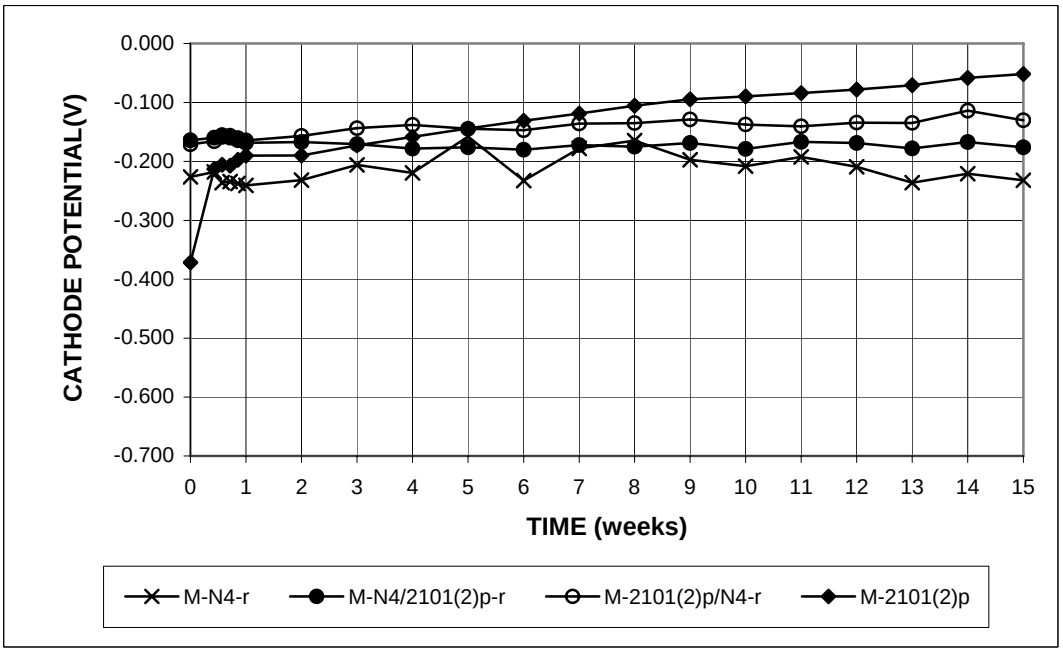

Figure 3.66b - Macrocell test. Average cathode corrosion potentials with respect to saturated calomel electrode for bare conventional steel, duplex steel, and combinations of the steels in simulated concrete pore solution with 1.6 molal ion NaCl.

Bare bar specimens in 6.04 m ion NaCl – Bare duplex stainless reinforcing bars were tested in simulated concrete pore solution containing 6.04 m ion NaCl without replacing the solution every five weeks. 2101(2)p, 2205, and 2205p steels were also tested in the high chloride concentration solution with the solution replaced every five weeks.

The average corrosion rates and total corrosion losses of bare conventional and duplex stainless steels subjected to the 6.04 m ion NaCl solution (without replacing the solution every five weeks) are shown in Figures 3.67 and 3.68, respectively.

Observations from the high NaCl concentration solution test are similar to those from the 1.6 m ion NaCl solution test, with the corrosion performance of the duplex stainless steels more clearly distinguished in the high chloride concentration solution. Conventional N2 steel had the highest corrosion rate, with values as high as 47 μm/yr during the first week and above 20 μm/yr throughout the test period. The two heats of nonpickled 2101 steel, 2101 and 2101(2), exhibited the next highest corrosion rates, between 10 and 20 μm/yr throughout the test period. The first heat of pickled 2101 steel, 2101p, exhibited average corrosion rates between 8 to 10 μm/yr for the first four weeks and corroded at a rate of about 5 μm/yr for the rest of the test period, while 2101(2)p steel corroded at below 0.25 μm/yr for the first 6 weeks, increasing to a maximum of 2 μm/yr at 12 weeks and ending with a value of about 1 μm/yr. The relatively poor performance of the first heat of 2101 steel in all likelihood was caused by the small cracks on the bar surface due to the lack of boron. Nonpickled 2205 steel corroded at a rate between 0 and 0.3 μm/yr for the first 5 weeks. The corrosion rate increased to values as high as 4 μm/yr at 10 weeks and then remained above 2.5 μm/yr for the rest of the test period. The pickled 2205 steel

showed the best corrosion performance, corroding at a rate below 0.3 μm/yr throughout the test.

The average corrosion rates and total corrosion losses at 15 weeks are summarized in Table 3.15 and 3.16, respectively. At 15 weeks, conventional N2 steel had the highest corrosion rate, 25.5 μm/yr, with a total corrosion loss of 9.8 μm, followed by the 2101 and 2101(2) steels, which had corrosion rates of 14 and 11 μm/yr and corrosion losses of 4.0 and 3.4 μm, respectively. 2101p steel had an average corrosion rate of 4.5 μm/yr and a total corrosion loss of 1.7 μm, while 2101(2)p steel had a corrosion rate of 1.0 μm/yr and a loss of 0.17 μm. Nonpickled 2205 exhibited a higher corrosion rate and corrosion loss than the 2101(2)p steel, with values of 2.5 μm/yr and 0.5 μm at 15 weeks, respectively, while the 2205p steel had the lowest corrosion rate, at 0.28 μm/yr, and the lowest corrosion loss, at 0.03 μm.

The results for the Student's t-test are presented in Tables C.7 through C.12. Table C.7 shows that the difference in the corrosion rates between N2 and 2101 steels is significant at $\alpha = 0.10$; the difference between N2 and 2101(2) steels is significant at $\alpha = 0.05$. Table C.8 shows that the differences in the corrosion losses between N2 steel and either 2101 or 2101(2) steel are significant at $\alpha = 0.02$.

Tables C.9 and C.10 show that the differences in both the corrosion rates and corrosion losses between all nonpickled steels and pickled steels are significant at $\alpha = 0.02$, with the exception that the difference in the corrosion rates between 2101 and 2101p steels is significant at $\alpha = 0.05$.

Table C.11 shows the results of the Student's t-test for comparing the average corrosion rates at 15 weeks between 2101(2)p steel and either 2205 or 2205p steel. The difference between 2101(2)p and 2205 steels is significant at $\alpha = 0.05$, while the difference between 2101(2)p and 2205p steels is not significant. Table C.12 shows

that the differences in the corrosion losses between 2101(2)p steel and either 2205 or 2205p steel are significant at $\alpha = 0.02$.

The average corrosion potentials of the anode and cathode for the duplex stainless steels in the high NaCl concentration solution are shown in Figures 3.69a and 3.69b, respectively. The anode corrosion potentials for the 2101, 2101(2) and 2101p steels dropped to values between –0.300 and –0.400 V by the end of the first week, indicating a high tendency to corrode. The 2101(2)p steel had anode corrosion potentials between –0.100 and –0.200 V for the first 10 weeks, dropping to values more negative than –0.200 V thereafter, while the anode corrosion potentials for the 2205 steel were more positive than –0.150 V for most of the first six weeks, dropping to about –0.220 V for the rest of the test period. In the high NaCl concentration test, 2101(2)p and 2205 steel exhibited active corrosion as the corrosion potentials became more negative than –0.200 V, as shown by the corrosion rates. The anode potential for the 2205 pickled bars remained around –0.150 V during the test. For all duplex stainless steels, the corrosion potentials of the cathodes were more positive than –0.200 V throughout the test period.

Table 3.15 - Average corrosion rates at 15 weeks for bare conventional and duplex stainless steels in concrete pore solution with 6.04 m ion NaCl in macrocell test

Specimen designation*	Steel type	Specimen corrosion rates (μm/yr)						Average (μm/yr)	Standard deviation
		1	2	3	4	5	6		
Bare bars in 6.04 m NaCl									
M-N2h	N2	33.87	37.80	12.17	24.51	18.96		25.46	10.52
M-2101h	2101	21.39	11.21	16.01	4.19	17.43		14.05	6.60
M-2101ph	2101p	2.63	3.03	2.08	9.13	5.40		4.46	2.91
M-2101(2)h	2101(2)	7.20	12.72	11.59	11.21	13.15	10.38	11.04	2.14
M-2101(2)ph	2101(2)p	3.47	0.23	0.00	0.00	1.82	0.23	0.96	1.41
M-2205h	2205	2.40	1.24	2.69	2.80	2.92	2.77	2.47	0.63
M-2205ph	2205p	0.14	0.20	0.23	0.40	0.43		0.28	0.13

*** A-B**

A: test method; M = macrocell test.

B: steel type and test condition; N3 and N4 = conventional steel; 2101 and 2101(2) = two heats of 2101 duplex stainless steel (21% chromium, 1% nickel), 2205 = 2205 duplex stainless steel (22% chromium, 5% nickle), p = pickled, h = 6.04 m ion NaCl concentration.

Table 3.16 - Average total corrosion losses at 15 weeks for bare conventional and stainless steels in concrete pore solution with 6.04 m ion NaCl in macrocell test

Specimen designation*	Steel type	Specimen total corrosion losses (μm)						Average (μm)	Standard deviation
		1	2	3	4	5	6		
Bare bars in 6.04 m NaCl									
M-N2h	N2	12.32	11.64	6.93	9.28	8.63		9.76	2.21
M-2101h	2101	3.98	3.64	4.58	2.00	5.61		3.96	1.33
M-2101ph	2101p	0.84	1.32	1.42	3.17	1.79		1.71	0.88
M-2101(2)h	2101(2)	2.17	3.74	3.79	3.70	3.22	3.59	3.37	0.62
M-2101(2)ph	2101(2)p	0.25	0.18	0.00	0.14	0.28	0.14	0.17	0.10
M-2205h	2205	0.51	0.34	0.52	0.34	0.62	0.65	0.49	0.13
M-2205ph	2205p	0.02	0.03	0.02	0.02	0.05		0.03	0.01

*** A-B**

A: test method; M = macrocell test.

B: steel type and test condition; N3 and N4 = conventional steel; 2101 and 2101(2) = two heats of 2101 duplex stainless steel (21% chromium, 1% nickel), 2205 = 2205 duplex stainless steel (22% chromium, 5% nickle), p = pickled, h = 6.04 m ion NaCl concentration.

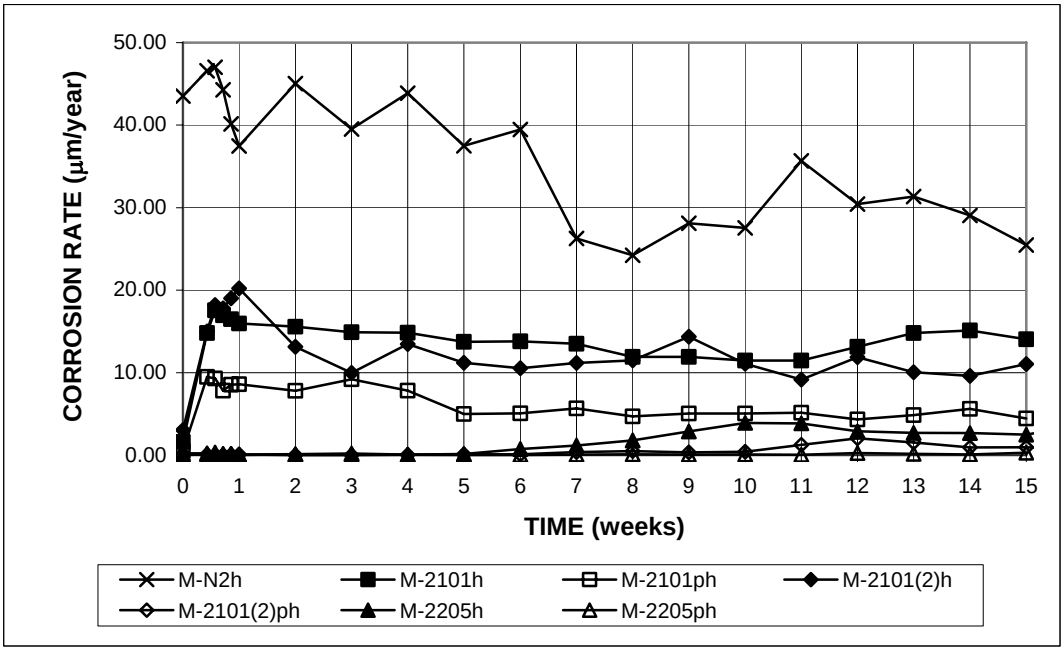

(a)

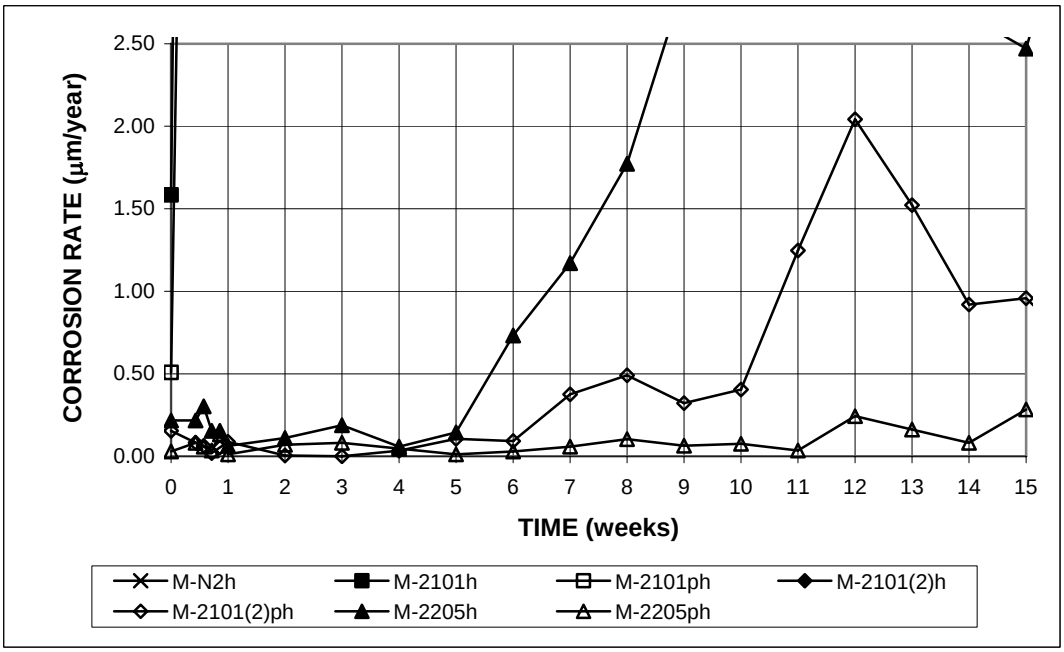

(b)

Figure 3.67 - Macrocell test. Average corrosion rates for bare conventional and duplex stainless steels in simulated concrete pore solution with 6.04 molal ion NaCl.

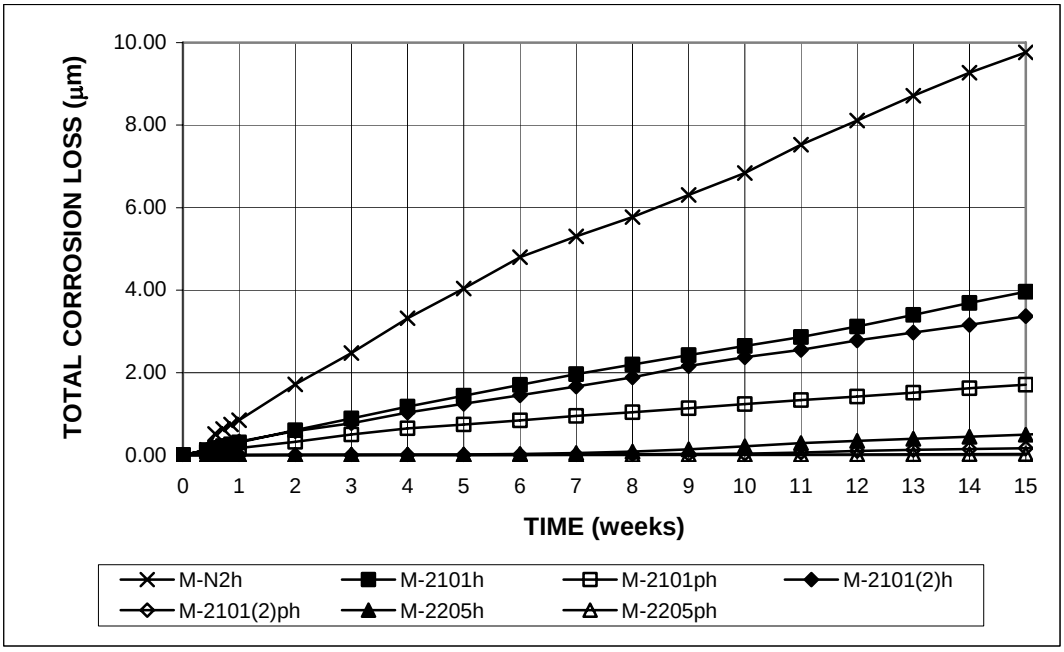

(a)

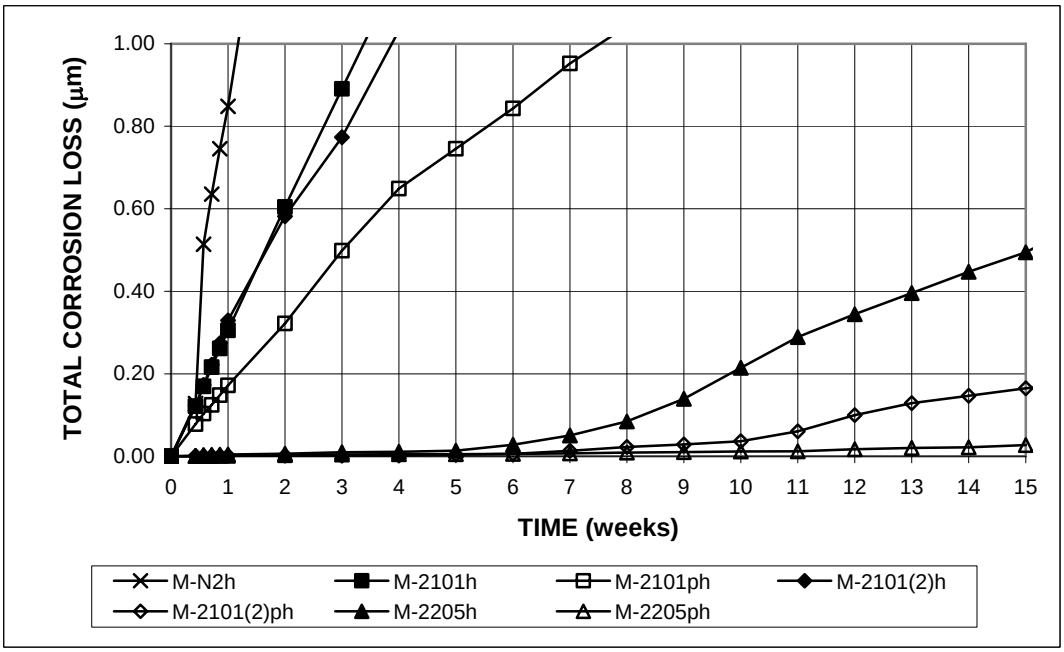

(b)

Figure 3.68 - Macrocell test. Average total corrosion losses for bare conventional and duplex stainless steels in simulated concrete pore solution with 6.04 molal ion NaCl.

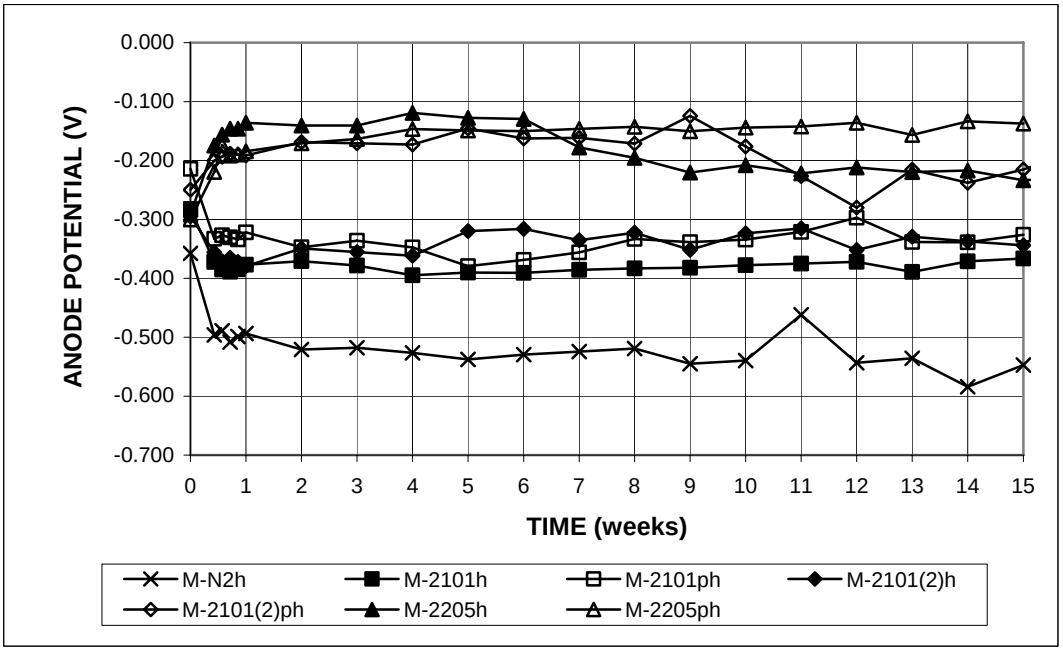

Figure 3.69a - Macrocell test. Average anode corrosion potentials with respect to saturated calomel electrode for bare conventional and duplex stainless steels in simulated concrete pore solution with 6.04 molal ion NaCl.

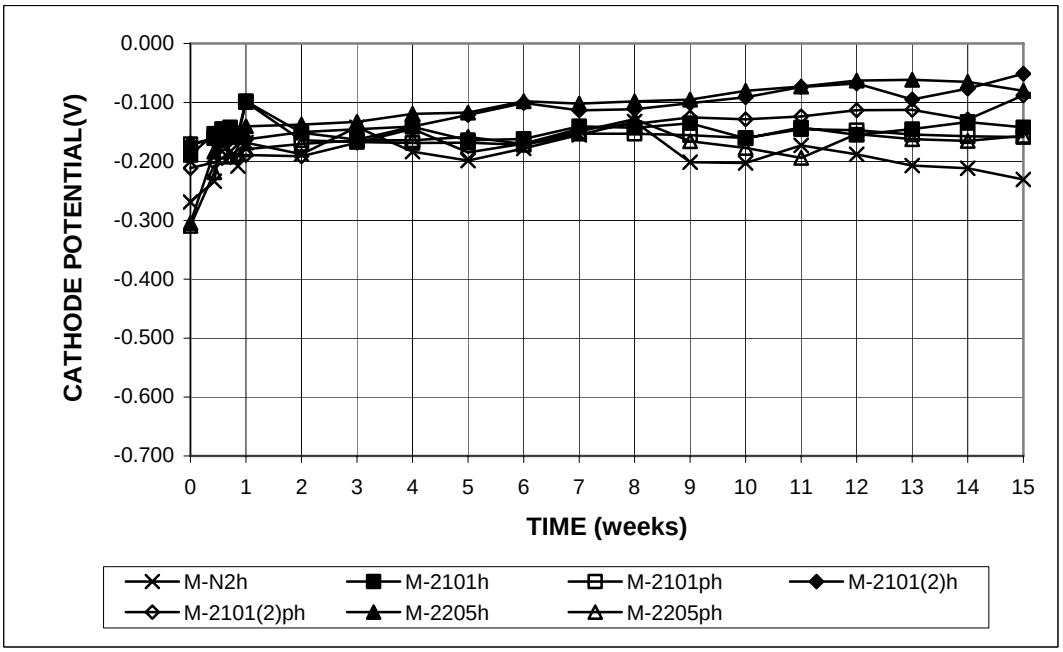

Figure 3.69b - Macrocell test. Average cathode corrosion potentials with respect to saturated calomel electrode for bare conventional and duplex stainless steels in simulated concrete pore solution with 6.04 molal ion NaCl.

The results for bare conventional N2 steel, and duplex stainless steels, 2101(2)p, 2205 and 2205p, subjected to a 6.04 m ion NaCl solution with the solution replaced every five weeks are shown in Figures 3.70a and 3.70b for the average corrosion rates and Figures 3.71a and 3.71b for the average total corrosion losses. The values at 15 weeks are summarized in Tables 3.17 and 3.18. The results of the Student's t-test are shown in Tables C.9 through C.12. The comparison between the tests with and without the solution replaced is presented in Section 3.5.

When replacing the test solutions every 5 weeks, 2101(2)p steel and 2205 steel exhibited maximum corrosion rates of 0.42 μm/yr and 1.7 μm/yr at 13 weeks, respectively. After 15 weeks, the corrosion rates were 0.13 μm/yr for 2101(2)p steel and 1.6 μm/yr for the 2205 steel. As before, the lowest corrosion rate was exhibited by pickled 2205 steel, below 0.10 μm/yr for the first 14 weeks of the test period and ending at 0.18 μm/yr, compared to a rate of 30 μm/yr exhibited by conventional steel at the end of the test. Pickled 2205 steel is the only steel that meets the requirement of the Kansas Department of Transportation Special Provision to the Standard Specifications on Stainless Steel Reinforcing Bars. The special provision requires that the average corrosion rate for a minimum of five specimens must at no time during the 15-week test period exceed 0.25 μm/yr, with no single specimen exceeding a corrosion rate of 0.5 μm/yr.

At 15 weeks, conventional steel had the highest corrosion loss, 8.9 μm, followed by the 2205 steel at 0.29 μm. At this point, the second heat of picked 2101 steel, 2101(2)p, exhibited a corrosion loss of 0.05 μm, while pickled 2205 steel, 2205p, had the lowest loss, 0.01 μm, corresponding to 0.1% of the value for conventional steel.

Tables C.9 and C.10 show that the differences in both the corrosion rates and losses between 2205 and 2205p steels are significant at $\alpha = 0.02$. Table C.11 and C.12 show that the differences in both the corrosion rates and losses between 2101(2)p and 2205 steels are significant at $\alpha = 0.02$, while the differences between 2101(2)p and 2205p steels are not statistically significant.

The average corrosion potentials of the anode and cathode for the duplex stainless steels in the high NaCl concentration solution (replaced every five weeks) are shown in Figures 3.72a and 3.72b, respectively. The anode corrosion potentials for the duplex steels remained, for the most part, between –0.135 and –0.200 V throughout the test, with 2205 steel showing values more negative than –0.200 V during the last few weeks of the test. At 15 weeks, the anode corrosion potentials were –0.183, –0.214, and –0.143 V for the 2101(2)p, 2205, and 2205p steels, respectively. The duplex stainless steels had corrosion potentials between –0.100 and –0.200 V at the cathode, and the corrosion potential became slightly more positive with time, with a value of –0.160 V for the 2101(2)p steel, –0.140 V for the 2205 steel, and –0.135 V for the 2205p steel at 15 weeks.

Table 3.17 - Average corrosion rates at 15 weeks for bare conventional and duplex stainless steels in simulated concrete pore solution with 6.04 m ion NaCl in macrocell test (solution replaced every five weeks).

Specimen designation*	Steel type	Specimen corrosion rates (μm/yr)						Average (μm/yr)	Standard deviation
		1	2	3	4	5	6		
Bare bars in 6.04 m NaCl									
M-N2h-r	N2	42.11	29.51	32.28	24.83	22.66	26.56	29.66	6.98
M-2101(2)ph-r	2101(2)p	0.00	0.06	0.00	0.03	0.00	0.66	0.13	0.27
M-2205h-r	2205	1.13	1.71	0.06	2.37	2.34	1.71	1.55	0.87
M-2205ph-r	2205p	0.12	0.12	0.09	0.35	0.26	0.14	0.18	0.10

*** A-B-C**

A: test method; M = macrocell test.

B: steel type and test condition; N3 and N4 = conventional steel; 2101(2) = the second heat of 2101 duplex stainless steel (21% chromium, 1% nickel), 2205 = 2205 duplex stainless steel (22% chromium, 5% nickle), p = pickled, h = 6.04 m ion NaCl concentration;

C: r = the test solutions are replaced every five weeks.

Table 3.18 - Average total corrosion losses at 15 weeks for bare conventional and duplex stainless steels in simulated concrete pore solution with 6.04 m ion NaCl in macrocell test (solution replaced every five weeks).

Specimen designation*	Steel type	Specimen total corrosion losses (μm)						Average (μm)	Standard deviation
		1	2	3	4	5	6		
Bare bars in 6.04 m NaCl									
M-N2h-r	N2	10.53	10.26	8.59	8.41	7.99	7.48	8.88	1.24
M-2101(2)ph-r	2101(2)p	0.04	0.02	0.02	0.01	0.01	0.20	0.05	0.07
M-2205h-r	2205	0.22	0.51	0.08	0.44	0.35	0.17	0.29	0.16
M-2205ph-r	2205p	0.02	0.01	0.01	0.01	0.01	0.00	0.01	0.00

*** A-B-C**

A: test method; M = macrocell test.

B: steel type and test condition; N3 and N4 = conventional steel; 2101(2) = the second heat of 2101 duplex stainless steel (21% chromium, 1% nickel), 2205 = 2205 duplex stainless steel (22% chromium, 5% nickle), p = pickled, h = 6.04 m ion NaCl concentration;

C: r = the test solutions are replaced every five weeks.

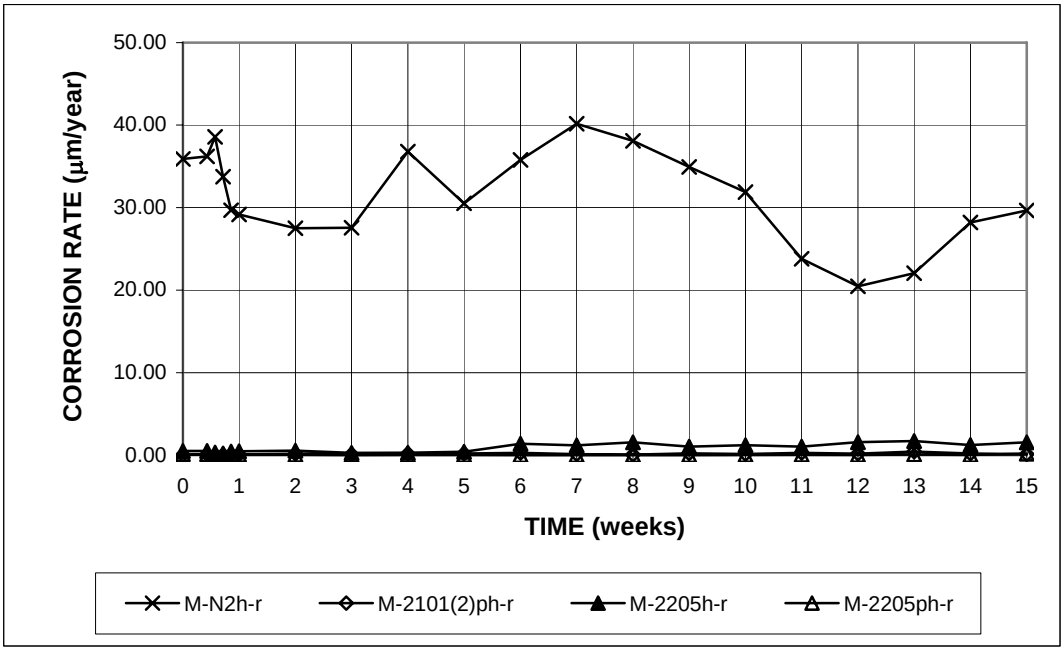

(a)

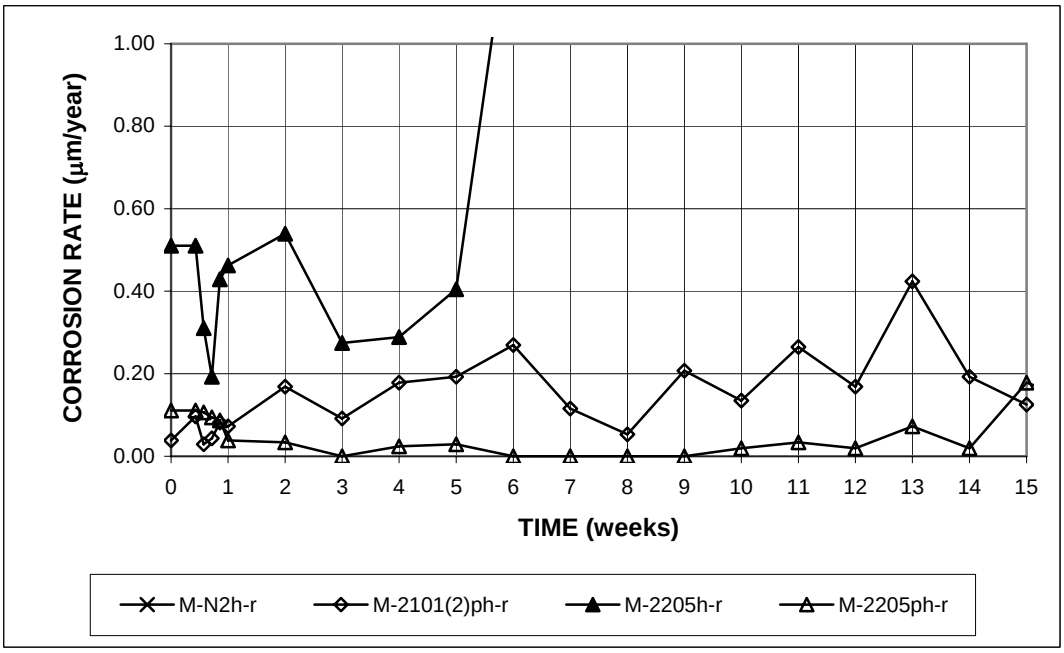

(b)

Figure 3.70 - Macrocell test. Average corrosion rates for bare conventional and duplex stainless steels in simulated concrete pore solution with 6.04 molal ion NaCl. Solutions are replaced every five weeks.

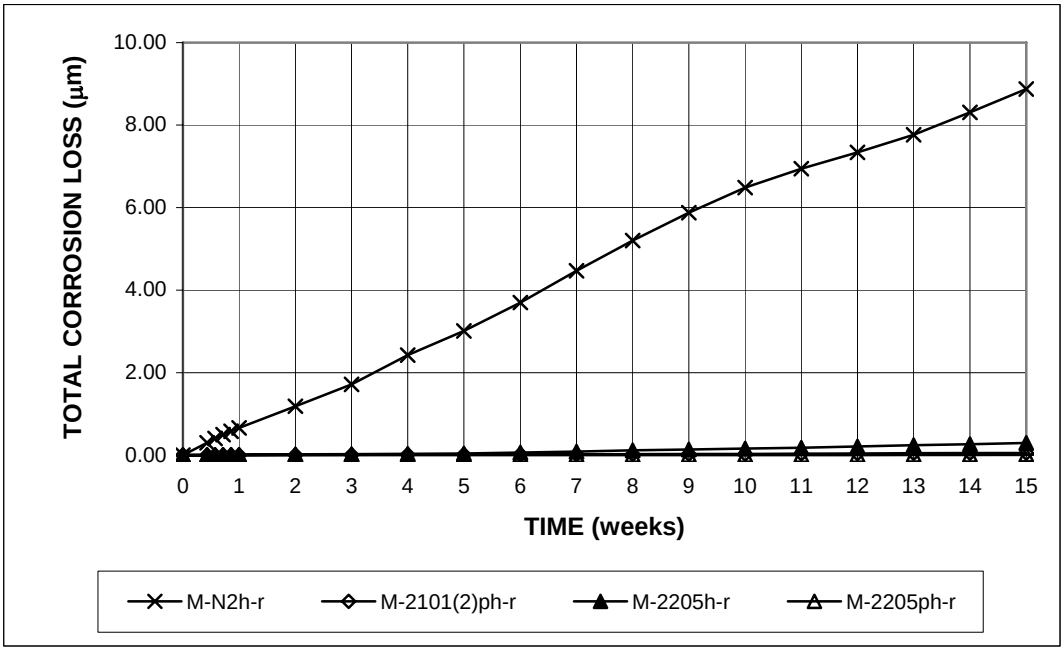

(a)

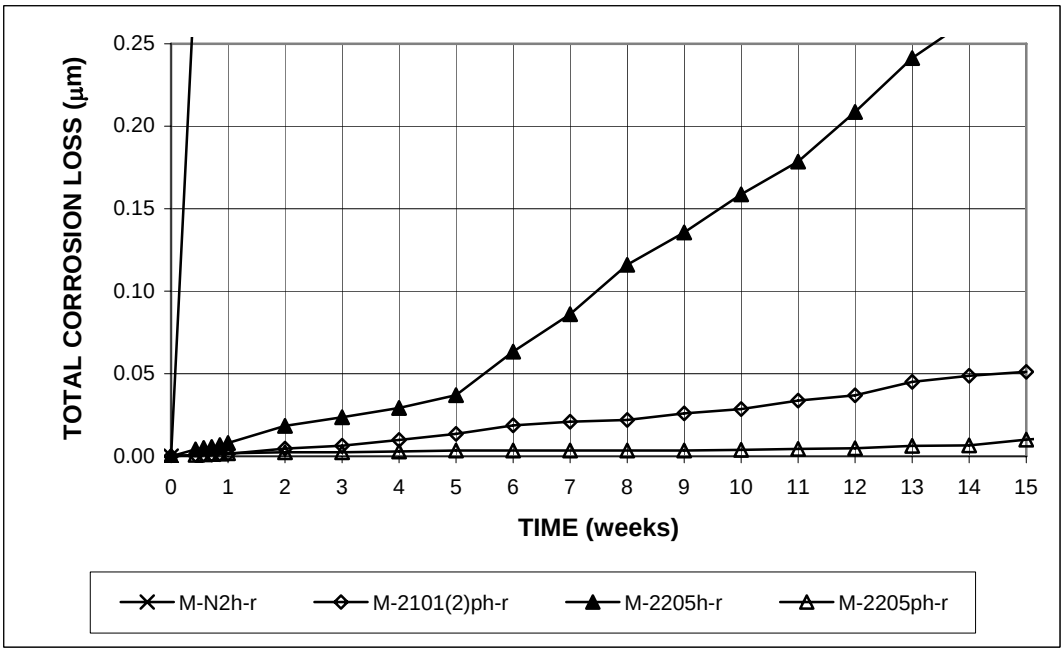

(b)

Figure 3.71 - Macrocell test. Average total corrosion losses for bare conventional and duplex stainless steels in simulated concrete pore solution with 6.04 molal ion NaCl. Solutions are replaced every five weeks.

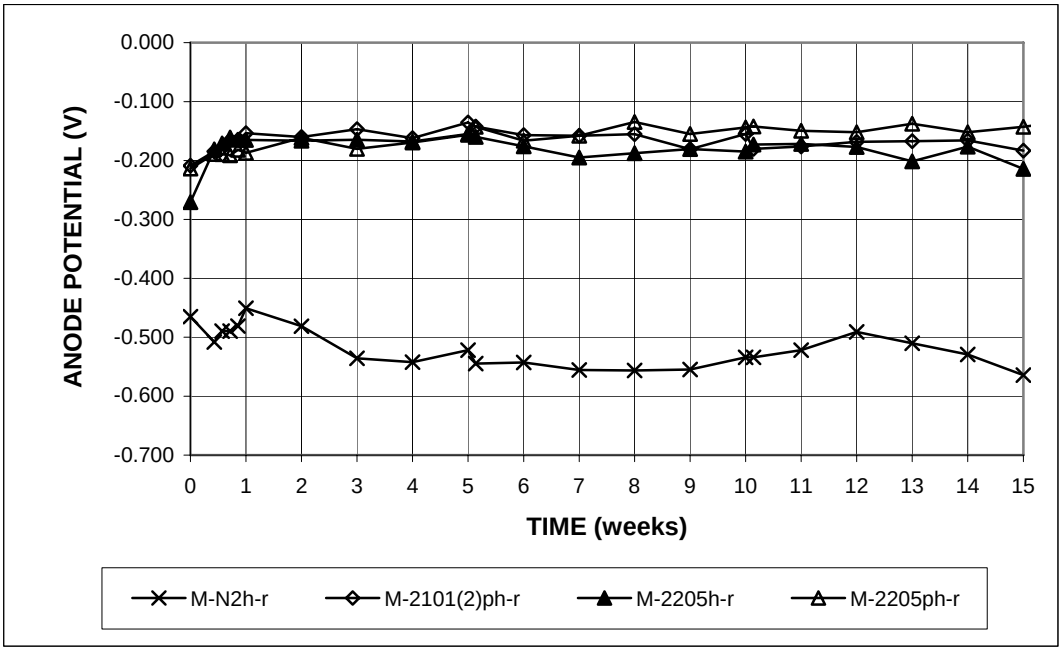

Figure 3.72a - Macrocell test. Average anode corrosion potentials with respect to saturated calomel electrode for bare conventional and duplex stainless steels in simulated concrete pore solution with 6.04 molal ion NaCl. Solutions are replaced every 5 weeks.

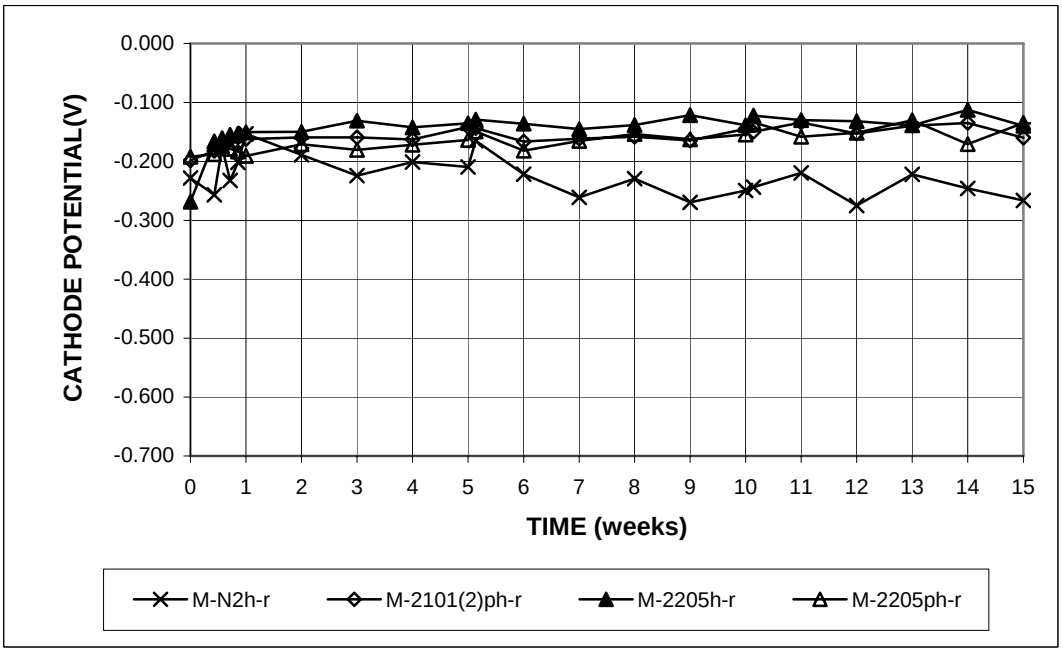

Figure 3.72b - Macrocell test. Average cathode corrosion potentials with respect to saturated calomel electrode for bare conventional and duplex stainless steels in simulated concrete pore solution with 6.04 molal ion NaCl. Solutions are replaced every 5 weeks.

Mortar-wrapped specimens – The average corrosion rates for the mortar-wrapped duplex stainless steel bars are shown in Figures 3.73a and 3.73b. The values at 15 weeks are summarized in Table 3.19. Solutions were not replaced in these tests.

Again, conventional steel exhibited the highest corrosion rate, followed by 2101 and 2101(2) steel, with values of 16.3 μm/yr for conventional steel, 8.7 μm/yr for the 2101 steel, and 5.1 μm/yr for the 2101(2) steel at 15 weeks (Table C.7 shows that the difference between conventional steel and 2101 steel is significant at $\alpha = 0.2$, while the difference between conventional steel and 2101(2) steel is significant at $\alpha = 0.02$). The average corrosion rates for the pickled 2101 steels and the nonpickled and pickled 2205 steels remained below 0.25 μm/yr for the duration of the test, ending with values of 0.11 μm/yr or less, less than or equal to 0.7% of the rate exhibited by conventional steel.

The average total corrosion losses are shown in Figures 3.74a and 3.74b, and the values at 15 weeks are summarized in Table 3.20. At 15 weeks, conventional steel exhibited the highest corrosion loss, 3.8 μm, followed by the nonpickled 2101 steels, 2101 and 2101(2), at about 1.0 and 0.80 μm, respectively (Table C.8 shows that the differences between conventional steel and either 2101 or 2101(2) steel are significant at $\alpha = 0.02$). At this point, the corrosion losses for the rest of the duplex steels were below 0.03 μm, corresponding to 0.8% of the value for conventional steel. Tables C.10 and C.12 show that the differences between 2205 and 2205p steels, and between 2101(2)p steel and either 2205 or 2205p steel are not statistically significant.

The average corrosion potentials of the anode and cathode for the mortar-wrapped duplex stainless steels are shown in Figures 3.75a and 3.75b, respectively. All duplex stainless steels exhibited anode corrosion potentials between –0.100 and –0.150 V, with the exception of the nonpickled 2101 steels, for which anode

corrosion potentials dropped to values below –0.200 V after four weeks for 2101(2) steel, and seven weeks for 2101 steel, ending with values of about –0.350 V. Compared to the cathode corrosion potential for conventional steel (around –0.200 V), the corrosion potentials for duplex stainless steels at the cathode were more positive, ranging from –0.100 to –0.150 V throughout the test period. The cathode corrosion potentials indicate that conventional steel and all duplex stainless steels at the cathode remained passive for the duration of the test.

Table 3.19 - Average corrosion rates at 15 weeks for mortar-wrapped conventional and duplex stainless steels in simulated concrete pore solution with 1.6 m ion NaCl in macrocell test

Specimen designation*	Steel type	Specimen corrosion rates (μm/yr)						Average (μm/yr)	Standard deviation
		1	2	3	4	5	6		
Mortar wrapped specimens in 1.6 m NaCl									
M-N2m	N2	17.43	19.02	24.83	5.49	14.65		16.28	7.09
M-2101m	2101	9.13	13.06	11.56	0.95			8.68	5.40
M-2101pm	2101p	0.00	0.00	0.03	0.06			0.02	0.03
M-2101(2)m	2101(2)	5.52	4.91	5.81	3.76	8.87	1.76	5.11	2.36
M-2101(2)pm	2101(2)p	0.09	0.03	0.12	0.03	0.17	0.20	0.11	0.07
M-2205m	2205	0.06	0.03	0.00	0.03	0.06	0.00	0.03	0.03
M-2205pm	2205p	0.09	0.00	0.00	0.12	0.14	0.00	0.06	0.07

*** A-B**

A: test method; M = macrocell test.

B: steel type and test condition; N3 and N4 = conventional steel; 2101 and 2101(2) = two heats of 2101 duplex stainless steel (21% chromium, 1% nickel), 2205 = 2205 duplex stainless steel (22% chromium, 5% nickle), p = pickled, m = mortar-wrapped specimens;

Table 3.20 - Average total corrosion losses at 15 weeks for mortar-wrapped conventional and duplex stainless steels in simulated concrete pore solution with 1.6 m ion NaCl in macrocell test

Specimen designation*	Steel type	Specimen total corrosion losses (μm)						Average (μm)	Standard deviation
		1	2	3	4	5	6		
Mortar wrapped specimens in 1.6 m NaCl									
M-N2m	N2	4.04	2.96	2.22	3.75	6.09		3.81	1.46
M-2101m	2101	0.75	1.95	0.94	0.32			0.99	0.69
M-2101pm	2101p	0.01	0.00	0.02	0.02			0.01	0.01
M-2101(2)m	2101(2)	1.15	0.50	0.77	0.54	1.21	0.64	0.80	0.31
M-2101(2)pm	2101(2)p	0.02	0.02	0.03	0.02	0.04	0.03	0.03	0.01
M-2205m	2205	0.03	0.03	0.02	0.02	0.03	0.02	0.03	0.01
M-2205pm	2205p	0.04	0.03	0.02	0.02	0.02	0.02	0.03	0.01

*** A-B**

A: test method; M = macrocell test.

B: steel type and test condition; N3 and N4 = conventional steel; 2101 and 2101(2) = two heats of 2101 duplex stainless steel (21% chromium, 1% nickel), 2205 = 2205 duplex stainless steel (22% chromium, 5% nickle), p = pickled, m = mortar-wrapped specimens;

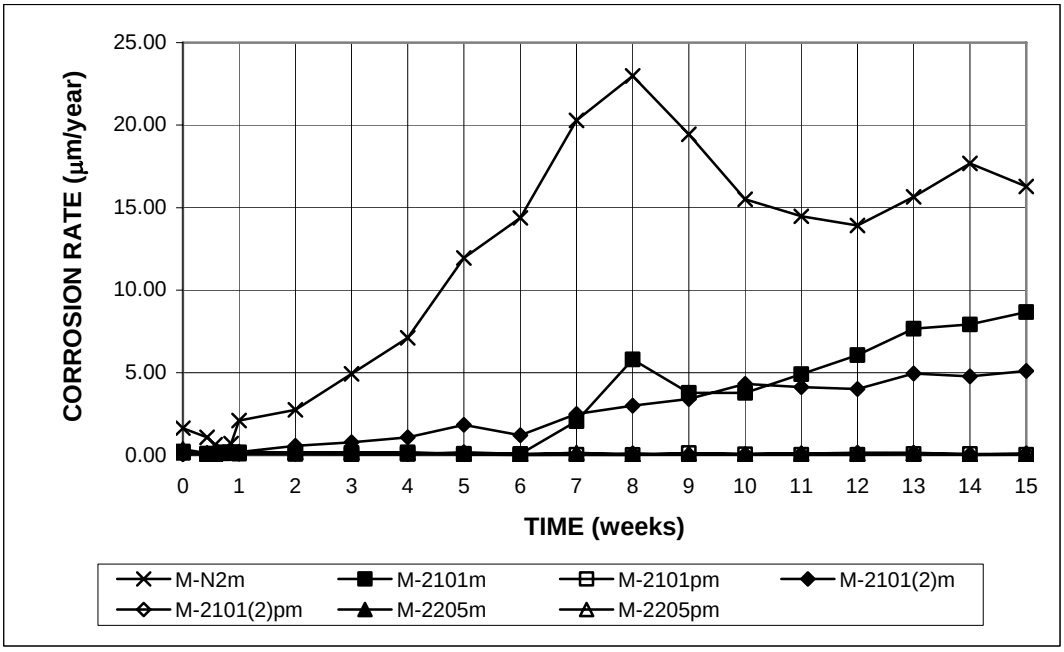

(a)

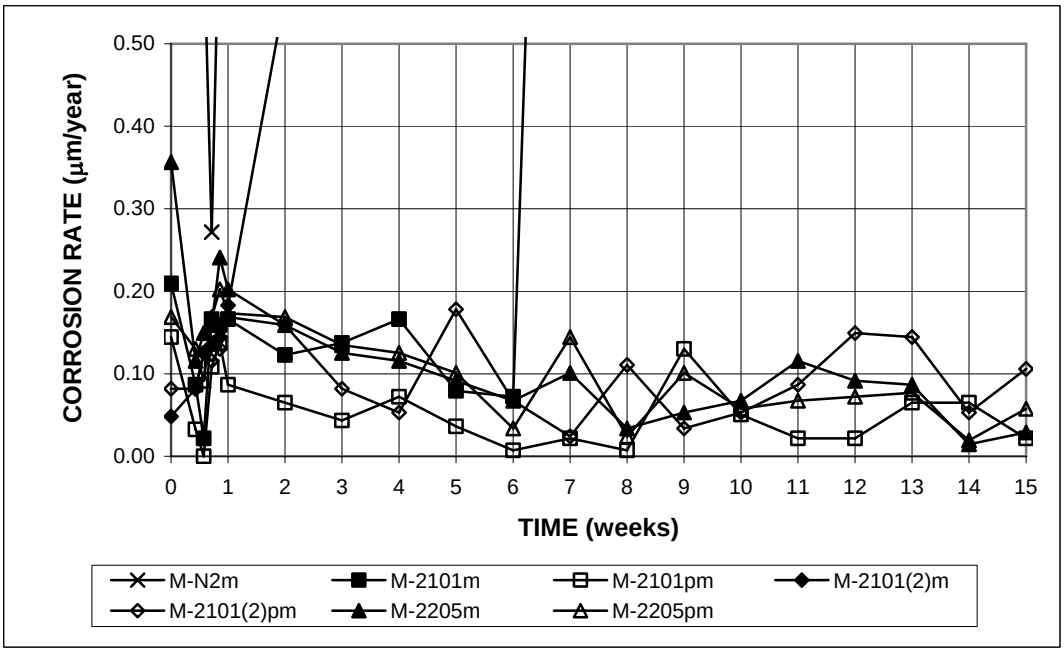

(b)

Figure 3.73 - Macrocell test. Average corrosion rates for morter-wrapped conventional and duplex stainless steels in simulated concrete pore solution with 1.6 molal ion NaCl.

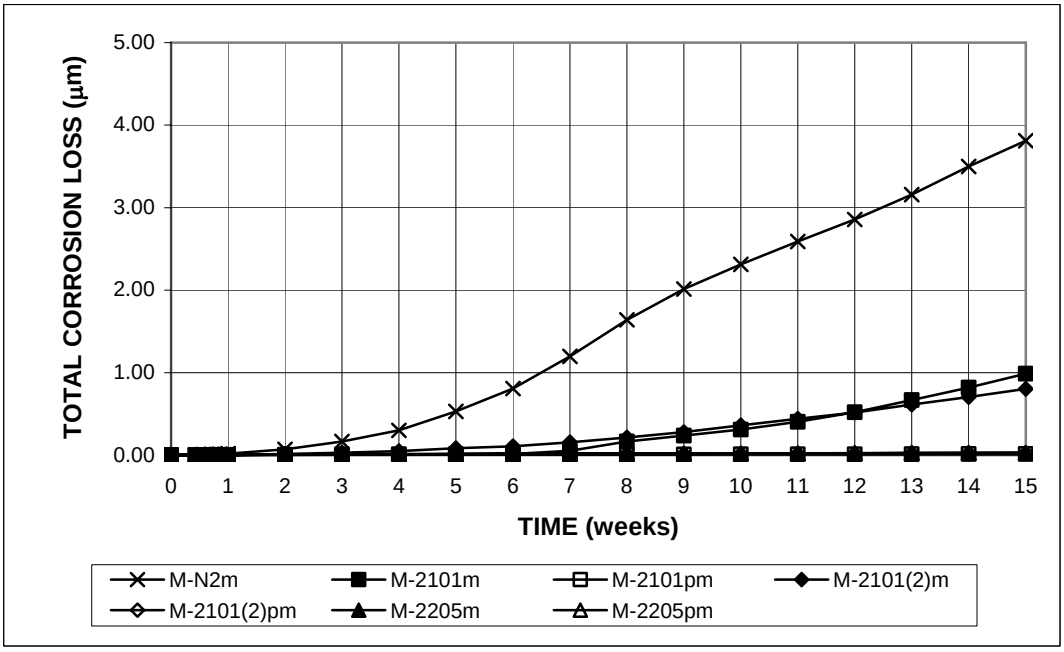

(a)

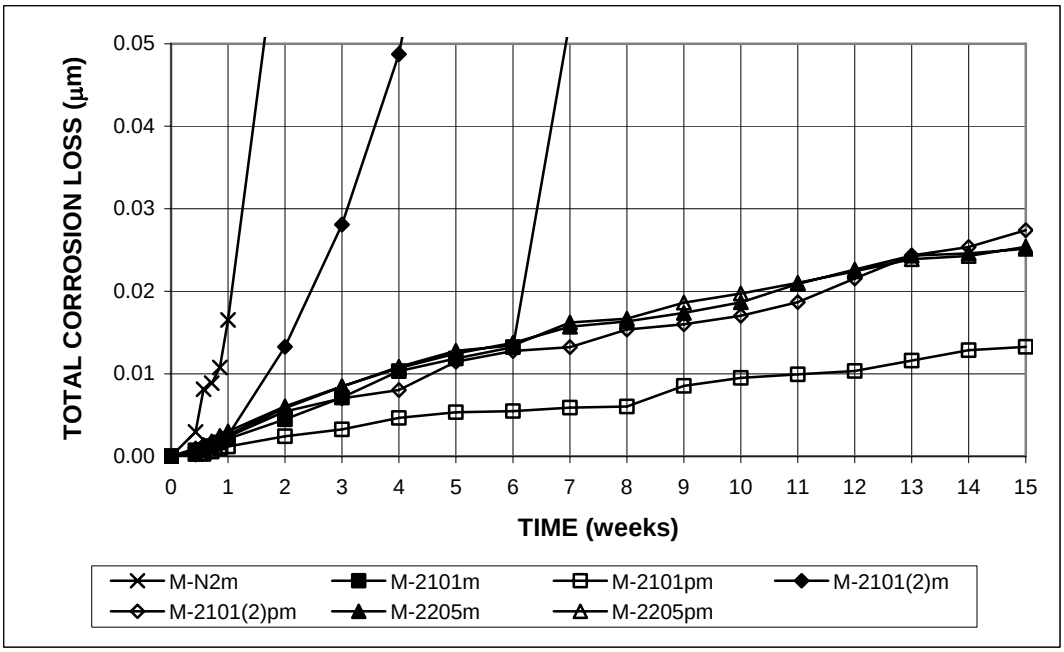

(b)

Figure 3.74 - Macrocell test. Average total corrosion losses for morter-wrapped conventional and duplex stainless steels in simulated concrete pore solution with 1.6 molal ion NaCl.

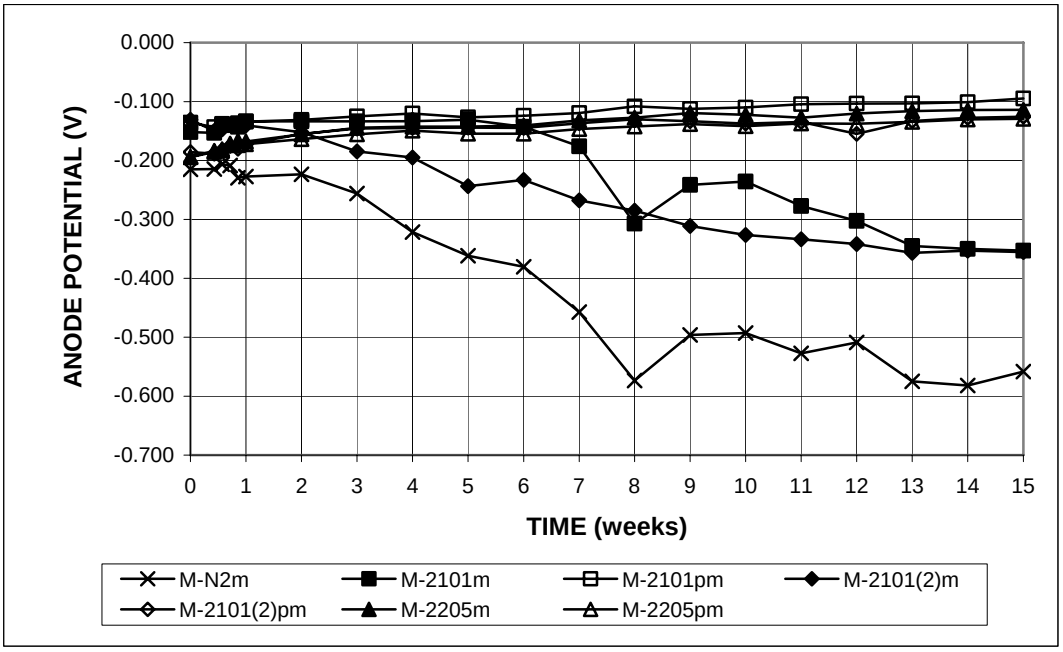

Figure 3.75a - Macrocell test. Average anode corrosion potentials with respect to saturated calomel electrode for mortar-wrapped conventional and duplex stainless steels in simulated concrete pore solution with 1.6 molal ion NaCl.

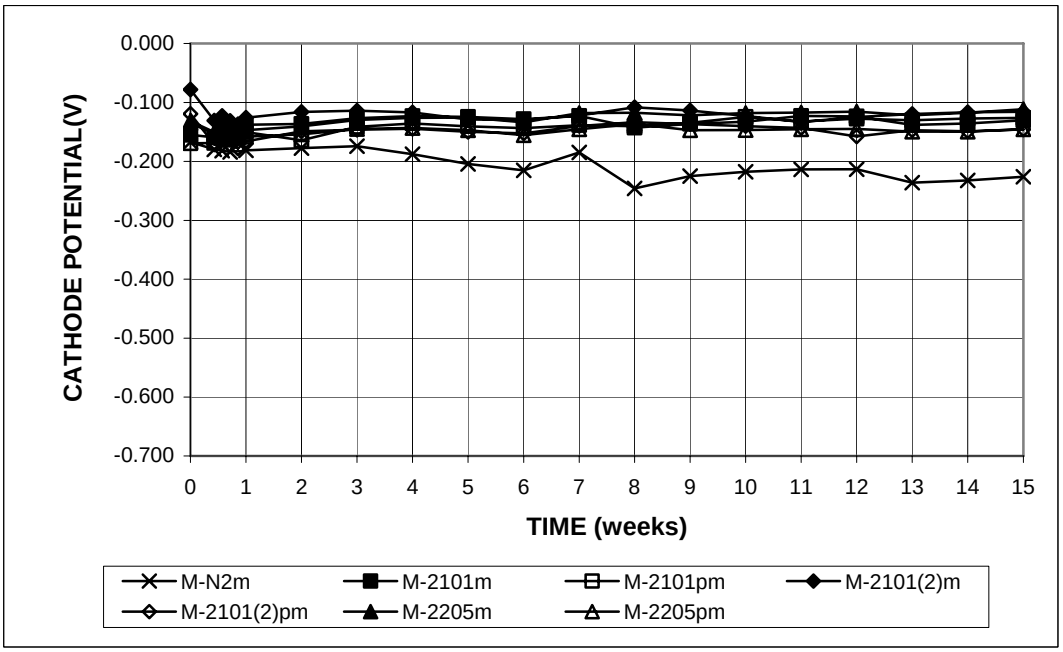

Figure 3.75b - Macrocell test. Average cathode corrosion potentials with respect to saturated calomel electrode for mortar-wrapped conventional and duplex stainless steels in simulated concrete pore solution with 1.6 molal ion NaCl.

Visual Inspection – At the end of the tests, the duplex stainless steels were visually inspected. As shown in Figures 3.76 and 3.77, corrosion products were observed on the bare anode bars for the 2101 and 2101(2) steels subjected to the 1.6 m ion NaCl solution, while the anode bars for the pickled 2101 steels and the nonpickled and pickled 2205 steels did not exhibited corrosion products in the low NaCl concentration solution.

Figure 3.76 – Corrosion products on bare 2101 steel anode bar (M-2101-5) in 1.6 m NaCl solution at 15 weeks

Figure 3.77 – Corrosion products on bare 2101(2) steel anode bar (M-2101(2)-5) in 1.6 m NaCl solution at 15 weeks.

Figures 3.78 through 3.82 show the corrosion products on the anode bars for the 2101, 2101(2), 2101p, 2101(2)p, and 2205 steels subjected to the 6.04 m ion NaCl solution. The pickled 2205 is the only steel that did not exhibited corrosion products in the high NaCl concentration solution, as shown in Figure 3.83.

Figure 3.78 – Corrosion products on bare 2101 steel anode bar (M-2101h-3) in 6.04 m NaCl solution at 15 weeks

Figure 3.79 – Corrosion products on bare 2101(2) steel anode bar [M-2101(2)h-3] in 6.04 m NaCl solution at 15 weeks

Figure 3.80 – Corrosion products on bare 2101p steel anode bar (M-2101ph-5) in 6.04 m NaCl solution at 15 weeks

Figure 3.81 – Corrosion products on bare 2101(2)p steel anode bar [M-2101(2)ph-6] in 6.04 m NaCl solution at 15 weeks

Figure 3.82 – Corrosion products on bare 2205 steel anode bar (M-2205h-2) in 6.04 m NaCl solution at 15 weeks

Figure 3.83 – No corrosion products on bare 2205p steel anode bar (M-2205ph-1) in 6.04 m NaCl solution at 15 weeks

For mortar-wrapped specimens, the mortar cover was removed; corrosion products were observed on anode bars for the 2101 and 2101(2) steels, as shown in Figure 3.84 and 3.85, respectively, while no corrosion products were observed on the anode bars for the 2101p, 2101(2)p, 2205, and 2205p steels.

Figure 3.84 – Corrosion products on 2101 steel anode bar (M-2101m-1) after removal of mortar cover at 15 weeks

Figure 3.85 – Corrosion products on 2101(2) steel anode bar [M-2101(2)m-1] after removal of mortar cover at 15 weeks

3.4.2 Bench-scale tests

All of the duplex stainless steels, 2101, 2101(2), 2101p, 2101(2)p, 2205, and 2205p, were tested with the same bars in both the top and bottom mats in the Southern Exposure and cracked beam tests. In addition, the combination of duplex stainless steel and conventional steel was evaluated in the Southern Exposure test using (1) nonpickled 2205 steel on the top mat and N2 steel on the bottom mat (SE-2205/N2), and (2) N2 steel on the top mat and nonpickled 2205 steel on the bottom mat (SE-N2/2205).

Southern Exposure test – Average corrosion rates versus time for specimens with the same duplex stainless steel in the top and bottom mats are shown in Figures 3.86a and 3.86b. The average corrosion rates at 96 weeks are summarized in Table 3.21. Conventional steel and the first heat of nonpickled 2101 steel exhibited the highest corrosion rates. The corrosion rate for N conventional steel began to increase from a negligible value at 3 weeks, peaking at 7.5 μm/yr at 43 weeks and ending with a value of 2.8 μm/yr at 96 weeks, while the 2101 steel started to corrode at 8 weeks, with a maximum corrosion rate of 5.5 μm/yr at 49 weeks, ending at 3.7 μm/yr at 96 weeks. The 2101p and 2101(2) steels exhibited significant corrosion during the second half of the test period, with 2101p steel corroding at 1.5 μm/yr and 2101(2) steel corroding at 0.39 μm/yr at the end of the test. 2205 steel began to show observable corrosion during the last few weeks of the test period, ending with a value of 0.2 μm/yr, less than 1/10 of the corrosion rate of the conventional steel. 2101(2)p and 2205p steel exhibited the lowest average corrosion rates, remaining below 0.1 μm/yr throughout the test period, although 2101(2)p steel showed a jump to 0.07 μm/yr during the last week due to one specimen that exhibited a corrosion rate of 0.24 μm/yr.

The results of the Student's t-test comparing the average corrosion rates at 96 weeks are presented in Tables C.7, C.9, and C.11. Table C.7 shows that the difference between N and 2101 steels is not statistically significant [the difference is also not significant at 70 weeks (Balma et al. 2005)], while the difference between N and 2101(2) steels is significant at $\alpha = 0.10$ [the difference is significant at $\alpha = 0.02$ at 70 weeks (Balma et al. 2005)].

Table C.9 shows that the differences between 2101 and 2101p steels, and between 2101(2) and 2101(2)p steels are significant at $\alpha = 0.20$, while the difference between 2205 and 2205p steels is not significant.

Table C.11 shows the differences between 2101(2)p steel and either 2205 or 2205p steel are not statistically significant.

The average total corrosion losses are shown in Figures 3.87a and 3.87b, and the values at 96 weeks are summarized in Table 3.22. At 96 weeks, conventional steel exhibited the highest corrosion loss, 7.6 μm, followed by the first heat of nonpickled 2101 steel at 4.2 μm; 2101p and 2101(2) steel had corrosion losses of 0.75 and 0.39 μm, respectively. At this point, the corrosion losses for the rest of the duplex steels were below 0.02 μm, less than 0.3% of the value for conventional steel.

The results of the Student's t-test comparing the average corrosion losses are presented in Tables C.8, C.10, and C.12. Table C.8 shows that the difference between N and 2101 steels is significant at $\alpha = 0.10$, while the difference between N and 2101(2) steels is significant at $\alpha = 0.02$.

Table C.10 shows that the difference between 2101 and 2101p steels is significant at $\alpha = 0.10$; the difference between 2101(2) and 2101(2)p steels is significant at $\alpha = 0.20$; and the difference between 2205 and 2205p steels is not statistically significant.

Table C.12 shows the differences between 2101(2)p steel and either 2205 or 2205p steel are not statistically significant.

The average corrosion potentials of the top and bottom mats of steel are presented in Figures 3.88a and 3.88b, respectively. The top mat of the conventional steel had a corrosion potential more negative than –0.350 V, indicating active corrosion, at seven weeks, followed the 2101 steel at 37 weeks, 2101p steel at 66 weeks, and 2101(2) at 86 weeks. The top mat corrosion potentials for the 2101(2)p, 2205, and 2205p steels remained more positive than –0.300 V for the duration of the test, indicating a low tendency to corrode. At the end of the test, the anode corrosion potentials were –0.593 V for the conventional steel, –0.479 V for 2101 steel, –0.440 V for 2101p steel, –0.372 for 2101(2) steel, –0.288 V for 2101(2)p steel, –0.238 V for 2205 steel, –0.183 for 2205p steel. With the exception of 2205p steel, the corrosion potential of all steels continued to become more negative as the test concluded. The bottom mat corrosion potentials for duplex stainless steels 2101, 2101p and 2101(2) remained around –0.300 V during the second half of the test period, while 2101(2)p, 2205 and 2205p steel had corrosion potentials that were more positive than –0.250 V for most of the test period.

The average mat-to-mat resistances for the Southern Exposure test specimens with duplex stainless steels are shown in Figure 3.89. For all steels, the mat-to-mat resistances had initial values of about 150 ohms, increasing with time at a nearly same rate for the first 40 weeks, reaching a value of about 500 ohms. During the second half of the test, in most cases, the mat-to-mat resistances for duplex steels continued to increase while exhibiting progressively larger scatter, with 2101(2), 2101(2)p, 2205, and 2205p steel showing higher values; the mat-to-mat resistances ranged from 312 ohms for 2101 steel to 1792 ohms for 2101(2) steel at 96 weeks; the

mat-to-mat resistance for conventional N steel increased to about 1200 ohms at 67 weeks and then dropped to 700 ohms at 96 weeks. As mentioned in Section 3.3.2, the changes in mat-to-mat resistances may be caused by the deposit of corrosion products on the bars, cracking of the concrete, and changes in the moisture content of the specimens.

The average corrosion rates and total corrosion losses for the Southern Exposure specimens containing both nonpickled 2205 duplex stainless steel and conventional steel are compared with those for specimens with these steels alone in Figures 3.90 and 3.91, respectively. Tables 3.21 and 3.22 summarize the average corrosion rates and total corrosion losses at 15 weeks. During the second half of the test, the 2205/N2 specimens exhibited slightly higher corrosion rates than the specimens with the 2205 steel alone, while the corrosion rates of the N2/2205 specimens were slightly lower than those of the specimens with conventional steel alone during most of the test period. After 96 weeks, the 2205/N2 specimens had an average total corrosion loss of 0.14 μm, compared to a value of 0.1 μm for the all 2205 specimens (the difference is not significant, as shown in Table C.8), while the total corrosion loss was 6.3 μm for the N2/2205 specimens and 7.6 μm for the all conventional steel specimens (the difference is not significant).

The average corrosion potentials of the top and bottom mats of steel for specimens with the combination of 2205 and conventional steel are shown in Figures 3.92a and 3.92b, respectively. The average top mat potential of the 2205/N2 specimens and bottom mat potential of the N2/2205 specimens were slightly more negative than those of the all 2205 specimens, respectively. Both of the corrosion potentials for the 2205 steel, however, remained more positive than –0.350 V,

indicating a low tendency to corrode for the 2205 steel in conjunction with conventional steel.

The average mat-to-mat resistances for the Southern Exposure specimens with the combination of 2205 and conventional steel are shown in Figure 3.93. Overall, the specimens exhibited increasing mat-to-mat resistances. The mat-to-mat resistances had similar initial values of about 150 ohms, reaching about 3500 ohms for the 2205/N2 specimens, 2000 ohms for the 2205 and N2/2205 specimens at the end of the test. As described before, the mat-to-mat resistance for the specimens with conventional steel alone increased to about 1200 ohms at 67 weeks and then dropped to 700 ohms at 96 weeks. The changes in mat-to-mat resistances may be caused by the deposit of corrosion products on the bars, cracking of the concrete, and changes in the moisture content of the specimens.

Table 3.21 - Average corrosion rates at 96 weeks for specimens with conventional and duplex stainless steels in Southern Exposure test

Specimen designation*	Steel type	Specimen corrosion rates (μm/yr)						Average (μm/yr)	Standard deviation
		1	2	3	4	5	6		
Southern Exposure test									
SE-N	N	5.11	0.00	0.00	1.67	5.35	4.52	2.77	2.52
SE-2101	2101	1.70	4.34	5.19				3.74	1.82
SE-2101p	2101p	0.47	3.39	0.54				1.47	1.67
SE-2101(2)	2101(2)	0.01	0.36	0.00	0.48	1.10		0.39	0.45
SE-2101(2)p	2101(2)p	0.01	0.02	0.07	0.00	0.24		0.07	0.10
SE-2205	2205	0.26	0.03	0.64	0.01	0.00		0.19	0.28
SE-2205p	2205p	0.00	0.00	0.02	0.01	0.01		0.01	0.01
SE-N2/2205	N2/2205	4.42	2.36	1.13				2.64	1.67
SE-2205/N2	2205/N2	0.05	0.00	0.25				0.10	0.13

*** A-B**

A: test method; SE = Southern Exposure test.

B: steel type and test condition; N = conventional steel; 2101 and 2101(2) = two heats of 2101 duplex stainles steel (21% chromium, 1% nickel), 2205 = 2205 duplex stainless steel (22% chromium, 5% nickle), N2/2205 = N2 steel at the top mat, 2205 steel at the bottom mat; 2205/N2 = 2205 steel at the top mat, N2 steel at the bottom mat; p = pickled.

Table 3.22 - Average total corrosion losses at 96 weeks for specimens with conventional and duplex stainless steels in Southern Exposure test

Specimen designation*	Steel type	Specimen total corrosion losses (μm)						Average (μm)	Standard deviation
		1	2	3	4	5	6		
Southern Exposure test									
SE-N	N	10.36	9.57	8.04	4.35	6.42	7.10	7.64	2.18
SE-2101	2101	2.03	4.68	5.93				4.21	1.99
SE-2101p	2101p	0.11	1.99	0.14				0.75	1.08
SE-2101(2)	2101(2)	0.22	0.18	0.01	0.56	0.99		0.39	0.39
SE-2101(2)p	2101(2)p	0.01	0.02	0.02	0.01	0.05		0.02	0.02
SE-2205	2205	0.05	0.11	0.33	0.01	0.00		0.10	0.13
SE-2205p	2205p	0.02	0.03	0.03	0.01	0.01		0.02	0.01
SE-N2/2205	N2/2205	4.74	5.54	8.48				6.25	1.96
SE-2205/N2	2205/N2	0.11	0.08	0.24				0.14	0.09

*** A-B**

A: test method; SE = Southern Exposure test.

B: steel type and test condition; N = conventional steel; 2101 and 2101(2) = two heats of 2101 duplex stainles steel (21% chromium, 1% nickel), 2205 = 2205 duplex stainless steel (22% chromium, 5% nickle), N2/2205 = N2 steel at the top mat, 2205 steel at the bottom mat; 2205/N2 = 2205 steel at the top mat, N2 steel at the bottom mat; p = pickled.

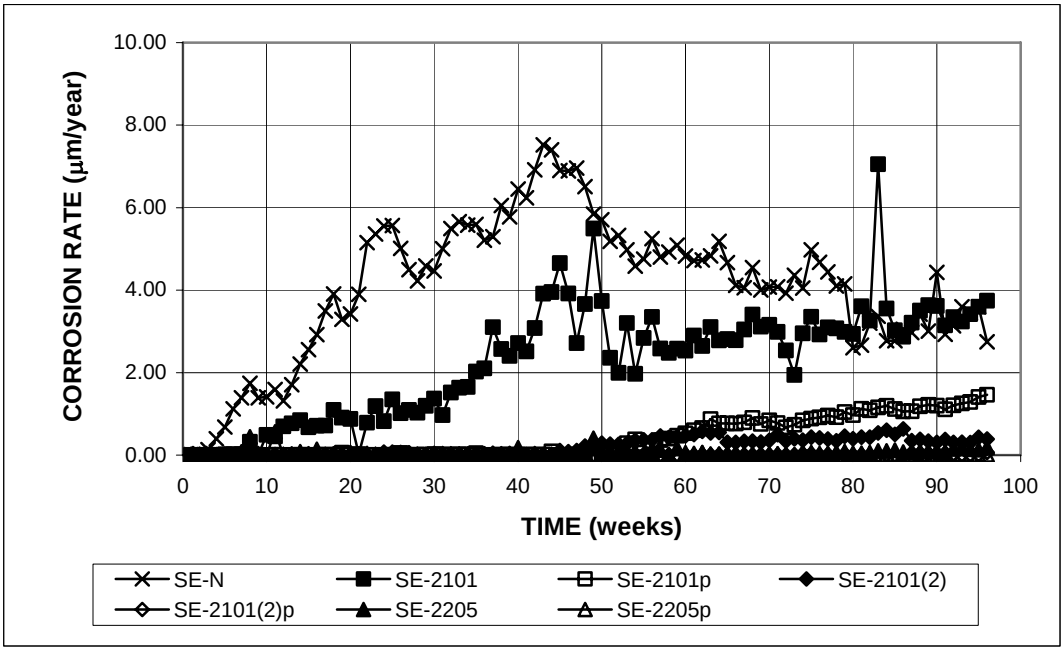

(a)

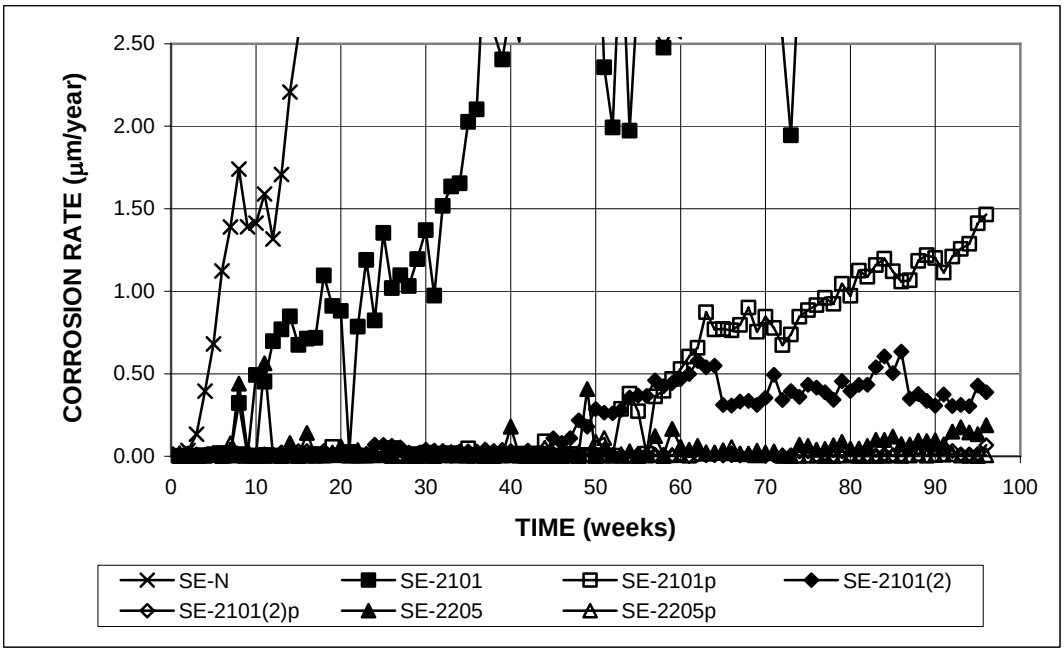

(b)

Figure 3.86 - Southern Exposure test. Average corrosion rates of conventional and duplex stainless steels, specimens w/c = 0.45, ponded with 15% NaCl solution.

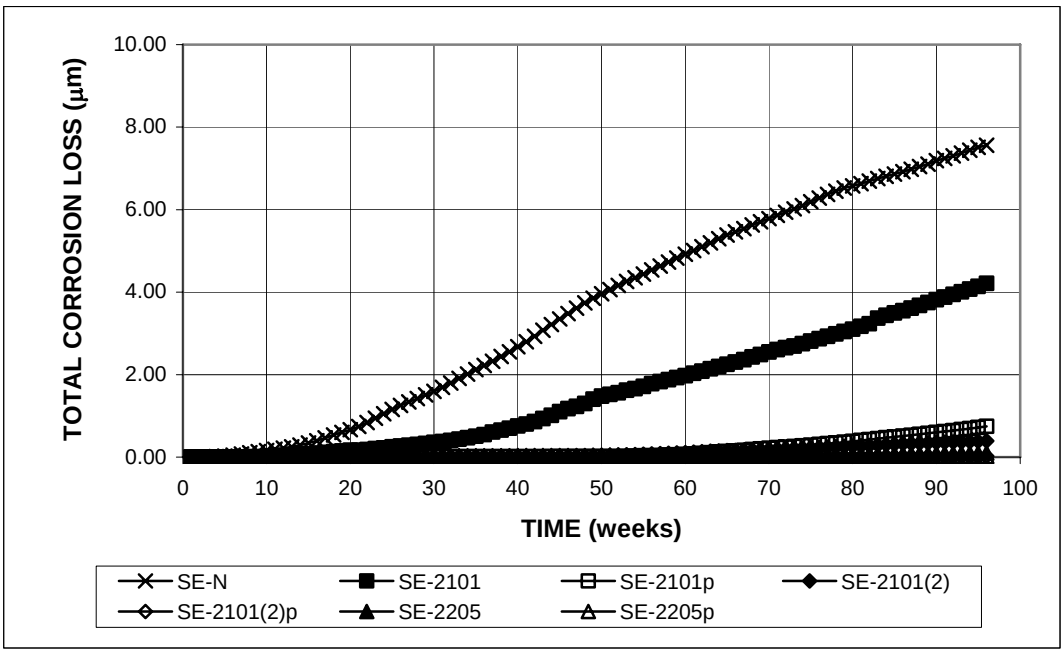

(a)

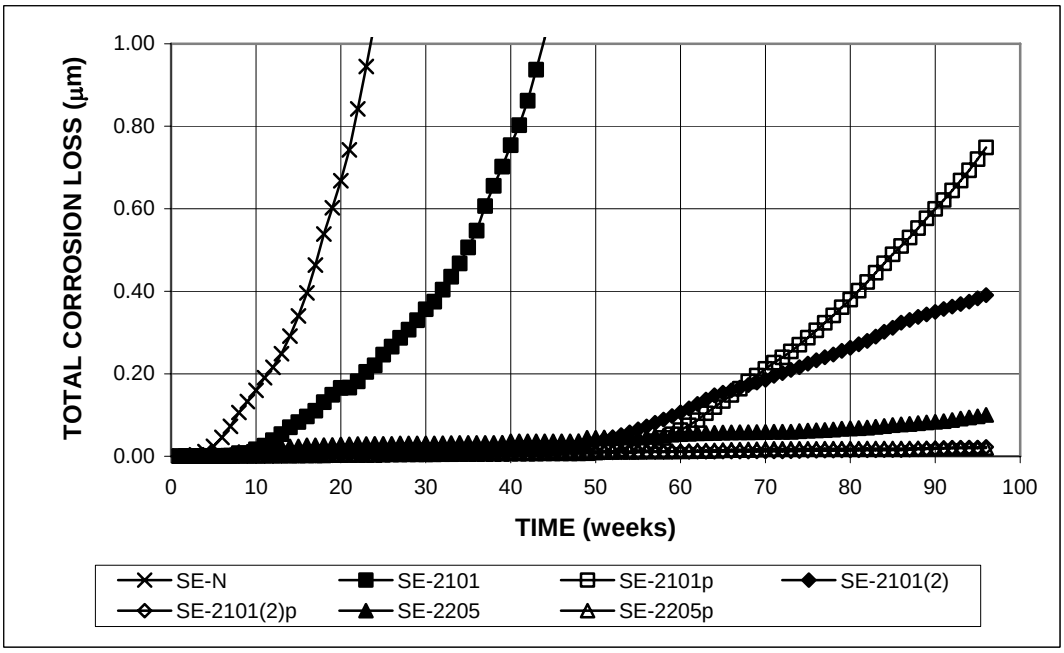

(b)

Figure 3.87 - Southern Exposure test. Average total corrosion losses of conventional and duplex stainless steels, specimens w/c = 0.45, ponded with 15% NaCl solution.

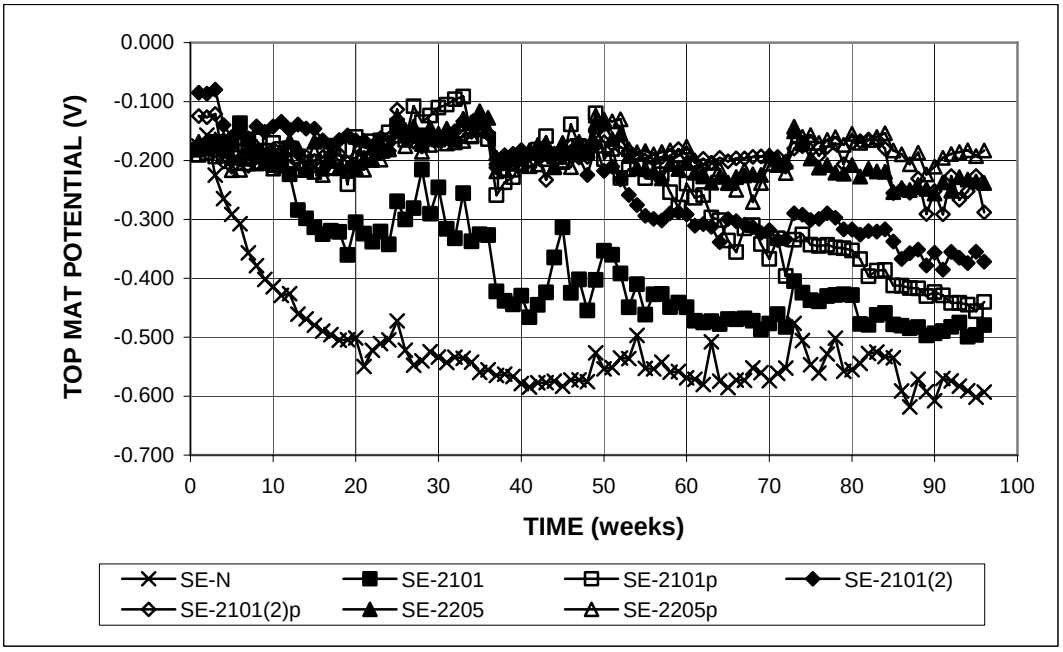

Figure 3.88a - Southern Exposure test. Average top mat corrosion potentials with respect to copper-copper sulfate electrode for conventional and duplex stainless steels, specimens w/c = 0.45, ponded with 15% NaCl solution.

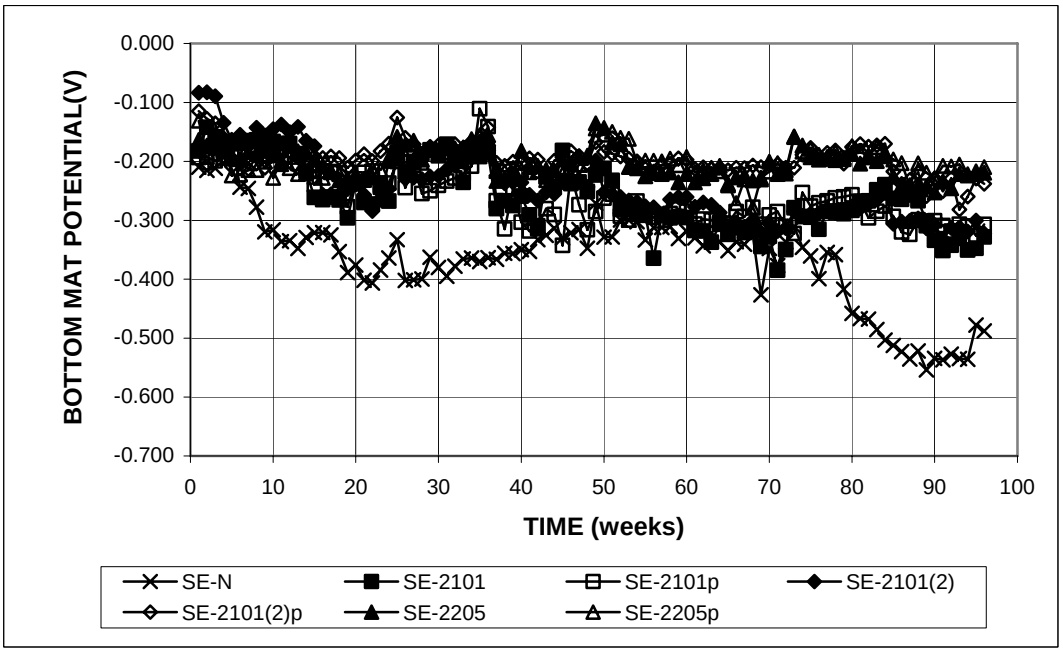

Figure 3.88b - Southern Exposure test. Average bottom mat corrosion potentials with respect to copper-copper sulfate electrode for conventional and duplex stainless steels, specimens w/c = 0.45, ponded with 15% NaCl solution.

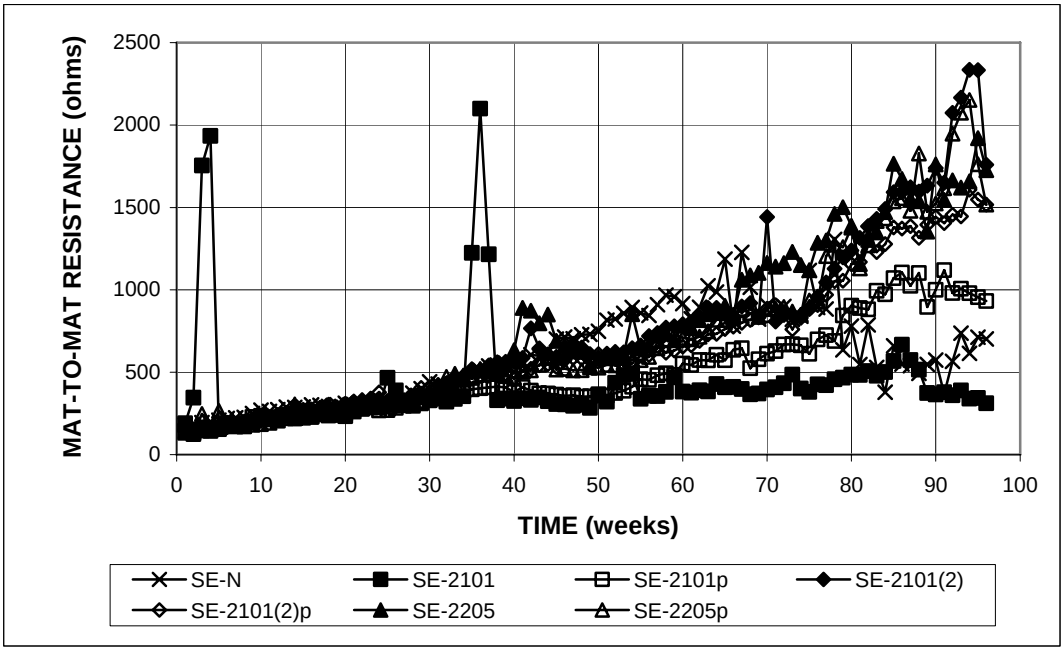

Figure 3.89 - Southern Exposure test. Average mat-to-mat resistances for specimens with conventional and duplex stainless steels, w/c = 0.45, ponded with 15% NaCl solution.

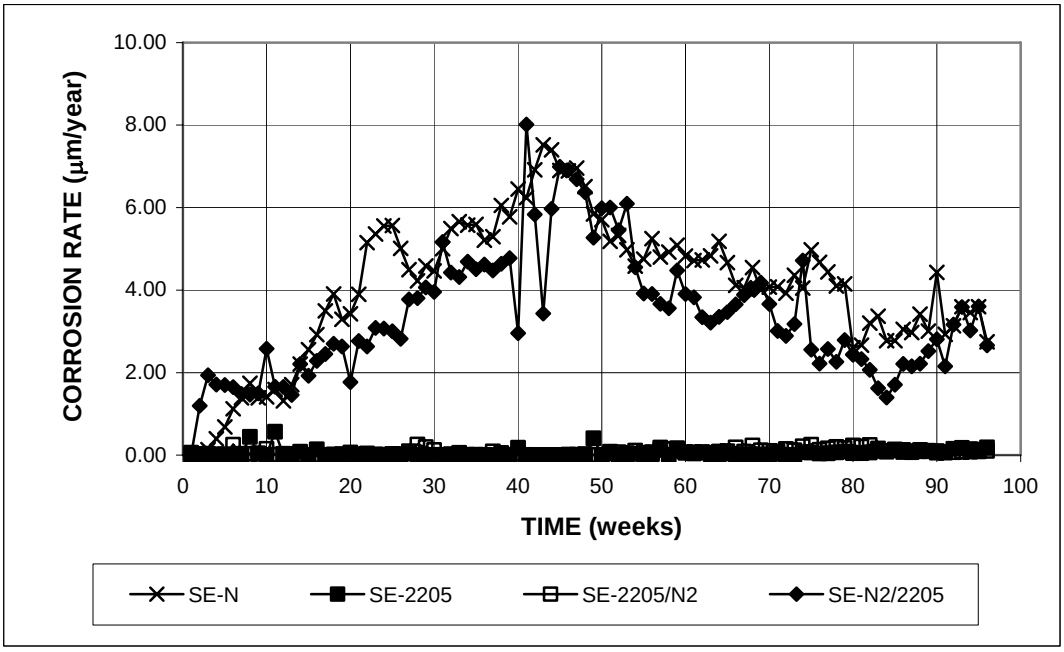

(a)

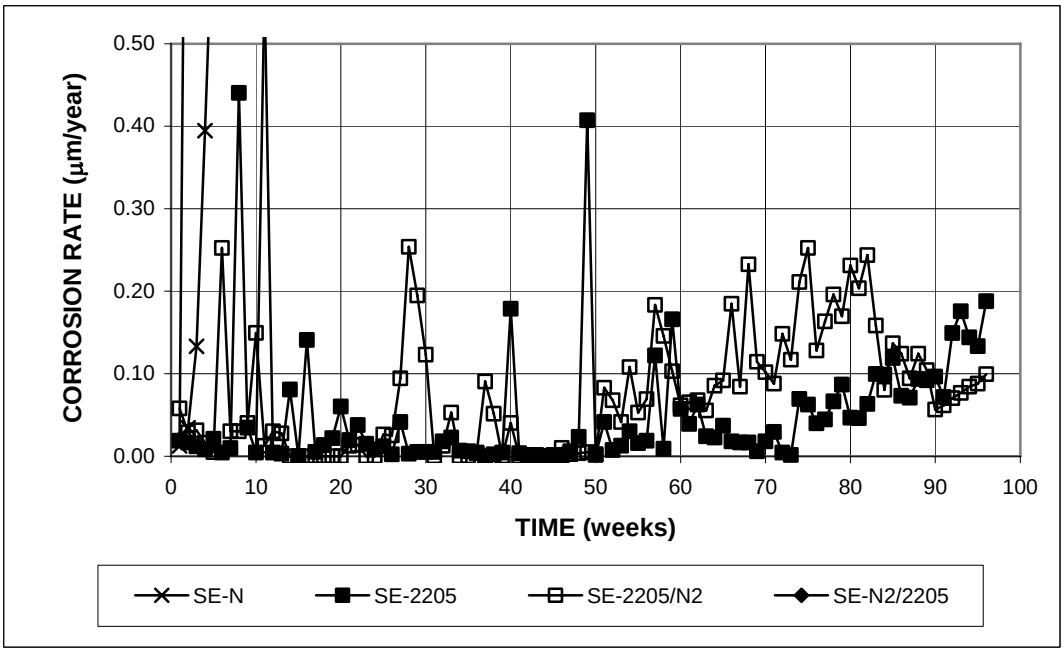

(b)

Figure 3.90 - Southern Exposure test. Average corrosion rates of conventional steel, duplex stainless steel, and the combination of the two steels, specimens w/c = 0.45, ponded with 15% NaCl solution.

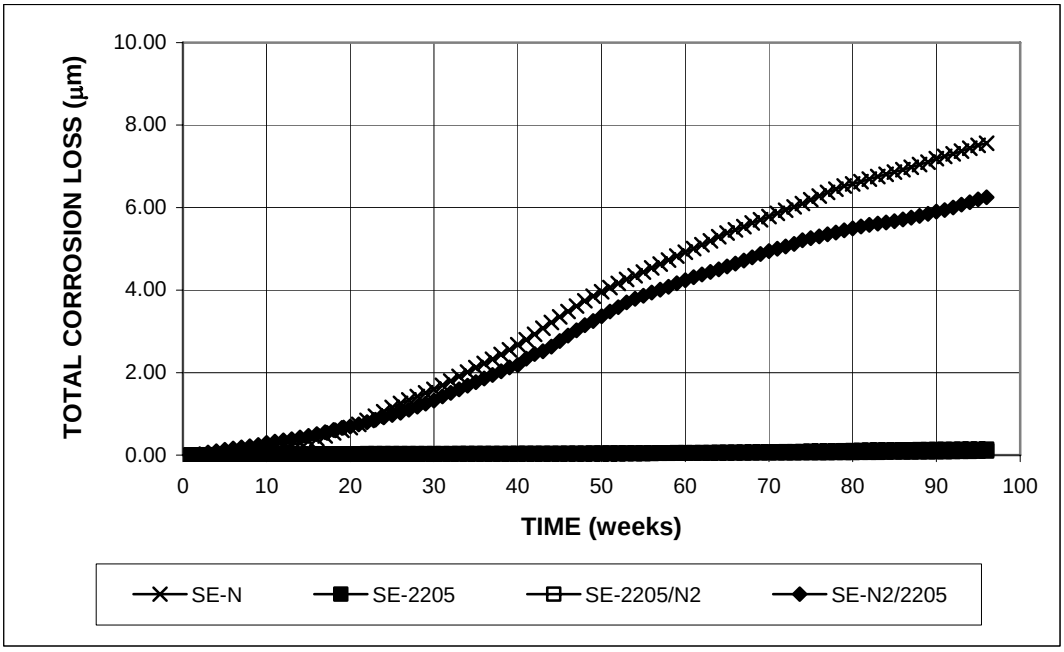

(a)

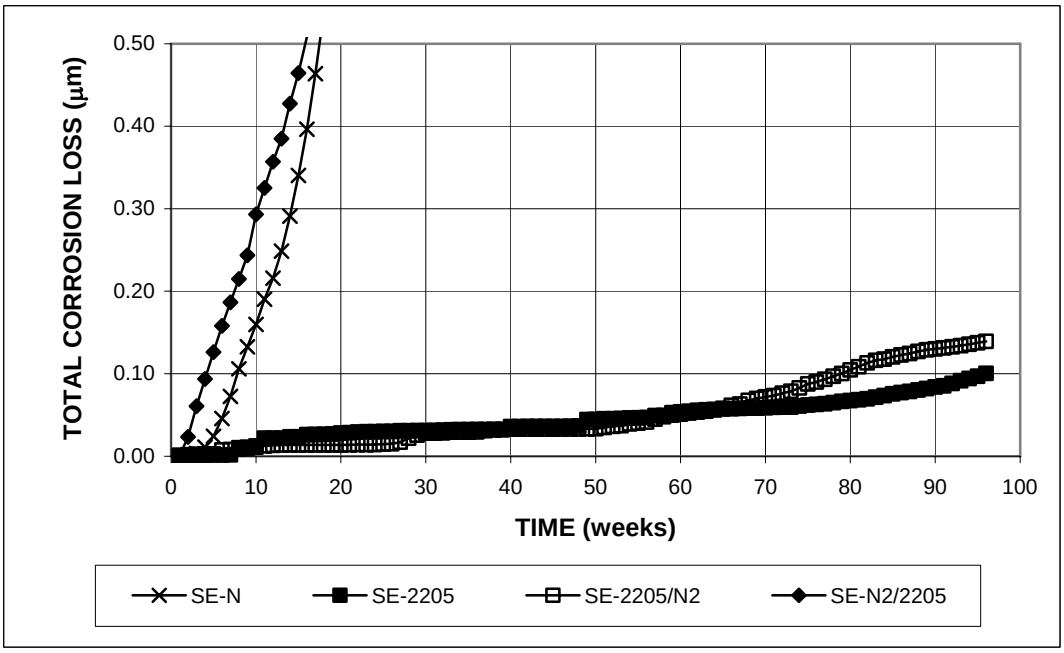

(b)

Figure 3.91 - Southern Exposure test. Average total corrosion losses of conventional steel, duplex stainless steel, and the combination of the two steels, specimens w/c = 0.45, ponded with 15% NaCl solution.

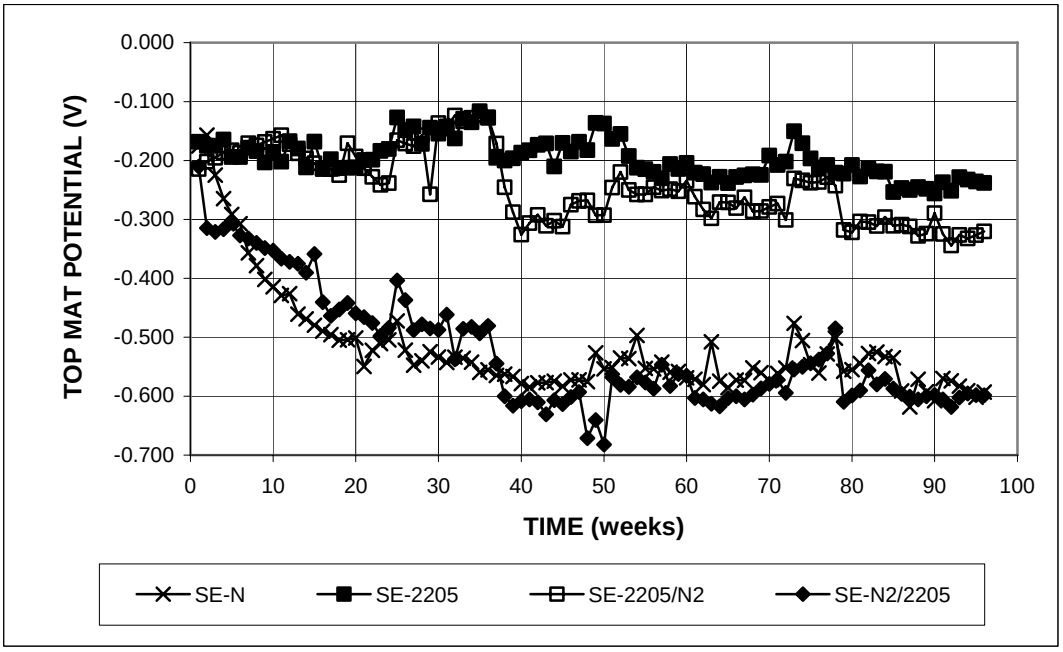

Figure 3.92a - Southern Exposure test. Average top mat corrosion potentials with respect to copper-copper sulfate electrode for conventional steel, duplex stainless steel, and the combination of the two steels, w/c = 0.45, ponded with 15% NaCl solution.

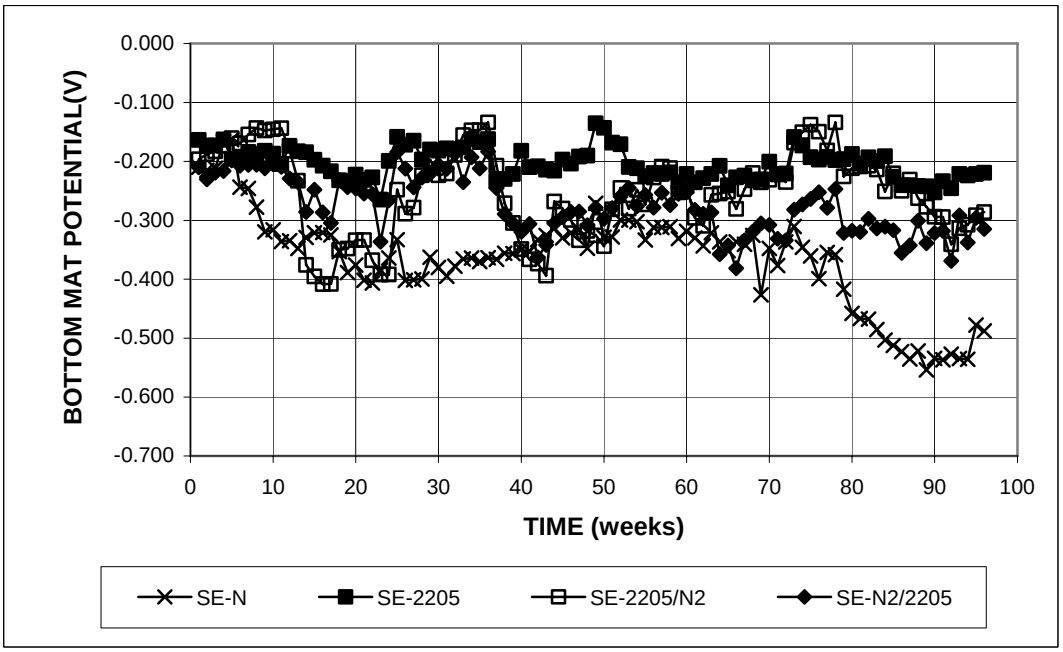

Figure 3.92b - Southern Exposure test. Average bottom mat corrosion potentials with respect to copper-copper sulfate electrode for conventional steel, duplex stainless steel, and the combination of the two steels, w/c = 0.45, ponded with 15% NaCl solution.

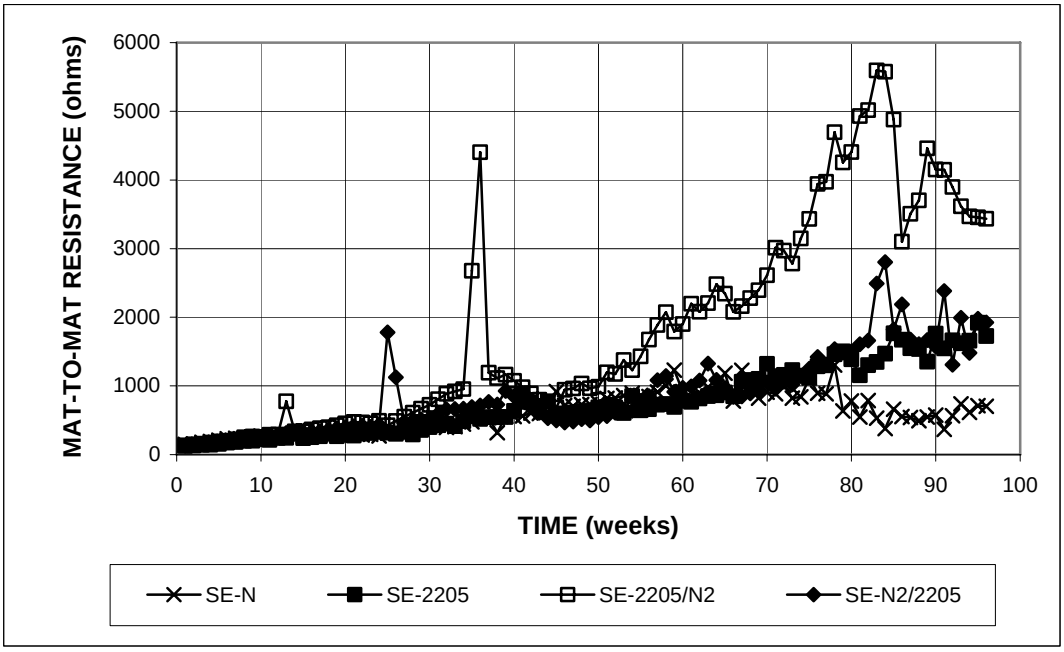

Figure 3.93 - Southern Exposure test. Average mat-to-mat resistances for specimens with conventional steel, duplex stainless steel, and the combination of the two steels, w/c = 0.45, ponded with 15% NaCl.

Cracked beam test – The average corrosion rates for the cracked beam specimens with the duplex stainless steels are shown in Figures 3.94a and 3.94b. Table 3.23 summarizes the average corrosion rates at 96 weeks. The relative corrosion performance of each kind of steel in the cracked beam test was similar to that shown in the bare bar macrocell and Southern Exposure tests. Conventional steel exhibited the highest corrosion rate, followed by the nonpickled 2101 steels, 2101 and 2101(2). The corrosion rates of the steels were relatively high (15, 7, and 6 μm/yr for conventional, 2101, and 2101(2) steels, respectively) within the first few weeks, dropping to stable values, about 3 μm/yr for conventional steel and 1.5 μm/yr for 2101 and 2101(2) steel, in the middle of the test period. During the second half of the test, the corrosion rate of conventional steel hit a few peaks, one as high as 8.6 μm/yr, ending with a value of 2.2 μm/yr; the corrosion rate of 2101 steel increased after 70

weeks, reaching 3.1 μm/yr at the end of the test, while 2101(2) steel corroded at a steady rate, ending at a value of 1.3 μm/yr. As explained in Section 3.1.2, the high initial corrosion rates are due to the fact that the steel is directly subjected to the 15% NaCl solution. As time progresses, corrosion products fill the slot above the steel and the corrosion rates reach stable values. The increase in the corrosion rate observed for conventional steel and 2101 steel during the later period of the test may be due to concrete cracking caused by the deposition of corrosion products, which exposes the bars to additional chlorides. For the rest of the duplex steels, the corrosion rate of 2101p steel remained below 1.0 μm/yr during the first 70 weeks, but increased to a value of 4.9 μm/yr at 96 weeks; the corrosion rate of 2205 steel was below 0.3 μm/yr for most of the first 80 weeks, but began to increase slowly, reaching a value of 0.73 μm/yr at 96 weeks, while the pickled 2101(2) and 2205 steels exhibited the best corrosion resistance, with the corrosion rates remaining below 0.05 μm/yr during most of the test period.

The results of the Student's t-test for comparing the average corrosion rates at 96 weeks are presented in Tables C.7, C.9, and C.11. Table C.7 shows that the differences between conventional steel and either 2101 or 2101(2) steel is not statistically significant [the differences are significant at α =0.05 at 70 weeks (Balma et al. 2005)].

Table C.9 shows that the differences between 2101 and 2101p steel, and between 2205 and 2205p steel are not significant, while the difference between 2101(2) and 2101(2)p steels is significant at α = 0.02.

Table C.11 shows the differences between 2101(2)p steel and either 2205 or 2205p steel are not statistically significant.

Figures 3.95a and 3.95b show the average total corrosion losses for the cracked beam specimens, and Table 3.24 summarizes the values at 96 weeks. At 96 weeks, conventional steel exhibited the highest corrosion loss, 10 μm, followed by the nonpickled 2101 steels, 2101 and 2101(2), at 4.4 and 3.7 μm, respectively; 2101p steel had an average corrosion loss of 2.3 μm. At this point, the corrosion loss for 2205 steel was below 0.5 μm, and the losses for 2101(2)p and 2205p steel equaled 0.05 μm, corresponding to 0.5% of that of conventional steel.

The results of the Student's t-test for comparing the average corrosion losses at 96 weeks are presented in Tables C.8, C.10, and C.12. Table C.8 shows that the differences between conventional steel and either 2101 or 2101(2) steel are significant at α =0.02.

Table C.10 shows that the difference between 2101 and 2101p steel is significant at α = 0.20; the difference between 2101(2) and 2101(2)p steel is significant at α = 0.02; the difference between 2205 and 2205p steel is not statistically significant.

Table C.12 shows the differences between 2101(2)p and either 2205 or 2205p steel are not statistically significant.

The average corrosion potentials of the top and bottom mats of steel for the cracked beam specimens are presented in Figures 3.96a and 3.96b, respectively. The conventional steel in the top mat had the most negative corrosion potentials, between –0.500 and –0.600 V for most of the test, followed by 2101 and 2101(2) steel, with values primarily between –0.400 and –0.500 V. These corrosion potentials (more negative than –0.350 V) indicate that steel was undergoing had active corrosion throughout the test. The top mat corrosion potential for 2101p steel dropped to values below –0.350 V after 12 weeks, ending with a value of about –0.500 V at 96 weeks.

2205 steel had top mat corrosion potentials between –0.200 and –0.300 V during most of the test, with values becoming more negative than –0.300 V after 84 weeks, while the top mat potential for 2101(2)p steel remained more positive than –0.300 V throughout the test, indicating a low tendency to corrode, although the potential was becoming progressively more negative after 60 weeks. The corrosion potential of 2205p steel remained more positive than –0.200 V throughout most of test period. For the bottom mat of steel, all of the duplex stainless steels exhibited corrosion potentials more positive than –0.350 V, with 2205p steel showing values of about –0.200 V during the 96 week period.

The average mat-to-mat resistances for the cracked beam specimens with the duplex stainless steels are shown in Figure 3.97. For all steels, the mat-to-mat resistances of the cracked beam specimens had initial values of about 300 ohms, twice those of the SE specimens. Similar to the pattern in Southern Exposure test, for the first half of the test period, the mat-to-mat resistance of the CB specimens increased with time and all specimens had similar values, reaching about 2000 ohms half way through the test period. For the second half of the test period, the mat-to-mat resistances exhibited larger scatter. The values for the specimens containing 2101, 2101(2), 2101(2)p, 2205, and 2205p steels continued to increase, with values ranging from 2600 ohms for 2205p steel to 7000 ohms for 2101 steel at 96 weeks, while the mat-to-mat resistance of the specimens with conventional and 2101p steels dropped during the later period of the test, with a value of 920 ohms for conventional steel and 220 ohms for the 2101p steel at the end of the test, the latter likely due to additional cracking of the specimens.

Table 3.23 - Average corrosion rates at 96 weeks for specimens with conventional and duplex stainless steels in cracked beam test

Specimen designation*	Steel type	Specimen corrosion rates (μm/yr)						Average (μm/yr)	Standard deviation
		1	2	3	4	5	6		
Cracked beam test									
CB-N	N	0.03	0.02	2.39	4.21	6.40	0.00	2.17	2.68
CB-2101	2101	8.23	0.90	0.30				3.14	4.41
CB-2101p	2101p	7.88	2.66	4.15				4.90	2.69
CB-2101(2)	2101(2)	0.78	0.87	0.84	2.12	1.67		1.25	0.60
CB-2101(2)p	2101(2)p	0.08	0.06	0.02	0.02	0.04		0.04	0.03
CB-2205	2205	0.20	2.90	0.47	0.08	0.03		0.73	1.22
CB-2205p	2205p	0.00	0.08	0.02	0.02	0.02		0.03	0.03

*** A-B**

A: test method; CB = Cracked beam test.

B: steel type and test condition; N = conventional steel; 2101 and 2101(2) = two heats of 2101 duplex stainles steel (21% chromium, 1% nickel), 2205 = 2205 duplex stainless steel (22% chromium, 5% nickle), N2/2205 = N2 steel at the top mat, 2205 steel at the bottom mat; 2205/N2 = 2205 steel at the top mat, N2 steel at the bottom mat; p = pickled.

Table 3.24 - Average total corrosion losses at 96 weeks for specimens with conventional and duplex stainless steels in cracked beam test

Specimen designation*	Steel type	Specimen total corrosion losses (μm)						Average* (μm)	Standard deviation**
		1	2	3	4	5	6		
Cracked beam test									
CB-N	N	12.63	10.09	6.48	10.91	13.68	6.25	10.01	3.09
CB-2101	2101	5.93	4.80	2.32				4.35	1.85
CB-2101p	2101p	3.37	1.62	1.77				2.25	0.97
CB-2101(2)	2101(2)	3.45	2.96	3.67	4.10	4.12		3.66	0.49
CB-2101(2)p	2101(2)p	0.09	0.02	0.05	0.03	0.04		0.05	0.03
CB-2205	2205	0.26	1.65	0.24	0.15	0.06		0.47	0.66
CB-2205p	2205p	0.04	0.11	0.03	0.02	0.04		0.05	0.03

*** A-B**

A: test method; CB = Cracked beam test.

B: steel type and test condition; N = conventional steel; 2101 and 2101(2) = two heats of 2101 duplex stainles steel (21% chromium, 1% nickel), 2205 = 2205 duplex stainless steel (22% chromium, 5% nickle), N2/2205 = N2 steel at the top mat, 2205 steel at the bottom mat; 2205/N2 = 2205 steel at the top mat, N2 steel at the bottom mat; p = pickled.

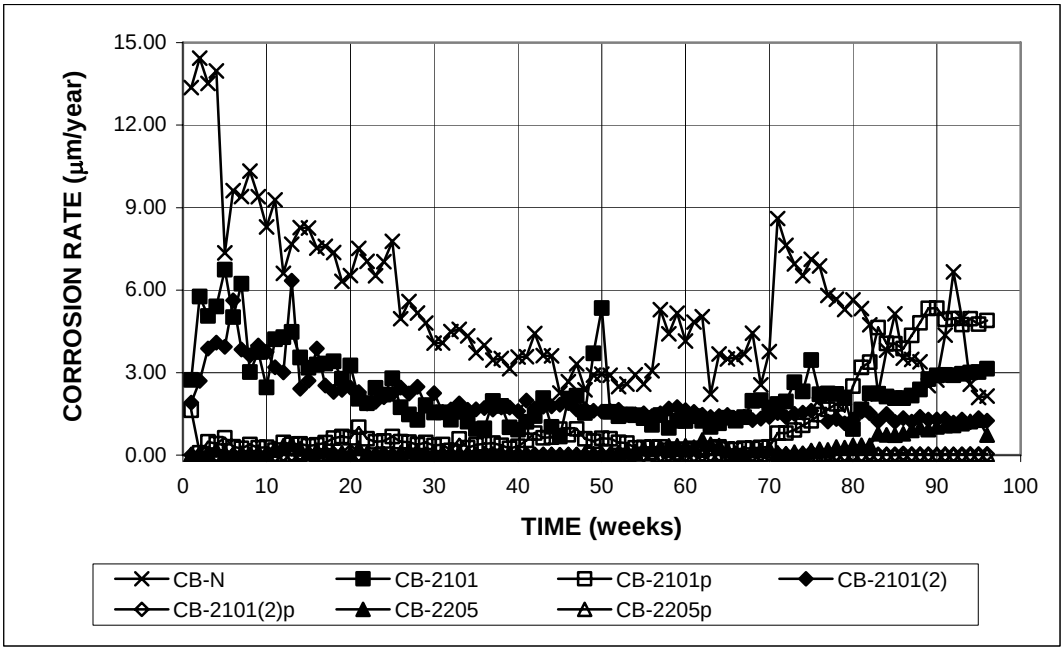

(a)

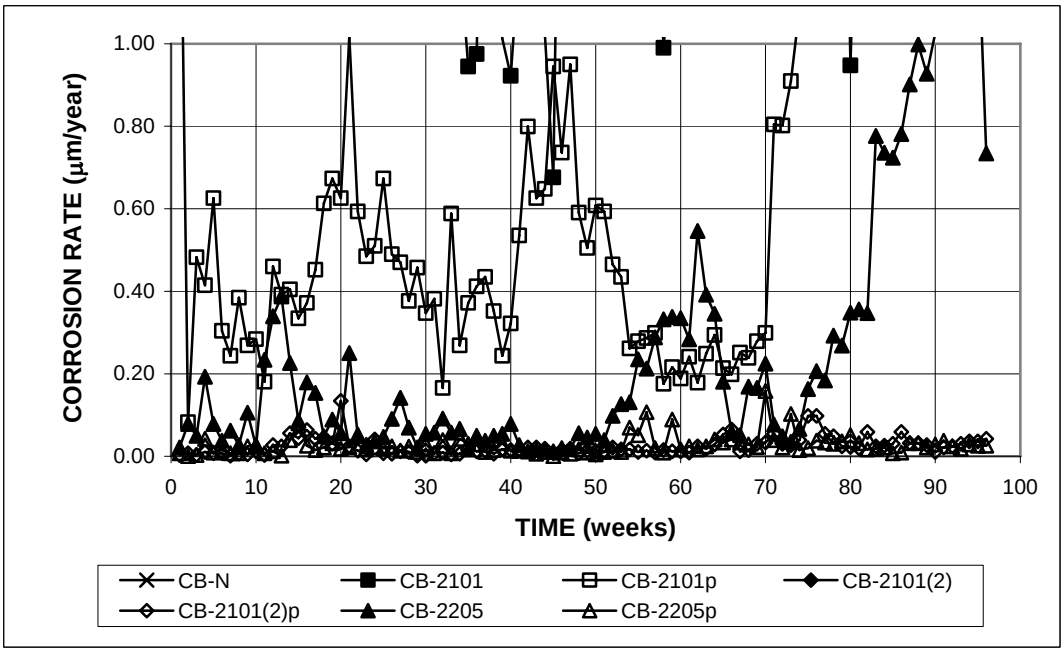

(b)

Figure 3.94 - Cracked beam test. Average corrosion rates of conventional and duplex stainless steels, specimens w/c = 0.45, ponded with 15% NaCl solution.

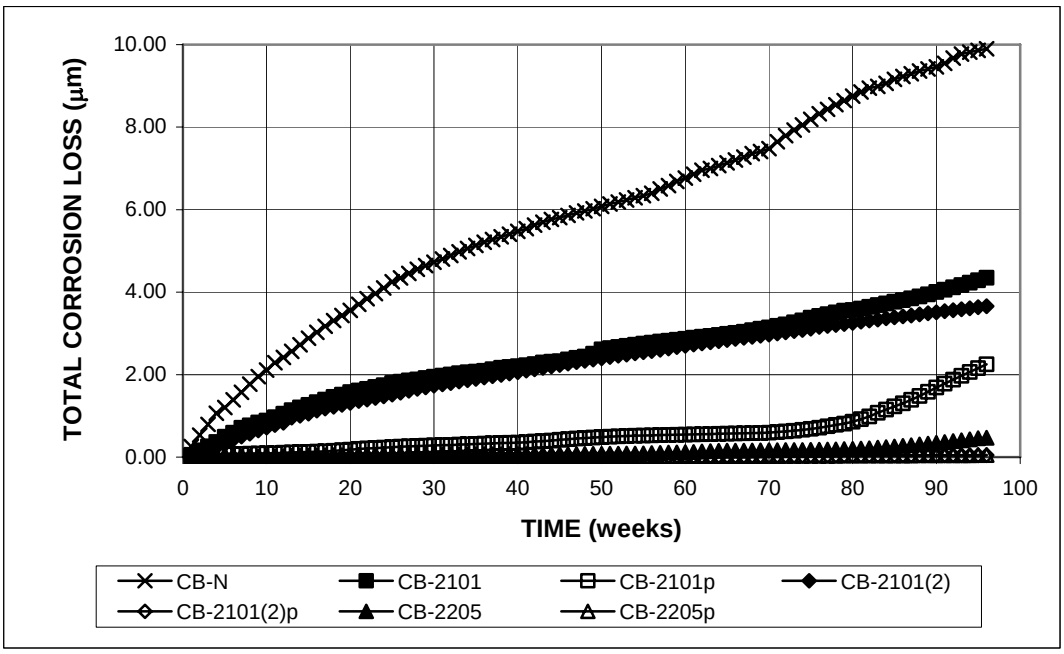

(a)

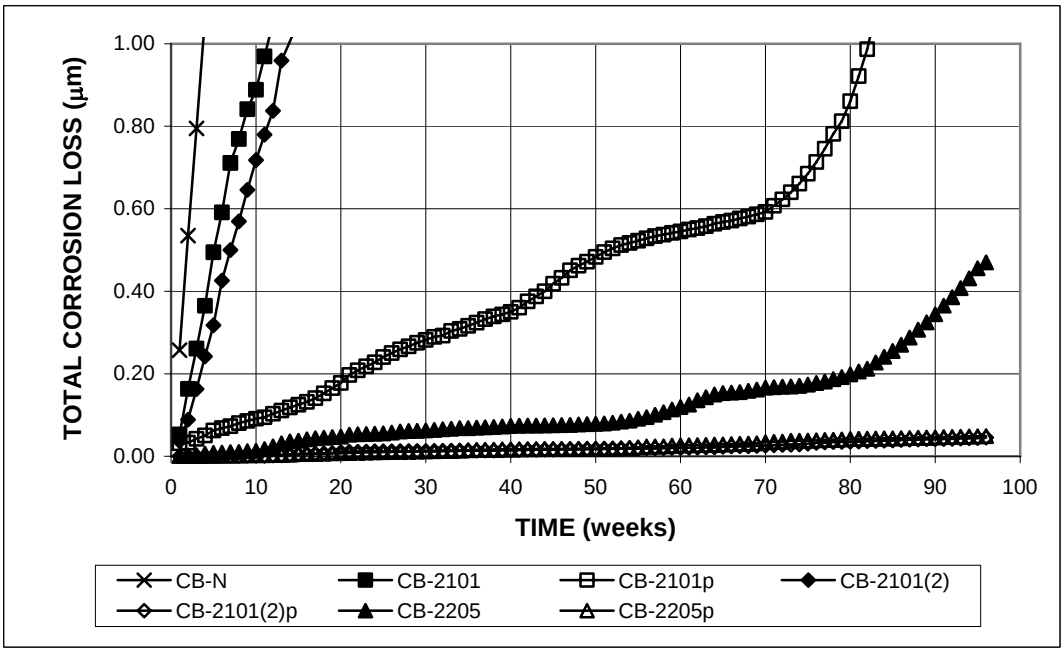

(b)

Figure 3.95 - Cracked beam test. Average total corrosion loess of conventional and duplex stainless steels, specimens w/c = 0.45, ponded with 15% NaCl solution.

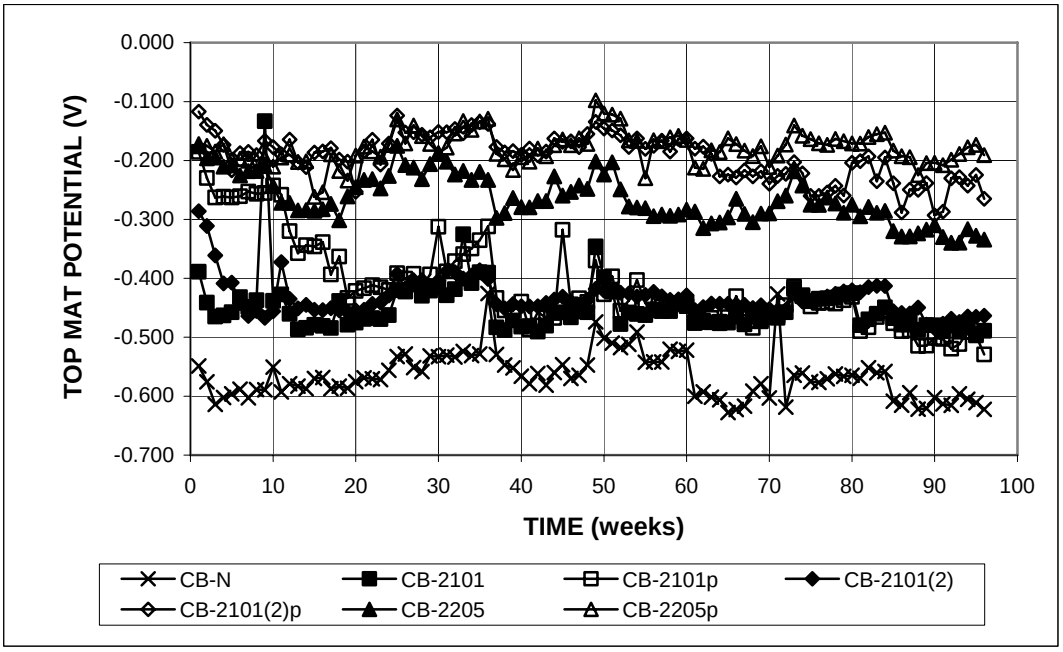

Figure 3.96a - Cracked beam test. Average top mat corrosion potentials with respect to copper-copper sulfate electrode for conventional and duplex stainless steels, specimens w/c = 0.45, ponded with 15% NaCl solution.

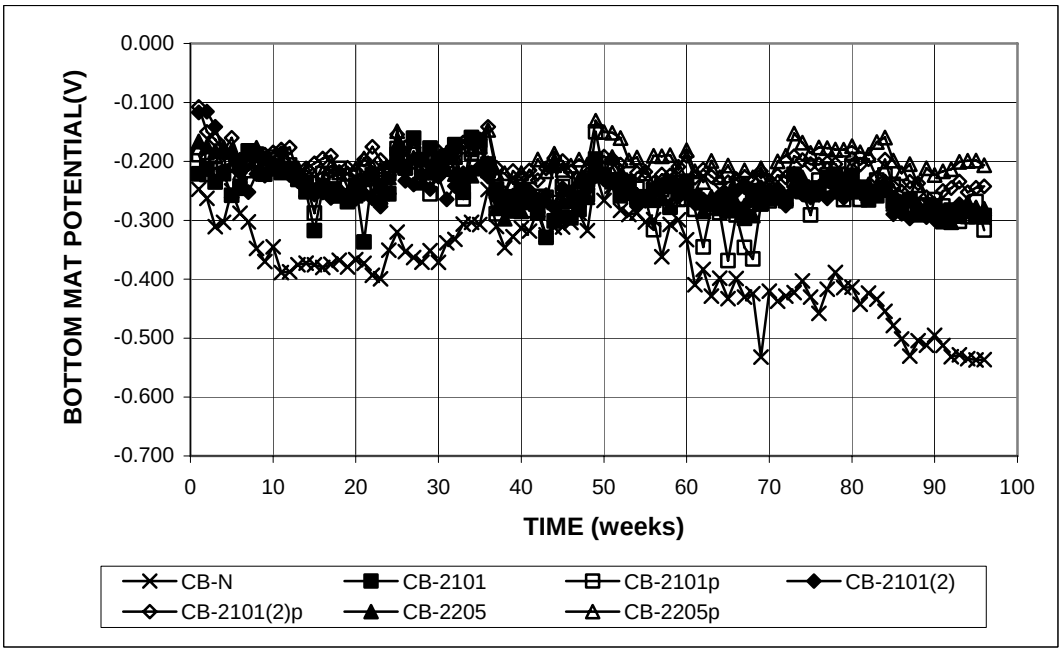

Figure 3.96b - Cracked beam test. Average bottom mat corrosion potentials with respect to copper-copper sulfate electrode for conventional and duplex stainless steels, specimens w/c = 0.45, ponded with 15% NaCl solution.

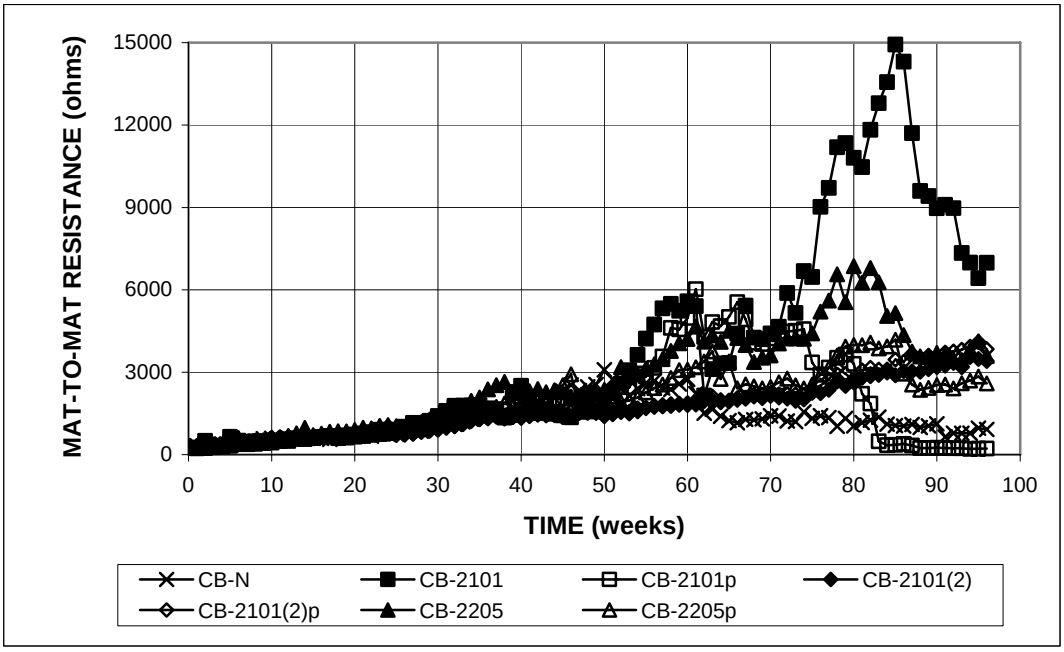

Figure 3.97 - Cracked beam test. Average mat-to-mat resistances for specimens with conventional and duplex stainless steels, w/c = 0.45, ponded with 15% NaCl solution.

Visual Inspection – At the end of the tests, the bars were removed from the concrete for visual inspection. For all SE specimens containing the 2101, 2101(2), and 2101p steels, the top mat bars exhibited corrosion products, as shown in Figures 3.98 through 3.100. For three of five SE specimens with the 2205 steel, some corrosion products were observed in the top mat bars, as shown in Figure 3.101. None of the 2101(2)p and 2205p top mat bars in SE specimens exhibited corrosion products, as shown in Figure 3.102 and 3.103.

Figure 3.98 – 2101 reinforcing bar from the top mat of an SE specimen (SE-2101-2) at 96 weeks, showing corrosion products.

Figure 3.99 – 2101p reinforcing bar from the top mat of an SE specimen (SE-2101p-2) at 96 weeks, showing corrosion products.

Figure 3.100 – 2101(2) reinforcing bar from the top mat of an SE specimen [SE-2101(2)-1] at 96 weeks, showing corrosion products.

Figure 3.101– 2205 reinforcing bar from the top mat of an SE specimen (SE-2205-3) at 96 weeks, showing corrosion products.

Figure 3.102 – 2101(2)p reinforcing bar from the top mat of an SE specimen [SE-2101(2)p-3] at 96 weeks, showing no corrosion products.

Figure 3.103 – 2205p reinforcing bar from the top mat of an SE specimen (SE-2205p-4) at 96 weeks, showing no corrosion products.

For the CB specimens containing the 2101, 2101(2) and 2101p steel, the top mat bars exhibited corrosion products, as shown in Figures 3.104 through 3.106. For the CB specimens containing 2205 steel, with the exception of one specimen (CB-2205-5), some corrosion products were observed on the top mat bars, as shown in Figure 3.107. Of the CB specimens containing 2101(2)p steel, only one top mat bar [CB-2101(2)p-1] exhibited any corrosion products, as shown in Figure 3.108. The remaining 2101(2)p bars and all 2205p bars from the top mat of CB specimens showed no corrosion products, as shown in Figures 3.109 and 3.110, respectively.

Figure 3.104 – 2101 reinforcing bar from the top mat of a CB specimen (CB-2101-2) at 96 weeks, showing corrosion products.

Figure 3.105 – 2101p reinforcing bar from the top mat of a CB specimen (CB-2101p-2) at 96 weeks, showing corrosion products.

Figure **3.106** – 2101(2) reinforcing bar from the top mat of a CB specimen [CB-2101(2)-3] at 96 weeks, showing corrosion products.

Figure **3.107** – 2205 reinforcing bar from the top mat of a CB specimen at 96 weeks (CB-2205-4), showing corrosion products.

Figure **3.108** – 2101(2)p reinforcing bar from the top mat of a CB specimen [CB-2101(2)p-1] at 96 weeks, showing corrosion products. Only 2101(2)p specimen to do so.

Figure **3.109** – 2101(2)p reinforcing bar from the top mat of a CB specimen [CB-2101(2)p-4] at 96 weeks, showing no corrosion products.

Figure 3.110 – 2205p reinforcing bar from the top mat of a CB specimen (CB-2205p-4) at 96 weeks, showing no corrosion products.

3.5 COMPARISON FOR RAPID MACROCELL TESTS WITH AND WITHOUT THE TEST SOLUTION REPLACED.

The average corrosion rates and losses for reinforcing steels in the rapid macrocell tests with and without the test solution replaced every five weeks are compared in Tables 3.25 and 3.26 and Figures 3.111 through 3.116. The results of the Student's t-test are shown in Tables C.13 and C.14 in Appendix C. As before, tests with the solution replaced is indicated by "r" in the specimen designation.

Bare bar specimens in 1.6 m NaCl solution – Bare conventional and MMFX reinforcing bars were tested in simulated concrete pore solution containing 1.6 m ion NaCl, replacing and without replacing the solution every five weeks. For conventional steel, the test without the solution replaced was performed for N3 steel, while the test with the solution replaced was performed for N2 and N4 steels.

The average corrosion rates and losses for the conventional and MMFX steels are shown in Figures 3.111 and 3.112, respectively, and the values at 15 weeks are summarized in Tables 3.25 and 3.26. The results of the Student's t-test are presented in Tables C.13 and C.14. The results show that without replacing the solutions, the conventional steel (N3) exhibited higher corrosion rates than the steels (N2 and N4) when replacing the solutions. N3 steel had average corrosion rates primarily above 30 μm/yr during the test, ending with a value of 36 μm/yr at 15 weeks, while N2 and N4 steel had rates primarily below 30 μm/yr during the test, with rates of 21 and 28 μm/yr at 15 weeks, respectively. The difference in the average corrosion rates at 15 weeks between N3 and N2 steels is significant at $\alpha = 0.20$, while the difference between N3 and N4 steels is not statistically significant.

The average corrosion rates for MMFX steel were between 4 and 20 μm/yr throughout the test period. During the last few weeks, the steel exhibited lower

corrosion rates when the test solutions were replaced than when they were not. At 15 weeks, without replacing the test solutions, the steel (MMFX) corroded at a rate of 19.8 μm/yr, while when replacing the test solutions, the steel (MMFX-r) corroded at a rate of 16.8 μm/yr. The difference is not statistically significant.

At 15 weeks, without replacing the test solutions every 5 weeks, the total corrosion loss was 2.52 μm for MMFX steel and 9.0 μm for N3 steel; when replacing the test solutions, the total corrosion loss was 2.81 μm for MMFX steel and 6.6 and 6.1 μm for N2 and N4 steel, respectively. Table C.14 shows that the difference in the corrosion losses between N3 and N4 steel is statistically significant at $\alpha = 0.20$, while the difference between N3 and N2 steel and the difference in the MMFX steel tests are not statistically significant.

The results show that although the difference is not significant in some cases, both conventional and MMFX steels exhibited lower average corrosion rates and average corrosion losses at the end of the test (except for the corrosion loss of MMFX steel) when the test solutions were replaced every five weeks. The reason is that replacing the test solution avoids the drop of the pH due to the carbonation, which causes an increasingly Cl^-/OH^- ratio in the anode solution.

Bare bar specimens in 6.04 m ion NaCl – Bare conventional N2 steel and duplex stainless steels, 2101(2)p, 2205 and 2205p, were tested in simulated concrete pore solution containing 6.04 m ion NaCl, with and without replacing the solution every five weeks.

The average corrosion rates and total corrosion losses of the steels are shown in Figures 3.113 and 3.114, respectively. The values at 15 weeks are summarized in Tables 3.25 and 3.26. The results of the Student's t-test are presented in Tables C.13 and C.14.

During most of the test period, conventional N2 steel corroded at a rate between 20 and 40 μm/yr, with lower values when the test solutions were replaced than when they were not. At 15 weeks, when the solutions were not replaced every five weeks, the steel had a corrosion rate of 25.5 μm/yr, with a total corrosion loss of 9.8 μm, while when the test solutions were replaced, the steel had a corrosion rate of 29.7 μm/yr, with a total corrosion loss of 8.9 μm. The differences in the corrosion rates and losses at the end of the test, however, are not statistically significant.

The effect of replacing the test solution on the duplex stainless steels is more apparent. During the second half of the test period, the 2101(2)p, 2205, and 2205p steels all exhibited lower average corrosion rates when the test solutions were replaced every five weeks than when they were not. As shown in Figure 3.113(b), when the test solutions were not replaced, 2101(2)p steel had a maximum rate of 2.0 μm/yr at 12 weeks, ending with a value of 0.96 μm/yr at 15 weeks; 2205 steel had a maximum rate of 3.9 μm/yr at 10 weeks, ending with a value of 2.5 μm/yr; and 2205p steel had a maximum rate of 0.28 μm/yr at 15 weeks; when the test solutions were replaced, 2101(2)p steel had a maximum rate of 0.42 μm/yr at 13 weeks, ending with a value of 0.13 μm/yr at 15 weeks; 2205 steel had a maximum rate of 1.7 μm/yr at 13 weeks, ending with a value of 1.6 μm/yr; and 2205p steel has a maximum rate of 0.18 μm/yr at 15 weeks. Table C.13 shows that the differences in the corrosion rates at 15 weeks with and without solution replacement are not statistically significant for 2101(2)p steel and are significant at $\alpha = 0.10$ for 2205 steel and at $\alpha = 0.20$ for 2205p steel.

The average total corrosion losses are summarized in Table 3.26, and the results of the Student's t-test are presented in Table C.14. At the end of the test, compared to values of 0.17 μm for 2101(2)p steel, 0.49 μm for 2205 steel, and 0.03

μm for 2205p steel when the test solutions were not replaced, the average corrosion losses were 0.05 μm for 2101(2)p steel, 0.29 μm for 2205 steel, and 0.01 μm for 2205p steel when the test solutions were replaced. The differences in the corrosion losses with and without solution replacement are significant at $\alpha = 0.05$ for 2101(2)p and 2205 steels and significant at $\alpha = 0.10$ for 2205p steel.

The results show that 2101(2)p, 2205, and 2205p steel exhibited lower corrosion rates and losses when the test solutions were replaced than they were not, indicating that not only does replacing the solutions help maintain the high pH of the test solutions but that steels with higher corrosion resistance are relatively more sensitive than conventional steel to the maintenance of a high pH.

*Mortar-wrapped specimen*s – Mortar-wrapped conventional N2 steel and MMFX steel were tested with and without test solution replacement.

The average corrosion rates and corrosion losses are shown in Figures 3.115 and 3.116, respectively, and the values at 15 weeks are summarized in Tables 3.25 and 3.26. The results of the Student's t-test are presented in Tables C.13 and C.14.

During the test period, N2 steel exhibited similar average corrosion rates in both cases, with the exception, between 6 and 10 weeks, that the corrosion rate was significantly higher when the test solutions were not replaced than they were. At the end of the test, without replacing the test solutions, N2 steel had an average corrosion rate of 16.3 μm/yr and a loss of 3.8 μm, while when replacing the test solutions every five weeks, the steel had an average corrosion rate of 17.1 μm/yr and a loss of 3.5 μm. The differences in the corrosion rates and losses are not statistically significant.

Without replacing the test solutions, the average corrosion rate for MMFX steel remained negligible for the first 2 weeks and then increased slowly with time,

peaking at 10.6 μm/yr at 15 weeks. When replacing the test solutions, MMFX steel began to exhibit significant corrosion at 5 weeks, reached a maximum corrosion rate of 4.4 μm/yr at 9 weeks, and completed the 15-week test with a corrosion rate of 1.4 μm/yr. The difference in the corrosion rates at 15 weeks is significant at $\alpha = 0.02$. At this point, the average corrosion loss for MMFX steel was 1.4 μm when not replacing the test solutions and 0.55 μm when replacing the test solutions. The difference is significant at $\alpha = 0.10$.

The results show that although buffering provided by the mortar cover and filler in the solutions can reduce carbonation, the effect of replacing the test solutions every five weeks is still apparent, as both conventional and MMFX steel exhibited less total corrosion losses at the end of test when the solutions were replaced.

Overall, in all macrocell tests, replacing the solutions helps maintain the pH, and thus, the Cl^-/OH^- ratio of the anode solution, and reduces the corrosion rate and loss of steel. Under any circumstances, to maintain a consistent pH throughout the test and allow for a fair evaluation of all reinforcing steels, it is recommended that the test solutions in rapid macrocell test be replaced every five weeks.

Table 3.25 - Average corrosion rates at 15 weeks for reinforcing steels in macrocell test with and without the test solutions replaced every five weeks

Specimen designation*	Steel type	Specimen corrosion rates (μm/yr)						Average (μm/yr)	Standard deviation
		1	2	3	4	5	6		
Bare bars in 1.6 m NaCl									
M-N3	N3	52.60	0.26	67.77	40.17	32.43	22.08	35.88	23.61
M-N2-r	N2	15.17	20.63	19.68	5.35	31.99	32.25	20.85	10.28
M-N4-r	N4	31.23	22.16	16.68	40.66	26.74	31.12	28.10	8.30
M-MMFX	MMFX	12.34	8.03	23.06	18.21	32.25	25.03	19.82	8.83
M-MMFX-r	MMFX	15.43	27.92	14.88	16.18	12.54	14.02	16.83	5.57
Bare bars in 6.04 m NaCl									
M-N2h	N2	33.87	37.80	12.17	24.51	18.96		25.46	10.52
M-N2h-r	N2	42.11	29.51	32.28	24.83	22.66	26.56	29.66	6.98
M-2101(2)ph	2101(2)p	3.47	0.23	0.00	0.00	1.82	0.23	0.96	1.41
M-2101(2)ph-r	2101(2)p	0.00	0.06	0.00	0.03	0.00	0.66	0.13	0.27
M-2205h	2205	2.40	1.24	2.69	2.80	2.92	2.77	2.47	0.63
M-2205h-r	2205	1.13	1.71	0.06	2.37	2.34	1.71	1.55	0.87
M-2205ph	2205p	0.14	0.20	0.23	0.40	0.43		0.28	0.13
M-2205ph-r	2205p	0.12	0.12	0.09	0.35	0.26	0.14	0.18	0.10
Mortar-wrapped specimens in 1.6 m NaCl									
M-N2m	N2	17.43	19.02	24.83	5.49	14.65		16.28	7.09
M-N2m-r	N2	17.28	22.89	18.96	11.96	14.51		17.12	4.19
M-MMFXm	MMFX	8.87	17.37	10.12	9.54	11.68	5.98	10.59	3.81
M-MMFXm-r	MMFX	0.09	0.06	5.40	0.12	0.72	1.88	1.38	2.09

*** A-B-C**

A: test method; M = macrocell test.

B: steel type and test condition; N2, N3, N4 = conventional steels; MMFX = mircrocomposite MMFX steel; 2101 and 2101(2) = two heats of 2101 duplex stainless steel (21% chromium, 1% nickel), 2205 = 2205 duplex stainless steel (22% chromium, 5% nickle); h = 6.04 m ion concentration; m = mortar-wrapped specimens

C: r = the test solutions are replaced every five weeks.

Table 3.26 - Average total corrosion losses at 15 weeks for reinforcing steels in macrocell test with and without the test solutions replaced every five weeks

Specimen designation*	Steel type	Specimen total corrosion losses (μm)						Average (μm)	Standard deviation
		1	2	3	4	5	6		
Bare bars in 1.6 m NaCl									
M-N3	N3	12.33	4.15	13.49	11.17	7.08	5.50	8.95	3.88
M-N2-r	N2	6.26	8.15	6.89	4.13	7.17	6.94	6.59	1.35
M-N4-r	N4	7.02	5.25	4.93	7.61	6.53	5.24	6.10	1.11
M-MMFX	MMFX	3.12	2.15	3.19	1.19	1.78	3.68	2.52	0.96
M-MMFX-r	MMFX	2.16	3.73	1.53	3.58	2.01	3.86	2.81	1.02
Bare bars in 6.04 m NaCl									
M-N2h	N2	12.32	11.64	6.93	9.28	8.63		9.76	2.21
M-N2h-r	N2	10.53	10.26	8.59	8.41	7.99	7.48	8.88	1.24
M-2101(2)ph	2101(2)p	0.25	0.18	0.00	0.14	0.28	0.14	0.17	0.10
M-2101(2)ph-r	2101(2)p	0.04	0.02	0.02	0.01	0.01	0.20	0.05	0.07
M-2205h	2205	0.51	0.34	0.52	0.34	0.62	0.65	0.49	0.13
M-2205h-r	2205	0.22	0.51	0.08	0.44	0.35	0.17	0.29	0.16
M-2205ph	2205p	0.02	0.03	0.02	0.02	0.05		0.03	0.01
M-2205ph-r	2205p	0.02	0.01	0.01	0.01	0.01	0.00	0.01	0.00
Mortar-wrapped specimens in 1.6 m NaCl									
M-N2m	N2	4.04	2.96	2.22	3.75	6.09		3.81	1.46
M-N2m-r	N2	3.09	4.72	2.41	3.35	3.75		3.47	0.86
M-MMFXm	MMFX	2.18	0.56	1.88	0.99	1.68	0.93	1.37	0.63
M-MMFXm-r	MMFX	0.02	0.02	1.77	0.02	0.36	1.15	0.55	0.74

*** A-B-C**

A: test method; M = macrocell test.

B: steel type and test condition; N2, N3, N4 = conventional steels; MMFX = mircrocomposite MMFX steel; 2101 and 2101(2) = two heats of 2101 duplex stainless steel (21% chromium, 1% nickel), 2205 = 2205 duplex stainless steel (22% chromium, 5% nickle); h = 6.04 m ion concentration; m = mortar-wrapped specimens

C: r = the test solutions are replaced every five weeks.

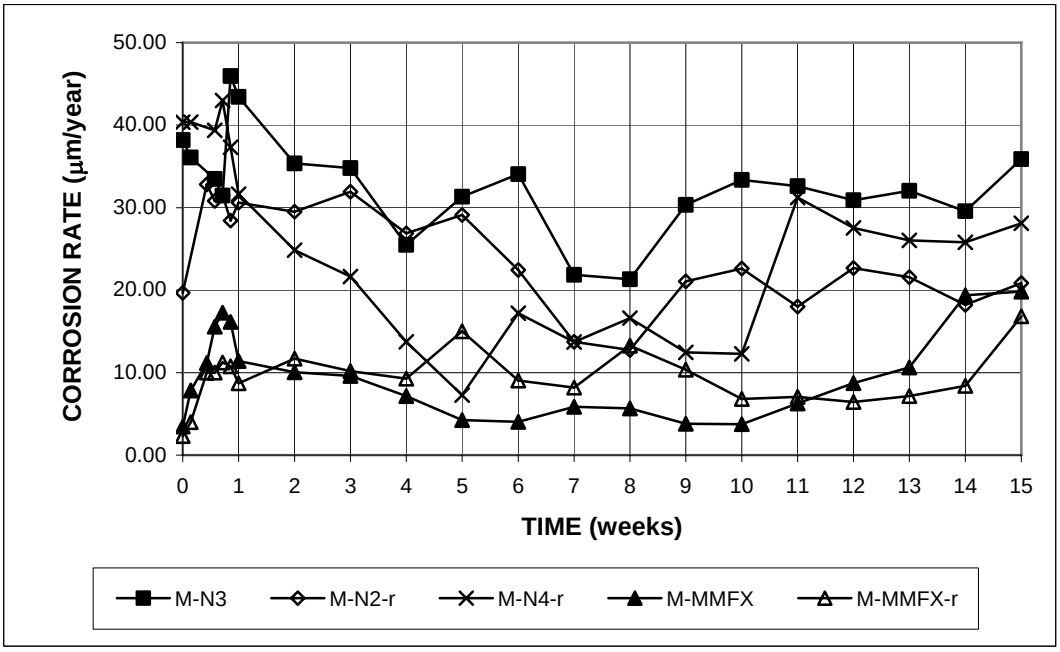

Figure 3.111 - Macrocell test. Average corrosion rates, bare conventional and MMFX steels in simulated concrete pore solution with 1.6 molal ion NaCl, replacing and without replacing the test solutions every five weeks

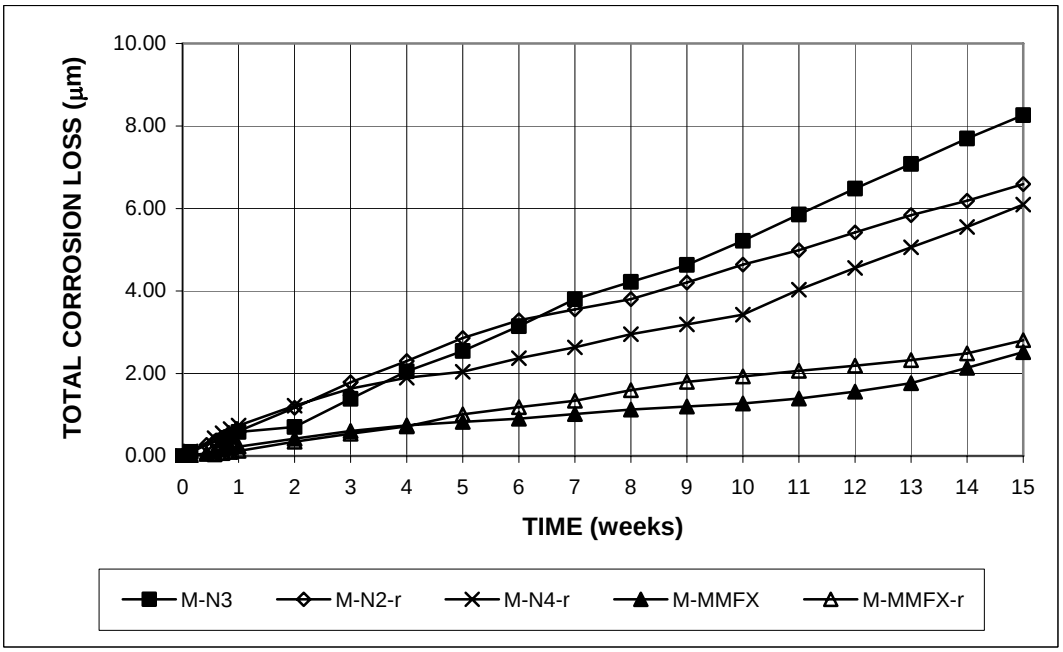

Figure 3.112 - Macrocell test. Average total corrosion losses, bare conventional and MMFX steels in simulated concrete pore solution with 1.6 molal ion NaCl, replacing and without replacing the test solutions every five weeks.

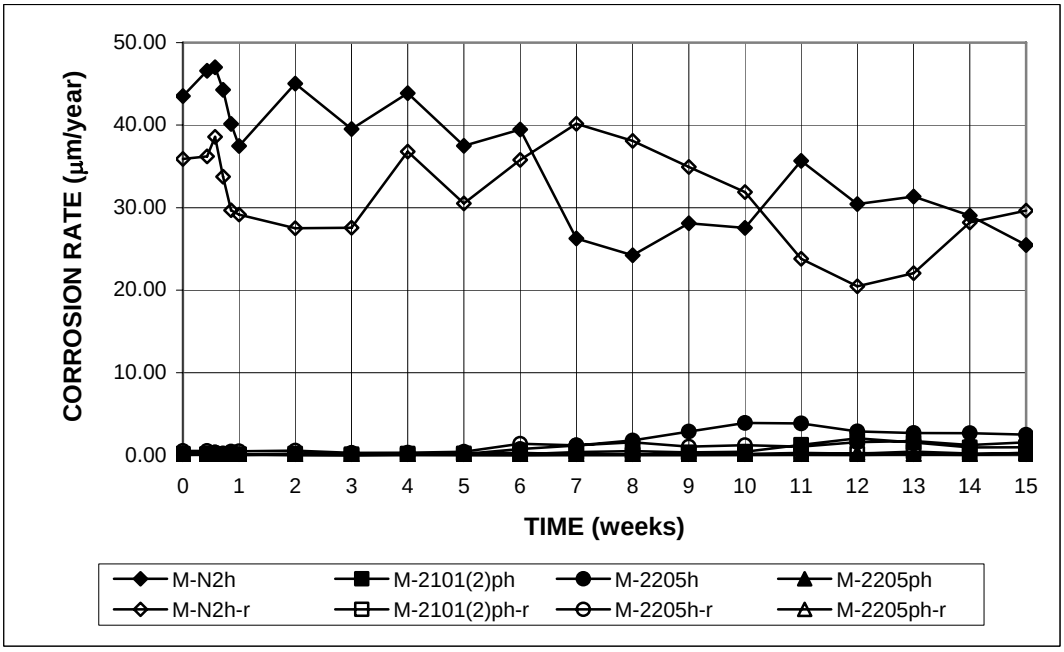

(a)

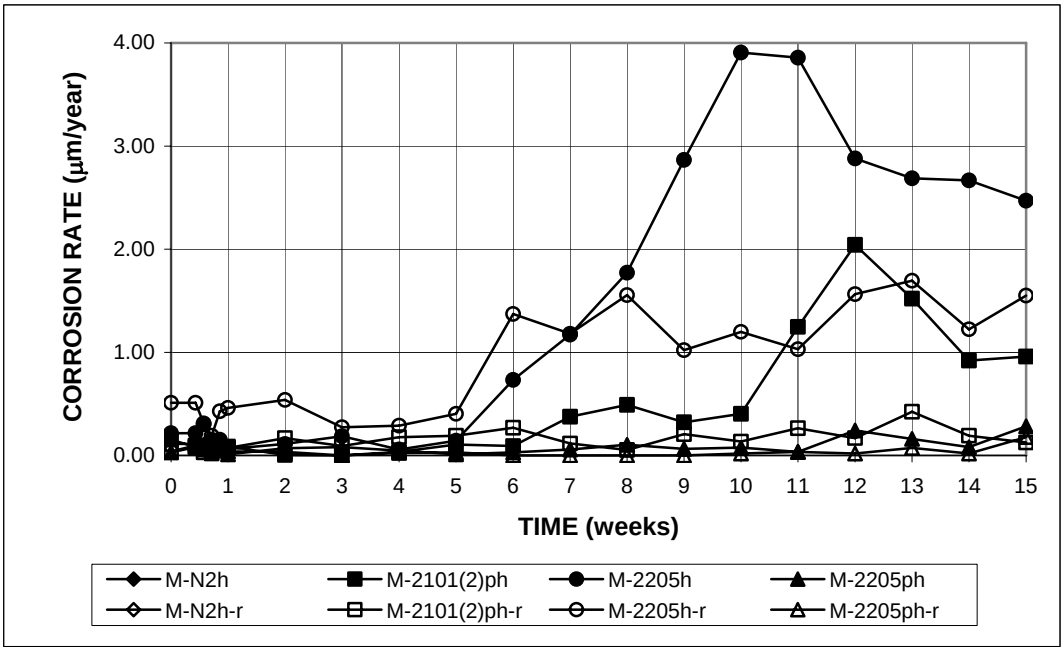

(b)

Figure 3.113 - Macrocell test. Average corrosion rates for bare conventional and duplex stainless steels in simulated concrete pore solution with 6.04 molal ion NaCl, replacing and without replacing the test solutions every five weeks.

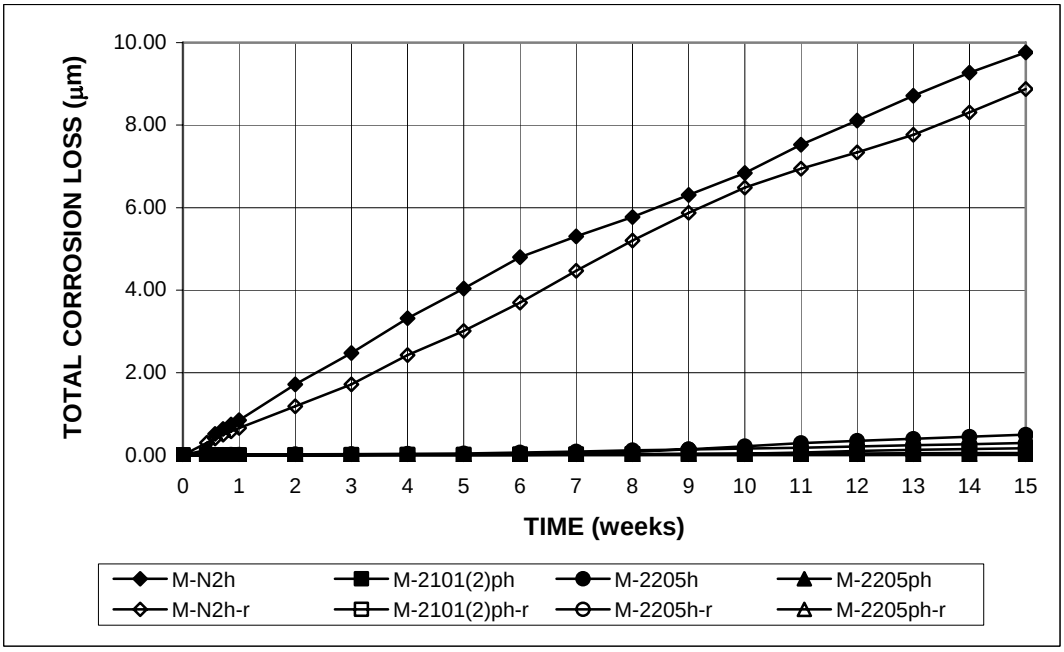

(a)

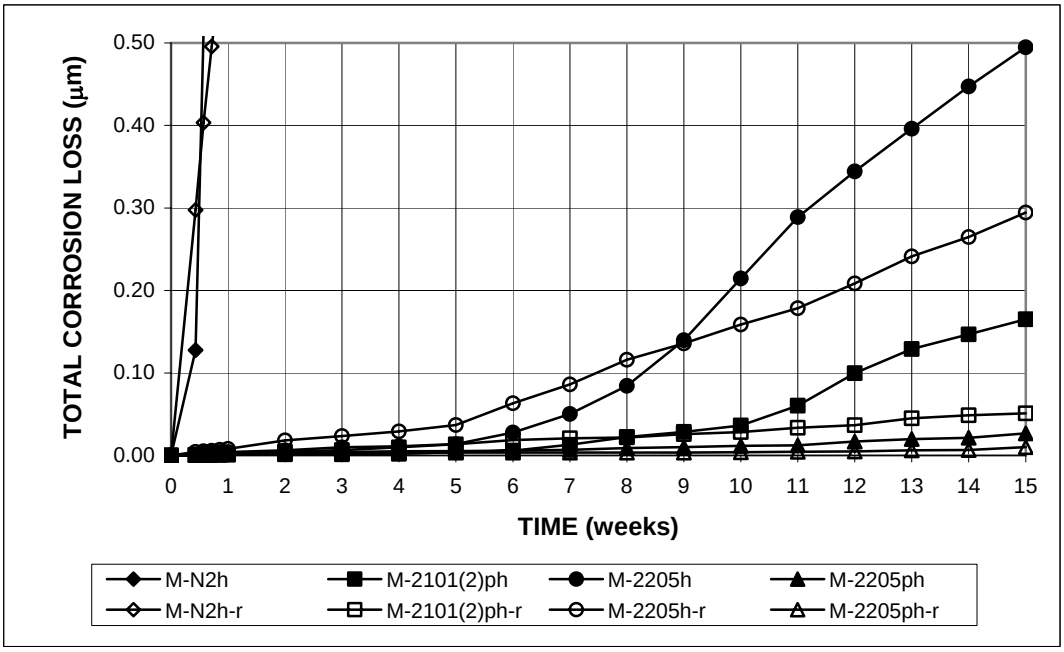

(b)

Figure 3.114 - Macrocell test. Average total corrosion losses for bare conventional and duplex stainless steels in simulated concrete pore solution with 6.04 molal ion NaCl, replacing and without replacing the test solutions every five weeks.

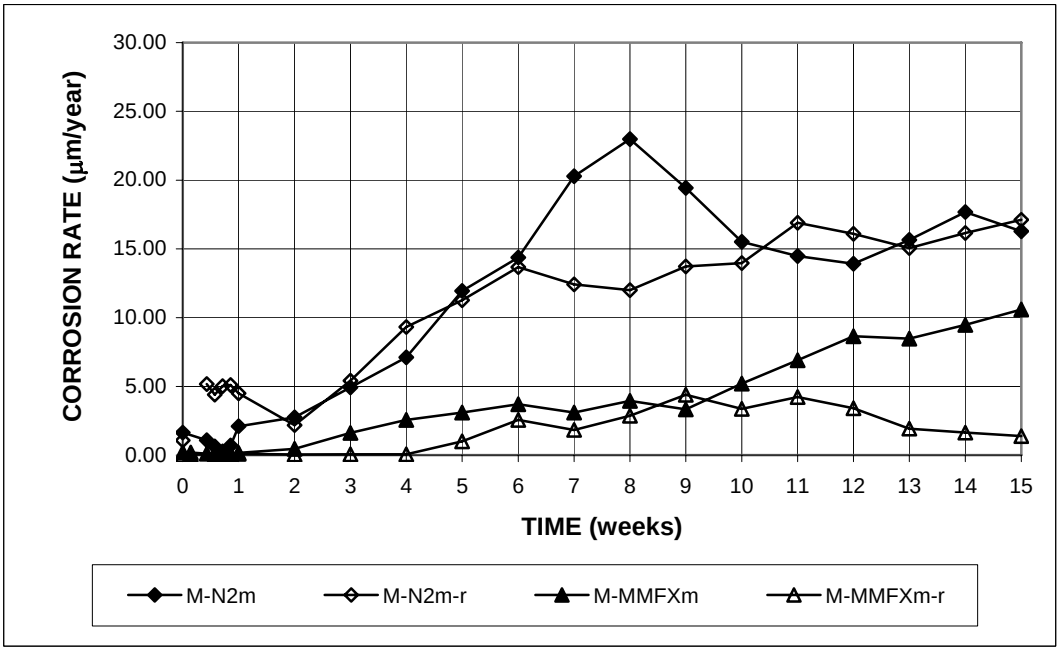

Figure 3.115 - Macrocell test. Average corrosion rates, mortar-wrapped conventional and MMFX steels in simulated concrete pore solution with 1.6 molal ion NaCl, replacing and without replacing the test solutions every five weeks.

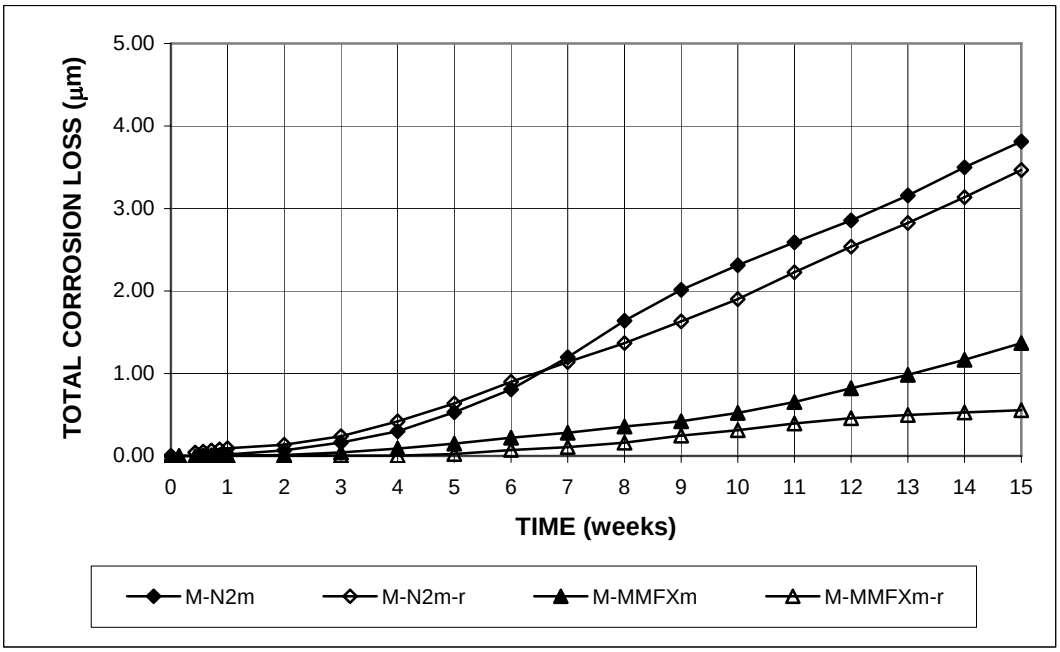

Figure 3.116 -Macrocell test. Average total corrosion losses, mortar-wrapped conventional and MMFX steels in simulated concrete pore solution with 1.6 molal ion NaCl, replacing and without replacing the test solutions every five weeks.

3.6 SUMMARY OF RESULTS

Conventional steel – Four batches of conventional reinforcing steel: N, N2, N3, and N4 were evaluated. Compared to the other steels in this study, the conventional steels exhibited the lowest corrosion resistance in all tests. Overall, there is no statistically significant difference between the conventional steels.

Epoxy-coated steel – Epoxy-coated steel was evaluated with both epoxy-coated and uncoated bars as the cathode. The epoxy coating was penetrated by four 3.2-mm (0.125-in.) diameter holes to simulate defects in the coating.

As shown in Tables 3.6 and 3.8, when uncoated steel was used as the cathode, the corrosion losses for epoxy-coated steel, based on the total area, were 7%, 12%, and 24% of (based on the exposed area, 7, 57, and 117 times) the values for conventional steel in the mortar-wrapped macrocell specimens, Southern Exposure, and cracked beam tests, respectively.

When epoxy-coated steel was used as the cathode, for the macrocell test with bare bars in 1.6 m ion NaCl solution, the corrosion loss for epoxy-coated steel was 6% of the value for conventional steel based on the total area and six times the value for conventional steel based on the exposed area; for the macrocell test with mortar wrapped specimens, the corrosion losses of epoxy-coated steel were 0.4% and 40% of the values for conventional steel, based on the total and exposed area, respectively.

The results demonstrate that the cathode area has great effect on the corrosion rate of the epoxy-coated steel and that it is important to use all epoxy-coated reinforcing steel on bridge decks, rather than just the top mat of steel.

MMFX steel – Microcomposite MMFX II steel was evaluated in the “as delivered” condition. In all evaluations, MMFX exhibited higher corrosion resistance than the conventional steels, with average corrosion losses at the end of the tests

between 16% and 66% of the values for conventional steel. The corrosion losses, however, were higher than the values exhibited by epoxy-coated steel based on the total area.

As shown in Table 3.10, in the macrocell test, without replacing the test solutions every five weeks, MMFX steel had average corrosion losses equal to 28% and 26% of the values for conventional steel for bare and mortar-wrapped specimens, respectively, in the 1.6 m ion NaCl solution. When the test solutions were replaced every five weeks, MMFX steel had average corrosion losses equal to 43%, 66%, and 16% of the values for conventional steel for bare bars in the 1.6 m ion NaCl solution, bare bars in the 6.04 m ion NaCl solution, and mortar-wrapped specimens, respectively.

As shown in Table 3.12, in the Southern Exposure and cracked beam tests, the average corrosion losses for MMFX steel were 26% and 37% of the values for conventional steel, respectively,.

The effect of the combining MMFX and conventional steels was evaluated using the macrocell (mortar-wrapped specimens) and Southern Exposure tests. The average total corrosion losses indicate that MMFX anode bars with MMFX steel as the cathode performed comparatively better than those with conventional steel as the cathode (it may be due to MMFX steel limits the activity at the cathode), indicating that MMFX steel can be used in conjunction with conventional steel.

Bent MMFX steel in the Southern Exposure test exhibited an average corrosion loss equal to 1.7 times the value of straight MMFX steel. However, it is not clear that bending MMFX steel, in fact, causes additional corrosion because only three bent MMFX specimens were evaluated, and the average corrosion rate of the specimens dropped significantly over time, from the highest during the first 12 weeks

to the lowest in the second half of the test period compared to the values for conventional and straight MMFX steels.

Of corrosion potential tests to evaluate conventional and MMFX steel as a function of chloride concentration in simulated concrete pore solution, bare conventional and MMFX bars exhibited active corrosion (corrosion potentials more negative than –0.275 V with respect to SCE) at molal ion concentrations of 0.5 m and above, corresponding to a critical Cl^-/OH^- ratio of 0.31 (as will be seen in Chapter 4, the critical chloride threshold for MMFX steel in concrete is three to four times the value for conventional steel). At the NaCl highest concentrations (1.6 and 6.04 m), the corrosion potentials for MMFX steel were only slightly more positive than conventional steel, ranging from –0.300 to –0.500 V. Overall, the corrosion potential test, along with the macrocell and bench-scale tests, show that MMFX and conventional steel have nearly identical corrosion potentials, indicating that both steels have a similar tendency to corrode.

Duplex stainless steels – Duplex stainless steels evaluated include two heats of 2101 steel and one heat of 2205 steel in both the “as-rolled” and pickled conditions. The bars in the first heat of 2101 steel (2101 and 2101p) were slightly deformed and had small cracks on the surface due to a lack of boron. The second heat [2101(2) and 2101(2)p] was provided to allow a fair evaluation of the steel. The results demonstrate that pickled 2101 steel [2101(2)p] and nonpickled and pickled 2205 steel (2205 and 2205p) exhibit significantly better corrosion resistance than conventional steel, while nonpickled 2101 steel [2101(2)] has similar corrosion resistance to MMFX steel. The corrosion resistance of duplex stainless steels depends on the chromium (Cr) and nickel (Ni) contents and whether the bars are pickled or nonpickled. Overall, 2205 steel (22% chromium and 5% nickel) has better corrosion

resistance than 2101 steel (21% chromium and 1% nickel) when evaluated in the same condition, pickled bars have higher corrosion resistance than nonpickled bars, and pickled 2101 steel has better corrosion resistance than nonpickled 2205 steel.

In the macrocell test, for bare and mortar-wrapped specimens in 1.6 m ion NaCl solution (Tables 3.14 and 3.20), nonpickled 2101 steel [2101(2)] had average corrosion losses equal to 16% and 21% of the values for conventional steel, respectively, while pickled 2101 steel and nonpickled and pickled 2205 steels remained passive throughout the test period, with corrosion losses less than 0.4% of the value of conventional steel for bare bars and 0.8% of the value of conventional steel for mortar-wrapped specimens.

In the macrocell test with bare bars in 6.04 m ion NaCl solution, the corrosion performance of duplex stainless steels are more clearly distinguished. Without replacing the test solutions every five weeks, the average corrosion losses for 2101(2), 2101(2)p, 2205, and 2205p steel were 35%, 2%, 5%, and 0.3% of the values for conventional steel, respectively (Table 3.16). When the test solutions were replaced every five weeks, the average corrosion losses for 2101(2)p, 2205, and 2205p steel were 0.6%, 3%, and 0.1% of the values for conventional steel, respectively (Table 3.18). In the high NaCl concentration test, the average anode corrosion potentials with respect to SCE for 2205 and 2101(2)p steels (Figure 3.69a and 72a) dropped from about –0.150 V to values more negative than –0.200 V during the second half of the test period, while the corrosion potential for 2205p steel remained around –0.150 V throughout the test.

In the Southern Exposure test, the average corrosion losses for 2101(2), 2101(2)p, 2205, and 2205p steel were 5%, 0.3%, 1.0%, and 0.3% of the values of conventional steel, respectively (Table 3.22). Although the pickled 2101 and 2205

steels exhibited the same corrosion loss at the end of the test, results for individual specimens show that one 2101(2)p specimen was corroding during the last few weeks, with the corrosion potentials of the top mat more negative than –0.350 V with respect to CSE (Figure A.178a), while all pickled 2205 bars remained passive throughout the test period. As discussed by Balma et al. (2005), the corrosion activity of the pickled 2101 steel may be caused by steel that is not fully pickled.

In the cracked beam test, the average corrosion losses for 2101(2), 2101(2)p, 2205, and 2205p steel were 37%, 0.5%, 5%, and 0.5% of the values of conventional steel, respectively (Table 3.24). The average corrosion potentials of the top mat for 2101(2)p, 2205, and 2205p steel were becoming progressively more negative, with the value for 2101(2)p steel slightly more positive than –0.300 V, the value for 2205 steel more negative than –0.300 V, and the value for 2205p steel more positive than –0.200 V at the end of the test (Figure 3.96a).

In all evaluations, pickled 2205 steel remained passive throughout the test period and exhibited the best corrosion resistance of the steels evaluated in this study.

The effect of the combining conventional steel and duplex stainless steels [2101(2)p and 2205] was evaluated using the macrocell and Southern Exposure tests. The results show that the corrosion resistance of specimens containing both duplex stainless steel and conventional steel is similar to that of specimens with these steels alone, indicating the use of duplex stainless steel in conjunction with conventional steel is not a problem.

CHAPTER 4

CHLORIDE DIFFUSION IN TEST SPECIMENS AND CRITICAL CHLORIDE THRESHOLDS

This chapter presents results and analysis of chloride diffusion in Southern Exposure specimens, including the diffusion coefficients and surface concentrations calculated based on chloride profiles in dummy SE specimens (specimens without reinforcing steel), and the critical chloride thresholds for conventional, MMFX microcomposite, and duplex stainless steels. In addition, values obtained using different chloride analysis methods are compared.

4.1 CHLORIDE ANALYSIS IN CONCRETE

As described in Section 2.5.1, chloride concentrations in 45 concrete samples from dummy SE specimens were analyzed using Procedure A in AASHTO T 260-97 for total chlorides (referred to in this report as *Method 1*), Procedure A in AASHTO T 260-97 for water-soluble chlorides (*Method 2*), and Procedure C in AASHTO T 260-94 for total chlorides (*Method 3*). Thirty of the samples were also tested by the Kansas Department of Transportation (KDOT) using *Method 2*. Based on the results, a relationship between *Method 1* and *Method 3* for total chloride analysis is established, the total and water-soluble chloride concentrations obtained using *Method 1* and *Method 2*, respectively, are compared, and the accuracy of the chloride analysis in this study is evaluated.

4.1.1 Procedures A and C in AASHTO T 260 for total chlorides

For Procedure A in AASHTO T 260-97 (*Method 1*), powdered concrete samples are digested using a nitric acid (HNO_3) solution, and the total chloride content is determined directly using potentiometric titration. For Procedure C in AASHTO T 260-94 (*Method 3*), concrete samples are digested using a mild acid solution, and the percent chloride content by weight of the concrete is determined based on a reading, taken with a millivoltmeter on the sample solution using a specific chloride ion electrode, in conjunction with a calibration equation, which represents the response of the electrode in combination with the millivoltmeter to chloride ion concentration. Because of the different digestion methods, the chloride content [referred to as *y* in Eq. (3) in AASHTO T 260-94] obtained from *Method 3* and the total chloride content from *Method 1* are different. The two chloride contents, however, have a unique linear relationship for each electrode and millivoltmeter combination, which can be established by running both methods for a set of concrete samples and comparing the results using linear regression analysis. Based on the linear relationship (a linear regression equation), an equivalent total chloride content can be calculated as follows:

$$\% \text{ Cl} = A + By \tag{4.1}$$

where

% Cl = equivalent total chloride content;

y = percent chloride content based on the millivolt reading and calibration equation of the electrode/meter combination from *Method 3*.

A and *B* = the intercept and the slope, respectively, in the regression equation.

According to Procedure C in AASHTO T 260-94, the equivalent chloride content, rather than the value *y*, is the total chloride content reported.

In this study, the total chloride concentrations from *Method 1* and those based on the millivolt reading from *Method 3* (*y*) for 45 concrete samples are tabulated in Table 4.1. The total chloride concentrations from *Method 1* are between 0.01 and 1.0% by weight of concrete [0.22 and 22.3 kg/m^3 (0.38 and 37.6 lb/yd^3)]. As will be seen later, these values cover the range of most of the chloride concentrations obtained in this study. Based on the regression analysis of the data using an Excel spreadsheet, a linear equation with an intercept of 0.0108 (*A*), a slope of 1.3143 (*B*), and a coefficient of determination R^2 of 0.9947 was obtained, as shown in Figure 4.1. The high coefficient of determination indicates a good linear correlation between *Method 1* and *Method 3*. Based on the values of *A* and *B*, the equivalent total chloride contents of the samples were obtained, also shown in Table 4.1. In this study, since the combination of the electrode and millivoltmeter did not change, the values of *A* and *B* were assumed to be constant; all total chloride contents obtained using *Method 3* are reported as equivalent chloride contents, converted from the values of *y* based on the *A* and *B*.

Table 4.1 – Total chloride concentrations from Procedure A in AASHTO T 260-97 (*Method 1*) and Procedure C in AASHTO T 260-94 (*Method 3*)

Sample[a]	Depth (mm)	Total Cl^- from Method 1		*y* from Method 3[b]	Total Cl^- from Method 3[c]	
		% wt. of concrete	kg/m^3	% wt. of concrete	% wt. of concrete	kg/m^3
X-1-0.5	13	0.278	6.24	0.166	0.229	5.13
X-1-1.0	25	0.028	0.62	0.012	0.027	0.60
X-1-1.5	38	0.014	0.31	0.028	0.047	1.06
X-1-3.0	76	0.010	0.22	0.003	0.015	0.34
X-1-5.5	140	0.012	0.28	0.004	0.016	0.37
Y-1-0.5	13	0.341	7.65	0.221	0.302	6.77
Y-1-1.0	25	0.015	0.33	0.008	0.021	0.47
Y-1-1.5	38	0.012	0.27	0.004	0.016	0.36
Y-1-3.0	76	0.014	0.30	0.004	0.016	0.37
Y-1-5.5	140	0.005	0.11	0.004	0.016	0.37
Z-1-0.5	13	0.243	5.46	0.153	0.212	4.75
Z-1-1.0	25	0.020	0.45	0.032	0.053	1.20
Z-1-1.5	38	0.020	0.45	0.010	0.024	0.53
Z-1-3.0	76	0.017	0.38	0.008	0.021	0.47
Z-1-5.5	140	0.017	0.38	0.007	0.020	0.45
X-2-0.5	13	0.756	16.96	0.539	0.719	16.13
X-2-1.0	25	0.312	7.00	0.211	0.289	6.47
X-2-1.5	38	0.021	0.46	0.011	0.025	0.56
X-2-3.0	76	0.010	0.22	0.004	0.017	0.37
X-2-5.5	140	0.019	0.44	0.005	0.017	0.38
Y-2-0.5	13	0.651	14.59	0.484	0.647	14.51
Y-2-1.0	25	0.198	4.44	0.136	0.190	4.26
Y-2-1.5	38	0.017	0.38	0.012	0.026	0.58
Y-2-3.0	76	0.009	0.21	0.007	0.020	0.45
Y-2-5.5	140	0.077	1.74	0.044	0.068	1.54
Z-2-0.5	13	0.758	17.01	0.601	0.800	17.95
Z-2-1.0	25	0.462	10.36	0.342	0.460	10.32
Z-2-1.5	38	0.144	3.22	0.091	0.130	2.92
Z-2-3.0	76	0.014	0.30	0.006	0.019	0.43
Z-2-5.5	140	0.010	0.23	0.004	0.017	0.37
X-3-0.5	13	0.846	18.97	0.678	0.902	20.23
X-3-1.0	25	0.592	13.29	0.442	0.591	13.26
X-3-1.5	38	0.371	8.32	0.272	0.368	8.26
X-3-3.0	76	0.017	0.38	0.003	0.015	0.34
X-3-5.5	140	0.367	8.24	0.267	0.362	8.12
Y-3-0.5	13	0.906	20.32	0.698	0.928	20.83
Y-3-1.0	25	0.621	13.92	0.497	0.665	14.91

Table 4.1 (con't) – Total chloride concentrations from Procedure A in AASHTO T 260-97 (*Method 1*) and Procedure C in AASHTO T 260-94 (*Method 3*)

Y-3-1.5	38	0.419	9.40	0.314	0.423	9.49
Y-3-3.0	76	0.023	0.52	0.007	0.019	0.43
Y-3-5.5	140	0.032	0.71	0.014	0.030	0.67
Z-3-0.5	13	0.994	22.30	0.707	0.940	21.09
Z-3-1.0	25	0.809	18.15	0.584	0.779	17.48
Z-3-1.5	38	0.527	11.83	0.404	0.541	12.14
Z-3-3.0	76	0.020	0.45	0.003	0.015	0.34
Z-3-5.5	140	0.053	1.20	0.024	0.043	0.96

a: A-B-C

A: X = the first dummy SE specimen, Y = the second specimen, Z = the third specimen.

B: 1 = the first sampling, 2 = the second sampling, 3 = the third sampling.

C: 0.5, 1.0, 1.5, 3.0, and 5.5 = the depths (in.) of the samples.

b: *y*, referred in Eq. (3) in AASHTO T290 -94, is the percent chloride content based on millivolt reading and calibaration equation of electorde and voltmeter.

c: The total chloride content is the equivalent value, equal to $A+By$. A and B are obtained by a regression analysis for the chloride contents from *Method 1* and the values of y from M*ethod 3*. In this study, based on 45 samples, A = 0.0108 and B = 1.3143.

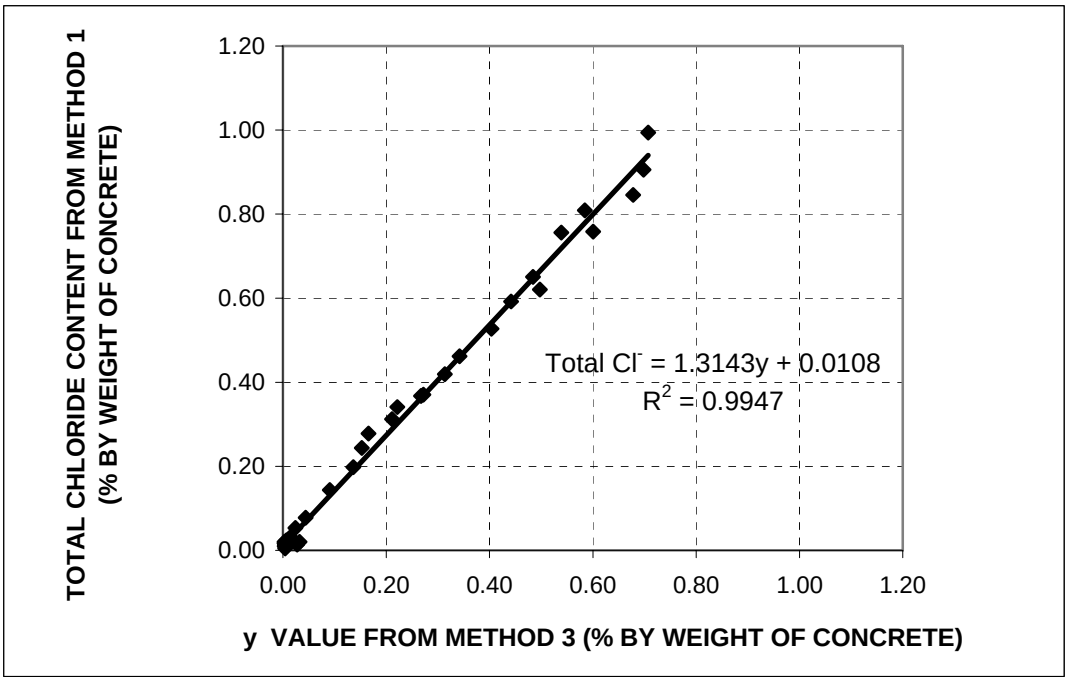

Figure 4.1 - Linear relationship between total Cl^- based on Procedure A in AASHTO T 260 - 97 (*Method 1*) and the value of *y* based on Procedure C in AASHTO T 260-94 (*Method 3*) for 45 concrete samples.

4.1.2 Comparison of total and water-soluble chloride contents

The total and water-soluble chloride contents of the 45 concrete samples, determined using *Method 1* and *Method 2*, respectively, are tabulated in Table 4.2. The table also includes test results obtained by the Materials laboratory of the Kansas Department of Transportation (KDOT) using *Method 2*.

Table 4.2 – Total chloride concentrations and water-soluble chloride concentrations based on Procedure A in AASHTO T 260-97 (*Method 1 and Method 2*) for concrete samples.

Samples[a]	Depth (mm)	Total chloride contents Method 1(kg/m^3)	Water-soluble chloride contents (kg/m^3)	
			Method 2	Method 2 by KDOT [b]
X-1-0.5	13	6.24	6.51	5.59
X-1-1.0	25	0.62	0.44	0.34
X-1-1.5	38	0.31	0.23	0.19
X-1-3.0	76	0.22	0.17	0.17
X-1-5.5	140	0.28	0.17	0.24
Y-1-0.5	13	7.65	7.46	7.46
Y-1-1.0	25	0.33	0.25	0.27
Y-1-1.5	38	0.27	0.23	0.00
Y-1-3.0	76	0.30	0.20	0.17
Y-1-5.5	140	0.11	0.12	0.00
Z-1-0.5	13	5.46	5.25	5.05
Z-1-1.0	25	0.45	0.35	0.29
Z-1-1.5	38	0.45	0.35	0.27
Z-1-3.0	76	0.38	0.20	0.22
Z-1-5.5	140	0.38	0.27	0.24
X-2-0.5	13	16.96	16.66	16.55
X-2-1.0	25	7.00	7.04	7.13
X-2-1.5	38	0.46	0.44	0.34
X-2-3.0	76	0.22	0.12	0.00
X-2-5.5	140	0.44	0.28	0.22
Y-2-0.5	13	14.59	14.67	14.52
Y-2-1.0	25	4.44	4.49	4.48
Y-2-1.5	38	0.38	0.41	0.41
Y-2-3.0	76	0.21	0.28	0.19
Y-2-5.5	140	1.74	1.74	1.64
Z-2-0.5	13	17.01	18.63	17.64
Z-2-1.0	25	10.36	10.10	10.16
Z-2-1.5	38	3.22	3.00	2.98

Table 4.2 (con't) – Total chloride concentrations and water-soluble chloride concentrations based on Procedure A in AASHTO T 260-97 (*Method 1 and Method 2*) for concrete samples.

Samples[a]	Depth (mm)	Total chloride contents Method 1(kg/m^3)	Water-soluble chloride contents (kg/m^3)	
			Method 2	Method 2 by KDOT [b]
Z-2-5.5	140	0.23	0.20	0.00
X-3-0.5	13	18.97	18.52	-
X-3-1.0	25	13.29	13.10	-
X-3-1.5	38	8.32	8.13	-
X-3-3.0	76	0.38	0.30	-
X-3-5.5	140	8.24	7.79	-
Y-3-0.5	13	20.32	19.72	-
Y-3-1.0	25	13.92	13.33	-
Y-3-1.5	38	9.40	9.03	-
Y-3-3.0	76	0.52	0.41	-
Y-3-5.5	140	0.71	0.56	-
Z-3-0.5	13	22.30	20.76	-
Z-3-1.0	25	18.15	17.33	-
Z-3-1.5	38	11.83	11.53	-
Z-3-3.0	76	0.45	0.30	-
Z-3-5.5	140	1.20	1.09	-

a: A-B-C
A: X = the first dummy SE specimen, Y = the second specimen, Z = the third specimen.
B: 1 = the first sampling, 2 = the second sampling, 3 = the third sampling.
C: 0.5, 1.0, 1.5, 3.0, and 5.5 = the depths (in.) of the samples.
b: Kansas Department of Transportation.

For comparison, the differences between the total and water-soluble chloride contents (excluding the KDOT results) are plotted versus the total chloride contents in Figure 4.2 and the ratios of the water-soluble to total chloride contents are plotted versus the total chloride contents in Figure 4.3.

Figure 4.2 shows that the total chloride contents are generally higher than the water-soluble chloride contents, with the exception of just a few samples (a result that may be a function of the natural variability of the test results). The difference between the total and water-soluble chloride contents, representing the bound chlorides, increases with the chloride content, indicating that as the chloride content increases, more chlorides are removed from the concrete pore solution by chloride binding.

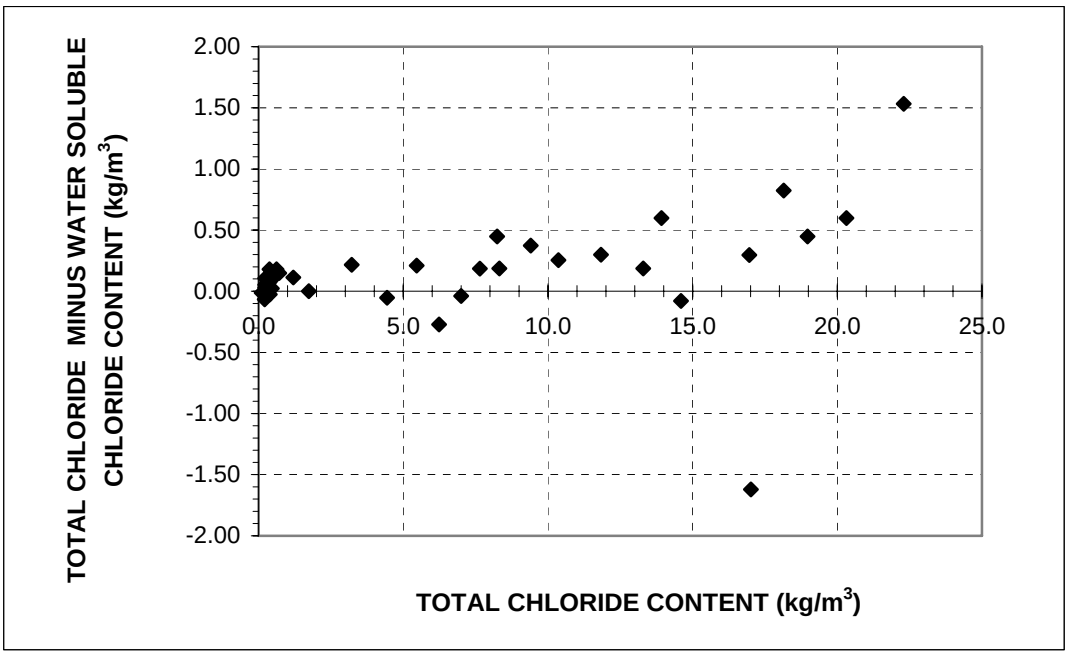

Figure 4.2 - Differences between the total and water-soluble chloride contents (the bound chlorides) versus the total chloride contents for 45 concrete samples.

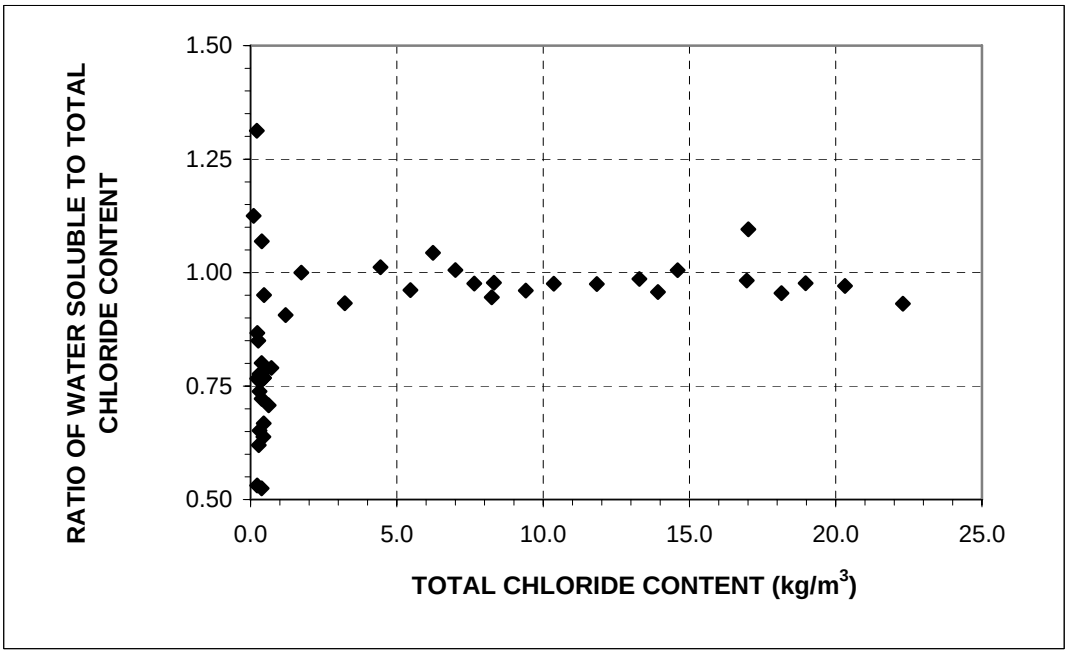

Figure 4.3 - Ratios of water-soluble chlorides to total chlorides for 45 concrete samples.

As shown in Figure 4.4, when the chloride content is low, say, less than 0.6 kg/m^3 (1.0 lb/yd^3), the ratios of the water-soluble chlorides to total chlorides exhibit large scatter. The values range from 0.52 to 1.31, with a comparatively low average of 0.8. The large scatter in the ratios reflects the effects of the variability of the tests, superimposed on the low chloride contents of samples. For chloride contents higher than 0.6 kg/m^3 (1.0 lb/yd^3), however, the ratios of the water-soluble chlorides to total chlorides appear to be quite constant, mostly between 0.9 and 1.0, with an average of 0.96. The higher ratio indicates that a smaller fraction of the higher chloride content is chemically bound. As mentioned in Chapter 1, chloride binding primarily occurs because of the reaction between chlorides and tricalcium aluminate (C_3A), one of the components of cement, to form calcium chloroaluminate ($3CaO{\cdot}Al_2O_3{\cdot}CaCl_2{\cdot}10H_2O$). In this study, when the measured chloride content in the concrete is low, the majority of the chlorides are likely those that are added into the concrete at the time of mixing [as will be seen later, the initial chloride content can reach 0.3 kg/m^3 (0.5 lb/yd^3)]. Therefore, a relatively high percentage of the chlorides can be bound during the initial hydration reaction. The concrete samples with a high chloride content represent mature concrete into which chloride from external sources is dominant. In this case, only a small fraction of the chlorides were bound since much less C_3A is available in hardened concrete than in cement. It is expected that the ratios of the water-soluble to total chlorides would have been lower if all of the chlorides had been added to concrete at the time of mixing.

4.1.3 Evaluation of the accuracy of the chloride analysis

Thirty of the 45 samples were sent to the Kansas Department of Transportation (KDOT) for testing for water-soluble chlorides using *Method 2*. The

results from KDOT are presented in Table 4.2. For comparison, the chloride contents tested by KDOT are plotted versus those tested in this study in Figure 4.4. The ratios of the values obtained in this study to those from KDOT are plotted versus the values in this study in Figure 4.5. The differences between the values in this study and those from KDOT are plotted in Figure 4.6.

Figure 4.4 shows that the chloride contents tested in this study have a good linear correlation with the values obtained by KDOT. The two group values range from 0 to 20 kg/m^3, yielding a linear equation with an intercept of –0.0477, a slope of 0.9789, and a coefficient of determination R^2 of 0.9947 based on a regression analysis.

Figure 4.5 shows that the ratios of the chloride contents tested in this study to those tested by KDOT are between 0.7 and 1.5, with an average of 1.10. When the chloride content is low [< 0.6 kg/m^3 (1.0 lb/yd^3)], the ratios range from 0.7 to 1.5, with an average of 1.15 and a standard deviation of 0.20, while when the chloride content is higher than 0.6 kg/m^3 (1.0 lb/yd^3), the ratios range from 0.99 to 1.16, with an average of 1.03 and a standard deviation of 0.05. The large scatter in the ratios, representing a large relative error of testing, occurs only when samples have a low chloride content (less than 0.6 kg/m^3).

As shown in Figure 4.6, most of the chloride results obtained in the lab are slightly higher than those obtained in KDOT. The differences between the values range form –0.1 to 1.0 kg/m^3 (–0.17 to 1.69 lb/yd^3), without any trend.

Overall, the chloride contents tested in this study are very close to the corresponding values tested by KDOT, indicating the chloride analyses in this study are reliable.

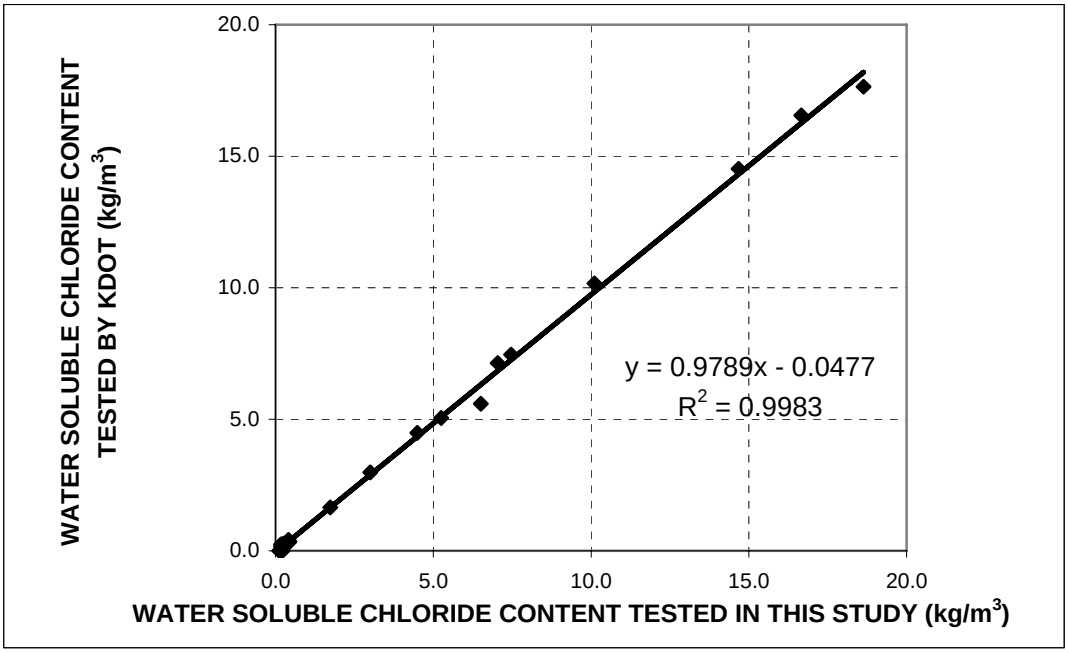

Figure 4.4 – Water-soluble chlorides tested in this study versus the chloride contents tested in KDOT for 30 concrete samples

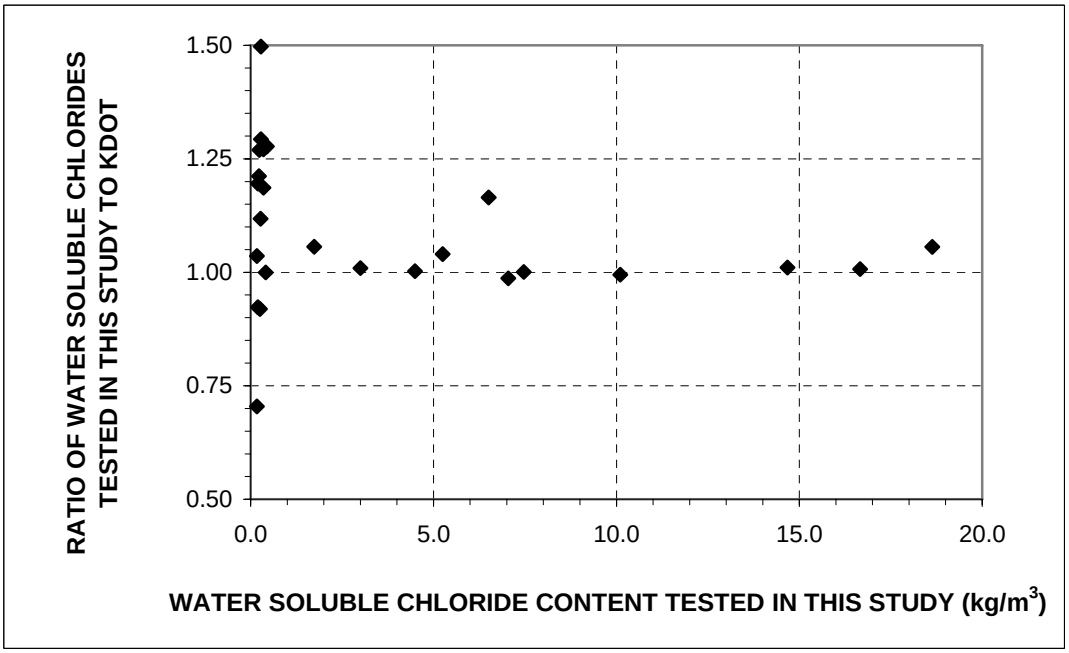

Figure 4.5 - Ratios of water-soluble chlorides tested in this study to KDOT versus the chloride contents tested in this study for 30 concrete samples

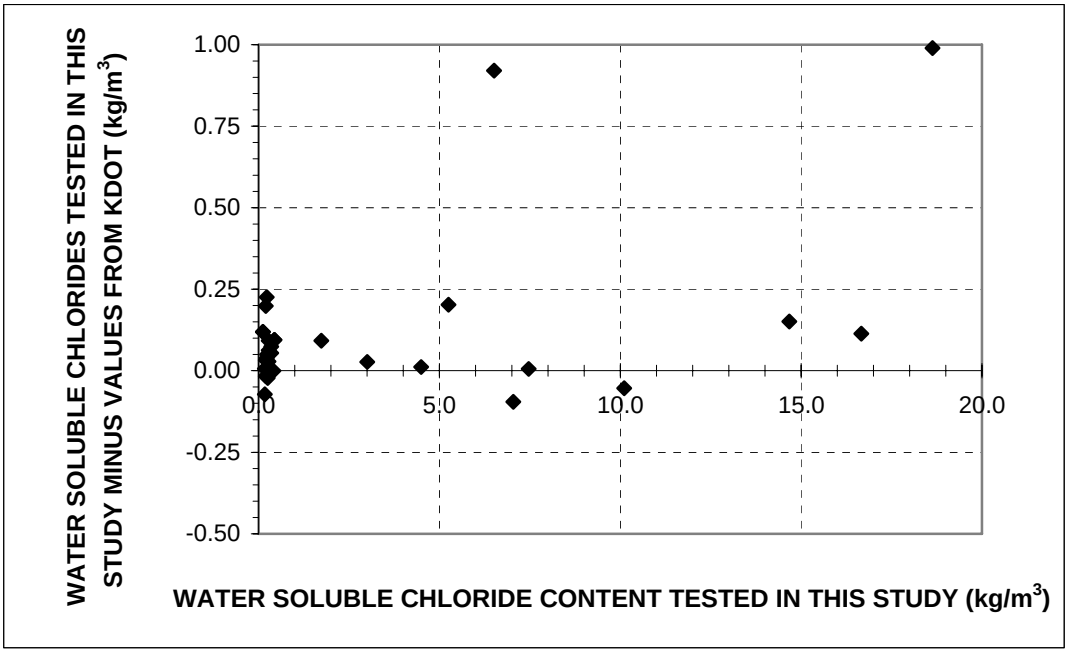

Figure 4.6 - Differences between the water-soluble chloride contents tested in this study and KDOT versus the chloride contents tested in this study for 30 concrete samples.

4.2 CHLORIDE PROFILES AND DIFFUSION EQUATIONS

As described in Section 2.5.2, the chloride profiles for three dummy SE specimens (SE-D1) in the first study and six dummy SE specimens (SE-D2) in the second study were obtained. In this section, the average chloride profile results are presented in Figures 4.7 through 4.9. Based the average values, three optimum diffusion equations, for total chlorides from the first study [Eq. (4.4)] and for total and water-soluble chlorides from the second study [Eq. (4.5) and (4.6)], were obtained using the least squares method.

4.2.1 Chloride profiles

The average total chloride concentrations at varying depths are plotted versus time in Figure 4.7 for the SE-D1 specimens (the individual results are presented in Table E.1 in Appendix E).

The figure shows that the chloride concentration decreases significantly as the depth increases, while increasing with time. At 6 weeks, the average chloride contents were 5.8, 1.9, 0.21, 0.18, and 0.17 kg/m^3 (9.7, 3.2, 0.36, 0.30, and 0.28 lb/yd^3) at depths of 13, 25, 38, 76, and 140 mm (0.5, 1, 1.5, 3, and 5.5 in.), respectively. At the end of the test, 96 weeks, the average chloride contents were 22.9, 19.9, 17.5, 3.4, and 5.2 kg/m^3 (38.6, 33.6, 29.5, 5.7, and 8.8 lb/yd^3) at depths of 13, 25, 38, 76, and 140 mm (0.5, 1, 1.5, 3, and 5.5 in.), respectively. The average chloride content at a depth of 140 mm (5.5 in.) remained very low (less than 0.6 kg/m^3) before 60 weeks and then increased to an unusually high level (even higher than that at a depth of 76 mm). The increase is attributed to high chloride contents at a depth of 140 mm (5.5 in.) from individual specimens, which may have been caused by capillary action of chloride ions from the bottom of specimens that had become contaminated with salt during the test. At depths of 25 mm (1 in.) and 38 mm (1.5 in.), the level o f reinforcing steel in SE specimens, the average chloride content was well above the threshold value for conventional steel, 0.6 to 0.9 kg/m^3 (1.0 to 1.5 lb/yd^3), by 6 and 24 weeks, respectively.

The average chloride contents taken from the SE-D2 specimens at varying depths are plotted versus time in Figure 4.8 for total chlorides and Figure 4.9 for water-soluble chlorides (the individual results are presented in Tables E.2 and E.3). Compared to the values from the SE-D1 specimens, most of the total chloride concentrations from the SE-D2 specimens are lower. As expected, the total chloride

contents are for the most part higher than the water-soluble chloride values due to chloride binding. At 96 weeks, the average chloride contents were 24.9, 16.8, 10.6, 0.51, and 2.1 kg/m^3 (42.0, 28.3, 17.9, 0.86, and 3.6 lb/yd^3) for total chlorides and 20.7, 14.7, 9.4, 0.50, and 2.2 kg/m^3 (34.9, 24.8, 15.8, 0.84, and 3.7 lb/yd^3) for water-soluble chlorides at depths of 13, 25, 38, 76, and 140 mm (0.5, 1, 1.5, 3, and 5.5 in.), respectively. For both total and water-soluble chlorides, the average chloride concentrations in the SE-D2 specimens exceeded 0.9 kg/m^3 (1.5 lb/yd^3) by 12 and 36 weeks at depths of 25 mm (1 in.) and 38 mm (1.5 in.), respectively. As with the SE-D1 specimens, chloride contents at a depth of 140 mm (5.5 in.) for the SE-D2 specimens jumped to unusually high values as the test progressed.

An initial chloride concentration was estimated for each specimen, taken as the average of the chloride contents at the depths of 76 mm (3 in.) and 140 mm (5.5 in.) at 6 weeks for SE-D1 specimens, and the average chloride content taken from the samples at 0 weeks for SE-D2 specimens. The results are tabulated in Table 4.3. The average initial total chloride concentration was 0.17 kg/m^3 (0.29 lb/yd^3) for the SE-D1 specimens. The average initial concentrations were 0.30 kg/m^3 (0.50 lb/yd^3) and 0.19 kg/m^3 (0.31 lb/yd^3) for total and water-soluble chlorides, respectively, for the SE-D2 specimens.

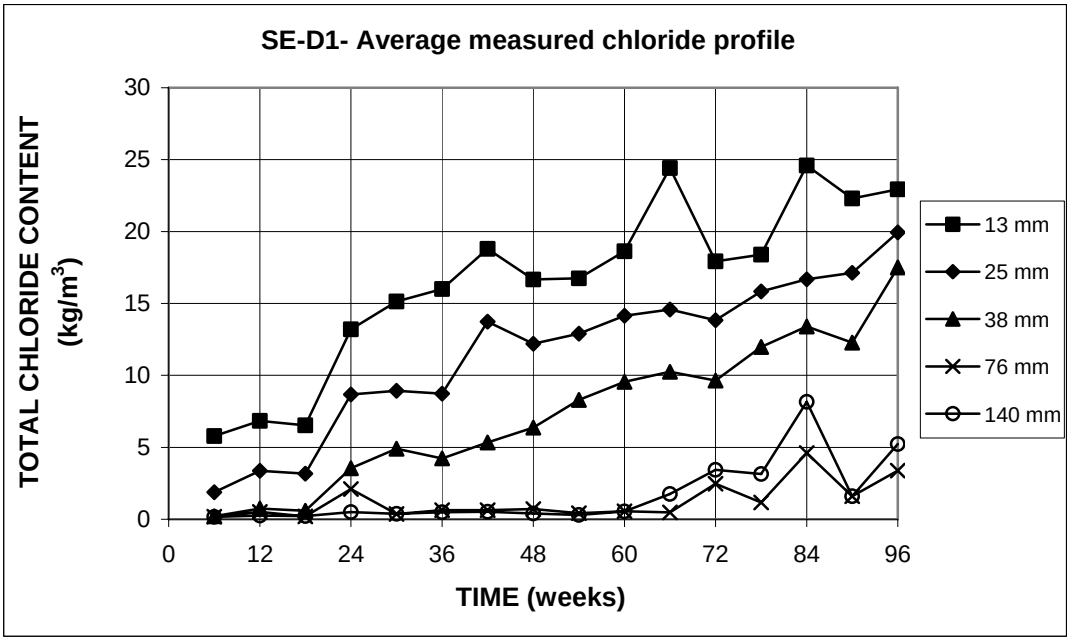

Figure 4.7 – Average total chloride contents versus time at five depths for dummy Southern Exposure specimens in the first study (SE-D1), w/c = 0.45, ponded with 15% NaCl.

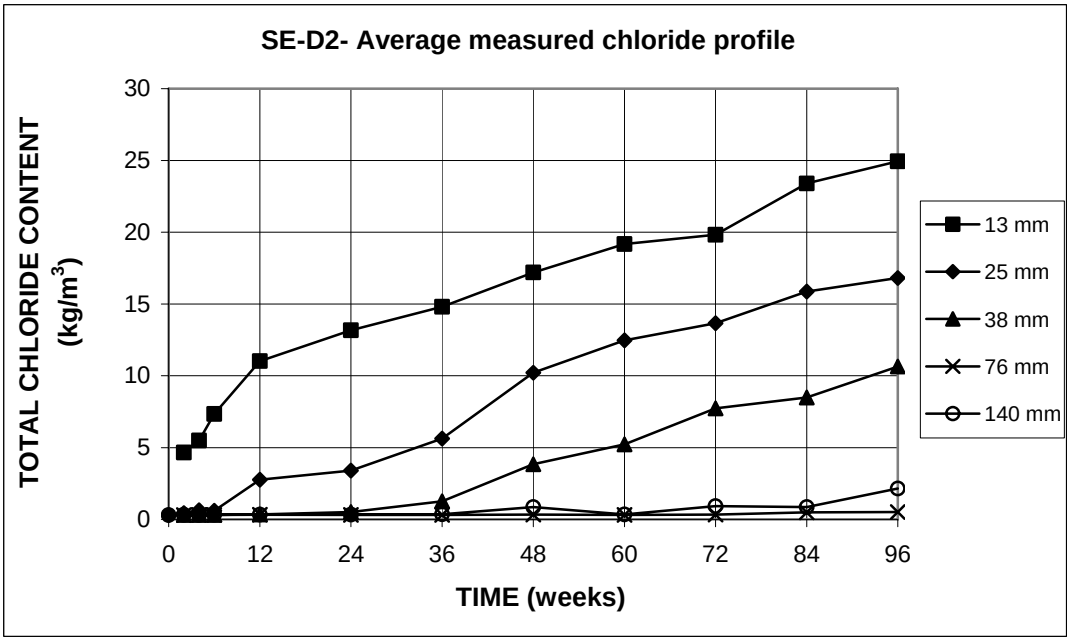

Figure 4.8 – Average total chloride contents versus time at five depths for dummy Southern Exposure specimens in the second study (SE-D2), w/c = 0.45, ponded with 15% NaCl.

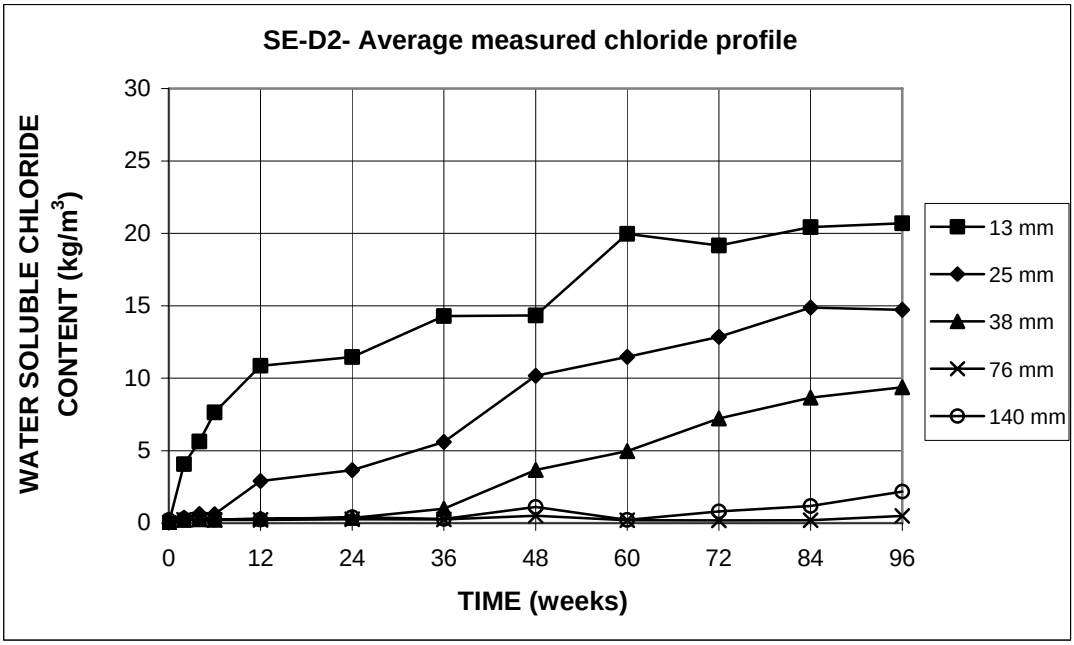

Figure 4.9 - Average water-soluble chloride contents versus time at five depths for dummy Southern Exposure specimens in the second study (SE-D2), w/c = 0.45, ponded with 15% NaCl.

Table 4.3 - Initial chloride concentrations for dummy SE specimens

Specimens[a]	Intial total chlorides (kg/m^3)	Initial water sloluble chlorides (kg/m^3)
SE-D1-1	0.145	-
SE-D1-2	0.181	-
SE-D1-3	0.196	-
Average	0.174	-
SE-D2-1	0.288	0.159
SE-D2-2	0.260	0.106
SE-D2-3	0.290	0.098
SE-D2-4	0.298	0.276
SE-D2-5	0.312	0.220
SE-D2-6	0.346	0.251
Average	0.299	0.185

a: SE = Southern Exposure test, D1, D2 = dummy SE specimens in the first and second study, respectively

4.2.2 Chloride diffusion equations

In this study, Fick's second law, assuming constant diffusion coefficient and surface concentration, Eq. (1.10), is used to model the penetration of chlorides into the SE specimens. This diffusion equation has four degrees of freedom, the effective diffusion coefficient D_c, surface concentration C_s, depth d, and time t. The diffusion coefficient and surface concentration can be determined by fitting Eq. (1.10) to measured chloride profiles by means of a nonlinear regression analysis using the least squares method. In the current study, a net chloride profile was obtained for each specimen by subtracting the initial chloride concentration from the measured chloride concentrations. In addition, the high chloride concentrations at the depth of 140 mm (5.5 in.), which may not result due to diffusion, were excluded (these values are marked with "*" in Tables E.1 through E.3 in Appendix E). Using the corrected chloride profile, two regression analyses were performed:

(1) The first consisted of minimizing the sum of square errors, S_t, based on the measured chloride concentrations at the varying depths for each time of exposure, t, to determine the values of the effective diffusion coefficient and surface concentration for each value of t.

$$S_t = \sum_{n=1}^{N} (C_m(n,t) - C_c(n,t))^2 \tag{4.2}$$

where

S_t = Sum of square errors to be minimized;

N = The number of samples, N = 5, or 4 if the value at the depth of 140 mm is excluded;

$C_m(n,t)$ = Measured chloride concentration at the n^{th} depth at time t ;

$C_c(n,t)$ = Calculated chloride concentration at the n^{th} depth at time t.

(2) The second consisted of minimizing the sum of the sum of square errors, *S*, based on all measured chloride concentrations at the varying depths at all time periods to determine a single value for the effective diffusion coefficient and surface concentration..

$$S = \sum_{t=1}^{T}\left(\sum_{n=1}^{N}(C_m(n,t) - C_c(n,t))^2\right) \qquad (4.3)$$

where

S = Sum of the Sum of square errors to be minimized;

T = The number of time periods, T = 16 for SE-D1 specimens,
and = 11 for SE-D2 specimens.

The minimization processes were performed using the solver function in Microsoft Excel Spreadsheet.

Based on the first least square analysis, a set of the best-fit effective diffusion coefficients and surface concentrations versus time were obtained. The results for individual specimens are presented in Figures E.1 through e.6 in Appendix E. The average effective diffusion coefficients and surface concentrations were determined based on the average chloride profiles (as shown in Figures 4.7 to 4.9) and are plotted versus time in Figures 4.10 and 4.11, respectively. The figures show that the effective diffusion coefficient and surface concentration exhibit very little time dependence.

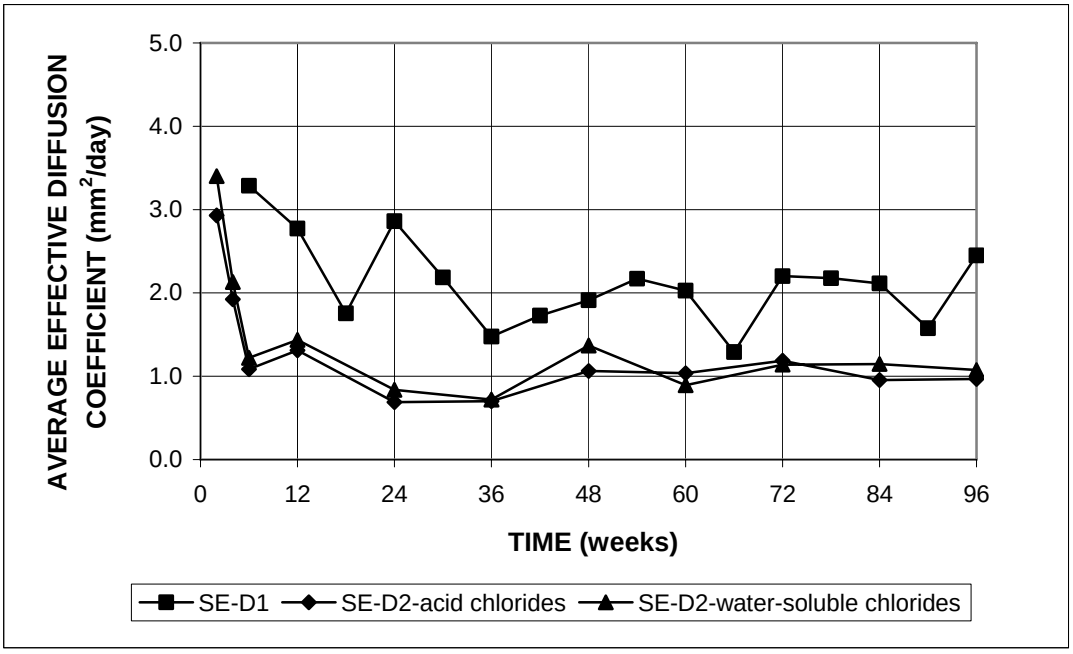

Figure 4.10 – Average effective diffusion coefficients versus time for dummy Southern Exposure specimens, w/c = 0.45, ponded with 15% NaCl.

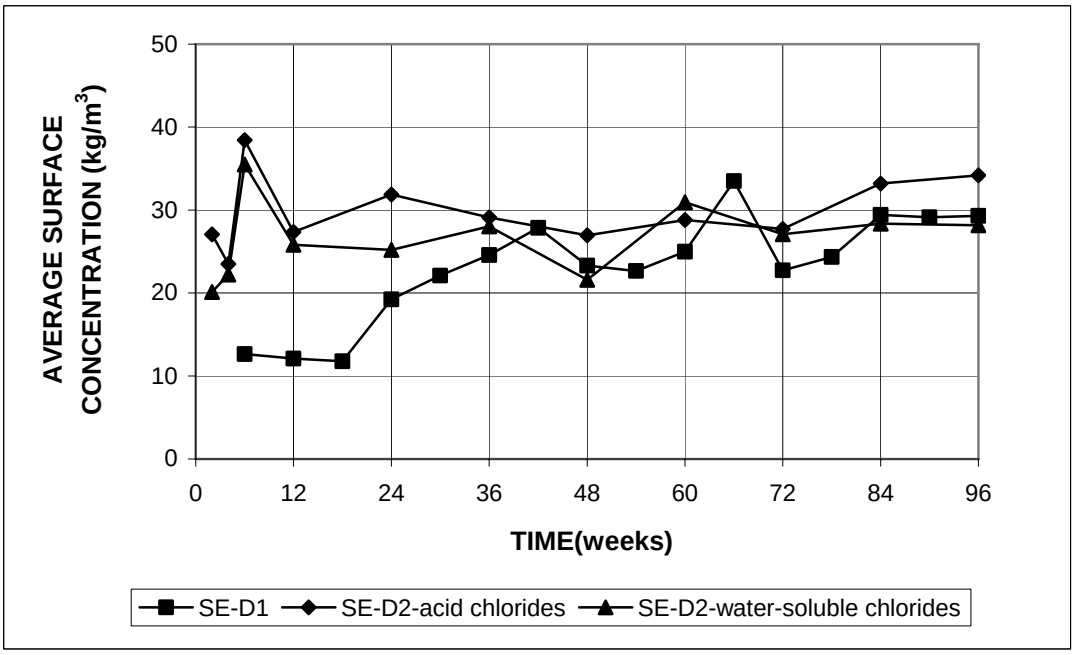

Figure 4.11 – Average surface concentrations versus time for dummy Southern Exposure specimens, specimens w/c = 0.45, ponded with 15% NaCl.

For the SE-D1 specimens, the average effective diffusion coefficient started with a value as high as 3.3 mm^2/day at 6 weeks and then dropped, varying little after 24 weeks, with values primarily around 2.0 mm^2/day. For the SE-D2 specimens, the diffusion coefficients based on total chlorides and water-soluble chlorides are very similar; the values also started high, at about 3.5 mm^2/day, and then dropped to about 0.8 mm^2/day at 24 weeks, remaining narrowly around 1.0 mm^2/day for the rest of the test period. The high initial diffusion coefficients indicate a high rate of chloride penetration into the specimens during the early period, which may be due to the absorption, rather than the diffusion of chlorides.

As shown in Figure 4.11, the average surface concentration for the SE-D1 specimens increased from an initial value of 13 kg/m^3 (22 lb/yd^3) at 6 weeks to 25 kg/m^3 (42 lb/yd^3) at 36 weeks, and then remained between 20 and 30 kg/m^3 (34 and 51 lb/yd^3), while the surface concentrations for the SE-D2 specimens appeared to be constant throughout the test period; the values based on total chlorides were between 24 to 38 kg/m^3 (40 to 64 lb/yd^3), slightly higher than those based on water-soluble chlorides, which ranged from 20 to 35 kg/m^3 (34 to 59 lb/yd^3).

Overall, for both the SE-D1 and SE-D2 specimens, the average effective diffusion coefficients and surface concentrations fluctuated within a narrow range during most of the test period. This demonstrates that assuming constant values for the diffusion coefficient and surface concentration is reasonable for these test specimens.

Following this assumption, the second least square analysis was performed [Eq. (4.3)]. The analysis produces a single effective diffusion coefficient and surface concentration based on the chloride profile over the full test period. The values from the analysis are then adopted to obtain the diffusion equation. The effective diffusion

coefficients and surface concentrations for individual specimens are tabulated in Table E.4. The average results based on the average chloride profiles (as shown in Figures 4.7 to 4.9) are presented in Table 4.4. The table also includes the sums of squared errors between the measured and calculated chloride concentrations, which can be used to evaluate the match of the calculated chloride profile to the measured chloride profile.

Table 4.4 – Average diffusion coefficients (D_c) and surface concentrations (C_s) for dummy SE specimens, by least squares analysis based on average chloride profiles at all time periods [Eq.(4.3)].

Specimens[a]	Unique values		Sum of square errors $(kg/m^3)^2$	Cl^-
	$D_c (mm^2/day)$	$C_s (kg/m^3)$		
SE-D1	1.66	26.7	283	total
SE-D2	1.00	30.2	80	total
SE-D2	1.11	26.8	70	water-soluble

a: SE = Southern Exposure test, D1, D2 = dummy SE specimens in the first and second study, respectively.

As shown in Table 4.4, the average effective diffusion coefficient and surface concentrations are, respectively, 1.66 mm^2/day and 26.7 kg/m^3 (45 lb/yd^3) for the SE-D1 specimens, 1.00 mm^2/day and 30.2 kg/m^3 (50.9 lb/yd^3) for the SE-D2 specimens based on total chlorides, and 1.11 mm^2/day and 26.8 kg/m^3 (45.2 lb/yd^3) for the SE-D2 specimens based on water-soluble chlorides. The results show that the SE-D1 specimens have a larger average diffusion coefficient and smaller surface concentration than the SE-D2 specimens. The difference may be attributed to variation in the properties of concrete cast at different times (about two years apart). For the SE-D2 specimens, the average surface concentration based on water-soluble chlorides is 11% lower than that based on total chlorides, while the diffusion coefficient is 11% higher. Based on these best-fit diffusion parameters from the

second least square analysis, as well as the initial chloride concentrations, the following diffusion equations are obtained:

$$C(x,t) = 26.7\left[1 - erf\left(\frac{x}{2\sqrt{1.66t}}\right)\right] + 0.17 \quad (4.4)$$

for the SE-D1 specimens based on total chlorides;

$$C(x,t) = 30.2\left[1 - erf\left(\frac{x}{2\sqrt{1.00t}}\right)\right] + 0.30 \quad (4.5)$$

for the SE-D2 specimens based on total chlorides;

$$C(x,t) = 26.8\left[1 - erf\left(\frac{x}{2\sqrt{1.11t}}\right)\right] + 0.19 \quad (4.6)$$

for the SE-D2 specimens based on water-soluble chlorides.

where

$C(x, t)$ = Chloride concentration at depth x (mm) and time t (day), kg/m^3;

erf = Error function.

Based on Eq. (4.4) to (4.6), the calculated chloride concentrations at varying depths are compared with the measured average chloride profiles versus time in Figures 4.12, 4.13, and 4.14 for the SE-D1 specimens, the SE-D2 specimens on an acid-soluble basis (total chlorides), and the SE-D2 specimens on a water-soluble basis, respectively.

The results show that for the SE-D1 specimens, the calculated total chloride concentrations at the depth of 25 mm (1.0 in.), are 0.67 kg/m^3 (1.13 lb/yd^3) at 5 weeks and 1.02 kg/m^3 (1.72 lb/yd^3) at 6 weeks, exceeding the lower and upper bounds of the typical chloride threshold values for conventional steel, respectively, while for SE-D2 specimens, the calculated chloride concentrations at the depth of 25 mm (1.0 in.) are

0.61 kg/m^3 (1.03 lb/yd^3) at 7 weeks and 1.01 (1.70 lb/yd^3) at 9 weeks, on an acid-soluble basis, and 0.60 kg/m^3 (1.01 lb/yd^3) at 7 weeks and 1.04 kg/m^3 (1.75 lb/yd^3) at 9 weeks, on a water-soluble basis. For all of the specimens, the calculated chloride concentrations at the depth of 140 mm (5 in.), the level of the bottom mat of steel in specimens, are between 0.19 and 0.30 kg/m^3 (0.32 and 0.51 lb/yd^3), only slightly higher than the initial chloride contents, indicating that the observed corrosion of the bottom mat of steel may not be caused by chlorides that reached the steel by diffusion through the concrete from upper surface.

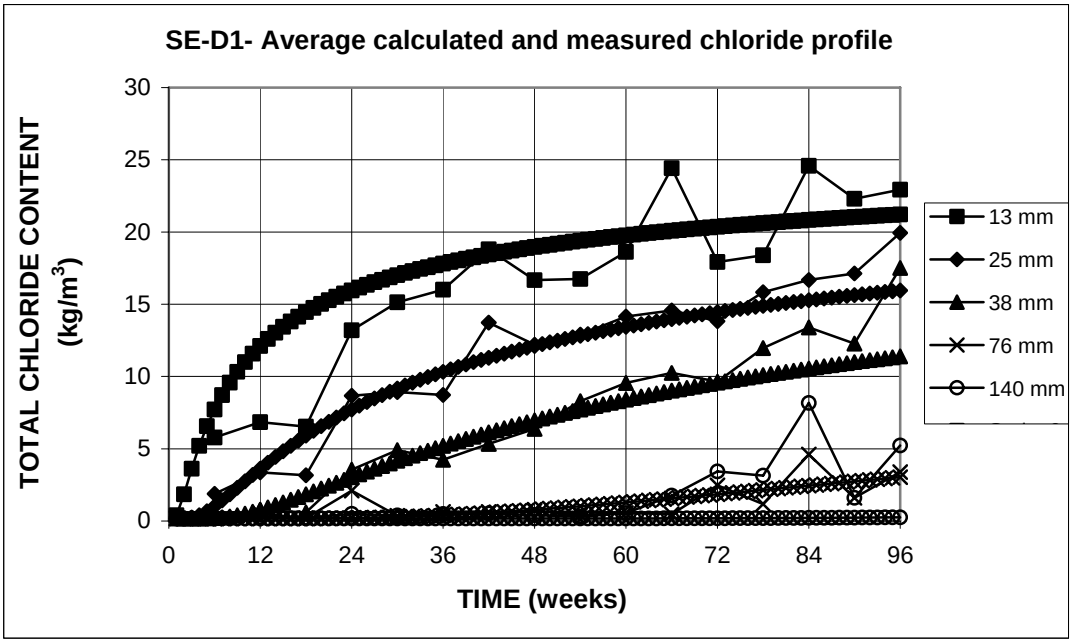

Figure 4.12 – Average calculated and measured total chloride contents versus time at five depths for dummy Southern Exposure specimens in the first study, w/c = 0.45, ponded with 15% NaCl.

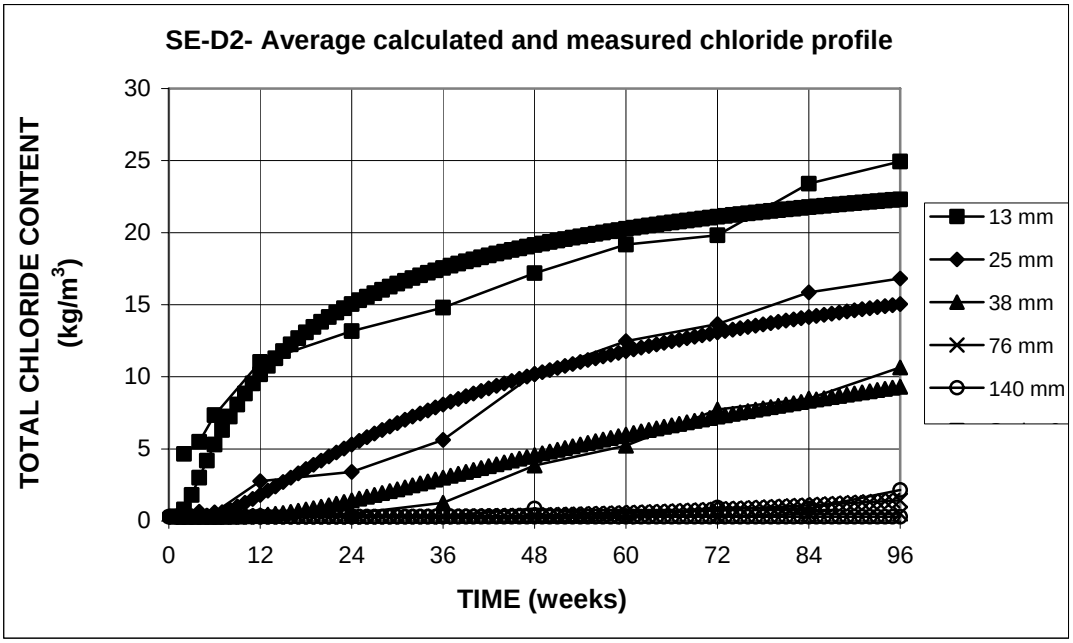

Figure 4.13 – Average calculated and measured total chloride contents versus time at five depths for dummy Southern Exposure specimens in the second study, w/c = 0.45, ponded with 15% NaCl.

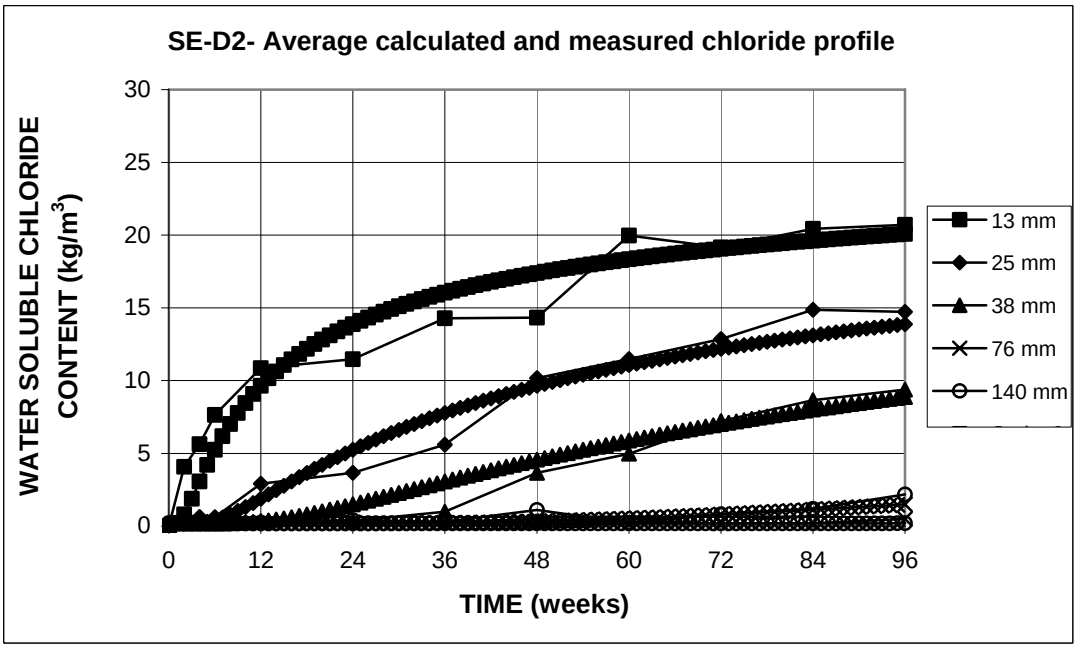

Figure 4.14 – Average calculated and measured water-soluble chloride contents versus time at five depths for dummy Southern Exposure specimens in the second study, w/c = 0.45, ponded with 15% NaCl.

4.3 CRITICAL CHLORIDE THRESHOLDS

The critical chloride thresholds for reinforcing steels in this study were determined based on both the diffusion equation and direct analysis of the chloride contents adjacent to the steel in normal Southern Exposure (SE), modified Southern Exposure (MSE), and beam specimens (B).

The advantage of the technique based on the diffusion equation is that the chloride threshold can be determined during the regular Southern Exposure test, without interfering with the evaluation of other corrosion resistance parameters because of sampling. As will be seen later, however, the results based on the diffusion equation can be greatly affected by variations in concrete properties. Direct chloride analysis is desirable if the representative concrete samples adjacent to the steel can be obtained (usually complicated by the nonhomogeneity of concrete). To ensure a reasonable average value, the modified Southern Exposure and beam specimens were used to obtain a high number chloride samples for a single bar. As described in Section 2.5.3, in the modified SE specimens, each top mat bar is connected to two bottom mat bars across a 10-ohm resistor. Ten samples are taken for each of the top bars. The beam specimens are cracked beam specimens without the simulated crack. Twenty samples are taken for the single top bar. Although the tests are only used to determine the critical chloride threshold, direct chloride analysis for the modified SE and beam specimens appears to be more applicable than the methods based on the diffusion equation and the normal SE specimens. The number of chloride samples taken for the modified SE and beam specimens will be justified based on statistical analysis, as will be demonstrated in Section 4.3.4.

As mentioned in Section 2.5.3, corrosion initiation is considered to have occurred for the specimens when either the corrosion potential of the top mat of steel

first shifts to a value more negative than –0.350 V with respect to a copper-saturated copper sulfate electrode (CSE) or the macrocorrosion rate first reaches a value greater than or equal to 0.3 μm/yr. The alternative requirement for the corrosion rate in this criterion increases the reliability of identifying corrosion initiation since active corrosion can occur when corrosion potentials are more positive than –0.350 V with respect to CSE, as will be seen later.

The critical thresholds based on the diffusion equations are presented in Tables 4.5, 4.6, and 4.7 for conventional (N and N3), MMFX, and duplex stainless steels, respectively. The results based on the direct chloride analysis for the normal SE specimens are presented in Table 4.8 for MMFX and duplex stainless steels. The results based on the direct chloride analysis for the modified SE and the beam specimens are presented in Tables 4.9 and 4.12 for conventional steel (N2), and Tables 4.10 and 4.13 for MMFX steel, respectively.

In the evaluations, the average chloride thresholds on a water-soluble basis ranged from 0.78 to 1.22 kg/m^3 (1.31 to 2.05 lb/yd^3) for the conventional steel and from 2.80 to 4.07 kg/m^3 (4.72 to 6.86 lb/yd^3) for MMFX steel, about three to four times the values of conventional steel; the average chloride threshold was 1.46 kg/m^3 (2.46 lb/yd^3) for 2101 steel and ranged from 3.33 to 7.29 kg/m^3 (5.61 to 12.3 lb/yd^3) for 2101(2) steel, from 9.55 to 9.75 kg/m^3 (16.1 to 16.4 lb/yd^3) for 2101p steel, from 11.8 to 16.1 kg/m^3 (19.9 to 27.1 lb/yd^3) for 2101(2)p steel, and from 11.6 to 15.1 kg/m^3 (19.6 to 25.4 lb/yd^3) for 2205 steel. Since no 2205p bars corroded, the chloride threshold for the pickled 2205 steel is estimated to be greater than 12.5 kg/m^3 (21.1 lb/yd^3), the chloride concentration at the depth of steel at 96 weeks based on the diffusion equation.

4.3.1 Critical chloride thresholds based on chloride diffusion equations

Using the diffusion equations based on the dummy specimens, the chloride thresholds of reinforcing steel in normal SE specimens (summarized in Table 2.6) were determined at the time of corrosion initiation. In this study, a depth of 29 mm (1.125 in.) [3.2 mm (0.125 in.) below the upper surface of the top bars] is regarded as a nominal depth of steel in the SE specimens. The chloride concentrations at the depth are tabulated with time in Table E.5 in Appendix E based on Eq. (4.4), (4.5), and (4.6).

The times to corrosion initiation, the corrosion rates, corrosion potentials, and the critical chloride thresholds based on the time-to-initiation and Eq. (4.4), (4.5), and (4.6) are presented in Table 4.5 for N and N3 conventional steels for six SE specimens for each steel.

At corrosion initiation, conventional N and N3 steels had average corrosion rates of 0.38 and 0.66 μm/yr, respectively, with the same average corrosion potential, –0.334 V, with respect to CSE. In this study, since the N steel SE specimens and the SE-D1 dummy specimens were cast at about the same time, with the same cement and aggregates, and the N3 steel specimens and the SE-D2 specimens were cast at about the same time and with the same materials, the chloride thresholds based on Eq. (4.4) will be used for N steel and those based on Eq. (4.5) and (4.6) are used for N3 steel.

The calculated critical chloride thresholds for the conventional steels exhibit a large scatter because of the high variability in the time-to-initiation, which ranged from 3 to 10 weeks for N steel and from 2 to 17 weeks for the N3 steel. For N steel, on a total chloride basis, the critical chloride thresholds range from 0.19 to 1.81 kg/m^3 (0.32 to 3.05 lb/yd^3), with an average of 0.65 kg/m^3 (1.09 lb/yd^3). For N3 steel, on a

total chloride basis, the chloride thresholds range from 0.30 to 2.23 kg/m^3 (0.50 to 3.75 lb/yd^3), with an average of 0.82 kg/m^3 (1.38 lb/yd^3); on a water-soluble basis, the chloride thresholds range from 0.19 to 2.30 kg/m^3 (0.32 to 3.88 lb/yd^3), with an average of 0.78 kg/m^3 (1.32 lb/yd^3).

Table 4.5 - Critical chloride thresholds for conventional steels N and N3 based on corrosion initiation time and diffusion equations in SE specimens.

Specimens[a]	Time-to-initiation (weeks)	Corrosion potentials (V)	Corrosion rates (μm/yr)	Chloride contents (kg/m^3)	
				total[b]	water-soluble[c]
Conventional N steel					
SE-N-1	7	-0.362	0.53	0.85	-
SE-N-2	3	-0.331	0.39	0.19	-
SE-N-3	4	-0.328	0.42	0.26	-
SE-N-4	3	-0.297	0.36	0.19	-
SE-N-5	10	-0.365	0.00	1.81	-
SE-N-6	6	-0.319	0.56	0.59	-
Average		**-0.334**	**0.38**	**0.65**	-
SD				0.63	-
COV				0.97	-
Conventional N3 steel					
SE-N3-1	8	-0.298	0.45	0.51	0.46
SE-N3-2	9	-0.342	0.56	0.63	0.61
SE-N3-3	3	-0.267	0.61	0.30	0.19
SE-N3-4	2	-0.361	1.05	0.30	0.19
SE-N3-5	11	-0.341	0.49	0.94	0.96
SE-N3-6	17	-0.396	0.81	2.23	2.30
Average		**-0.334**	**0.66**	**0.82**	**0.78**
SD				0.73	0.80
COV				0.90	1.02

a: SE = Southern Exposure test. SD = Standard deviation; COV = Coefficient of variation.
b: The total chloride contents are based on Eq. (4.4) for N steel and Eq. (4.5) for N3 steel as discussed in the text.
c: The water-soluble chloride contents are based on Eq. (4.6), which is the most appropriate for N3 steel as discussed in the text.

The times to corrosion initiation, corrosion rates, corrosion potentials, and the critical chloride thresholds based on the time-to-initiation and the diffusion equations

for MMFX steel are presented in Table 4.6 for six SE specimens. Since the time of fabrication of the specimens was close to that of the SE-D2 dummy specimens, Eq. (4.5) and (4.6) are used for MMFX steel.

Compared to conventional steel, MMFX steel has a longer time-to-initiation which ranges from 11 to 26 weeks. The average corrosion potentials and corrosion rates at corrosion initiation were –0.358 V with respect to CSE and 0.51 μm/yr, respectively.

Table 4.6 - Critical chloride thresholds for MMFX steel based on corrosion initiation time and diffusion equations in SE specimens.

Specimens[a]	Time-to-initiation (weeks)	Corrosion potentials (V)	Corrosion rates (μm/yr)	Chloride contents (kg/m^3)	
				total[b]	water-soluble[c]
SE-MMFX-1	11	-0.374	0.72	0.94	0.96
SE-MMFX-2	26	-0.329	1.45	4.35	4.35
SE-MMFX-3	16	-0.346	0.41	1.99	2.07
SE-MMFX-4	11	-0.383	0.10	0.94	0.96
SE-MMFX-5	26	-0.393	0.01	4.35	4.35
SE-MMFX-6	25	-0.323	0.38	4.12	4.14
Average		**-0.358**	**0.51**	**2.78**	**2.80**
SD				1.68	1.67
COV				0.60	0.59

a: SE = Southern Exposure test. SD = Standard deviation; COV = Coefficient of variation.
b: The total chloride contents are based on Eq. (4.5), which is the most appropriate for MMFX steel.
d: The water soluble chloride contents are based on Eq. (4.6), which is the most appropriate for MMFX steel.

The critical chloride thresholds on a total chloride basis for the MMFX bars ranged from 0.94 to 4.35 kg/m^3 (1.59 to 7.32 lb/yd^3), with an average of 2.78 kg/m^3 (4.69 lb/yd^3), 3.4 times the value exhibited by the conventional N3 steel, 0.82 kg/m^3 (1.38 lb/yd^3), and 4.3 times the value shown by the N steel, 0.65 kg/m^3 (1.09 lb/yd^3). On a water-soluble basis, the chloride threshold for MMFX steel ranged from 0.96 to 4.35 kg/m^3 (1.62 and 7.32 lb/yd^3), with an average of 2.80 kg/m^3 (4.72 lb/yd^3), which is 3.6 times the value for the conventional N3 steel.

The times to corrosion initiation, corrosion rates, corrosion potentials, and corresponding chloride thresholds for the duplex stainless steels in Southern Exposure specimens are presented in Table 4.7.

Like the specimens with N3 and MMFX steel, the specimens with the duplex stainless steels were fabricated at about same time as the SE-D2 dummy specimens. Thus, the chloride thresholds based on Eq. (4.5) and (4.6) are applicable.

Table 4.7 - Critical chloride thresholds for duplex stainless steels based on corrosion initiation time and diffusion equations in SE specimens.

Specimens[a]	Time-to-initiation (weeks)	Corrosion potentials (V)	Corrosion rates (μm/yr)	Chloride contents (kg/m^3)	
				total[b]	water-soluble[c]
2101 steel					
SE-2101-1	13	-0.305	0.34	1.33	1.38
SE-2101-2	18	-0.207	0.43	2.47	2.54
SE-2101-3	8	-0.256	0.93	0.51	0.46
Average		**-0.256**	**0.56**	**1.43**	**1.46**
SD				0.98	1.04
COV				0.69	0.71
2101p steel (pickled)					
SE-2101p-1	66	-0.354	0.03	10.8	10.2
SE-2101p-2	52	-0.378	0.01	9.04	8.63
SE-2101p-3	69	-0.381	0.20	11.1	10.5
Average		**-0.371**	**0.08**	**10.3**	**9.75**
SD				1.11	0.98
COV				0.11	0.10
2101(2) steel					
SE-2101(2)-1	48	-0.266	0.39	8.45	8.11
SE-2101(2)-2	71 (53)*	-0.387 (-0.276)*	0.01 (0.02)*	11.3 (9.17)*	10.6 (8.75)*
SE-2101(2)-3	96 (37)*	-0.369 (-0.310)*	0.00 (0.00)*	13.4 (6.61)*	12.5 (6.45)*
SE-2101(2)-4	57	-0.315	0.33	9.71	9.22
SE-2101(2)-5	24	-0.234	0.35	3.89	3.92
Average		**-0.314 (-0.280)***	**0.22 (0.22)***	**9.36 (7.57)***	**8.88 (7.29)***
SD				3.58 (2.37)*	3.22 (2.16)*
COV				0.38 (0.31)*	0.36 (0.30)*

Table 4.7 (con't) - Critical chloride thresholds for duplex stainless steels, based on corrosion initiation time and diffusion equations in SE specimens.

Specimens[a]	Time-to-initiation (weeks)	Corrosion potentials (V)	Corrosion rates (μm/yr)	Chloride contents (kg/m^3)	
				total[b]	water-soluble[c]
2101(2)p steel (pickled)					
SE-2101(2)p-1	> 96	-0.221**	0.01**	> 13.4	> 12.5
SE-2101(2)p-2	> 96	-0.182**	0.02**	> 13.4	> 12.5
SE-2101(2)p-3	> 96	-0.339**	0.07**	> 13.4	> 12.5
SE-2101(2)p-4	> 96	-0.204**	0.00**	> 13.4	> 12.5
SE-2101(2)p-5	85	-0.436**	0.09**	12.6	11.8
2205 steel					
SE-2205-1	>96	-0.305**	0.26**	> 13.4	> 12.5
SE-2205-2	> 96	-0.208**	0.03**	> 13.4	> 12.5
SE-2205-3	83	-0.291**	0.34**	12.4	11.6
SE-2205-4	> 96	-0.180**	0.01**	> 13.4	> 12.5
SE-2205-5	> 96	-0.188**	0.00**	> 13.4	> 12.5
2205p steel (pickled)					
SE-2205p-1	> 96	-0.170**	0.00**	> 13.4	> 12.5
SE-2205p-2	> 96	-0.176**	0.00**	> 13.4	> 12.5
SE-2205p-3	> 96	-0.194**	0.02**	> 13.4	> 12.5
SE-2205p-4	> 96	-0.199**	0.01**	> 13.4	> 12.5
SE-2205p-5	> 96	-0.176**	0.01**	> 13.4	> 12.5

a: SE = Southern Exposure test; SD = standard deviation, COV = coefficient of variation.
b: The total chloride contents are based on Eq. (4.5) which is the most appropriate for duplex steels.
d: The water soluble chloride contents are based on Eq. (4.6), which is the most appropriate for duplex steels.
*: The value in parenthesis is based on the criterion that corrosion initiation is considered to have occurred when the corrosion potential becomes more negative than –0.275 V (rather than –0.350 V) with respect to CSE for SE-2101(2)-2 and -3 specimens.
**: Corrosion did not initiate with 96-week test period.

The times-to-initiation for the first batch of 2101 steel (the steel was slightly deformed and had small cracks on the surface due to a lack of boron) ranged from 8 to 18 weeks. At the initiation of corrosion, compared to conventional and MMFX steels, the steel had more positive corrosion potentials, with an average of –0.260 V with respect to CSE. The average chloride thresholds for the steel are approximately two times those for conventional N3 steel and half of those for MMFX steel. On a total chloride basis, the critical chloride thresholds for the 2101 steel ranged from

0.51 to 2.47 kg/m^3 (0.86 to 4.15 lb/yd^3), with an average of 1.43 kg/m^3 (2.42 lb/yd^3). On a water-soluble basis, the chloride thresholds for the steel ranged from 0.46 to 2.54 kg/m^3 (0.78 to 4.28 lb/yd^3), with an average of 1.46 kg/m^3 (2.46 lb/yd^3).

The corrosion of the first batch of 2101 pickled steel (2101p) initiated from 53 to 69 weeks after the test had begun. At the time, the steel had an average corrosion potential of –0.371 V and an average corrosion rate of 0.08 μm/yr. The low corrosion rate was due to corrosion of bottom mat of steel in these specimens (as shown in Appendix A.172b) which reduced the difference of the corrosion potentials between the top and bottom mats, thus the macrocorrosion rate. On a total chloride basis, the critical chloride thresholds for the 2101p steel ranged from 9.04 to 11.1 kg/m^3 (15.2 to 18.7 lb/yd^3), with an average of 10.3 kg/m^3 (17.4 lb/yd^3), 12.6 times the value for conventional N3 steel. On a water-soluble basis, the chloride thresholds for 2101p steel ranged from 8.63 to 10.5 kg/m^3 (14.5 to 17.6 lb/yd^3), with an average of 9.75 kg/m^3 (16.4 lb/yd^3), 12.4 times the value for the conventional steel.

The times to corrosion initiation for the second batch of 2101 steel [2101(2)] ranged from 24 to 96 weeks. The corresponding average chloride thresholds are 9.36 kg/m^3 (15.8 lb/yd^3) on a total chloride basis and 8.88 kg/m^3 (15.0 lb/yd^3) on a water-soluble basis, only slightly less than the values for 2101p steel. The times-to-initiation for specimens SE-2101(2)-2 and SE-2101(2)-3, however, equal to 71 and 96 weeks, respectively, may be overestimated. The reason is that the bottom mats of steel in the two specimens exhibited active corrosion earlier than the top mats. Thus, a corrosion potential more negative than –0.350 V was used as the indicator of the corrosion initiation. This corrosion potential may be too high because the other specimens for the steel, SE-2101(2)-1, SE-2101(2)-4, SE-2101(2)-5, exhibited active corrosion (corrosion rates of 0.39, 0.33, and 0.35 μm/yr) at corrosion potentials of –0.266,

–0.315, and –0.234 V, respectively. If corrosion potential more negative than –0.275 V with respect to CSE is considered to be indicate depassivation for 2101(2) steel, the times-to-initiation for specimens SE-2101(2)-2 and SE-2101(2)-3 become 53 and 37 weeks, respectively. With the more conservative consideration, the chloride threshold on a total chloride basis for 2101(2) steel ranges from 3.9 to 9.7 kg/m^3 (6.6 to 16.4 lb/yd^3), with an average of 7.6 kg/m^3 (12.8 lb/yd^3), while, on a water-soluble basis, the chloride threshold ranges from 3.9 to 9.2 kg/m^3 (6.6 to 15.5 lb/yd^3), with an average of 7.3 kg/m^3 (12.3 lb/yd^3), about 9 times the value for conventional N3 steel.

For the second batch of 2101 picked steel [(2101(2)p], only one specimen corroded. This occurred at 85 weeks, with a corrosion potential of –0.436 V (–0.168 V at 83 weeks and –0.259 V at 84 weeks) and a corrosion rate of 0.09 μm/yr (the bars at the bottom mat were still passive). Using Eq. (4.5), 2101(2)p steel has a minimum chloride threshold of 12.6 kg/m^3 (21.2 lb/yd^3) on a total chloride basis, while using Eq. (4.6), on a water-soluble basis, the chloride threshold was at least 11.8 kg/m^3 (19.8 lb/yd^3), which represent values that are 15 times the value for conventional N3 steel. Since only one specimen corroded and the others remained passive throughout the test, the average chloride threshold for 2101(2)p steel is expected to be higher.

The results for nonpickled 2205 steel are similar to those of 2101(2)p steel, with one specimen corroding at 83 weeks and the others remaining passive for the duration of the test. At the initiation of corrosion, the corrosion potential and corrosion rate for the specimen were –0.291 V and 0.34 μm/yr, respectively. The minimum chloride thresholds for the steel are 12.4 kg/m^3 (20.9 lb/yd^3) on a total chloride basis using Eq. (4.5) and 11.6 kg/m^3 (19.6 lb/yd^3) on a water-soluble basis using Eq. (4.6).

Pickled 2205 steel (2205p) exhibited the best corrosion resistance, with no specimen corroding during the test. The critical chloride threshold on a total chloride basis for the steel is, thus, greater than 13.4 kg/m^3 (22.6 lb/yd^3), while the threshold on an water-soluble basis is greater than 12.5 kg/m^3 (21.1 lb/yd^3), at least 16 times the value for conventional N3 steel.

Overall, based on the time-to-corrosion in the Southern Exposure test and the diffusion equations, a reasonable estimate of critical chloride thresholds for reinforcing steel can be obtained. Since the diffusion equations are obtained from dummy specimens rather than the specimens containing bars, it is important to minimize differences in concrete properties between specimens to ensure that the test and dummy specimens exhibit similar diffusion rates.

4.3.2 Direct determination of critical chloride thresholds in normal SE specimens

In this study, concrete samples were taken from the normal SE specimens at the times of corrosion initiation. Fifteen SE specimens were sampled, four for MMFX steel, three for 2101p steel, five for 2101(2) steel, one for 2101(2)p steel, and two for 2205 steel. (For other specimens, the corrosion did not initiate during the test or samples were not taken.) The critical chloride thresholds on a water-soluble basis are presented for these steels in Table 4.10 and compared with the values based on the diffusion equation for water-soluble chlorides, Eq. (4.6).

The chloride thresholds for MMFX steel based on the direct chloride analysis ranged from 1.90 to 5.77 kg/m^3 (3.20 to 9.72 lb/yd^3), with an average of 3.09 kg/m^3 (5.21 lb/yd^3), compared to an average of 3.73 kg/m^3 (6.29 lb/yd^3) based on the diffusion equation.

Table 4.8 – Critical chloride threshold for reinforcing steels in normal Southern Exposure specimens

Specimens[a]	Time-to-initiation (weeks)	Water-soluble chlorides (kg/m^3)	
		direct determination	based on diffusion equation[c]
MMFX steel			
SE-MMFX-45N-2	26	5.77	4.35
SE-MMFX-45N-3	16	1.90	2.07
SE-MMFX-45N-5	26	2.36	4.35
SE-MMFX-45N-6	25	2.33	4.14
Average		**3.09**	**3.73**
SD		1.80	1.11
COV		0.58	0.30
2101p steel (pickled)			
SE-2101p-45N-1	66	10.3	10.2
SE-2101p-45N-2	52	7.66	8.63
SE-2101p-45N-3	69	10.7	10.5
Average		**9.55**	**9.75**
SD		1.65	0.98
COV		0.17	0.10
2101(2) steel			
SE-2101(2)-45N-1	48	4.89	8.11
SE-2101(2)-45N-2	71	6.39	10.6
SE-2101(2)-45N-3	96	8.96	12.5
SE-2101(2)-45N-4	57	3.92	9.22
SE-2101(2)-45N-5	24	1.18	3.92
Average		**5.11 (3.33)** [b]	**9.07 (7.08)** [b]
SD		2.89 (1.93)[b]	3.22 (2.80)[b]
COV		0.57 (0.58)[b]	0.36 (0.4)[b]
2101(2)p steel (pickled)			
SE-2101(2)p-45N-5	85	16.1	11.8
2205 steel			
SE-2205-45N-3	83	15.1	11.6

a: SE = Southern Exposure test; SD = standard deviation; COV = coefficient of variation.
b: The value in parenthesis is based on specimens SE-2101(2)-1, 4, 5.
c: using the diffusion equation, Eq. (4.6), for water-soluble chlorides.

The threshold values for 2101p steel are 7.66, 10.3, and 10.7 kg/m^3 (12.9, 17.3, and 18.1 lb/yd^3), with an average of 9.55 kg/m^3 (16.1 lb/yd^3), which are very similar to the values based on the diffusion equation.

The chloride thresholds for 2101(2) steel based on the direct chloride analysis are 1.18, 3.92, 4.89, 6.39, and 8.96 kg/m^3 (1.98, 6.61, 8.24, 10.8, 15.1 lb/yd^3). As discussed in Section 4.3.1, the time to corrosion initiation for specimens SE-2101(2)-2 and SE-2101(2)-3 may be overestimated. Disregarding the values from these specimens, 6.39 and 8.96 kg/m^3 (10.8 and 15.1 lb/yd^3), the average chloride threshold for 2101(2) steel is 3.33 kg/m^3 (5.61 lb/yd^3), slightly higher than the average value for MMFX steel, 3.09 kg/m^3 (5.21 lb/yd^3). Compared to the corresponding values based on the diffusion equation, which average 7.08 kg/m^3 (11.9 lb/yd^3), the threshold values based on the direct chloride analysis are much lower (and may be more applicable). The difference between values based on direct readings and diffusion analyses may have occured if the SE specimens had lower diffusion coefficients than the dummy specimens. If this is the case, the chloride threshold would be overestimated if the diffusion equations based on the dummy specimens were used for the normal specimens.

Based on the direct chloride analysis for the only 2101(2)p specimen to corrode, the chloride threshold for the steel is 16.1 kg/m^3 (27.1 lb/yd^3), higher than the value based on the diffusion equation, 11.8 kg/m^3 (19.8 kg/m^3).

Based on the direct chloride analysis for the 2205 specimen corroding at 83 weeks, the chloride threshold for 2205 steel is 15.1 kg/m^3 (25.4 lb/yd^3), also higher than the corresponding value based on the diffusion equation, which is 11.6 kg/m^3 (19.6 lb/yd^3).

4.3.3 Direct determination of chloride threshold using modified SE and beam specimens

Modified Southern Exposure specimens – Six modified Southern Exposure specimens were fabricated to determine the chloride threshold of N2 conventional steel and MMFX steel. In these specimens, the two top bars were monitored individually. Chloride samples (10 samples in most cases) were taken at the initiation of corrosion for each bar (except for one bar in conventional steel specimens 1 and 2 and MMFX specimen 3, which were subjected to trial sampling using other methods, and two bars in MMFX specimen 5 that were contaminated from the outside). The average value from the individual samples is regarded as the chloride threshold for the bar.

The times-to-initiation, corrosion rates, corrosion potentials, and individual and average critical chloride contents on a water-soluble basis for conventional N2 steel (10 bars) are presented in Table 4.9.

The conventional bars had times-to-initiation ranging from 8 to 20 weeks, with corrosion rates ranging from 0.35 to 3.51 μm/yr (in the latter case, the corrosion rate was 0.05 μm/yr one week before reaching 3.51 μm/yr; the jump in the corrosion rate reflects the nature of the steel corrosion) and corresponding corrosion potentials ranging from –0.280 to –0.421 V with respect to CSE. The average critical chloride thresholds for the 10 bars are 0.92, 1.31, 0.71, 1.18, 0.54, 0.62, 0.91, 0.53, 1,23, and 1.17 kg/m^3 (1.56, 2.21, 1.20, 1.99, 0.91, 1.05, 1.54, 0.90, 2.07, and 1.97 lb/yd^3), with an average of 0.91 kg/m^3 (1.54 lb/yd^3).

For each of the 10 conventional bars, the individual chloride contents range from lows of 0.41, 0.56, 0.37, 0.60, 0.34, 0.36, 0.43, 0.39, 0.79, and 0.67 kg/m^3 (0.69, 0.94, 0.63, 1.01, 0.58, 0.60, 0.73, 0.65, 1.33, and 1.13 lb/yd^3) to highs of 1.61, 2.84,

1.53, 2.17, 0.81, 0.99, 1.38, 0.95, 1.90, and 1.79 kg/m^3 (2.71, 4.78, 2.58, 3.65, 1.37, 1.67, 2.39, 1.60, 3.21, and 3.02 lb/yd^3), respectively. The coefficients of variation for the individual bars range from 0.28 to 0.70. The scatter in the individual results is likely due to the non-homogeneity of concrete, which causes the uneven ingress of chlorides.

The times-to-initiation, corrosion rates, corrosion potentials, and individual and average critical chloride thresholds on a water-soluble basis for MMFX reinforcing steel (9 bars) are presented in Table 4.10.

The times-to-initiation for MMFX steel ranged from 17 to 39 weeks, with corrosion rates ranging from 0.01 to 2.00 μm/yr (the corrosion rate was 0.02 μm/yr one week before reaching 2.00 μm/yr; as discussed earlier, the jump in the corrosion rate reflects the nature of corrosion of reinforcing steel in concrete) and corrosion potentials ranging from –0.333 to –0.460 V with respect to CSE. The average critical chloride thresholds for the MMFX bars were 5.34, 3.01, 4.80, 5.43, 3.23, 2.97, 2.66, 2.75 and 3.11 kg/m^3 (9.00, 5.08, 8.08, 9.16, 5.45, 5.00, 4.47, 4.64, and 5.23 lb/yd^3), with an average of 3.70 kg/m^3 (6.23 lb/yd^3), four times the value for conventional steel.

For each of the 9 bars, the individual chloride contents range from lows of 3.21, 1.57, 2.88, 4.41, 1.49, 1.87, 1.27, 1.61, and 1.84 kg/m^3 (5.41, 2.64, 4.85, 7.43, 2.52, 3.15, 2.14, 2.71, and 3.10 lb/yd^3) to highs of 6.98, 4.37, 6.32, 7.77, 4.86, 3.74, 3.96, 4.28, and 4.03 kg/m^3 (11.8, 7.4, 10.65, 13.1, 8.18, 6.29, 6.67, 7.21, and 6.80 lb/yd^3), respectively. The coefficients of variation for the individual bars ranged from 0.19 to 0.34, lower than exhibited by the individual bars for conventional steel, indicating a more even distribution of chlorides at higher chloride contents.

The critical chloride thresholds based on the direct chloride analysis for modified SE specimens are compared with values calculated using the diffusion equation, Eq. (4.6), in Table 4.11 for each of the conventional N2 and MMFX bars in modified SE specimens.

Based on direct chloride analysis, the critical chloride thresholds for conventional steel range from 0.54 to 1.31 kg/m^3 (0.91 to 2.21 lb/yd^3), with an average of 0.91 kg/m^3 (1.54 lb/yd^3) and a coefficient of variation of 0.33, compared to values based on the diffusion equation from dummy specimens, which range from 0.46 to 3.01 kg/m^3 (0.78 to 5.07 lb/yd^3), with an average of 1.38 kg/m^3 (2.33 lb/yd^3) and a coefficient of variation of 0.61. The critical chloride thresholds based on direct chloride analysis for MMFX steel range from 2.66 to 5.43 kg/m^3 (4.47 to 9.16 lb/yd^3), with an average of 3.70 kg/m^3 (6.23 lb/yd^3) and a coefficient of variation of 0.31, while the values based on the diffusion equation range from 2.30 to 6.78 kg/m^3 (3.88 to 11.4 lb/yd^3), with an average of 4.23 kg/m3 (7.13 lb/yd^3) and coefficient of variation of 0.34.

Compared to the values based on direct chloride analysis, which have an average of 0.91 kg/m^3 (1.54 lb/yd^3) and a coefficient of variation of 0.33 for conventional steel and an average of 3.70 kg/m^3 (6.23 lb/yd^3) and a coefficient of variation of 0.31 for MMFX steel, the critical chloride thresholds based on the diffusion equation exhibit larger scatter, with an average of 1.38 kg/m^3 (2.33 lb/yd^3) and a coefficient of variation of 0.61 for conventional steel and an average of 4.23 kg/m3 (7.13 lb/yd^3) and coefficient of variation of 0.34 for MMFX steel. The larger scatter in the values based on the diffusion equation is due to the scatter in the times-to-initiation, which is greatly effected by variations in concrete properties. The critical chloride thresholds based on direct chloride analysis for the modified SE

specimens should carry more weight than the values obtained using the diffusion equation.

Table 4.9 – Critical chloride thresholds for N2 conventional steel based on the direct analysis of the chloride content in modified Southern Exposure specimens.

Specimens[a]	Bar No.	Initiation time (weeks)	Corrosion rate (μm/yr)	Corrosion potentials (V)	Water soluble Cl^- (kg/m^3)			
					1	2	3	4
MSE-N2-1	1[b]	-	-	-	-	-	-	-
	2	8	0.84	-0.273	0.41	0.90	0.99	1.61
MSE-N2-2	1[b]	-	-	-	-	-	-	-
	2	12	2.89	-0.396	0.56	1.42	0.76	2.84
MSE-N2-3	1	15	1.96	-0.404	0.41	0.49	0.37	0.49
	2	14	1.79	-0.380	2.17	1.01	0.60	0.78
MSE-N2-4	1	9	1.76	-0.379	0.46	0.61	0.50	0.51
	2	9	3.51	-0.421	0.47	0.62	0.99	0.36
MSE-N2-5	1	14	0.82	-0.332	1.01	1.38	1.42	0.97
	2	9	0.35	-0.280	0.52	0.50	0.39	0.61
MSE-N2-6	1	20	1.52	-0.361	0.90	0.82	1.08	1.57
	2	17	1.84	-0.379	1.61	1.08	1.08	1.79

Specimens[a]	Bar No.	Water soluble Cl^- (kg/m^3)						Average (kg/m^3)	SD[c]	COV [c]
		5	6	7	8	9	10			
MSE-N2-1	1[b]	-	-	-	-	-	-	-	-	-
	2	0.71	-	-	-	-	-	0.92	0.44	0.48
MSE-N2-2	1[b]	-	-	-	-	-	-	-	-	-
	2	0.97	-	-	-	-	-	1.31	0.91	0.70
MSE-N2-3	1	0.56	1.08	0.75	1.53	-	-	0.71	0.40	0.57
	2	1.34	-	-	-	-	-	1.18	0.62	0.52
MSE-N2-4	1	0.46	0.46	0.34	0.76	0.46	0.81	0.54	0.15	0.28
	2	0.46	0.60	0.50	0.82	0.46	0.97	0.62	0.23	0.36
MSE-N2-5	1	1.08	0.67	0.90	0.54	0.43	0.71	0.91	0.33	0.36
	2	0.41	0.52	0.43	0.43	0.95	0.56	0.53	0.16	0.31
MSE-N2-6	1	1.90	0.79	1.79	0.86	1.34	1.23	1.23	0.41	0.34
	2	1.68	0.67	0.69	0.78	1.31	1.01	1.17	0.41	0.35
						Average		**0.91**		

a: MSE = modified Southern Exposure specimen; N2 = conventional steel N2.
b: The samples for the bar are not available because the specimen was subjected to trial sampling using other methods.
c: SD = standard deviation; COV = coefficient of variation.

Table 4.10 – Critical chloride thresholds for MMFX steel based on the direct analysis of the chloride content in modified Southern Exposure specimens

Specimens[a]	Bar No.	Initiation time (weeks)	Corrosion rate (μm/yr)	Corrosion potentials (V)	Water soluble Cl^- (kg/m^3)			
					1	2	3	4
MSE-MMFX-1	1	23	0.50	-0.390	3.21	3.55	3.38	4.71
	2	17	0.60	-0.362	1.57	1.76	2.32	2.20
MSE-MMFX-2	1	23	0.41	-0.333	3.47	2.88	5.98	5.33
	2	28	0.01	-0.363	4.41	5.19	5.57	5.42
MSE-MMFX-3	1[b]	-	-	-	-	-	-	-
	2	17	1.95	-0.460	1.49	2.43	2.56	2.99
MSE-MMFX-4	1	30	0.57	-0.348	1.87	3.03	3.14	3.74
	2	29	2.00	-0.367	2.91	2.35	2.05	3.96
MSE-MMFX-5[c]	-	-	-	-	-	-	-	-
MSE-MMFX-6	1	26	1.20	-0.359	2.99	1.61	2.09	2.54
	2	39	0.68	-0.368	2.51	2.91	3.32	3.18

Specimens[a]	Bar No.	Water soluble Cl^- (kg/m^3)						Average (kg/m^3)	SD[d]	COV[d]
		5	6	7	8	9	10			
MSE-MMFX-1	1	5.83	6.1	6.57	6.84	6.27	6.98	5.34	1.49	0.28
	2	2.76	4.37	3.66	3.88	4.30	3.32	3.01	1.03	0.34
MSE-MMFX-2	1	6.32	-	-	-	-	-	4.80	1.54	0.32
	2	5.98	5.19	7.77	4.97	4.89	4.97	5.43	0.92	0.17
MSE-MMFX-3	1[b]	-	-	-	-	-	-	-	-	-
	2	3.40	4.48	3.70	4.86	2.99	3.44	3.23	0.98	0.30
MSE-MMFX-4	1	3.36	3.36	2.28	-	-	-	2.97	0.66	0.22
	2	3.03	1.27	1.57	3.85	3.32	2.24	2.66	0.91	0.34
MSE-MMFX-5[c]	-	-	-	-	-	-	-	-	-	-
MSE-MMFX-6	1	2.54	4.28	2.24	2.73	3.62	2.88	2.75	0.76	0.28
	2	3.09	3.36	4.03	3.50	1.84	3.32	3.11	0.59	0.19
						Average		3.70		

a: MSE = modified Southern Exposure specimen; MMFX = MMFX steel

b: The samples for the bar were not available because the specimen was subjected to trial sampling using other methods.

c: The specimen was contaminated from outside.

d: SD = standard deviation; COV = coefficient of variation.

Table 4.11 - Critical chloride thresholds for conventional and MMFX steels in modified Southern Exposure specimens based on the direct chloride analysis and the diffusion equation equation.

Specimens[a]	Bar No.	Time-to-initiation (weeks)	Water-soluble chlorides (kg/m^3)	
			direct determination	based on diffusion equation[b]
Conventional N2 steel				
MSE-N2-1	1	-	-	-
	2	8	0.92	0.46
MSE-N2-2	1	-	-	-
	2	12	1.31	1.16
MSE-N2-3	1	15	0.71	1.83
	2	14	1.18	1.60
MSE-N2-4	1	9	0.54	0.61
	2	9	0.62	0.61
MSE-N2-5	1	14	0.91	1.60
	2	9	0.53	0.61
MSE-N2-6	1	20	1.23	3.01
	2	17	1.17	2.30
Average			**0.91**	**1.38**
SD			0.30	0.85
COV			0.33	0.61
MMFX steel				
MSE-MMFX-1	1	23	5.34	3.69
	2	17	3.01	2.30
MSE-MMFX-2	1	23	4.80	3.69
	2	28	5.43	4.77
MSE-MMFX-3	1	-	-	-
	2	17	3.23	2.30
MSE-MMFX-4	1	30	2.97	5.17
	2	29	2.66	4.97
MSE-MMFX-5	-	-	-	-
MSE-MMFX-6	1	26	2.75	4.35
	2	39	3.11	6.78
Average			**3.70**	**4.23**
SD			1.14	1.43
COV			0.31	0.34

a: MSE = modified Southern Exposure specimens; N2 = conventional steel, MMFX = MMFX steel; SD = standard deviation, COV. = coefficient of variation.

b: Water soluble chloride contents are based on the diffusion equation (4.6).

Beam specimens – As described in Section 2.5.3, three beam specimens (one bar in each specimen) were fabricated to determine the chloride threshold of N2 conventional steel and MMFX steel. At the initiation of corrosion, 20 chloride samples were taken from each specimen.

The times-to-initiation, corrosion rates, corrosion potentials, and individual and average critical chloride contents on a water-soluble basis are presented in Table 4.12 for conventional steel and Table 4.13 for MMFX steel.

The conventional N2 steel had times-to-initiation ranging from 14 to 21 weeks, with an average corrosion rate of 1.12 μm/yr and average corrosion potential of –0.365 V with respect to CSE. The average chloride threshold for all three specimens was 1.22 kg/m^3 (2.05 lb/yd^3), about one-third higher than obtained in modified SE specimens, 0.91 kg/m^3 (1.54 lb/yd^3). The individual chloride contents ranged from 0.56 to 2.59 kg/m^3 (0.95 to 4.36 lb/yd^3), with an average of 1.19 kg/m^3 (2.01 lb/yd^3) and a coefficient of variation of 0.40, for specimen 1, from 0.51 to 2.85 kg/m^3 (0.85 to 4.81 lb/yd^3), with an average of 1.23 kg/m^3 (2.08 lb/yd^3) and a coefficient of variation of 0.44, for specimen 2, and from 0.49 to 2.35 kg/m^3 (0.82 to 3.96 lb/yd^3), with an average of 1.23 kg/m^3 (2.07 lb/yd^3) and a coefficient of variation of 0.38, for specimen 3.

Table 4.13 shows that the times-to-corrosion for MMFX steel ranged from 26 to 51 weeks. At initiation, the average corrosion rate and corrosion potential were 0.93 μm/yr and –0.343 V, respectively. The average chloride threshold for the three specimens was 4.07 kg/m^3 (6.86 lb/yd^3), about 3.3 times the value for conventional steel. The individual critical chloride contents ranged from 3.85 to 6.23 kg/m^3 (6.48 to 10.5 lb/yd^3), with an average of 5.36 kg/m^3 (9.03 lb/yd^3) and a coefficient of variation of 0.14, for specimen 1, from 1.27 to 5.57 kg/m^3 (2.14 to 9.38 lb/yd^3), with an average

of 2.96 kg/m^3 (4.98 lb/yd^3) and a coefficient of variation of 0.38, for specimen 2, and from 1.72 to 6.46 kg/m^3 (2.90 to 10.9 lb/yd^3), with an average of 3.89 kg/m^3 (6.56 lb/yd^3) and a coefficient of variation of 0.26, for specimen 3.

The critical chloride thresholds based on the direct chloride analysis are compared with the values calculated using Eq. (4.6) in Table 4.14 for the conventional and MMFX steel beam specimens.

Compared to the values based on the direct chloride analysis, which have an average of 1.22 kg/m^3 (2.05 lb/yd^3) with a coefficient of variation of 0.02 for conventional steel and an average of 4.07 kg/m^3 (6.86 lb/yd^3) with a coefficient of variation of 0.30 for MMFX steel, the critical chloride thresholds based on the diffusion equation are much higher, with an average of 2.85 kg/m^3 (4.80 lb/yd^3) and a coefficient of variation of 0.39 for conventional steel and an average of 6.38 kg/m^3 (10.8 lb/yd^3) and an coefficient of variation of 0.33 for MMFX steel. As discussed earlier, the high values based on the diffusion equation are attributed to the long times-to-initiation which may be caused by the variations in concrete properties.

Table 4.12 – Critical chloride thresholds for conventional steel N2, based on the direct analysis of the chloride content in beam specimens

Specimens[a]	Sides[b]	Initiation time (weeks)	Corrosion rates (μm/yr)	Corrosion potentials (V)	Water soluble Cl^- (kg/m^3)			
					1	2	3	4
B-N2-1	1	21	1.17	-0.358	0.90	1.46	0.75	1.34
	2				2.59	1.36	1.16	1.37
B-N2-2	1	23	1.17	-0.392	1.34	0.51	1.08	0.99
	2				0.67	1.61	1.61	1.64
B-N2-3	1	14	1.02	-0.344	1.34	0.62	1.12	1.64
	2				1.27	1.83	0.93	1.72

Specimens[a]	Sides[b]		Water soluble Cl^- (kg/m^3)					Average (kg/m^3)	SD[c]	COV [c]
		5	6	7	8	9	10			
B-N2-1	1	0.82	1.83	1.12	0.97	1.16	0.93			
	2	0.86	1.79	0.56	0.83	1.31	0.72	1.19	0.48	0.40
B-N2-2	1	0.77	0.80	0.88	0.92	0.80	0.92			
	2	1.53	1.69	1.38	0.92	1.76	2.85	1.23	0.54	0.44
B-N2-3	1	2.35	1.49	0.67	1.12	1.49	0.90			
	2	1.31	0.49	0.71	1.53	1.12	0.93	1.23	0.47	0.38
						Average		**1.22**		

a: = beam specimens; N2 = conventional steel N2;

b: 10 chloride samples were taken for each side of the bar in one specimen;

c: SD = standard deviation; COV = coefficient of variation.

Table 4.13 – Critical chloride thresholds for MMFX steel, based on the direct analysis of the chloride content in beam specimens

Specimens[a]	Sides[b]	Initiation time (weeks)	Corrosion rates (μm/yr)	Corrosion potentials (V)	Water soluble Cl^- (kg/m^3)			
					1	2	3	4
B-MMFX-1	1	51	1.02	-0.36	4.33	5.49	5.71	5.11
	2				5.90	5.87	6.23	6.01
B-MMFX-2	1	26	1.22	-0.341	1.27	1.46	1.87	1.85
	2				2.28	2.84	3.36	3.29
B-MMFX-3	1	36	0.56	-0.329	3.81	3.74	4.02	4.76
	2				4.97	3.66	2.73	3.51

Specimens[a]	Sides[b]	Water soluble Cl^- (kg/m^3)						Average (kg/m^3)	SD[c]	COV[c]
		5	6	7	8	9	10			
B-MMFX-1	1	5.53	6.16	6.16	4.28	4.33	4.82			
	2	4.79	5.90	5.71	4.93	6.09	3.85	5.36	0.75	0.14
B-MMFX-2	1	3.14	1.61	2.24	2.43	3.51	3.14			
	2	3.06	3.40	4.52	5.57	4.44	3.89	2.96	1.12	0.38
B-MMFX-3	1	4.36	3.10	3.10	4.63	6.46	2.95			
	2	3.17	4.74	4.93	1.72	3.88	3.60	3.89	1.03	0.26
						Average		**4.07**		

a: B = beam specimens; MMFX = MMFX microcomposite steel;
b: 10 chloride samples were taken for each side of the bar in one specimen.
c: SD = standard deviation; COV = coefficient of variation.

Table 4.14 – Critical chloride thresholds for conventional and MMFX steels in beam specimen, based on the direct chloride analysis and the diffusion equation.

Specimens[a]	Bar No.	Time-to-initiation (weeks)	Water-soluble chlorides (kg/m^3)	
			direct determination	based on diffusion equation[b]
Conventional steel N2				
B-N2-1	1	21	1.19	3.24
B-N2-2	1	23	1.23	3.69
B-N2-3	1	14	1.23	1.60
Average			**1.22**	**2.85**
SD			0.02	1.10
COV			0.02	0.39
MMFX steel				
B-MMFX-1	1	51	5.36	8.50
B-MMFX-2	1	26	2.96	4.35
B-MMFX-3	1	36	3.89	6.28
Average			**4.07**	**6.38**
SD			1.21	2.08
COV			0.30	0.33

a: B = beam specimens; N2 = conventional steel, MMFX = MMFX steel; SD= standard deviation, COV = coefficient of variation.
b: the water soluble chloride contents are based on the diffusion equation (4.6).

4.4 STATISTICAL ANALYSIS FOR SAMPLING FREQUENCY

A primary concern in direct sampling for chloride content is the need to determine how representative the concrete samples are or, more appropriately, how many concrete samples need to be taken to ensure a reasonable estimate of the true average chloride content in the concrete adjacent to the steel. Statistically, the sample size needed can be determined based on the confidence level desired, the acceptable error, and the standard deviation.

According to the central limit theorem (Walpole and Myers 1993), for large size *n*, the mean ($\overline{X}$) of a random sample taken from a population with mean μ and variance σ^2 is approximately normally distributed with mean μ and variance σ^2/n. As a result, the distribution of the random variable

$$Z = \frac{\overline{X} - \mu}{\sigma / \sqrt{n}} \tag{4.7}$$

is a standard normal distribution $N(0,1)$, which means that if the mean, $\overline{X}$, is used as an estimate of μ, we can assert with (1-α)100% confidence that the error of the estimate, ε (equal to $\left|\overline{X} - \mu\right|$), satisfies

$$\frac{\left|\overline{X} - \mu\right|}{\sigma / \sqrt{n}} \leq z_{\alpha/2} \tag{4.8}$$

where α equals to 0.05 and $z_{\alpha/2}$ equals to 1.96 for a 95% confidence level.

Based on Eq. (4.8), if we wish to estimate the mean of the population, μ, within a specified error ε with (1-α)100% confidence, the required sample size is

$$n = \left(\frac{z_{\alpha/2}\sigma}{\varepsilon} \right)^2 \tag{4.9}$$

Based on Eq. (4.9), the required sample size increases as the acceptable error decreases, and as the specified confidence level and standard deviation increase.

In this study, the average chloride content ($\overline{X}$) of the concrete samples for each bar is used as the estimate of the true average chloride content (the mean of the population, μ) at the level of the steel; the population variation σ^2 is unknown, but can be replaced with the variation of the samples (in most cases 10 samples for MSE specimens and 20 samples for beam specimens), s^2. Several acceptable errors of estimate were selected, including 30, 25, 20, 15, and 10% of the average chloride content of the samples, along with three absolute values, 1.0, 0.5, and 0.25 kg/m^3. The sample size for 95% confidence that the estimate of the true average chloride content is within the selected errors is calculated using Eq. (4.9). The results are presented in Table 4.15 for conventional and MMFX steels in modified SE specimens and Table 4.16 for the same steels in beam specimens.

Table 4.15 shows that for the ten conventional bars in the modified SE specimens, the average required sample sizes are 8, 12, 19, 34, 76 for specified errors of 30, 25, 20, 15, and 10% of the average chloride contents of the samples and 1, 3, and 13 for the errors of 1.0, 0.5, and 0.25 kg/m^3, respectively, while for the nine MMFX bars in modified SE specimens, the average required sample sizes are 3, 5, 7, 13, 30 for specified errors of 30, 25, 20, 15, and 10% of the average chloride contents of the samples and 4, 17, and 66 for the errors of 1.0, 0.5, and 0.25 kg/m^3.

Table 4.16 shows that for the three conventional bars in the beam specimens, the average required sample sizes are 7, 10, 16, 28, 64 for specified errors of 30, 25, 20, 15, and 10% of the average chloride contents of the samples and 1, 4, and 15 for the errors of 1.0, 0.5, and 0.25 kg/m^3, respectively, while for the three MMFX bars in beam specimens, the average required sample sizes are 3, 5, 7, 13, 30 for specified

errors of 30, 25, 20, 15, and 10% of the average chloride contents of the samples and 4, 15, and 59 for the errors of 1.0, 0.5, and 0.25 kg/m^3.

The results show that the required sample sizes for two specimen types are very close. This is likely due to similarity in the types of test specimen.

Based on the above statistical analysis on the required sample size, for the modified SE specimens, it can be asserted with 95% confidence that the difference between the average chloride content for the 10 samples in a single specimen and the true value does not exceed a value between 0.25 and 0.5 kg/m^3 (0.42 and 0.84 lb/yd^3) or about 25 to 30% of the average value of the samples for conventional steel and between 0.50 and 1.0 kg/m^3 (0.84 and 1.7 lb/yd^3) or about 15 to 20% of the average value of the samples for MMFX steel. For the beam specimens, it can be asserted with 95% confidence that the difference between the average chloride content for the 20 samples in a single specimen and the true value does not exceed a value of at most 0.25 kg/m^3 (0.42 lb/yd^3) or 25% of the average value of the samples for conventional steel and at most 0.50 kg/m^3 (0.84 lb/yd^3) or 15% of the average value of the samples for MMFX steel. For the full data (all samples from all specimens listed in Tables 4.15 and 4.16), the average values are, with 95% confidence, within 10% and 0.25 kg/m^3 (0.42 lb/yd^3) of the true values in all cases.

Finally, the analysis shows that, for the 95% confidence level, the maximum error, ε, associated with a single sample is 1.96σ, equal to 0.8 to 1.0 kg/m^3 (1.4 to 1.7 lb/yd^3) for an average concentration of about 1.0 kg/m^3 (1.7 lb/yd^3) and equal to about 2.0 kg/m^3 (3.4 lb/yd^3) for an average concentration of about 4.0 kg/m^3 (6.8 lb/yd^3) in the current tests.

Table 4.15 - Sample sizes for 95% confidence that the difference between the average chloride content of the samples and the true value is within the selected errors for modified Southern Exposure specimens.

Specimens[a]	Bar No.	Average (kg/m^3)	SD[b]	Sample size within acceptable errors							
				% of average value					kg/m^3		
				30	25	20	15	10	1.0	0.5	0.25
Conventional N2 steel											
MSE-N2-1	2	0.92	0.44	10	14	22	39	88	1	3	12
MSE-N2-2	2	1.31	0.91	21	30	47	83	186	3	13	51
MSE-N2-3	1	0.71	0.40	14	20	31	55	124	1	3	10
	2	1.18	0.62	12	17	26	47	105	1	6	23
MSE-N2-4	1	0.54	0.15	3	5	7	13	29	0	0	1
	2	0.62	0.23	6	8	13	22	50	0	1	3
MSE-N2-5	1	0.91	0.33	6	8	13	23	51	0	2	7
	2	0.53	0.16	4	6	9	16	36	0	0	2
MSE-N2-6	1	1.23	0.41	5	7	11	19	43	1	3	10
	2	1.17	0.41	5	8	12	21	47	1	3	10
Average		**0.91**	**0.40**	**8**	**12**	**19**	**34**	**76**	**1**	**3**	**13**
MMFX steel											
MSE-MMFX-1	1	5.34	1.49	3	5	8	13	30	9	34	137
	2	3.01	1.03	5	7	11	20	45	4	16	66
MSE-MMFX-2	1	4.80	1.54	4	6	10	18	39	9	36	145
	2	5.43	0.92	1	2	3	5	11	3	13	52
MSE-MMFX-3	2	3.23	0.98	4	6	9	16	36	4	15	60
MSE-MMFX-4	1	2.97	0.66	2	3	5	8	19	2	7	27
	2	2.66	0.91	5	7	11	20	45	3	13	51
MSE-MMFX-6	1	2.75	0.76	3	5	7	13	30	2	9	36
	2	3.11	0.59	2	2	4	6	14	1	5	22
Average		**3.70**	**1.01**	**3**	**5**	**7**	**13**	**30**	**4**	**17**	**66**

a: MSE = modified Southern Exposure specimen;

b: SD = standard deviation of the samples. The average of the standard deviations is a statistical average standard deviation, which is calculated in accordance with the following formula:

$$\overline{S} = \left[\frac{\sum_{i=1}^{k} (n_i - 1) S_i^2}{\left(\sum_{i=1}^{k} n_i \right) - k} \right]^{1/2}$$

where k is the number of the tested bars; n is the number of the samples for each bar; s_i is the standard deviation of the samples for the i^{th} bar.

Table 4.16 - Sample sizes for 95% confidence that the difference between the average chloride content of the samples and the true value is within the selected errors for beam specimens.

Specimens[a]	Average (kg/m^3)	SD[b]	Sample size within acceptable errors							
			% of average value					kg/m^3		
			30	25	20	15	10	1.0	0.5	0.25
Conventional N2 steel										
B-N2-1	1.19	0.48	7	10	15	27	61	1	3	14
B-N2-2	1.23	0.47	6	9	14	24	55	1	3	13
B-N2-3	1.23	0.54	8	12	19	33	74	1	5	18
Average	**1.22**	**0.50**	**7**	**10**	**16**	**28**	**64**	**1**	**4**	**15**
MMFX steel										
B-MMFX-1	5.36	0.75	1	1	2	3	7	2	9	34
B-MMFX-2	2.96	1.12	6	9	14	24	55	5	19	77
B-MMFX-3	3.89	1.03	3	4	7	12	27	4	16	65
Average	**4.07**	**0.98**	**3**	**5**	**7**	**13**	**30**	**4**	**15**	**59**

a: B = beam specimen;
b: SD = standard deviation of the samples. The average of the standard deviations is a statistical average standard deviation, which is calculated in accordance with the following formula:

$$\overline{S} = \left[\frac{\sum_{i=1}^{k} (n_i - 1) S_i^2}{\left(\sum_{i=1}^{k} n_i \right) - k} \right]^{1/2}$$

where k is the number of the tested bars; n is the number of the samples for each bar; s_i is the standard deviation of the samples for the i^{th} bar.

4.5 SUMMARY OF THE CRITICAL CHLORIDE THRESHOLDS

In this section, the critical chloride thresholds for conventional, MMFX, and duplex stainless steels are summarized. The chloride thresholds will be used for service life prediction of decks containing conventional, MMFX, 2101(2)p, 2205, and 2205p steels.

Conventional steels - Based on diffusion analysis, the critical chloride thresholds on a total chloride basis for conventional N steel range from 0.19 to 1.81 kg/m^3 (0.32 to 3.05 lb/yd^3), with an average of 0.65 kg/m^3 (1.10 lb/yd^3). For conventional N3 steel, the threshold ranges from 0.30 to 2.23 kg/m^3 (0.51 to 3.76

lb/yd^3), with an average of 0.82 kg/m^3 (1.38 lb/yd^3) on a total chloride basis and from 0.19 to 2.30 kg/m^3 (0.32 to 3.88 lb/yd^3), with an average of 0.78 kg/m^3 (1.31 lb/yd^3) on a water-soluble basis.

Based on the direct chloride analysis, the critical chloride threshold on a water-soluble basis for conventional N2 steel ranges from 0.53 to 1.31 kg/m^3 (0.89 to 2.21 lb/yd^3), with an average of 0.91 kg/m^3 (1.53 lb/yd^3) for the modified SE specimens, and from 1.19 to 1.23 kg/m^3 (2.01 to 2.07 lb/yd^3), with an average of 1.22 kg/m^3 (2.06 lb/yd^3) for the beam specimens.

The chloride threshold values based on the diffusion equation show larger scatter than the values based on the direct chloride analysis due to the variation in concrete properties. The latter appears to be more applicable.

The average chloride threshold for all 83 samples from the modified SE specimens and 60 samples from the beam specimens, on a water-soluble basis, will be used as the chloride threshold for conventional steel in the service life prediction of bridge decks. The value, equal to (0.91×83+1.22×60)/143 = 1.04 kg/m^3 (1.75 lb/yd^3), is close to that obtained in earlier studies [0.6 to 0.9 kg/m^3 (1.0 to 1.5 lb/yd^3) on a total chloride basis].

MMFX steel - Based on diffusion analysis, the critical chloride threshold for MMFX steel ranges from 0.94 to 4.35 kg/m^3 (1.58 to 7.33 lb/yd^3), with an average of 2.78 kg/m^3 (4.68 lb/yd^3) on a total chloride basis and from 0.96 to 4.35 kg/m^3 (1.62 to 7.33 lb/yd^3), with an average of 2.80 kg/m^3 (4.72 lb/yd^3) on a water-soluble basis based on the diffusion equation.

Based on direct chloride analysis, the critical chloride threshold on a water-soluble basis for MMFX steel ranges from 1.90 to 5.77 kg/m^3 (3.20 to 9.72 lb/yd^3), with an average of 3.09 kg/m^3 (5.21 lb/yd^3) for the normal SE specimens, from 2.75

to 5.43 kg/m^3 (4.63 to 9.15 lb/yd^3), with an average of 3.70 kg/m^3 (6.23 lb/yd^3) for the modified SE specimens, and from 2.96 to 5.36 kg/m^3 (4.99 to 9.03 lb/yd^3), with an average of 4.07 kg/m^3 (6.86 lb/yd^3) for the beam specimens.

The chloride threshold values based on the diffusion equation also show larger scatter than the values based on the direct chloride analysis.

The average chloride threshold for all four samples from the normal SE specimens, 82 samples from the modified SE specimens, and 60 samples from the beam specimens, on a water-soluble basis, will be used as the chloride threshold for MMFX steel in the service life prediction of bridge decks. The value, equal to (3.09×4+3.70×82+4.07×60)/146 = 3.84 kg/m^3 (6.46 lb/yd^3), matches values obtained in earlier studies [3.8 kg/m^3 (6.4 lb/yd^3) (Clemeña 2003) and 4.6 kg/m^3 (7.7 lb/yd^3) (Trejo and Pillai 2003) on a total chloride basis].

Duplex stainless steels – The critical chloride thresholds for duplex stainless steels were determined based on the diffusion equation and the direct chloride analysis for the normal Southern Exposure specimens.

Based on diffusion analysis, the critical chloride threshold for 2101 steel ranges from 0.51 to 2.47 kg/m^3 (0.86 to 4.16 lb/yd^3), with an average of 1.43 kg/m^3 (2.41 lb/yd^3), on a total chloride basis and from 0.46 to 2.54 kg/m^3 (0.78 to 4.28 lb/yd^3), with an average of 1.46 kg/m^3 (2.46 lb/yd^3), on a water-soluble basis.

Based on diffusion analysis, the critical chloride threshold for 2101p steel ranges from 9.04 to 11.1 kg/m^3 (15.2 to 18.7 lb/yd^3), with an average of 10.3 kg/m^3 (17.4 lb/yd^3), on a total chloride basis and from 8.63 to 10.5 kg/m^3 (14.5 to 17.7 lb/yd^3), with an average of 9.75 kg/m^3 (16.4 lb/yd^3), on a water-soluble basis.

Based on the direct chloride analysis for the normal SE specimens, the critical chloride threshold for 2101p steel ranges from 7.66 to 10.7 kg/m^3 (12.9 to 18.0 lb/yd^3), with an average of 9.55 kg/m^3 (16.1 lb/yd^3), on a water-soluble basis.

Based on diffusion analysis, the critical chloride threshold for 2101(2) steel ranges from 3.89 to 9.71 kg/m^3 (6.55 to 16.4 lb/yd^3), with an average of 7.57 kg/m^3 (12.8 lb/yd^3), on a total chloride basis and from 3.92 to 9.22 kg/m^3 (6.61 to 15.5 lb/yd^3), with an average of 7.29 kg/m^3 (12.3 lb/yd^3), on a water-soluble basis.

Based on the direct chloride analysis for the normal SE specimens, the critical chloride threshold for 2101(2) steel ranges from 1.18 to 4.89 kg/m^3 (1.99 to 8.24 lb/yd^3), with an average of 3.33 kg/m^3 (5.61 lb/yd^3), on a water-soluble basis.

Only one 2101(2)p SE specimen (six specimens in total) corroded. Based on diffusion analysis, the chloride threshold for the steel is 12.6 kg/m^3 (21.2 lb/yd^3) on a total chloride basis and 11.8 kg/m^3 (19.8 lb/yd^3) on a water-soluble basis. Based on the direct chloride analysis for the specimen, the chloride threshold for the steel is 16.1 kg/m^3 (27.1 lb/yd^3) on a water-soluble basis. Since only one specimen corroded and the others remained passive throughout the test, the average chloride threshold for 2101(2)p steel is expected to be higher. Because of the limited data, conservatively, the average of the threshold values on a water-soluble basis based on the only specimen to corrode will be used as the chloride threshold for 2101(2)p steel for service life prediction, which is equal to (11.8+16.1)/2 = 14.0 kg/m^3 (23.5 lb/yd^3).

Only one 2205 SE specimen (six specimens in total) corroded. Based on diffusion analysis, the chloride threshold for the steel is 12.4 kg/m^3 (20.9 lb/yd^3) on a total chloride basis and 11.6 kg/m^3 (19.6 lb/yd^3) on a water-soluble basis. Based on the direct chloride analysis for the specimen, the chloride threshold for the steel is 15.1 kg/m^3 (25.4 lb/yd^3) on a water-soluble basis. As with 2101(2)p steel, the average

of the threshold values on a water-soluble basis based on the only specimen to corrode, (11.6+15.1)/2 = 13.4 kg/m^3 (22.5 lb/yd^3), will be used for service life prediction.

Pickled 2205 steel (2205p) exhibited the best corrosion resistance, with no specimen corroding during the test. Based on diffusion analysis, the critical chloride threshold for the steel is greater than 13.4 kg/m^3 (22.6 lb/yd^3) on a total chloride basis and 12.5 kg/m^3 (21.1 lb/yd^3) on a water-soluble basis, which are the chloride concentrations at the depth of the steel at the end of the test. Since 2205p steel has better corrosion resistance than 2101(2)p steel, conservatively, the chloride threshold for 2101(2)p steel, 14.0 kg/m^3 (23.5 lb/yd^3), will be used for the service life prediction of decks containing 2205p steel.

CHAPTER 5

SERVICE LIFE PREDICTION AND LIFE CYCLE COST ANALYSIS

In this chapter, the service lives (the times to first repair) of bridge decks containing conventional, epoxy-coated, MMFX, pickled 2101 [2101(2)p], nonpickled 2205, and pickled 2205 (2205p) steels are estimated based on the laboratory results for critical chloride thresholds and corrosion rates, along with data from bridge deck surveys performed by Miller and Darwin (2000) and Lindquist, Darwin, and Browning (2005). The service life of bridge decks containing epoxy-coated reinforcing steel is also estimated based on the experience of the Kansas Department of Transportation (KDOT) and the South Dakota Department of Transportation (SDDOT). Based on the service lives and 25-year cycles between repairs, a life cycle cost analysis is performed to compare the cost effectiveness of the steels for bridge decks over a 75-year economic life following the procedures used by Kepler et al. (2000), Darwin et al. (2002), and Balma et al. (2005). The bridge decks used in the comparison include a typical 230-mm (9.0 in.) concrete bridge deck with 76 mm (3.0 in.) of concrete cover over the top mat of steel for all of the steels, a 216-mm (8.5 in.) concrete bridge deck with 65 mm (2.5 in.) of concrete cover for pickled 2101 and nonpickled and pickled 2205 steels, and a 191-mm (7.5 in.) concrete subdeck with a 38-mm (1.5 in.) silica fume concrete overlay for conventional, epoxy-coated, and MMFX steels. Total costs for construction and repair over the 75-year economic life are compared on a present-cost basis.

5.1 SERVICE LIFE PREDICTION

In this study, the service life of reinforced concrete bridge decks is estimated based on both analysis and experience.

Based on analysis, the service life of bridge decks can be estimated by determining the time it takes for chlorides to penetrate the concrete cover and reach the threshold concentration at the depth of the embedded steel, causing corrosion to initiate (the time to corrosion initiation), plus the time it takes after corrosion initiation for corrosion products to crack and spall the concrete (the time to concrete cracking).

The time to corrosion initiation – the time to corrosion initiation is determined based on the penetration rates of the chlorides at crack locations on bridge decks from field surveys (Miller and Darwin 2000, Lindquist, Darwin, and Browning 2005) and the critical chloride thresholds of steel obtained in the current study.

As described in Section 1.5, Miller and Darwin (2000) and Lindquist et al. (2005) reported water-soluble chloride concentrations from 59 reinforced concrete bridge decks with ages ranging from several months to 20 years. Forty of the decks were sampled at two different times. Samples were obtained at crack locations and in uncracked concrete. The results of both studies were summarized by Lindquist et al. The chloride concentrations at depths of 25.4 mm (1.0 in.), 50.8 mm (1.5 in.), 63.5 mm (2.5 in.), and 76.2 mm (3.0 in.), which were linearly interpolated from the raw data, were obtained versus time. Since the surveys showed that reinforced concrete bridge decks exhibited significant cracking parallel to and above the reinforcing bars, the chloride concentrations obtained at the crack locations are used to estimate the time to corrosion initiation in the current study. The chloride concentrations versus time at depths of 76.2 mm (3 in.) and 63.5 mm (2.5 in.) for bridges with an annual

average daily traffic (AADT) greater than 7500 (high traffic bridges) are shown in Figures 5.1 (a) and (b) , respectively.

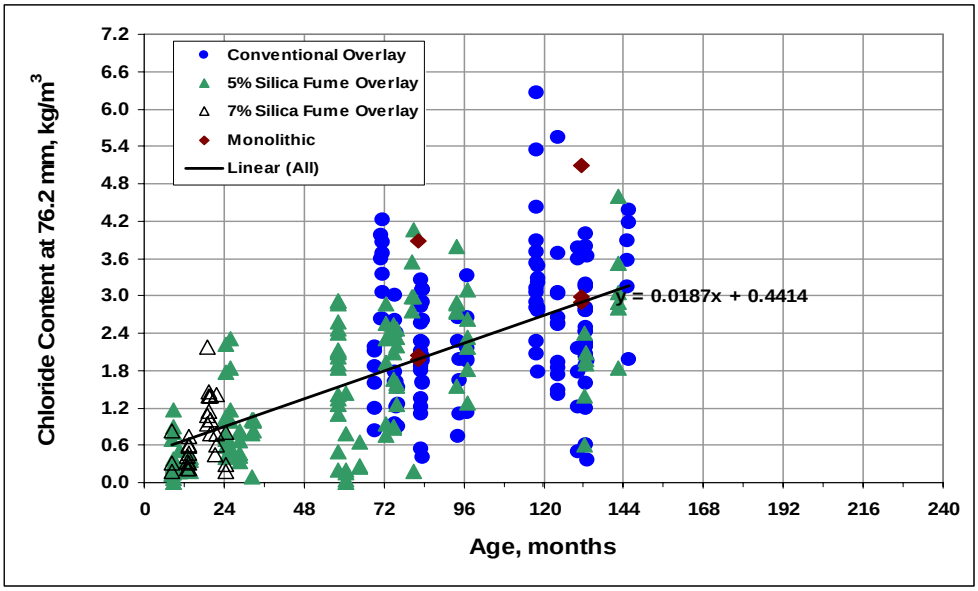

(a)

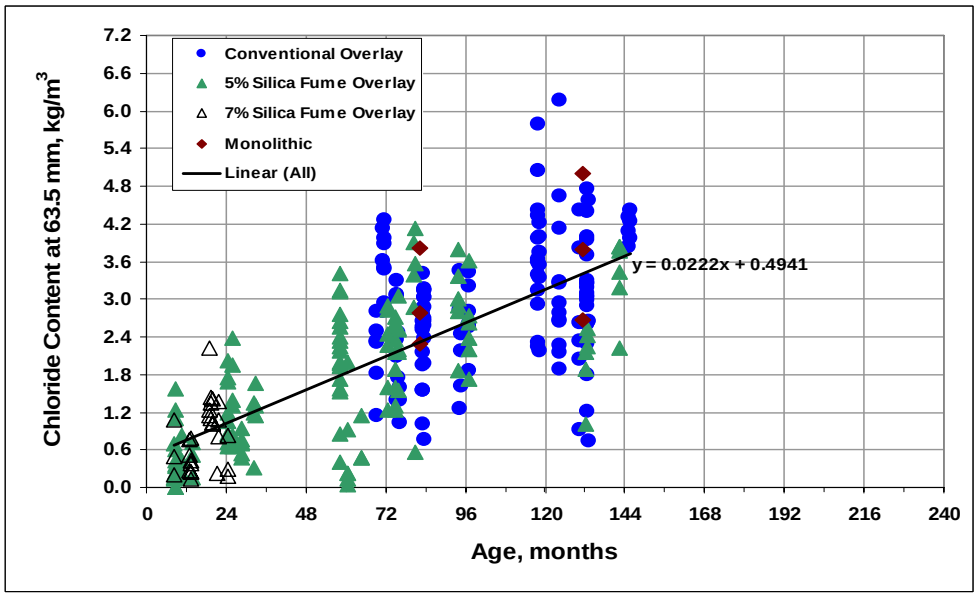

(b)

Figure 5.1 - Chloride content taken on cracks interpolated at depths of 76.2 mm (3 in.) (a) and 63.5 mm (2.5 in.) (b) versus placement age for bridges with an AADT greater than 7500.

The figures show that the chloride concentrations at crack locations increase nearly linearly with age and decrease as the sample depth increases. Linear trend lines of the chloride concentrations versus time can be expressed as:

$$C = 0.0187t + 0.4414 \text{ at a depth of 76.2 mm (3.0 in.)} \quad (5.1)$$

$$C = 0.0222t + 0.4941 \text{ at a depth of 63.5 mm (2.5 in.)} \quad (5.2)$$

where

C = water-soluble chloride concentration, kg/m^3;

t = time, months;

As presented in Chapter 4, the critical chloride thresholds, on a water-soluble basis, used for the service life estimate are 1.04 kg/m^3 (1.75 lb/yd^3) for conventional steel and 3.84 kg/m^3 (6.46 lb/yd^3) for MMFX steel, based on the average values from direct chloride analyses. The chloride thresholds for the other steels are 13.4 kg/m^3 (22.5 lb/yd^3) for 2205 steel and 14.0 kg/m^3 (23.5 lb/yd^3) for pickled 2101 and 2205 [2101(2)p and 2205p] steels; these values are based on the only specimens to corrode [one 2205 SE specimen and one 2101(2)p SE specimen which is used for both 2101(2)p and 2205p steel], representing conservative estimates. Using the critical chloride thresholds, in conjunction with Eq. (5.1) and (5.2), the times to corrosion initiation are calculated to be 2.7 years for conventional steel, 15.2 years for MMFX steel, 57.7 years for 2205 steel, and 60.4 years for 2101(2)p and 2205p steels with a concrete cover of 76.2 mm (3.0 in.) and 48.4 years for 2205 steel and 50.7 years for 2101(2)p and 2205p steels with a concrete cover of 63.5 mm (2.5 in.). The time to corrosion initiation for epoxy-coated steel with a damaged coating is same as that for conventional steel since the steels have the same critical chloride thresholds.

The time to concrete cracking after corrosion initiation– The time to concrete cracking after corrosion initiation for uncoated steels is determined based on the

corrosion rates of the steels measured in the current study and the estimate that a thickness loss of 25 μm (0.001 in.) of steel will result in a volume of corrosion products that will crack concrete (McDonald, Pfeifer, and Sherman 1998, Pfeifer 2000, Darwin et al. 2002).

The average corrosion rates for different steels are presented in Chapter 3. Since the Southern Exposure (SE) and cracked beam (CB) specimens simulate a portion of concrete bridge decks (uncracked and cracked concrete deck, respectively), the average of the corrosion rates obtained from the specimens is selected as the most realistic to estimate service life.

For conventional and MMFX steels, all individual specimens corroded in the bench-scale tests. The average corrosion rates versus time are shown in Figures 3.10 and 3.49 for the SE specimens and Figures 3.13 and 3.53 for the CB specimens, respectively. The results show that the average corrosion rates varied, depending on the progress of corrosion. For example, the SE specimens exhibited progressively higher corrosion rates during the first half of the test period, while the CB specimens exhibited relatively high initial rates, which then declined. To select reasonable (or representative) corrosion rates for the steels, the average values of the corrosion rates between 60 and 70 weeks for the SE specimens, and between 30 and 40 weeks for the CB specimens are used (the conventional and MMFX steels corroded steadily during these periods). For conventional N, N3, and MMFX steels, these values are 4.57, 9.27, and 2.45 μm/yr for the SE specimens, and 3.94, 4.78, and 2.55 μm/yr for the CB specimens, with averages of 4.26, 7.03, and 2.50 μm/yr, respectively. These values do not represent corrosion rates in bridge decks, however. Since the steels are usually subjected to a more severe environment in the accelerated laboratory tests than in the actual structure, corrosion rates equal to one-half of those measured in the bench-

scale tests are used to estimate service life (the value is selected to match estimated service life for conventional steel based on experience, as will be discussed later). This gives a corrosion rate of 2.82 μm/yr [0.5(4.26+7.03)/2 = 2.82] for conventional steel, based on the values of both N and N3 steel, and 1.25 μm/yr (2.50/2 = 1.25) for MMFX steel. Using these modified corrosion rates, along with the estimate that concrete will crack when the thickness loss of steel reaches 25 μm (0.001 in.) (McDonald, Pfeifer, and Sherman 1998, Pfeifer 2000, Darwin et al. 2002), the time to concrete cracking after corrosion initiation is estimated to be 8.9 years for conventional steel and 20 years for MMFX steel.

For pickled 2101 and nonpickled 2205 steels, not all of the bench-scale specimens corroded during the 96-week test period. Conservatively, the corrosion rates at the end of the test for the corroding specimens, rather than the average values for all individual specimens, are selected to estimate the service life. For pickled 2101 steel, as shown in Figures A.176 and A.200, one Southern Exposure specimen [SE-2101(2)p-5] corroded, with a corrosion rate of 0.24 μm/yr at 96 weeks and two cracked beam specimens [CB-2101(2)p-1 and CB-2101(2)p-5] corroded, with corrosion rates of 0.08 and 0.04 μm/yr and an average of 0.06 μm/yr at 96 weeks. For nonpickled 2205 steel, as shown in Figures A.179 and A.204, one Southern Exposure specimen [SE-2205-3] corroded, with a corrosion rate of 0.64 μm/yr at 96 weeks and four cracked beam specimens [CB-2205-1, 2, 3, and 4] corroded, with corrosion rates of 0.20, 2.9, 0.47 and 0.08 μm/yr and an average of 0.91 μm/yr at 96 weeks. By averaging the corrosion rates of the SE and CB specimens, a corrosion rate of 0.15 μm/yr [(0.24+0.06)/2 = 0.15] is obtained for pickled 2101 steel and a corrosion rate of 0.78 μm/yr [(0.64+0.91)/2 = 0.78] is obtained for nonpickled 2205 steel. Considering that corrosion of these steels occurred during the later period of the test

and that the corrosion rates might have continued to increase had the tests been continued, conservatively, these values are not modified as they were for conventional and MMFX steels. Using the corrosion rates, along with the estimate that concrete will crack when a thickness loss of steel reaches 25 μm (0.001 in.), the time to concrete cracking after corrosion initiation is estimated to be 167 years for pickled 2101 steel and 32 years for nonpickled 2205 steel.

For pickled 2205 steel, none of specimens corroded in the bench-scale tests. The corrosion rate after the corrosion initiation is, actually, unknown for the steel. Since pickled 2205 steel has better corrosion resistance than pickled 2101 steel, however, the time to concrete cracking after corrosion initiation for the steel can be estimated to be at least 167 years.

The time to concrete cracking after corrosion initiation for damaged epoxy-coated steel is estimated based on the corrosion rate obtained from the bench-scale specimens with the steel [with four 3.2-mm (0.125 in.) diameter drilled holes in the coating) in both mats in a follow-on study (Gong et al. 2005) and the local corrosion losses of the steel needed to crack the concrete cover in a Southern Exposure specimen, which can be calculated based on the empirical equation [Eq. (1.26)] presented by Torres-Acosta and Sagues (2004).

As discussed in Chapter 1, when only a fraction of the reinforcing bar (a ring region on the bar) corrodes, the local corrosion loss needed to crack the concrete cover can be expressed as:

$$x_{crit} = 11\left(\frac{C}{\phi}\right)\left(\frac{C}{L}+1\right)^2 \tag{1.26}$$

where

x_{crit} = thickness loss of steel needed to crack concrete cover, μm;

C = concrete cover, mm;

ϕ = reinforcing bar diameter, mm;

L = anodic length, the length of the anodic ring region, mm;

Based on Eq. (1.26), for a bar with an anodic length (L) equal to 3.2 mm (0.125 in.) (the diameter of the drilled holes for epoxy-coated steel) in the SE specimen, the thickness loss needed to crack the concrete cover is equal to 1426 μm (0.056 in.) using a concrete cover (C) of 25 mm (1.0 in.) and a bar diameter (ϕ) of 16 mm (0.5 in.). For an epoxy-coated bar, however, the corrosion occurs at holes in the epoxy on one side of the bar, rather than a ring region. Assuming that the tensile stress caused by the volume of the corrosion products from one hole on one side of the epoxy-coated bar is half of the stress caused by the corrosion products over a ring shaped region with length L equal to the diameter of the hole, a thickness loss of the epoxy-coated bar required to crack the concrete cover in the SE specimen is estimated to be 2852 μm, twice the corrosion loss (x_{crit}) given by Eq. (1.26) over the ring shaped region.

Using the local corrosion loss of 2852 μm to cause concrete cracking, along with a corrosion rate of 1.75 μm/year based on the exposed area in the coating from the follow-on study by Gong et al. (2005), the time to concrete cracking after corrosion initiation is estimated to be 1630 years for damaged epoxy-coated steel. This figure suggests that bridge decks with concrete covers of 76 and 63 mm (3.0 and 2.5 in.) containing reinforcing steel with a damaged epoxy coating will never undergo cracking caused by corrosion of the exposed steel. The calculations do not, however, consider the potential effect of loss of adhesion between the epoxy and the steel, which may greatly reduce the time to first repair (Sagues et al. 1994).

To consider the effects of adhesion loss, the service life for bridge decks containing epoxy-coated steel is also estimated based on the experience of the Bridge Management Engineers at the Kansas Department of Transportation (KDOT) and the South Dakota Department of Transportation (SDDOT) (Darwin et al. 2002). In both states, bridge decks containing epoxy-coated reinforcing steel that were constructed in the late 1970s have never required repair due to corrosion-induced damage. Engineers at KDOT estimated the service life of bridge decks with epoxy-coated steel to be 30 years, while SDDOT estimated the service life to be 40 years. Both figures were used in the life cycle cost analysis by Darwin et al. (2002) and Balma et al. (2005). In the current study, considering that bridge decks containing epoxy-coated steel have not required repair due to the corrosion of the steel, as of the date of this report, and thus, have the service life very likely over 30 years, a value of 40 years is used in the following economic analysis. For completeness, in addition to 40 years, a value of 50 years is also included.

The service lives of bridge decks with different steels, including the times to corrosion initiation plus the times after corrosion initiation to concrete cracking based on the analysis and the values based on the experience are summarized in Table 5.1.

The results show that, based on the analysis, the average service life of bridge decks containing conventional steel is 12 years. The value matches the experience in many states that bridge decks with conventional steel require repair in 10 to 25 years, depending on exposure conditions (Darwin et al. 2002); the service life of bridge decks containing MMFX steel is 35 years, compared to 27 years estimated in an earlier study (Darwin et al. 2002); the service lives of bridge decks containing pickled 2101 and nonpickled and pickled 2205 steels are over 75 years, even if the decks have a thickness of 216 mm (8.5 in.), corresponding to a concrete cover of 65 mm (2.5 in.).

Table 5.1 - The times to corrosion initiation, the times to concrete cracking after corrosion initiation, and the service lives (the times to first repair) for bridge decks with different steels

Bridge decks[a]	Type of Steel[b]	Corrosion thresholds (kg/m^3)	Corrosion rates (μm/yr)	Time to corrosion initiation (years)	Time to concrete cracking[c] (years)	Service life (years)
230-mm and 191-mm + 38-mm SFO	Conv.	1.04	2.82	2.7	8.9	12
	MMFX	3.84	1.25	15.2	20.0	35
	ECR	1.04	-	-	-	40[d]
		1.04	-	-	-	50[d]
		1.04	1.75	2.7	1630	>75
230-mm	2205	13.4	0.78	57.7	32	>75
	2101(2)p	14.0	0.15	60.4	167	>75
	2205p	14.0	< 0.15	> 60.4	> 167	>75
216-mm	2205	13.4	0.78	48.4	32	>75
	2101(2)p	14.0	0.15	50.7	167	>75
	2205p	14.0	< 0.15	> 50.7	> 167	>75

a: Types of bridge decks compared:
230-mm = 230-mm (9.0 in.) concrete bridge deck with 76 mm (3.0 in.) of concrete cover over the top mat;
216-mm = 216-mm (8.5 in.) concrete bridge deck with 65 mm (3.0 in.) of concrete cover over the top mat;
191-mm + 38-mm SFO = 191-mm (7.5 in.) concrete subdeck with a 38 mm (1.5 in.) silica fume concrete overlay (SFO).
b: Steel types:
Conv. = conventional steel; MMFX = Microcomposite MMFX II steel;
2101(2)p = the second heat of pickled 2101 duplex stainless steel (21% chromium, 1% nickel);
2205 = 2205 duplex stainless steel (22% chromium, 5% nickel), 2205p = pickled 2205 steel;
ECR = epoxy-coated reinforcing steel.
c: after corrosion initiation.
d: estimated based on the experience.

5.2 LIFE CYCLE COST ANALYSIS

The cost effectiveness of conventional, MMFX, pickled 2101 [2101(2)p], nonpickled 2205, and pickled 2205 (2205p) steels are compared based on a life cycle cost analysis for bridge decks over a 75-year economic life. The bridge decks include a 230-mm (9.0-in.) concrete bridge deck for all of the steels, a 216-mm (8.5-in.) concrete bridge deck for 2101p, 2205 and 2205p steels, since a decrease in concrete cover may be accepted for the stainless steels, and a 191-mm (7.5-in.) concrete

subdeck with a 38-mm (1.5-in.) silica fume concrete overlay for conventional, MMFX, and epoxy-coated steel. The silica fume overly deck with epoxy-coated steel is the most common bridge deck type used in Kansas for high-traffic, high-salt exposure conditions. The life cycle cost analysis, following the procedures used by Kepler et al. (2000), Darwin et al. (2002), and Balma et al. (2005), includes:

1) Determining new bridge deck costs in dollars per square meter, considering the in-place costs of concrete and steel, with an estimate that the same steel content will be used for all decks, based on a value of 143 kg/m^3 (241 lb/yd^3) of reinforcing steel in the 230-mm (9.0-in.) decks.

2) Determining repair costs, including full-depth and partial-depth repairs (considering that, on the average, 6% of a bridge deck will receive a full-depth repair and 22% will receive a partial-depth repair), machine preparation, a 38-mm silica fume overlay, and incidental costs. The repair costs for bridge decks with different steels are considered same.

3) Determining repair schedules based on the service life (the time to first repair) and the times between repairs over a 75-year economic life. The service life is estimated based on analysis and experience, as described in Section 5.1. A fixed value of 25 years is used as the time between repairs for all types of reinforcing steel.

4) Comparing cost effectiveness based on the present value of the costs for bridge decks using discount rates of 2, 4, and 6%. The present values consist of the new bridge deck costs and the present values of the repair costs.

5.2.1 NEW BRIDGE DECK COSTS

Based on average bid items obtained from KDOT for 2000 to 2003 (Balma et al. 2005), the in-place cost of a monolithic concrete deck or subdeck is \$475.30/m^3

and the in-place cost of the silica fume overlay is $1148/m^3$ [$43.60/$m^2$ for a thickness of 38 mm (1.5 in.)].

The in-place cost of steel consists of the cost of the steel at the mill plus the cost of fabrication, delivery, and placement. The values used in the current study are based on data provided by manufacturers and fabricators in 2004 and 2005 and analysis from an early study (Balma et al. 2005).

For conventional steel, the cost at the mill is $0.55/kg ($0.25/lb), and the cost for fabrication, delivery, and placement is $1.30/kg ($0.59/lb), giving an in-place cost of $1.85/kg ($0.84/lb)

For MMFX steel, two prices at the mill, $1.81/kg and $2.20/kg ($0.82/lb and $1.00/lb), are used in the analysis. The cost for fabrication, delivery, and placement is also $1.30/kg ($0.59/lb). The in-place costs for the steel are, thus, $3.11/kg and $3.50/kg ($1.41/lb and $1.59/lb).

For epoxy-coated steel, the cost after application of the epoxy is $0.68/kg ($0.31/lb), and the cost for fabrication, delivery, and placement is $1.41/kg ($0.64/lb), giving an in-place cost of $2.09/kg ($0.95/lb).

For pickled 2101 steel, three different prices at the mill, $2.46/kg, $3.01/kg, and $4.00/kg ($1.12/lb, $1.37/lb, and $1.82/lb), are used, based on the difference in cost between pickled 2101 and 2205 steels calculated by Balma et al. (2005). For pickled 2205 steel, the costs at the mill are $3.96/kg, $4.51/kg, and $5.50/kg ($1.80/lb, $2.05/lb, and $2.50/lb), which were obtained by manufacturers. For nonpickled 2205 steel, the costs are $3.87/kg, $4.42/kg, and $5.41/kg ($1.76/lb, $2.01/lb, and $2.46/lb), based on the costs of the pickled 2205 steel minus the cost of pickling process done at the mill, $0.09/kg ($0.04/lb) (Larsen 2005). Using these values, along with the cost for fabrication, delivery and placement of stainless steel

estimated to be \$1.39/kg (\$0.63/lb), the in-place costs are \$3.85/kg, \$4.40/kg and \$5.39/kg (\$1.75/lb, \$2.00/lb, and \$2.45/lb) for pickled 2101 steel, \$5.26/kg, \$5.81/kg, and \$6.80/kg (\$2.39/lb, \$2.64/lb, and \$3.09/lb) for nonpickled 2205 steel, and \$5.35/kg, \$5.90/kg and \$6.89/kg (\$2.43/lb, \$2.68/lb, and \$3.13/lb) for pickled 2205 steel.

Based on the in-place costs of the concretes and steels, the average amount of steel used in a 230-mm (9.0 in.) concrete deck (143 kg/m^3), and the thickness of the decks, the new deck costs in dollars per square meter can be calculated as follows:

New deck cost (\$/m^2) = in-place cost of concrete (\$/m^3) × thickness of the concrete (m) + in-place cost of steel (\$/kg) × the amount of steel (143 kg/m^3) × 0.230 (m).

The costs of the new bridge decks with the various options of reinforcing steel are shown in Table 5.2.

The results show that, for the 230-mm concrete bridge deck, the new deck costs are \$170.15/m^2 for conventional reinforcement, \$211.59/m^2 to \$224.42/m^2 for MMFX reinforcement, depending on the cost of the steel, and \$178.04/m^2 for epoxy-coated reinforcement. The new deck costs are \$235.93/m^2, \$254.02/m^2, and \$286.58/m^2 for 2101(2)p steel, \$282.30/m^2, \$300.39/m^2, and \$332.95/m^2 for 2205 steel, and \$285.26/m^2, \$303.35/m^2, and \$335.91/m^2 for 2205p steel, depending on the costs of the steels. Decks with 2101(2)p steel cost \$49.34/m^2 less than decks with 2205p steel, while decks with 2205 steel cost \$2.96/m^2 less than decks with 2205p steel. For the 216-mm concrete bridge deck, the new deck costs are \$6.60/m^2 less than the costs for the 230-mm bridge decks with the same steel. The new deck costs for the 191-mm (7.5-in.) concrete subdeck with a 38-mm (1.5-in.) silica fume concrete overlay are \$25.10/m^2 more than the costs for the 230-mm bridge deck with

the same steel. The silica fume overlay deck containing epoxy-coated steel is $\$203.14/m^2$, slightly lower than the cost of the 230-mm (9.0 in.) concrete deck containing MMFX steel.

Table 5.2 - The costs of new bridge decks with different steels

Bridge decks[a]	In-place cost of concrete ($/m^3)	Cost of concrete per square meter of decks ($/m^2)	Type of Steel[b]	In-place cost of steel ($/m^3)	Cost of steel per square meter of decks ($/m^2)	Cost of new deck ($/m^2)
230-mm	475.3	475.3 × 0.230 =109.30	**Conv.**	1.85	60.85	**170.15**
			MMFX	3.11	102.29	**211.59**
				3.50	115.12	**224.42**
			ECR	2.09	68.74	**178.04**
			2101(2)p	3.85	126.63	**235.93**
				4.40	144.72	**254.02**
				5.39	177.28	**286.58**
			2205	5.26	173.00	**282.30**
				5.81	191.09	**300.39**
				6.80	223.65	**332.95**
			2205p	5.35	175.96	**285.26**
				5.90	194.05	**303.35**
				6.89	226.61	**335.91**
216-mm	475.3	475.3 × 0.216 =102.70	**2101(2)p**	3.85	126.63	**229.33**
				4.40	144.72	**247.42**
				5.39	177.28	**279.98**
			2205	5.26	173.00	**275.70**
				5.81	191.09	**293.79**
				6.80	223.65	**326.35**
			2205p	5.35	175.96	**278.66**
				5.90	194.05	**296.75**
				6.89	226.61	**329.31**
191-mm + 38-mm SFO	475.3 for concrete, 1148 for SFO	475.3 × 0.191 + 1148 × 0.038 = 134.40	**Conv.**	1.85	60.85	**195.25**
			MMFX	3.11	102.29	**236.69**
				3.50	115.12	**249.52**
			ECR	2.09	68.74	**203.14**

a: Types of bridge decks compared:
230-mm = 230-mm (9.0 in.) concrete bridge deck with 76 mm (3.0 in.) of concrete cover over the top mat;
216-mm = 216-mm (8.5 in.) concrete bridge deck with 65 mm (3.0 in.) of concrete cover over the top mat;
191-mm + 38-mm SFO = 191-mm (7.5 in.) concrete subdeck with a 38 mm (1.5 in.) silica fume concrete overlay (SFO).

b: Steel types:
Conv. = conventional steel; MMFX = Microcomposite MMFX II steel;
ECR = epoxy-coated reinforcing steel;
2101(2)p = the second heat of pickled 2101 duplex stainless steel (21% chromium, 1% nickel);
2205 = 2205 duplex stainless steel (22% chromium, 5% nickel), 2205p = pickled 2205 steel;

5.2.2 REPAIR COSTS

The repair costs for all bridge decks are considered to be the same.

Based on an earlier study (Kepler et al. 2000), it is estimated that the repair of bridge decks consists of full-depth repair for 6% of the deck area and partial-depth repair for 22% of the deck area. A 38-mm (1.5 in.) silica fume overlay is also placed over the deck as part of the repair, a standard repair practice in Kansas.

The repair cost in dollars per square meter is determined by summing the full-depth and partial-depth repairs, machine preparation, a 38-mm silica fume overlay, and incidental costs. Based on the average low-bid costs for the years 2000 to 2003 reported by KDOT, the costs of full depth and partial-depth repairs are $\$380.30/m^2$ and $\$125.80/m^2$ (based on repaired area), respectively, the cost of machine preparation is $\$13.10/m^2$, the cost of a 38-mm silica fume overlay is $\$43.60/m^2$, and incidental costs are $\$154.89/m^2$. Based on these costs, the average repair cost for a bridge deck is calculated as follows:

$$0.06 \times \frac{\$380.30}{m^2} + 0.22 \times \frac{\$125.80}{m^2} + \frac{\$13.10}{m^2} + \frac{\$43.60}{m^2} + \frac{\$1540.9}{m^2} = \$262.30/m^2$$

5.2.3 COST EFFECTIVENESS

Based on the service lives determined in Section 5.1 and 25-year cycles between repairs, over a 75-year economic life, the repair schedules for bridge decks are determined: bridge decks with conventional steel need to be repaired at 12 years, 37 years, and 62 years; bridge decks with MMFX steel need to be repaired at 35 years and 60 years; bridge decks with epoxy-coated steel need to be repaired at 40 years and 65 years if the service life is 40 years, at 50 years if the service life is 50 years,

and do not need to be repaired if the service life is over 75 years; bridge decks with 2101(2)p, 2205, and 2205p steels do not need repairs.

The cost effectiveness of the steels is compared based on the present values of the total costs for the bridge decks over the 75-year economic life. The total present cost consists of the new bridge deck costs and the present values of the repair costs, calculated using discount rates of 2, 4, and 6%. Present value is calculated using Eq. (5.3):

$$P = F \times (1+i)^{-n} \tag{5.3}$$

where

P = present value ($/m^2);

F = repair cost($/m^2) ;

i = discount rate (%/100);

n = time to repair (years).

The repair schedules and the present values of the total costs for the bridge decks with the various options are summarized in Table 5.3.

The results show that the present costs of the bridge decks containing conventional, MMFX, and epoxy-coated steels vary, depending on the cost of new decks, the service life estimated, and the discount rate, while the present costs of the decks containing the duplex stainless steels equal to the costs of new decks, since none of the decks needs repair during a 75-year economic life.

Of all evaluated bridge decks, at all discount rates, the lowest cost and the second lowest cost options are, respectively, the 230-mm concrete deck and the silica fume overlay deck containing epoxy-coated reinforcing steel, if their service lives can reach 75 years, which have total present costs of $178.04/m^2 and $203.14/m^2. The

highest and the second highest cost options are the silica fume overlay deck and the 230-mm concrete deck containing conventional steel, with present costs of $604.97/m^2 and $579.87/m^2 at discount rate of 2%, $443.59/m^2 and $418.49/m^2 at discount rate of 4%, and $363.05/m^2 and $337.95/m^2 at discount rate of 6%, respectively.

The present costs of bridge decks with pickled 2101 steel are lower than the costs of decks with nonpickled 2205 steel, which are less than decks with pickled 2205 steel. The present costs for the 216-mm concrete bridge decks are less than the costs for the 230-mm bridge decks with the same steel. For the bridge decks with the duplex stainless steels, the present costs range from 229.33/m^2 (the 216-mm deck containing pickled 2101 steel, using the low end of the steel price) to $335.91/m^2 (the 230-mm deck containing pickled 2205 steel, using the high end of the steel price). Although pickled 2101 and nonpickled 2205 steel are more cost effective than pickled 2205 steel in this analysis, both steels exhibited some corrosion activity in the laboratory tests, which is not recognized in the current analysis and may represent a potential problem.

At a discount rate of 2%, for service lives of 40 and 50 years, respectively, the present costs of the 230-mm concrete deck with epoxy-coated steel are $369.24/m^2 and $275.49/m^2, while the costs of the silica fume overlay decks with epoxy-coated steel are $394.3/m^2 and $300.59/m^2. These costs are lower than those of decks with MMFX steel, which are $422.69/m^2 and $435.52/m^2 for the 230-mm concrete deck, and $447.79/m^2 and $460.62/m^2 for the silica fume overlay deck depending on the price of the steel. At discount rates of 4% and 6%, similarly, bridge decks (with and without a silica fume overlay) containing epoxy-coated steel are more cost effective

than bridge decks containing MMFX steel, even without a silica fume overlay and using the low price of the steel.

As discount rates increase, the present costs of bridge decks containing MMFX and epoxy-coated steels decrease. At a discount rate of 2%, all of the decks (with and without the silica fume overlay) containing MMFX steel and epoxy-coated steel with a service life of 40 years are less cost effective than all of the options with the duplex stainless steels. The 230-mm concrete deck and the silica fume overlay deck containing epoxy-coated steel with a service life of 50 years ($275.49/m^2 and $300.59/m^2) are less cost effective than the 230-mm deck with pickled 2101 steel ($254.02/m^2) and the 216-mm deck with pickled 2205 steel ($296.75/m^2) using the intermediate price for the steels, respectively. At a discount rate of 4%, more decks containing non-stainless steels become more cost effective than decks with duplex stainless steels. For example, the present cost of the 230-mm concrete deck containing epoxy-coated steel with a service life of 50 years, $214.95/m^2, is less than the costs of all decks with the duplex stainless steels, while the present cost of the 230-mm deck with a service life of 40 years, $253.17/m^2, is lower than the cost of the deck with pickled 2101 steel using the intermediate price for the steel, $254.02/m^2; the present cost of the 230-mm deck containing MMFX steel, $315.82/m^2, is lower than the cost of the 216-mm deck with nonpickled 2205 steel, $326.35/m^2, using the high prices for the steels, while the present cost of the silica fume overlay deck containing MMFX steel using the low end of the steel prices, $328.09/m^2, is lower than the cost of the 216-mm deck with pickled 2205 steel using the high price of the steel, $329.31/m^2. At a discount rate of 6%, decks (with and without a silica fume overlay) containing epoxy-coated steel with a service life of 40 years ($209.48/m^2 and $234.58/m^2) become the lowest cost option, compared to all decks with other types of

steel; the present costs of decks containing MMFX steel, from $253.67/m^2 for the 230-mm deck using the low price of the steel to $291.59/m^2 for the silica fume overlay deck using the high price of the steel, are lower than the costs of all decks containing nonpickled and pickled 2205 steel using the intermediate and high prices of the steels. States such as Kansas and South Dakota, however, tend to use discount rates at or just below 2%.

Overall, the highest cost option is represented by the decks containing conventional steel. Bridge decks containing MMFX steel do not appear to be more cost effective than decks containing epoxy-coated steel. Bridge decks containing pickled 2101 steel are more cost effective than decks containing nonpickled 2205 steel, which has higher cost and lower corrosion resistance. Although bridge decks with pickled 2101 steel are also more cost effective than decks with pickled 2205 steel, it is important to consider the fact that pickled 2101 steel exhibited some corrosion activity, while pickled 2205 steel did not. The lowest cost option of bridge decks depends on the service life estimated and the discount rate. A bridge deck containing epoxy-coated steel represents the lowest cost option if its service life can reach 75 years, or if it has a service life of 50 year at a discount rate of 4% or above.

Table 5.3 - Life cycle cost analysis for bridge decks containing conventional, MMFX, epoxy-coated, and duplex stainless steels

Type of deck	Type of steel	Cost of new decks ($/m^2)	Time to repair 1 (years)	Cost of repair 1 ($/m^2)	Time to repair 2 (years)	Cost of repair 2 ($/m^2)	Time to repair 3 (years)	Cost of repair 3 ($/m^2)	Present cost i = 2% ($/m^2)	Present cost i = 4% ($/m^2)	Present cost i = 6% ($/m^2)
230-mm	Conv.	170.15	12	262.30	37	262.30	62	262.30	579.87	418.49	337.95
	MMFX	211.59	35	262.30	60	262.30			422.69	302.99	253.67
		224.42	35	262.30	60	262.30			435.52	315.82	266.49
	ECR	178.04	40	262.30	65	262.30			369.24	253.17	209.48
			50	262.30					275.49	214.95	192.28
			>75						178.04	178.04	178.04
191-mm + 38-mm SFO	Conv.	195.25	12	262.30	37	262.30	62	262.30	604.97	443.59	363.05
	MMFX	236.69	35	262.30	60	262.30			447.79	328.09	278.77
		249.52	35	262.30	60	262.30			460.62	340.92	291.59
	ECR	203.14	40	262.30	65	262.30			394.34	278.27	234.58
			50	262.30					300.59	240.05	217.38
			>75						203.14	203.14	203.14
230-mm	2101(2)p	235.93	>75						235.93	235.93	235.93
		254.02	>75						254.02	254.02	254.02
		286.58	>75						286.58	286.58	286.58
	2205	282.30	>75						282.30	282.30	282.30
		300.39	>75						300.39	300.39	300.39
		332.95	>75						332.95	332.95	332.95
	2205p	285.26	>75						285.26	285.26	285.26
		303.35	>75						303.35	303.35	303.35
		335.91	>75						335.91	335.91	335.91

Table 5.3 (con't) - Life cycle cost analysis for bridge decks containing conventional, MMFX, epoxy-coated, and duplex stainless steels

216-mm	2101(2)p	229.33	>75	229.33	229.33	229.33
		247.42	>75	247.42	247.42	247.42
		279.98	>75	279.98	279.98	279.98
	2205	275.70	>75	275.70	275.70	275.70
		293.79	>75	293.79	293.79	293.79
		326.35	>75	326.35	326.35	326.35
	2205p	278.66	>75	278.66	278.66	278.66
		296.75	>75	296.75	296.75	296.75
		329.31	>75	329.31	329.31	329.31

a: Types of bridge decks compared:

230-mm = 230-mm (9.0 in.) concrete bridge deck; 216-mm = 216-mm (8.5 in.) concrete bridge deck; 191-mm + 38-mm SFO = 191-mm (7.5 in.) concrete subdeck with a 38 mm (1.5 in.) silica fume concrete (SFO).

b: Steel types:

Conv. = conventional steel; MMFX = Microcomposite MMFX II steel; ECR = epoxy-coated reinforcing steel.

2101(2)p = the second heat of pickled 2101 duplex stainless steel (21% chromium, 1% nickel);

2205 = 2205 duplex stainless steel (22% chromium, 5% nickel), 2205p = pickled 2205 steel;

CHAPTER 6

SUMMARY, CONCLUSIONS, AND RECOMMENDATIONS

6.1 SUMMARY

The purpose of this study is to evaluate the corrosion resistance and the cost effectiveness of duplex stainless steels and MMFX microcomposite compared to epoxy-coated and conventional reinforcing steel for bridges decks using laboratory tests.

The reinforcing steels evaluated include: (1) four heats of conventional ASTM A 615 reinforcing steel (N, N2, N3, and N4); (2) epoxy-coated N3 reinforcing steel: ECR; (3) Microcomposite MMFX II steel: MMFX; (4) two heats of 2101 duplex stainless steel “as rolled” [2101 and 2101(2)], and pickled to remove the mill scale [2101p and 2101(2)p]; (5) 2205 duplex stainless steel “as rolled” (2205), and pickled (2205p). The bars in the first heat of 2101 steel, 2101 and 2101p, were slightly deformed and had small cracks on the surface due to a lack of boron. The second heat, 2101(2) and 2101(2)p, was provided to allow a fair evaluation of the steel.

The rapid macrocell test (with and without mortar cover on the steel) and two bench-scale tests, the Southern Exposure and cracked beam tests, are used to evaluate the reinforcing steels. The corrosion rates, corrosion potentials, total corrosion losses (an integral of the corrosion rate over time), and mat-to-mat resistances for the bench-scale specimens are reported. The Student’s t-test is used to determine whether the differences in the average corrosion rates and losses are statistically significant.

During the study, the macrocell test was modified by replacing the solutions at the anode and the cathode every five weeks to limit the effects of changes in the pH of the simulated pore solution due to carbonation. An additional set of corrosion

potential tests were performed to compare conventional and MMFX steels in simulated concrete pore solutions with various NaCl concentrations.

The critical chloride thresholds for the reinforcing steels are determined based on both a diffusion equation and direct analysis of the chloride contents adjacent to the steel in normal Southern Exposure (SE), modified Southern Exposure (MSE), and beam specimens (B) at the time of corrosion initiation.

Based on laboratory results for critical chloride thresholds and corrosion rates, along with data from bridge deck surveys (Miller and Darwin 2000, Lindquist et al. 2005) and field experience, the service lives (the times to first repair) of bridge decks containing conventional, epoxy-coated, MMFX, 2101(2)p, 2205, and 2205p steels are estimated. A life cycle cost analysis is performed to compare the cost effectiveness of the steels for bridge decks over a 75-year economic life.

6.2 CONLUSIONS

The following conclusions are based on the results and analyses presented in this report.

1. Compared to the other steels in this study, conventional steel has the lowest corrosion resistance. The average chloride thresholds for the steel, on a water-soluble basis, were 0.78 kg/m^3 (1.31 lb/yd^3) based on diffusion analysis and 0.91 and 1.22 kg/m^3 (1.53 and 2.05 lb/yd^3) based on direct chloride analysis for the modified SE and beam specimens, respectively.
2. Epoxy-coated steel [with four 3.2-mm (0.125-in.) diameter holes in the coating to simulate defects] exhibits low corrosion rates based on total steel area. The cathode area has a great effect on the corrosion rate. When uncoated steel was used as the cathode, the corrosion losses of epoxy-coated steel

ranged from 7% to 24% of the values of conventional steel. When epoxy-coated steel was used as the cathode, the corrosion losses of epoxy-coated steel ranged from 0.4 and 6% of the values of conventional steel.

3. MMFX microcomposite steel exhibits higher corrosion resistance than conventional steel, with corrosion losses between 16% and 66% of the value of conventional reinforcing steel.
4. MMFX and conventional steel exhibit nearly identical corrosion potentials, indicating that both steels have a similar tendency to corrode. For bare bars in the simulated concrete pore solution with NaCl, both MMFX and conventional steel exhibited a critical Cl^-/OH^- ratio of 0.31.
5. Based on the statistical analyses of samples taken for direct chloride analysis, the average required sample sizes for the errors of 1.0, 0.5, and 0.25 kg/m^3, with 95% confidence, are 1, 3, and 13 for the modified SE specimens and 1, 4, and 15 for the beam specimens for an average concentration of about 1.0 kg/m^3 (1.7 lb/yd^3), and 4, 17, and 66 for the modified SE specimen and 4, 15, and 59 for the beam specimen for an average concentration of about 4.0 kg/m^3 (6.8 lb/yd^3).
6. The chloride threshold of MMFX microcomposite steel is three to four times that of conventional steel. The average threshold values for MMFX steel, on a water-soluble basis, are 2.80 kg/m^3 (4.72 lb/yd^3) based on diffusion analysis and 3.70 and 4.07 kg/m^3 (6.23 and 6.86 lb/yd^3) based on direct chloride analysis for the modified SE and beam specimens, respectively.
7. Chloride thresholds based on direct chloride analysis for the modified SE and beam specimens exhibit less scatter, and thus, should carry more weight than

the values based on the diffusion equation, which is greatly effected by variations in concrete properties.

8. Based on the statistical analysis on the chloride samples from the modified SE and beam specimens, the average chloride contents (for all samples from all specimens in each case) are, with 95% confidence, within 10% and 0.25 kg/m^3 (0.42 lb/yd^3) of the true average chloride content at the level of the steel.
9. Pickled 2101 steel [2101(2)p] and nonpickled and pickled 2205 steel (2205 and 2205p) exhibit significantly better corrosion resistance than conventional steel, while nonpickled 2101 steel [2101(2)] has similar corrosion resistance to MMFX steel. The corrosion losses for 2101(2), 2101(2)p, 2205, and 2205p steel, respectively, ranged from 5% to 37%, 0.4% to 2%, 0.4% to 5%, and 0.2% to 0.5% of the value for conventional steel.
10. Conservatively, based on the only Southern Exposure specimen to corrode (a single specimen for each steel type), the chloride thresholds for 2101(2)p and 2205 steel, on a water-soluble basis, were 11.8 and 11.6 kg/m^3 (19.8 lb/yd^3 and 19.6 lb/yd^3) based on diffusion analysis, and 16.1 and 15.1 kg/m^3 (27.1 and 25.4 lb/yd^3) based on direct chloride analysis, respectively. The chloride thresholds are more than 10 times the value of conventional steel.
11. The corrosion resistance of duplex stainless steels depends on the chromium (Cr) and nickel (Ni) contents and whether the bars are pickled or nonpickled. Overall, 2205 steel (22% chromium and 5% nickel) has better corrosion resistance than 2101 steel (21% chromium and 1% nickel) when evaluated in the same condition, pickled bars have higher corrosion resistance than

nonpickled bars, and pickled 2101 steel has better corrosion resistance than nonpickled 2205 steel.

12. The use of duplex stainless steel in conjunction with conventional steel does not increase the rate of corrosion for either steel.
13. In all evaluations, pickled 2205 steel remained passive throughout the test period and exhibited the best corrosion resistance of the steels evaluated. Pickled 2205 steel is the only steel that meets the corrosion requirements of the Kansas Department of Transportation Special Provision to the Standard Specifications on Stainless Steel Reinforcing Bars. The special provision requires that, during the rapid macrocell test, the average corrosion rate for a minimum of five specimens must at no time exceed 0.25 μm/yr, with no single specimen exceeding a corrosion rate of 0.5 μm/yr.
14. In all macrocell tests, replacing the solutions helps maintain the pH, and thus, the Cl^-/OH^- ratio of the anode solution, and reduces the corrosion rate and loss of steel, allowing a fair evaluation of all reinforcing steels.
15. Based on critical chloride thresholds and corrosion rates, along with data from bridge deck surveys, the service lives (the times to first repair) of bridge decks containing conventional and MMFX steel are estimated to be 12 and 35 years, respectively; the service lives for bridge decks containing epoxy-coated, 2101(2)p, 2205, and 2205p steels are estimated to be more than 75 years. The analysis for epoxy-coated steel did not, however, consider the potential effect of loss of adhesion between the epoxy and the steel, which may greatly reduce the time to first repair.
16. Bridge decks containing MMFX steel do not appear to be more cost effective than decks containing epoxy-coated steel.

17. Bridge decks containing pickled 2101 steel are more cost effective than decks containing nonpickled 2205 steel, which has higher cost and lower corrosion resistance.
18. Bridge decks containing epoxy-coated steel represent the lowest cost option if the service life can reach 75 years. If the bridge deck has a service life of 50 year, at a discount rate of 4% or above, it is still the lowest cost option, while at a discount rate of 2% or below, usually used by states such as Kansas and South Dakota, the lowest cost option is bridge deck containing pickled 2101 steel.
19. Although bridge decks containing pickled 2101 steel are more cost effective than decks containing pickled 2205 steel, it is important to consider the fact that pickled 2101 steel exhibited some corrosion activity in the laboratory tests, which is not recognized in the current analysis and may represent a potential problem.

6.3 RECOMMENDATIONS

1. Bridge decks containing MMFX steel do not appear to be more cost effective than decks containing epoxy-coated steel. MMFX Microcomposite steel should not be used as a direct replacement for epoxy-coated steel.
2. Epoxy-coated steel has good corrosion resistance. The cathode area has great effect on the corrosion rate of epoxy-coated steel and it is important to use all epoxy-coated reinforcing steel on bridge decks, rather than just the top mat of steel.

3. To develop more accurate service life prediction models for epoxy-coated reinforcement, the effect of loss of adhesion between the epoxy and the steel should be included in the analysis.
4. Pickled 2101 and pickled 2205 duplex stainless steels are recommended for use in reinforced concrete bridge decks. Pickled 2205 steel can provide better corrosion protection than pickled 2101 steel.
5. To reduce the cost, it is recommended to investigate the use of pickled 2101 and 2205 steels as the top mat in conjunction with epoxy-coated steel as the bottom mat in bridge decks in the future studies.
6. In all macrocell tests, replacing the solutions helps maintain the pH, and thus, the Cl^-/OH^- ratio of the anode solution. Under any circumstances, to maintain a consistent pH throughout the test and allow for a fair evaluation of all reinforcing steels, it is recommended that the test solutions in rapid macrocell tests be replaced every five weeks.
7. Statistically, effective chloride thresholds for reinforcing steel can be determined based on chloride samples from the modified Southern Exposure and beam specimens. For steels with high chloride thresholds, such as duplex stainless steels, it is recommended that more rapid test methods be developed.

REFERENCES

AASHTO T 260-94 (1994). "Standard Test Method for Sampling and Testing for Chloride Ion in Concrete and Concrete Raw Materials," *Standard Specifications for Transportation Materials and Methods of Sampling and Testing*, 17th Edition, Part II Tests, 1995, American Association of State Highway and Transportation Officials, pp. 650-664.

AASHTO T 260-97 (1997). "Standard Test Method for Sampling and Testing for Chloride Ion in Concrete and Concrete Raw Materials," *Standard Specifications for Transportation Materials and Methods of Sampling and Testing*, 19th Edition, Part II Tests, 1998, American Association of State Highway and Transportation Officials, pp. 925-931.

ACI Committee 222 (2001). "Protection of Metals in Concrete Against Corrosion (ACI 222R-01)," *ACI Manual of Concrete Practice 2005*, American Concrete Institute, Farmington Hills, MI, Part 1.

ASTM A 276-95. "Standard Specification for Stainless Steel Bars and Shapes," *2004 Annual Book of ASTM Standards*, Vol. 03.02, American Society for Testing and Materials, West Conshohocken, PA.

ASTM A 955M-96. "Standard Specification for Deformed and Plain Stainless Steel Bars for Concrete Reinforcement," *2004 Annual Book of ASTM Standards*, Vol. 03.02, American Society for Testing and Materials, West Conshohocken, PA.

ASTM C 876-91. "Standard Test Method for Half-Cell Potentials of Uncoated Reinforcing Steel in Concrete," *2004 Annual Book of ASTM Standards*, Vol. 03.02, American Society for Testing and Materials, West Conshohocken, PA.

ASTM G 109-99a. "Standard Test Method for Determining the Effects of Chemical Admixtures on the Corrosion of Embedded Steel Reinforcement in Concrete Exposed to Chloride Environments," *2004 ASTM Annual Book of ASTM Standards*, Vol. 04.02, American Society for Testing and Materials, West Conshohocken, PA.

Alonso, C., Andrade, C., Castellote, M., and Castro, P. (2000). "Chloride Threshold Values to Depassivate Reinforcing Bars Embedded in a Standardized OPC Mortar," *Cement and Concrete Research*, Vol. 30, pp. 1047-1055.

Andrade, C., Alonso, C. with contributions from J. Gulikers, R. Polder, R. Cigna, Ø. Vennesland, M. Salta, A. Raharinaivo and B. Elsener Bayer (2004). "RILEM TC-154-EMC: 'Electrochemical Techniques for Measuring Metallic Corrosion' Recommendations: - Test Methods for On-site Corrosion Rate Measurement of Steel Reinforcement in Concrete by means of the Polarization Resistance Method," *Materials and Structures*, Vol. 37, No. 273, pp. 461-471.

Andrade, C., and Gonzales, J. A. (1978). "Quantitative Measurements of Corrosion Rate of Reinforcing Steels Embedded in Concrete Using Polarization Resistance Measurements," *Materials and Corrosion*, Vol. 29, No. 8, Aug., pp. 515-519.

Balma, J., Darwin, D., Browning, J. P., and Locke, C. E. (2002). "Evaluation of the Corrosion Resistance of Microalloyed Reinforcing Steel," *SM Report* No. 71, University of Kansas Center for Research, Inc., Lawrence, KS, 171 pp.

Balma, J., Darwin, D., Browning, J. P., and Locke, C. E. (2005). "Evaluation of Corrosion Protection Systems and Corrosion Testing Methods for Reinforcing Steel in Concrete," *SM Report* No. 76, University of Kansas Center for Research, Inc., Lawrence, KS, 517 pp.

Bamforth, P. B. (1999). "The Derivation of Input Data for Modeling Chloride Ingress from Eight-Year U.K. Coastal Exposure Trials," *Magazine of Concrete Research*, Vol. 51, No. 2, pp. 87-96.

Berke, N. B., Hicks, M. C. (1994). "Predicting Chloride Profiles in Concrete," *Corrosion*, Vol. 50, No. 3, pp. 234-239.

Bertolini, L., Elsener, B., Pedeferri, P., and Polder, R. (2004). *Corrosion of Steel in Concrete – Prevention, Diagnosis, Repair*, WILEY-VCH Verlag GmbH & Co. KGaA, Weinheim, 392 pp.

Boddy, A., Bentz, E., Thomas, M. D. A., and Hooton, R. D. (1999). "An Overview and Sensitivity Study of a Multi-Mechanistic Chloride Transport Model," *Cement and Concrete Research*, Vol. 29, pp. 827-837.

Broomfield, J. P. (1997). *Corrosion of Steel in Concrete: Understanding, Investigation, and Repair*, E & FN Spon, London, 240 pp.

Broomfield, J. P., Rodriguez, J., Ortega, L. M., and Garcia, A. M. (1993). "Corrosion Rate Measurement and Life Prediction for Reinforced Concrete Structures," *Proceedings of the Structural Faults and Repair - 93*, University of Edinburgh, Scotland, Vol. 2, pp. 155-164.

Brown, M. C., Weyers, R. E., and Via, C. E. (2003) "Corrosion Protection Service Life of Epoxy-Coated Reinforcing Steel in Virginia Bridge Decks," *Final Report* VTRC 04-CR7, Virginia Transportation Research Council, Charlottesville, Va., 63 pp.

Cady, P. D., and Gannon, E. J. (1992). "Condition Evaluation of Concrete Bridges Relative to Reinforcement Corrosion. Volume 8: Procedure Manual," *Report* No.

SHRP-S/FR-92-110, Strategic Highway Research Program, National Research Council, Washington, D. C., 124 pp.

Castellote, M., Andrade, C., and Alonso, C. (2002). "Accelerated Simultaneous Determination of the Chloride Depassivation Threshold and of the Non-Stationary Diffusion Coefficient Values," *Corrosion Science*, Vol. 44, No.11, Nov., pp. 2409-2424.

Chappelow, C. C., McElroy, A. D., Blackburn, R. R., Darwin, D., DeNoyelles, F. G. and Locke, C. E. (1992). *Handbook of Test Methods for Evaluating Chemical Deicers*, Strategic Highway Research Program, National Research Council, Washington, D. C., 312 pp.

Clear, K. C. (1989). "Measuring Rate of Corrosion of Steel in Field Concrete Structures," *Transportation Research Record* No. 1211, Transportation Research Board, Washington, D. C., pp. 28-37.

Clear, K. C. (1992) "Effectiveness of Epoxy-Coated Reinforcing Steel," *Concrete International*, Vol. 14, No. 5, May, pp. 58-64.

Clear, K. C., Hartt, W. H., McIntyre, J. and Lee, S. K. (1995) "Performance of Epoxy-Coated Reinforcing Steel in Highway Bridges," *NCHRP Report* No. 370, Transportation Research Board, Washington, D. C., 159 pp.

Clemeña, G. G. and Virmani, Y. P. (2002). "Testing of Selected Metallic Reinforcing Bars for Extending the Service Life of Future Concrete Bridges: Testing in Outdoor Concrete Blocks," *Final Report* VTRC 03-R6, Virginia Transportation Research Council, Charlottesville, Va., Dec., 24 pp.

Clemeña, G. G. (2003). "Investigation of the resistance of Several New Metallic Reinforcing Bars to Chloride-induced Corrosion in Concrete," *Interim Report* VTRC 04-R7, Virginia Transportation Research Council, Charlottesville, Va., Dec., 24 pp.

Committee on the Comparative Costs of Rock Salt and Calcium Magnesium Acetate (CMA) for Highway Deicing (1991). "Highway Deicing: Comparing Salt and Calcium Magnesium Acetate," *Transportation Research Board Special Report* 235, Transportation Research Board, National Research Council, Washington, D. C., 163 pp.

Darwin, D. (1995). "Corrosion-Resistant Reinforcing Steel," *SL Report* 95-2, University of Kansas Center for Research, Inc., Lawrence, KS, 22 pp.

Darwin, D., Locke, C. E., Balma, J. and Kahrs, J. T. (1999). "Evaluation of Stainless Steel Clad Reinforcing Bars," *SL Report* 99-3, University of Kansas Center for Research, Inc., Lawrence, KS, July, 43 pp.

Darwin, D., Browning, J. P., Nguyen, T. V., and Locke, C. E. (2002). "Mechanical and Corrosion Properties of a High-Strength, High Chromium Reinforcing Steel for Concrete," *SM Report* No. 66, University of Kansas Center for Research, Inc., Lawrence, KS, 142 pp.

Diamond, S. (1986). "Chloride Concentrations in Concrete Pore Solutions Resulting From Calcium and Sodium Chloride Admixtures," *Cement, Concrete, and Aggregates*, Vol. 8, No. 2, pp. 97-102.

Elsener, B. with contributions from Andrade, C., Gulikers, J., Polder, R. and Raupach, M. (2003). "RILEM TC-154-EMC: 'Electrochemical Techniques for Measuring Metallic Corrosion' Recommendations: Half-cell Potential Measurements - Potential Mapping on Reinforcing Concrete Structures," *Materials and Structures*, Vol. 36, No. 261, pp. 461-471.

Escalante, E., Cohen, M., and Kahn, A. H. (1984). "Measuring the Corrosion Rate of Reinforcing Steel in Concrete," *Report* No. NBSIR-84-2853, National Bureau of Standards, Washington, D. C., 50 pp.

Fils, J., Sehgal, A., Li, D., Kho, Y-T., Sabol, S., Pickering, H., Osseo-Asare, K., and Cady, P. D. (1992). "Condition Evaluation of Concrete Bridges Relative to Reinforcement Corrosion. Volume 2: Method for Measuring Corrosion Rate of Reinforcing Steel," *Report* No. SHRP-S/FR-92-104, Strategic Highway Research Program, National Research Council, Washington, D. C., 105 pp.

Freemantle, M. (2002). "Stainless Steel Failure Explained," *Chemical & Engineering News*, February 18, pp. 11.

Ge, B., Darwin, D., Locke, C. E., and Browning, J. P. (2004). "Evaluation of Corrosion Protection Systems And Testing Methods for Conventional Reinforcing Steel," *SM Report* No. 73, University of Kansas Center for Research, Inc, Lawrence, KS, 213 pp.

Glass, G. K. and Buenfeld, N. R. (1997). "The Presentation of the Chloride Threshold Level for Corrosion of Steel in Concrete," *Corrosion Science*, Vol. 39, No. 5, pp. 1001-1013.

Gong, L., Darwin, D., Browning, J. P., and Locke, C. E. (2002). "Evaluation of Mechanical and Corrosion Properties of MMFX Reinforcing Steel in Concrete," *SM Report* No. 70, University of Kansas Center for Research, Inc, Lawrence, KS, 112 pp.

Gong, L. (2006). “Multiple Corrosion Protection Systems for Reinforced Concrete Bridge Components,” Dissertation in progress, University of Kansas, Lawrence, KS.

Goni, S. and Andrade, C. (1990). “Synthetic Concrete Pore Solution Chemistry and Rebar Corrosion Rate in the Presence of Chlorides,” *Cement and Concrete Research*, Vol. 20, No. 4, Apr., pp. 525-539.

Gouda, V. K. (1970). “Corrosion and Corrosion inhibition of Reinforcing Steel, I. Immersed in Alkaline Solutions,” *British Corrosion Journal*, Vol. 5, Sept., pp. 198-203.

Hartt, W. H., Powers, R. G., Leroux, V., and Lysogorski, D. K (2004). “A Critical Literature Review of High-Performance Corrosion Reinforcement in Concrete Bridge Applications,” *Report* No. FHWA-HRT-04-093, Federal Highway Administration, McLean, VA, 773 pp.

Hansson, C. M. and Sorensen, B. (1990) “The Threshold Concentration of Chloride in Concrete for the Initiation of Reinforcement Corrosion,” *Corrosion Rates of Steel in Concrete*, ASTM STP 1065, N. S. Berke, V. Chaker, and D. Whiting, eds., American Society for Testing and Materials, West Conshohocken, PA, pp. 3-16.

Hausmann, D. A. (1967). “Steel Corrosion in Concrete,” *Materials Protection*, Vol. 6, Nov., pp. 19-23.

Hope, B. B. and Ip, A. K. C. (1986). “Chloride Corrosion Threshold in Concrete,” *ACI Materials Journal*, Vol. 84, No. 4, July-Aug., pp. 306-314.

Hussain, S. E., Al-Gahtani, A. S., and Rasheeduzzafar (1996). “Chloride Threshold for Corrosion of Reinforcement in Concrete,” *ACI Materials Journal*, Vol. 94, No. 6, Nov.-Dec., pp. 534-538.

Jones, D. A. (1996). *Principles and Prevention of Corrosion*, Macmillan Publishing Company, New York, NY, 572 pp.

Kahrs, J., Darwin, D., and Locke, C. E. (2001). “Evaluation of Corrosion Resistance of Type 304 Stainless Steel Clad Reinforcing Bars,” *SM Report* No. 65, University of Kansas Center for Research, Inc., Lawrence, KS, 76 pp.

Kenneth C. Clear Inc. (1992). “Part I, ‘Effectiveness of Epoxy Coated Reinforcing Steel,’” and Wiss, Janney, Elstner Associates. Inc., “Part II, ‘A Review of Report Effectiveness of Epoxy-Coated Reinforcing Steel and Proposed Investigation of Testes Specimens from this CRSI-Sponsored Study at Kenneth C. Clear Inc. for

CRSI,'" *CRSI Performance Research: Epoxy Coated Reinforcing Steel, Interim Report*, Concrete Reinforcing Steel Institute, Schaumburg, IL, 108 pp.

Kepler, J., Darwin, D., Locke, C. E. (2000). "Evaluation of Corrosion Protection Methods for Reinforced Concrete Highway Structures," *SM Report* No. 58, University of Kansas Center for Research, Inc., Lawrence, KS, 219 pp.

Khan, M. S. (1997) "Chloride Ion Analysis by AASHTO Method," *Concrete International*, Vol. 19, No. 10, Oct., pp. 67-69.

Koch, G. H., Broongers, M. P. H., Thompson, N. G., Virmani, Y. P., and Payer, J. H. (2001). "Corrosion Cost and Preventive Strategies in the United States," *Report* No. FHWA-RD-01-156, Federal Highway Administration, McLean, VA, 773 pp.

Lambert, P. P., Page, C. L. and Vassie, P. R. W. (1991). "Investigation of Reinforcement Corrosion 2. Electrochemical Monitoring of Steel in Chloride Contaminated Concrete," *Materials and Structures*, Vol. 24, No. 143, pp. 351-358.

Lee, S-K. and Krauss, P. D. (2004). "Long-Term Performance of Epoxy-Coated Reinforcing Steel in Heavy Salt-Contaminated Concrete," *Report* No. FHWA-HRT-04-090, Federal Highway Administration, McLean, VA, 132 pp.

Lindquist, W. D., Darwin, D., Browning, J. P. (2005). "Cracking and Chloride Contents in Reinforced Concrete Bridge Decks," *SM Report* No. 78, University of Kansas Center for Research, Inc., Lawrence, KS, 453 pp.

Liu, Y. and Weyers, R. E. (1998) "Modeling the Time-to-Corrosion Cracking in Chloride Contaminated Reinforcing Concrete Structures," *ACI Materials Journal*, Vol. 95, No. 6, Nov.-Dec., pp. 675-681.

Lorentz, T. E., French, C. W., and Leon, R. T. (1992). "Corrosion of Coated and Uncoated Reinforcing Steel in Concrete," *Structural Engineering Report* No. 92-03, University of Minnesota Center of Transportation Studies, 204 pp.

Manning, D. G. (1996). "Corrosion Performance of Epoxy-Coated Reinforcing Steel: North American Experience," *Construction and Building Materials*, Vol. 10, No.5, July, pp. 349-365.

Mangat, P. S. and Molloy, B. T. (1994). "Prediction of Long Term Chloride Concentration in Concrete," *Materials and Structures*, Vol. 27, pp. 338-346.

Martinez, S. L., Darwin, D., McCabe, S. L., and Locke, Carl E., Jr. (1990). "Rapid Test for Corrosion Effects of Deicing Chemicals in Reinforced Concrete," *SL Report* 90-4, University of Kansas Center for Research, Inc., Lawrence, KS, 61 pp.

McDonald, D. B., Pfeifer, D. W., and Blake, G. T. (1996). "The Corrosion Performance of Inorganic-, Ceramic-, and Metallic-Clad Reinforcing Bars and Solid Metallic Reinforcing Bars in Accelerated Screening Tests," *Report* No. FHWA-RD-96-085, Federal Highway Administration, Washington, D. C., 112 pp.

McDonald, D. B., Pfeifer, D. W., and Sherman, M. R. (1998). "Corrosion Evaluation of Epoxy-Coated, Metallic-Clad and Solid Metallic Reinforcing Bars in Concrete," *Publication* No. FHWA-RD-98-153, Federal Highway Administration, McLean, VA, 137 pp.

MMFX Steel Corporation of America (2002). *Product Bulletin*, February, Charlotte, NC.

Miller, G. and Darwin, D. (2000). "Performance and Constructability of Silica Fume Bridge Deck Overlays," *SM Report* No. 57, University of Kansas Center for Research, Inc., Lawrence, KS, 423 pp.

Mindess, S., Young, J. F., and Darwin, D. (2003). *Concrete*, Pearson Education, Inc. NJ. 644 pp.

Nurnberger, U. (1996). "Stainless Steel in Concrete - State of the Art Report," *European Federation of Corrosion Publications* No. 18, the Institute of Materials, London, 30 pp.

Oh, B. H., Jang, S. Y., and Shin, Y. S. (2003). "Experimental Investigation of the Threshold Chloride Concentration for Corrosion Initiation in Reinforced Concrete Structures," *Magazine of Concrete Research*, Vol. 55, No. 2, pp. 117-124.

Peterson, J. E., Sohanghpurwala, A. A., Scannell, W. T., Islam, M., Weyers, R. E., Via, C. E., and Khan, M. S. (1998) "Letters - Chloride Ion Analysis," *Concrete International*, Vol. 20, No. 6, June, pp. 7-11.

Pfeifer, D. W. (2000). "High Performance Concrete and Reinforcing Steel with a 100-Year Service Life," *PCI Journal*, Vol. 45, No. 3, May-June, pp. 46-54.

Pfeifer, D. W., Landgren, R. J., and Zoob, A. (1987). "Protective Systems for New Prestressed and Substructure Concrete," *Report* No. FHWA/RD-86/193, Federal Highway Administration, McLean, VA, Apr., 133 pp.

Pfeifer, D. W. and Scali, M. J. (1981). "Concrete Sealers for Protection of Bridge Structures," *National Cooperative Highway Research Board Program Report* 244, Transportation Research Board, National Research Council, Washington, D.C., 138 pp.

Pyc, W. A., Weyers, R. E., Weyers, R. M., Mokarem, D. W., Zemajtis, J., Sprinkel, M. M., and Dillard, J. G. (2000). "Field Performance of Epoxy-Coated Reinforcing Steel in Virginia Bridge Decks," *Final Report* VTRC 00-R16, Virginia Transportation Research Council, Charlottesville, VA, 38 pp.

Salt Institute website (2005). – http://www.saltinstitute.org.

Sagues, A. A., Powers, R. G., and Zayed, A. (1990). "Marine Environment Corrosion of Epoxy-Coated Reinforcing Steel," *Corrosion of Reinforcement in Concrete*, C. Page, K. Treadaway, and P. Bamforth, Editors, Elsevier Applied Science, London-New York, pp. 539-549.

Sagues, A. A., Powers, R. G., and Kessler, R. (1994). "Corrosion Processes and Field Performance of Epoxy-Coated Reinforcing Steel in Marine Structures," *Corrosion 94*, Paper No. 299, National Association of Corrosion Engineers, Houstion, TX, 15 pp.

Schmitt, T. R. and Darwin, D. (1995). "Cracking in Concrete Bridge Decks," *SM Report* No. 39, University of Kansas Center for Research, Inc., Lawrence, KS, 151 pp.

Schwensen, S. M., Darwin, D., and Locke, C. E. (1995). "Rapid Evaluation of Corrosion-Resistant Concrete Reinforcing Steel in the Presence of Deicers," *SL Report* 95-6, University of Kansas Center for Research, Inc., Lawrence, KS, 90 pp.

Sedriks, A. J. (1996). Corrosion of Stainless Steels, Second Edition, John Wiley & Sons. Inc., NY, 437 pp.

Senecal, M. R., Darwin, D., and Locke, C. E. (1995). "Evaluation of Corrosion-Resistant Steel Reinforcing Bars," *SM Report* No. 40, University of Kansas Center for Research, Inc., Lawrence, KS, 142 pp.

Sherman, M. R., McDonald, D. B., and Pfeifer, D. W. (1996). "Durability Aspects of Precast Prestressed Concrete – Part 2: Chloride Permeability Study," *PCI Journal*, Vol. 41, No. 4, July –Aug., pp. 75-95.

Smith, F. N. and Tullman, M. (1999). "Using Stainless Steel as Long-Lasting Rebar Material," *Materials Performance*, Vol. 38, No. 5, pp. 72-76.

Smith, J. L., Darwin, D., and Locke, C. E. (1995). "Corrosion-Resistant Steel Reinforcing Bars Initial Tests," *SL Report* 95-1, University of Kansas Center for Research, Inc., Lawrence, KS, 43 pp.

Smith, J. L. and Virmani, Y. P. (1996). "Performance of Epoxy Coated Rebars in Bridge Decks." *Report* No. FHWA-RD-96-092, Federal Highway Administration, Washington, D. C., 100 pp.

Smith, J. L. and Virmani, Y. P. (2000). "Materials and Methods for Corrosion Control of Reinforced and Prestressed Concrete Structures in New Construction." *Report* No. FHWA-RD-00-081, Federal Highway Administration, Washington, D. C., 82 pp.

Taylor, P. C., Nagi, M. A. and Whiting, D. A. (1999). "A Literature Review of the Threshold Chloride Content Needed to Promote Steel Corrosion in Concrete," *PCA R&D Serial* No. 2169, Portland Cement Association, Skokie, IL, 32 pp.

Thomas, M. (1996). "Chloride Threshold in Marine Concrete," *Cement and Concrete Research*, Vol. 26. No. 4, pp. 513-519.

Thomas, M. (2002). "Determining the Corrosion Resistance of Steel Reinforcement for Concrete," the website of MMFX Steel Corporation of America.

Thomas, M. D. A. and Bamforth, P. B. (1999). "Modeling Chloride Diffusion in Concrete: Effect of Fly Ash and Slag," *Cement and Concrete Research*, Vol. 29, pp. 487-495.

Torres-Acosta, A. A. and Sagues, A. A. (2004). "Concrete Cracking by Localized Steel Corrosion – Geometric Effects," *ACI Materials Journal*, Vol. 101, No. 6, Nov.-Dec., pp. 501-507.

Trejo, D. (2002). "Evaluation of the Critical Chloride Threshold and Corrosion Rate for Different Steel Reinforcement Types," *Interim Report*, Texas Engineering Experimental Station, July, 38 pp.

Trejo, D., Monteiro, P. J. M., Gerwick, B. and Thomas, G. (2000). "Microstructural Design of Concrete Reinforcing Bars for Improved Corrosion Performance," *ACI Materials Journal*, Vol. 97, No. 1, Jan.-Feb., pp. 78-83.

Trejo, D., Monteiro, P. J. M., Thomas, G., and Wang, X. (1994). "Mechanical Properties and Corrosion Susceptibility of Dual Phase Steel in Concrete," *Cement and Concrete Research*, Vol. 24, No. 7, pp. 1245-1254.

Trejo, D. and Pillai, R. G. (2003). "Accelerated Chloride Threshold Testing: Part I – ASTM A 615 and A 706 Reinforcement," *ACI Materials Journal*, Vol. 100, No. 6, Nov.-Dec., pp. 519-527.

Trejo, D. and Pillai, R. G. (2004). “Accelerated Chloride Threshold Testing: Part II – Corrosion-Resistant Reinforcement,” *ACI Materials Journal*, Vol. 101, No. 1, Jan.-Feb., pp. 57-64.

Uji, K., Matsuoka, Y., and Maruya, T. (1990). “Formulation of an Equation for Surface Chloride Content of Concrete due to Permeation of Chloride”, *Corrosion of Reinforcement in Concrete*, Page, C. L., Treadaway, K. W. J., and Bamforth, P. B., eds, Elsevier Applied Science, New York, pp. 258-267.

Virmani, Y. P. (1990). "Effectiveness of Calcium Nitrite Admixture as a Corrosion Inhibitor," *Public Roads*, Vol. 54, No. 1, pp. 171-182.

Virmani Y. P. and Clemena G. G. (1998). “Corrosion Protection – Concrete Bridges,” *Report* No. FHWA-RD-98-088, Federal Highway Administration, McLean, VA, April, 133 pp.

Walpole, Ronald E. and Myers, Raymond H. (1993) “Probability and Statistics for Engineers and Scientists,” Prentice-Hall, Inc., Englewood Cliffs, New Jersey, 766 pp.

Weyers, R. E., Pyc, W., Zemajtis, J., Liu, Y., Mokarem, D., and Sprinkel, M. M. (1997). “Field Investigation of Corrosion-Protection Performance of Bridge Decks Constructed With Epoxy-Coated Reinforcing Steel in Virginia,” *Transportation Research Record*, No. 1597, pp. 82-90.

Weyers, R. E. (1998) “Service life model for concrete structures in chloride laden environment”, *ACI Materials Journal*, Vol. 95, No. 4, July-Aug., pp. 445-453.

Weyers, R. E., Fitch, M. G., Larsen, E. P., Al-Quadi, I. L., Chamberlin, W. P., and Hoffman, P. C. (1994). “Concrete Bridge Protection and Rehabilitation: Chemical Physical Techniques, Service Life Estimates,” *Report* No. SHRP-S-668, Strategic Highway Research Program, National Research Council, Washington, D.C., 357 pp.

APPENDIX A

CORROSION RATES, TOTAL CORROSION LOSSES, AND CORROSION POTENTIALS FOR INDIVIDUAL SPECIMENS

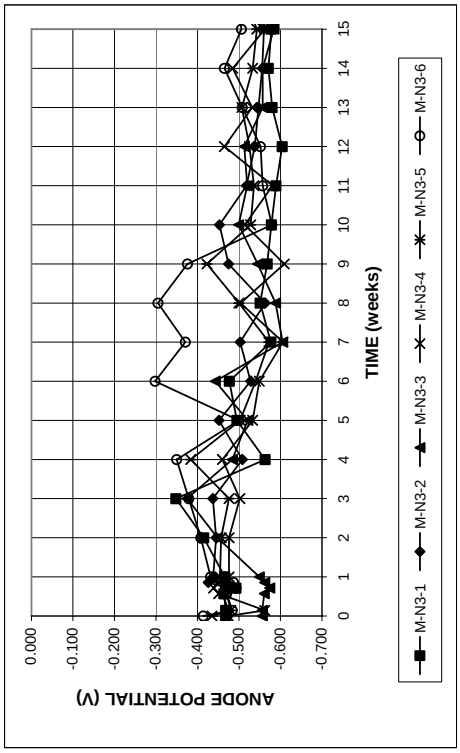

Figure A.3a - Macrocell test. Anode corrosion potentials with respect to saturated calomel electrode for bare conventional N3 steel in simulated concrete pore solution with 1.6 molal ion NaCl.

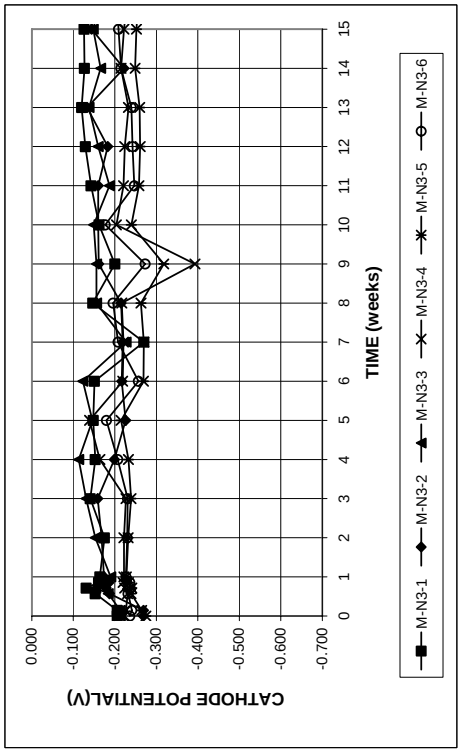

Figure A.3b - Macrocell test. Cathode corrosion potentials with respect to saturated calomel electrode for bare conventional N3 steel in simulated concrete pore solution with 1.6 molal ion NaCl.

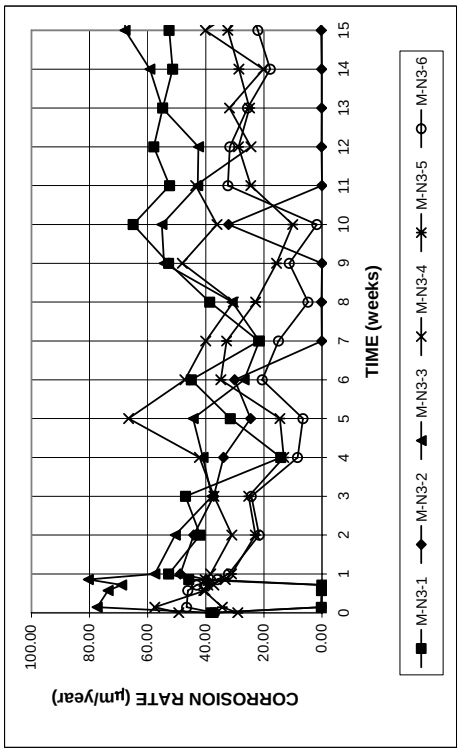

Figure A.1 - Macrocell test. Corrosion rates for bare conventional N3 steel in simulated concrete pore solution with 1.6 molal ion NaCl.

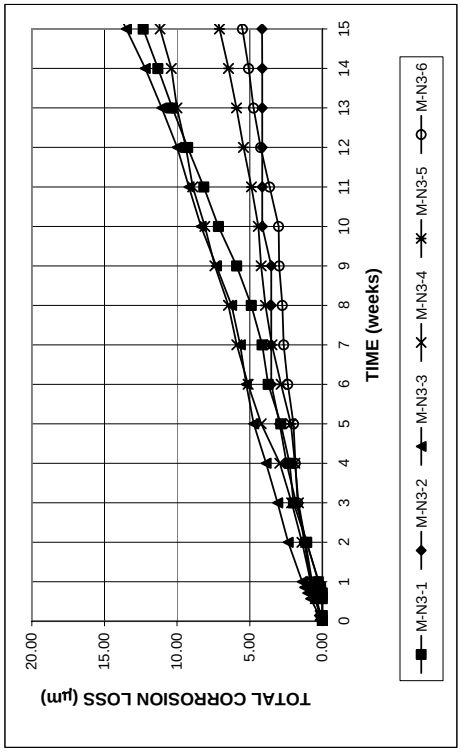

Figure A.2 - Macrocell test. Total corrosion losses for bare conventional N3 steel in simulated concrete pore solution with 1.6 molal ion NaCl.

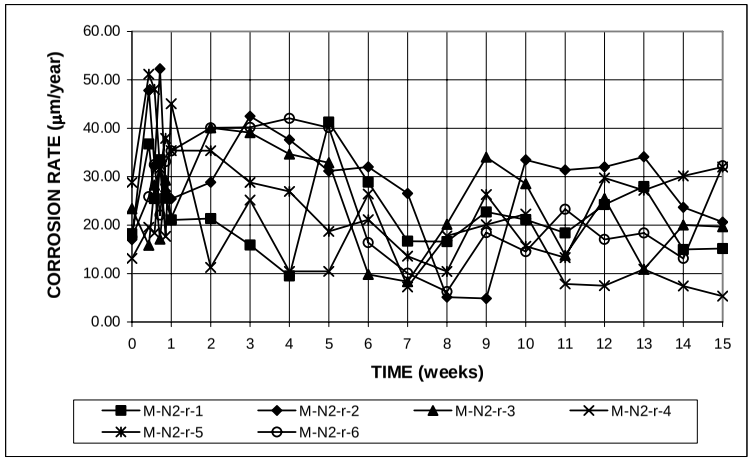

Figure A.4 - Macrocell test. Corrosion rates for bare conventional N2 steel in simulated concrete pore solution with 1.6 molal ion NaCl. Solutlions are replaced every 5 weeks.

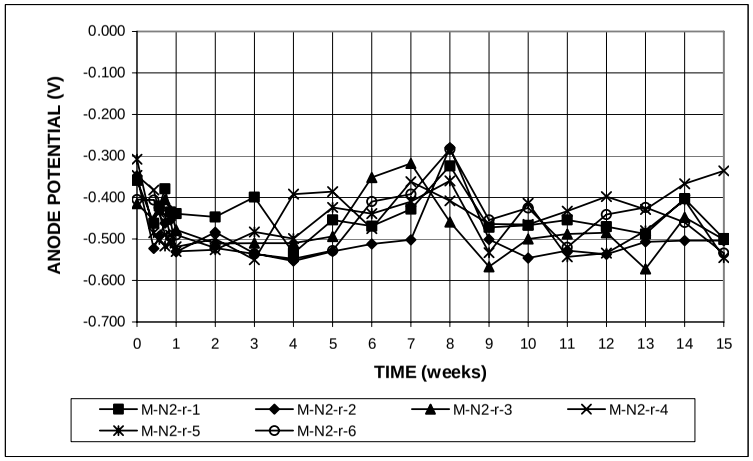

Figure A.6a - Macrocell test. Anode corrosion potentials with respect to saturated calomel electrode for bare conventional N2 steel in simulated concrete pore solution with 1.6 molal ion NaCl. Solutions are replaced every 5 weeks.

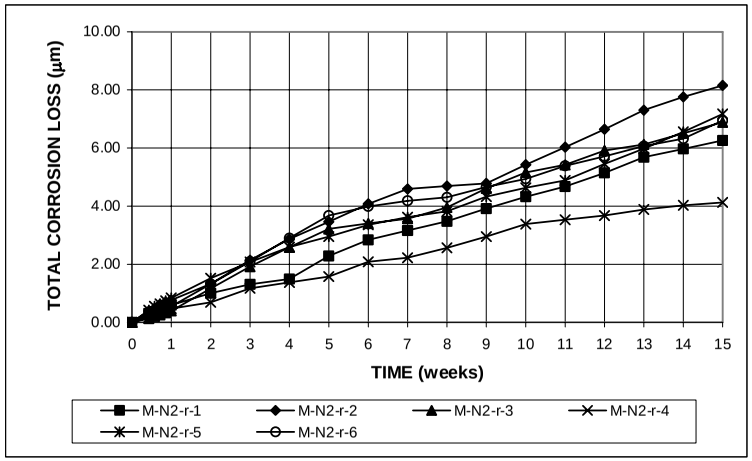

Figure A.5 - Macrocell test. Total corrosion losses for bare conventional N2 steel in simulated concrete pore solution with 1.6 molal ion NaCl. Solutions are replaced every 5 weeks.

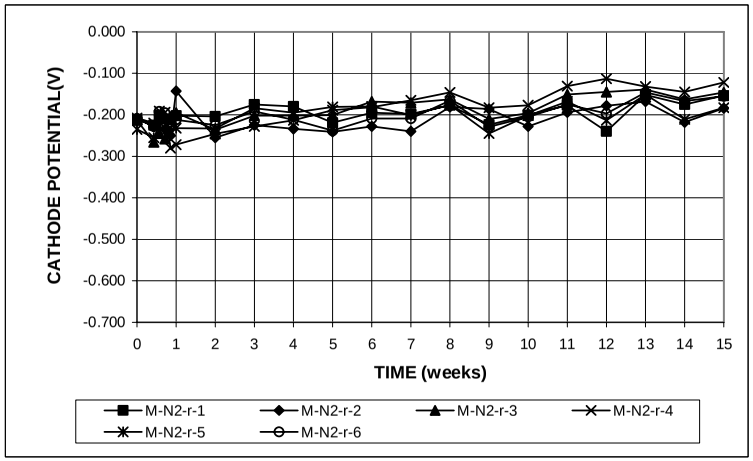

Figure A.6b - Macrocell test. Cathode corrosion potentials with respect to saturated calomel electrode for bare conventional N2 steel in simulated concrete pore solution with 1.6 molal ion NaCl. Solutions are replaced every 5 weeks.

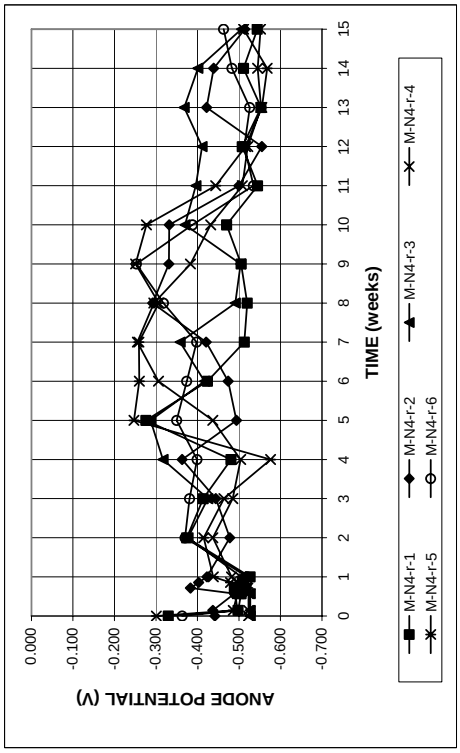

Figure A.9a - Macrocell test. Anode corrosion potentials with respect to saturated calomel electrode for bare conventional N4 steel in simulated concrete pore solution with 1.6 molal ion NaCl. Solutions are replaced every 5 weeks.

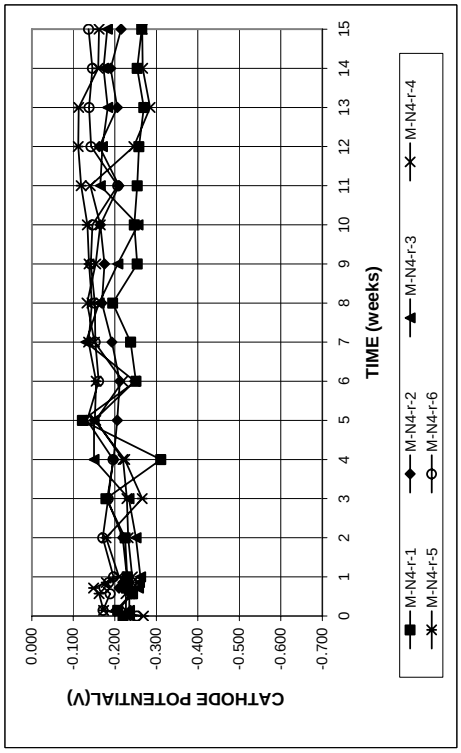

Figure A.9b - Macrocell test. Cathode corrosion potentials with respect to saturated calomel electrode for bare conventional N4 steel in simulated concrete pore solution with 1.6 molal ion NaCl. Solutions are replaced every 5 weeks.

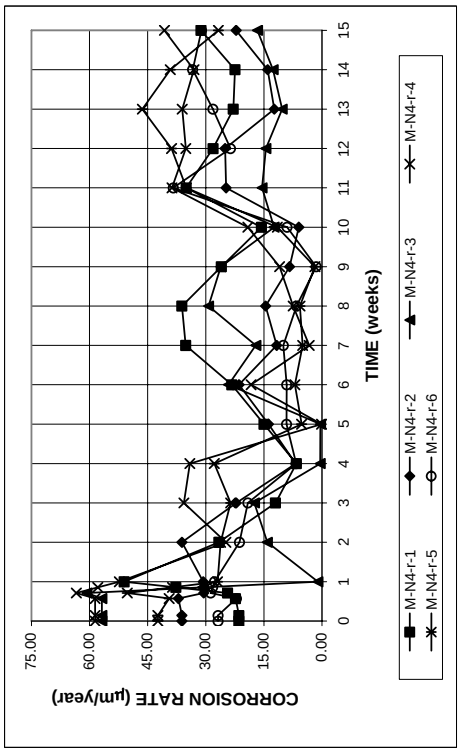

Figure A.7 - Macrocell test. Corrosion rates for bare conventional N4 steel in simulated concrete pore solution with 1.6 molal ion NaCl. Solutions are replaced every 5 weeks.

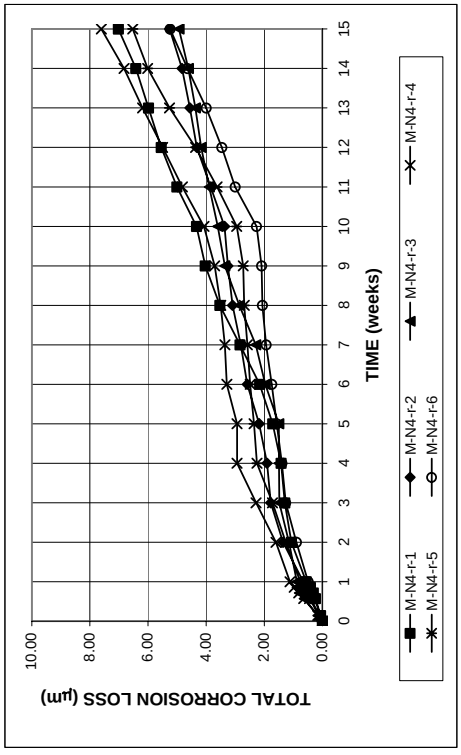

Figure A.8 - Macrocell test. Total corrosion losses for bare conventional N4 steel in simulated concrete pore solution with 1.6 molal ion NaCl. Solutions are replaced every 5 weeks.

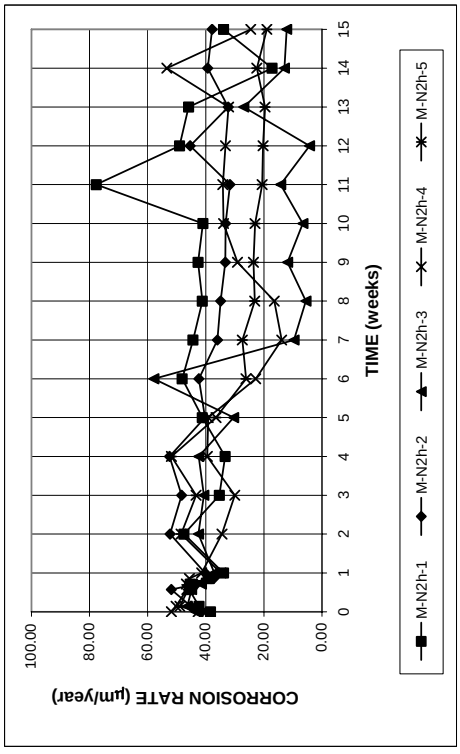

Figure A.10 - Macrocell test. Corrosion rates for bare conventional N2 steel in simulated concrete pore solution with 6.04 molal ion NaCl.

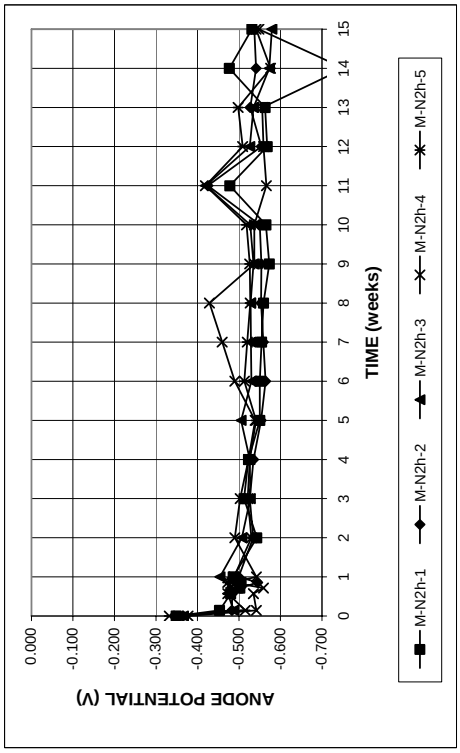

Figure A.12a - Macrocell test. Anode corrosion potentials with respect to saturated calomel electrode for bare conventional N2 steel in simulated concrete pore solution with 6.04 molal ion NaCl.

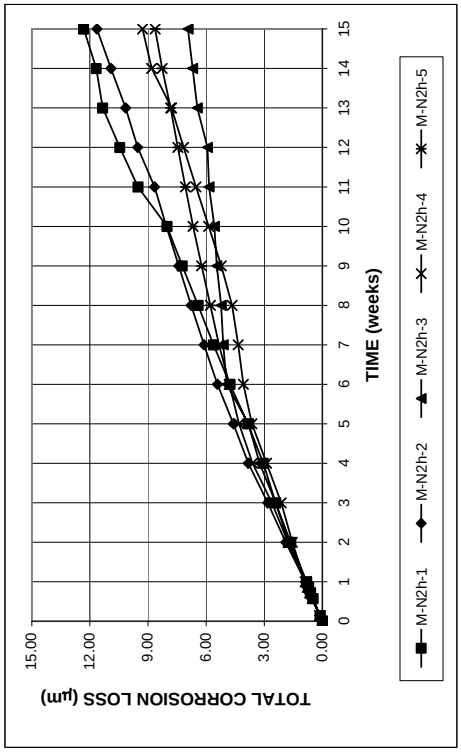

Figure A.11 - Macrocell test. Total corrosion losses for bare conventional N2 steel in simulated concrete pore solution with 6.04 molal ion NaCl.

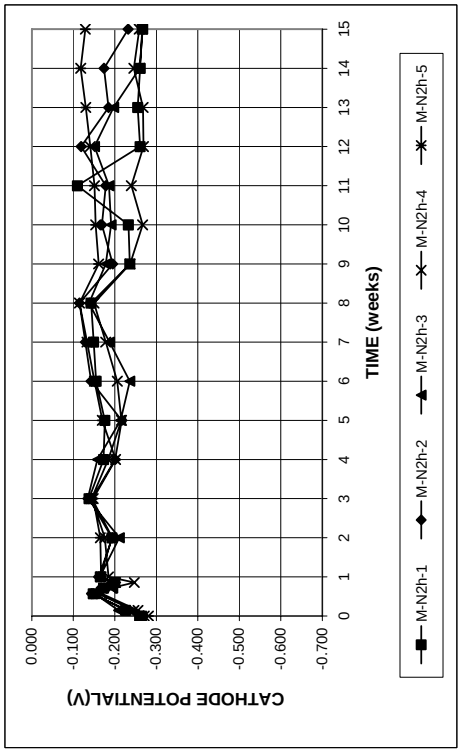

Figure A.12b - Macrocell test. Cathode corrosion potentials with respect to saturated calomel electrode for bare conventional N2 steel in simulated concrete pore solution with 6.04 molal ion NaCl.

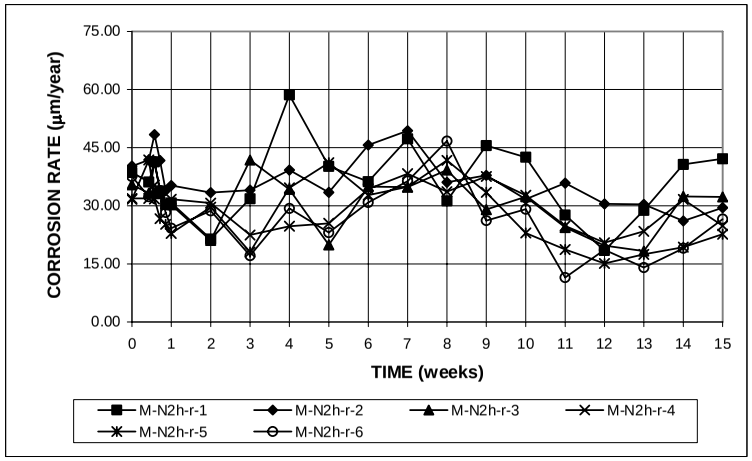

Figure A.13 - Macrocell test. Corrosion rates for bare conventional N2 steel in simulated concrete pore solution with 6.04 molal ion NaCl. Solutlions are replaced every 5 weeks.

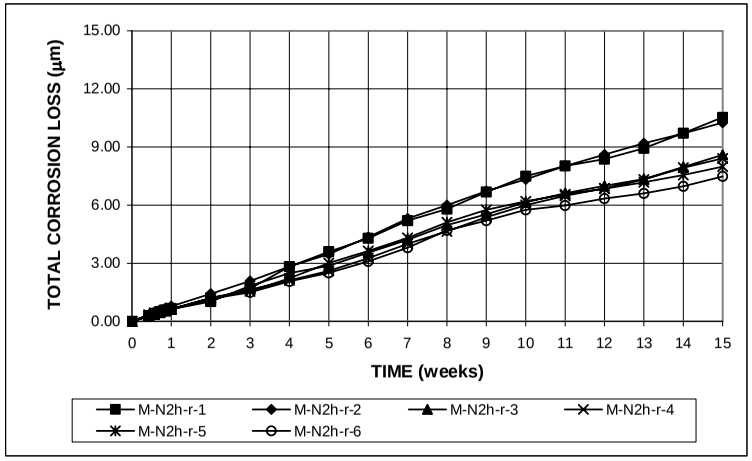

Figure A.14 - Macrocell test. Total corrosion losses for bare conventional N2 steel in simulated concrete pore solution with 6.04 molal ion NaCl. Solutions are replaced every 5 weeks.

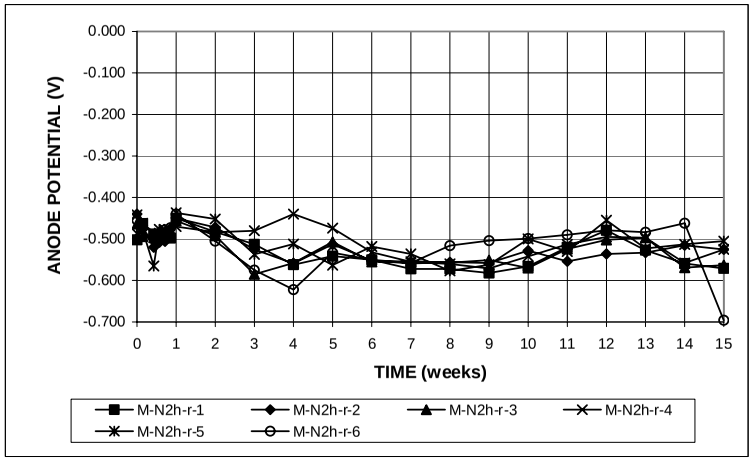

Figure A.15a - Macrocell test. Anode corrosion potentials with respect to saturated calomel electrode for bare conventional N2 steel in simulated concrete pore solution with 6.04 molal ion NaCl. Solutions are replaced every 5 weeks.

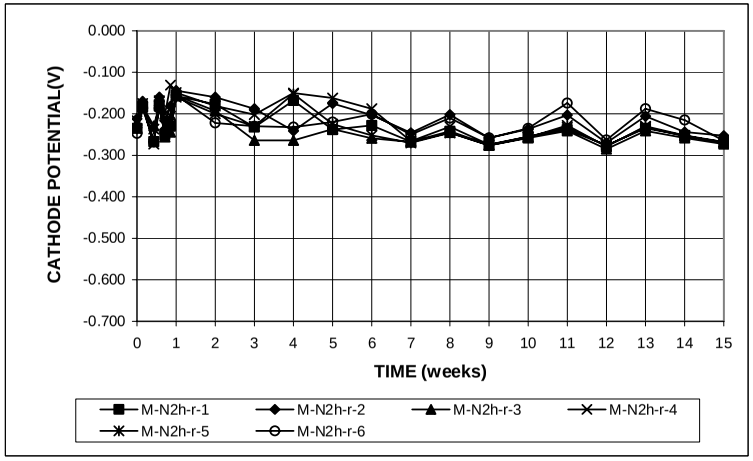

Figure A.15b - Macrocell test. Cathode corrosion potentials with respect to saturated calomel electrode for bare conventional N2 steel in simulated concrete pore solution with 6.04 molal ion NaCl. Solutions are replaced every 5 weeks.

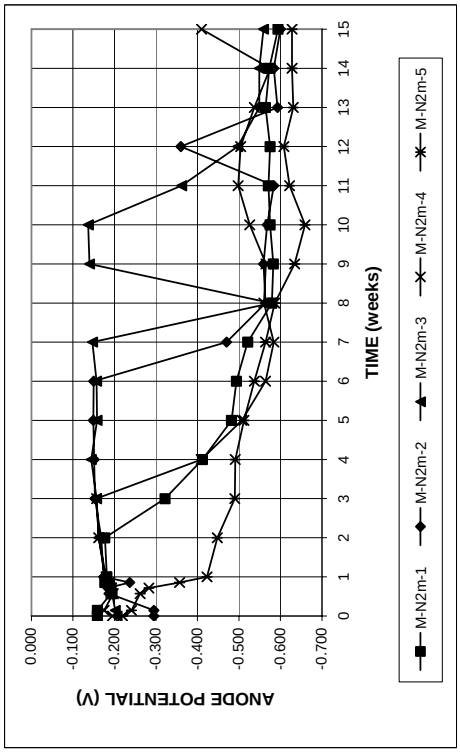

Figure A.18a - Macrocell test. Anode corrosion potentials with respect to saturated calomel electrode for mortar-wrapped conventional N2 steel in simulated concrete pore solution with 1.6 molal ion NaCl.

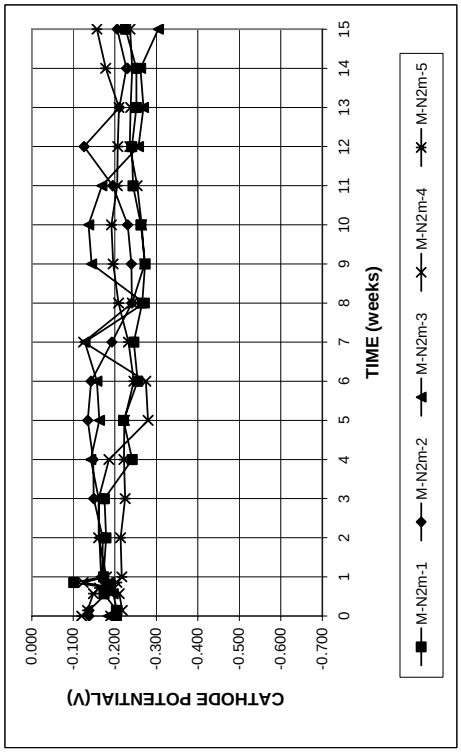

Figure A.18b - Macrocell test. Cathode corrosion potentials with respect to saturated calomel electrode for mortar-wrapped conventional N2 steel in simulated concrete pore solution with 1.6 molal ion NaCl.

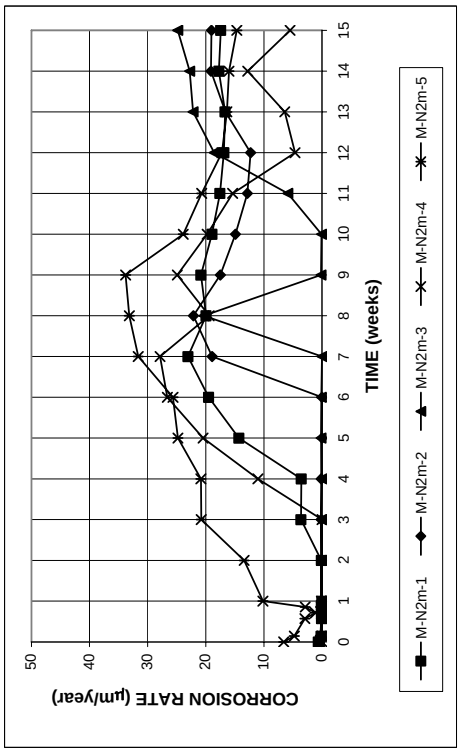

Figure A.16 - Macrocell test. Corrosion rates for mortar-wrapped conventional N2 steel in simulated concrete pore solution with 1.6 molal ion NaCl.

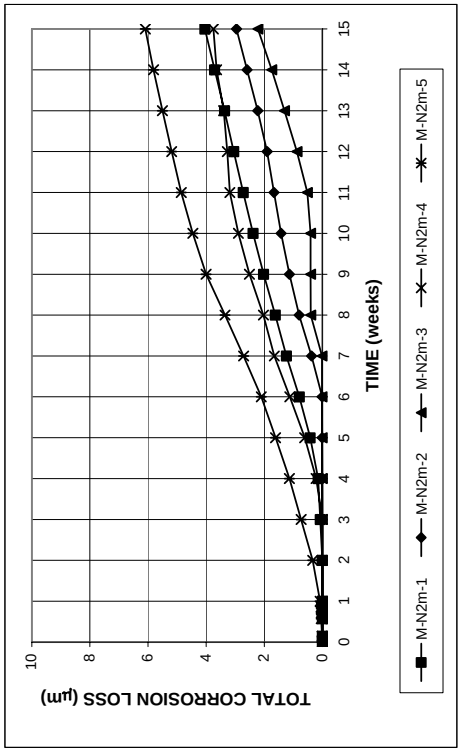

Figure A.17 - Macrocell test. Total corrosion losses for mortar-wrapped conventional N2 steel in simulated concrete pore solution with 1.6 molal ion NaCl.

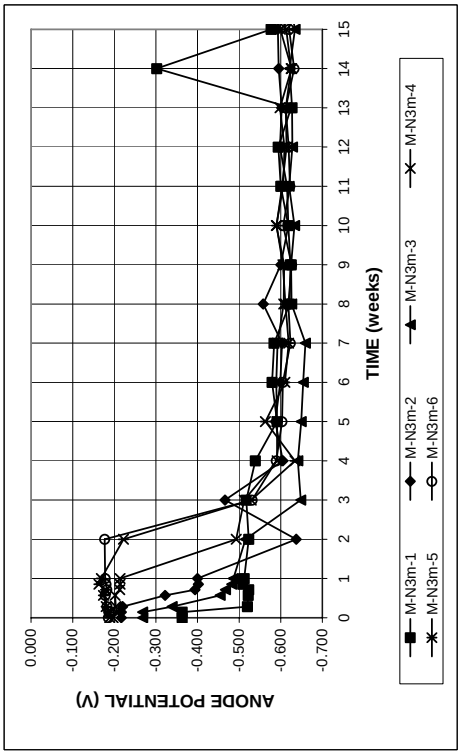

Figure A.21a - Macrocell test. Anode corrosion potentials with respect to saturated calomel electrode for mortar-wrapped conventional N3 steel in simulated concrete pore solution with 1.6 molal ion NaCl.

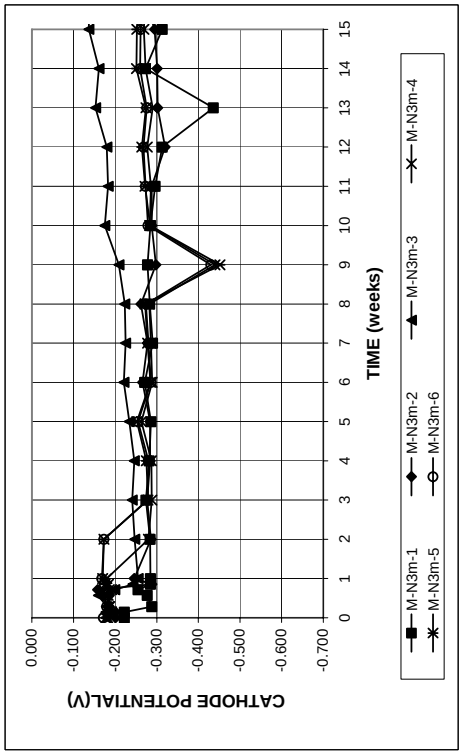

Figure A.21b - Macrocell test. Cathode corrosion potentials with respect to saturated calomel electrode for mortar-wrapped conventional N3 steel in simulated concrete pore solution with 1.6 molal ion NaCl.

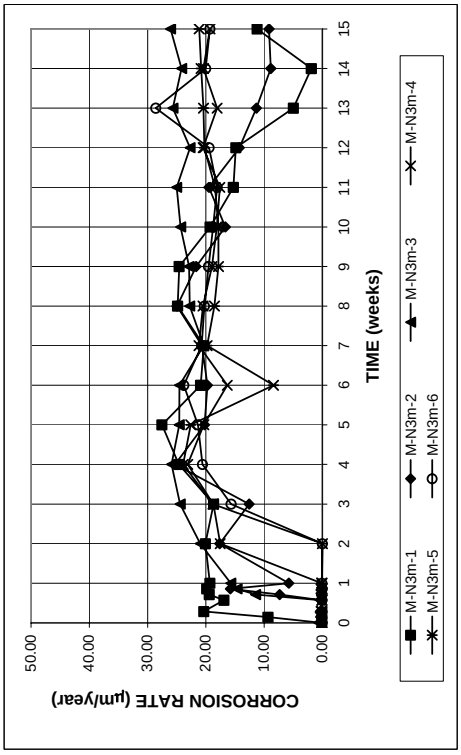

Figure A.19 - Macrocell test. Corrosion rates for mortar-wrapped conventional N3 steel in simulated concrete pore solution with 1.6 molal ion NaCl.

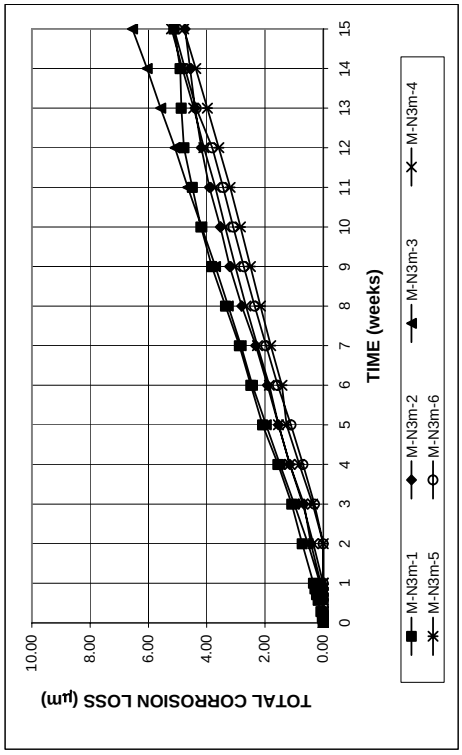

Figure A.20 - Macrocell test. Total corrosion losses for mortar-wrapped conventional N3 steel in simulated concrete pore solution with 1.6 molal ion NaCl.

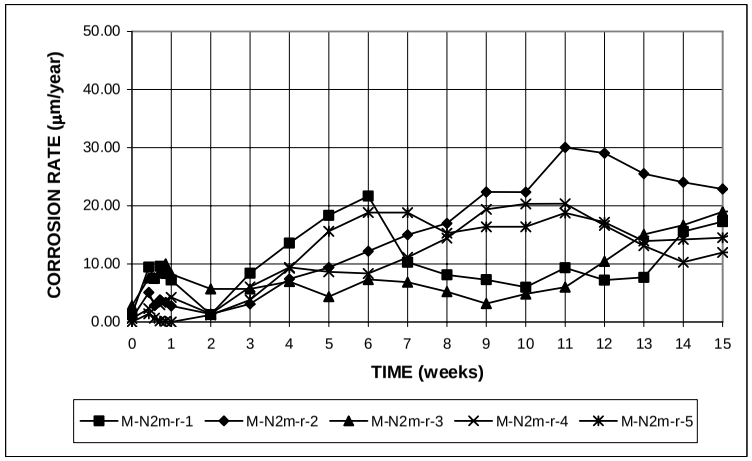

Figure A.22 - Macrocell test. Corrosion rates for mortar-wrapped conventional N2 steel in simulated concrete pore solution with 1.6 molal ion NaCl. Solutions are replace every 5 weeks.

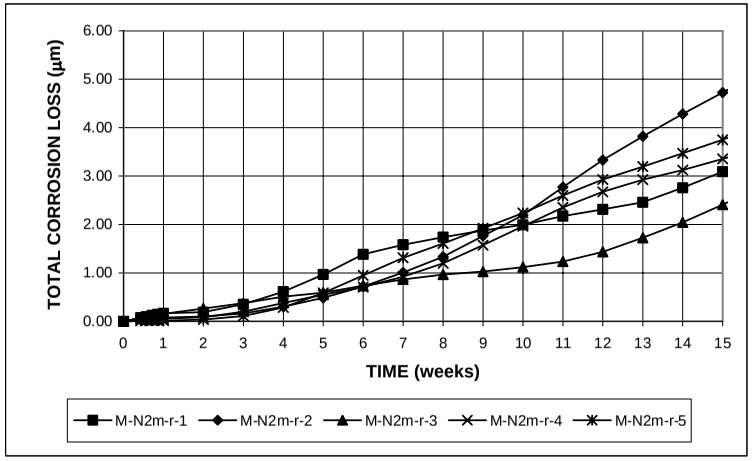

Figure A.23 - Macrocell test. Total corrosion losses for mortar-wrapped conventional N2 steel in simulated concrete pore solution with 1.6 molal ion NaCl. Solutions are replaced every 5 weeks.

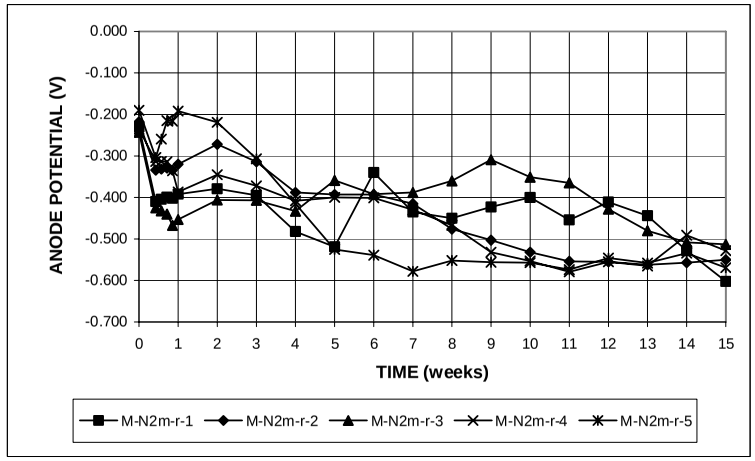

Figure A.24a - Macrocell test. Anode corrosion potentials with respect to saturated calomel electrode for mortar-wrapped conventional N2 steel in simulated concrete pore solution with 1.6 molal ion NaCl. Solutions are replaced every 5 weeks.

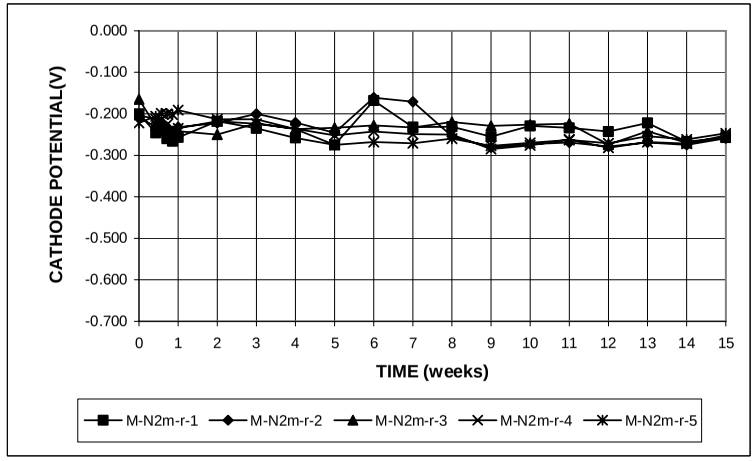

Figure A.24b - Macrocell test. Cathode corrosion potentials with respect to saturated calomel electrode for mortar-wrapped conventional N2 steel in simulated concrete pore solution with 1.6 molal ion NaCl. Solutions are replaced every 5 weeks.

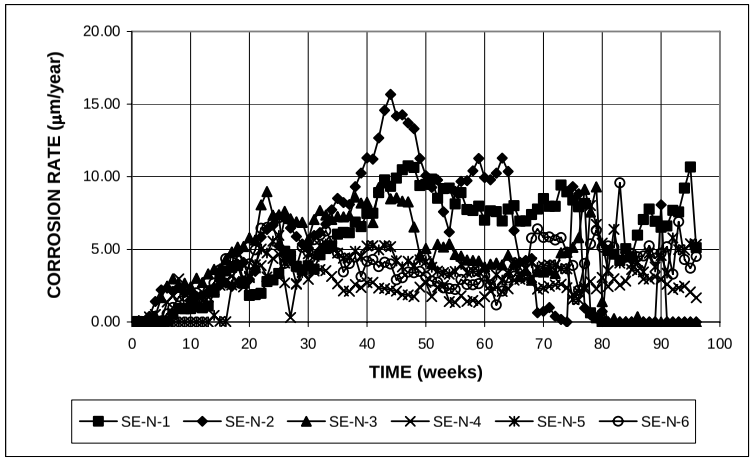

Figure A.25 - Southern Exposure test. Corrosion rates for conventional N steel, specimens w/c = 0.45, ponded with 15% NaCl solution.

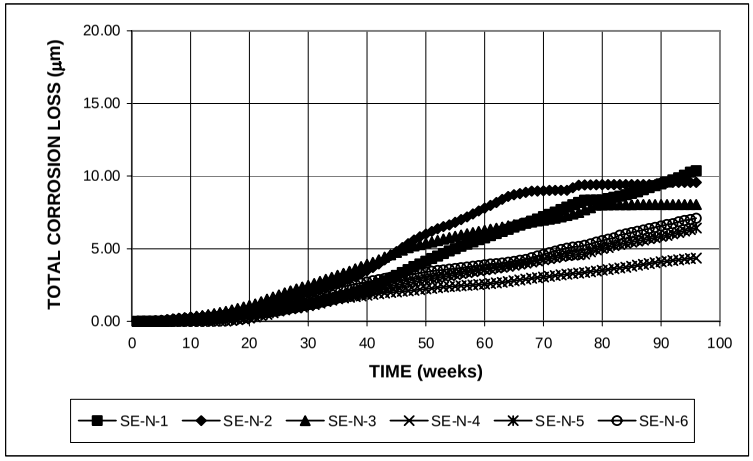

Figure A.26 - Southern Exposure test. Total corrosion losses of conventional N steel, specimens w/c = 0.45, ponded with 15% NaCl solution.

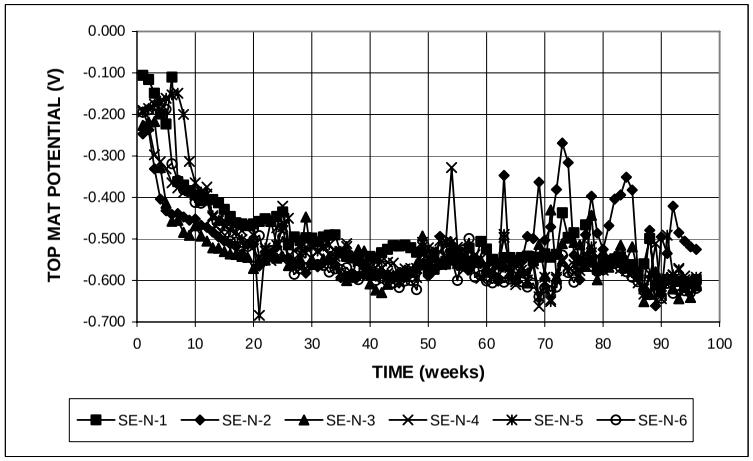

Figure A.27a - Southern Exposure test. Top mat corrosion potentials with respect to copper-copper sulfate electrode for conventional N steel, specimens w/c = 0.45, ponded with 15% NaCl solution.

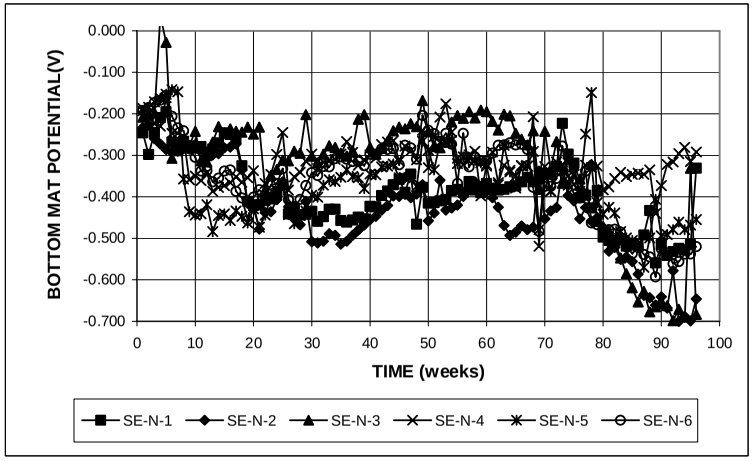

Figure A.27b - Southern Exposure test. Bottom mat corrosion potentials with respect to copper-copper sulfate electrode for conventional N steel, specimens w/c = 0.45, ponded with 15% NaCl solution.

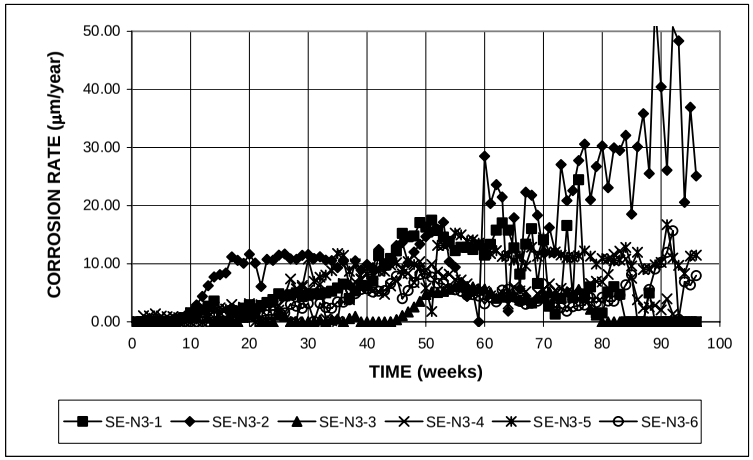

Figure A.28 -Southern Exposure test. Corrosion rates for conventional N3 steel, specimens w/c = 0.45, ponded with 15% NaCl solution.

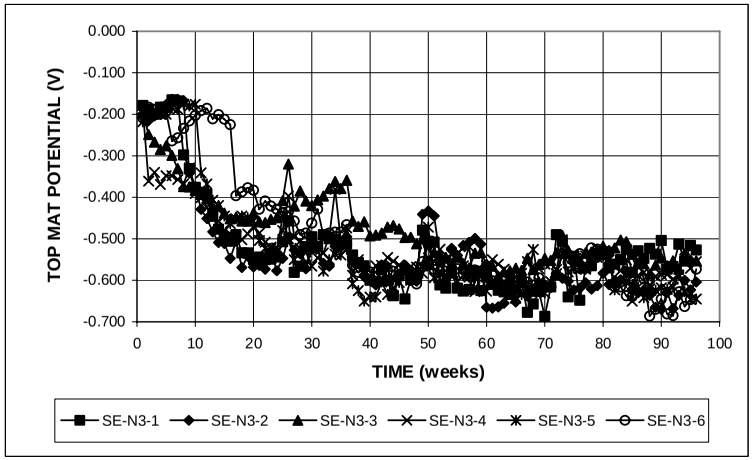

Figure A.30a - Southern Exposure test. Top mat corrosion potentials with respect to copper-copper sulfate electrode for conventional N3 steel, specimens w/c = 0.45, ponded with 15% NaCl solution.

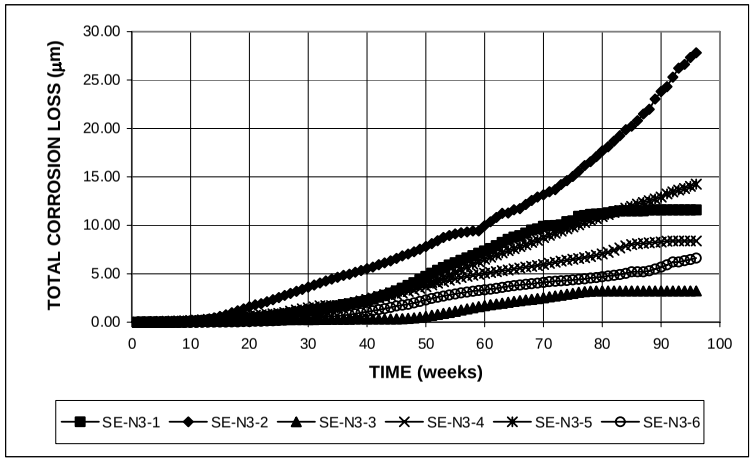

Figure A.29 - Southern Exposure test. Total corrosion losses of conventional N3 steel, specimens w/c = 0.45, ponded with 15% NaCl solution.

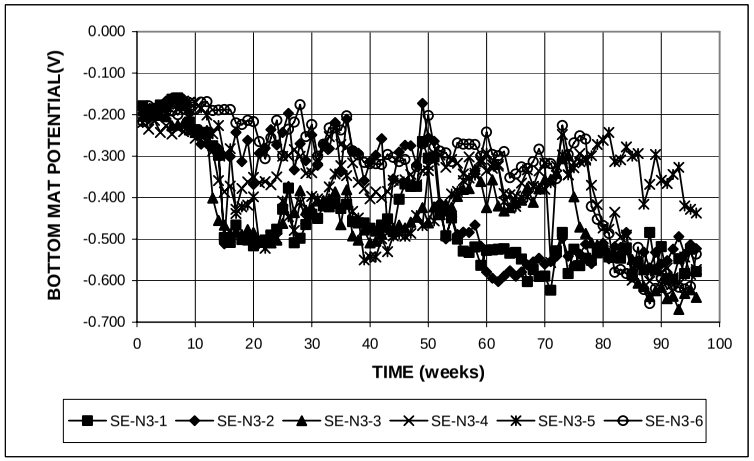

Figure A.30b - Southern Exposure test. Bottom mat corrosion potentials with respect to copper-copper sulfate electrode for conventional N3 steel, specimens w/c = 0.45, ponded with 15% NaCl solution.

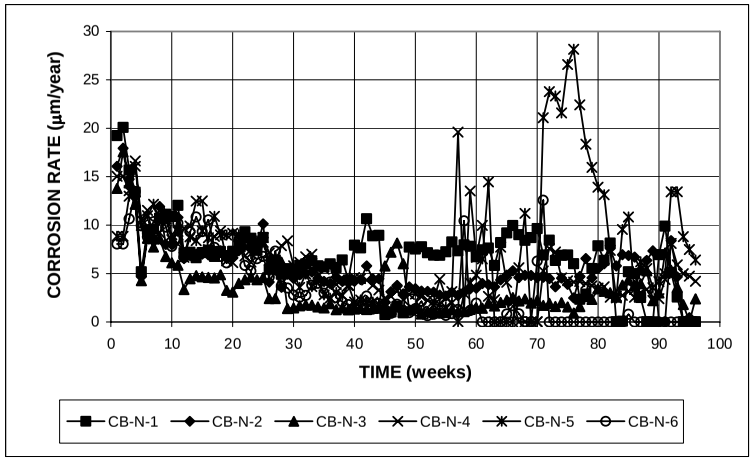

Figure A.31 - Cracked beam test. Corrosion rates for conventional N steel, specimens w/c= 0.45, ponded with 15% NaCl solution.

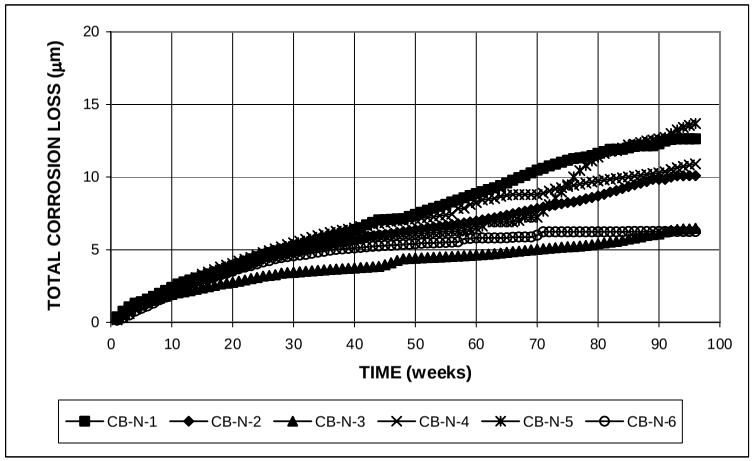

Figure A.32 -Cracked beam test. Total corrosion losses for conventional N steel, specimens w/c = 0.45, ponded with 15% NaCl solution.

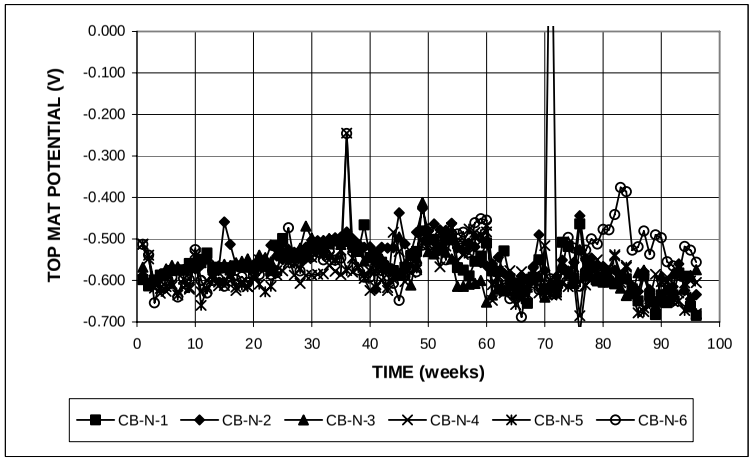

Figure A.33a - Cracked beam test. Top mat corrosion potentials with respect to copper-copper sulfate electrode for conventional N steel, specimens w/c = 0.45, ponded with 15% NaCl solution.

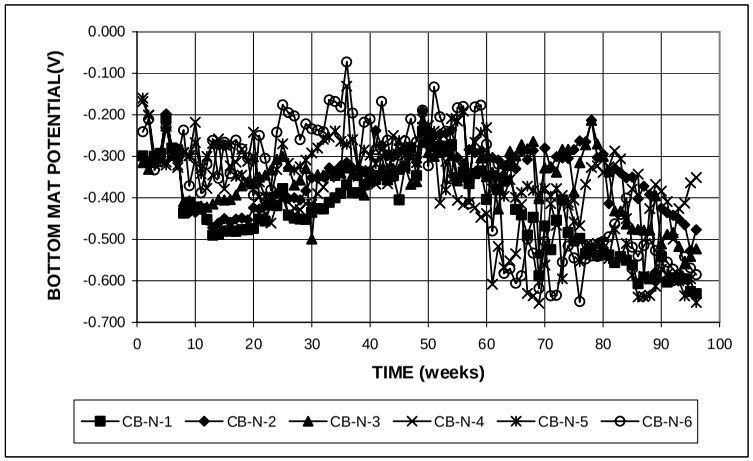

Figure A.33b - Cracked beam test. Bottom mat corrosion potentials with respect to copper-copper sulfate electrode for conventional N steel, specimens w/c = 0.45, ponded with 15% NaCl solution.

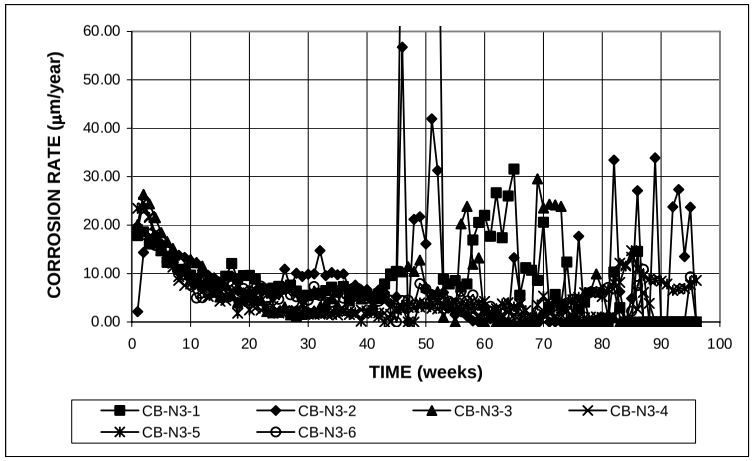

Figure A.34 - Cracked beam test. Corrosion rates for conventional N3 steel, specimens w/c = 0.45, ponded with 15% NaCl solution.

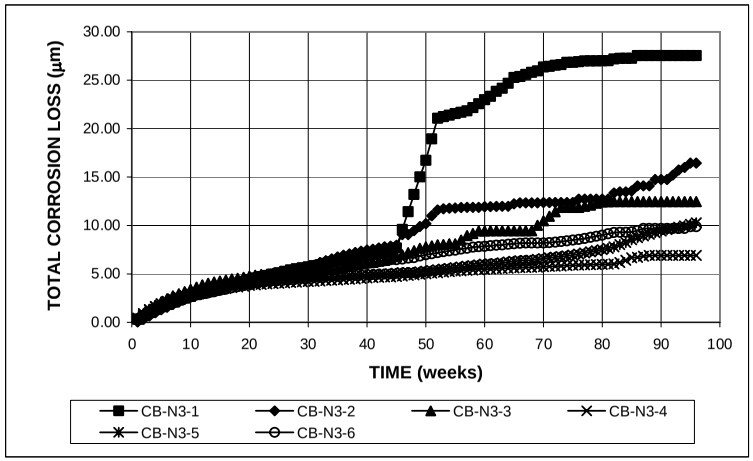

Figure A.35 -Cracked beam test. Total corrosion losses for conventional N3 steel, specimens w/c = 0.45, ponded with 15% NaCl solution.

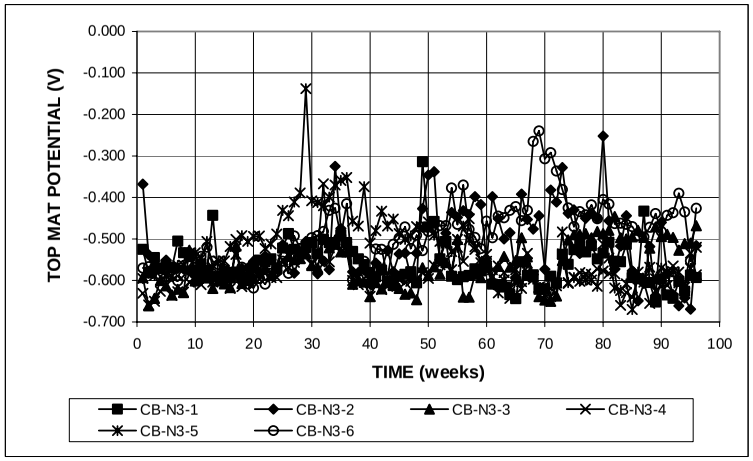

Figure A.36a - Cracked beam test. Top mat corrosion potentials with respect to copper-copper sulfate electrode for conventional N3 steel, specimens w/c = 0.45, ponded with 15% NaCl solution.

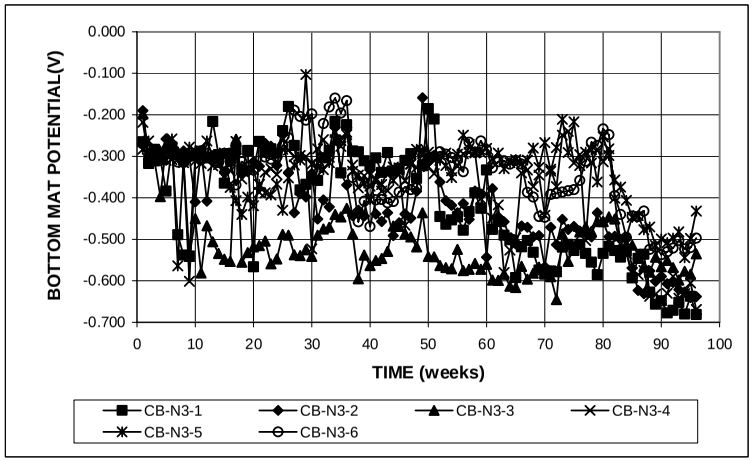

Figure A.36b - Cracked beam test. Bottom mat corrosion potentials with respect to copper-copper sulfate electrode for conventional N3 steel, specimens w/c = 0.45, ponded with 15% NaCl solution.

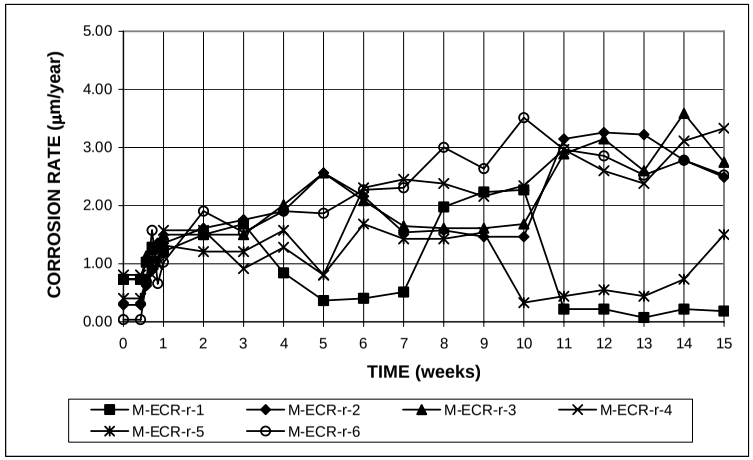

Figure A.37 - Macrocell Test. Corrosion rates based on total area of bar exposed to solution for bare epoxy-coated steel in simulated concrete pore solution with 1.6 molal ion NaCl. Solutions are replaced every 5 weeks.

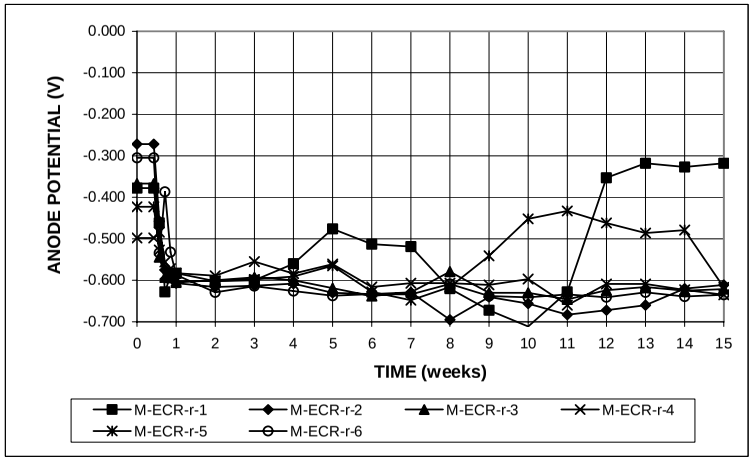

Figure A.39a - Macrocell Test. Anode corrosion potentials with respect to saturated calomel electrode for bare epoxy-coated steel in simulated concrete pore solution with 1.6 molal ion NaCl. Solutions are replaced every 5 weeks.

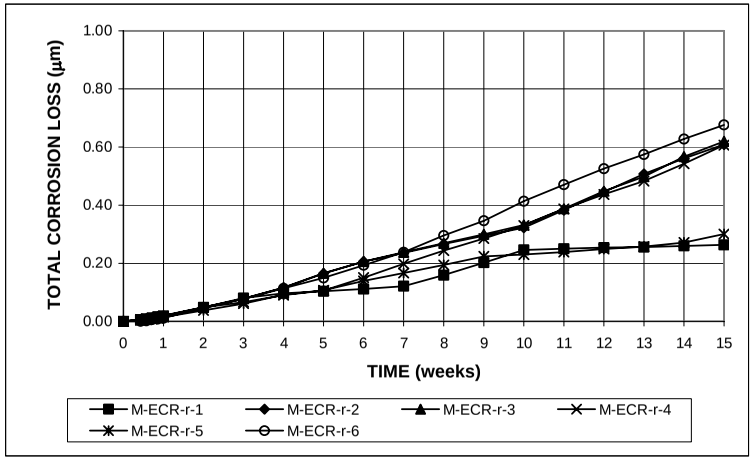

Figure A.38 - Macrocell Test. Total corrosion losses based on total area of bar exposed to solution for bare epoxy-coated steel in simulated concrete pore solution with 1.6 molal ion NaCl. Solutions are replaced every 5 weeks.

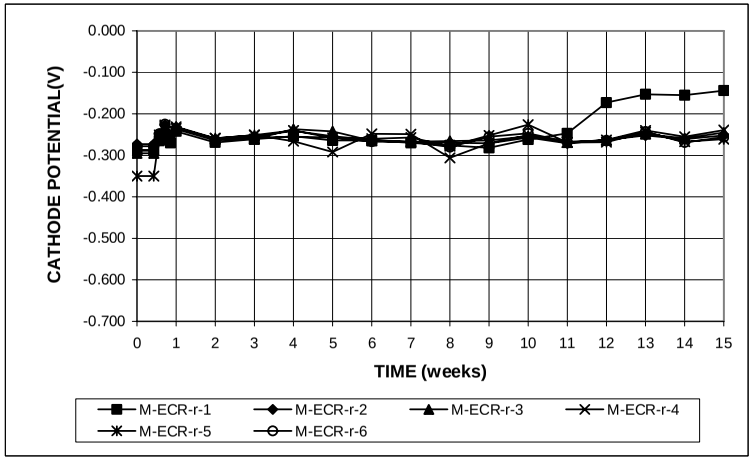

Figure A.39b - Macrocell Test. Cathode corrosion potentials with respect to saturated calomel electrode for bare epoxy-coated steel in simulated concrete pore solution with 1.6 molal ion NaCl. Solutions are replaced every 5 weeks.

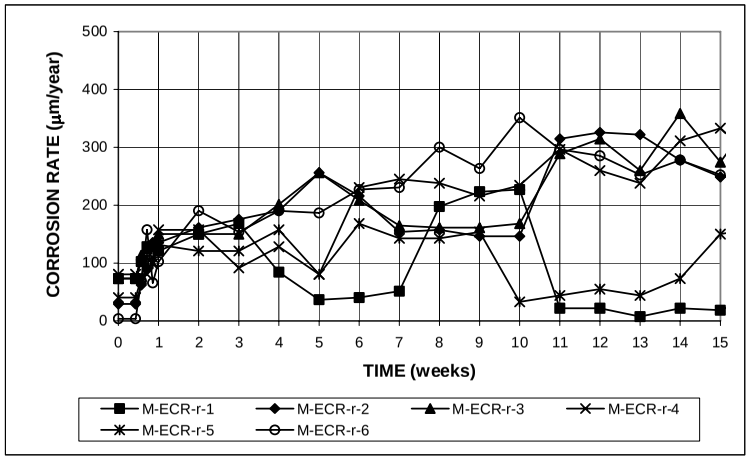

Figure A.40 - Macrocell Test. Corrosion rates based on exposed area of four 3.2-mm (0.125 in.) diameter holes in the coating for bare epoxy-coated steel in simulated concrete pore solution with 1.6 molal ion NaCl. Solutions are replaced every 5 weeks.

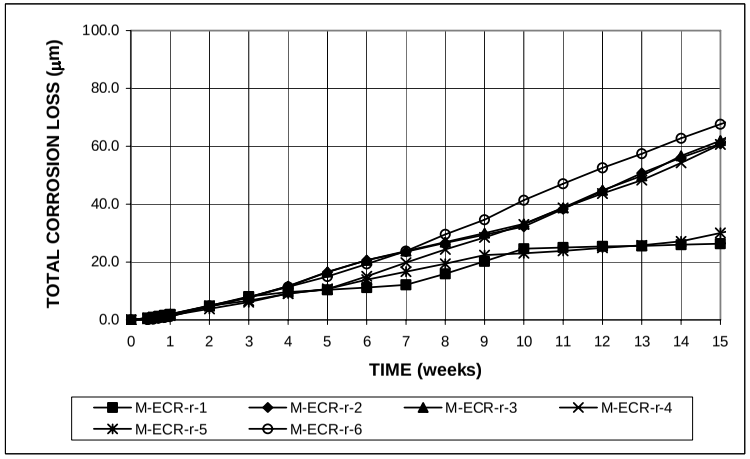

Figure A.41 - Macrocell Test. Total corrosion losses based on exposed area of four 3.2-mm (0.125 in.) diameter holes in the coating for bare epoxy-coated steel in simulated concrete pore solution with 1.6 molal ion NaCl. Solutions are replaced every 5 weeks.

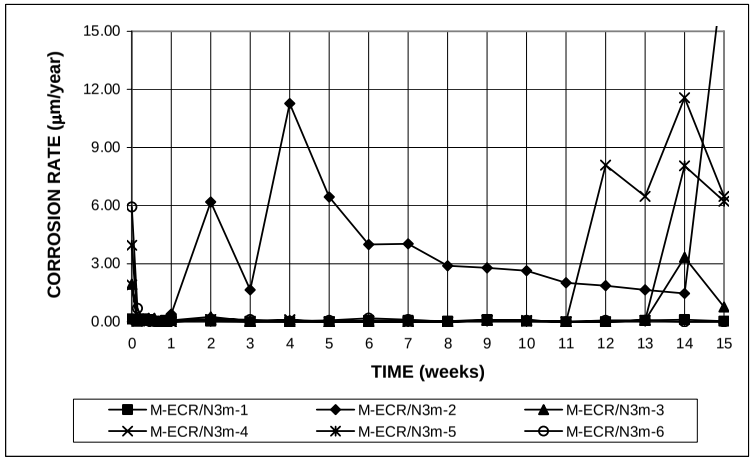

Figure A.42 - Macrocell Test. Corrosion rates based on total area of bar exposed to solution for mortar-wrapped epoxy-coated steel in simulated concrete pore solution with 1.6 molal ion NaCl, with mortar-wrapped conventional steel as the cathode.

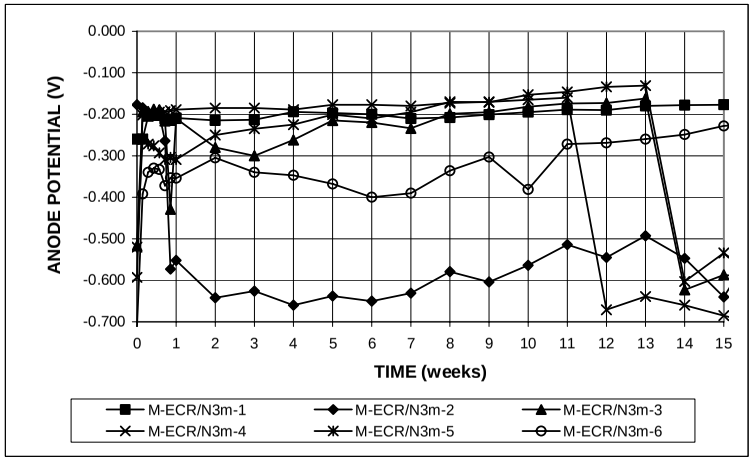

Figure A.44a - Macrocell Test. Anode corrosion potentials with respect to saturated calomel electrode, mortar-wrapped epoxy-coated steel as the anode in simulated concrete pore solution with 1.6 molal ion NaCl, mortar-wrapped conventional steel as the cathode.

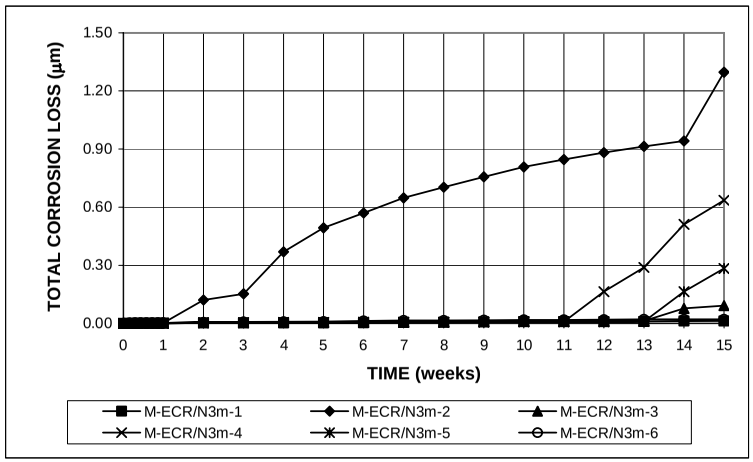

Figure A.43 - Macrocell Test. Total corrosion losses based on total area of bar exposed to solution for mortar-wrapped epoxy-coated steel in simulated concrete pore solution with 1.6 molal ion NaCl, with mortar-wrapped conventional steel as the cathode.

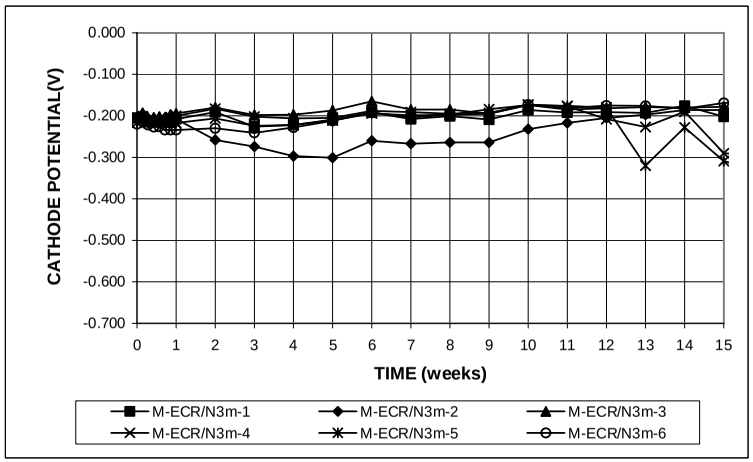

Figure A.44b - Macrocell Test. Cathode corrosion potentials with respect to saturated calomel electrode, mortar-wrapped epoxy-coated steel as the anode in simulated concrete pore solution with 1.6 molal ion NaCl, mortar-wrapped conventional steel as the cathode.

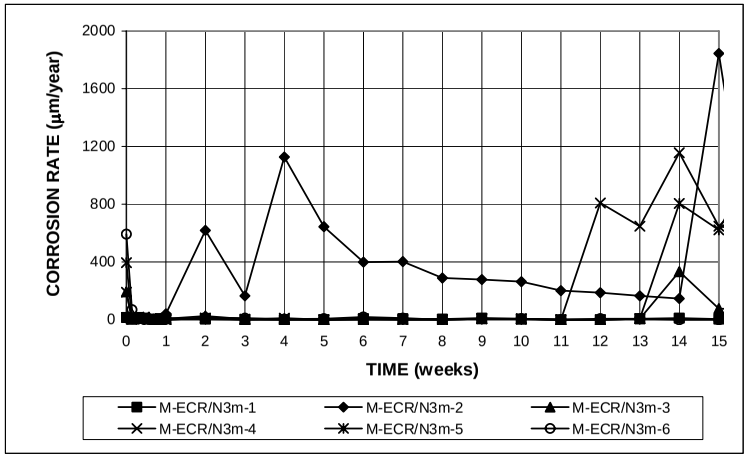

Figure A.45 - Macrocell Test. Corrosion rates based on exposed area of four 3.2-mm (0.125 in.) diameter holes in the coating for mortar-wrapped epoxy-coated steel in simulated concrete pore solution with 1.6 molal ion NaCl, with mortar-wrapped conventional steel as the cathode.

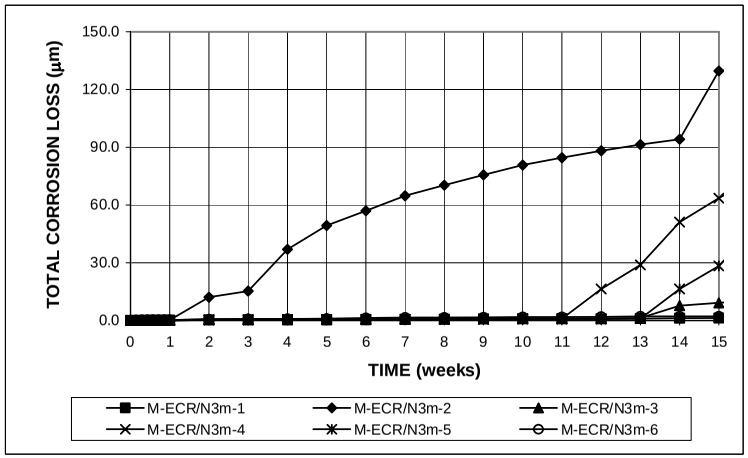

Figure A.46 - Macrocell Test. Total corrosion losses based on exposed area of four 3.2-mm (0.125 in.) diameter holes in the coating for mortar-wrapped epoxy-coated steel in simulated concrete pore solution with 1.6 molal ion NaCl, with mortar-wrapped conventional steel as the cathode.

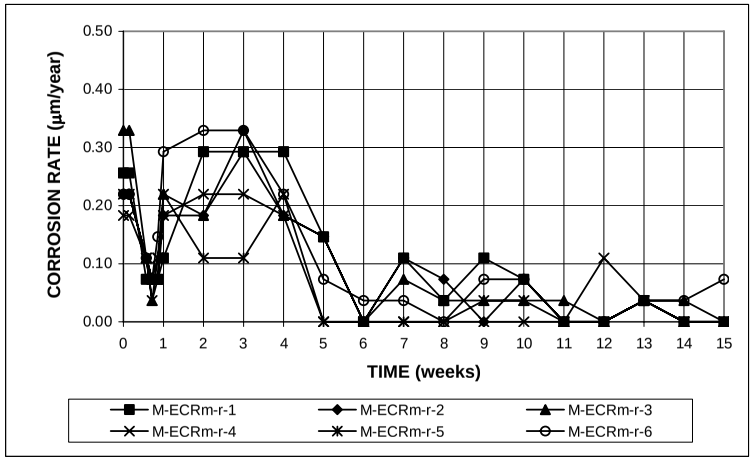

Figure A.47 - Macrocell Test. Corrosion rates based on total area of bar exposed to solution for mortar-wrapped epoxy-coated steel in simulated concrete pore solution with 1.6 molal ion NaCl. Solutions are replaced every 5 weeks.

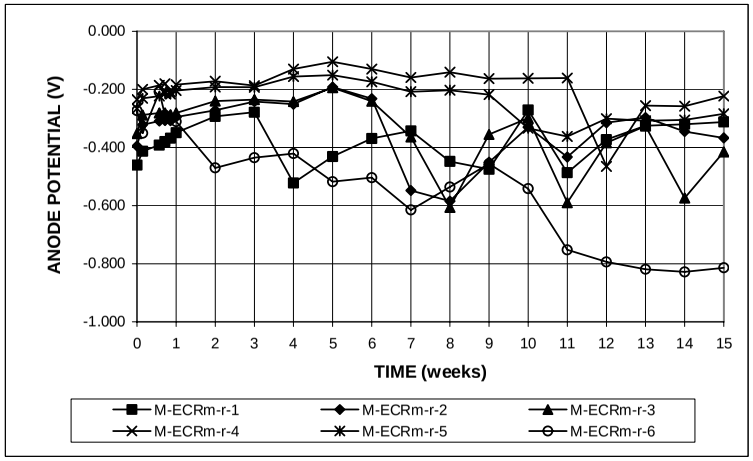

Figure A.49a - Macrocell Test. Anode corrosion potentials with respect to saturated calomel electrode for mortar-wrapped epoxy-coated steel in simulated concrete pore solution with 1.6 molal ion NaCl. Solutions are replaced every 5 weeks.

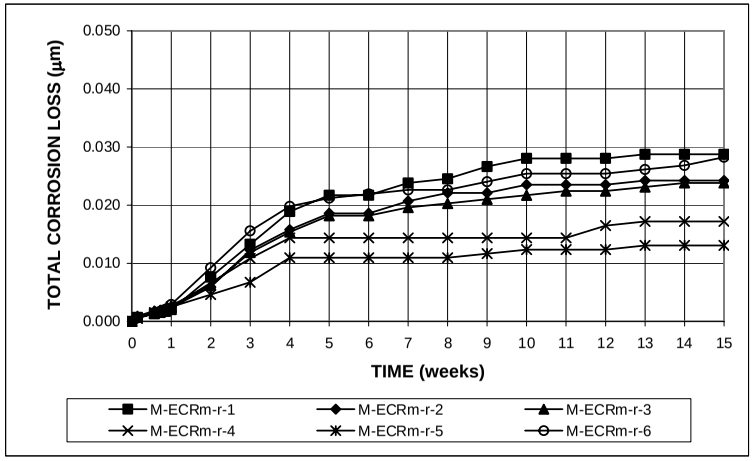

Figure A.48 - Macrocell Test. Total corrosion losses based on total area of bar exposed to solution for mortar-wrapped epoxy-coated steel in simulated concrete pore solution with 1.6 molal ion NaCl. Solutions are replaced every 5 weeks.

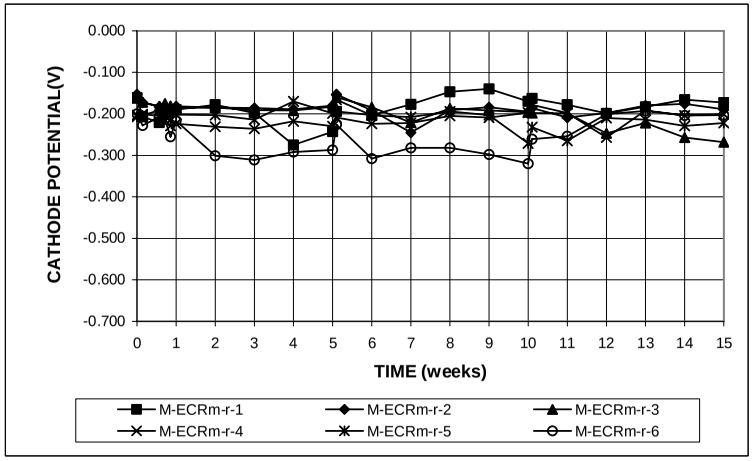

Figure A.49b - Macrocell Test. Cathode corrosion potentials with respect to saturated calomel electrode for mortar-wrapped epoxy-coated steel in simulated concrete pore solution with 1.6 molal ion NaCl. Solutions are replaced every 5 weeks.

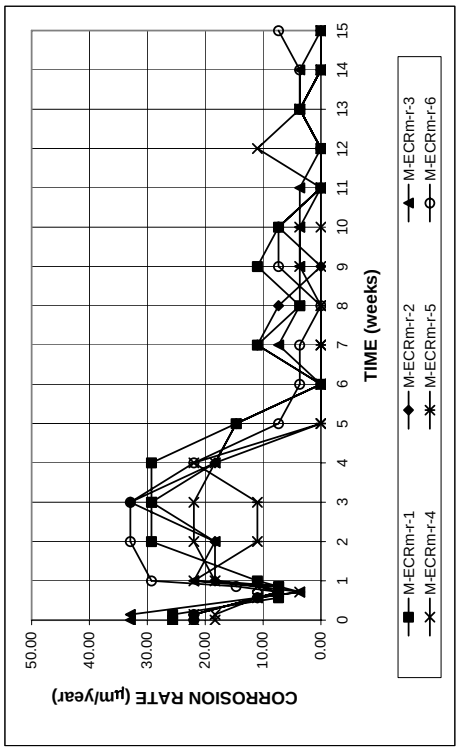

Figure A.50 - Macrocell Test. Corrosion rates based on exposed area of four 3.2-mm (0.125 in.) diameter holes in the coating for mortar-wrapped epoxy-coated steel in simulated concrete pore solution with 1.6 molal ion NaCl. Solutions are replaced every 5 weeks.

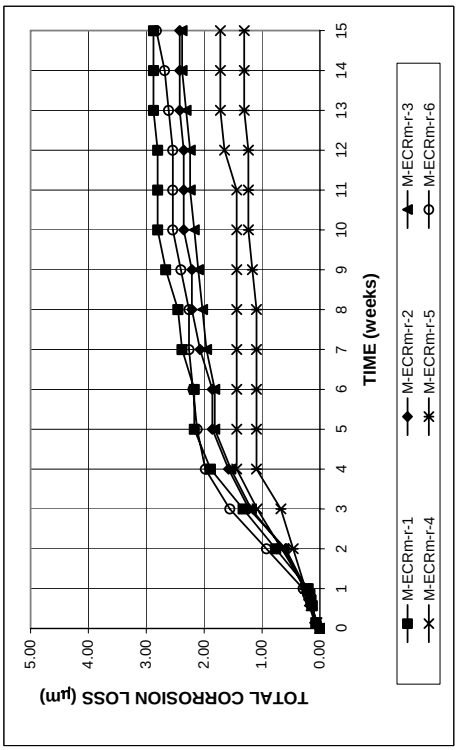

Figure A.51 - Macrocell Test. Total corrosion losses based on exposed area of four 3.2-mm (0.125 in.) diameter holes in the coating for mortar-wrapped epoxy-coated steel in simulated concrete pore solution with 1.6 molal ion NaCl. Solutions are replaced every 5 weeks.

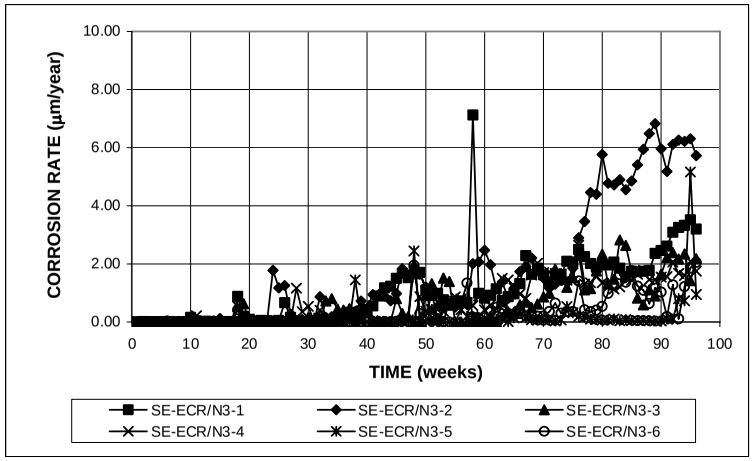

Figure A.52 - Southern Exposure test. Corrosion rates based on total area of the bar for epoxy-coated steel, specimens w/c = 0.45, ponded with 15% NaCl solution, conventional steel at the bottom mat.

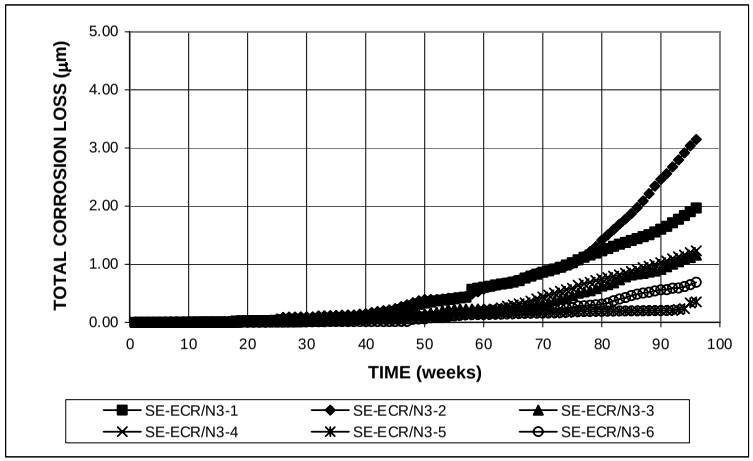

Figure A.53 - Southern Exposure test. Total corrosion losses based on total area of the bar for epoxy-coated steel, specimens w/c = 0.45, ponded with 15% NaCl solution, conventional steel at the bottom mat.

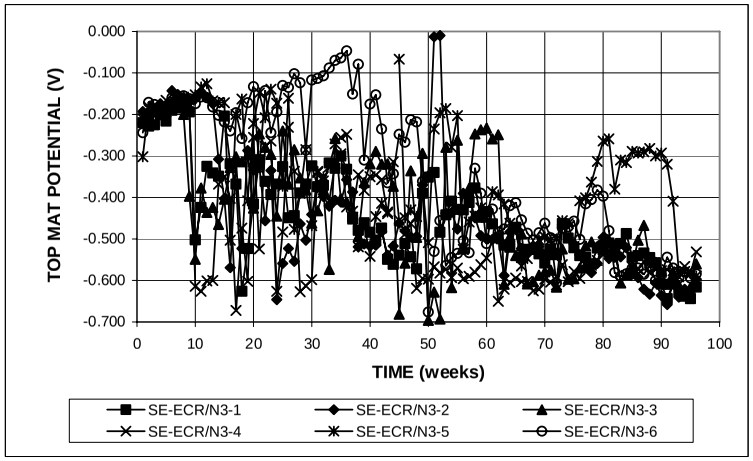

Figure A.54a - Southern Exposure test. Top mat corrosion potentials with respect to copper-copper sulfate electrode, epoxy-coated steel at the top mat, conventional steel at the bottom mat, specimens w/c = 0.45, ponded with 15% NaCl solution.

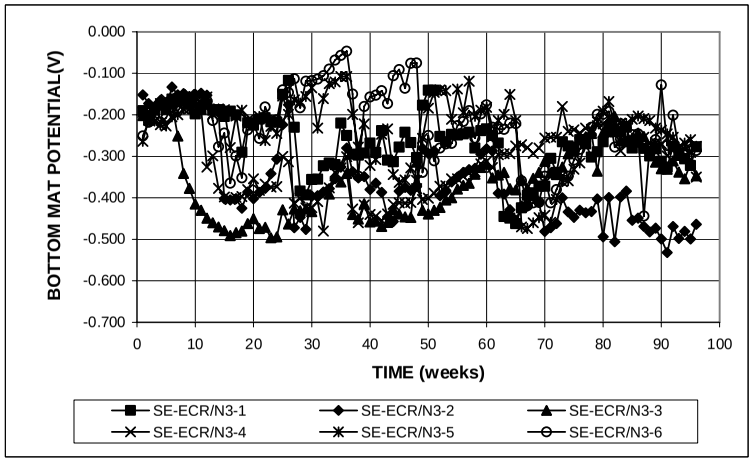

Figure A.54b - Southern Exposure test. Bottom mat corrosion potentials with respect to copper-copper sulfate electrode, epoxy-coated steel at the top mat, conventional steel at the bottom mat, specimens w/c = 0.45, ponded with 15% NaCl solution.

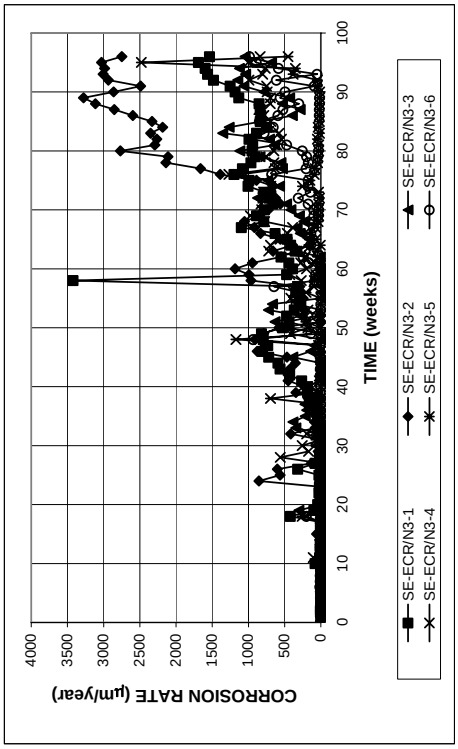

Figure A.55 - Southern Exposure test. Corrosion rates based on exposed area of four 3.2 mm (0.125 in.) diameter holes in the coating for epoxy-coated steel, specimens w/c = 0.45, ponded with 15% NaCl solution, conventional steel at the bottom mat.

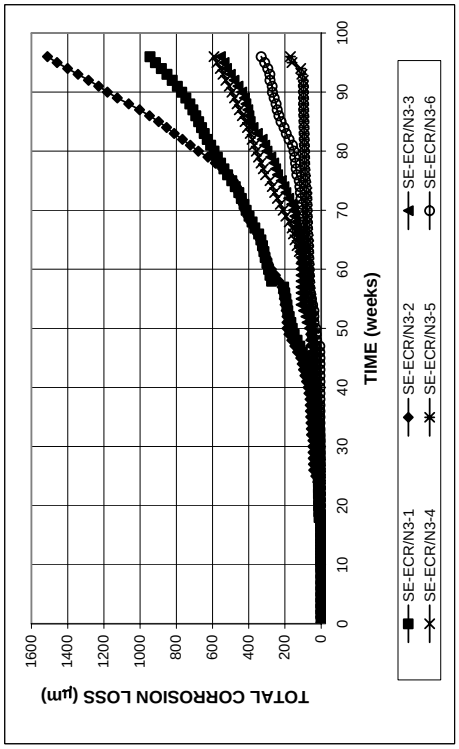

Figure A.56 - Southern Exposure test. Total corrosion losses based on exposed area of four 3.2 mm (0.125 in.) diameter holes in the coating for epoxy-coated steel, specimens w/c = 0.45, ponded with 15% NaCl solution, conventional steel at the bottom mat.

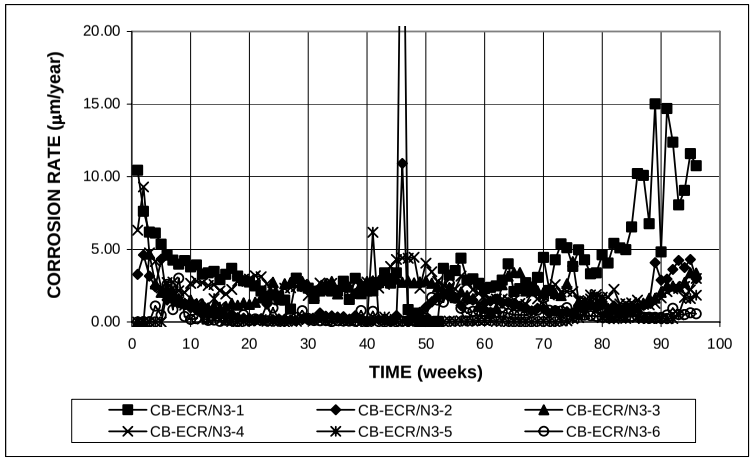

Figure A.57 - Cracked beam test. Corrosion rates based on total area of the bar for epoxy-coated steel, specimens w/c = 0.45, ponded with 15% NaCl solution, conventional steel at the bottom mat.

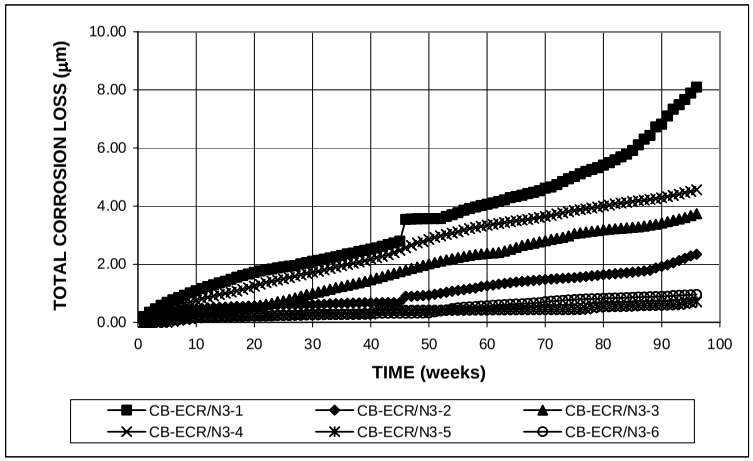

Figure A.58 - Cracked beam test. Total corrosion losses based on total area of the bar for epoxy-coated steel, specimens w/c = 0.45, ponded with 15% NaCl solution, conventional steel at the bottom mat.

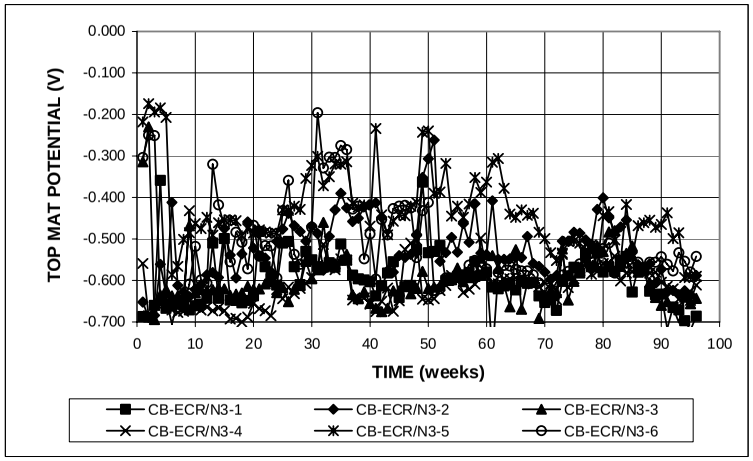

Figure A.59a - Cracked beam test. Top mat corrosion potentials with respect to copper-copper sulfate electrode, epoxy-coated steel at the top mat, conventional steel at the bottom mat, specimens w/c = 0.45, ponded with 15% NaCl solution.

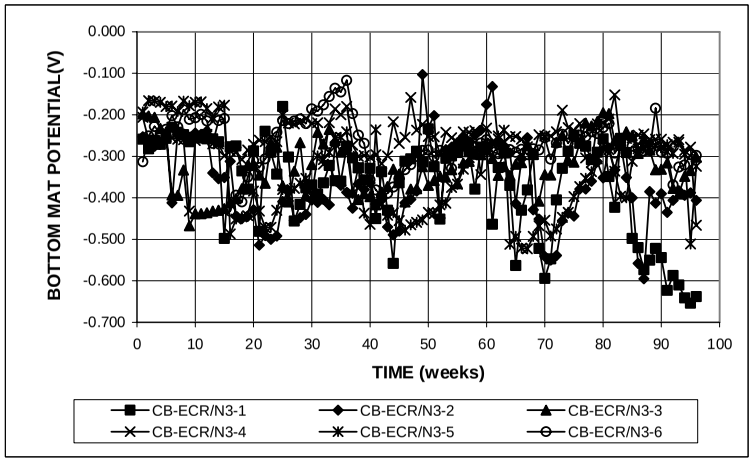

Figure A.59b - Cracked beam test. Bottom mat corrosion potentials with respect to copper-copper sulfate electrode, epoxy-coated steel at the top mat, conventional steel at the bottom mat, specimens w/c = 0.45, ponded with 15% NaCl solution.

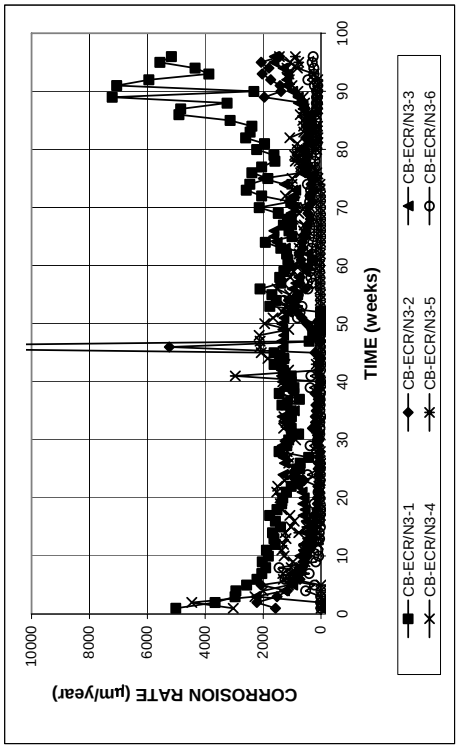

Figure A.60 - Cracked beam test. Corrosion rates based on exposed area of four 3.2 mm (0.125 in.) diameter holes in the coating for epoxy-coated steel, specimens w/c = 0.45, ponded with 15% NaCl solution, conventional steel at the bottom mat.

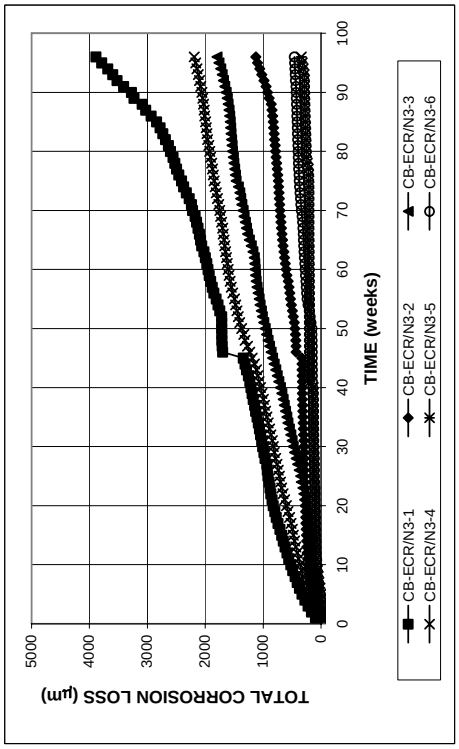

Figure A.61 - Cracked beam test. Total corrosion losses based on exposed area of four 3.2 mm (0.125 in.) diameter holes in the coating for epoxy-coated steel, specimens w/c = 0.45, ponded with 15% NaCl solution, conventional steel at the bottom mat.

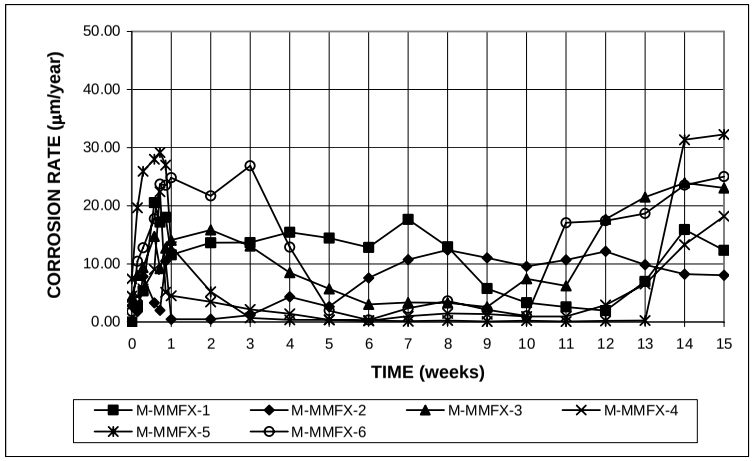

Figure A.62 - Macrocell test. Corrosion rates for bare MMFX steel in simulated concrete pore solution with 1.6 molal ion NaCl.

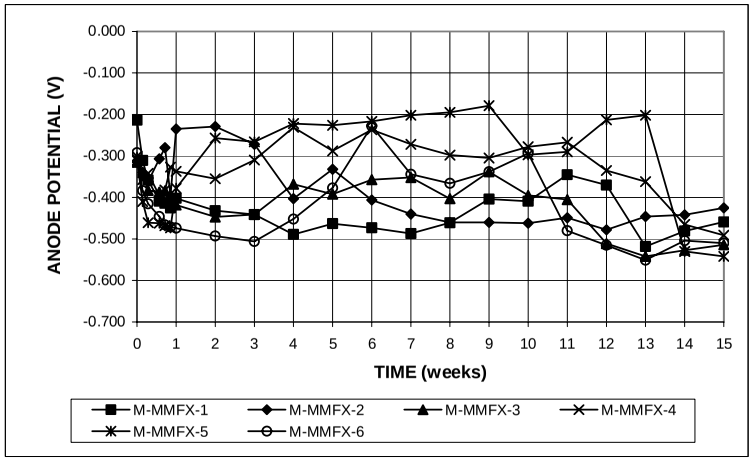

Figure A.64a - Macrocell test. Anode corrosion potentials with respect to saturated calomel electrode for bare MMFX steel in simulated concrete pore solution with 1.6 molal ion NaCl.

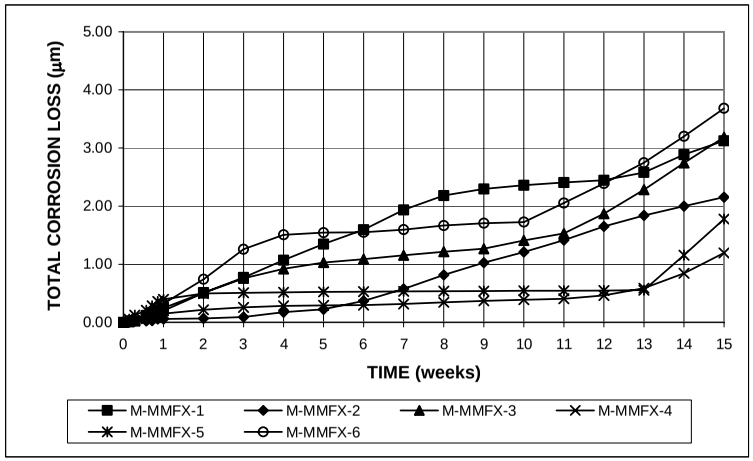

Figure A.63 - Macrocell test. Total corrosion losses for bare MMFX steel in simulated concrete pore solution with 1.6 molal ion NaCl.

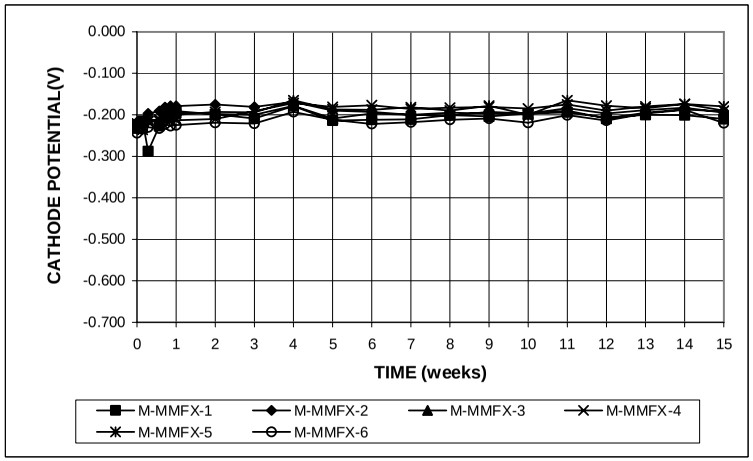

Figure A.64b - Macrocell test. Cathode corrosion potentials with respect to saturated calomel electrode for bare MMFX steel in simulated concrete pore solution with 1.6 molal ion NaCl.

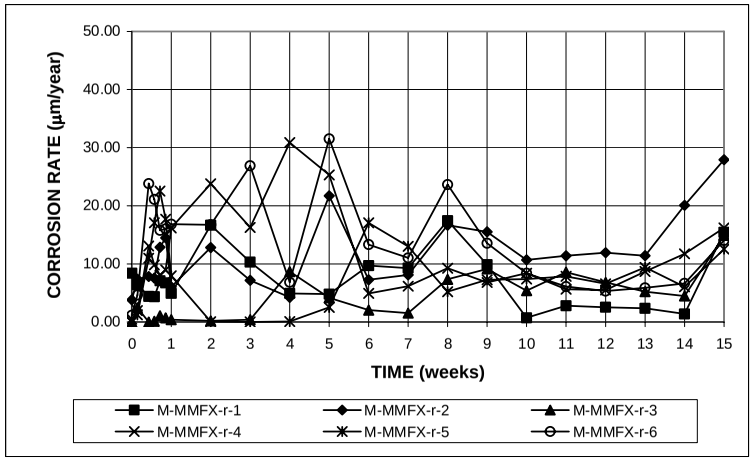

Figure A.65 - Macrocell test. Corrosion rates for bare MMFX steel in simulated concrete pore solution with 1.6 molal ion NaCl. Solutlions are replaced every 5 weeks.

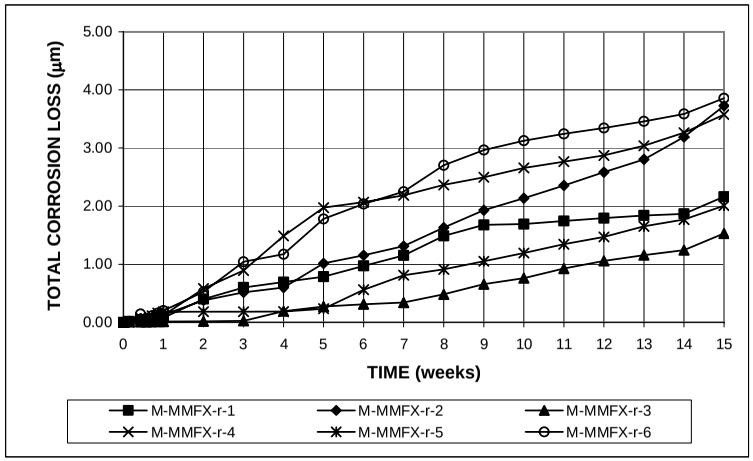

Figure A.66 - Macrocell test. Total corrosion losses for bare MMFX steel in simulated concrete pore solution with 1.6 molal ion NaCl. Solutions are replaced every 5 weeks.

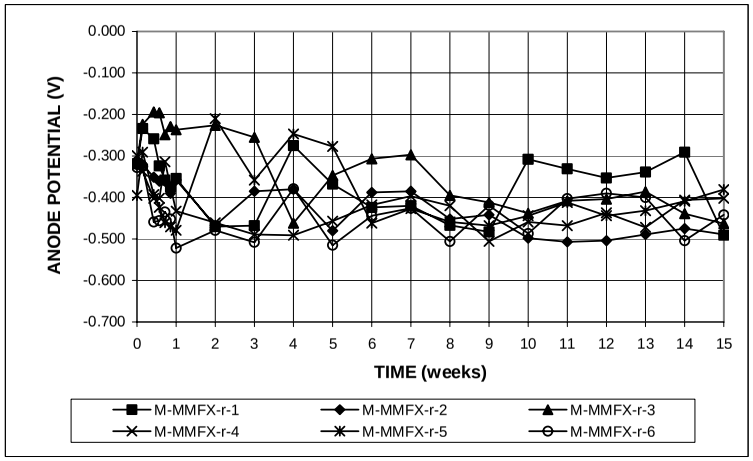

Figure A.67a - Macrocell test. Anode corrosion potentials with respect to saturated calomel electrode for bare MMFX steel in simulated concrete pore solution with 1.6 molal ion NaCl. Solutions are replaced every 5 weeks.

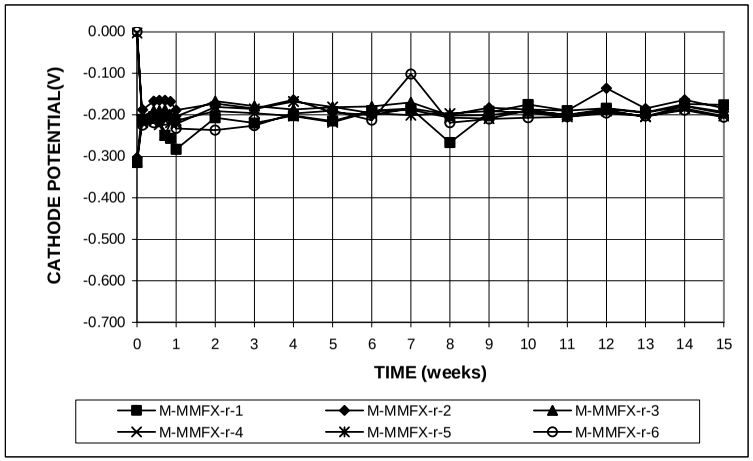

Figure A.67b - Macrocell test. Cathode corrosion potentials with respect to saturated calomel electrode for bare MMFX steel in simulated concrete pore solution with 1.6 molal ion NaCl. Solutions are replaced every 5 weeks.

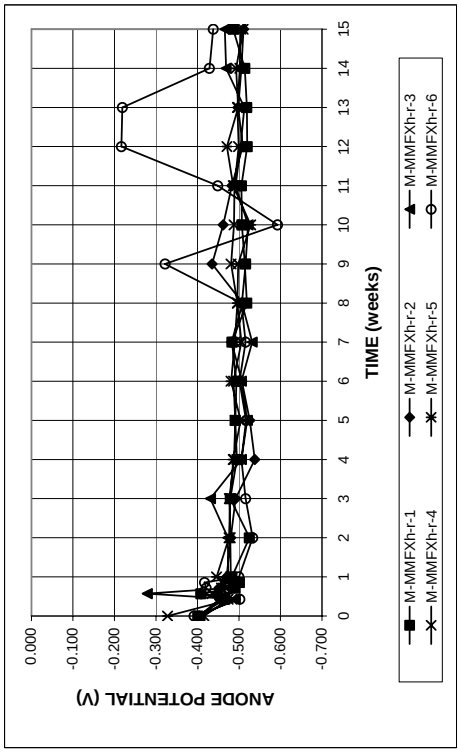

Figure A.70a - Macrocell test. Anode corrosion potentials with respect to saturated calomel electrode for bare MMFX steel in simulated concrete pore solution with 6.04 molal ion NaCl. Solutions are replaced every 5 weeks.

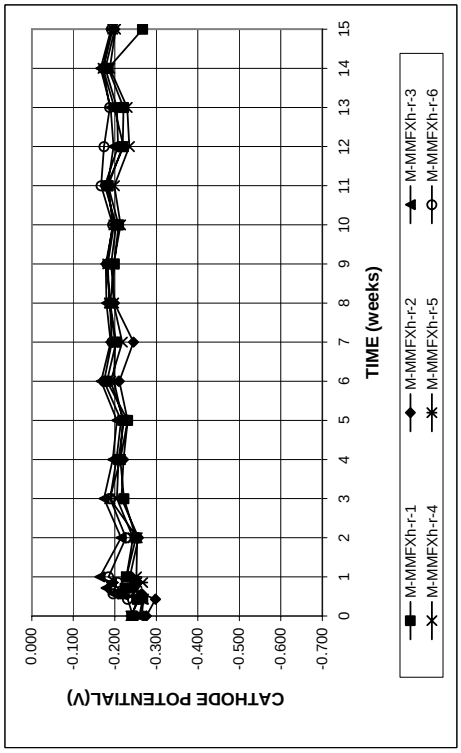

Figure A.70b - Macrocell test. Cathode corrosion potentials with respect to saturated calomel electrode for bare MMFX steel in simulated concrete pore solution with 6.04 molal ion NaCl. Solutions are replaced every 5 weeks.

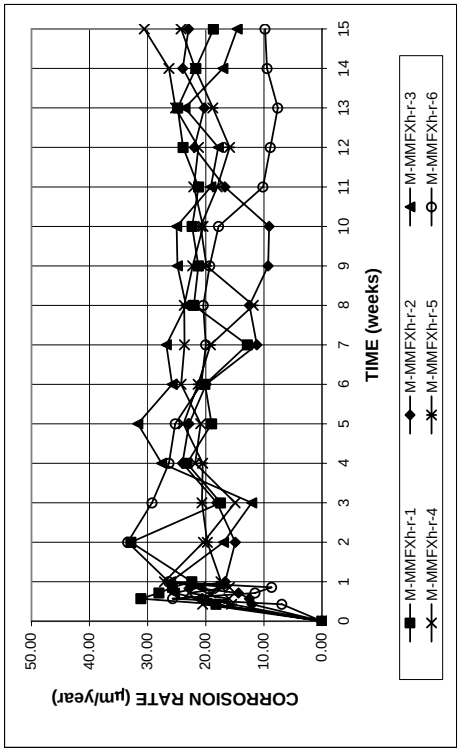

Figure A.68 - Macrocell test. Corrosion rates for bare MMFX steel in simulated concrete pore solution with 6.04 molal ion NaCl. Solutions are replaced every 5 weeks.

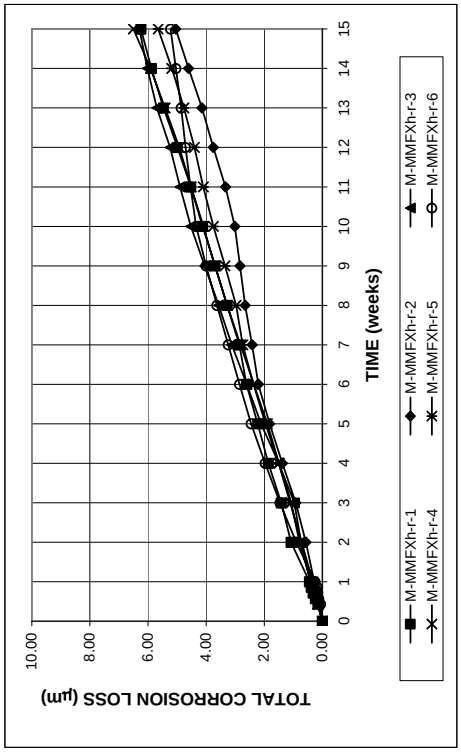

Figure A.69 - Macrocell test. Total corrosion losses for bare MMFX steel in simulated concrete pore solution with 6.04 molal ion NaCl. Solutions are replaced every 5 weeks.

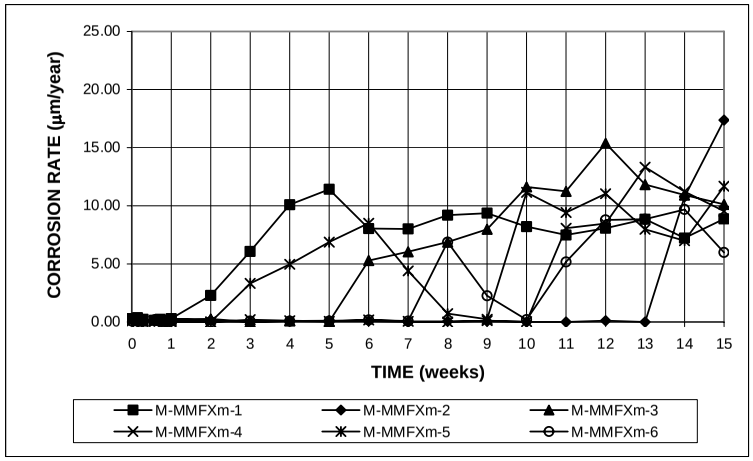

Figure A.71 - Macrocell test. Corrosion rates for mortar-wrapped MMFX steel in simulated concrete pore solution with 1.6 molal ion NaCl.

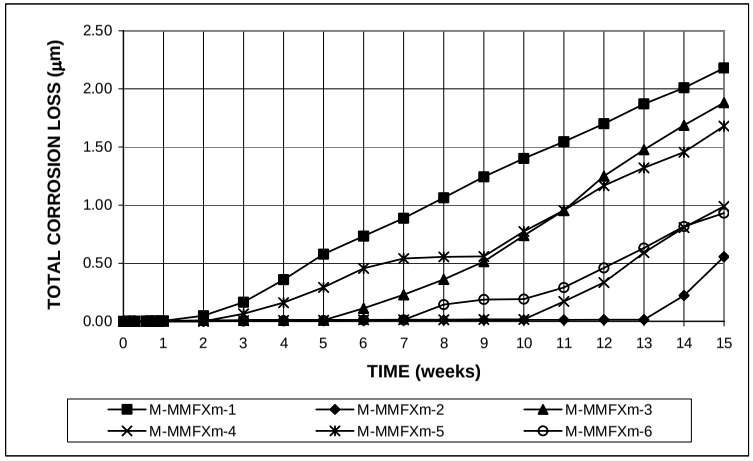

Figure A.72 - Macrocell test. Total corrosion losses for mortar-wrapped MMFX steel in simulated concrete pore solution with 1.6 molal ion NaCl.

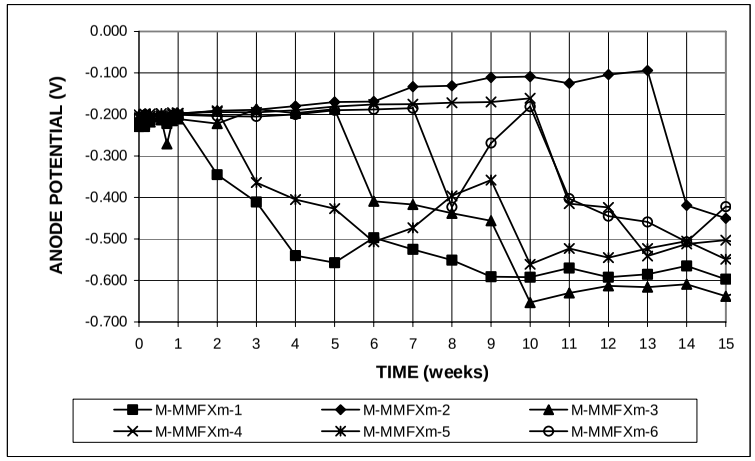

Figure A.73a -Macrocell test. Anode corrosion potentials with respect to saturated calomel electrode for mortar-wrapped MMFX steel in simulated concrete pore solution with 1.6 molal ion NaCl.

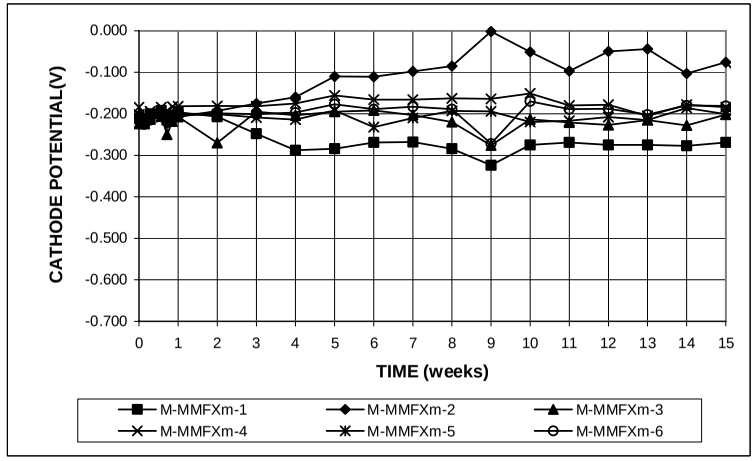

Figure A.73b - Macrocell test. Cathode corrosion potentials with respect to saturated calomel electrode for mortar-wrapped MMFX steel in simulated concrete pore solution with 1.6 molal ion NaCl.

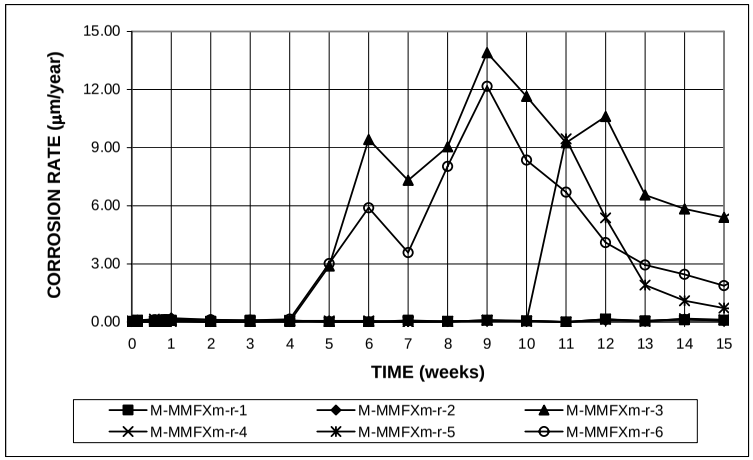

Figure A.74 -Macrocell test. Corrosion rates for mortar-wrapped MMFX steel in simulated concrete pore solution with 1.6 molal ion NaCl. Solutions are replaced every 5 weeks.

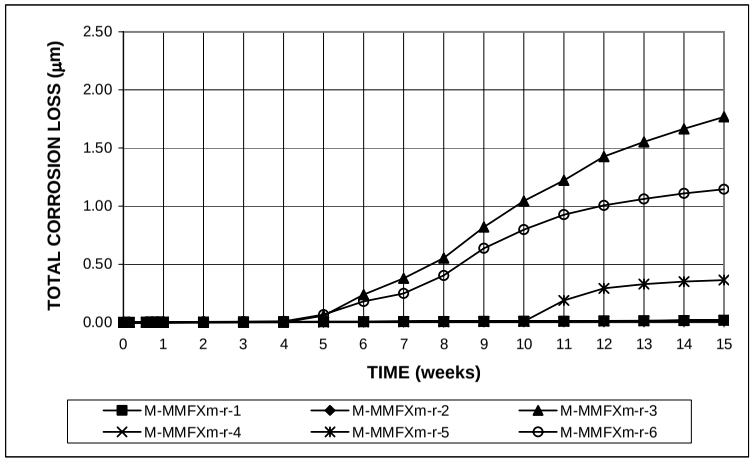

Figure A.75 - Macrocell test. Total corrosion losses for mortar-wrapped MMFX steel in simulated concrete pore solution with 1.6 molal ion NaCl. Solutions are replaced every 5 weeks.

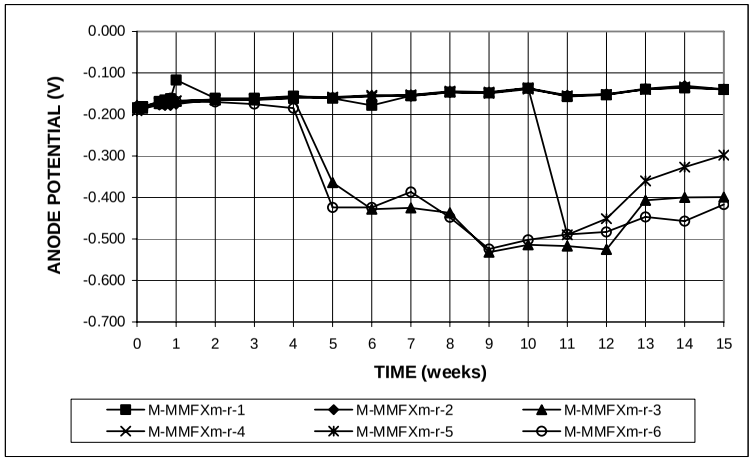

Figure A.76a - Macrocell test. Anode corrosion potentials with respect to saturated calomel electrode for mortar-wrapped MMFX steel in simulated concrete pore solution with 1.6 molal ion NaCl. Solutions are replaced every 5 weeks.

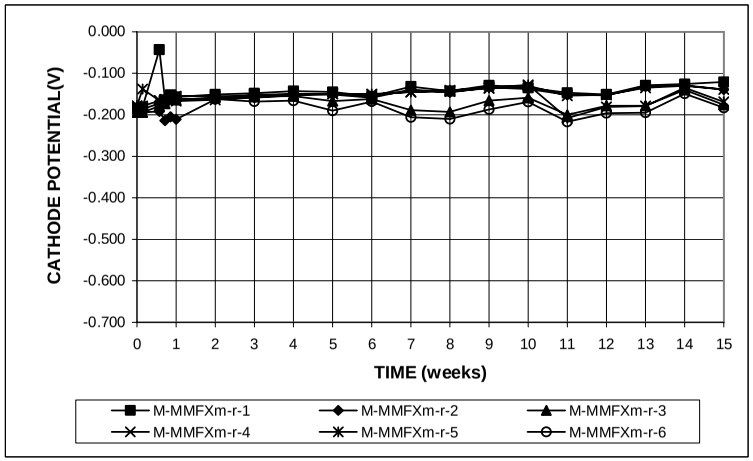

Figure A.76b - Macrocell test. Cathode corrosion potentials with respect to saturated calomel electrode for mortar-wrapped MMFX steel in simulated concrete pore solution with 1.6 molal ion NaCl. Solutions are replaced every 5 weeks.

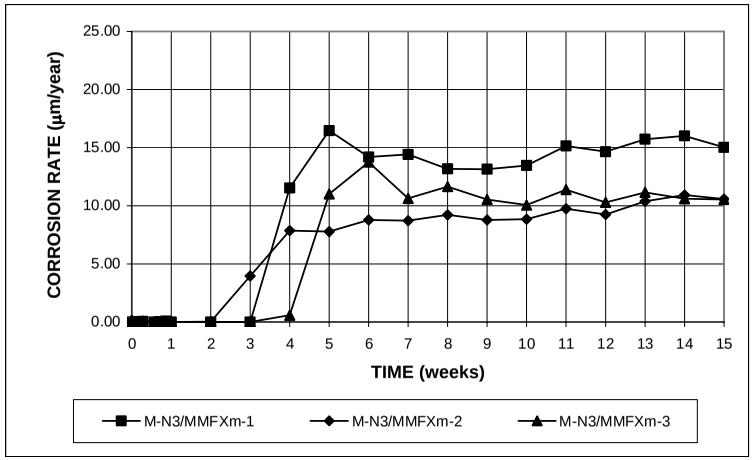

Figure A.77 - Macrocell Test. Corrosion rates for mortar-wrapped conventional N3 steel in simulated concrete pore solution with 1.6 molal ion NaCl, with mortar-wrapped MMFX steel as the cathode.

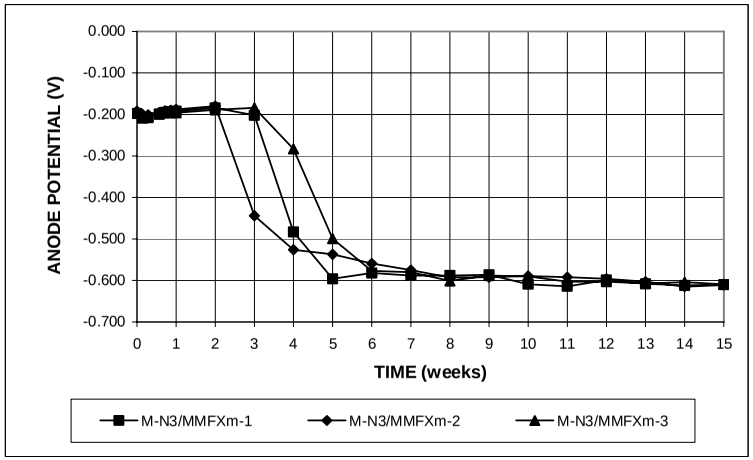

Figure A.79a -Macrocell Test. Anode corrosion potentials with respect to saturated calomel electrode, mortar-wrapped conventional N3 steel as the anode in simulated concrete pore solution with 1.6 molal ion NaCl, mortar-wrapped MMFX steel as the cathode.

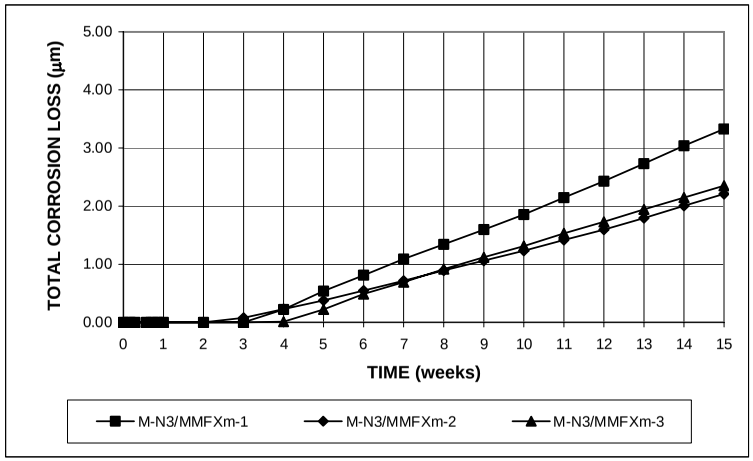

Figure A.78 - Macrocell Test. Total corrosion losses for mortar-wrapped conventional N3 steel in simulated concrete pore solution with 1.6 molal ion NaCl, with mortar-wrapped MMFX steel as the cathode.

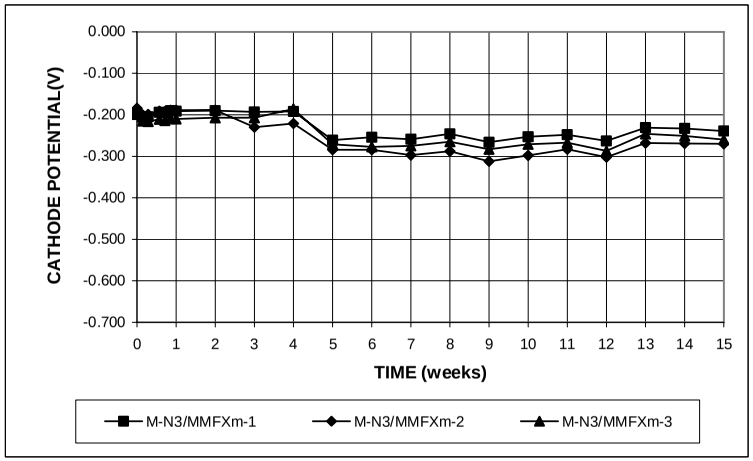

Figure A.79b - Macrocell Test. Cathode corrosion potentials with respect to saturated calomel electrode, mortar-wrapped conventional N3 steel as the anode in simulated concrete pore solution with 1.6 molal ion NaCl, mortar-wrapped MMFX steel as the cathode.

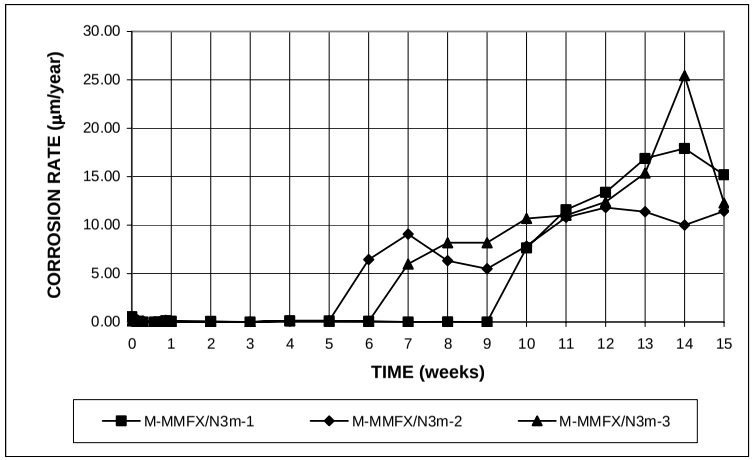

Figure A.80 - Macrocell Test. Corrosion rates for mortar-wrapped MMFX steel in simulated concrete pore solution with 1.6 molal ion NaCl, with mortar-wrapped conventional N3 steel as the cathode.

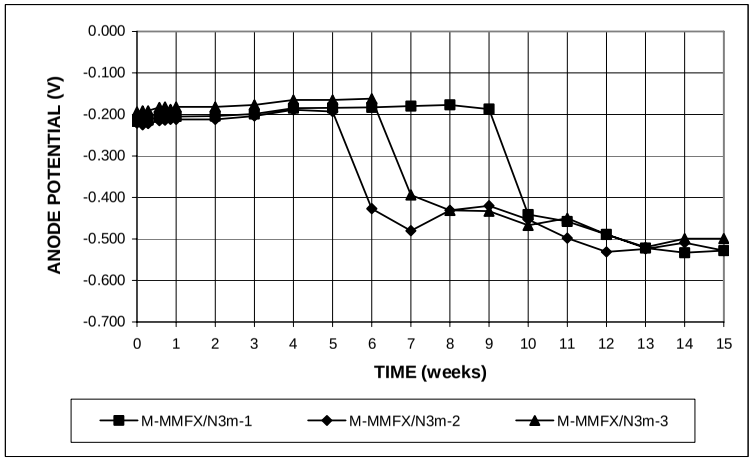

Figure A.82a -Macrocell Test. Anode corrosion potentials with respect to saturated calomel electrode, mortar-wrapped MMFX steel as the anode in simulated concrete pore solution with 1.6 molal ion NaCl, mortar-wrapped conventional N3 steel as the cathode.

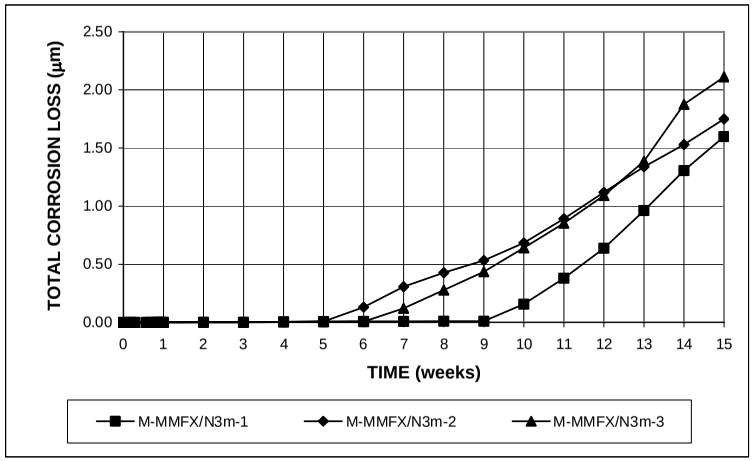

Figure A.81 - Macrocell Test. Total corrosion losses for mortar-wrapped MMFX steel in simulated concrete pore solution with 1.6 molal ion NaCl, with mortar-wrapped conventional steel as the cathode.

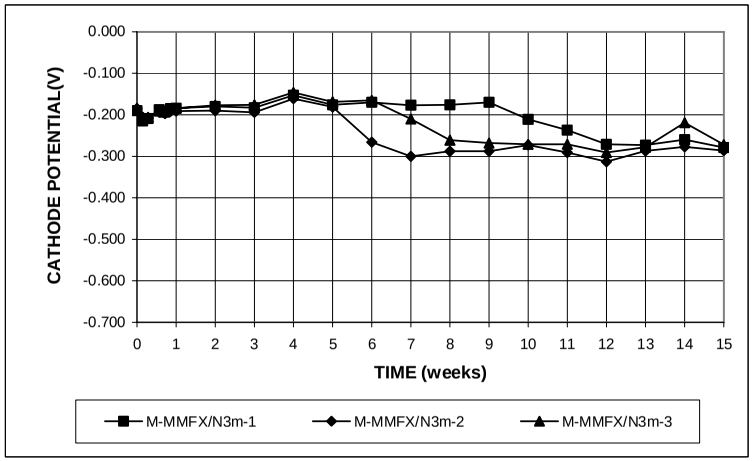

Figure A.82b - Macrocell Test. Cathode corrosion potentials with respect to saturated calomel electrode, mortar-wrapped MMFX steel as the anode in simulated concrete pore solution with 1.6 molal ion NaCl, mortar-wrapped conventional N3 steel as the cathode.

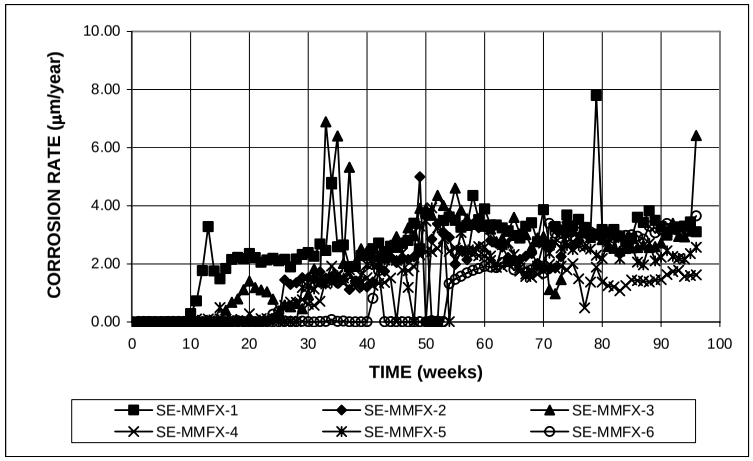

Figure A.83 - Southern Exposure test. Corrosion rates for MMFX steel, specimens w/c = 0.45, ponded with 15% NaCl solution.

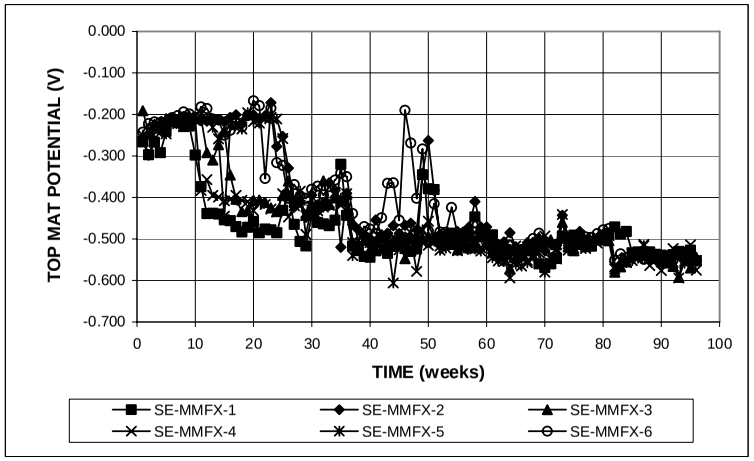

Figure A.85a - Southern Exposure test. Top mat corrosion potentials with respect to copper-copper sulfate electrode for MMFX steel, specimens w/c = 0.45, ponded with 15% NaCl solution.

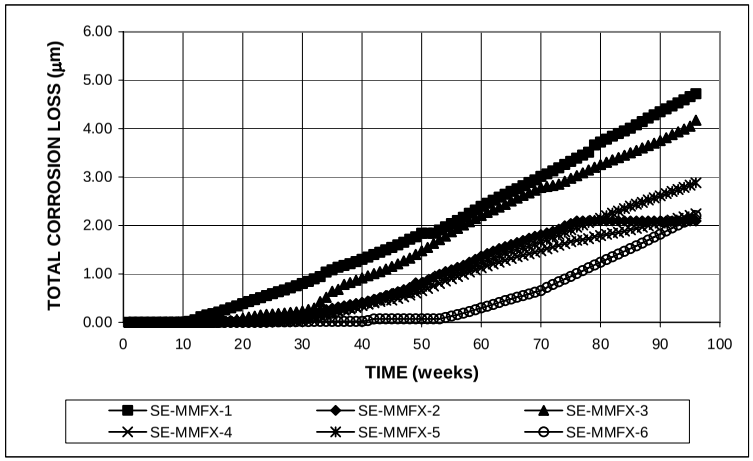

Figure A.84 - Southern Exposure test. Total corrosion losses of MMFX steel, specimens w/c = 0.45, ponded with 15% NaCl solution.

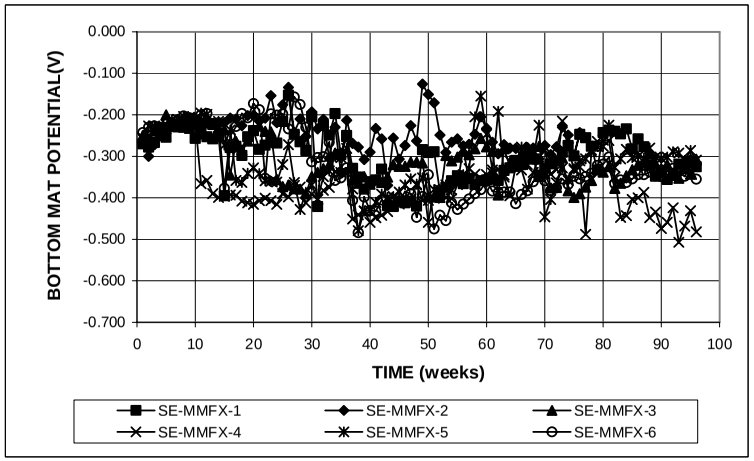

Figure A.85b - Southern Exposure test. Bottom mat corrosion potentials with respect to copper-copper sulfate electrode for MMFX steel, specimens w/c = 0.45, ponded with 15% NaCl solution.

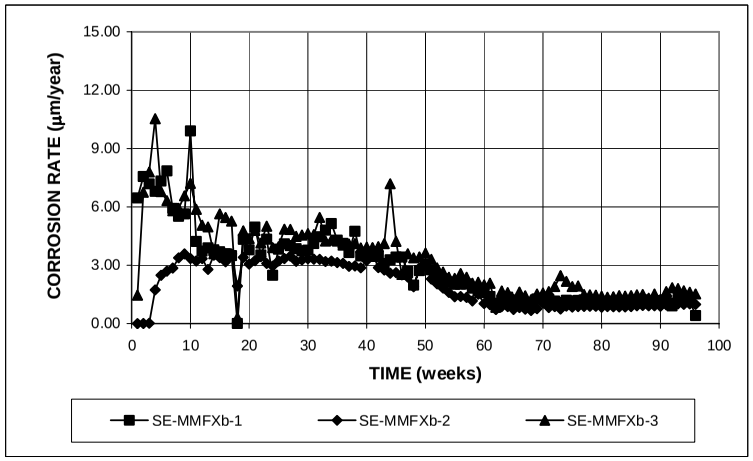

Figure A.86 - Southern Exposure test. Corrosion rates for bent MMFX steel, specimens w/c = 0.45, ponded with 15% NaCl solution, straight MMFX steel at the bottom mat.

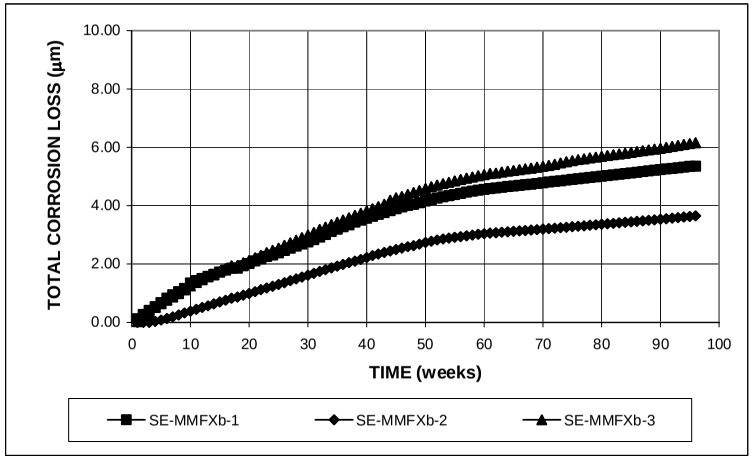

Figure A.87 - Southern Exposure test. Total corrosion losses of bent MMFX steel, specimens w/c = 0.45, ponded with 15% NaCl solution, straight MMFX steel at the bottom mat.

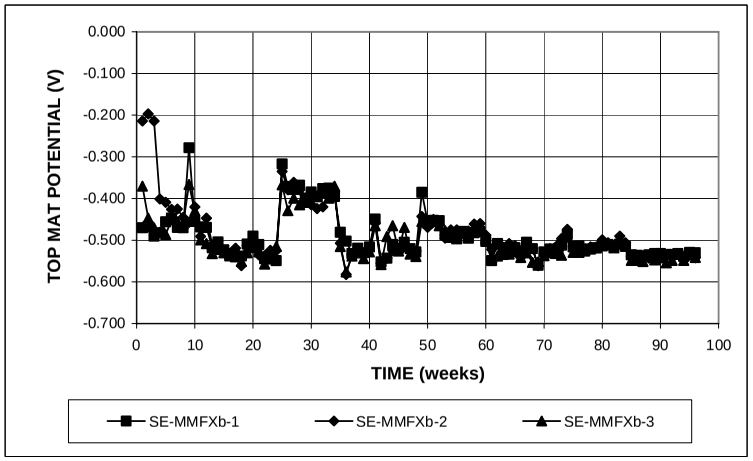

Figure A.88a - Southern Exposure test. Top mat corrosion potentials with respect to copper-copper sulfate electrode, bent MMFX steel at the top mat, straight MMFX steel at the bottom mat, specimens w/c = 0.45, ponded with 15% NaCl solution.

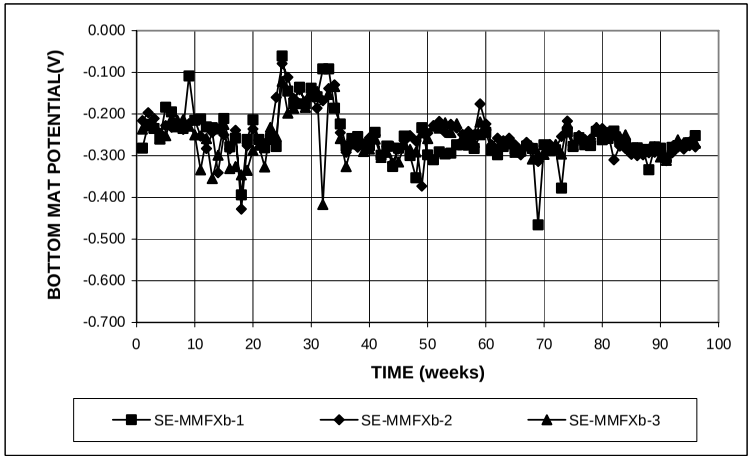

Figure A.88b - Southern Exposure test. Bottom mat corrosion potentials with respect to copper-copper sulfate electrode, bent MMFX steel at the top mat, straight MMFX steel at the bottom mat, specimens w/c = 0.45, ponded with 15% NaCl solution.

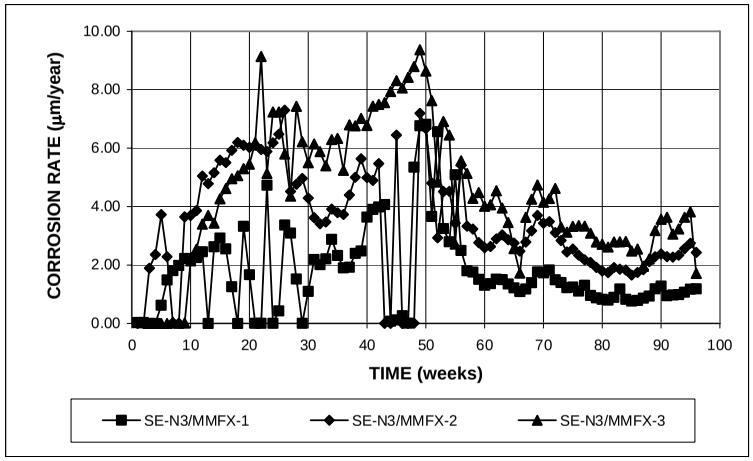

Figure A.89 - Southern Exposure test. Corrosion rates for conventional N3 steel, specimens w/c = 0.45, ponded with 15% NaCl solution, MMFX steel at the bottom mat.

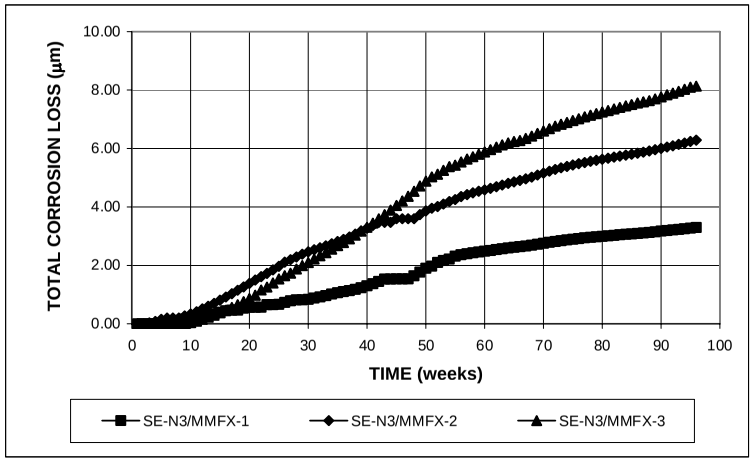

Figure A.90 - Southern Exposure test. Total corrosion losses of conventional N3 steel, specimens w/c = 0.45, ponded with 15% NaCl solution, MMFX steel at the bottom mat.

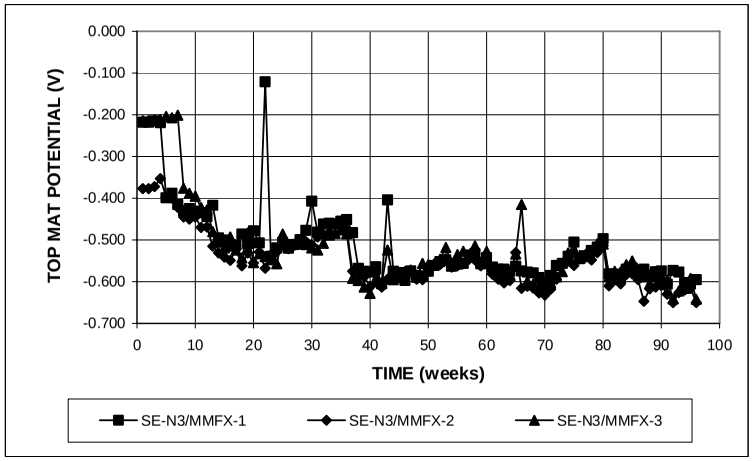

Figure A.91a - Southern Exposure test. Top mat corrosion potentials with respect to copper-copper sulfate electrode, conventional N3 steel at the top mat, MMFX steel at the bottom mat, specimens w/c = 0.45, ponded with 15% NaCl solution.

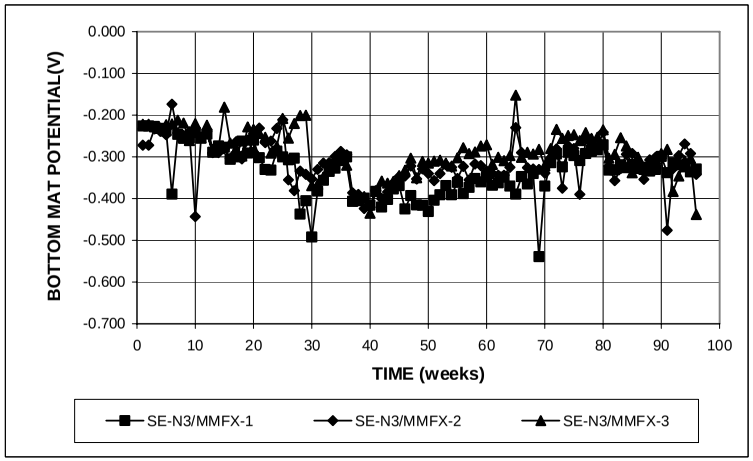

Figure A.91b - Southern Exposure test. Bottom mat corrosion potentials with respect to copper-copper sulfate electrode, conventional N3 steel at the top mat, MMFX steel at the bottom mat, specimens w/c = 0.45, ponded with 15% NaCl solution.

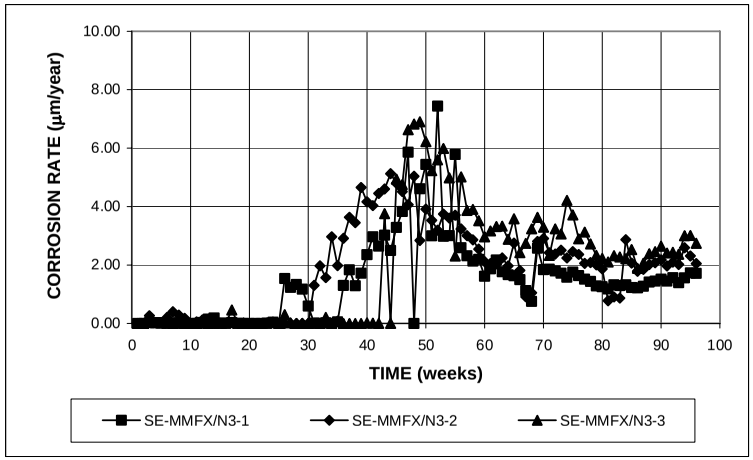

Figure A.92 - Southern Exposure test. Corrosion rates for MMFX steel, specimens w/c = 0.45, ponded with 15% NaCl solution, conventional N3 steel at the bottom mat.

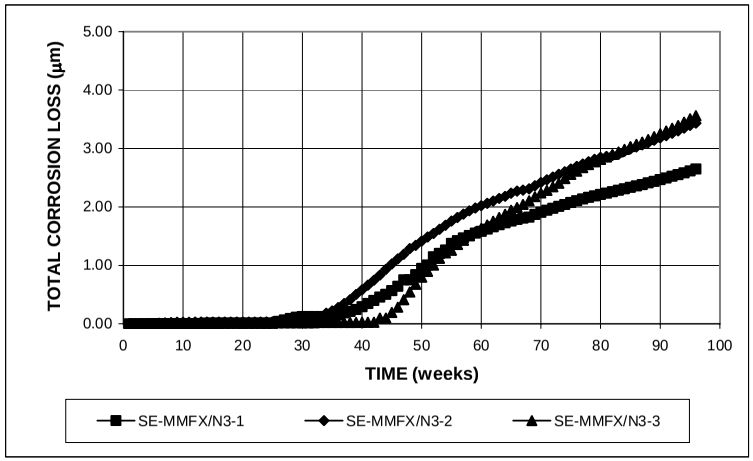

Figure A.93 - Southern Exposure test. Total corrosion losses of MMFX steel, specimens w/c = 0.45, ponded with 15% NaCl solution, conventional N3 steel at the bottom mat.

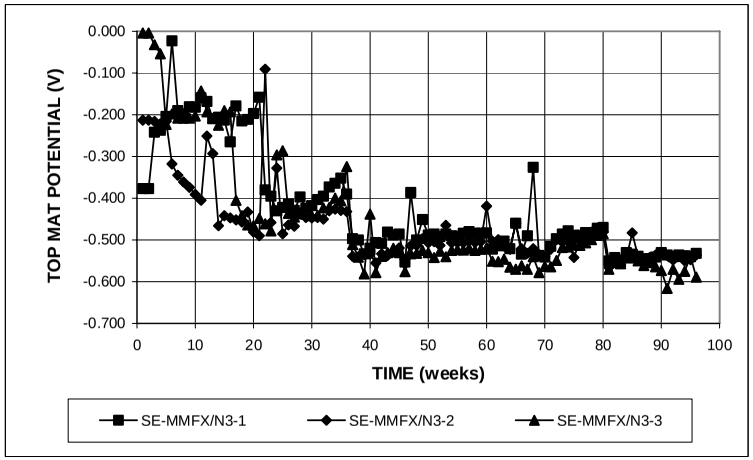

Figure A.94a - Southern Exposure test. Top mat corrosion potentials with respect to copper-copper sulfate electrode, MMFX steel at the top mat, conventional N3 steel at the bottom, specimens w/c = 0.45, ponded with 15% NaCl solution.

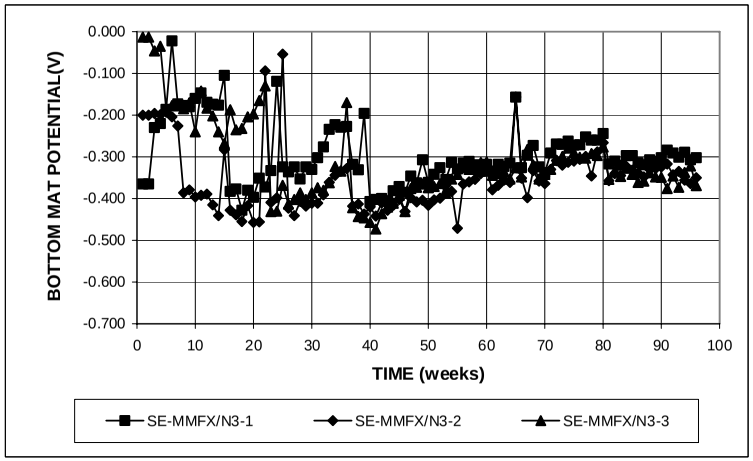

Figure A.94b - Southern Exposure test. Bottom mat corrosion potentials with respect to copper-copper sulfate electrode, MMFX steel at the top mat, conventional N3 steel at the bottom, specimens w/c = 0.45, ponded with 15% NaCl solution.

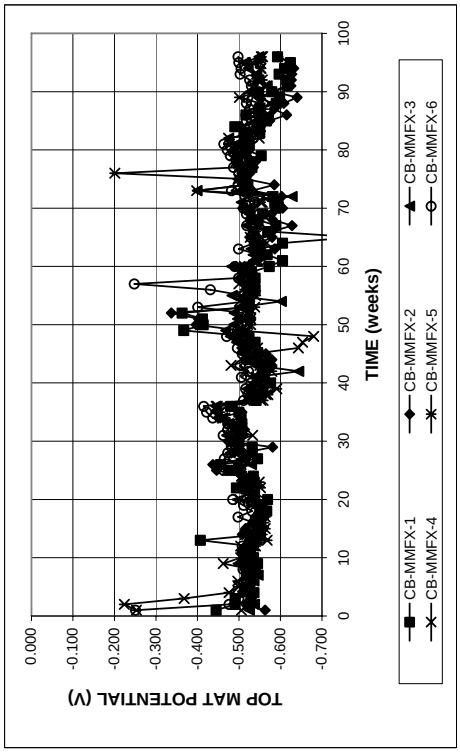

Figure A.97a - Cracked beam test. Top mat corrosion potentials with respect to copper-copper sulfate electrode for MMFX steel, specimens w/c = 0.45, ponded with 15% NaCl solution.

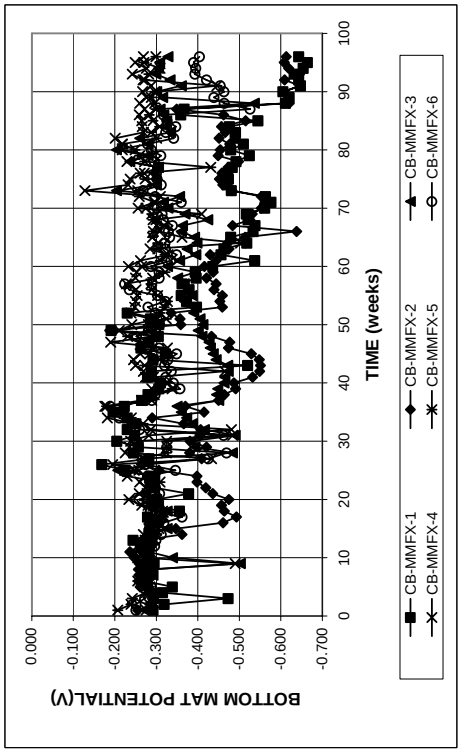

Figure A.97b - Cracked beam test. Bottom mat corrosion potentials with respect to copper-copper sulfate electrode for MMFX steel, specimens w/c = 0.45, ponded with 15% NaCl solution.

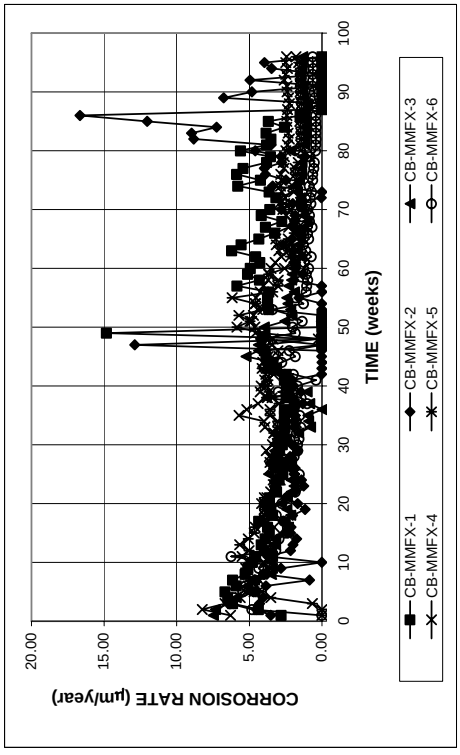

Figure A.95 - Cracked beam test. Corrosion rates for MMFX steel, specimens w/c = 0.45, ponded with 15% NaCl solution.

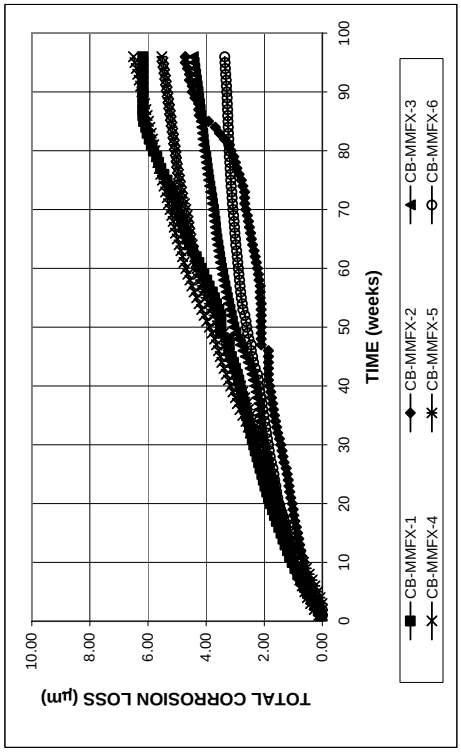

Figure A.96 -Cracked beam test. Total corrosion losses for MMFX steel, specimens w/c = 0.45, ponded with 15% NaCl solution.

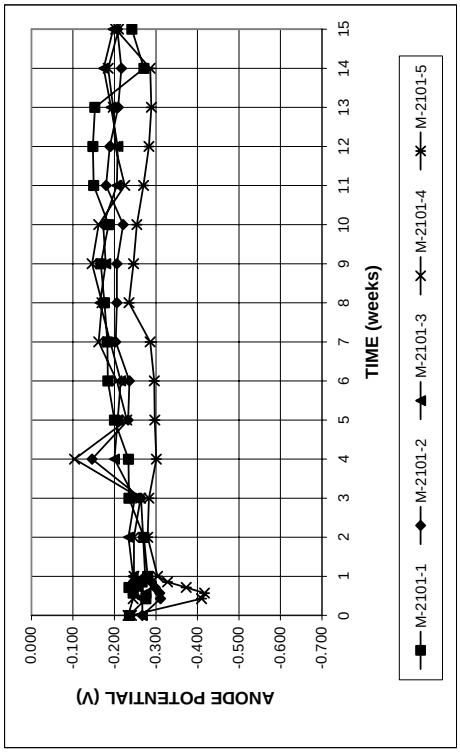

Figure A.100a - Macrocell test. Anode corrosion potentials with respect to saturated calomel electrode for bare 2101 duplex steel in simulated concrete pore solution with 1.6 molal ion NaCl.

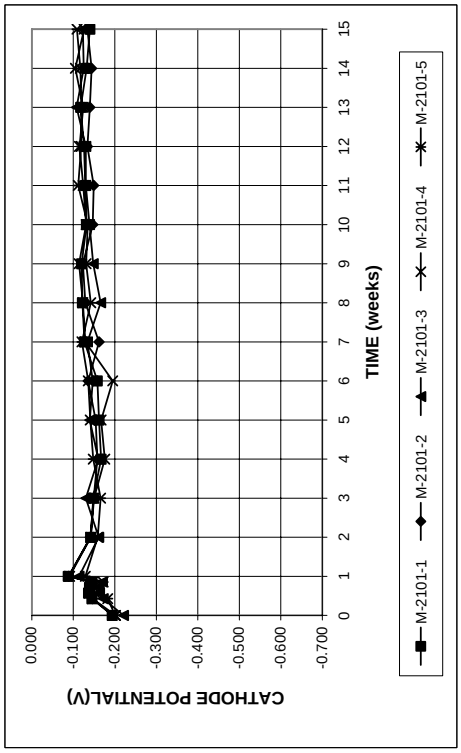

Figure A.100b - Macrocell test. Cathode corrosion potentials with respect to saturated calomel electrode for bare 2101 duplex steel in simulated concrete pore solution with 1.6 molal ion NaCl.

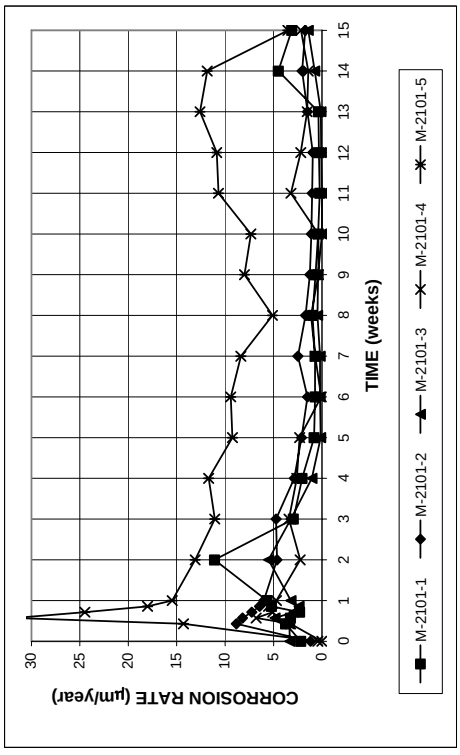

Figure A.98 - Macrocell test. Corrosion rates for bare 2101 duplex steel in simulated concrete pore solution with 1.6 molal ion NaCl.

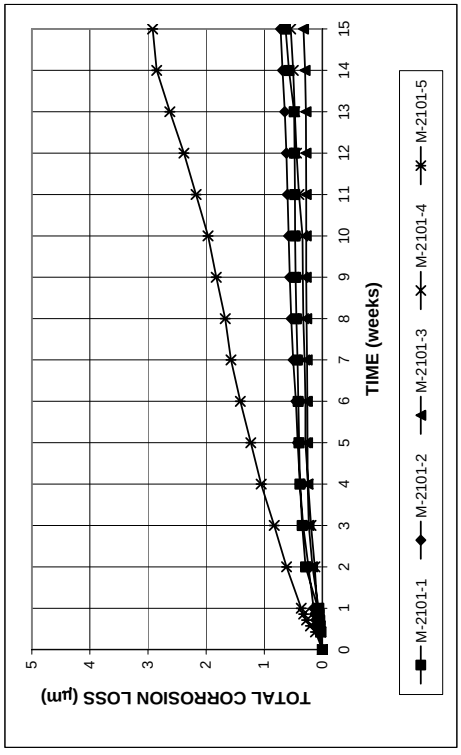

Figure A.99 - Macrocell test. Total corrosion losses for bare 2101 duplex steel in simulated concrete pore solution with 1.6 molal ion NaCl.

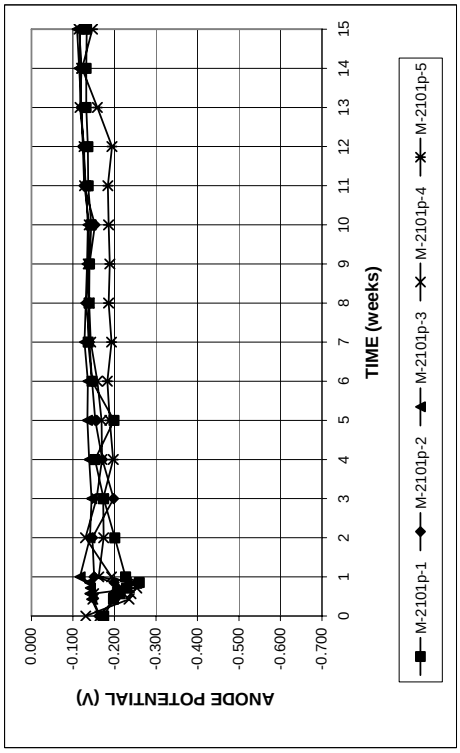

Figure A.103a - Macrocell test. Anode corrosion potentials with respect to saturated calomel electrode for bare pickled 2101 duplex steel in simulated concrete pore solution with 1.6 molal ion NaCl.

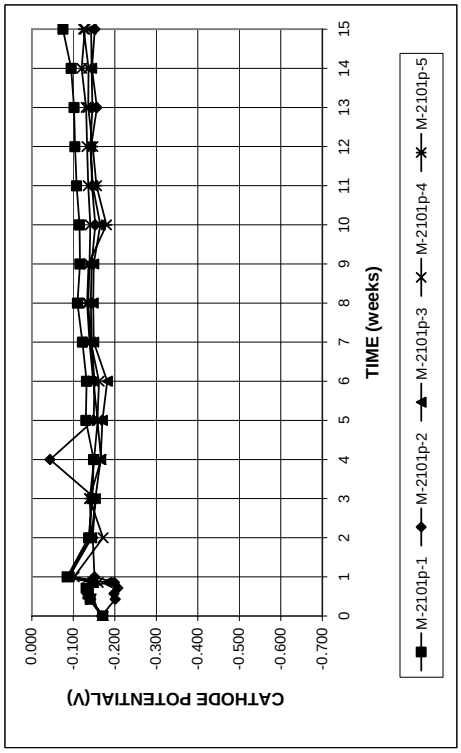

Figure A.103b - Macrocell test. Cathode corrosion potentials with respect to saturated calomel electrode for bare pickled 2101 duplex steel in simulated concrete pore solution with 1.6 molal ion NaCl.

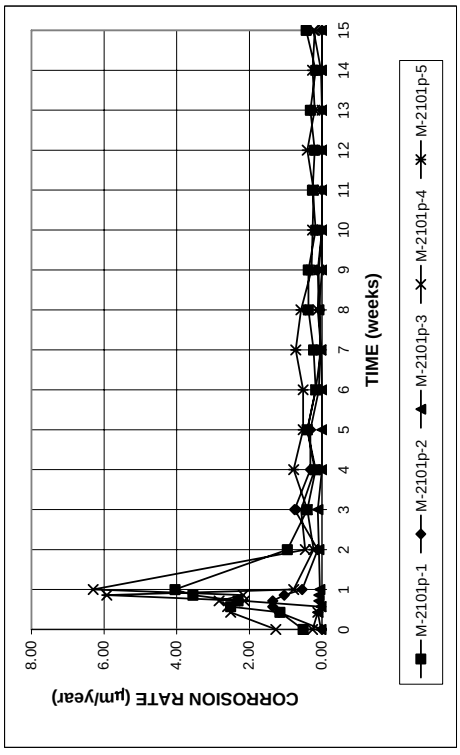

Figure A.101 - Macrocell test. Corrosion rates for bare pickled 2101 duplex steel in simulated concrete pore solution with 1.6 molal ion NaCl.

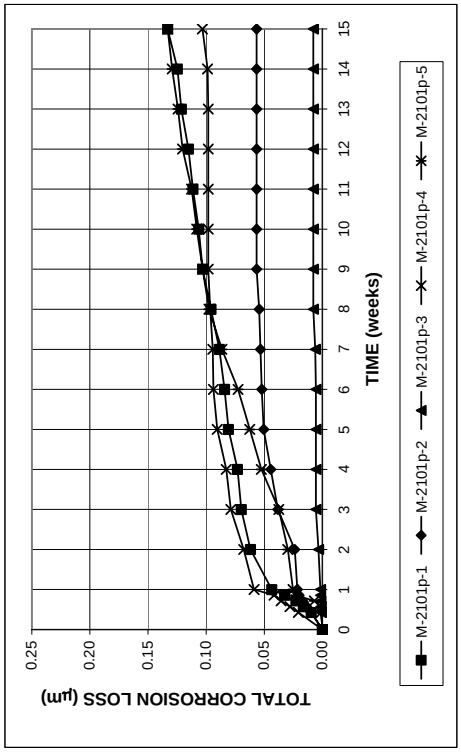

Figure A.102 - Macrocell test. Total corrosion losses for bare pickled 2101 duplex steel in simulated concrete pore solution with 1.6 molal ion NaCl.

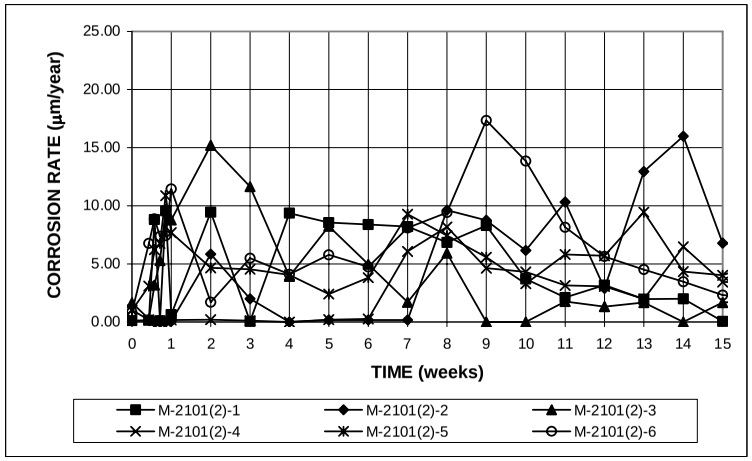

Figure A.104 - Macrocell test. Corrosion rates for bare 2101(2) duplex steel in simulated concrete pore solution with 1.6 molal ion NaCl.

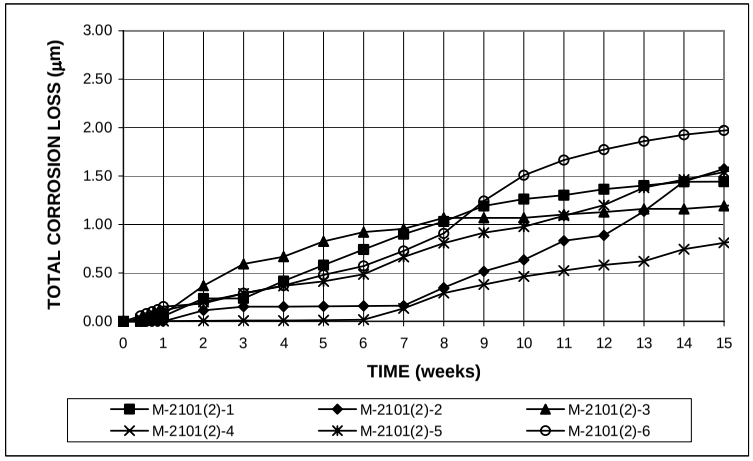

Figure A.105 - Macrocell test. Total corrosion losses for bare 2101(2) duplex steel in simulated concrete pore solution with 1.6 molal ion NaCl.

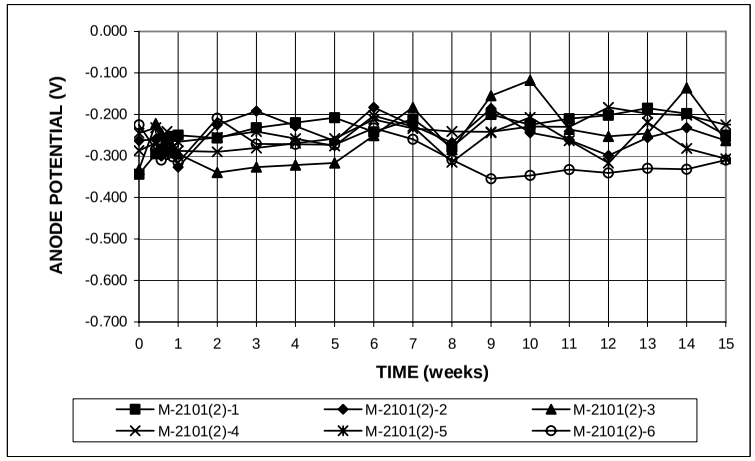

Figure A.106a - Macrocell test. Anode corrosion potentials with respect to saturated calomel electrode for bare 2101(2) duplex steel in simulated concrete pore solution with 1.6 molal ion NaCl.

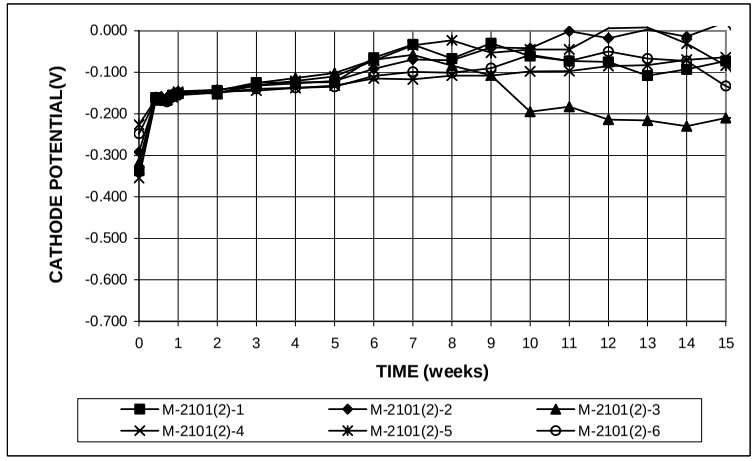

Figure A.106b - Macrocell test. Cathode corrosion potentials with respect to saturated calomel electrode for bare 2101(2) duplex steel in simulated concrete pore solution with 1.6 molal ion NaCl.

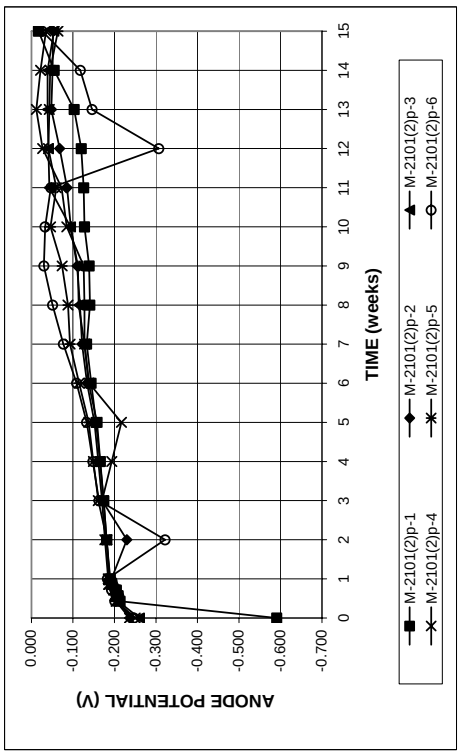

Figure A.109a - Macrocell test. Anode corrosion potentials with respect to saturated calomel electrode for bare pickled 2101(2) duplex steel in simulated concrete pore solution with 1.6 molal ion NaCl.

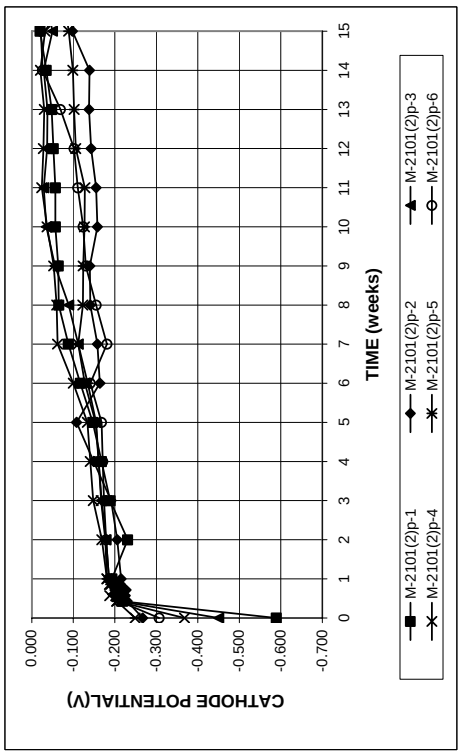

Figure A.109b - Macrocell test. Cathode corrosion potentials with respect to saturated calomel electrode for bare pickled 2101(2) duplex steel in simulated concrete pore solution with 1.6 molal ion NaCl.

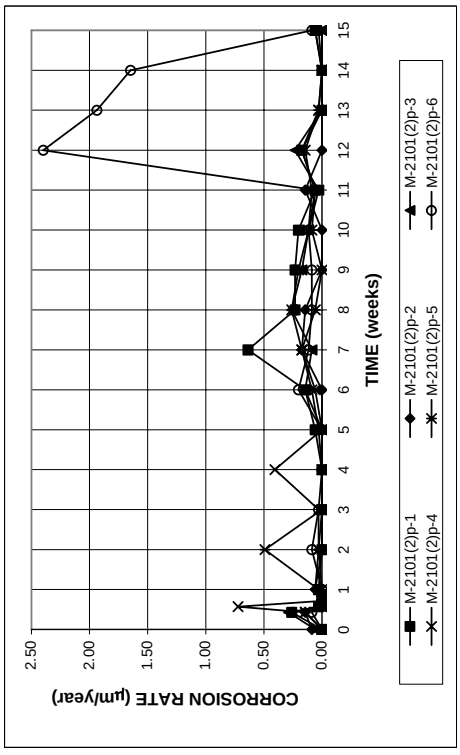

Figure A.107 - Macrocell test. Corrosion rates for bare pickled 2101(2) duplex steel in simulated concrete pore solution with 1.6 molal ion NaCl.

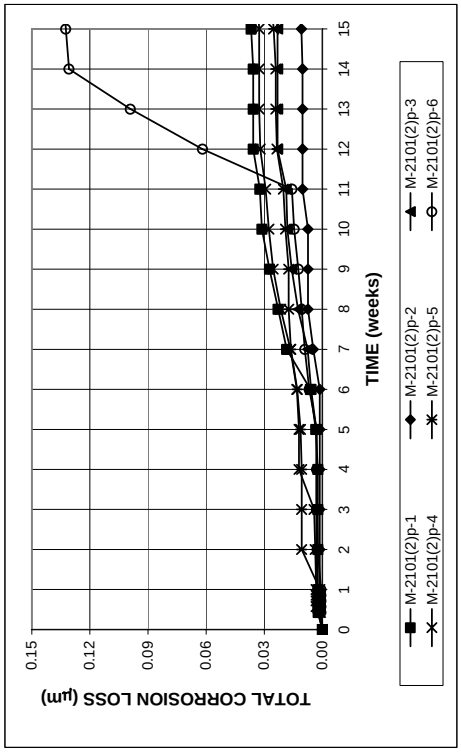

Figure A.108 - Macrocell test. Total corrosion losses for bare pickled 2101(2) duplex steel in simulated concrete pore solution with 1.6 molal ion NaCl.

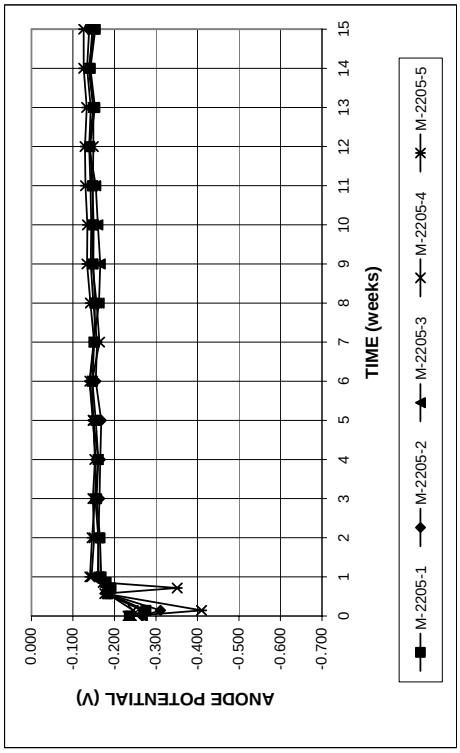

Figure A.112a - Macrocell test. Anode corrosion potentials with respect to saturated calomel electrode for bare 2205 duplex steel in simulated concrete pore solution with 1.6 molal ion NaCl.

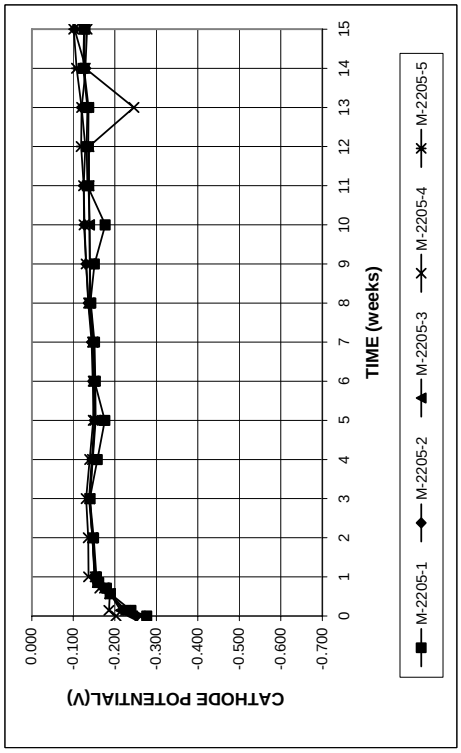

Figure A.112b - Macrocell test. Cathode corrosion potentials with respect to saturated calomel electrode for bare 2205 duplex steel in simulated concrete pore solution with 1.6 molal ion NaCl.

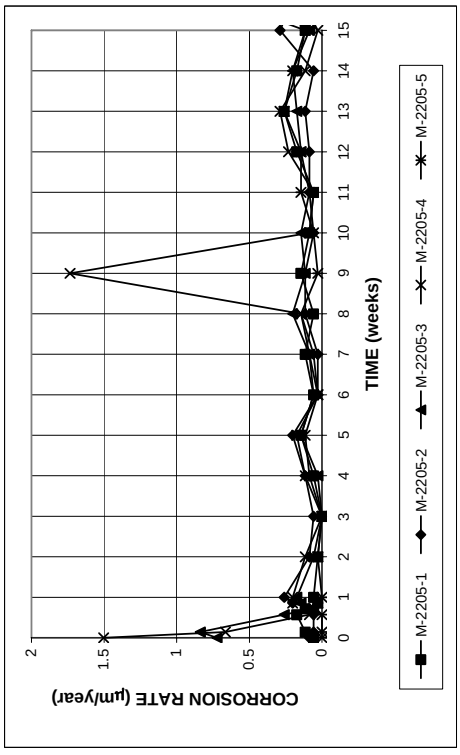

Figure A.110 - Macrocell test. Corrosion rates for bare 2205 duplex steel in simulated concrete pore solution with 1.6 molal ion NaCl.

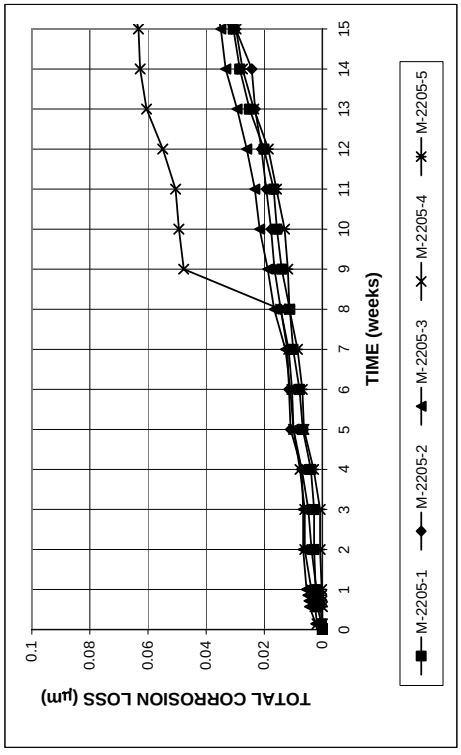

Figure A.111 - Macrocell test. Total corrosion losses for bare 2205 duplex steel in simulated concrete pore solution with 1.6 molal ion NaCl.

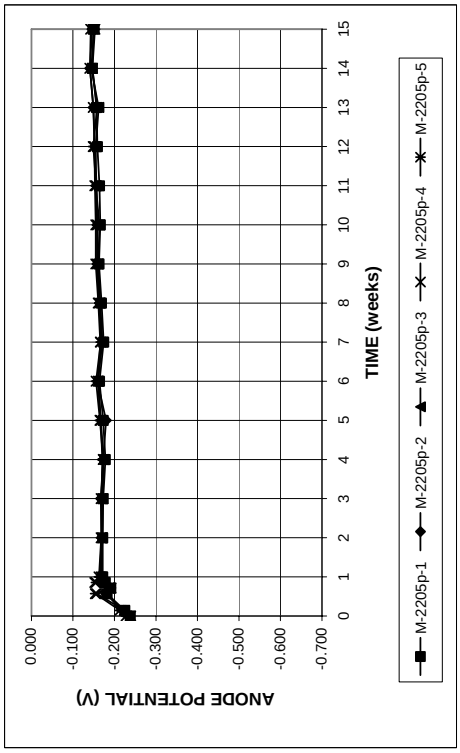

Figure A.115a - Macrocell test. Anode corrosion potentials with respect to saturated calomel electrode for bare pickled 2205 duplex steel in simulated concrete pore solution with 1.6 molal ion NaCl.

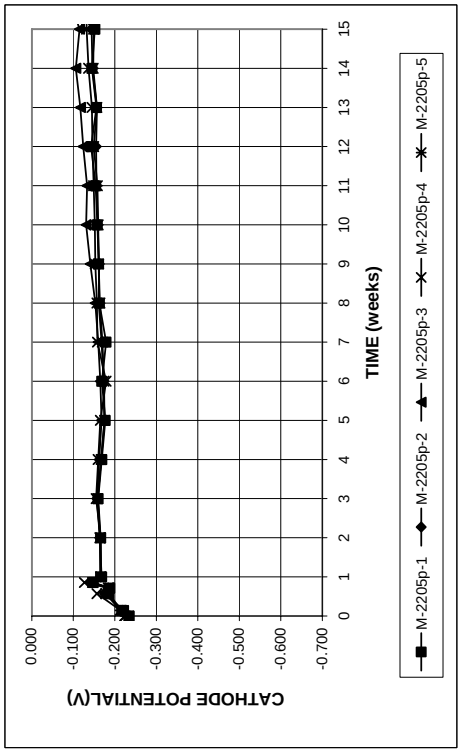

Figure A.115b - Macrocell test. Cathode corrosion potentials with respect to saturated calomel electrode for bare pickled 2205 duplex steel in simulated concrete pore solution with 1.6 molal ion NaCl.

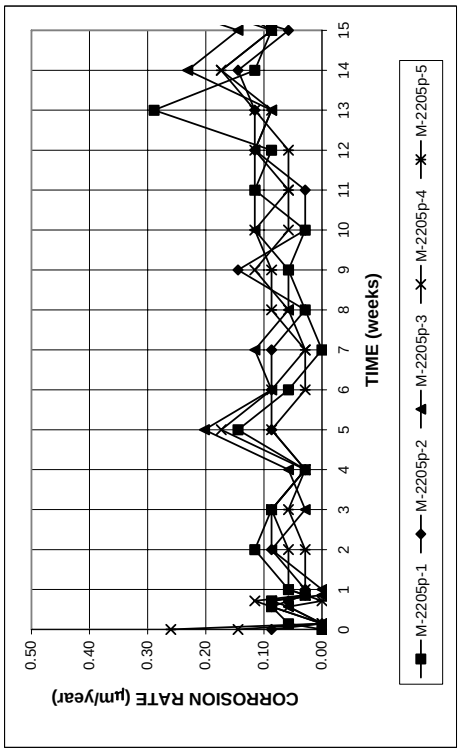

Figure A.113 - Macrocell test. Corrosion rates for bare pickled 2205 duplex steel in simulated concrete pore solution with 1.6 molal ion NaCl.

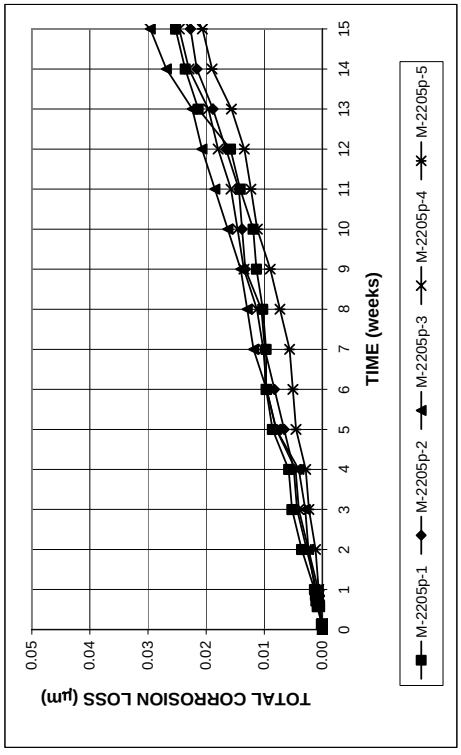

Figure A.114 - Macrocell test. Total corrosion losses for bare pickled 2205 duplex steel in simulated concrete pore solution with 1.6 molal ion NaCl.

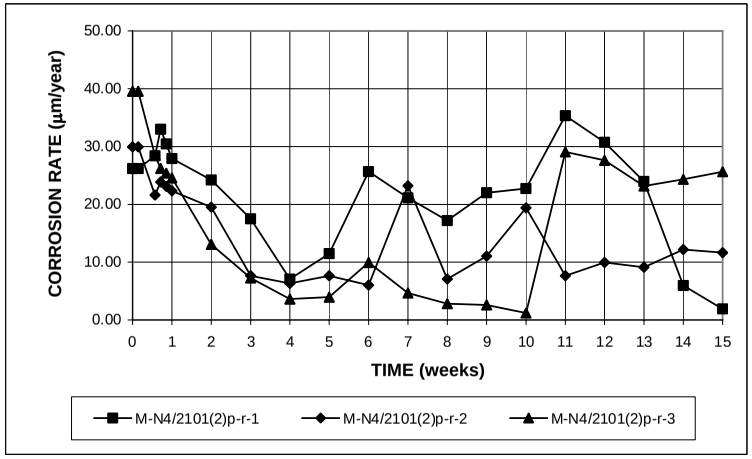

Figure A.116 - Macrocell Test. Corrosion rates for bare conventional N4 steel in simulated concrete pore solution with 1.6 molal ion NaCl, with bare pickled 2101(2) duplex steel as the cathode. Solutions are replaced every 5 weeks.

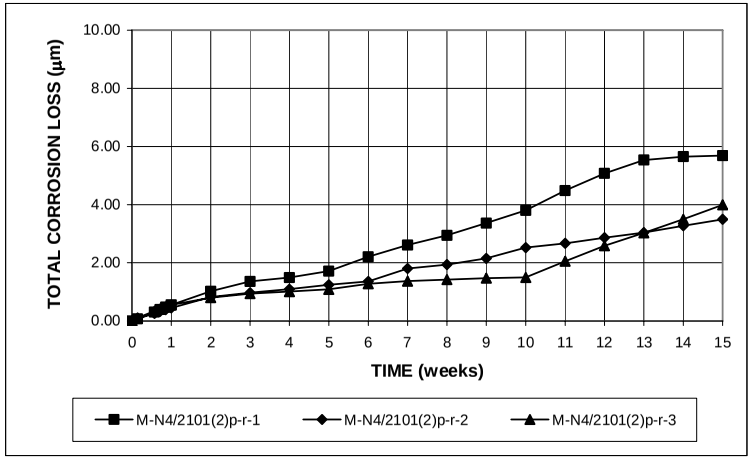

Figure A.117 - Macrocell Test. Total corrosion losses for bare conventional N4 steel in simulated concrete pore solution with 1.6 molal ion NaCl, with bare pickled 2101(2) duplex steel as the cathode. Solutions are replaced every 5 weeks.

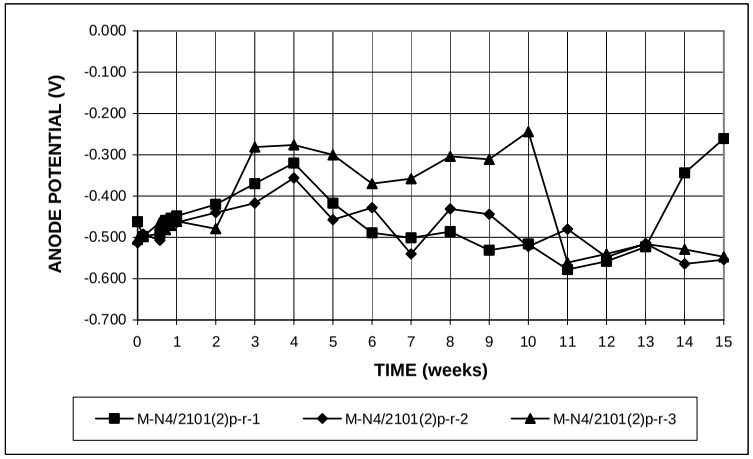

Figure A.118a -Macrocell Test. Anode corrosion potentials vs. saturated calomel electrode, bare conventional N4 steel as the anode in simulated concrete pore solution with 1.6 molal ion NaCl, bare pickled 2101(2) steel as the cathode. Solutions are replaced every 5 weeks.

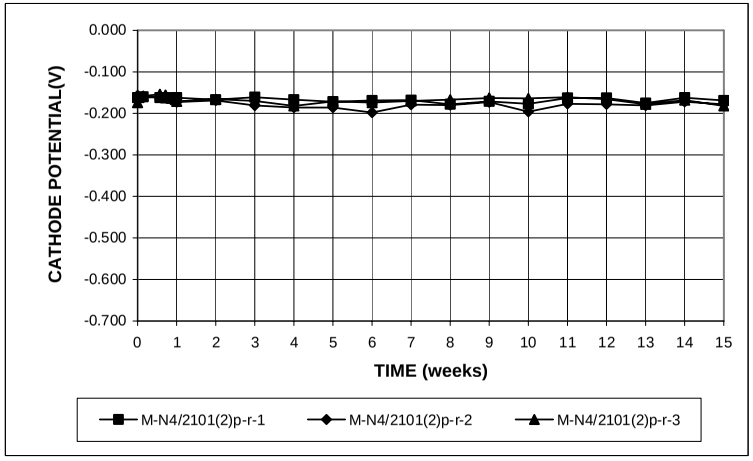

Figure A.118b - Macrocell Test. Cathode corrosion potentials vs. saturated calomel electrode, bare conventional N4 steel as the anode in simulated concrete pore solution with 1.6 molal ion NaCl, pickled 2101(2) steel as the cathode. Solutions are replaced every 5 weeks.

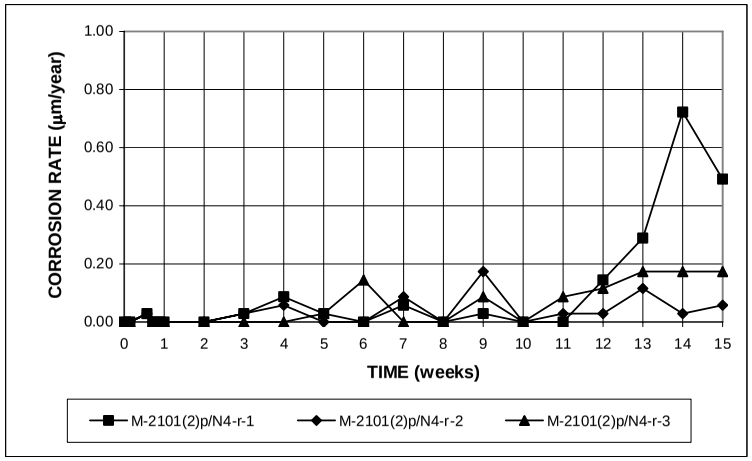

Figure A.119 - Macrocell Test. Corrosion rates for bare pickled 2101(2) steel in simulated concrete pore solution with 1.6 molal ion NaCl, with bare conventional N4 steel as the cathode. Solutions are replaced every 5 weeks.

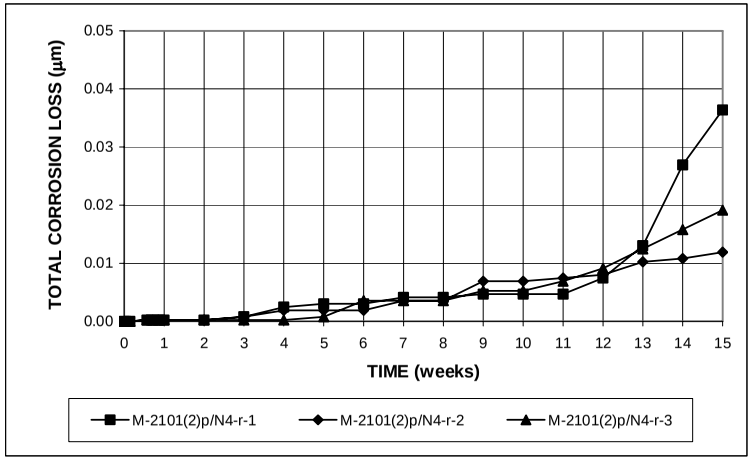

Figure A.120 - Macrocell Test. Total corrosion losses for bare pickled 2101(2) steel in simulated concrete pore solution with 1.6 molal ion NaCl, with bare conventional N4 steel as the cathode. Solutions are replaced every 5 weeks.

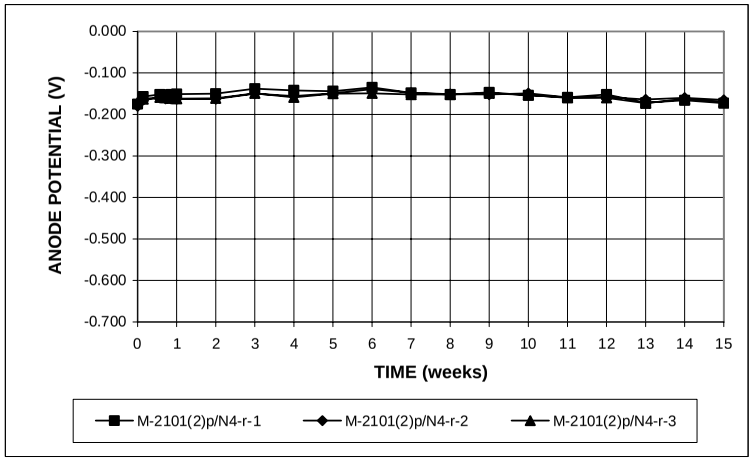

Figure A.121a -Macrocell Test. Anode corrosion potentials vs. saturated calomel electrode, bare pickled 2101(2) steel as the anode in simulated concrete pore solution with 1.6 molal ion NaCl, conventional N4 steel as the cathode. Solutions are replaced every 5 weeks.

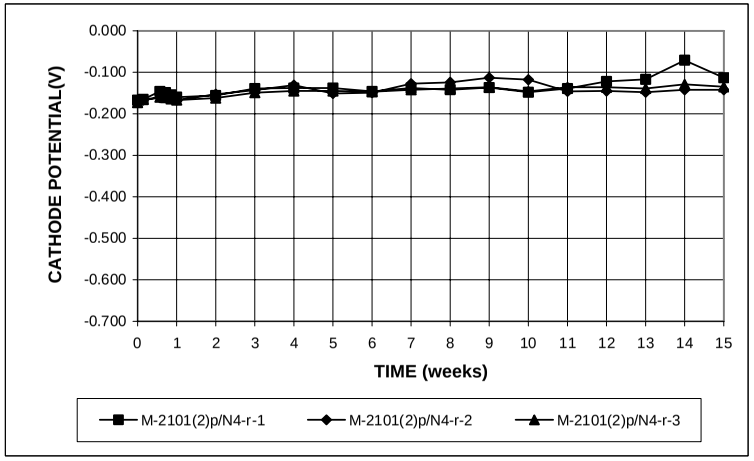

Figure A.121b - Macrocell Test. Anode corrosion potentials vs. saturated calomel electrode, bare pickled 2101(2) steel as the anode in simulated concrete pore solution with 1.6 molal ion NaCl, conventional N4 steel as the cathode. Solutions are replaced every 5 weeks.

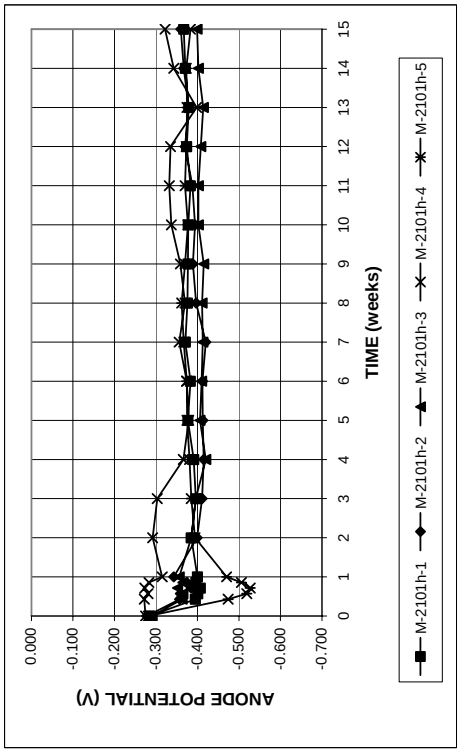

Figure A.124a - Macrocell test. Anode corrosion potentials with respect to saturated calomel electrode for bare 2101 duplex steel in simulated concrete pore solution with 6.04 molal ion NaCl.

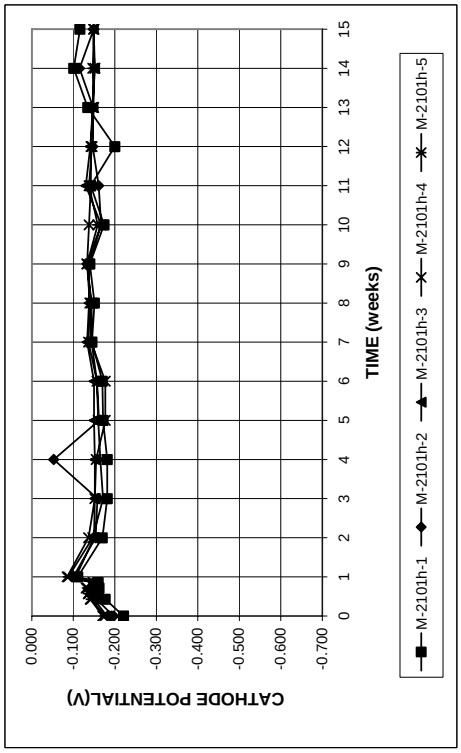

Figure A.124b - Macrocell test. Cathode corrosion potentials with respect to saturated calomel electrode for bare 2101 duplex steel in simulated concrete pore solution with 6.04 molal ion NaCl.

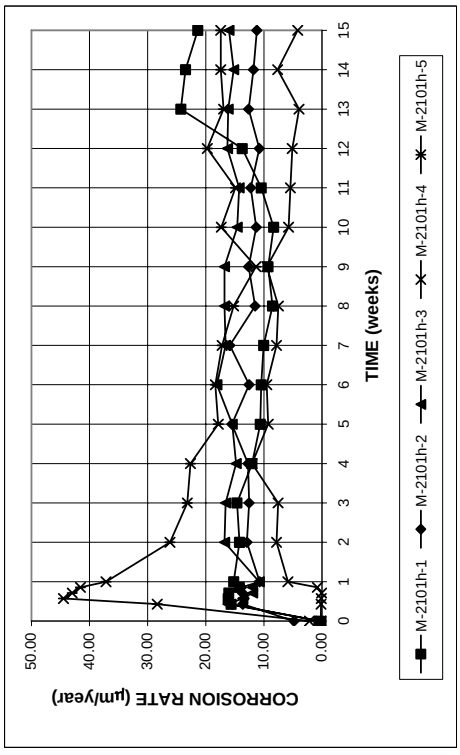

Figure A.122 - Macrocell test. Corrosion rates for bare 2101 duplex steel in simulated concrete pore solution with 6.04 molal ion NaCl.

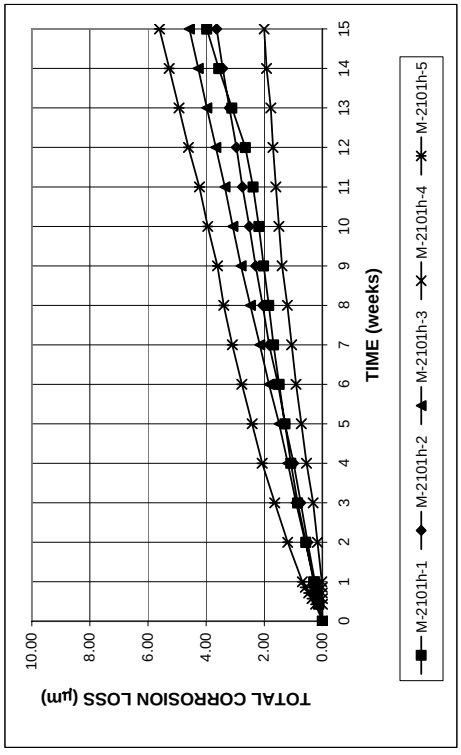

Figure A.123 - Macrocell test. Total corrosion losses for bare 2101 duplex steel in simulated concrete pore solution with 6.04 molal ion NaCl.

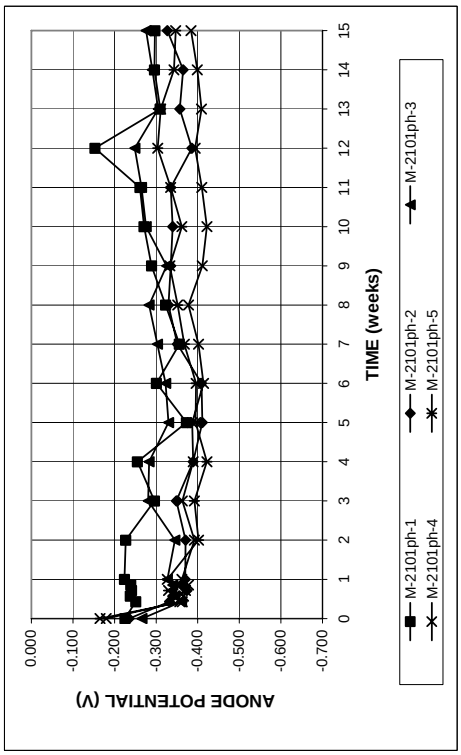

Figure A.127a - Macrocell test. Anode corrosion potentials with respect to saturated calomel electrode for bare pickled 2101 duplex steel in simulated concrete pore solution with 6.04 molal ion NaCl.

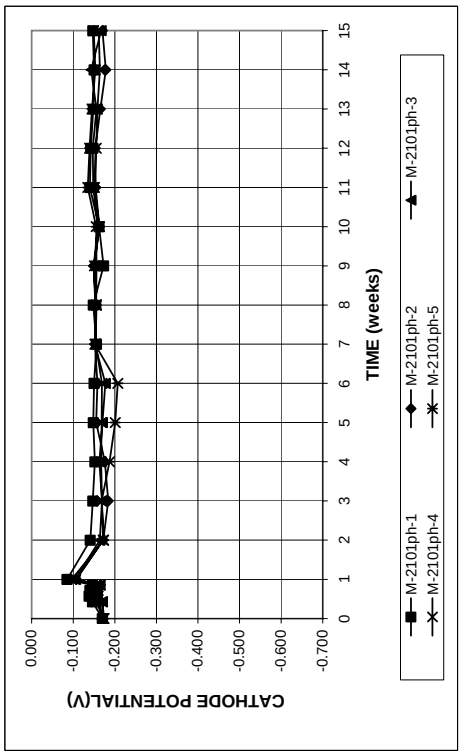

Figure A.127b - Macrocell test. Cathode corrosion potentials with respect to saturated calomel electrode for bare pickled 2101 duplex steel in simulated concrete pore solution with 6.04 molal ion NaCl.

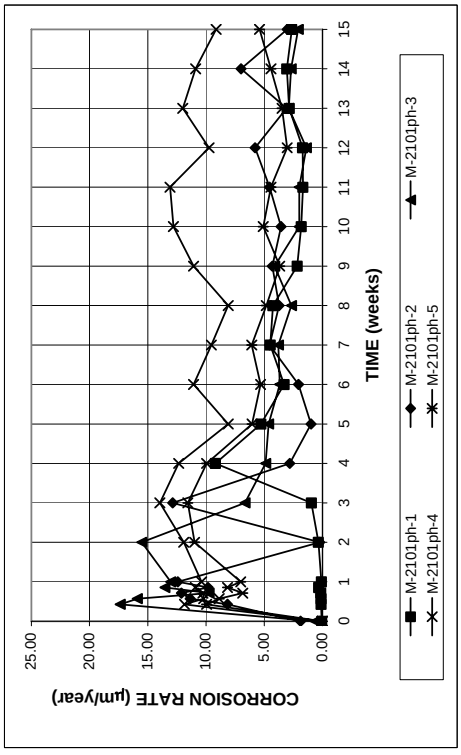

Figure A.125 - Macrocell test. Corrosion rates for bare pickled 2101 duplex steel in simulated concrete pore solution with 6.04 molal ion NaCl.

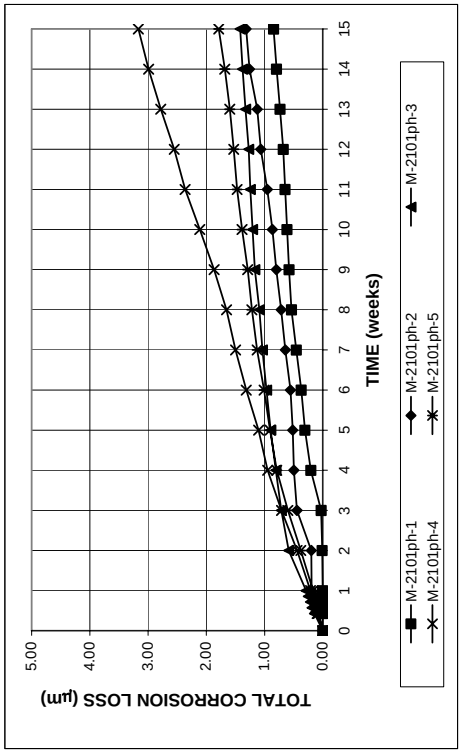

Figure A.126 - Macrocell test. Total corrosion losses for bare pickled 2101 duplex steel in simulated concrete pore solution with 6.04 molal ion NaCl.

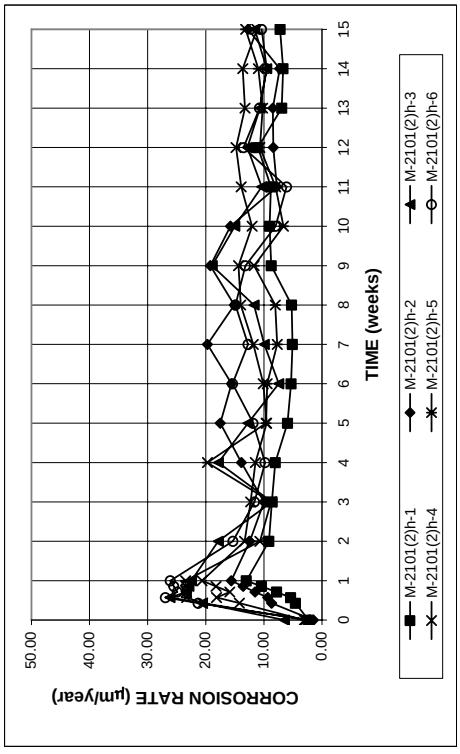

Figure A.128 - Macrocell test. Corrosion rates for bare 2101(2) duplex steel in simulated concrete pore solution with 6.04 molal ion NaCl.

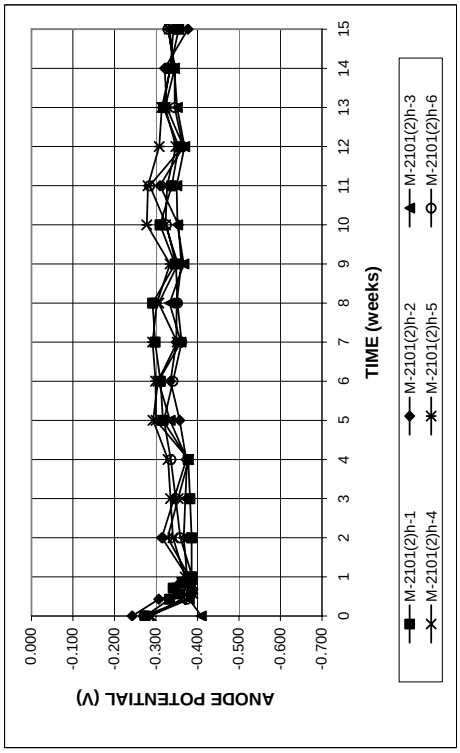

Figure A.130a - Macrocell test. Anode corrosion potentials with respect to saturated calomel electrode for bare 2101(2) duplex steel in simulated concrete pore solution with 6.04 molal ion NaCl.

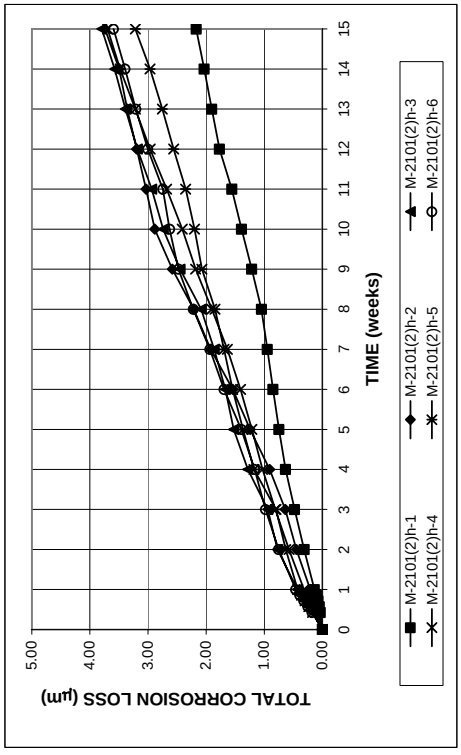

Figure A.129 - Macrocell test. Total corrosion losses for bare 2101(2) duplex steel in simulated concrete pore solution with 6.04 molal ion NaCl.

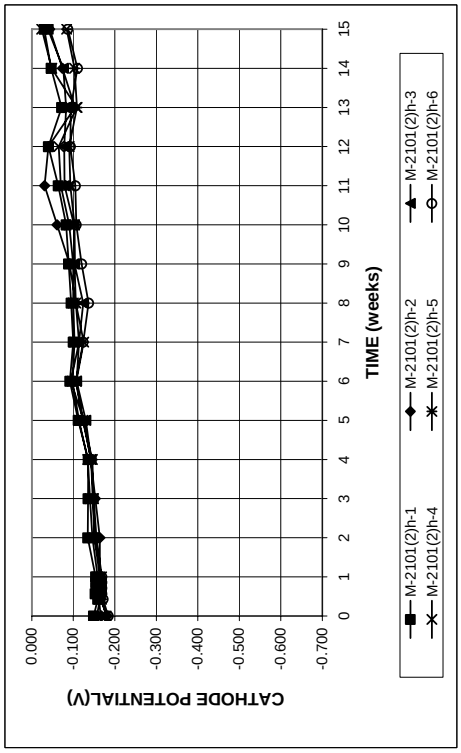

Figure A.130b - Macrocell test. Cathode corrosion potentials with respect to saturated calomel electrode for bare 2101(2) duplex steel in simulated concrete pore solution with 6.04 molal ion NaCl.

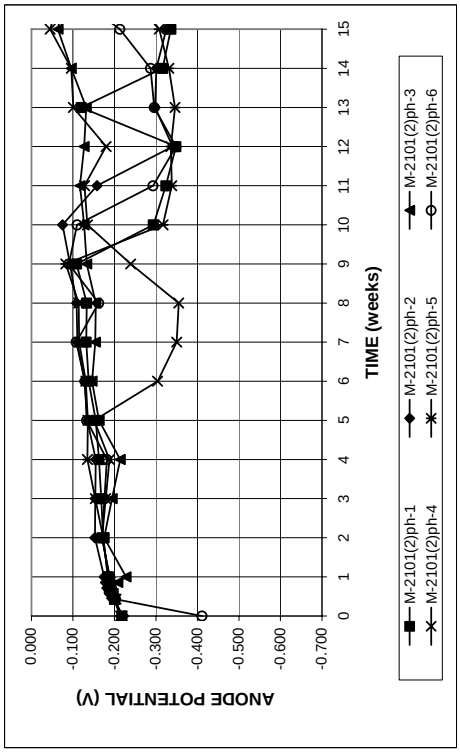

Figure A.133a - Macrocell test. Anode corrosion potentials with respect to saturated calomel electrode for bare pickled 2101(2) duplex steel in simulated concrete pore solution with 6.04 molal ion NaCl.

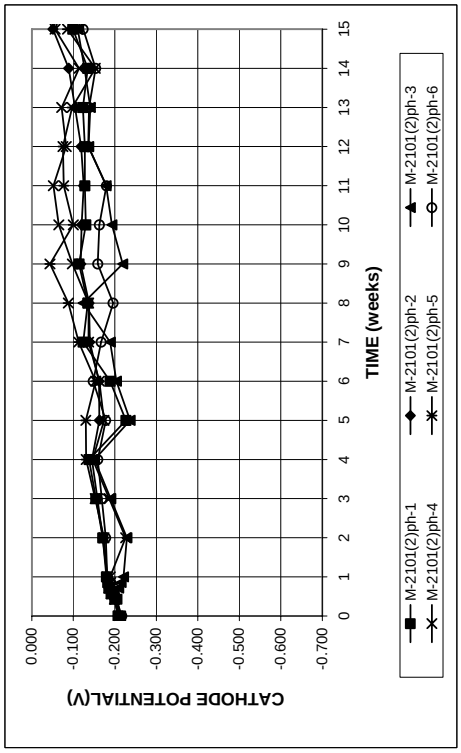

Figure A.133b - Macrocell test. Cathode corrosion potentials with respect to saturated calomel electrode for bare pickled 2101(2) duplex steel in simulated concrete pore solution with 6.04 molal ion NaCl.

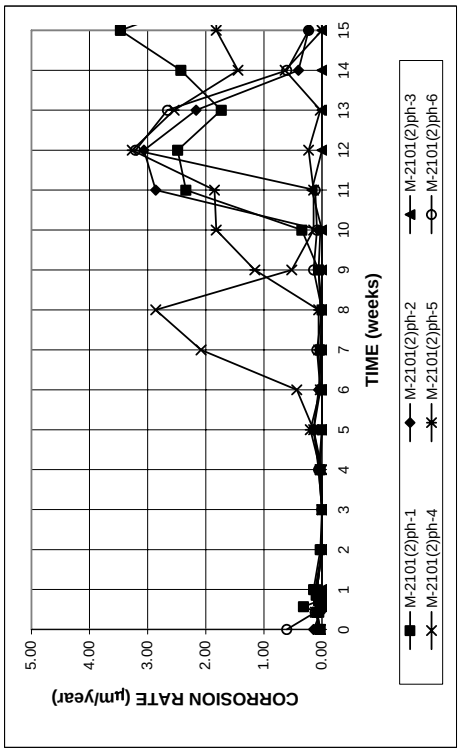

Figure A.131 - Macrocell test. Corrosion rates for bare pickled 2101(2) duplex steel in simulated concrete pore solution with 6.04 molal ion NaCl.

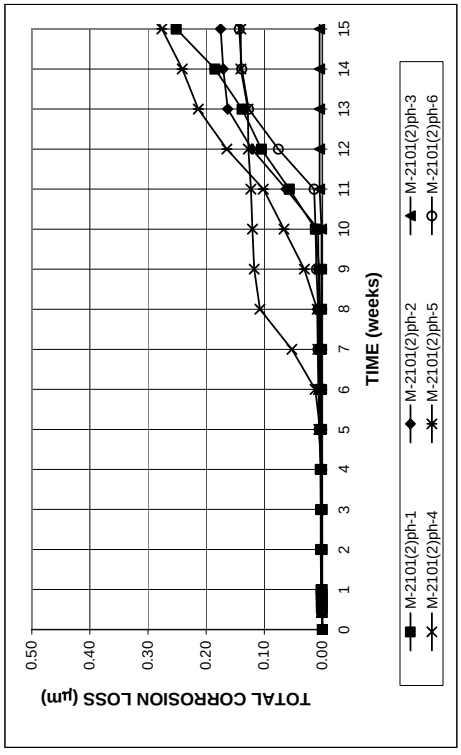

Figure A.132 - Macrocell test. Total corrosion losses for bare pickled 2101(2) duplex steel in simulated concrete pore solution with 6.04 molal ion NaCl.

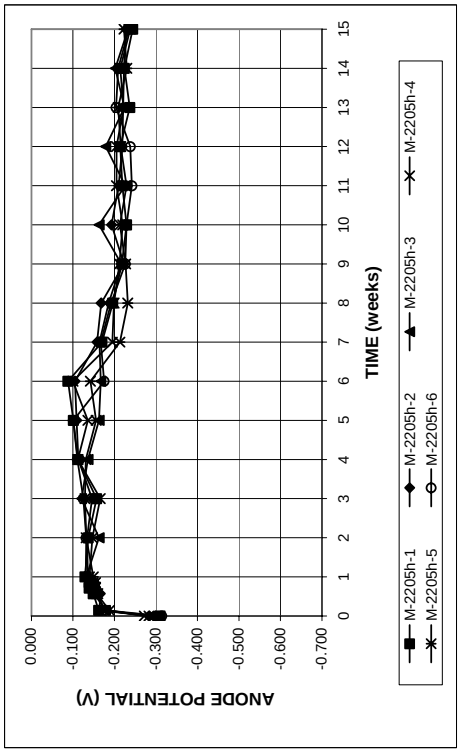

Figure A.136a - Macrocell test. Anode corrosion potentials with respect to saturated calomel electrode for bare 2205 duplex steel in simulated concrete pore solution with 6.04 molal ion NaCl.

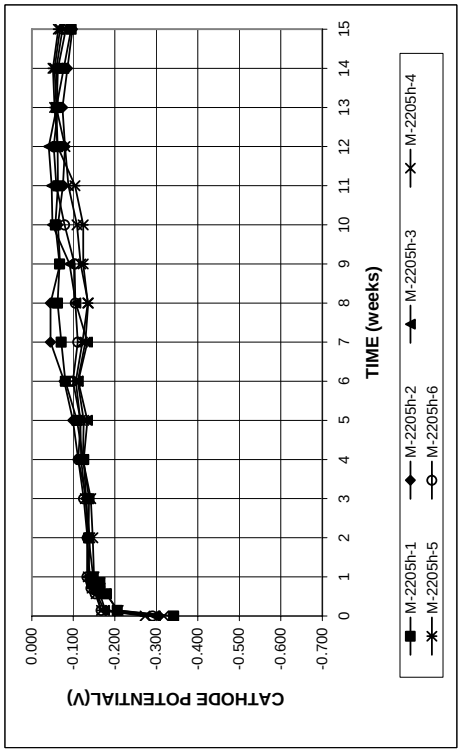

Figure A.136b - Macrocell test. Cathode corrosion potentials with respect to saturated calomel electrode for bare 2205 duplex steel in simulated concrete pore solution with 6.04 molal ion NaCl.

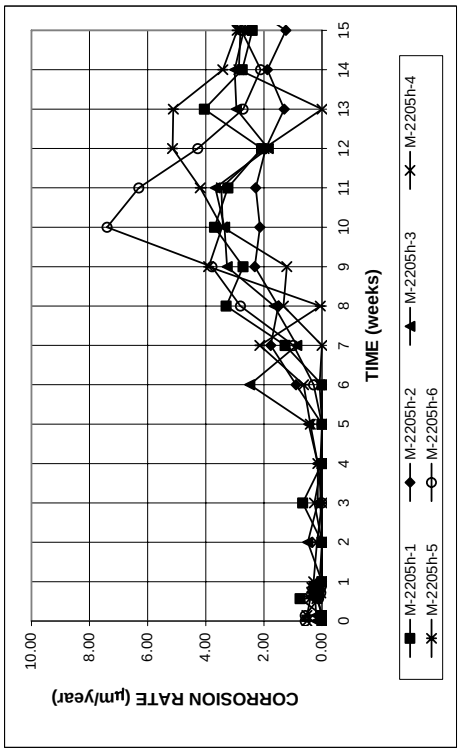

Figure A.134 - Macrocell test. Corrosion rates for bare 2205 duplex steel in simulated concrete pore solution with 6.04 molal ion NaCl.

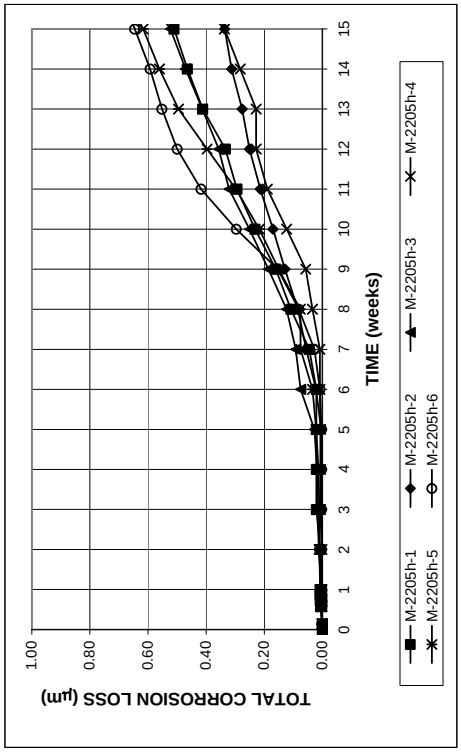

Figure A.135 -Macrocell test. Total corrosion losses for bare 2205 duplex steel in simulated concrete pore solution with 6.04 molal ion NaCl.

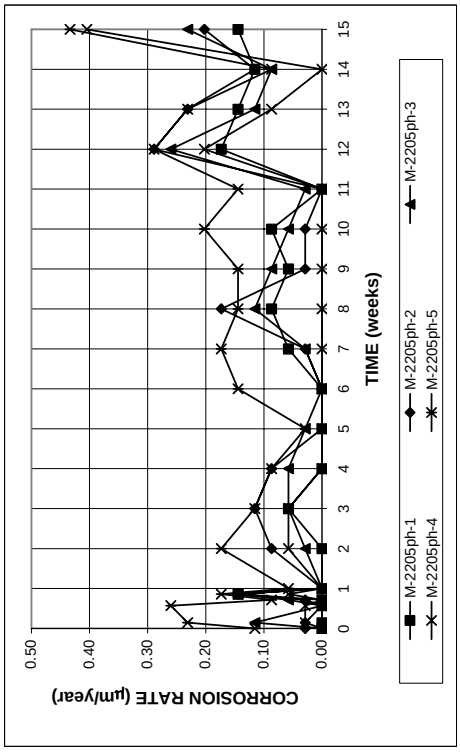

Figure A.137 - Macrocell test. Corrosion rates for bare pickled 2205 duplex steel in simulated concrete pore solution with 6.04 molal ion NaCl.

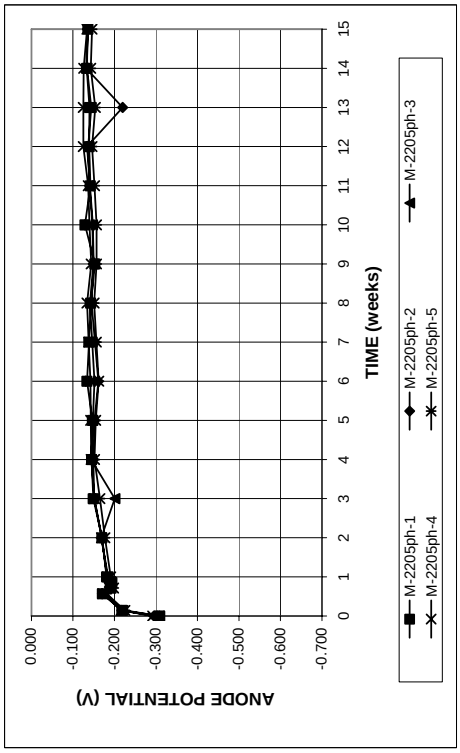

Figure A.139a - Macrocell test. Anode corrosion potentials with respect to saturated calomel electrode for bare pickled 2205 duplex steel in simulated concrete pore solution with 6.04 molal ion NaCl.

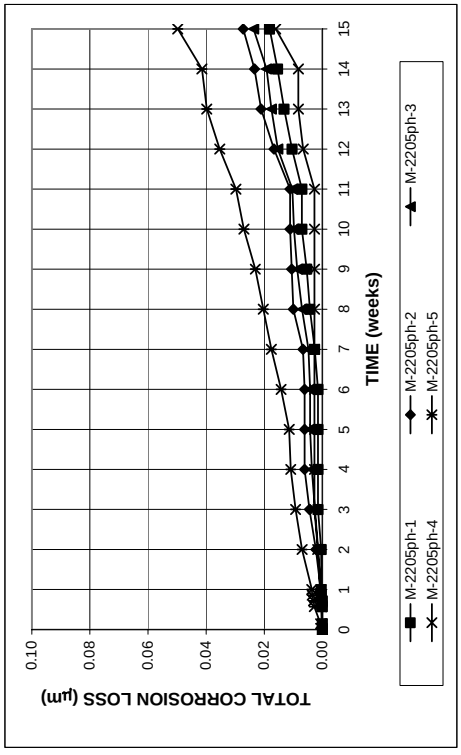

Figure A.138 - Macrocell test. Total corrosion losses for bare pickled 2205 duplex steel in simulated concrete pore solution with 6.04 molal ion NaCl.

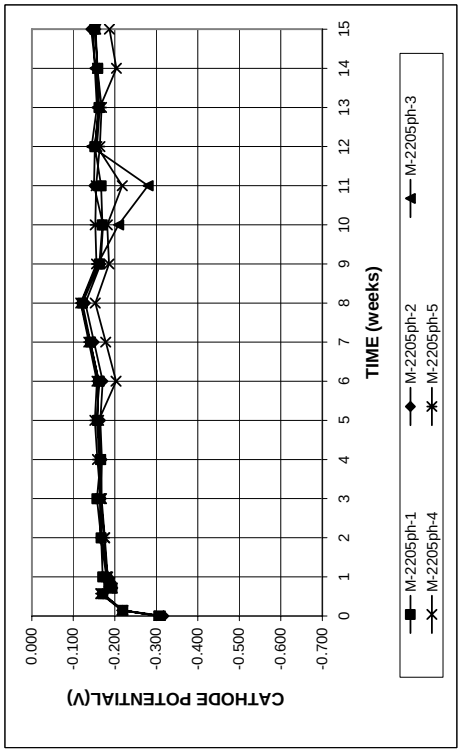

Figure A.139b - Macrocell test. Cathode corrosion potentials with respect to saturated calomel electrode for bare pickled 2205 duplex steel in simulated concrete pore solution with 6.04 molal ion NaCl.

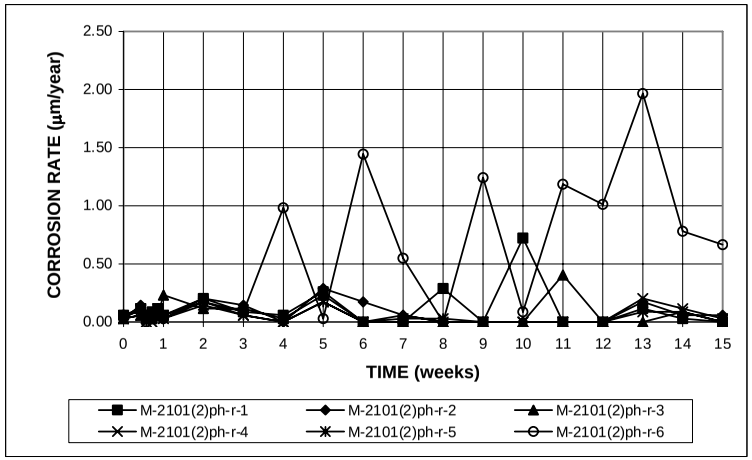

Figure A.140 - Macrocell test. Corrosion rates for bare pickled 2101(2) duplex steel in simulated concrete pore solution with 6.04 molal ion NaCl. Solutions are replaced every 5 weeks.

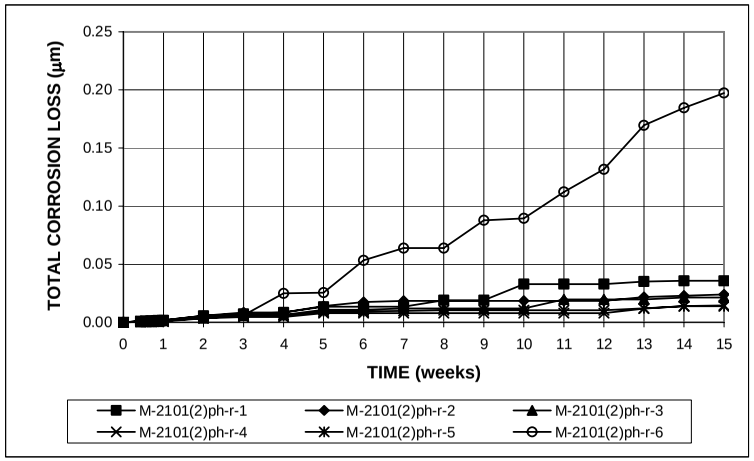

Figure A.141 - Macrocell test. Total corrosion losses for bare pickled 2101(2) duplex steel in simulated concrete pore solution with 6.04 molal ion NaCl. Solutions are replaced every 5 weeks.

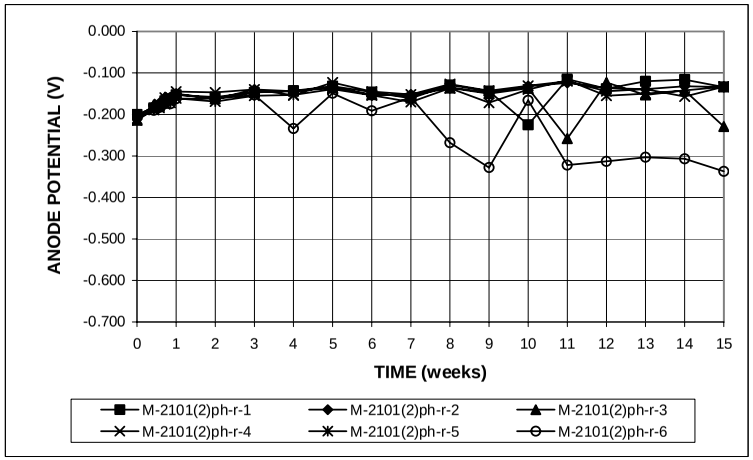

Figure A.142a - Macrocell test. Anode corrosion potentials with respect to saturated calomel electrode for bare pickled 2101(2) duplex steel in simulated concrete pore solution with 6.04 molal ion NaCl. Solutions are replaced every 5 weeks.

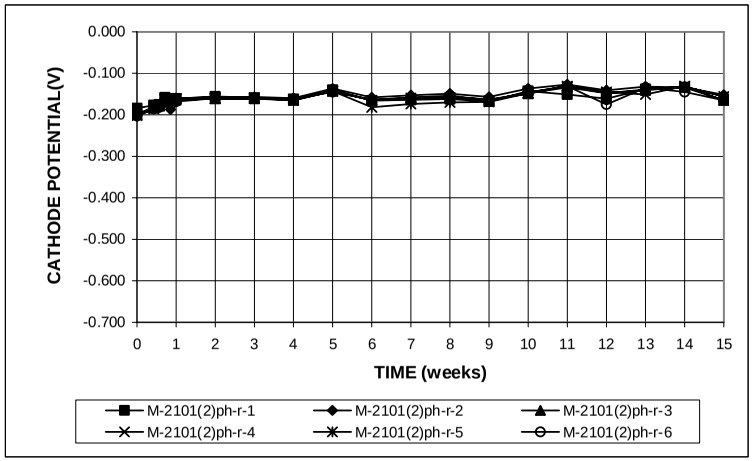

Figure A.142b - Macrocell test. Cathode corrosion potentials with respect to saturated calomel electrode for bare pickled 2101(2) duplex steel in simulated concrete pore solution with 6.04 molal ion NaCl. Solutions are replaced every 5 weeks.

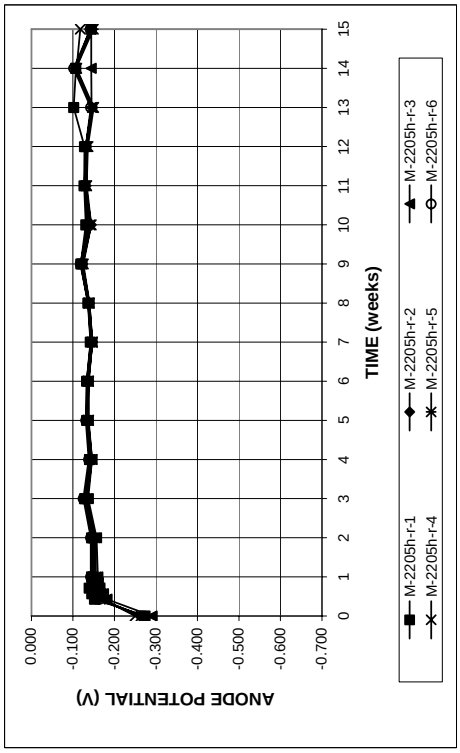

Figure A.145a - Macrocell test. Anode corrosion potentials with respect to saturated calomel electrode for bare 2205 duplex steel in simulated concrete pore solution with 6.04 molal ion NaCl. Solutions are replaced everay 5 weeks.

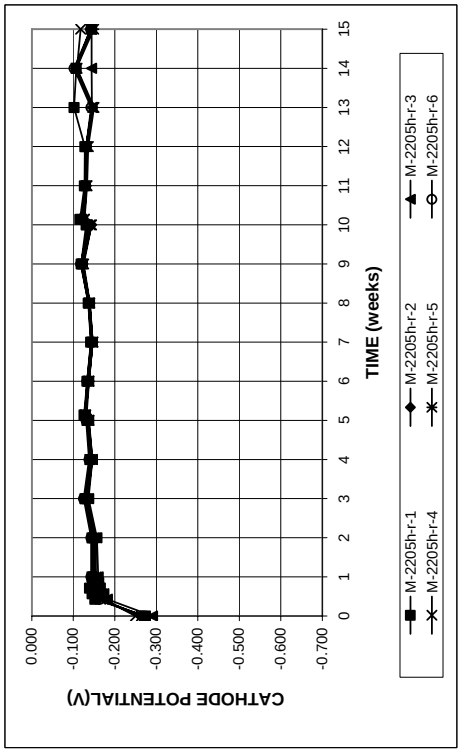

Figure A.145b - Macrocell test. Cathode corrosion potentials with respect to saturated calomel electrode for bare 2205 duplex steel in simulated concrete pore solution with 6.04 molal ion NaCl. Solutions are replaced everay 5 weeks.

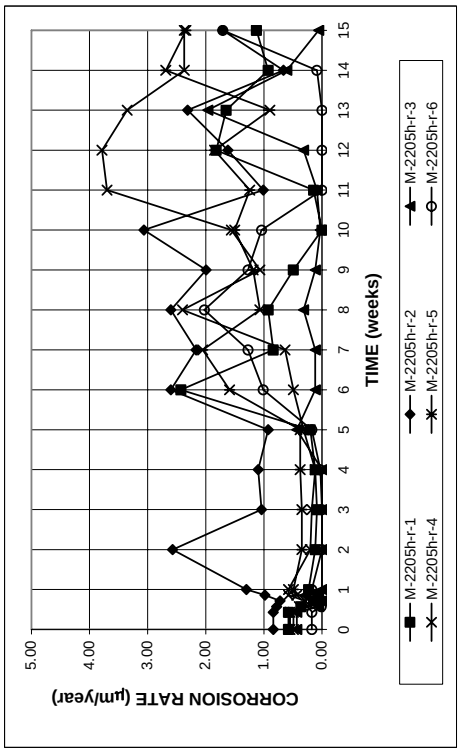

Figure A.143 - Macrocell test. Corrosion rates for bare 2205 duplex steel in simulated concrete pore solution with 6.04 molal ion NaCl. Solutions are replaced everay 5 weeks.

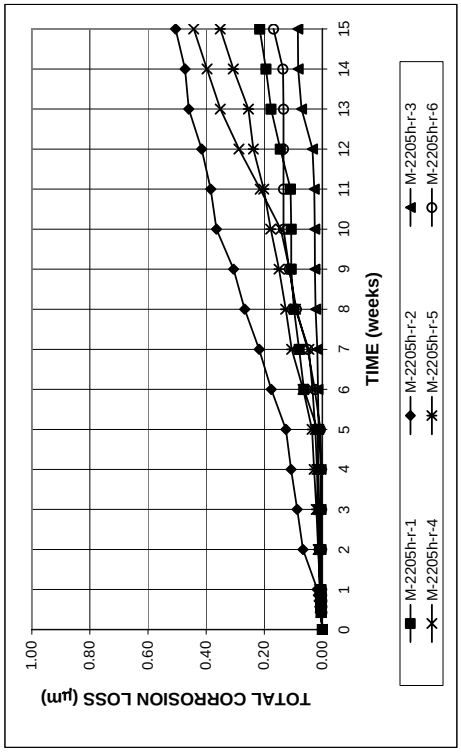

Figure A.144 -Macrocell test. Total corrosion losses for bare 2205 duplex steel in simulated concrete pore solution with 6.04 molal ion NaCl. Solutions are replaced everay 5 weeks.

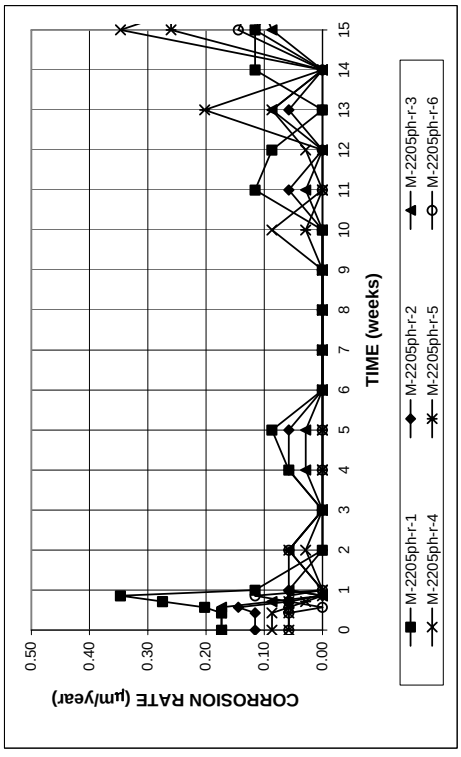

Figure A.146 - Macrocell test. Corrosion rates for bare pickled 2205 duplex steel in simulated concrete pore solution with 6.04 molal ion NaCl. Solutions are replaced every 5 weeks.

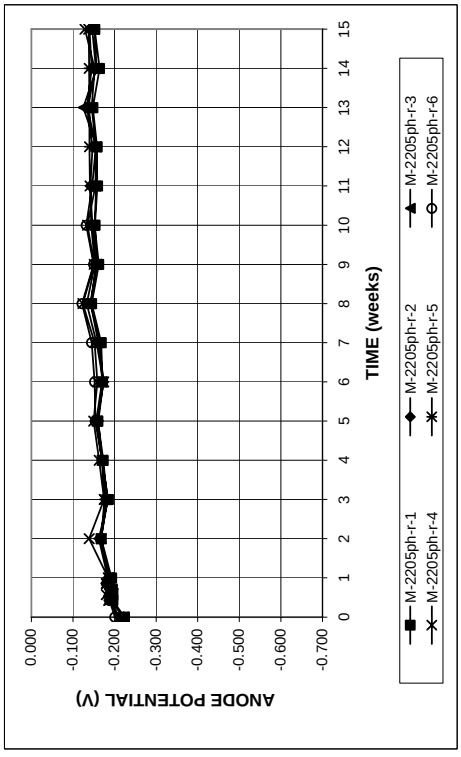

Figure A.148a - Macrocell test. Anode corrosion potentials with respect to saturated calomel electrode for bare pickled 2205 duplex steel in simulated concrete pore solution with 6.04 molal ion NaCl. Solutions are replaced every 5 weeks.

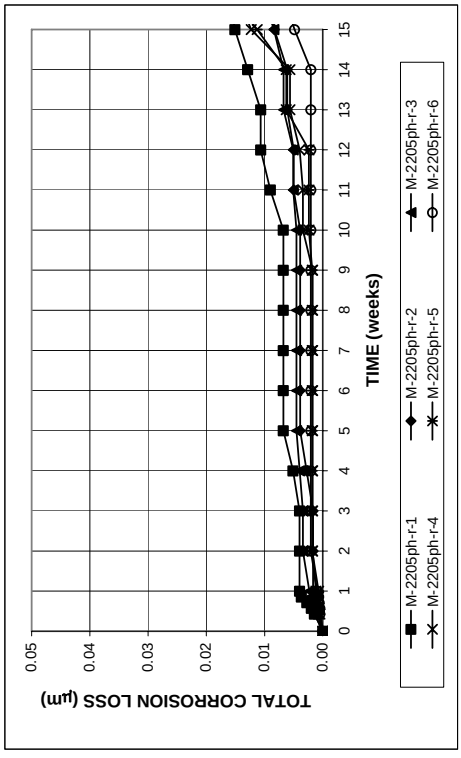

Figure A.147 - Macrocell test. Total corrosion losses for bare pickled 2205 duplex steel in simulated concrete pore solution with 6.04 molal ion NaCl. Solutions are replaced every 5 weeks.

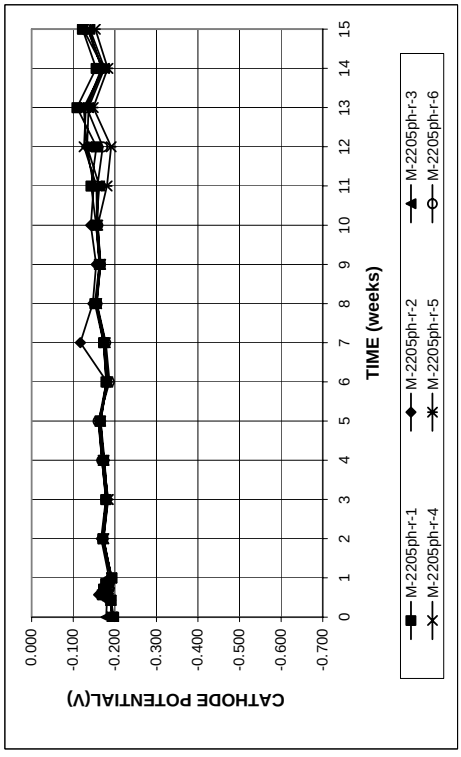

Figure A.148b - Macrocell test. Cathode corrosion potentials with respect to saturated calomel electrode for bare pickled 2205 duplex steel in simulated concrete pore solution with 6.04 molal ion NaCl. Solutions are replaced every 5 weeks.

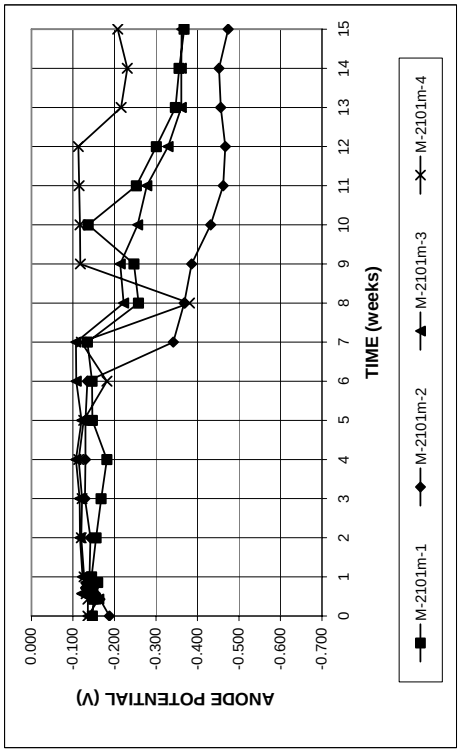

Figure A.151a - Macrocell test. Anode corrosion potentials with respect to saturated calomel electrode for mortar-wrapped 2101 duplex steel in simulated concrete pore solution with 1.6 molal ion NaCl.

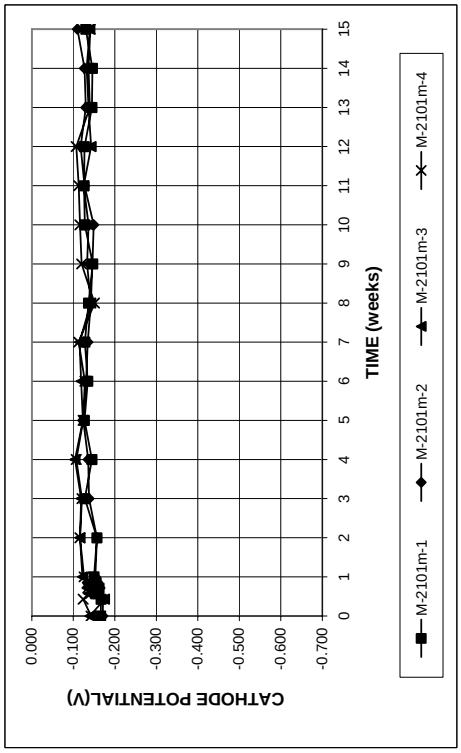

Figure A.151b - Macrocell test. Cathode corrosion potentials with respect to saturated calomel electrode for mortar-wrapped 2101 duplex steel in simulated concrete pore solution with 1.6 molal ion NaCl.

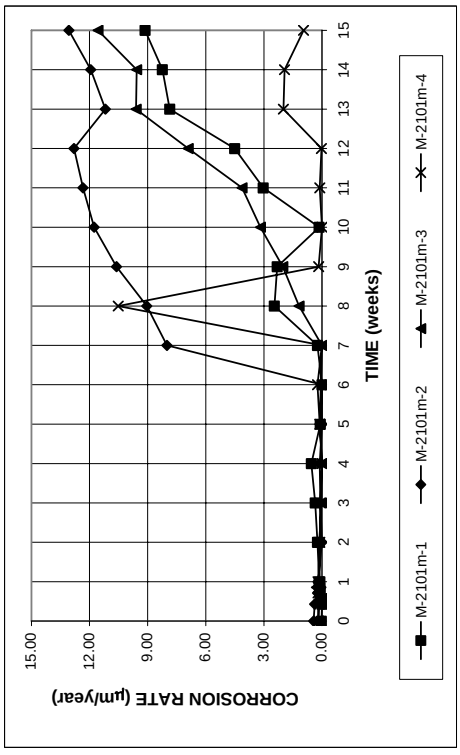

Figure A.149 - Macrocell test. Corrosion rates for mortar-wrapped 2101 duplex steel in simulated concrete pore solution with 1.6 molal ion NaCl.

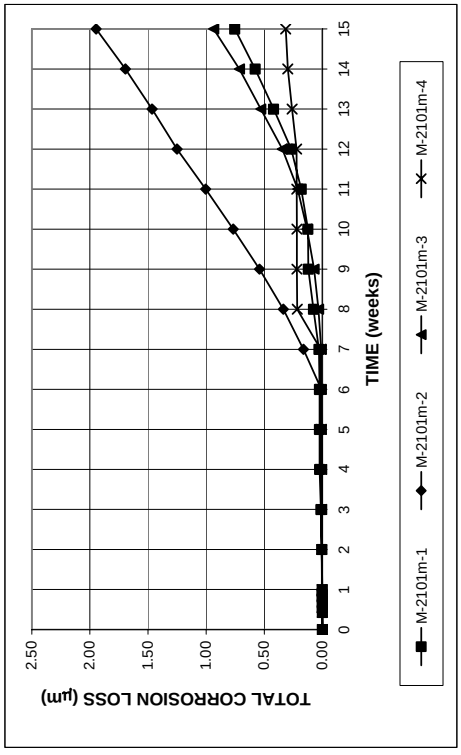

Figure A.150 - Macrocell test. Total corrosion losses for mortar-wrapped 2101 duplex steel in simulated concrete pore solution with 1.6 molal ion NaCl.

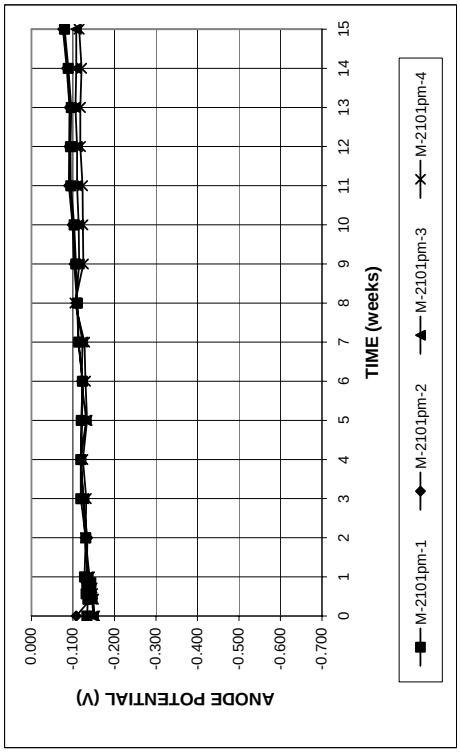

Figure A.154a - Macrocell test. Anode corrosion potentials with respect to saturated calomel electrode for mortar-wrapped pickled 2101 duplex steel in simulated concrete pore solution with 1.6 molal ion NaCl.

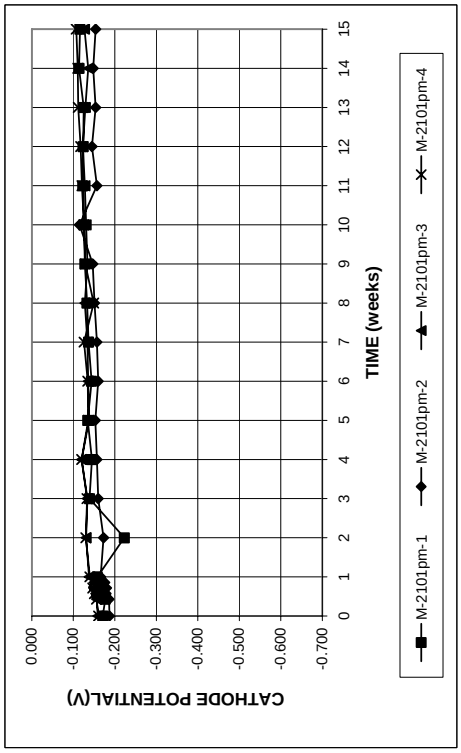

Figure A.154b - Macrocell test. Cathode corrosion potentials with respect to saturated calomel electrode for mortar-wrapped pickled 2101 duplex steel in simulated concrete pore solution with 1.6 molal ion NaCl.

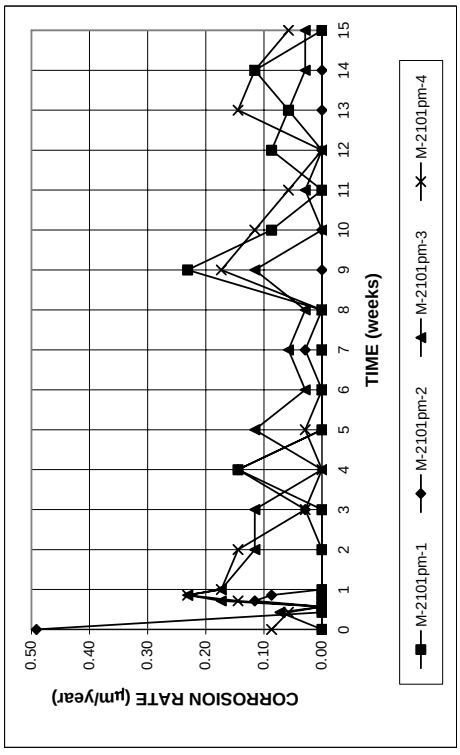

Figure A.152 - Macrocell test. Corrosion rates for mortar-wrapped pickled 2101 duplex steel in simulated concrete pore solution with 1.6 molal ion NaCl.

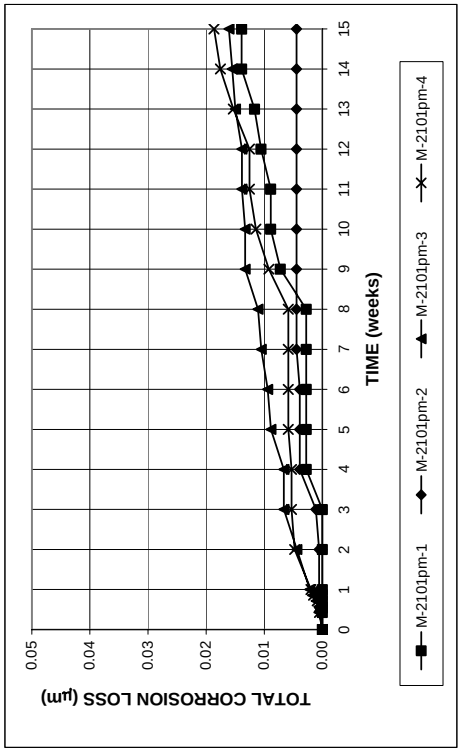

Figure A.153 - Macrocell test. Total corrosion losses for mortar-wrapped pickled 2101 duplex steel in simulated concrete pore solution with 1.6 molal ion NaCl.

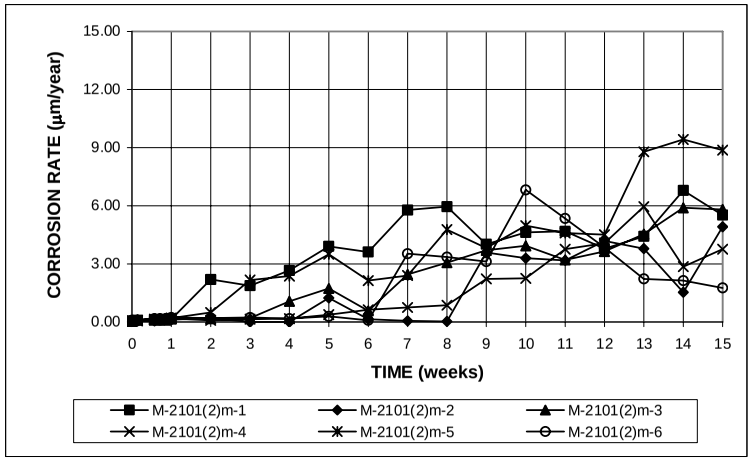

Figure A.155 - Macrocell test. Corrosion rates for mortar-wrapped 2101(2) duplex steel in simulated concrete pore solution with 1.6 molal ion NaCl.

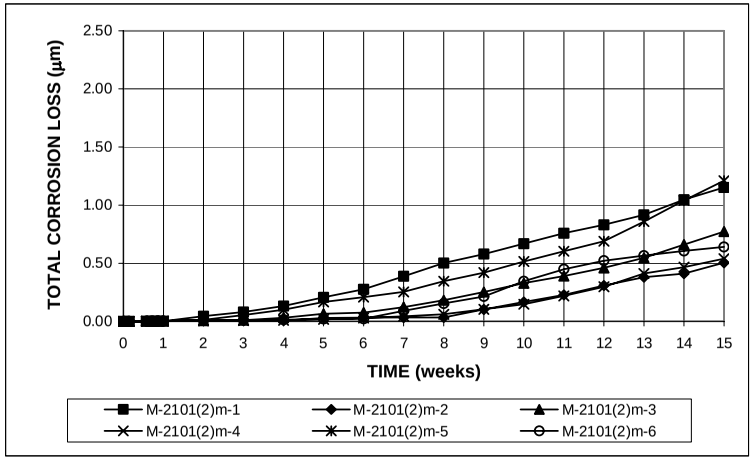

Figure A.156 - Macrocell test. Total corrosion losses for mortar-wrapped 2101(2) duplex steel in simulated concrete pore solution with 1.6 molal ion NaCl.

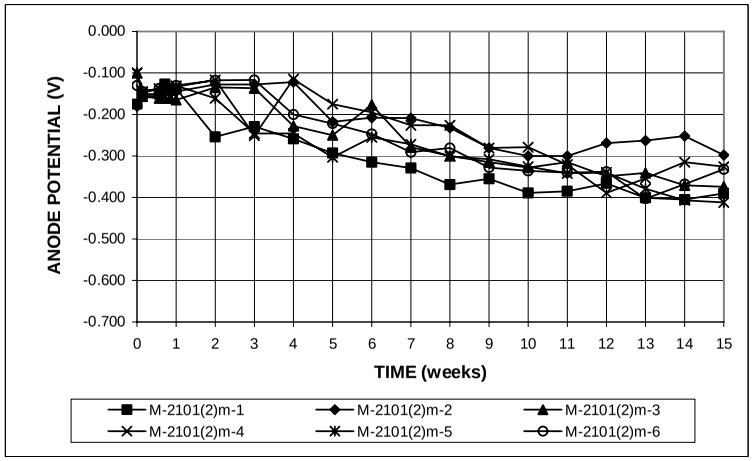

Figure A.157a - Macrocell test. Anode corrosion potentials with respect to saturated calomel electrode for mortar-wrapped 2101(2) duplex steel in simulated concrete pore solution with 1.6 molal ion NaCl.

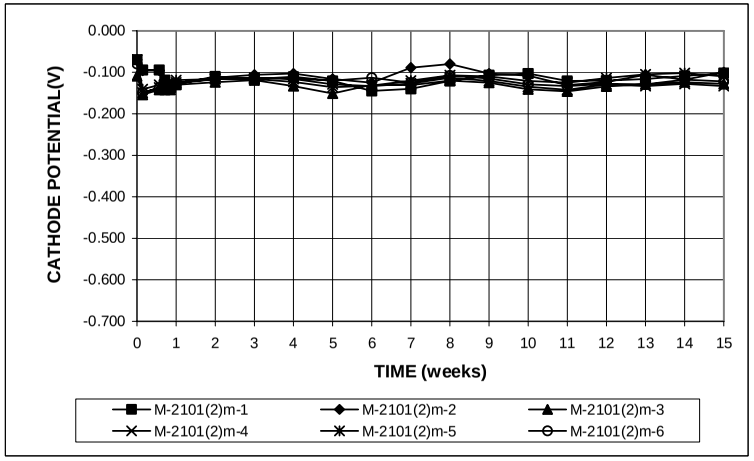

Figure A.157b - Macrocell test. Cathode corrosion potentials with respect to saturated calomel electrode for mortar-wrapped 2101(2) duplex steel in simulated concrete pore solution with 1.6 molal ion NaCl.

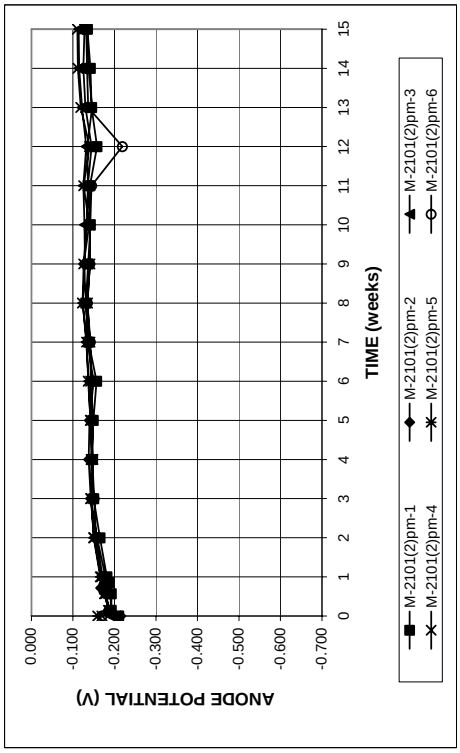

Figure A.160a - Macrocell test. Anode corrosion potentials with respect to saturated calomel electrode for mortar-wrapped pickled 2101(2) duplex steel in simulated concrete pore solution with 1.6 molal ion NaCl.

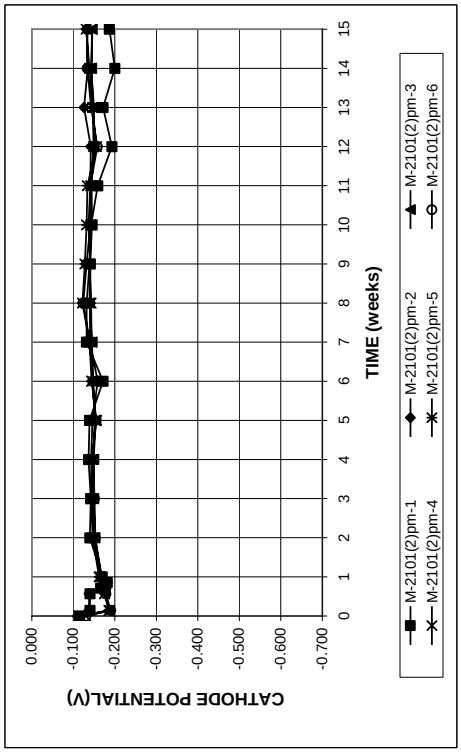

Figure A.160b - Macrocell test. Cathode corrosion potentials with respect to saturated calomel electrode for mortar-wrapped pickled 2101(2) duplex steel in simulated concrete pore solution with 1.6 molal ion NaCl.

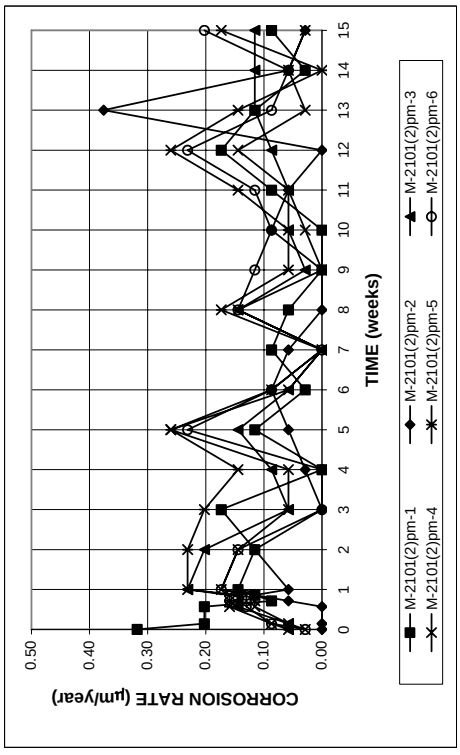

Figure A.158 - Macrocell test. Corrosion rates for mortar-wrapped pickled 2101(2) duplex steel in simulated concrete pore solution with 1.6 molal ion NaCl.

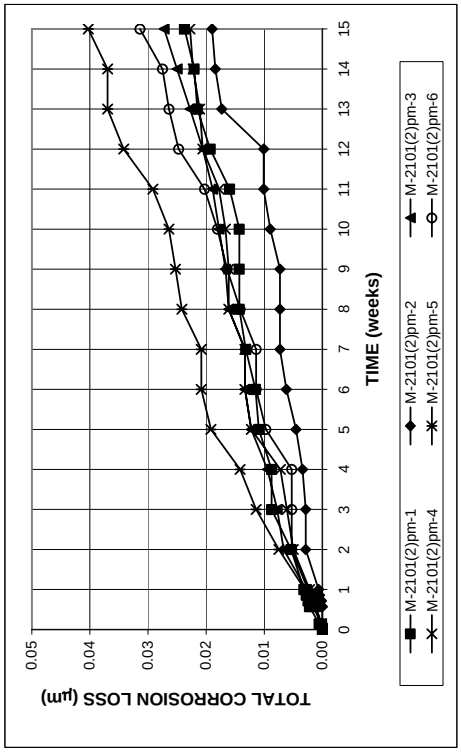

Figure A.159 - Macrocell test. Total corrosion losses for mortar-wrapped pickled 2101(2) duplex steel in simulated concrete pore solution with 1.6 molal ion NaCl.

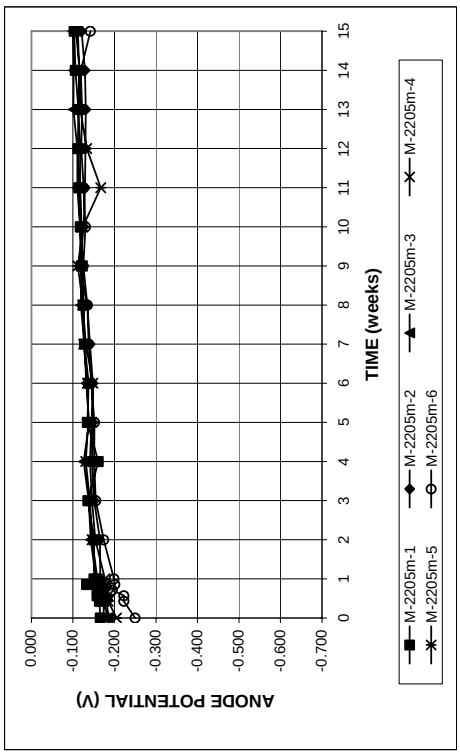

Figure A.163a - Macrocell test. Anode corrosion potentials with respect to saturated calomel electrode for mortar-wrapped 2205 duplex steel in simulated concrete pore solution with 1.6 molal ion NaCl.

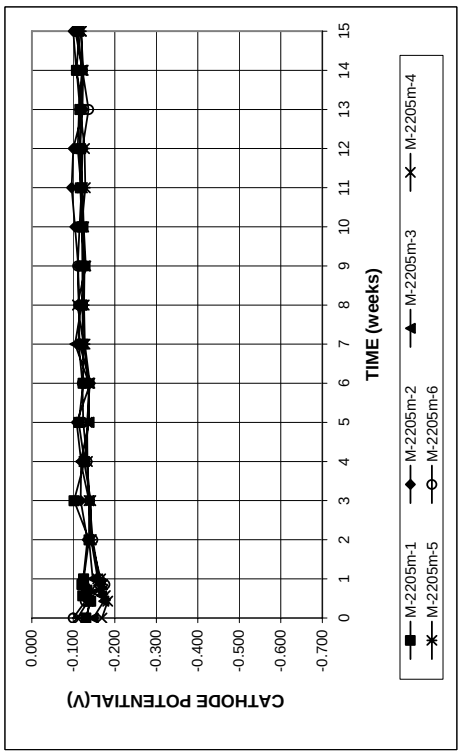

Figure A.163b - Macrocell test. Cathode corrosion potentials with respect to saturated calomel electrode for mortar-wrapped 2205 duplex steel in simulated concrete pore solution with 1.6 molal ion NaCl.

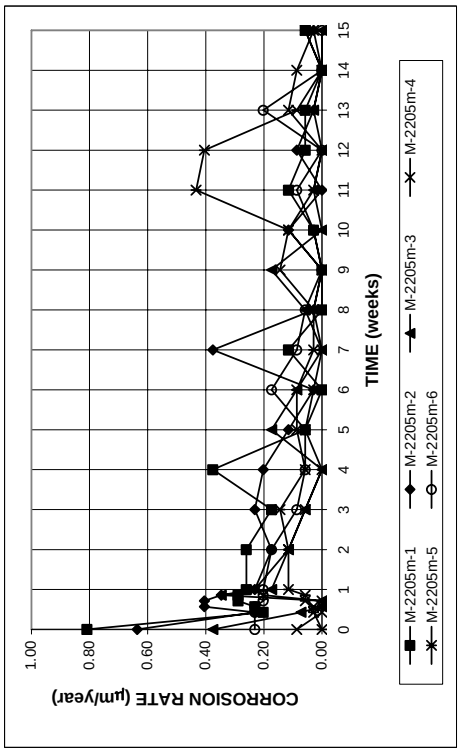

Figure A.161 - Macrocell test. Corrosion rates for mortar-wrapped 2205 duplex steel in simulated concrete pore solution with 1.6 molal ion NaCl.

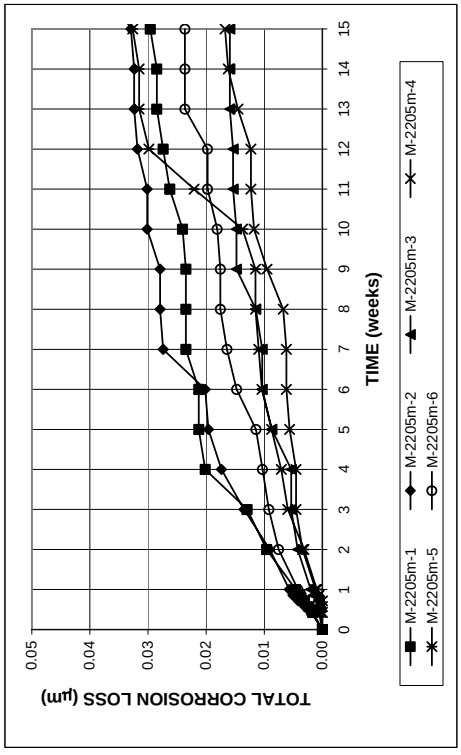

Figure A.162 - Macrocell test. Total corrosion losses for mortar-wrapped 2205 duplex steel in simulated concrete pore solution with 1.6 molal ion NaCl.

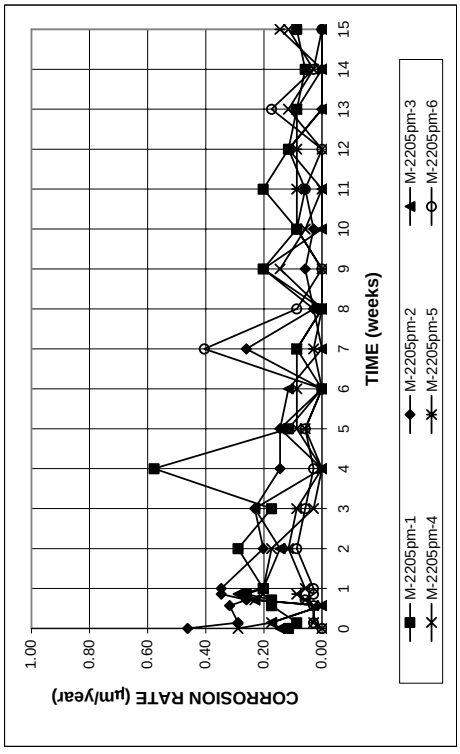

Figure A.164 - Macrocell test. Corrosion rates for mortar-wrapped pickled 2205 duplex steel in simulated concrete pore solution with 1.6 molal ion NaCl.

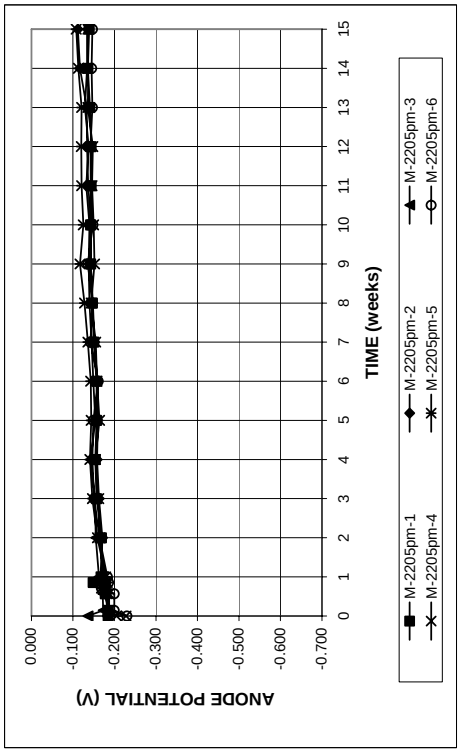

Figure A.166a - Macrocell test. Anode corrosion potentials with respect to saturated calomel electrode for mortar-wrapped pickled 2205 duplex steel in simulated concrete pore solution with 1.6 molal ion NaCl.

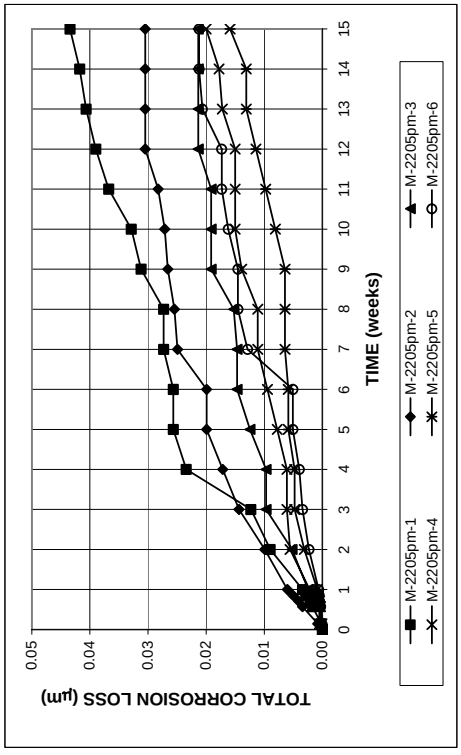

Figure A.165 - Macrocell test. Total corrosion losses for mortar-wrapped pickled 2205 duplex steel in simulated concrete pore solution with 1.6 molal ion NaCl.

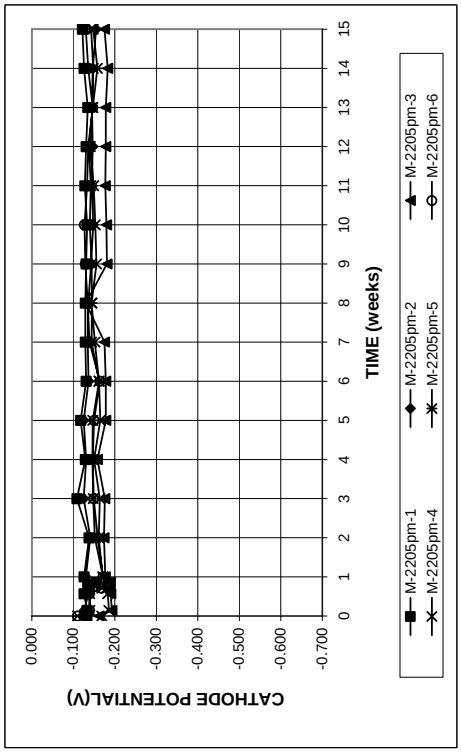

Figure A.166b - Macrocell test. Cathode corrosion potentials with respect to saturated calomel electrode for mortar-wrapped pickled 2205 duplex steel in simulated concrete pore solution with 1.6 molal ion NaCl.

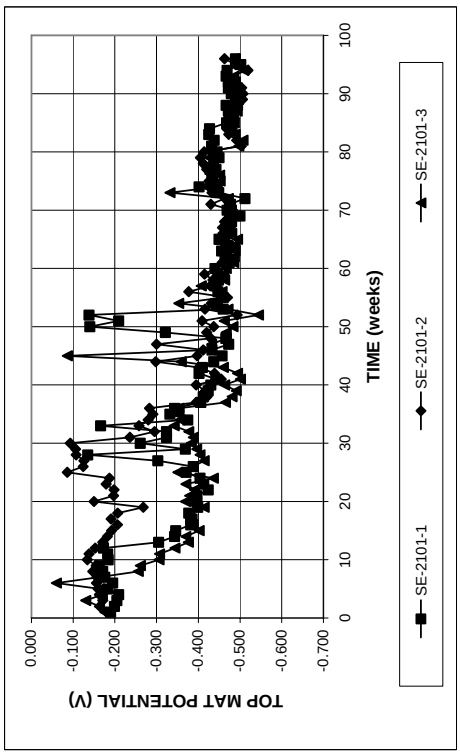

Figure A.169a -Southern Exposure test. Top mat corrosion potentials with respect to copper-copper sulfate electrode for 2101 duplex steel, specimens w/c = 0.45, ponded with 15% NaCl solution.

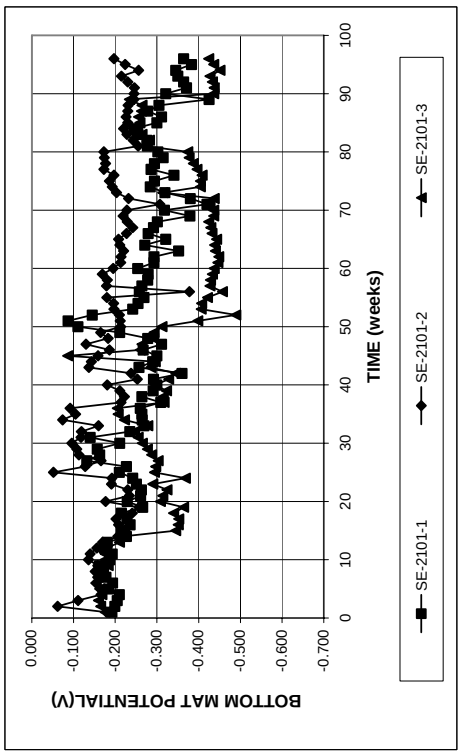

Figure A.169b - Southern Exposure test. Bottom mat corrosion potentials with respect to copper-copper sulfate electrode for 2101 duplex steel, specimens w/c = 0.45, ponded with 15% NaCl solution.

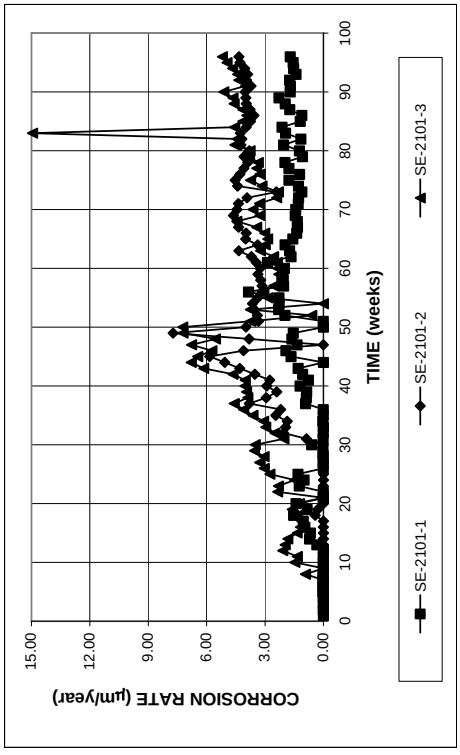

Figure A.167 -Southern Exposure test. Corrosion rates for 2101 duplex steel, specimens w/c = 0.45, ponded with 15% NaCl solution.

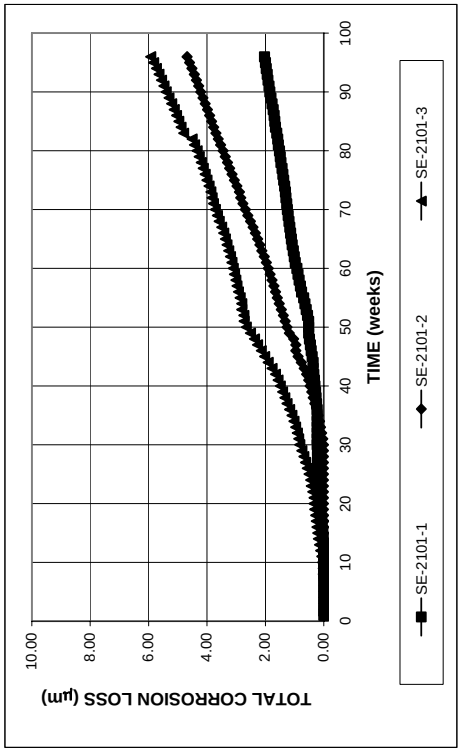

Figure A.168 - Southern Exposure test. Total corrosion losses of 2101 duplex steel, specimens w/c = 0.45, ponded with 15% NaCl solution.

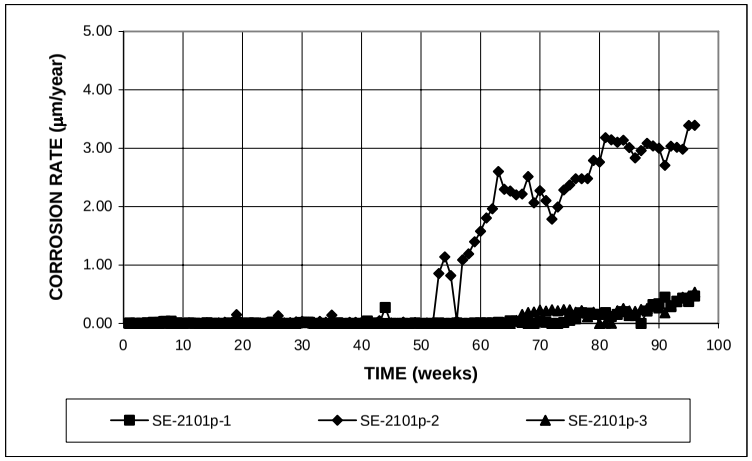

Figure A.170 -Southern Exposure test. Corrosion rates for pickled 2101 duplex steel, specimens w/c = 0.45, ponded with 15% NaCl solution.

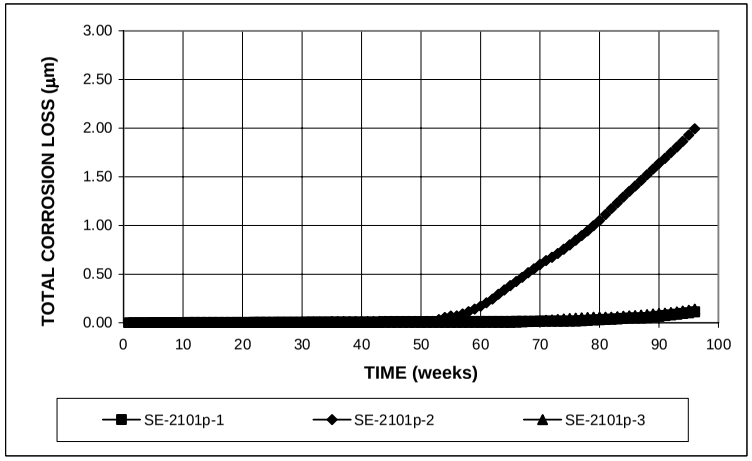

Figure A.171 - Southern Exposure test. Total corrosion losses of pickled 2101 duplex steel, specimens w/c = 0.45, ponded with 15% NaCl solution.

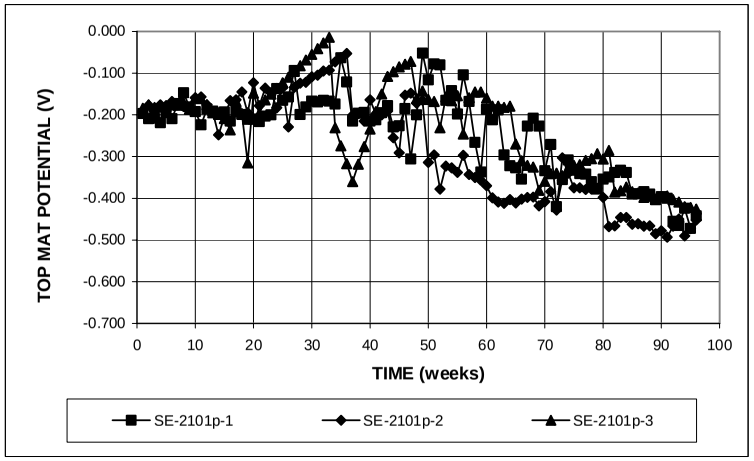

Figure A.172a - Southern Exposure test. Top mat corrosion potentials with respect to copper-copper sulfate electrode for pickled 2101 duplex steel, specimens w/c = 0.45, ponded with 15% NaCl solution.

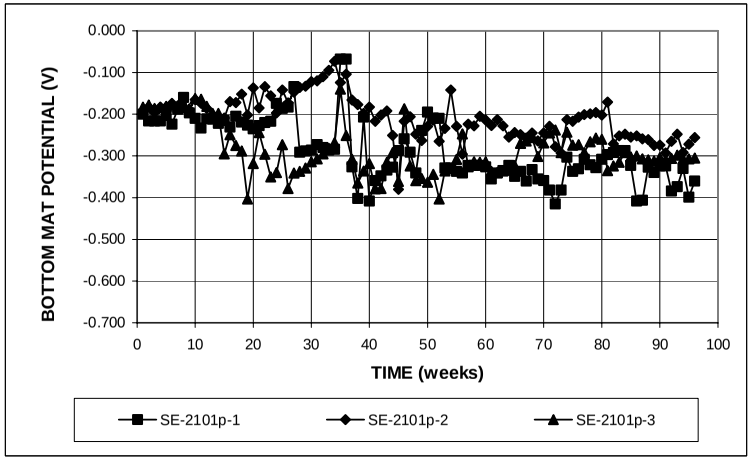

Figure A.172b - Southern Exposure test. Bottom mat corrosion potentials with respect to copper-copper sulfate electrode for pickled 2101 duplex steel, specimens w/c = 0.45, ponded with 15% NaCl solution.

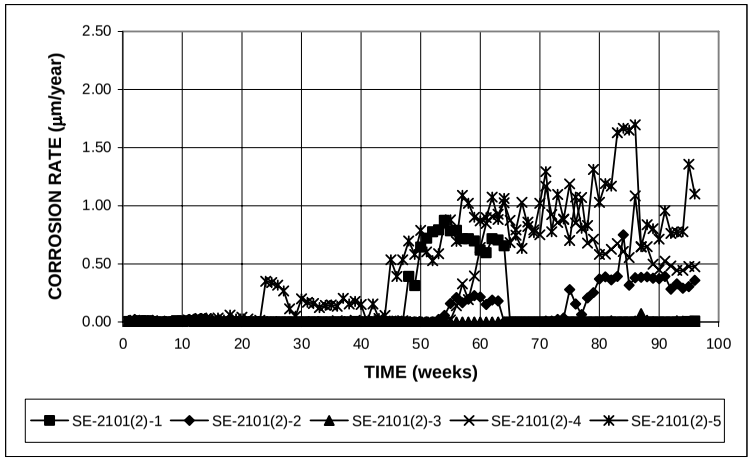

Figure A.173 -Southern Exposure test. Corrosion rates for 2101(2) duplex steel, specimens w/c = 0.45, ponded with 15% NaCl solution.

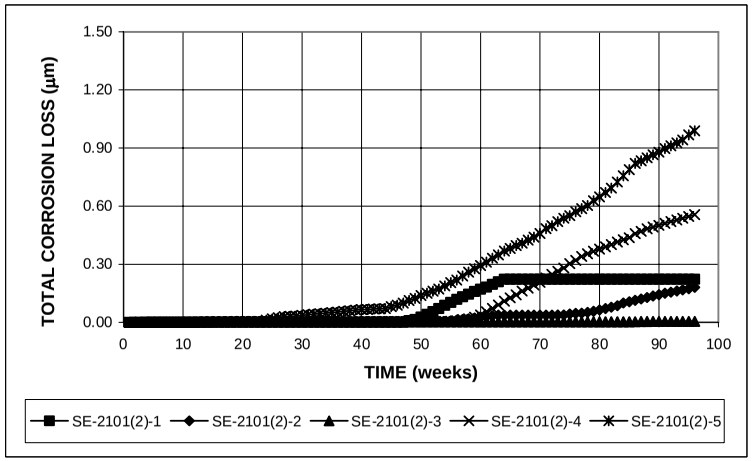

Figure A.174 - Southern Exposure test. Total corrosion losses of 2101(2) duplex steel, specimens w/c = 0.45, ponded with 15% NaCl solution.

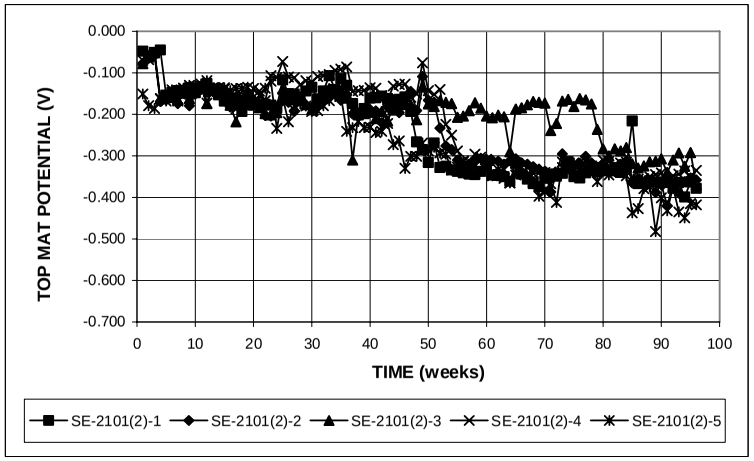

Figure A.175a - Southern Exposure test. Top mat corrosion potentials with respect to copper-copper sulfate electrode for 2101(2) duplex steel, specimens w/c = 0.45, ponded with 15% NaCl solution.

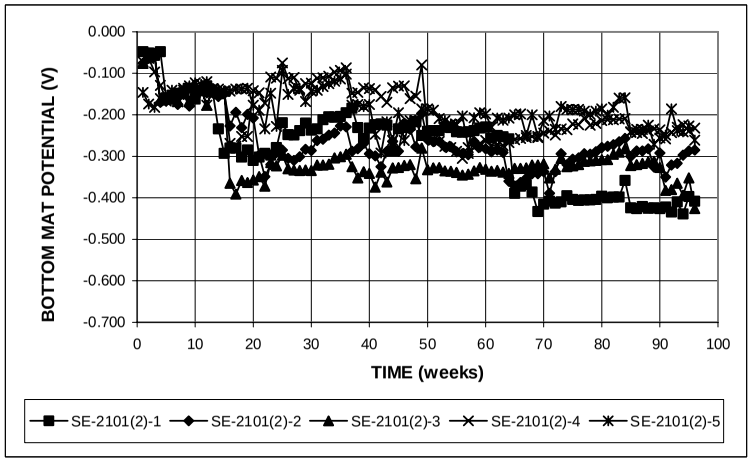

Figure A.175b - Southern Exposure test. Bottom mat corrosion potentials with respect to copper-copper sulfate electrode for 2101(2) duplex steel, specimens w/c = 0.45, ponded with 15% NaCl solution.

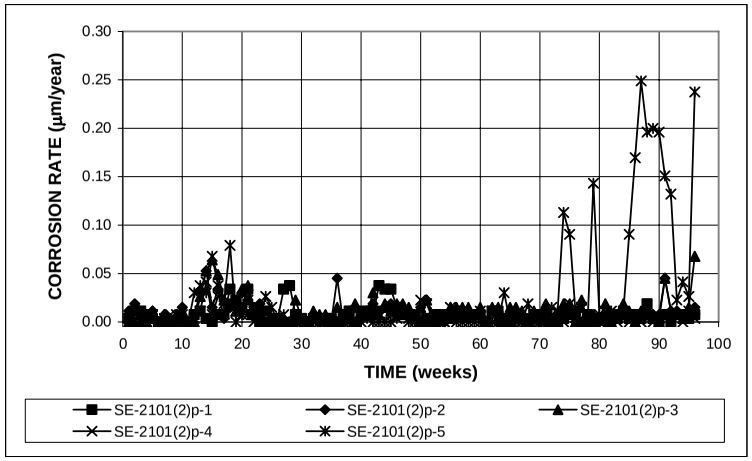

Figure A.176 - Southern Exposure test. Corrosion rates for pickled 2101(2) duplex steel, specimens w/c = 0.45, ponded with 15% NaCl solution.

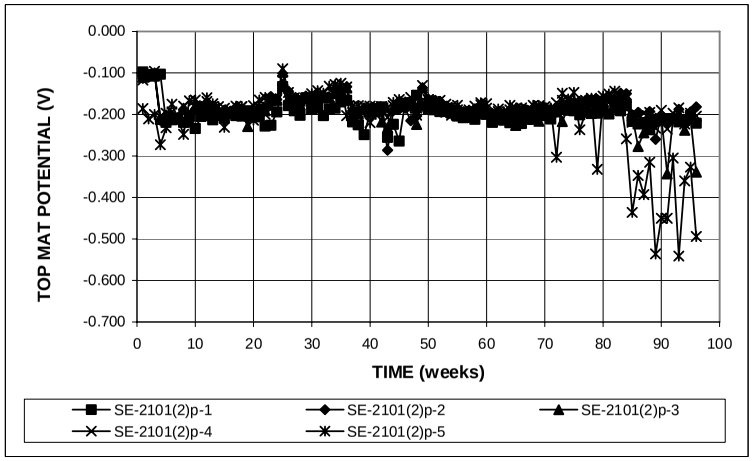

Figure A.178a - Southern Exposure test. Top mat corrosion potentials with respect to copper-copper sulfate electrode for pickled 2101(2) duplex steel, specimens w/c = 0.45, ponded with 15% NaCl solution.

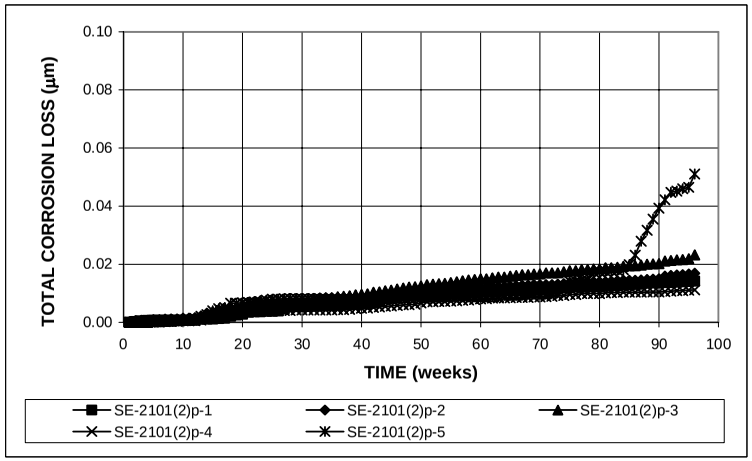

Figure A.177 - Southern Exposure test. Total corrosion losses of pickled 2101(2) duplex steel, specimens w/c = 0.45, ponded with 15% NaCl solution.

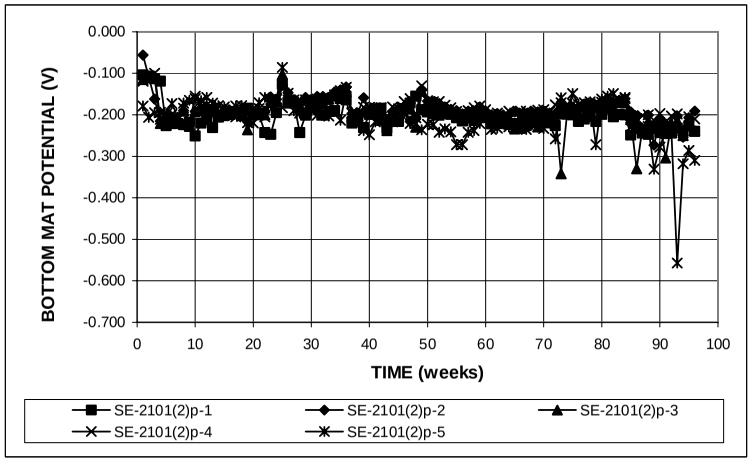

Figure A.178b - Southern Exposure test. Bottom mat corrosion potentials with respect to copper-copper sulfate electrode for pickled 2101(2) duplex steel, specimens w/c = 0.45, ponded with 15% NaCl solution.

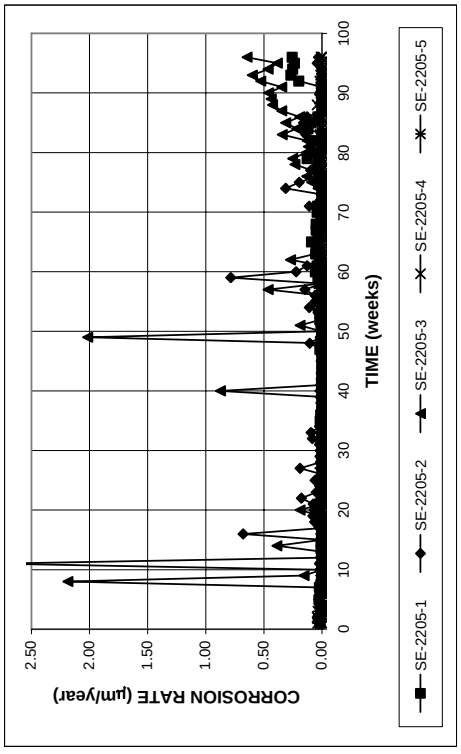

Figure A.179 -Southern Exposure test. Corrosion rates for 2205 duplex steel, specimens w/c = 0.45, ponded with 15% NaCl solution.

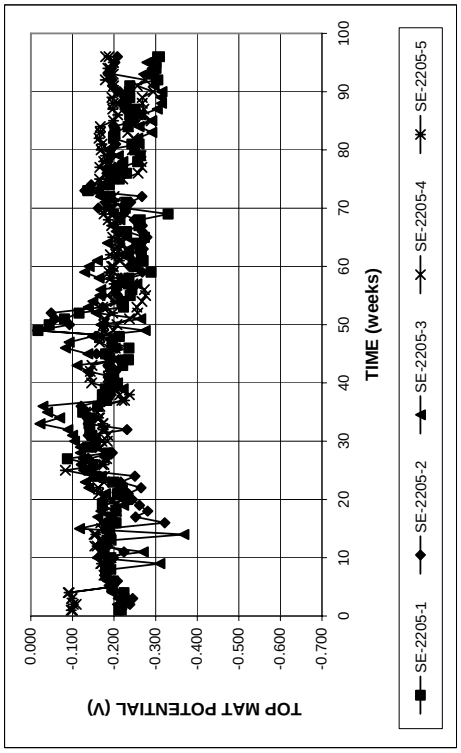

Figure A.181a - Southern Exposure test. Top mat corrosion potentials with respect to copper-copper sulfate electrode for 2205 duplex steel, specimens w/c = 0.45, ponded with 15% NaCl solution.

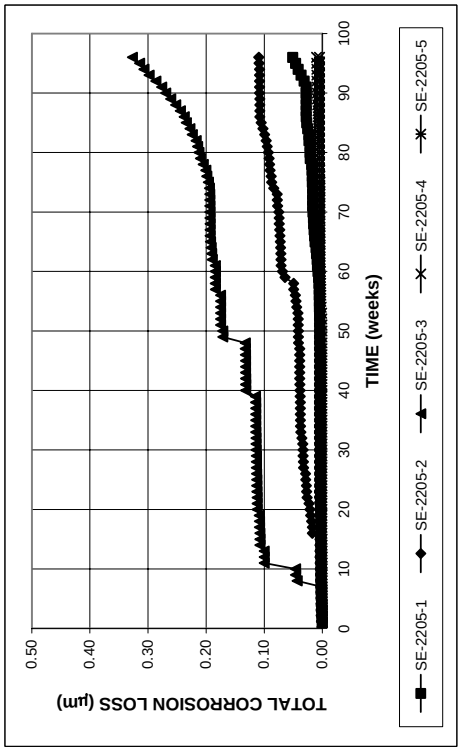

Figure A.180 - Southern Exposure test. Total corrosion losses of 2205 duplex steel, specimens w/c = 0.45, ponded with 15% NaCl solution.

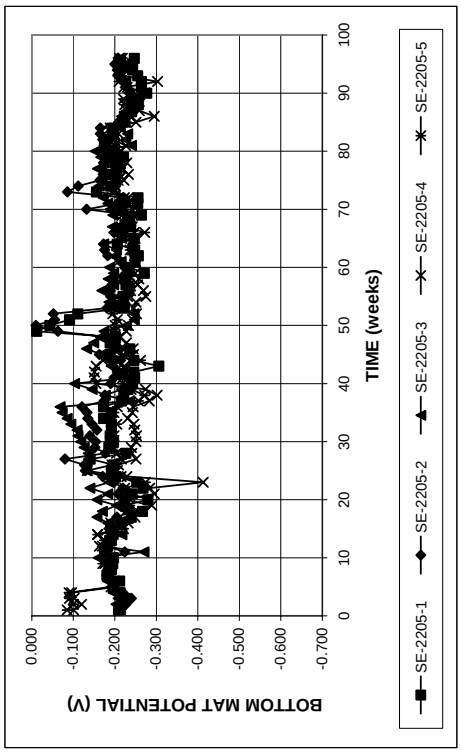

Figure A.181b - Southern Exposure test. Bottom mat corrosion potentials with respect to copper-copper sulfate electrode for 2205 duplex steel, specimens w/c = 0.45, ponded with 15% NaCl solution.

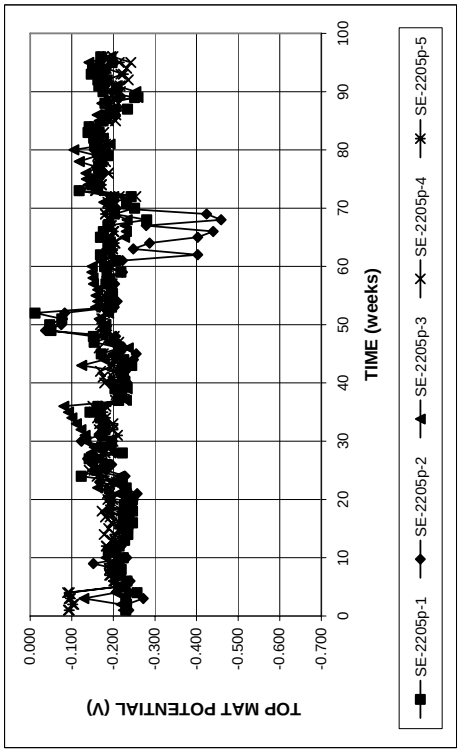

Figure A.184a - Southern Exposure test. Top mat corrosion potentials with respect to copper-copper sulfate electrode for pickled 2205 duplex steel, specimens w/c = 0.45, ponded with 15% NaCl solution.

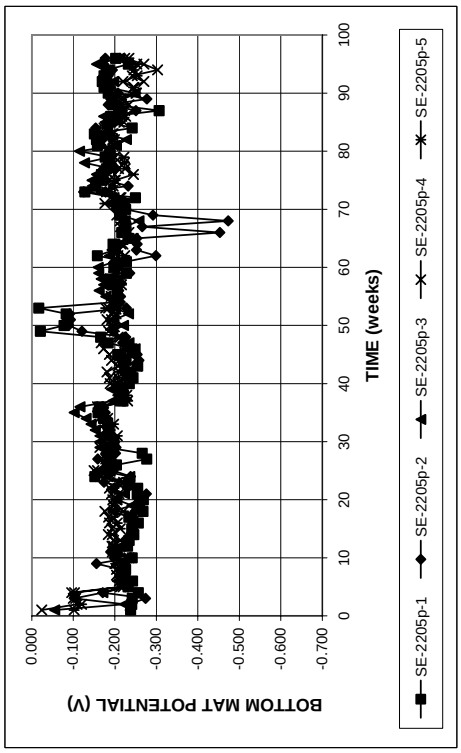

Figure A.184b - Southern Exposure test. Bottom mat corrosion potentials with respect to copper-copper sulfate electrode for pickled 2205 duplex steel, specimens w/c = 0.45, ponded with 15% NaCl solution.

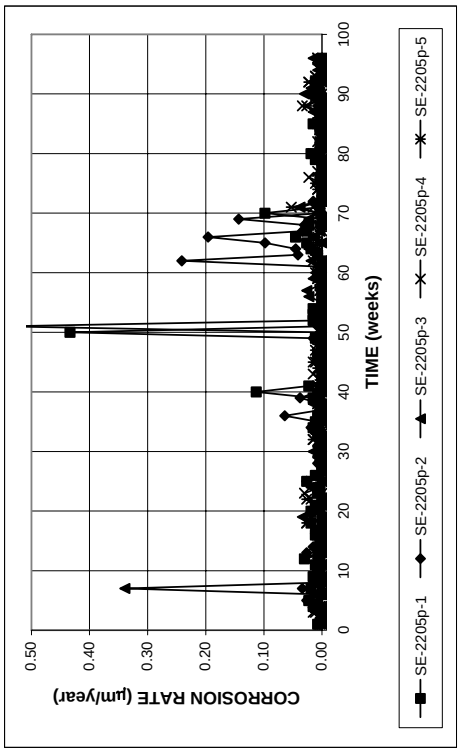

Figure A.182 -Southern Exposure test. Corrosion rates for pickled 2205 duplex steel, specimens w/c = 0.45, ponded with 15% NaCl solution.

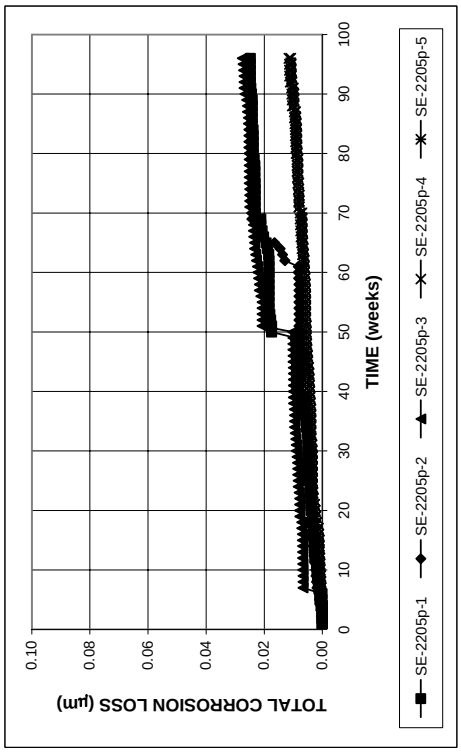

Figure A.183 - Southern Exposure test. Total corrosion losses of pickled 2205 duplex steel, specimens w/c = 0.45, ponded with 15% NaCl solution.

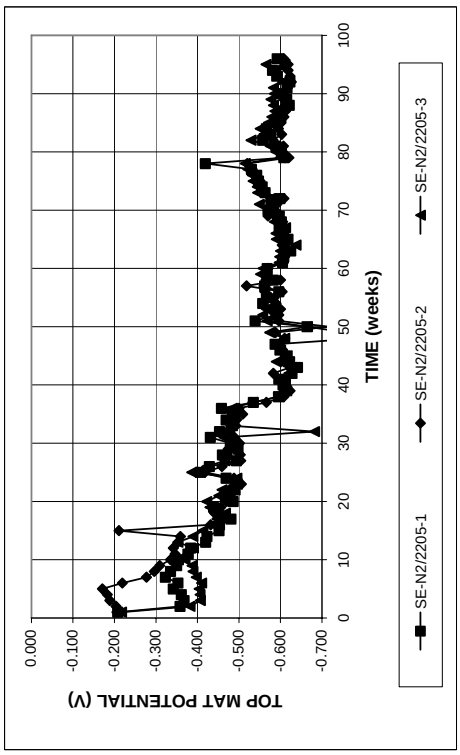

Figure A.187a - Southern Exposure test. Top mat corrosion potentials with respect to copper-copper sulfate electrode, conventional N2 steel at the top mat, 2205 steel at the bottom mat, specimens w/c = 0.45, ponded with 15% NaCl solution.

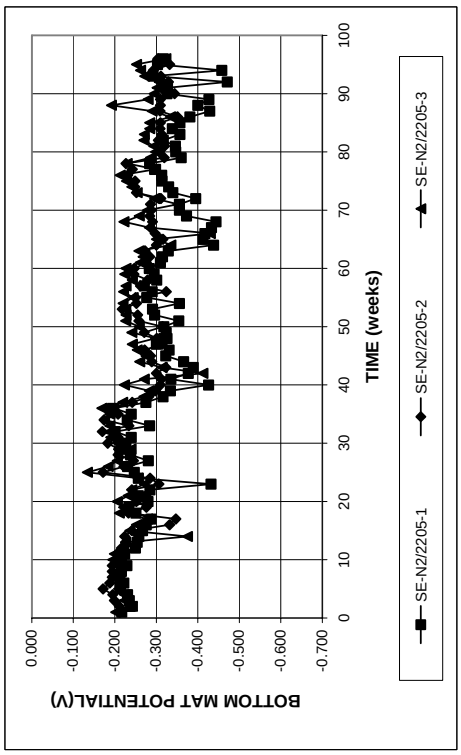

Figure A.187b - Southern Exposure test. Bottom mat corrosion potentials with respect to copper-copper sulfate electrode, conventional N2 steel at the top mat, 2205 steel at the bottom mat, specimens w/c = 0.45, ponded with 15% NaCl solution.

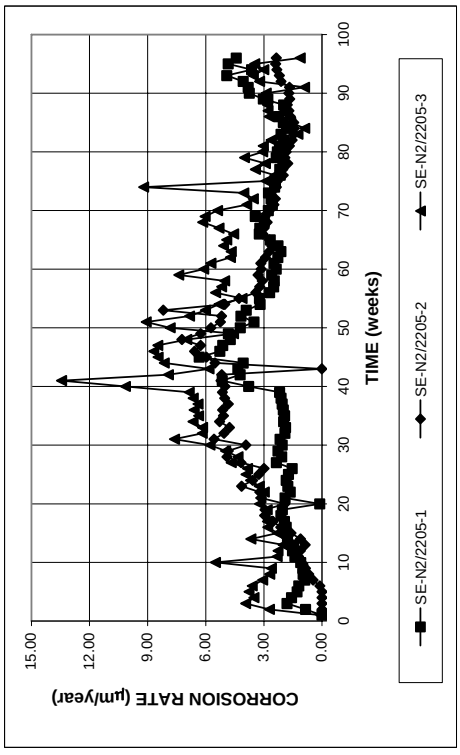

Figure A.185 - Southern Exposure test. Corrosion rates for conventional N2 steel, specimens w/c = 0.45, ponded with 15% NaCl solution, 2205 steel at the bottom mat.

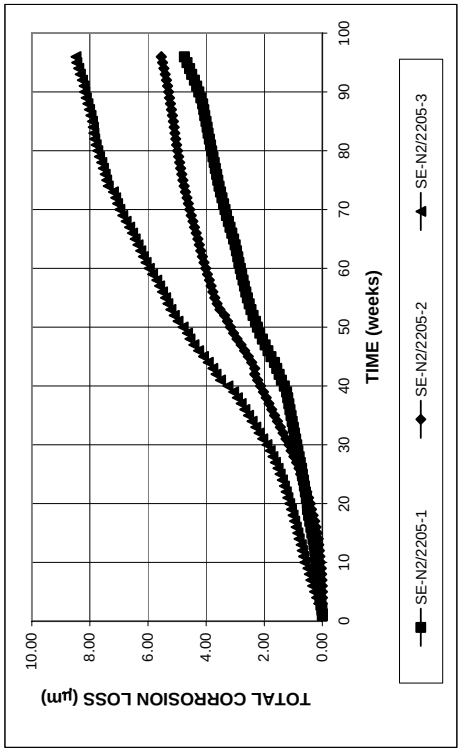

Figure A.186 - Southern Exposure test. Total corrosion losses of conventional N2 steel, specimens w/c = 0.45, ponded with 15% NaCl solution, 2205 steel at the bottom mat.

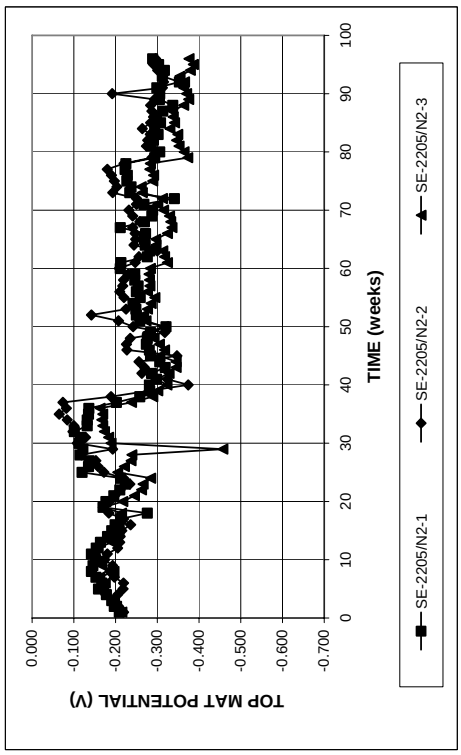

Figure A.190a - Southern Exposure test. Top mat corrosion potentials with respect to copper-copper sulfate electrode, 2205 steel at the top mat, conventional N2 steel at the bottom mat, specimens w/c = 0.45, ponded with 15% NaCl solution.

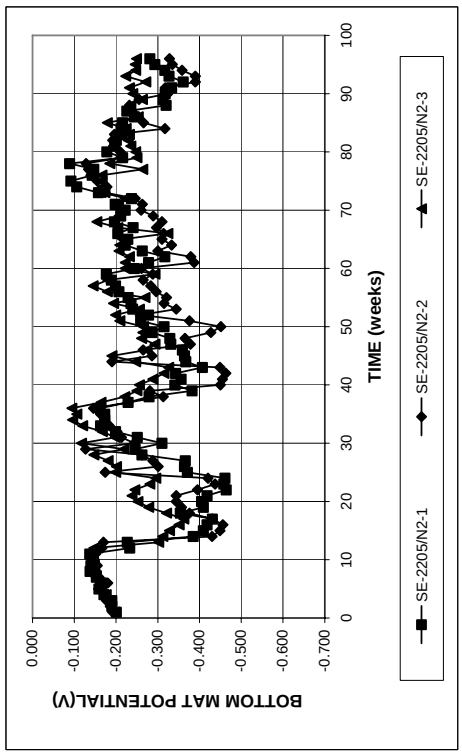

Figure A.190b - Southern Exposure test. Bottom mat corrosion potentials with respect to copper-copper sulfate electrode, 2205 steel at the top mat, conventional N2 steel at the bottom mat, specimens w/c = 0.45, ponded with 15% NaCl solution.

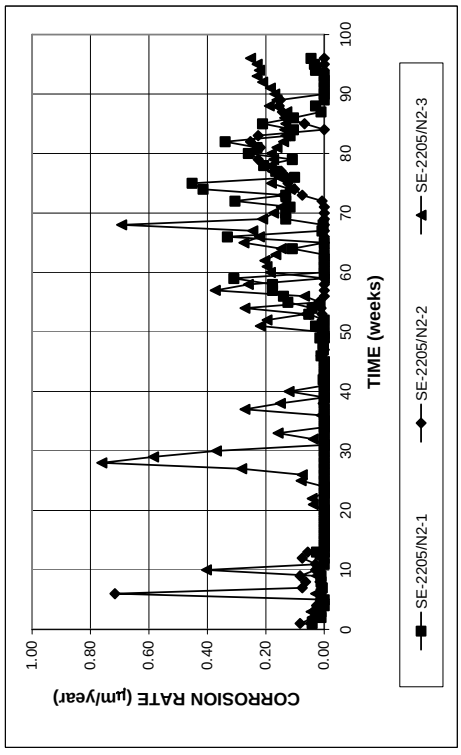

Figure A.188 - Southern Exposure test. Corrosion rates for 2205 steel, specimens w/c = 0.45, ponded with 15% NaCl solution, conventional N2 steel at the bottom mat.

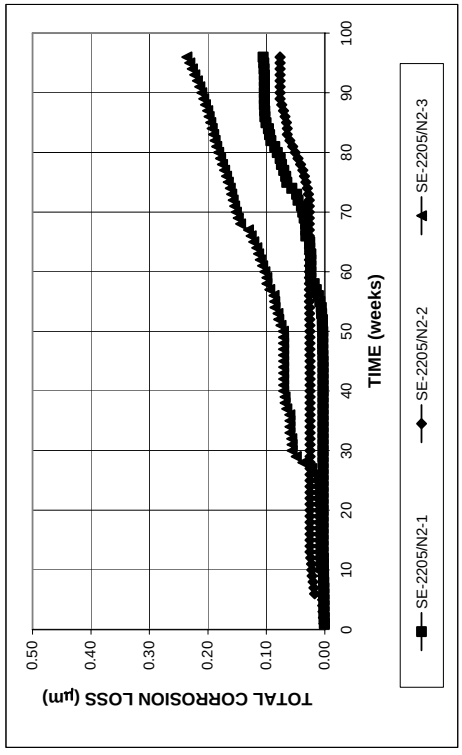

Figure A.189 - Southern Exposure test. Total corrosion losses of 2205 steel, specimens w/c = 0.45, ponded with 15% NaCl solution, conventional N2 steel at the bottom mat.

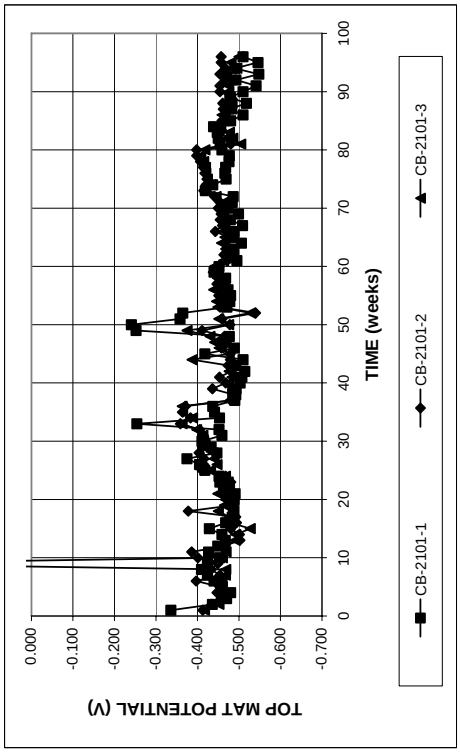

Figure A.193a - Cracked beam test. Top mat corrosion potentials with respect to copper-copper sulfate electrode for 2101 steel, specimens w/c = 0.45, ponded with 15% NaCl solution.

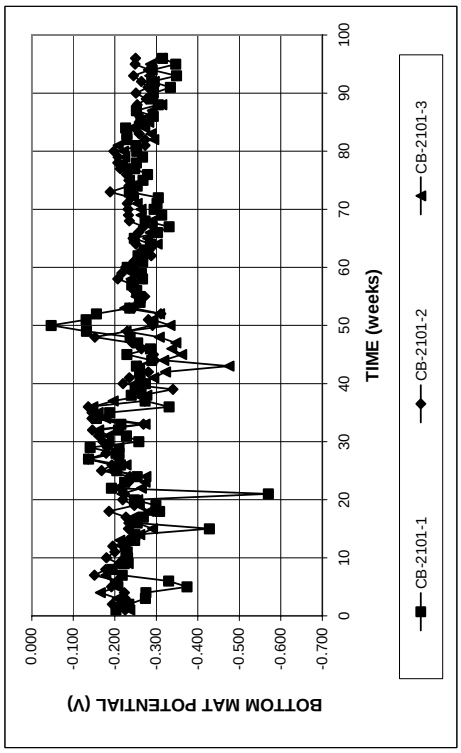

Figure A.193b - Cracked beam test. Bottom mat corrosion potentials with respect to copper-copper sulfate electrode for 2101 steel, specimens w/c = 0.45, ponded with 15% NaCl solution.

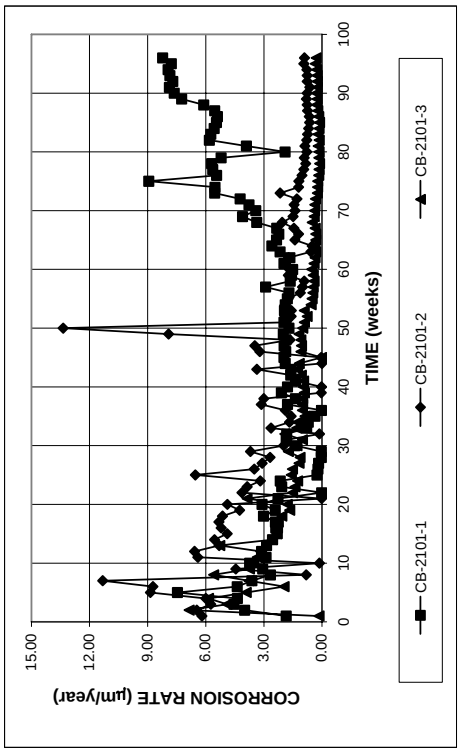

Figure A.191 - Cracked beam test. Corrosion rates for 2101 steel, specimens w/c = 0.45, ponded with 15% NaCl solution.

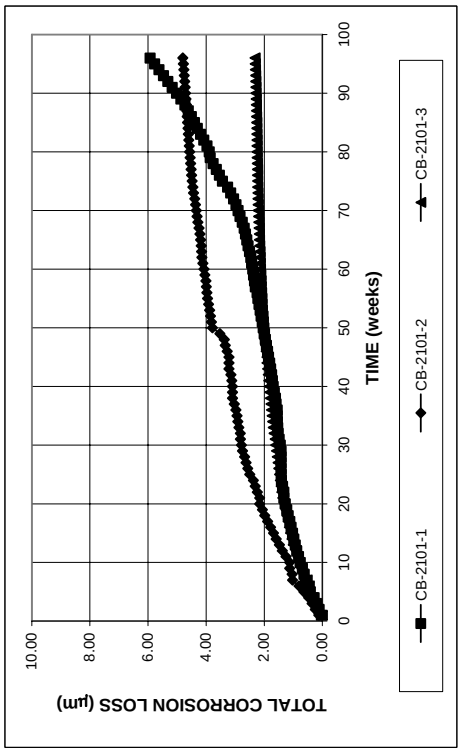

Figure A.192 -Cracked beam test. Total corrosion losses for 2101 steel, specimens w/c = 0.45, ponded with 15% NaCl solution.

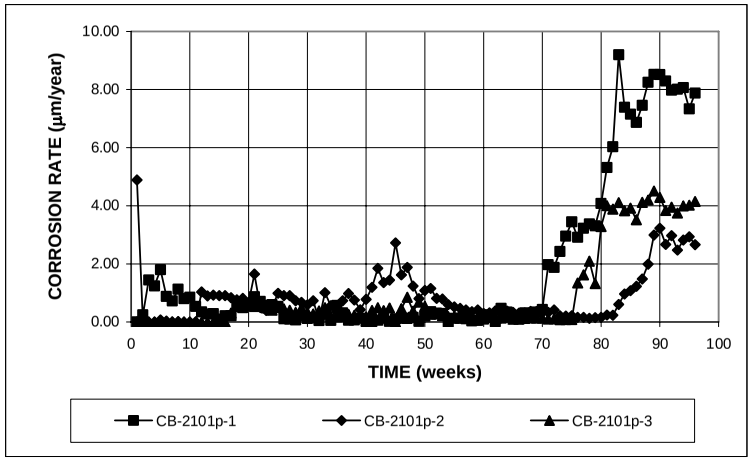

Figure A.194 - Cracked beam test. Corrosion rates for pickled 2101 steel, specimens w/c = 0.45, ponded with 15% NaCl solution.

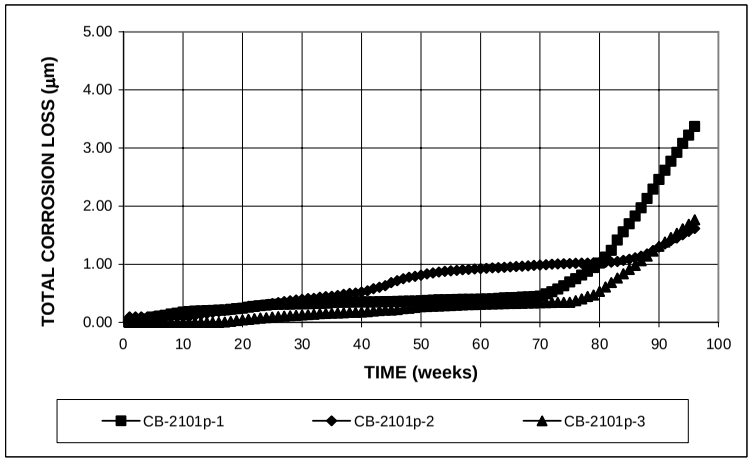

Figure A.195 -Cracked beam test. Total corrosion losses for pickled 2101 steel, specimens w/c = 0.45, ponded with 15% NaCl solution.

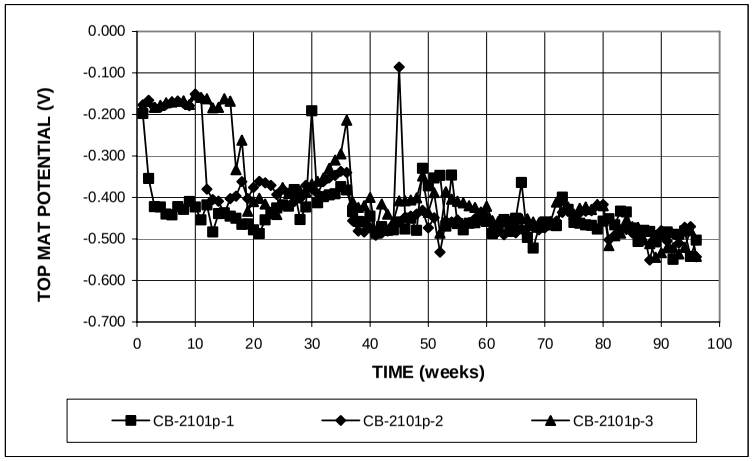

Figure A.196a - Cracked beam test. Top mat corrosion potentials with respect to copper-copper sulfate electrode for pickled 2101 steel, specimens w/c = 0.45, ponded with 15% NaCl solution.

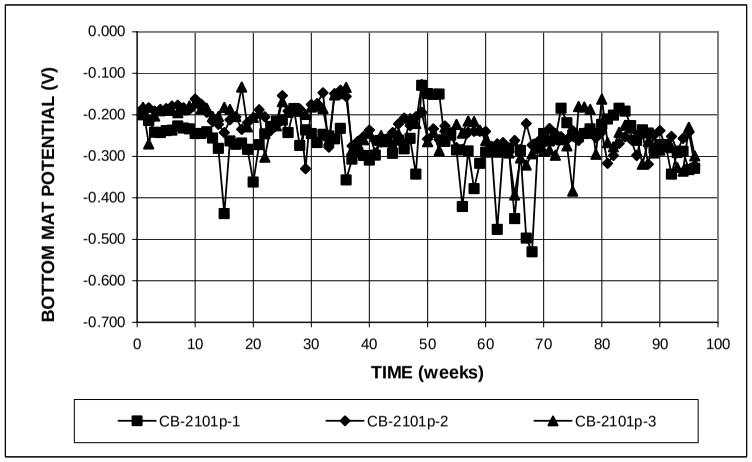

Figure A.196b - Cracked beam test. Bottom mat corrosion potentials with respect to copper-copper sulfate electrode for pickled 2101 steel, specimens w/c = 0.45, ponded with 15% NaCl solution.

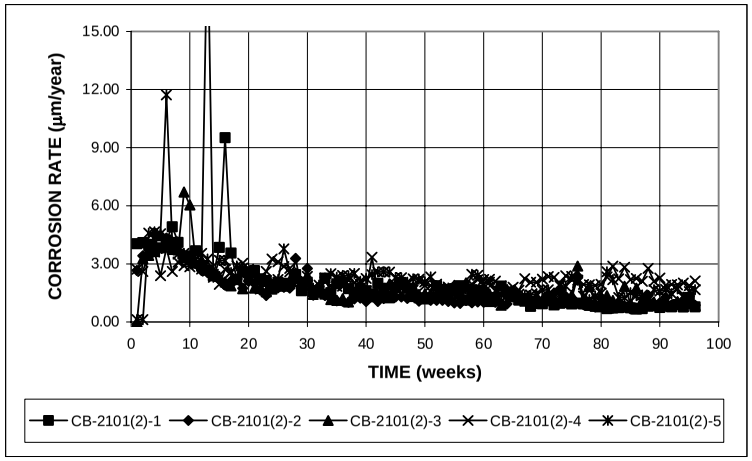

Figure A.197 - Cracked beam test. Corrosion rates for 2101(2) steel, specimens w/c = 0.45, ponded with 15% NaCl solution.

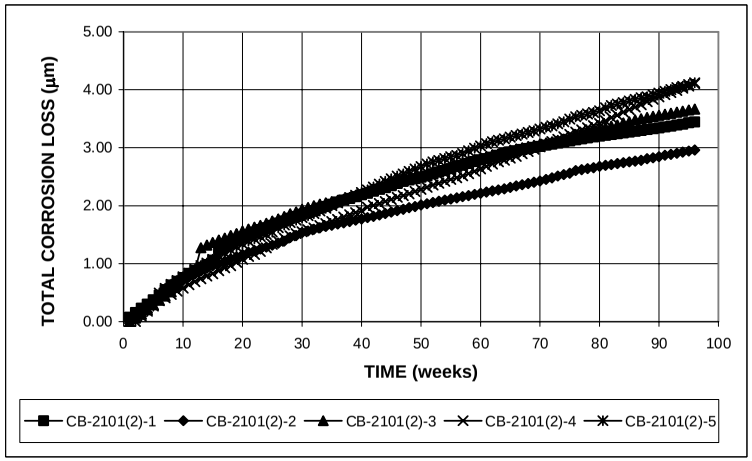

Figure A.198 -Cracked beam test. Total corrosion losses for 2101(2) steel, specimens w/c = 0.45, ponded with 15% NaCl solution.

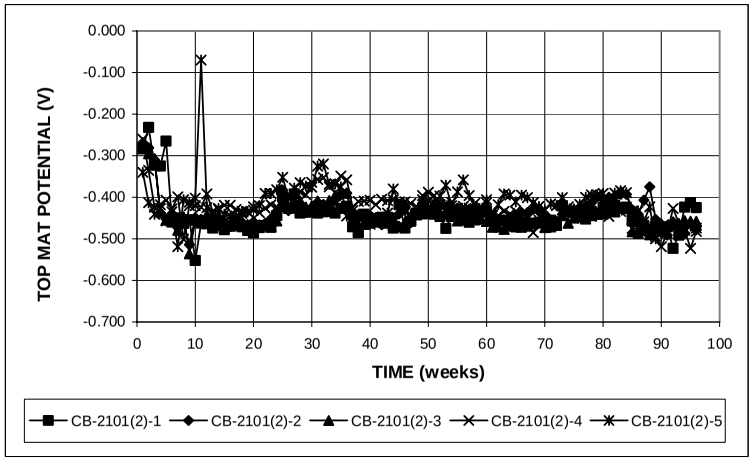

Figure A.199a - Cracked beam test. Top mat corrosion potentials with respect to copper-copper sulfate electrode for 2101(2) steel, specimens w/c = 0.45, ponded with 15% NaCl solution.

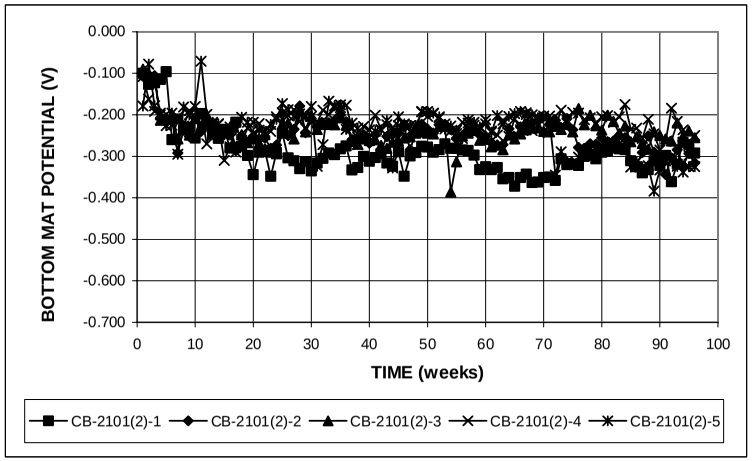

Figure A.199b - Cracked beam test. Bottom mat corrosion potentials with respect to copper-copper sulfate electrode for 2101(2) steel, specimens w/c = 0.45, ponded with 15% NaCl solution.

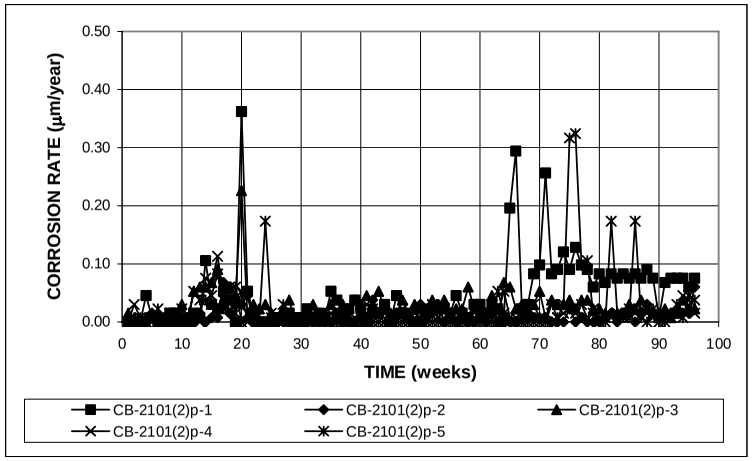

Figure A.200 - Cracked beam test. Corrosion rates for pickled 2101(2) steel, specimens w/c = 0.45, ponded with 15% NaCl solution.

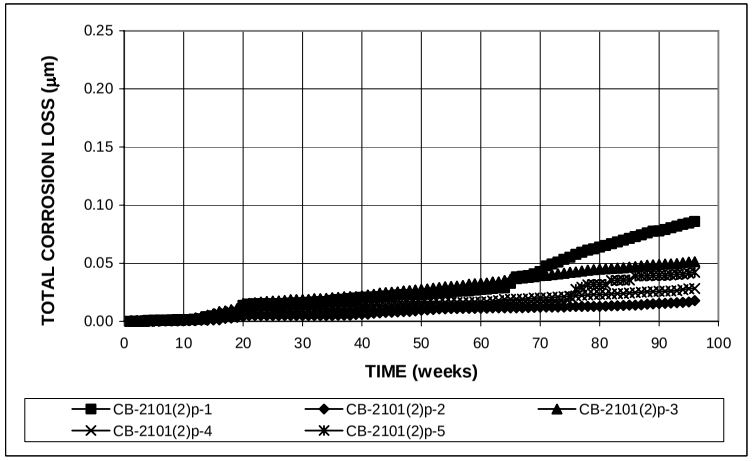

Figure A.201 -Cracked beam test. Total corrosion losses for pickled 2101(2) steel, specimens w/c = 0.45, ponded with 15% NaCl solution.

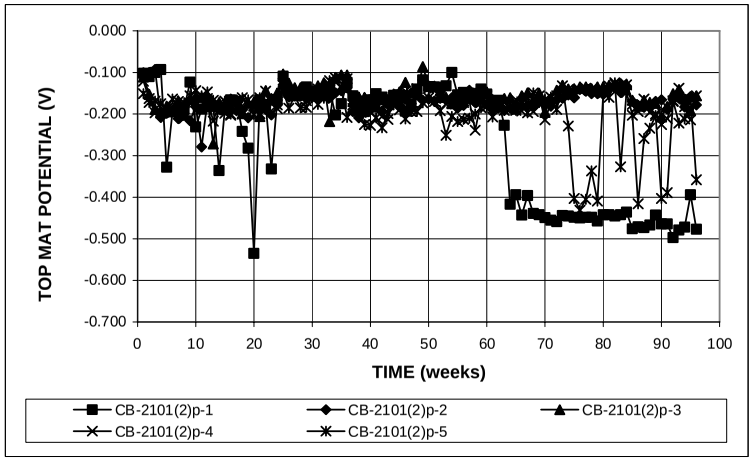

Figure A.202a - Cracked beam test. Top mat corrosion potentials with respect to copper-copper sulfate electrode for pickled 2101(2) steel, specimens w/c = 0.45, ponded with 15% NaCl solution.

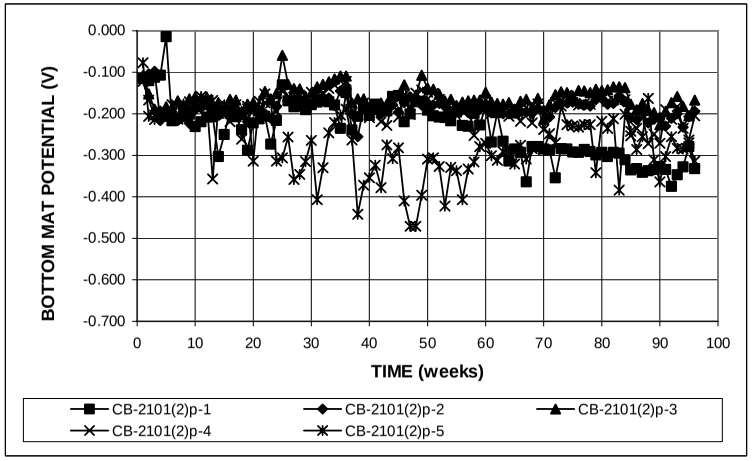

Figure A.202b - Cracked beam test. Bottom mat corrosion potentials with respect to copper-copper sulfate electrode for pickled 2101(2) steel, specimens w/c = 0.45, ponded with 15% NaCl solution.

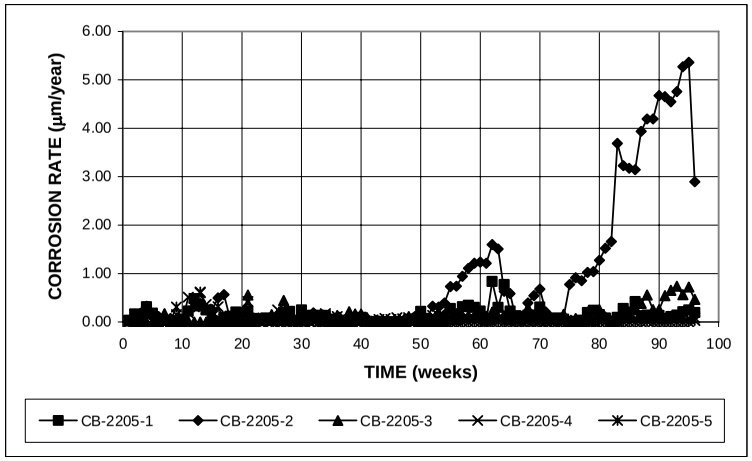

Figure A.204 - Cracked beam test. Corrosion rates for 2205 steel, specimens w/c = 0.45, ponded with 15% NaCl solution.

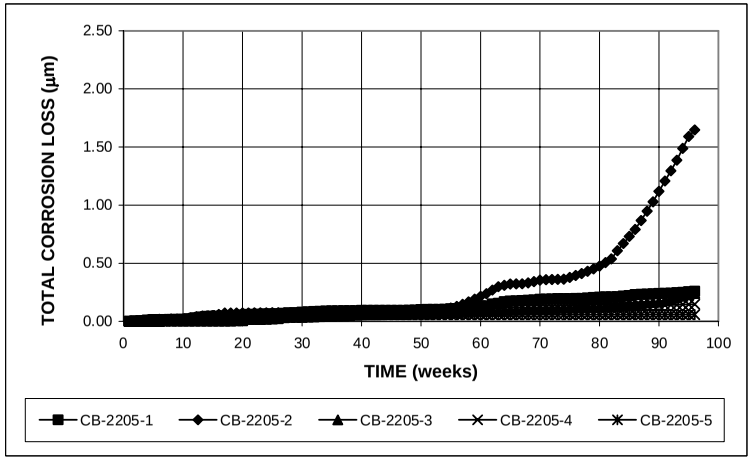

Figure A.205 -Cracked beam test. Total corrosion losses for 2205 steel, specimens w/c = 0.45, ponded with 15% NaCl solution.

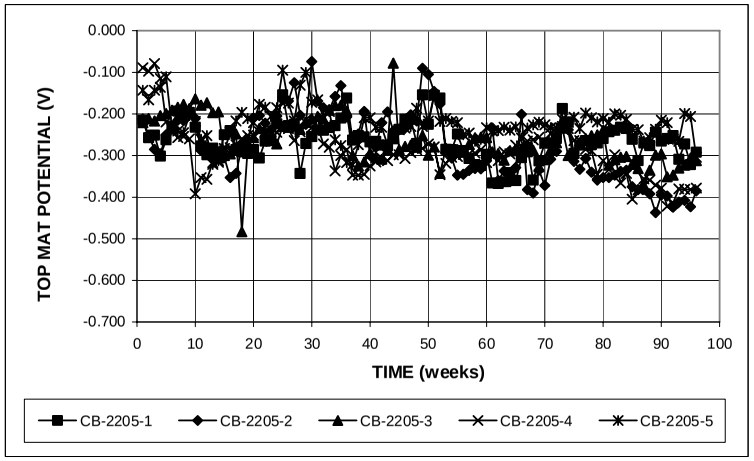

Figure A.206a - Cracked beam test. Top mat corrosion potentials with respect to copper-copper sulfate electrode for 2205 steel, specimens w/c = 0.45, ponded with 15% NaCl solution.

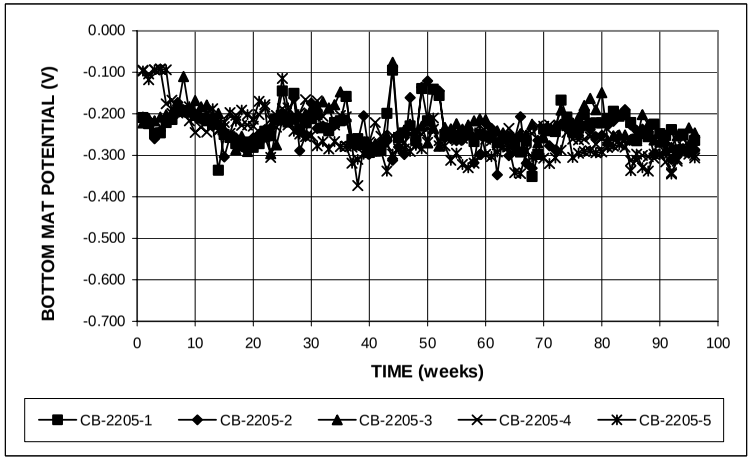

Figure A.206b - Cracked beam test. Bottom mat corrosion potentials with respect to copper-copper sulfate electrode for 2205 steel, specimens w/c = 0.45, ponded with 15% NaCl solution.

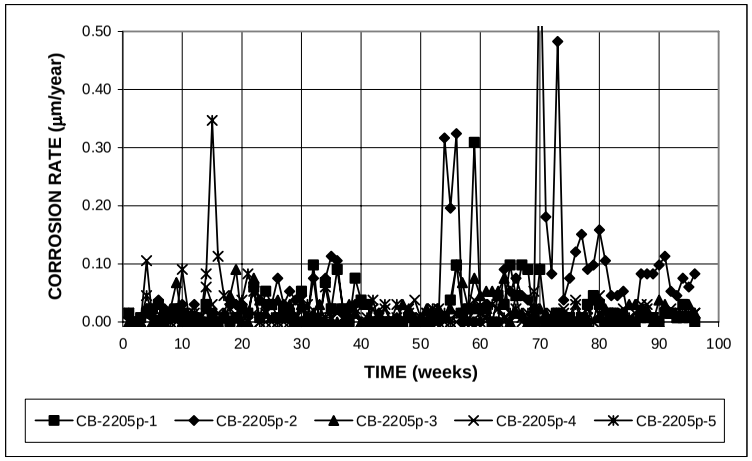

Figure A.207 - Cracked beam test. Corrosion rates for pickled 2205 steel, specimens w/c = 0.45, ponded with 15% NaCl solution.

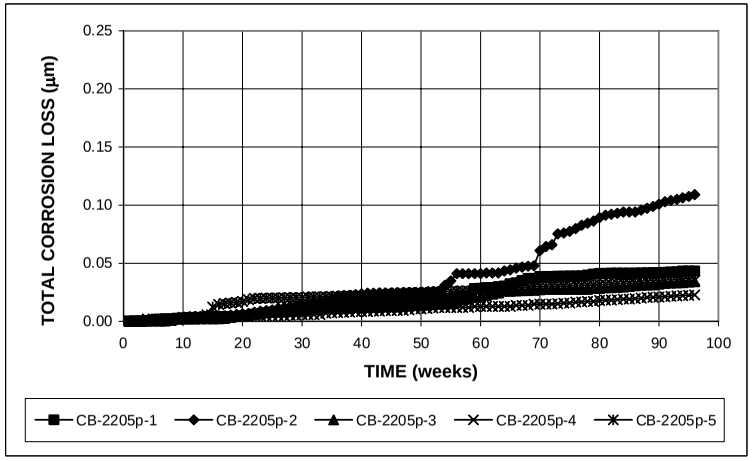

Figure A.208 -Cracked beam test. Total corrosion losses for pickled 2205 steel, specimens w/c = 0.45, ponded with 15% NaCl solution.

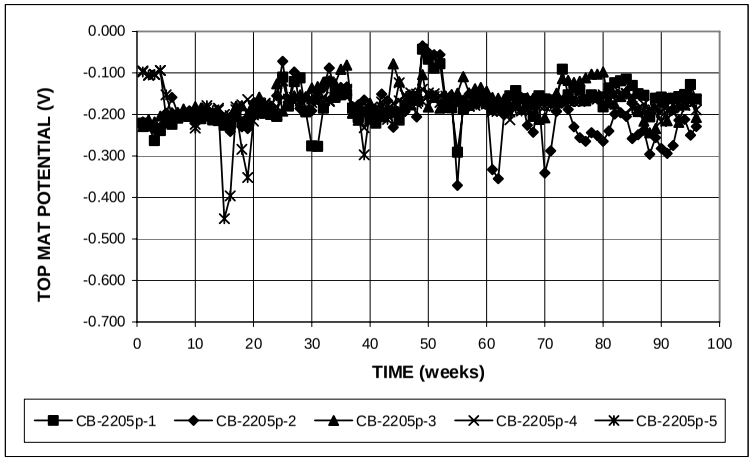

Figure A.209a - Cracked beam test. Top mat corrosion potentials with respect to copper-copper sulfate electrode for pickled 2205 steel, specimens w/c = 0.45, ponded with 15% NaCl solution.

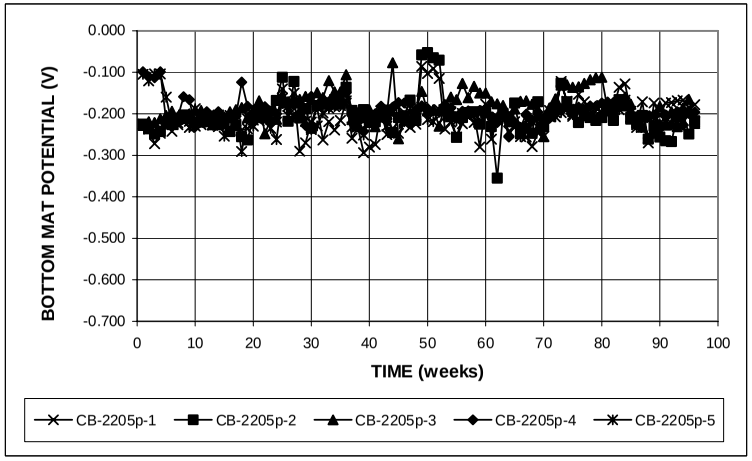

Figure A.209b - Cracked beam test. Bottom mat corrosion potentials with respect to copper-copper sulfate electrode for pickled 2205 steel, specimens w/c = 0.45, ponded with 15% NaCl solution.

APPENDIX B

MAT-TO-MAT RESISTANCES FOR INDIVIDUAL SPECIMENS

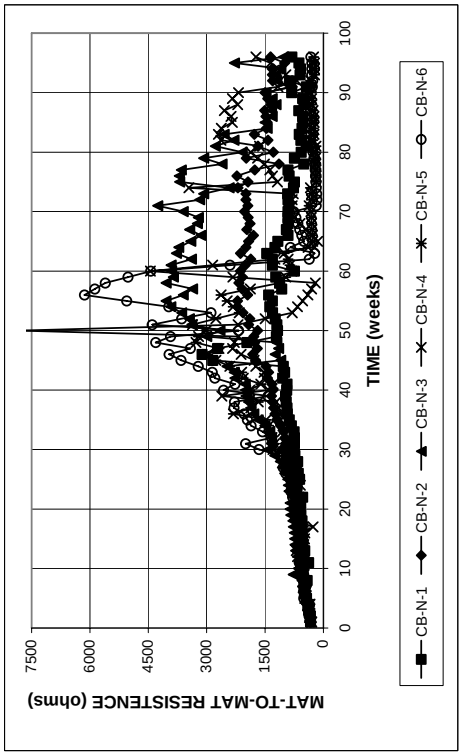

Figure B.3 - Cracked beam test. Mat-to-mat resistances for specimens with conventional N steel, specimens w/c = 0.45, ponded with 15% NaCl solution.

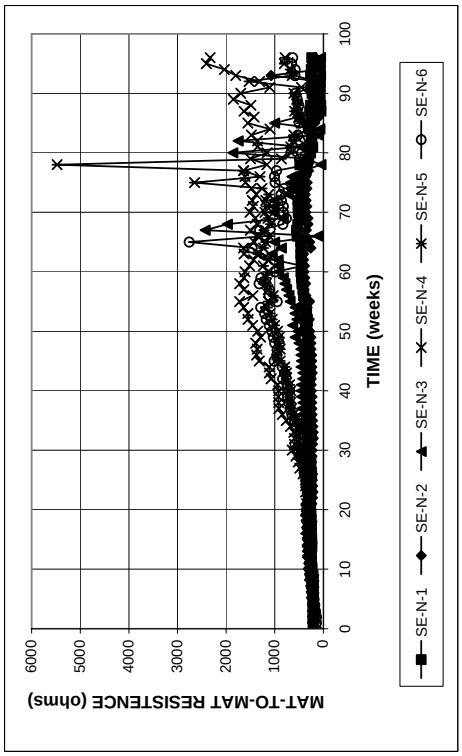

Figure B.1 - Southern Exposure test. Mat-to-mat resistances for specimens with conventional N steel, specimens w/c = 0.45, ponded with 15% NaCl solution.

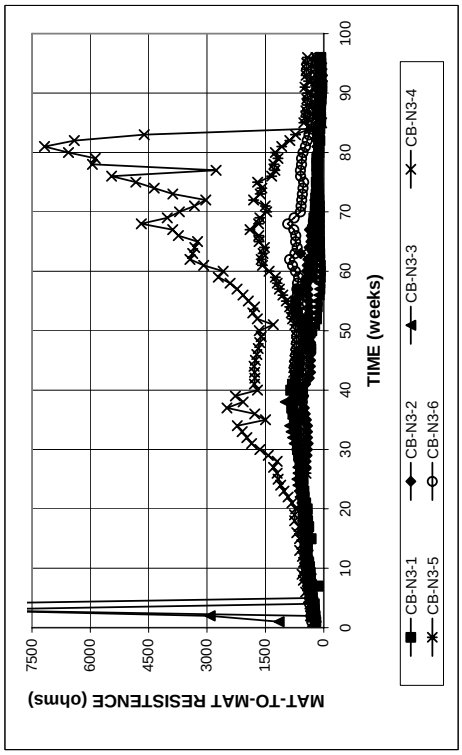

Figure B.4 - Cracked beam test. Mat-to-mat resistances for specimens with conventional N3 steel, specimens w/c = 0.45, ponded with 15% NaCl solution.

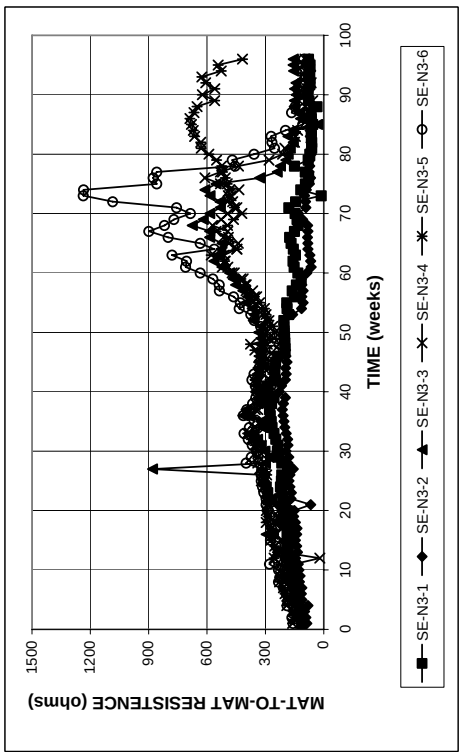

Figure B.2 - Southern Exposure test. Mat-to-mat resistances for specimens with conventional N3 steel, specimens w/c = 0.45, ponded with 15% NaCl solution.

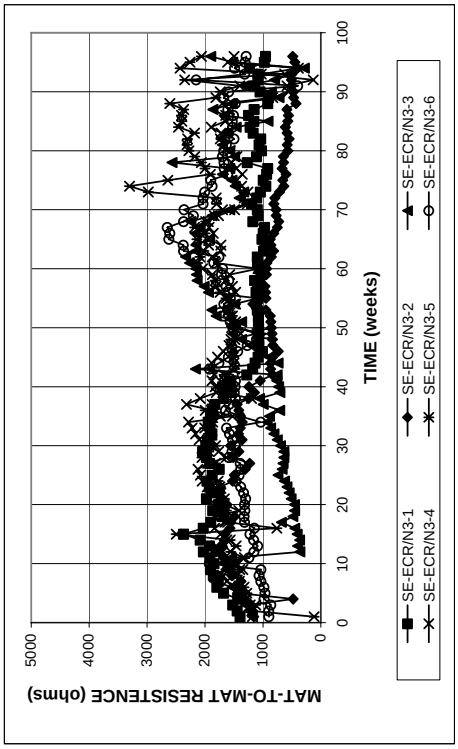

Figure B.5 - Southern Exposure test. Mat-to-mat resistances for specimens with epoxy-coated steel, specimens w/c = 0.45, ponded with 15% NaCl solution.

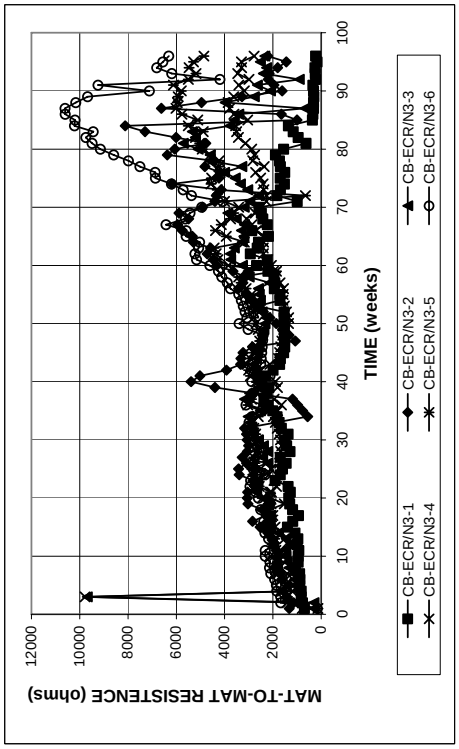

Figure B.6 - Cracked beam test. Mat-to-mat resistances for specimens with epoxy-coated steel, specimens w/c = 0.45, ponded with 15% NaCl solution.

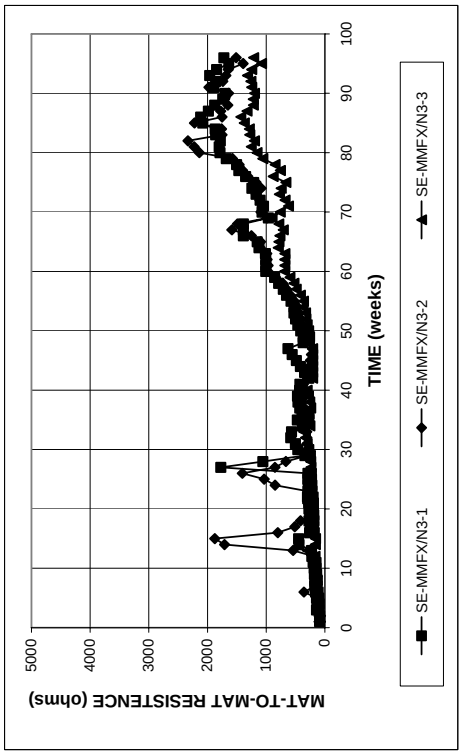

Figure B.9 - Southern Exposure test. Mat-to-mat resistances for specimens with MMFX steel at the top mat and conventional N3 steel at the bottom mat, specimens w/c = 0.45, ponded with 15% NaCl solution.

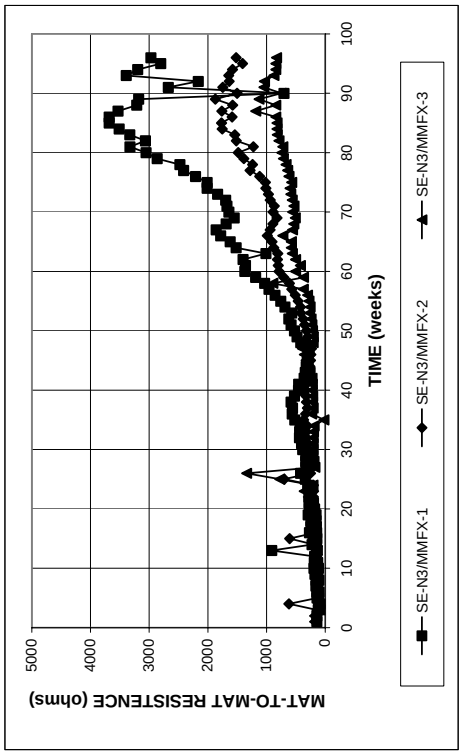

Figure B.10 - Southern Exposure test. Mat-to-mat resistances for specimens with MMFX steel at the bottom mat and conventional N3 steel at the top mat, specimens w/c = 0.45, ponded with 15% NaCl solution.

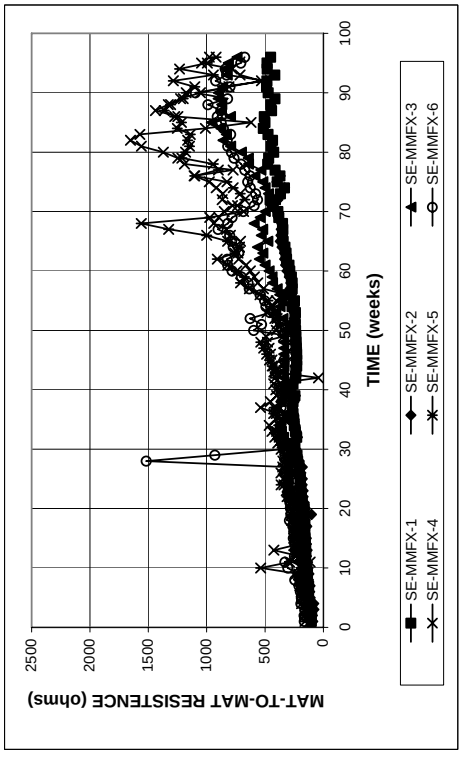

Figure B.7 - Southern Exposure test. Mat-to-mat resistances for specimens with MMFX steel, specimens w/c = 0.45, ponded with 15% NaCl solution.

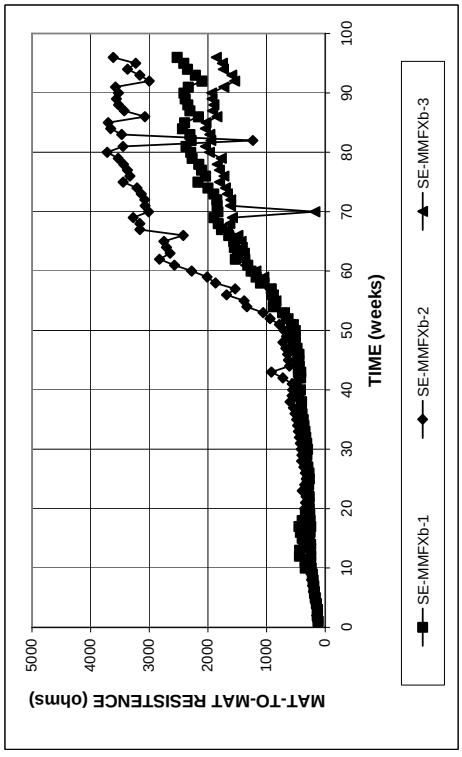

Figure B.8 - Southern Exposure test. Mat-to-mat resistances for specimens with bent MMFX steel, specimens w/c = 0.45, ponded with 15% NaCl solution.

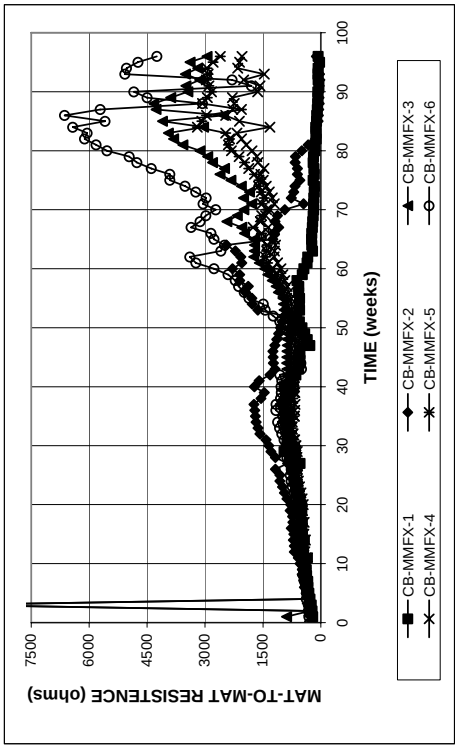

Figure B.11 - Cracked beam test. Mat-to-mat resistances for specimens with MMFX steel, specimens w/c = 0.45, ponded with 15% NaCl solution.

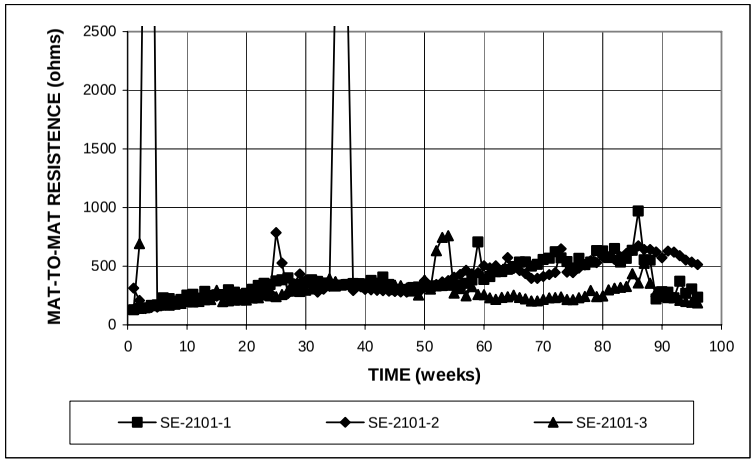

Figure B.12 - Southern Exposure test. Mat-to-mat resistances for specimens with 2101 duplex steel, specimens w/c = 0.45, ponded with 15% NaCl solution.

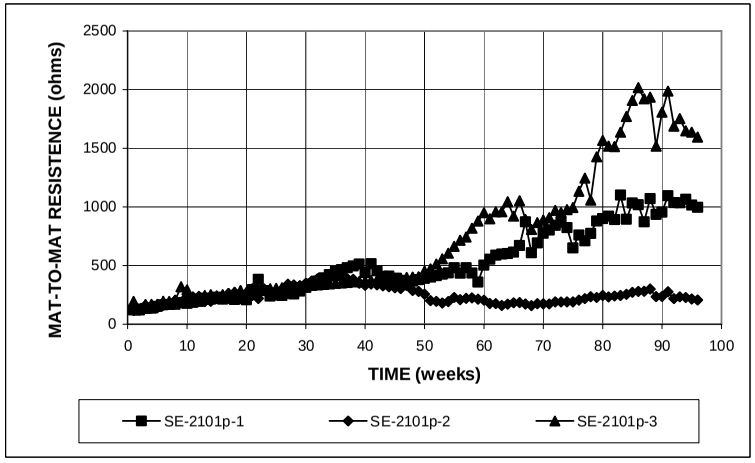

Figure B.13 - Southern Exposure test. Mat-to-mat resistances for specimens with pickled 2101 duplex steel, specimens w/c = 0.45, ponded with 15% NaCl solution.

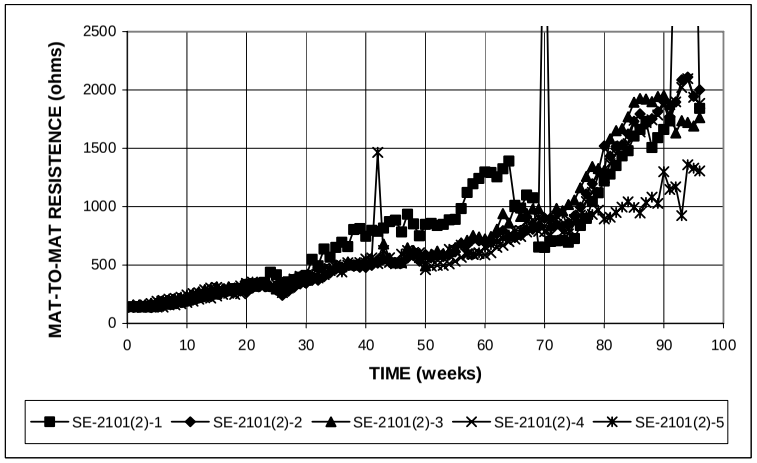

Figure B.14 - Southern Exposure test. Mat-to-mat resistances for specimens with 2101(2) duplex steel, specimens w/c = 0.45, ponded with 15% NaCl solution.

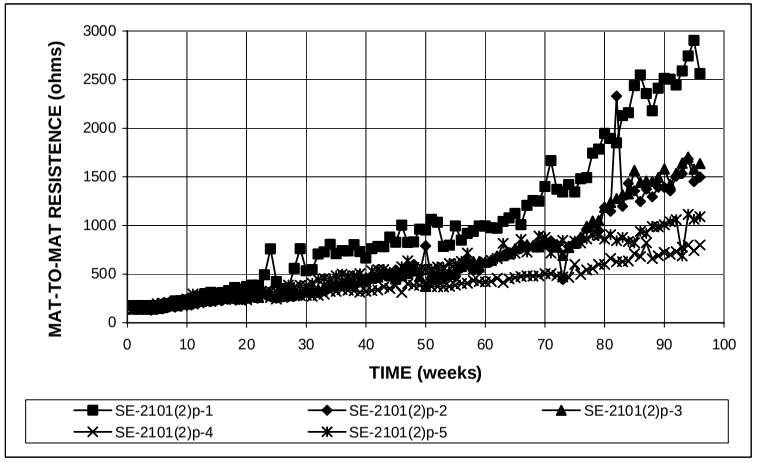

Figure B.15 - Southern Exposure test. Mat-to-mat resistances for specimens with pickled 2101(2) duplex steel, specimens w/c = 0.45, ponded with 15% NaCl solution.

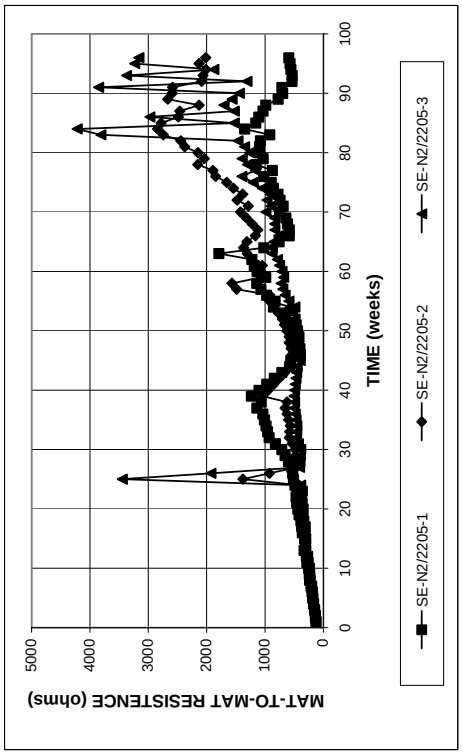

Figure B.18 - Southern Exposure test. Mat-to-mat resistances for specimens with 2205 steel at the bottom mat and conventional N2 steel at the top mat, specimens w/c = 0.45, ponded with 15% NaCl solution.

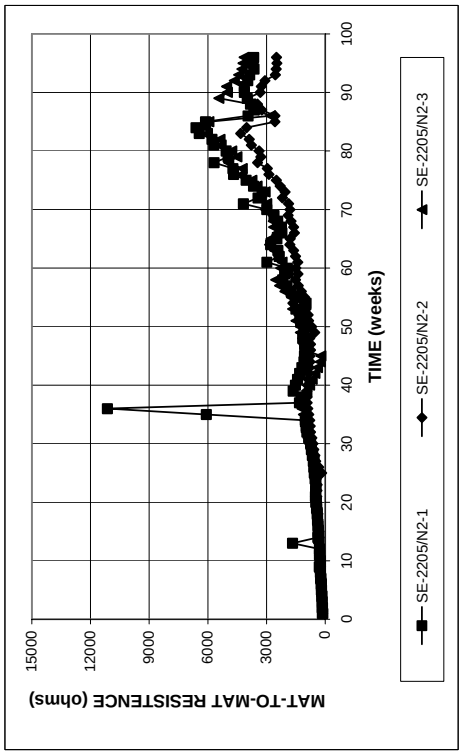

Figure B.19 - Southern Exposure test. Mat-to-mat resistances for specimens with 2205 steel at the top mat and conventional N2 steel at the bottom mat, specimens w/c = 0.45, ponded with 15% NaCl solution.

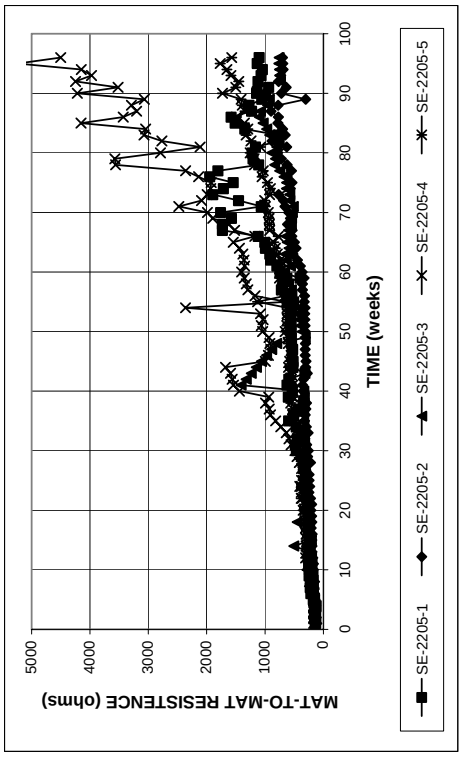

Figure B.16 - Southern Exposure test. Mat-to-mat resistances for specimens with 2205 duplex steel, specimens w/c = 0.45, ponded with 15% NaCl solution.

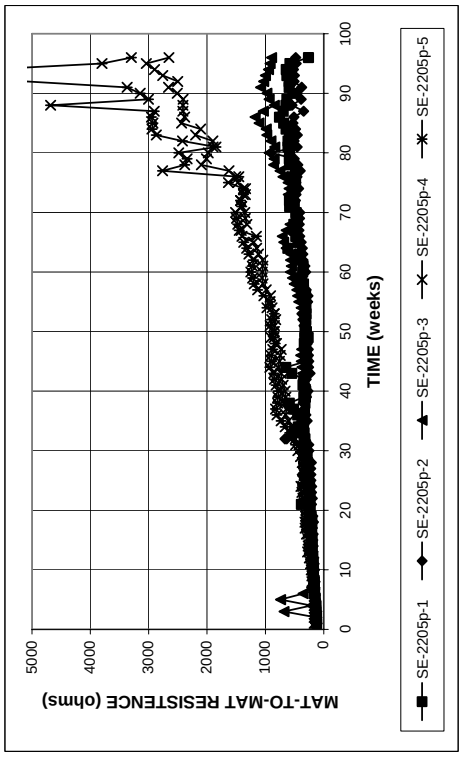

Figure B.17 - Southern Exposure test. Mat-to-mat resistances for specimens with pickled 2205 duplex steel, specimens w/c = 0.45, ponded with 15% NaCl solution.

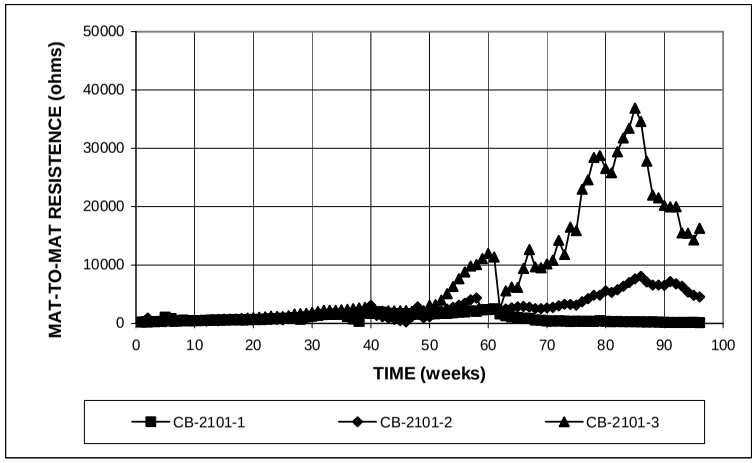

Figure B.20 - Cracked beam test. Mat-to-mat resistances for specimens with 2101 steel, specimens w/c = 0.45, ponded with 15% NaCl solution.

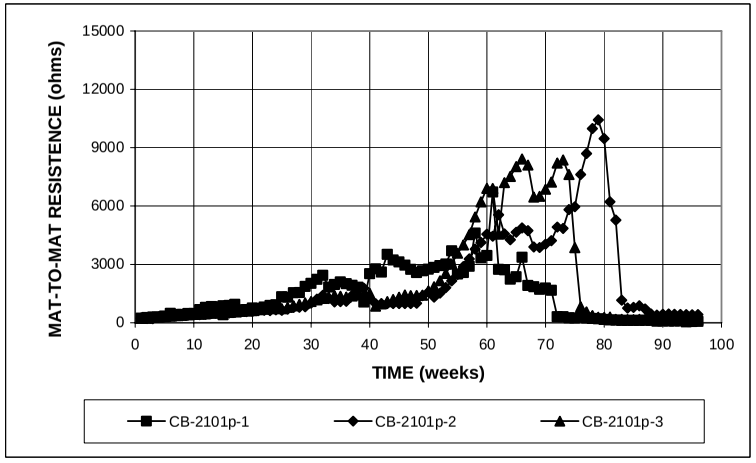

Figure B.21 - Cracked beam test. Mat-to-mat resistances for specimens with pickled 2101 steel, specimens w/c = 0.45, ponded with 15% NaCl solution.

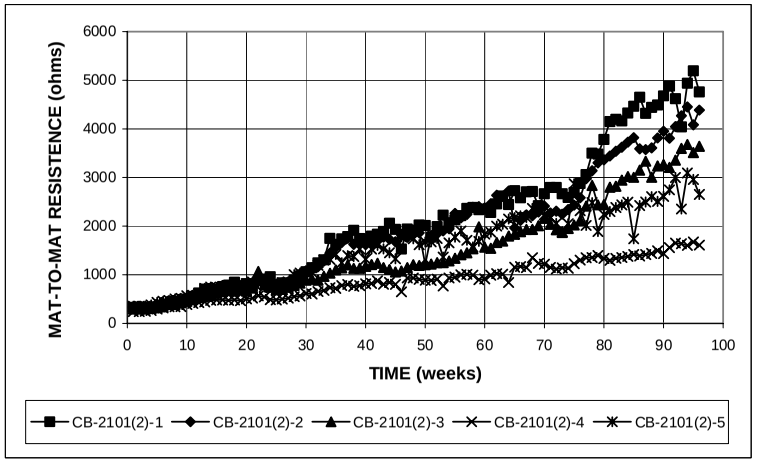

Figure B.22 - Cracked beam test. Mat-to-mat resistances for specimens with 2101(2) steel, specimens w/c = 0.45, ponded with 15% NaCl solution.

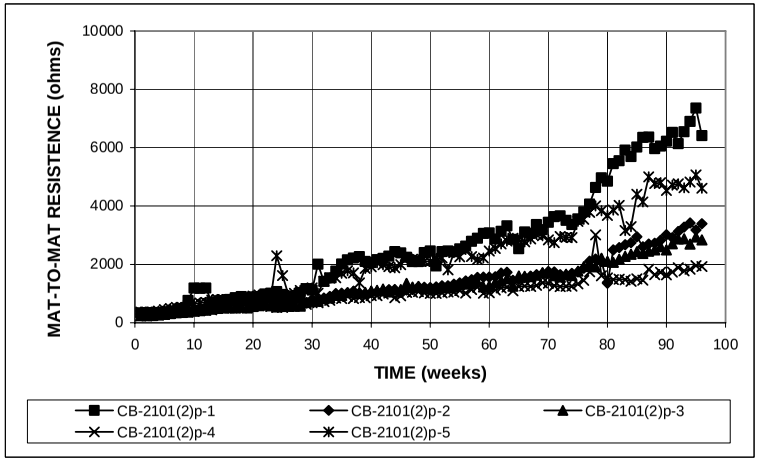

Figure B.23 - Cracked beam test. Mat-to-mat resistances for specimens with pickled 2101(2) steel, specimens w/c = 0.45, ponded with 15% NaCl solution.

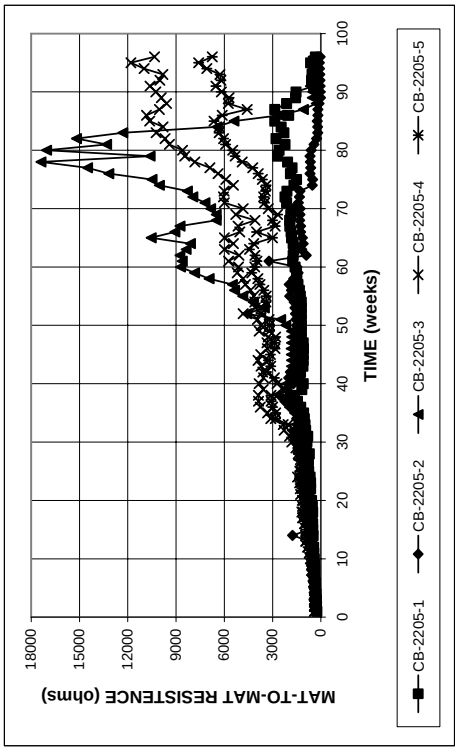

Figure B.24 - Cracked beam test. Mat-to-mat resistances for specimens with 2205 steel, specimens w/c = 0.45, ponded with 15% NaCl solution.

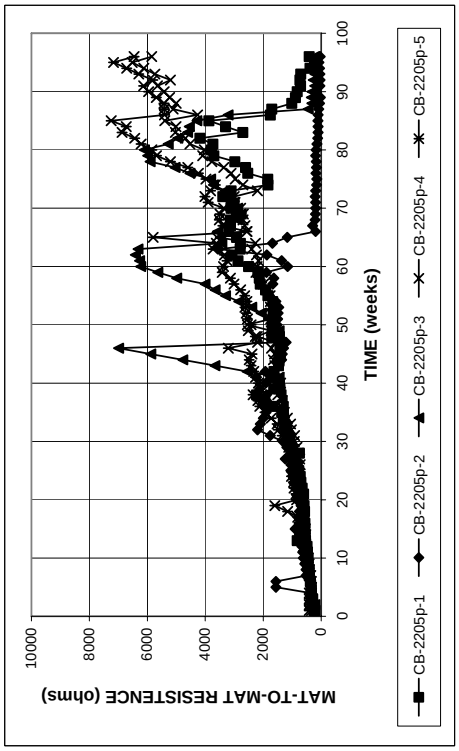

Figure B.25 - Cracked beam test. Mat-to-mat resistances for specimens with pickled 2205 steel, specimens w/c = 0.45, ponded with 15% NaCl solution.

APPENDIX C
STUDENT'S T-TEST

The Student's t-test is often used to assess if the means of two normally distributed populations are statistically different when the sample size is small and the population variances are unknown. Specifically, a statistical value *t* (t_{stat}) is calculated based on the means, the variances, and the sizes of two sample groups. The value is compared to a critical value [t_α (one side) or $t_{\alpha/2}$ (two sides)] at a level of significance, α, or a level of confidence (X%, equal to 1- α) from the t-distribution. The critical *t* values are tabulated in most statistics books in terms of the level of significance and the number of degrees of freedom of samples. If the absolute value of t_{stat} is greater than $t_{\alpha/2}$ at a given level of α, the difference in the means is statistically significant at the level of significance. If the absolute value of t_{stat} is smaller than $t_{\alpha/2}$, the difference in the means is not statistically significant at the level of α.

In this study, the t-test was performed at four levels of significance: 0.20, 0.10, 0.05, and 0.02, corresponding to confidence levels of 80, 90, 95, and 98%, respectively. The values of t_{stat} for the two groups being compared are obtained using the t-test data analysis function in Microsoft Excel spreadsheet (assuming unequal variances). The results of the t-tests are presented in Tables C.1 to C.14. The tables identify the specimens being compared, and show the values of t_{stat} and the values of $t_{\alpha/2}$ at each level of significance. A "Y" next to the value of $t_{\alpha/2}$ indicates that the absolute value of t_{stat} is greater than $t_{\alpha/2}$ at the given level of α, and thus, the difference in the means of the compared groups is statistically significant. An "N" indicates that the difference in the means is not significant.

Table C.1 – Student's t-test for comparing the average corrosion rates at the end of the test between specimens with different conventional steels

Specimens [a]		t_{stat} [b]	$t_{\alpha/2}$ [c] X%:	80%	90%	95%	98%
			α:	0.20	0.10	0.05	0.02
Macrocell test with bare specimens							
M-N2-r	M-N4-r	-1.344		1.372 N	1.812 N	2.228 N	2.764 N
Macrocell test with mortar specimens							
M-N2m	M-N3m	-0.346		1.397 N	1.860 N	2.306 N	2.896 N
Southern Exposure test							
SE-N	SE-N3	-1.109		1.440 N	1.943 N	2.447 N	3.143 N
Cracked beam test							
CB-N	CB-N3	0.415		1.383 N	1.833 N	2.262 N	2.821 N

[a] **A – B – C**
A: test method: M = macrocell test, SE = Southern Exposure test; CB = cracked beam test.
B: steel type and test condition → N, N2, N3, and N4: conventional steel; m: mortar-wrapped specimens.
C: r = the test solutions are replaced every five weeks
[b] t_{stat} : the calculated statistic t value obtained from the t-test with two-sample assuming unequal variances.
[c] $t_{\alpha/2}$: t value for Student's t-distribution at the given value of α, α: level of significance, X%: level of confidence.
Y: statistically significant difference between groups;
N: not a statistically significant difference between groups

Table C.2 – Student's t-test for comparing the average corrosion losses at the end of the test between specimens with different conventional steels.

Specimens [a]		t_{stat} [b]	$t_{\alpha/2}$ [c] X%:	80%	90%	95%	98%
			α:	0.20	0.10	0.05	0.02
Macrocell test with bare specimens							
M-N2-r	M-N4-r	0.737		1.383 N	1.833 N	2.262 N	2.821 N
Macrocell test with mortar specimens							
M-N2m	M-N3m	-2.043		1.476 Y	2.015 Y	2.571 N	3.365 N
Southern Exposure test							
SE-N	SE-N3	-1.192		1.440 N	1.943 N	2.447 N	3.143 N
Cracked beam test							
CB-N	CB-N3	-1.197		1.383 N	1.833 N	2.262 N	2.821 N

a: **A – B -C**
A: test method: M = macrocell test, SE = Southern Exposure test; CB = cracked beam test.
B: steel type and test condition → N, N2, N3, and N4: conventional steel; m: mortar-wrapped specimens.
C: r = the test solutions are replaced every five weeks
[b] t_{stat} : the calculated statistic t value obtained from the t-test with two-sample assuming unequal variances.
[c] $t_{\alpha/2}$: t value for Student's t-distribution at the given value of α, α: level of significance, X%: level of confidence.
Y: statistically significant difference between groups;
N: not a statistically significant difference between groups

Table C.3 – Student's t-test for comparing average corrosion rates at the end of the test between conventional uncoated and epoxy-coated steel

Specimens [a]		t_{stat} [b]	$t_{\alpha/2}$ [c]			
		X%:	**80%**	**90%**	**95%**	**98%**
		α:	**0.20**	**0.10**	**0.05**	**0.02**
Macrocell test with mortar specimens						
M-N3m	M-ECR/N3m^{T}	3.183	1.372 Y	1.812 Y	2.228 Y	2.764 Y
M-N3m	M-ECRm-r^{E}	5.747	1.415 Y	1.895 Y	2.365 Y	2.998 Y
Southern Exposure test						
SE-N3	SE-ECR/N3^{T}	1.161	1.476 N	2.015 N	2.571 N	3.365 N
Cracked beam test						
CB-N3	CB-ECR/N3^{T}	-1.136	1.372 N	1.812 N	2.228 N	2.764 N

[a] **A – B - C**
A: test method: M = macrocell test, SE = Southern Exposure test; CB = cracked beam test.
B: steel type and test condition → N3: conventional steel; ECR: epoxy-coated steel; ECR/N3 = ECR steel as the anode, N3 steel as the cathode; T: based on the total area; m: mortar-wrapped specimen.
[b] t_{stat} : the calculated statistic t value obtained from the t-test with two-sample assuming unequal variances.
[c] $t_{\alpha/2}$: t value for Student's t-distribution at the given value of α, α: level of significance, X%: level of confidence.
Y: statistically significant difference between groups;
N: not a statistically significant difference between groups.

Table C.4 – Student's t-test for comparing average corrosion losses at the end of the test between conventional uncoated and epoxy-coated steel

Specimens [a]		t_{stat} [b]	$t_{\alpha/2}$ [c]			
		X%:	**80%**	**90%**	**95%**	**98%**
		α:	**0.20**	**0.10**	**0.05**	**0.02**
Macrocell test with mortar specimens						
M-N3m	M-ECR/N3m^{T}	14.342	1.383 Y	1.833 Y	2.262 Y	2.821 Y
M-N3m	M-ECRm-r^{E}	8.084	1.372 Y	1.812 Y	2.228 Y	2.764 Y
Southern Exposure test						
SE-N3	SE-ECR/N3^{T}	2.969	1.476 Y	2.015 Y	2.571 Y	3.365 N
Cracked beam test						
CB-N3	CB-ECR/N3^{T}	3.269	1.440 Y	1.943 Y	2.447 Y	3.143 Y

[a] **A - B**
A: test method: M = macrocell test, SE = Southern Exposure test; CB = cracked beam test.
B: steel type and test condition → N3: conventional steel; ECR: epoxy-coated steel; ECR/N3 = ECR steel as the anode, N3 steel as the cathode; T: based on the total area; m: mortar-wrapped specimen.
[b] t_{stat} : the calculated statistic t value obtained from the t-test with two-sample assuming unequal variances.
[c] $t_{\alpha/2}$: t value for Student's t-distribution at the given value of α, α: level of significance, X%: level of confidence.
Y: statistically significant difference between groups;
N: not a statistically significant difference between groups.

Table C.5 – Student's t-test for comparing the average corrosion rates at the end of the test between conventional and MMFX microcomposite steels.

Specimens [a]		t_{stat} [b]	$t_{\alpha/2}$ [c]			
		X%:	**80%**	**90%**	**95%**	**98%**
		α:	**0.20**	**0.10**	**0.05**	**0.02**
Macrocell test with bare specimens in 1.6 m ion NaCl						
M-N3	M-MMFX	1.561	1.440 Y	1.943 N	2.447 N	3.143 N
M-N2-r	M-MMFX-r	0.842	1.397 N	1.860 N	2.306 N	2.896 N
Macrocell test with bare specimens in 6.04 m ion NaCl						
M-N2h-r	M-MMFXh-r	2.290	1.372 Y	1.812 Y	2.228 Y	2.764 N
Macrocell test with mortar specimens						
M-N3m	M-MMFXm	2.349	1.397 Y	1.860 Y	2.306 Y	2.896 N
M-N2m-r	M-MMFXm-r	7.651	1.440 Y	1.943 Y	2.447 Y	3.143 Y
M-N3m	M-N3/MMFXm	1.888	1.415 Y	1.895 N	2.365 N	2.998 N
M-MMFXm	M-MMFX/N3m	-1.236	1.415 N	1.895 N	2.365 N	2.998 N
Southern Exposure test						
SE-N3	SE-MMFX-45	0.987	1.476 N	2.015 N	2.571 N	3.365 N
SE-N3	SE-N3/MMFX	1.385	1.476 N	2.015 N	2.571 N	3.365 N
SE-MMFX	SE-MMFX/N3	1.619	1.415 Y	1.895 N	2.365 N	2.998 N
SE-MMFX	SE-MMFXb	3.210	1.415 Y	1.895 Y	2.365 Y	2.998 Y
Cracked beam test						
CB-N3	CB-MMFX	0.266	1.440 N	1.943 N	2.447 N	3.143 N

a **A – B –C**

A: test method: M = macrocell test, SE = Southern Exposure test; CB = cracked beam test.

B: steel type and test condition → N2 and N3 = conventional steel; MMFX = MMFX II microcomposite steel; MMFX/N3 = MMFX steel as the anode, N3 steel as the cathode; N3/MMFX = N3 steel as the anode, MMFX steel as the cathode; b = bent bars at the anode; h = 6.04 m ion NaCl concentration; m = mortar-wrapped specimens.

C: r = the test solutions are replaced every five weeks

[b] t_{stat} : the calculated statistic t value.

[c] $t_{\alpha/2}$: t value for Student's t-distribution at the given value of α, α: level of significance, X%: level of confidence.

Y: statistically significant difference between groups;

N: not a statistically significant difference between groups.

Table C.6 – Student's t-test for comparing the average corrosion losses at the end of the test between conventional and MMFX microcomposite steels.

Specimens [a]		t_{stat} [b]	$t_{\alpha/2}$ [c]			
		X%:	**80%**	**90%**	**95%**	**98%**
		α:	**0.20**	**0.10**	**0.05**	**0.02**
Macrocell test with bare specimens in 1.6 m ion NaCl						
M-N3	M-MMFX	3.940	1.440 Y	1.943 Y	2.447 Y	3.143 Y
M-N2-r	M-MMFX-r	5.462	1.383 Y	1.833 Y	2.262 Y	2.821 Y
Macrocell test with bare specimens in 6.04 m ion NaCl						
M-N2h-r	M-MMFXh-r	5.409	1.415 Y	1.895 Y	2.365 Y	2.998 Y
Macrocell test with mortar specimens						
M-N3m	M-MMFXm	10.380	1.372 Y	1.812 Y	2.228 Y	2.764 Y
M-N2m-r	M-MMFXm-r	5.976	1.397 Y	1.860 Y	2.306 Y	2.896 Y
M-N3m	M-N3/MMFXm	5.925	1.533 Y	2.132 Y	2.776 Y	3.747 Y
M-MMFXm	M-MMFX/N3m	-1.499	1.415 Y	1.895 N	2.365 N	2.998 N
Southern Exposure test						
SE-N3	SE-MMFX-45	2.505	1.476 Y	2.015 Y	2.571 N	3.365 N
SE-N3	SE-N3/MMFX	1.598	1.440 Y	1.943 N	2.447 N	3.143 N
SE-MMFX	SE-MMFX/N3	-0.286	1.415 N	1.895 N	2.365 N	2.998 N
SE-MMFX	SE-MMFXb	-2.289	1.533 Y	2.132 Y	2.776 N	3.747 N
Cracked beam test						
CB-N3-45	CB-MMFX-45	2.883	1.476 Y	2.015 Y	2.571 Y	3.365 N

[a] **A – B – C**

A: test method: M = macrocell test, SE = Southern Exposure test; CB = cracked beam test.

B: steel type and test condition → N2 and N3 = conventional steel; MMFX = MMFX II microcomposite steel; MMFX/N3 = MMFX steel as the anode, N3 steel as the cathode; N3/MMFX = N3 steel as the anode, MMFX steel as the cathode; b = bent bars at the anode; h = 6.04 m ion NaCl concentration; m = mortar-wrapped specimens.

C: r = the test solutions are replaced every five weeks

[b] t_{stat} : the calculated statistic t value obtained from the t-test with two-sample assuming unequal variances.

[c] $t_{\alpha/2}$: t value for Student's t-distribution at the given value of α, α: level of significance, X%: level of confidence.

Y: statistically significant difference between groups;

N: not a statistically significant difference between groups.

Table C.7 – Student's t-test for comparing the average corrosion rates at the end of the test between conventional and 2101 duplex stainless steels.

Specimens [a]		t_{stat} [b]	$t_{\alpha/2}$ [c]			
		X%:	**80%**	**90%**	**95%**	**98%**
		α:	**0.20**	**0.10**	**0.05**	**0.02**
Macrocell test with bare specimens in 1.6 m ion NaCl						
M-N3	M-2101	3.472	1.476 Y	2.015 Y	2.571 Y	3.365 Y
M-N3	M-2101(2)	3.391	1.476 Y	2.015 Y	2.571 Y	3.365 Y
M-N4-r	M-N4/2101(2)p-r	1.959	1.638 Y	2.353 N	3.182 N	4.541 N
M-2101(2)p	M-2101(2)p/N4-r	-1.552	1.886 N	2.920 N	4.303 N	6.965 N
Macrocell test with bare specimens in 6.04 m ion NaCl						
M-N2h	M-2101h	2.055	1.415 Y	1.895 Y	2.365 N	2.998 N
M-N2h	M-2101(2)h	3.013	1.533 Y	2.132 Y	2.776 Y	3.747 N
Macrocell test with mortar specimens						
M-N2m	M-2101m	1.827	1.415 Y	1.895 N	2.365 N	2.998 N
M-N2m	M-2101(2)m	3.374	1.476 Y	2.015 Y	2.571 Y	3.365 Y
Southern Exposure test						
SE-N	SE-2101	-0.660	1.440 N	1.943 N	2.447 N	3.143 N
SE-N	SE-2101(2)	2.276	1.476 Y	2.015 Y	2.571 N	3.365 N
SE-N	SE-N2/2205	0.099	1.440 N	1.943 N	2.447 N	3.143 N
SE-2205	SE-2205/N2	0.605	1.440 N	1.943 N	2.447 N	3.143 N
Cracked beam test						
CB-N	CB-2101	-0.350	1.638 N	2.353 N	3.182 N	4.541 N
CB-N	CB-2101(2)	0.815	1.440 N	1.943 N	2.447 N	3.143 N

[a] **A – B – C**

A: test method: M = macrocell test, SE = Southern Exposure test; CB = cracked beam test.

B: steel type and test condition → N, N2 , N3, and N4 = conventional steel; 2101 and 2101(2) = the first and second batches of 2101 duplex stainless steel (21% chromium, 1% nickel); 2205 = 2205 duplex stainless steel (25% chromium, 5% nickel); p = pickled; 2101(2)p/N4 = 2101(2)p steel as the anode, N4 steel as the cathode; N4/2101(2)p = N4 steel as the anode, 2101(2)p steel as the cathode; 2205/N2 = 2205 steel as the anode, N2 steel as the cathode; N2/2205 = N2 steel as the anode, 2205 steel as the cathode; h = 6.04 m ion NaCl concentration; m = mortar-wrapped specimens.

C: r = the test solutions are replaced every five weeks

[b] t_{stat} : the calculated statistic t value obtained from the t-test with two-sample assuming unequal variances.

[c] $t_{\alpha/2}$: t value for Student's t-distribution at the given value of α, α: level of significance, X%: level of confidence.

Y: statistically significant difference between groups;

N: not a statistically significant difference between groups.

Table C.8 – Student's t-test for comparing the average corrosion losses at the end of the test between conventional and 2101 duplex stainless steels

Specimens [a]		t_{stat} [b]	$t_{\alpha/2}$ [c]			
		X%:	**80%**	**90%**	**95%**	**98%**
		α:	**0.20**	**0.10**	**0.05**	**0.02**
Macrocell test with bare specimens in 1.6 m ion NaCl						
M-N3	M-2101	4.787	1.440 Y	1.943 Y	2.447 Y	3.143 Y
M-N3	M-2101(2)	4.727	1.476 Y	2.015 Y	2.571 Y	3.365 Y
M-N4-r	M-N4/2101(2)p-r	2.123	1.533 Y	2.132 N	2.776 N	3.747 N
M-2101(2)p	M-2101(2)p/N4-r	1.074	1.440 N	1.943 N	2.447 N	3.143 N
Macrocell test with bare specimens in 6.04 m ion NaCl						
M-N2h	M-2101h	5.031	1.415 Y	1.895 Y	2.365 Y	2.998 Y
M-N2h	M-2101(2)h	6.261	1.476 Y	2.015 Y	2.571 Y	3.365 Y
Macrocell test with mortar specimens						
M-N2m	M-2101m	3.824	1.440 Y	1.943 Y	2.447 Y	3.143 Y
M-N2m	M-2101(2)m	4.524	1.533 Y	2.132 Y	2.776 Y	3.747 Y
Southern Exposure test						
SE-N	SE-2101	2.355	1.533 Y	2.132 Y	2.776 N	3.747 N
SE-N	SE-2101(2)	7.979	1.476 Y	2.015 Y	2.571 Y	3.365 Y
SE-N	SE-N2/2205	0.960	1.476 N	2.015 N	2.571 N	3.365 N
SE-2205	SE-2205/N2	-0.504	1.440 N	1.943 N	2.447 N	3.143 N
Cracked beam test						
CB-N	CB-2101	3.424	1.440 Y	1.943 Y	2.447 Y	3.143 Y
CB-N	CB-2101(2)	4.957	1.476 Y	2.015 Y	2.571 Y	3.365 Y

[a] **A – B – C**

A: test method: M = macrocell test, SE = Southern Exposure test; CB = cracked beam test.

B: steel type and test condition → N, N2 , N3, and N4 = conventional steel; 2101 and 2101(2) = the first and second batches of 2101 duplex stainless steel (21% chromium, 1% nickel); 2205 = 2205 duplex stainless steel (25% chromium, 5% nickel); p = pickled; 2101(2)p/N4 = 2101(2)p steel as the anode, N4 steel as the cathode; N4/2101(2)p = N4 steel as the anode, 2101(2)p steel as the cathode; 2205/N2 = 2205 steel as the anode, N2 steel as the cathode; N2/2205 = N2 steel as the anode, 2205 steel as the cathode; h = 6.04 m ion NaCl concentration; m = mortar-wrapped specimens.

C: r = the test solutions are replaced every five weeks

[b] t_{stat} : the calculated statistic t value obtained from the t-test with two-sample assuming unequal variances.

[c] $t_{\alpha/2}$: t value for Student's t-distribution at the given value of α, α: level of significance, X%: level of confidence.
Y: statistically significant difference between groups;
N: not a statistically significant difference between groups.

Table C.9 – Student's t-test for comparing the average corrosion rates at the end of the test between nonpickled and pickled duplex stainless steels.

Specimens [a]		t_{stat} [b]	$t_{\alpha/2}$ [c]			
		X%:	**80%**	**90%**	**95%**	**98%**
		α:	**0.20**	**0.10**	**0.05**	**0.02**
Macrocell test with bare specimens						
M-2101	M-2101p	5.395	1.533 Y	2.132 Y	2.776 Y	3.747 Y
M-2101(2)	M-2101(2)p	3.204	1.476 Y	2.015 Y	2.571 Y	3.365 N
M-2205	M-2205p	0.759	1.476 N	2.015 N	2.571 N	3.365 N
Macrocell test with bare specimens in 6.04 m ion NaCl						
M-2101h	M-2101ph	2.973	1.476 Y	2.015 Y	2.571 Y	3.365 N
M-2101(2)h	M-2101(2)ph	9.650	1.383 Y	1.833 Y	2.262 Y	2.821 Y
M-2205h	M-2205ph	8.343	1.476 Y	2.015 Y	2.571 Y	3.365 Y
M-2205h-r	M-2205ph-r	3.855	1.476 Y	2.015 Y	2.571 Y	3.365 Y
Macrocell test with mortar specimens						
M-2101m	M-2101pm	3.207	1.638 Y	2.353 Y	3.182 Y	4.541 N
M-2101(2)m	M-2101(2)pm	5.184	1.476 Y	2.015 Y	2.571 Y	3.365 Y
M-2205m	M-2205pm	-1.000	1.415 N	1.895 N	2.365 N	2.998 N
Southern Exposure test						
SE-2101	SE-2101p	1.600	1.533 Y	2.132 N	2.776 N	3.747 N
SE-2101(2)	SE-2101(2)p	1.561	1.533 Y	2.132 N	2.776 N	3.747 N
SE-2205	SE-2205p	1.469	1.533 N	2.132 N	2.776 N	3.747 N
Cracked beam test						
CB-2101	CB-2101p	-0.587	1.638 N	2.353 N	3.182 N	4.541 N
CB-2101(2)	CB-2101(2)p	4.479	1.533 Y	2.132 Y	2.776 Y	3.747 Y
CB-2205	CB-2205p	1.299	1.533 N	2.132 N	2.776 N	3.747 N

[a] **A – B – C**

A: test method: M = macrocell test, SE = Southern Exposure test; CB = cracked beam test.

B: steel type and test condition → 2101 and 2101(2) = the first and second batches of 2101 duplex stainless steel (21% chromium, 1% nickel); 2205 = 2205 duplex stainless steel (25% chromium, 5% nickel); p = pickled; h = 6.04 m ion NaCl concentration; m = mortar-wrapped specimens.

C: r = the test solutions are replaced every five weeks

[b] t_{stat} : the calculated statistic t value obtained from the t-test with two-sample assuming unequal variances.

[c] $t_{\alpha/2}$: t value for Student's t-distribution at the given value of α, α: level of significance, X%: level of confidence.
Y: statistically significant difference between groups;
N: not a statistically significant difference between groups.

Table C.10 – Student's t-test for comparing the average corrosion losses at the end of the test between nonpickled and pickled duplex stainless steels.

Specimens [a]		t_{stat} [b]	$t_{\alpha/2}$ [c]			
		X%:	**80%**	**90%**	**95%**	**98%**
		α:	**0.20**	**0.10**	**0.05**	**0.02**
Macrocell test with bare specimens						
M-2101	M-2101p	1.970	1.533 Y	2.132 N	2.776 N	3.747 N
M-2101(2)	M-2101(2)p	8.576	1.476 Y	2.015 Y	2.571 Y	3.365 Y
M-2205	M-2205p	1.975	1.533 Y	2.132 N	2.776 N	3.747 N
Macrocell test with bare specimens in 6.04 m ion NaCl						
M-2101h	M-2101ph	3.166	1.415 Y	1.895 Y	2.365 Y	2.998 Y
M-2101(2)h	M-2101(2)ph	12.464	1.476 Y	2.015 Y	2.571 Y	3.365 Y
M-2205h	M-2205ph	8.545	1.476 Y	2.015 Y	2.571 Y	3.365 Y
M-2205h-r	M-2205ph-r	4.229	1.476 Y	2.015 Y	2.571 Y	3.365 Y
Macrocell test with mortar specimens						
M-2101m	M-2101pm	2.826	1.638 Y	2.353 Y	3.182 N	4.541 N
M-2101(2)m	M-2101(2)pm	6.169	1.476 Y	2.015 Y	2.571 Y	3.365 Y
M-2205m	M-2205pm	-0.027	1.383 N	1.833 N	2.262 N	2.821 N
Southern Exposure test						
SE-2101	SE-2101p	2.651	1.638 Y	2.353 Y	3.182 N	4.541 N
SE-2101(2)	SE-2101(2)p	2.109	1.533 Y	2.132 N	2.776 N	3.747 N
SE-2205	SE-2205p	1.344	1.533 N	2.132 N	2.776 N	3.747 N
Cracked beam test						
CB-2101	CB-2101p	1.739	1.638 Y	2.353 N	3.182 N	4.541 N
CB-2101(2)	CB-2101(2)p	16.586	1.533 Y	2.132 Y	2.776 Y	3.747 Y
CB-2205	CB-2205p	1.419	1.533 N	2.132 N	2.776 N	3.747 N

[a] **A – B – C**

A: test method: M = macrocell test, SE = Southern Exposure test; CB = cracked beam test.

B: steel type and test condition → 2101 and 2101(2) = the first and second batches of 2101 duplex stainless steel (21% chromium, 1% nickel); 2205 = 2205 duplex stainless steel (25% chromium, 5% nickel); p = pickled; h = 6.04 m ion NaCl concentration; m = mortar-wrapped specimens.

C: r = the test solutions are replaced every five weeks

[b] t_{stat} : the calculated statistic t value obtained from the t-test with two-sample assuming unequal variances.

[c] $t_{\alpha/2}$: t value for Student's t-distribution at the given value of α, α: level of significance, X%: level of confidence.
Y: statistically significant difference between groups;
N: not a statistically significant difference between groups.

Table C.11 – Student's t-test for comparing the average corrosion rates at the end of the test between 2101(2) pickled steel and 2205 nonpickled and pickled steels.

Specimens [a]		t_{stat} [b]	$t_{\alpha/2}$ [c]			
		X%:	**80%**	**90%**	**95%**	**98%**
		α:	**0.20**	**0.10**	**0.05**	**0.02**
Macrocell test with bare specimens						
M-2205	M-2101(2)p	1.938	1.476 Y	2.015 N	2.571 N	3.365 N
M-2205p	M-2101(2)p	2.682	1.383 Y	1.833 Y	2.262 Y	2.821 N
Macrocell test with bare specimens in 6.04 m ion NaCl						
M-2205h	M-2101(2)ph	2.401	1.415 Y	1.895 Y	2.365 Y	2.998 N
M-2205ph	M-2101(2)ph	-1.168	1.476 N	2.015 N	2.571 N	3.365 N
M-2205h-r	M-2101(2)ph-r	3.855	1.440 Y	1.943 Y	2.447 Y	3.143 Y
M-2205ph-r	M-2101(2)ph-r	0.456	1.440 N	1.943 N	2.447 N	3.143 N
Macrocell test with mortar specimens						
M-2205m	M-2101(2)pm	-2.457	1.440 Y	1.943 Y	2.447 Y	3.143 N
M-2205pm	M-2101(2)pm	-1.206	1.372 N	1.812 N	2.228 N	2.764 N
Southern Exposure test						
SE-2205	SE-2101(2)p	0.924	1.476 N	2.015 N	2.571 N	3.365 N
SE-2205p	SE-2101(2)p	-1.358	1.533 N	2.132 N	2.776 N	3.747 N
Cracked beam test						
CB-2205	CB-2101(2)p	1.269	1.533 N	2.132 N	2.776 N	3.747 N
CB-2205p	CB-2101(2)p	-0.897	1.397 N	1.860 N	2.306 N	2.896 N

[a] **A – B – C**

A: test method: M = macrocell test, SE = Southern Exposure test; CB = cracked beam test.

B: steel type and test condition → 2101(2) = the second batch of 2101 duplex stainless steel (21% chromium, 1% nickel); 2205 = 2205 duplex stainless steel (25% chromium, 5% nickel); p = pickled; h = 6.04 m ion NaCl concentration; m = mortar-wrapped specimens.

C: r = the test solutions are replaced every five weeks

[b] t_{stat} : the calculated statistic t value obtained from the t-test with two-sample assuming unequal variances.

[c] $t_{\alpha/2}$: t value for Student's t-distribution at the given value of α, α: level of significance, X%: level of confidence.

Y: statistically significant difference between groups;

N: not a statistically significant difference between groups.

Table C.12 – Student's t-test for comparing the average corrosion losses at the end of the test between 2101(2) pickled steel and 2205 nonpickled and pickled steels.

Specimens [a]		t_{stat} [b]	$t_{\alpha/2}$ [c]			
		X%:	**80%**	**90%**	**95%**	**98%**
		α:	**0.20**	**0.10**	**0.05**	**0.02**
Macrocell test with bare specimens						
M-2205	M-2101(2)p	-0.301	1.440 N	1.943 N	2.447 N	3.143 N
M-2205p	M-2101(2)p	-1.038	1.476 N	2.015 N	2.571 N	3.365 N
Macrocell test with bare specimens in 6.04 m ion NaCl						
M-2205h	M-2101(2)ph	4.905	1.383 Y	1.833 Y	2.262 Y	2.821 Y
M-2205ph	M-2101(2)ph	-3.463	1.476 Y	2.015 Y	2.571 Y	3.365 Y
M-2205h-r	M-2101(2)ph-r	3.316	1.415 Y	1.895 Y	2.365 Y	2.998 Y
M-2205ph-r	M-2101(2)ph-r	-1.396	1.476 N	2.015 N	2.571 N	3.365 N
Macrocell test with mortar specimens						
M-2205m	M-2101(2)pm	-0.489	1.372 N	1.812 N	2.228 N	2.764 N
M-2205pm	M-2101(2)pm	-0.392	1.383 N	1.833 N	2.262 N	2.821 N
Southern Exposure test						
SE-2205	SE-2101(2)p	1.282	1.533 N	2.132 N	2.776 N	3.747 N
SE-2205p	SE-2101(2)p	-0.405	1.440 N	1.943 N	2.447 N	3.143 N
Cracked beam test						
CB-2205	CB-2101(2)p	1.433	1.533 N	2.132 N	2.776 N	3.747 N
CB-2205p	CB-2101(2)p	0.197	1.415 N	1.895 N	2.365 N	2.998 N

[a] **A – B – C**

A: test method: M = macrocell test, SE = Southern Exposure test; CB = cracked beam test.

B: steel type and test condition → 2101(2) = the second batch of 2101 duplex stainless steel (21% chromium, 1% nickel); 2205 = 2205 duplex stainless steel (25% chromium, 5% nickel); p = pickled; h = 6.04 m ion NaCl concentration; m = mortar-wrapped specimens.

C: r = the test solutions are replaced every five weeks

[b] t_{stat} : the calculated statistic t value obtained from the t-test with two-sample assuming unequal variances.

[c] $t_{\alpha/2}$: t value for Student's t-distribution at the given value of α, α: level of significance, X%: level of confidence.

Y: statistically significant difference between groups;

N: not a statistically significant difference between groups.

Table C.13 – Student's t-test for comparing the average corrosion rates at the end of the rapid macrocell test between replacing and without replacing the test solutions

Specimens [a]		t_{stat} [b]	$t_{\alpha/2}$ [c]			
		X%:	**80%**	**90%**	**95%**	**98%**
		α:	**0.20**	**0.10**	**0.05**	**0.02**
Macrocell test with bare specimens in 1.6 m ion NaCl						
M-N3	M-N2-r	1.431	1.415 Y	1.895 N	2.365 N	2.998 N
M-N3	N-N4-r	0.762	1.440 N	1.943 N	2.447 N	3.143 N
M-MMFX	M-MMFX-r	0.702	1.397 N	1.860 N	2.306 N	2.896 N
Macrocell test with bare specimens in 6.04 m ion NaCl						
M-N2h	M-N2h-r	-0.762	1.415 N	1.895 N	2.365 N	2.998 N
M-2101(2)ph	M-2101(2)ph-r	1.423	1.476 N	2.015 N	2.571 N	3.365 N
M-2205h	M-2205h-r	2.108	1.383 Y	1.833 Y	2.262 N	2.821 N
M-2205ph	M-2205ph-r	1.479	1.397 Y	1.860 N	2.306 N	2.896 N
Macrocell test with mortar specimens						
M-N2m	M-N2m-r	-0.228	1.440 N	1.943 N	2.447 N	3.143 N
M-MMFXm	M-MMFXm-r	5.190	1.397 Y	1.860 Y	2.306 Y	2.896 Y

[a] **A – B – C**

A: test method: M = macrocell test.

B: steel type and test condition → N2, N3, and N4 = conventional steel; MMFX = MMFX II microcomposite steel; 2101(2) = the second batch of 2101 duplex stainless steel (21% chromium, 1% nickel); 2205 = 2205 duplex stainless steel (25% chromium, 5% nickel); p = pickled; h = 6.04 m ion NaCl concentration; m = mortar-wrapped specimens.

C: r = the test solutions are replaced every five weeks

[b] t_{stat} : the calculated statistic t value obtained from the t-test with two-sample assuming unequal variances.

[c] $t_{\alpha/2}$: t value for Student's t-distribution at the given value of α, α: level of significance, X%: level of confidence.
Y: statistically significant difference between groups;
N: not a statistically significant difference between groups.

Table C.14 – Student's t-test for comparing the average corrosion losses at the end of the rapid macrocell test between replacing and without replacing the test solutions

Specimens [a]		t_{stat} [b]	$t_{\alpha/2}$ [c]			
		X%:	**80%**	**90%**	**95%**	**98%**
		α:	**0.20**	**0.10**	**0.05**	**0.02**
Macrocell test with bare specimens in 1.6 m ion NaCl						
M-N3	M-N2-r	1.408	1.440 N	1.943 N	2.447 N	3.143 N
M-N3	N-N4-r	1.734	1.440 Y	1.943 N	2.447 N	3.143 N
M-MMFX	M-MMFX-r	-0.508	1.372 N	1.812 N	2.228 N	2.764 N
Macrocell test with bare specimens in 6.04 m ion NaCl						
M-N2h	M-N2h-r	0.797	1.440 N	1.943 N	2.447 N	3.143 N
M-2101(2)ph	M-2101(2)ph-r	2.317	1.383 Y	1.833 Y	2.262 Y	2.821 N
M-2205h	M-2205h-r	2.313	1.372 Y	1.812 Y	2.228 Y	2.764 N
M-2205ph	M-2205ph-r	2.727	1.533 Y	2.132 Y	2.776 N	3.747 N
Macrocell test with mortar specimens						
M-N2m	M-N2m-r	0.457	1.440 N	1.943 N	2.447 N	3.143 N
M-MMFXm	M-MMFXm-r	2.050	1.372 Y	1.812 Y	2.228 N	2.764 N

[a] **A – B – C**

A: test method: M = macrocell test.

B: steel type and test condition → N2, N3, and N4 = conventional steel; MMFX = MMFX II microcomposite steel; 2101(2) = the second batch of 2101 duplex stainless steel (21% chromium, 1% nickel); 2205 = 2205 duplex stainless steel (25% chromium, 5% nickel); p = pickled; h = 6.04 m ion NaCl concentration; m = mortar-wrapped specimens.

C: r = the test solutions are replaced every five weeks

[b] t_{stat} : the calculated statistic t value obtained from the t-test with two-sample assuming unequal variances.

[c] $t_{\alpha/2}$: t value for Student's t-distribution at the given value of α, α: level of significance, X%: level of confidence.
Y: statistically significant difference between groups;
N: not a statistically significant difference between groups

APPENDIX D

CORROSION POTENTIAL TEST TO EVALUATE CONVENTIONAL AND MMFX STEEL AS A FUNCTION OF CHLORIDE CONCENTRATION IN SIMULATED CONCRETE PORE SOLUTION

To determine the relative tendency of conventional and MMFX steel to corrode, the corrosion potentials of bare conventional and MMFX bars were compared in simulated concrete pore solution at NaCl molal ion concentrations of 0.2, 0.4, 0.5, 0.6, 0.7, 1.0, 1.6, and 6.04 m. The corrosion potential test provides a relative measure of Cl^-/OH^- ratio at which corrosion will be initiated.

D.1 TEST METHOD

When fabricating specimens, No. 16 [No. 5] reinforcing bars are cut with a band saw to a length of 127 mm (5 in.). The sharp edges on the bar ends are removed by grinding. The bars are then cleaned with acetone to remove grease and dirt from the surface.

The bare test specimens are placed in a 3.8-L (four-quart) cylindrical plastic container (three bars of the same type in one container), along with simulated concrete pore solution containing a 0.2, 0.4, 0.5, 0.6, 0.7, 1.0, 1.6 or 6.04 m ion concentration of sodium chloride (NaCl). The solution depth exposes 76 mm (3 in.) of a bar below the level of the solution. Plastic lids are placed just above the surface of the solution to hold the specimens in place and reduce the evaporation of the solution (four holes are cut in the lids to introduce the specimens and a saturated calomel electrode). The test solutions are replaced every five weeks to maintain the pH.

During the test, the corrosion potential of each bar is measured daily for the first week and weekly thereafter. The test lasts 15 weeks. Potential readings are taken with a high-impedance voltmeter with respect to a saturated calomel electrode (SCE), which is immersed in the solution around tested specimens. Potential more negative than –0.275 V indicates that the steel is corroding.

The plastic container, the voltmeter, the saturated calomel electrode, and the concrete pore solution are described in Section 2.3.3. The test solutions are prepared by adding 5.7, 11.4, 14.3, 17.1, 20.0, 28.5, 45.6 or 172.1g of NaCl to one liter of the simulated concrete pore solution to obtain a 0.2, 0.4, 0.5, 0.6, 0.7, 1.0, 1.6 or 6.04 molal ion concentration solution, which correspond Cl^-/OH^- ratios of 0.13, 0.25, 0.31, 0.38, 0.44, 0.61, 1.0, or 3.8, respectively.

In this study, three each conventional N2 and MMFX reinforcing bars are tested for each concentration.

D.2 TEST RESULTS

The average corrosion potentials for conventional N2 and MMFX steels in simulated concrete pore solution with 0.2, 0.4, 0.5, 0.6, 0.7, 1.0, 1.6 and 6.04 molal ion concentrations of NaCl are plotted versus time in Figures D.1 through D.8. The values at 15 weeks, the end of the test, are summarized in Table D.1. The individual results as a function of time are presented in Figures D.8 through D.16.

The results show that the average corrosion potentials for the two steels become progressively more negative, indicating a higher tendency to corrode, as the NaCl concentration increases.

At 0.2 and 0.4 m ion NaCl concentrations, as shown in Figures D.1 and D.2, the average corrosion potentials for conventional and MMFX steel were more

positive than –0.275 V during most of the test period, indicating a passive condition, with MMFX steel exhibiting slightly more negative potentials than conventional steel. At 15 weeks, the corrosion potentials for conventional and MMFX steel were –0.118 and –0.152 V at 0.2 m ion NaCl concentration and –0.136 V and –0.225 V at 0.4 m concentration, respectively.

Both conventional and MMFX steel exhibited active corrosion (corrosion potentials more negative than –0.275 V with respect to SCE) at NaCl molal ion concentrations of 0.5 m and above, corresponding to a critical Cl^-/OH^- ratio of 0.31.

At 0.5 m ion NaCl concentration, as shown in Figure D.3, conventional and MMFX steel has similar average corrosion potentials about –0.300 V throughout the test period, with an exception that the corrosion potential for conventional steel was more negative than MMFX steel, ranging from –0.300 to –0.400 V between 6 and 9 weeks.

At 0.6 m ion NaCl concentration, as shown in Figure D.4, the average corrosion potential for conventional steel were about –0.300 V during the first 9 weeks and then dropped to values more negative than –0.400 V, while the corrosion potential for MMFX steel was more negative than –0.300 V (primarily between –0.350 and –0.400 V) during the first five weeks and then became generally more positive, reaching –0.226 V at 15 weeks.

At 0.7 m ion NaCl concentration, as shown in Figure D.5, the average corrosion potential for conventional steel fluctuated between –0.300 and –0.400 V during most of the test period, while the corrosion potential for MMFX steel also ranged from –0.300 to –0.400 V, but with values generally become more positive with time, reaching –0.219 V at the end of the test.

At 1.0 m ion NaCl concentration, as shown in Figure D.6, the average corrosion potential for conventional steel ranged from –0.300 to –0.400 V during the first 9 weeks and then dropped to values between –0.400 and –0.500 V, while the corrosion potential for MMFX steel ranged from –0.300 to –0.400 V during the first 10 weeks and then became about –0.400 V. Both of the steels ended with a corrosion potential of about –0.360 V.

At 1.6 and 6.04 m ion NaCl concentrations, as shown in Figures D.7 and D.8, respectively, conventional steel exhibited slightly more negative average corrosion potentials than MMFX steel. At 1.6 m ion NaCl concentration, the corrosion potentials ranged from –0.400 to –0.500 V for conventional steel and ranged from –0.300 to –0.400 V for MMFX steel throughout the test period. At 6.04 m ion NaCl concentration, the corrosion potentials were about –0.500 V for conventional steel, with some points more negative than –0.500 V in the middle of the test, while the corrosion potentials for MMFX steel ranged from –0.400 to –0.500 V. The average corrosion potentials for both steels in the corrosion potential tests (1.6 and 6.04 m) were similar to the anode corrosion potentials exhibited by the steels in the corresponding macrocell tests, as shown in Figures 3.36a and 3.39a.

Overall, the corrosion potentials for conventional and MMFX steels are nearly identical, indicating that both steels have a similar tendency to corrode. The corrosion tendency, however, does not provide an indication of the corrosion rate, which is a function of the full electrochemical behavior of the steel.

Table D.1 - Average corrosion potentials at 15 weeks for conventional N2 and MMFX steels in corrosion potential test

Specimen designation*	NaCl ion Conc. (m)	Cl^-/OH^- ratios	Specimen corrosion potentials (V)			Average (V)	Standard deviation
			1	2	3		
Conventional N2 steel							
CP-N2(0.2)	0.2	0.13	-0.187	-0.081	-0.085	-0.118	0.06
CP-N2(0.4)	0.4	0.25	-0.146	-0.100	-0.163	-0.136	0.03
CP-N2(0.5)	0.5	0.31	-0.313	-0.181	-0.433	-0.309	0.13
CP-N2(0.6)	0.6	0.38	-0.468	-0.430	-0.401	-0.433	0.03
CP-N2(0.7)	0.7	0.44	-0.320	-0.388	-0.231	-0.313	0.08
CP-N2(1.0)	1.0	0.62	-0.359	-0.379	-0.327	-0.355	0.03
CPN2(1.6)	1.6	1.0	-0.414	-0.497	-0.420	-0.444	0.05
CP-N2(6.04)	6.04	3.8	-0.392	-0.371	-0.441	-0.401	0.04
MMFX steel							
CP-MMFX(0.2)	0.2	0.13	-0.160	-0.153	-0.142	-0.152	0.01
CP-MMFX(0.4)	0.4	0.25	-0.167	-0.222	-0.285	-0.225	0.06
CP-MMFX(0.5)	0.5	0.31	-0.270	-0.271	-0.283	-0.275	0.01
CP-MMFX(0.6)	0.6	0.38	-0.230	-0.293	-0.155	-0.226	0.07
CP-MMFX(0.7)	0.7	0.44	-0.210	-0.160	-0.288	-0.219	0.06
CP-MMFX(1.0)	1	0.62	-0.343	-0.372	-0.358	-0.358	0.01
CP-MMFX(1.6)	1.6	1.0	-0.342	-0.376	-0.354	-0.357	0.02
CP-MMFX(6.04)	6.04	3.8	-0.446	-0.467	-0.503	-0.472	0.03

*** A-B(C)**

A: test method; CP = corrosion potential test.

B: steel type; N2 = conventional steels; MMFX = mircrocomposite MMFX steel;

C: NaCl ion concentration in simulated concrete pore solutions.

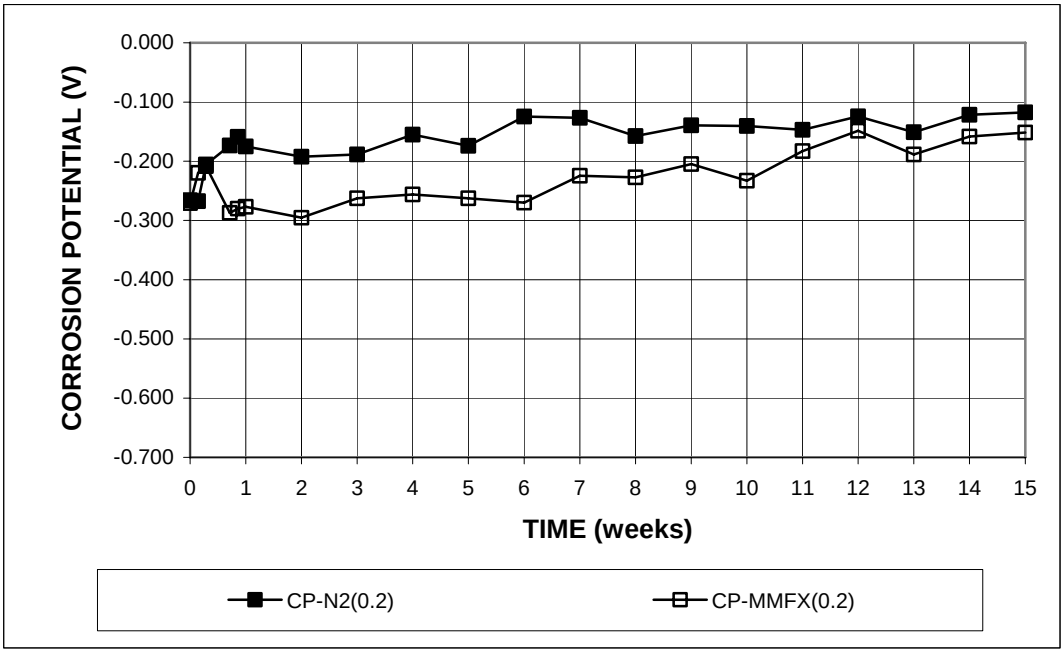

Figure D.1 -Corrosion potential test. Average corrosion potentials with respect to saturated calomel electrode for conventional N2 and MMFX steels in simulated concrete pore solution with 0.2 molal ion NaCl. Solutions are replaced every 5 weeks.

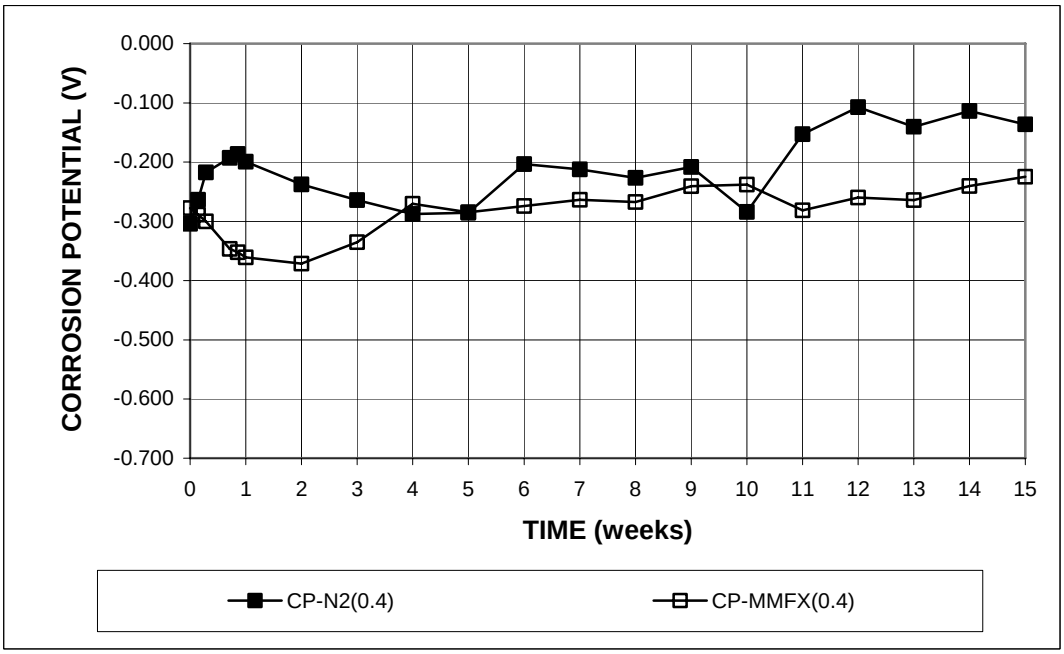

Figure D.2 -Corrosion potential test. Average corrosion potentials with respect to saturated calomel electrode for conventional N2 and MMFX steels in simulated concrete pore solution with 0.4 molal ion NaCl. Solutions are replaced every 5 weeks.

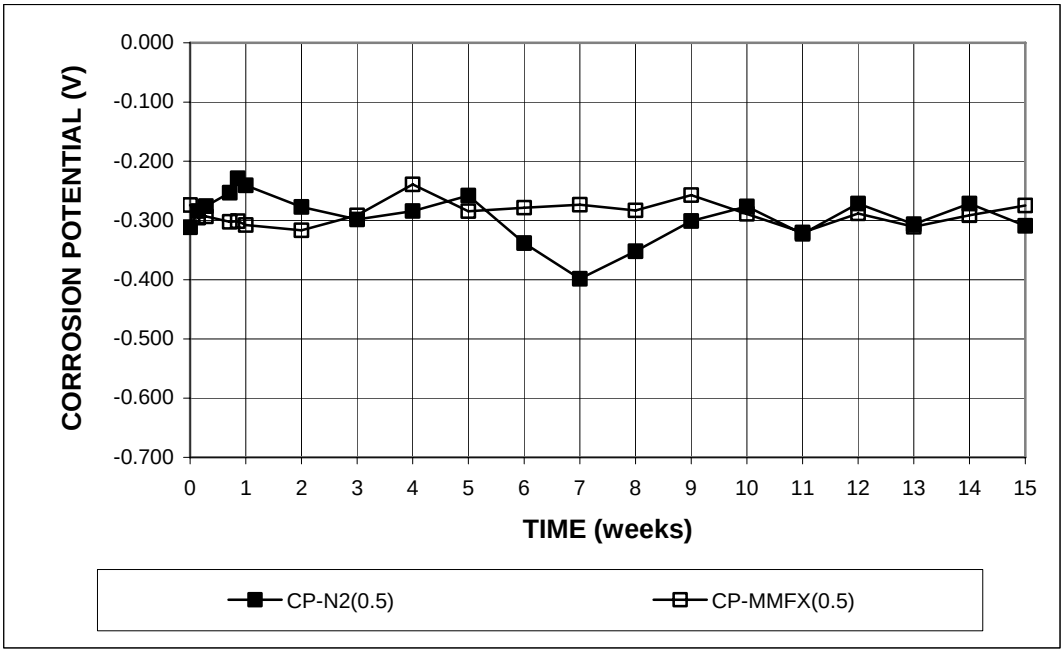

Figure D.3 -Corrosion potential test. Average corrosion potentials with respect to saturated calomel electrode for conventional N2 and MMFX steels in simulated concrete pore solution with 0.5 molal ion NaCl. Solutions are replaced every 5 weeks.

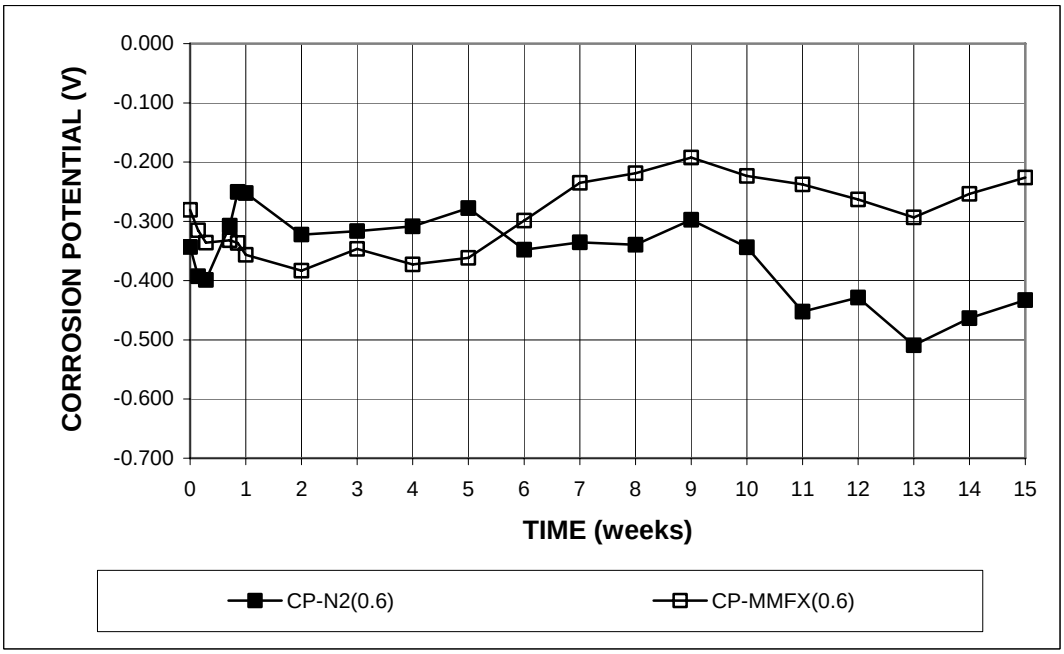

Figure D.4 -Corrosion potential test. Average corrosion potentials with respect to saturated calomel electrode for conventional N2 and MMFX steels in simulated concrete pore solution with 0.6 molal ion NaCl. Solutions are replaced every 5 weeks.

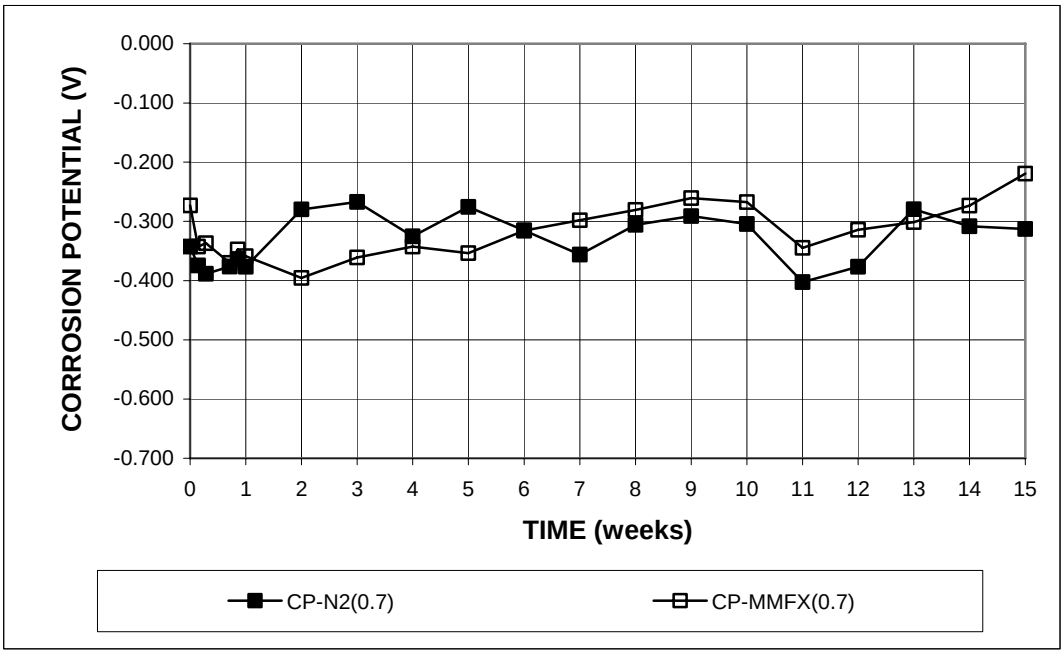

Figure D.5 -Corrosion potential test. Average corrosion potentials with respect to saturated calomel electrode for conventional N2 and MMFX steels in simulated concrete pore solution with 0.7 molal ion NaCl. Solutions are replaced every 5 weeks.

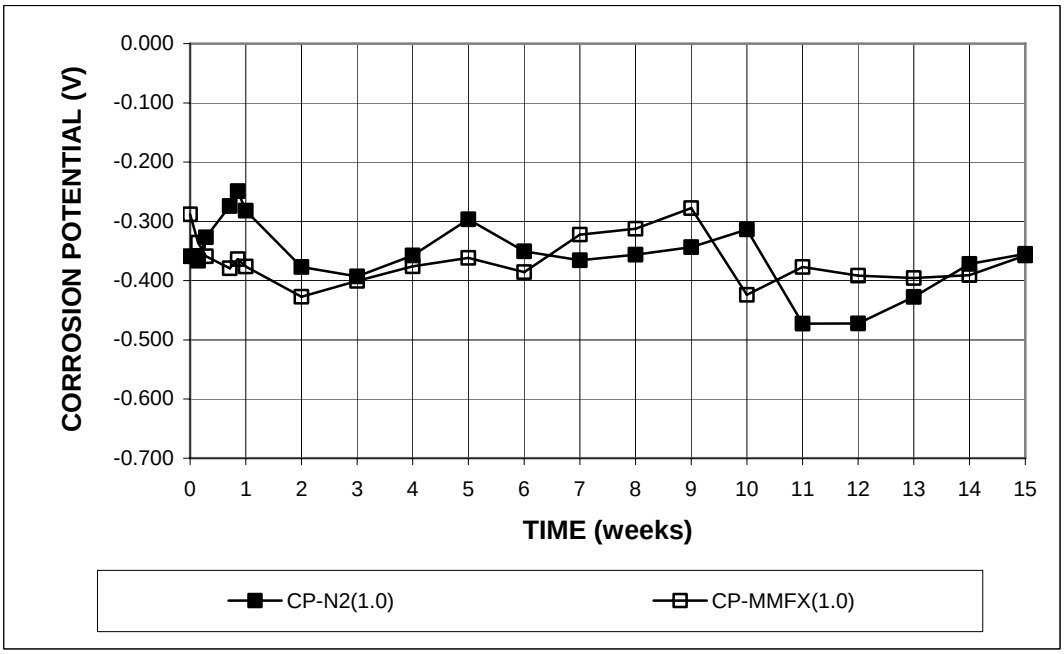

Figure D.6 -Corrosion potential test. Average corrosion potentials with respect to saturated calomel electrode for conventional N2 and MMFX steels in simulated concrete pore solution with 1.0 molal ion NaCl. Solutions are replaced every 5 weeks.

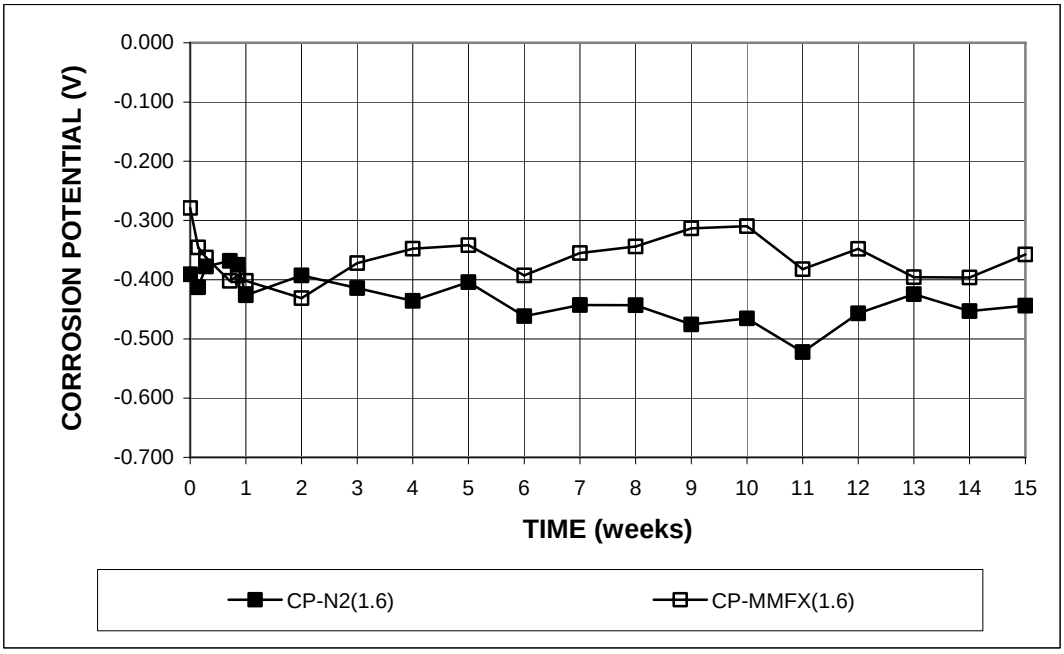

Figure D.7 -Corrosion potential test. Average corrosion potentials with respect to saturated calomel electrode for conventional N2 and MMFX steels in simulated concrete pore solution with 1.6 molal ion NaCl. Solutions are replaced every 5 weeks.

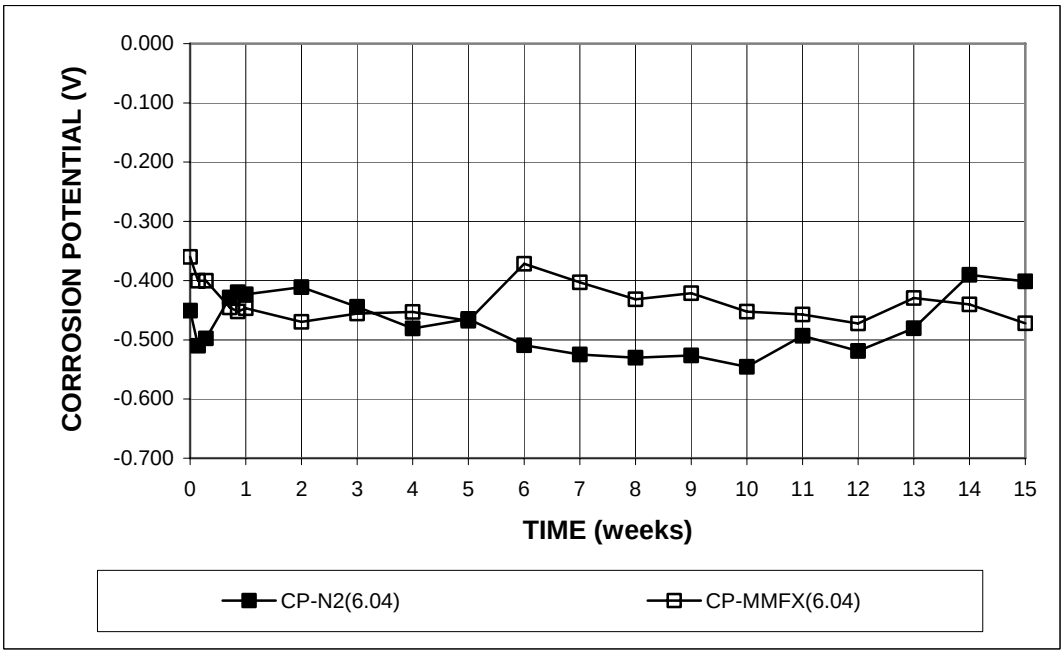

Figure D.8 -Corrosion potential test. Average corrosion potentials with respect to saturated calomel electrode for conventional N2 and MMFX steels in simulated concrete pore solution with 6.04 molal ion NaCl. Solutions are replaced every 5 weeks.

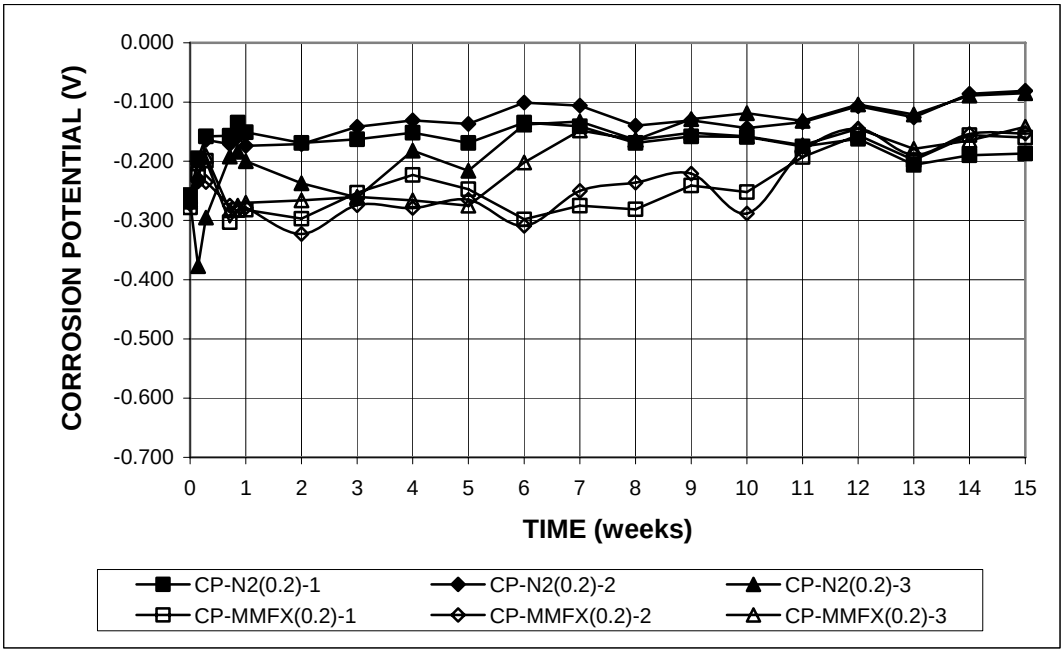

Figure D.9 -Corrosion potential test. Corrosion potentials with respect to saturated calomel electrode for conventional N2 and MMFX steels in simulated concrete pore solution with 0.2 molal ion NaCl. Solutions are replaced every 5 weeks.

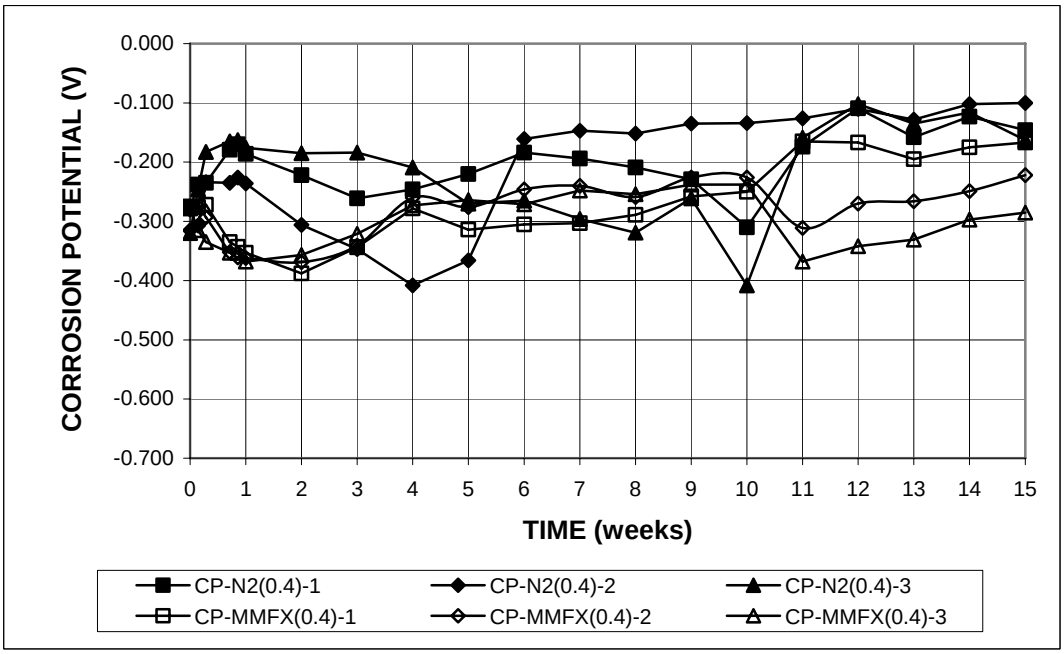

Figure D.10 -Corrosion potential test. Corrosion potentials with respect to saturated calomel electrode for conventional N2 and MMFX steels in simulated concrete pore solution with 0.4 molal ion NaCl. Solutions are replaced every 5 weeks.

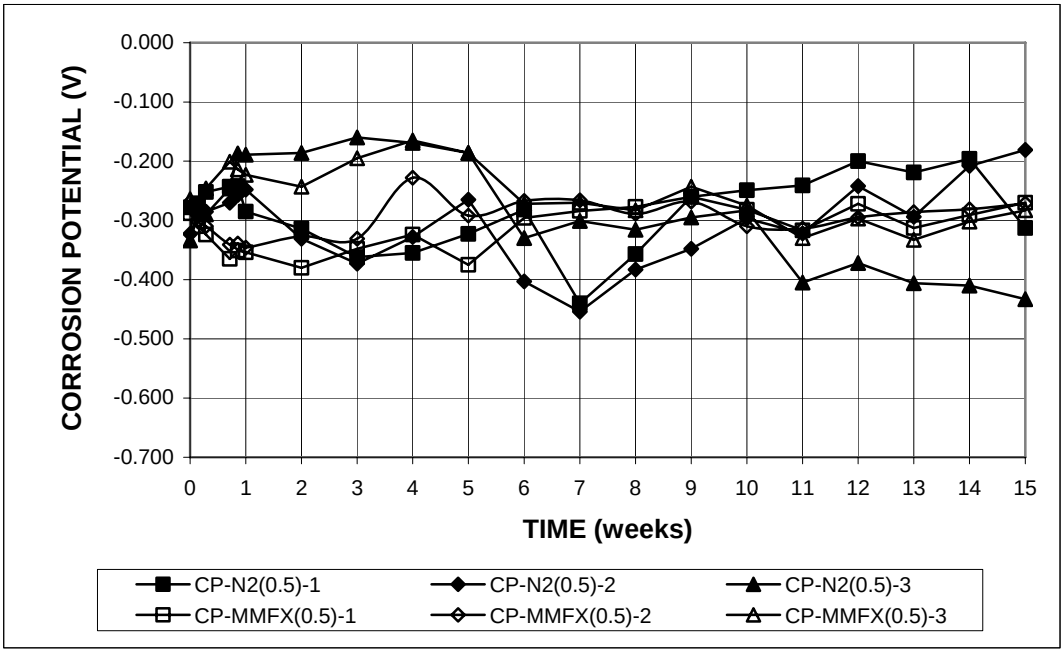

Figure D.11 -Corrosion potential test. Corrosion potentials with respect to saturated calomel electrode for conventional N2 and MMFX steels in simulated concrete pore solution with 0.5 molal ion NaCl. Solutions are replaced every 5 weeks.

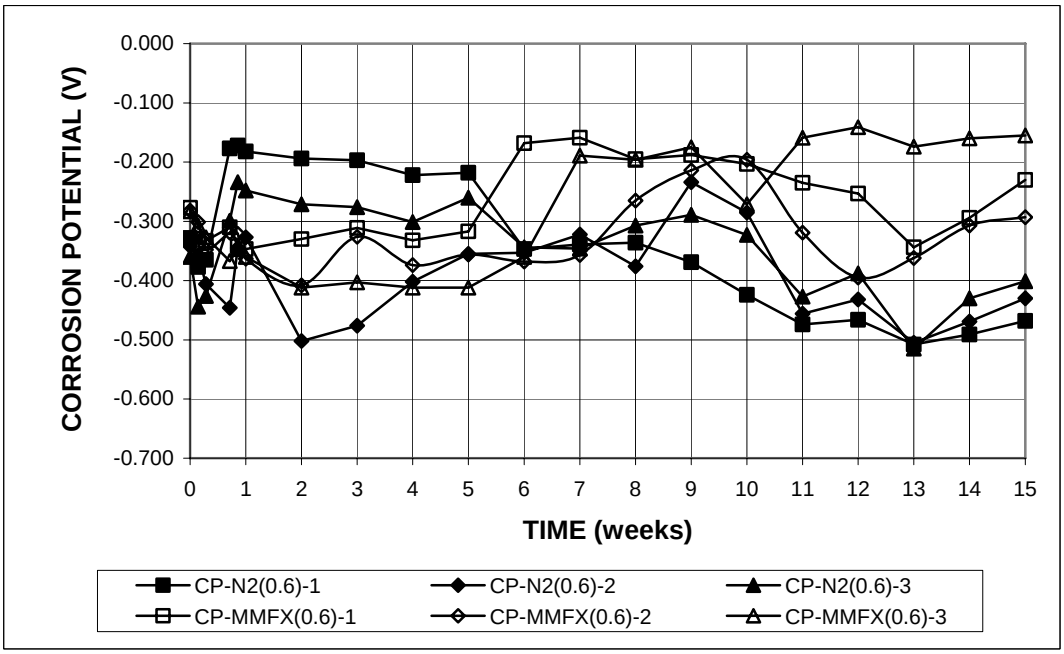

Figure D.12 -Corrosion potential test. Corrosion potentials with respect to saturated calomel electrode for conventional N2 and MMFX steels in simulated concrete pore solution with 0.6 molal ion NaCl. Solutions are replaced every 5 weeks.

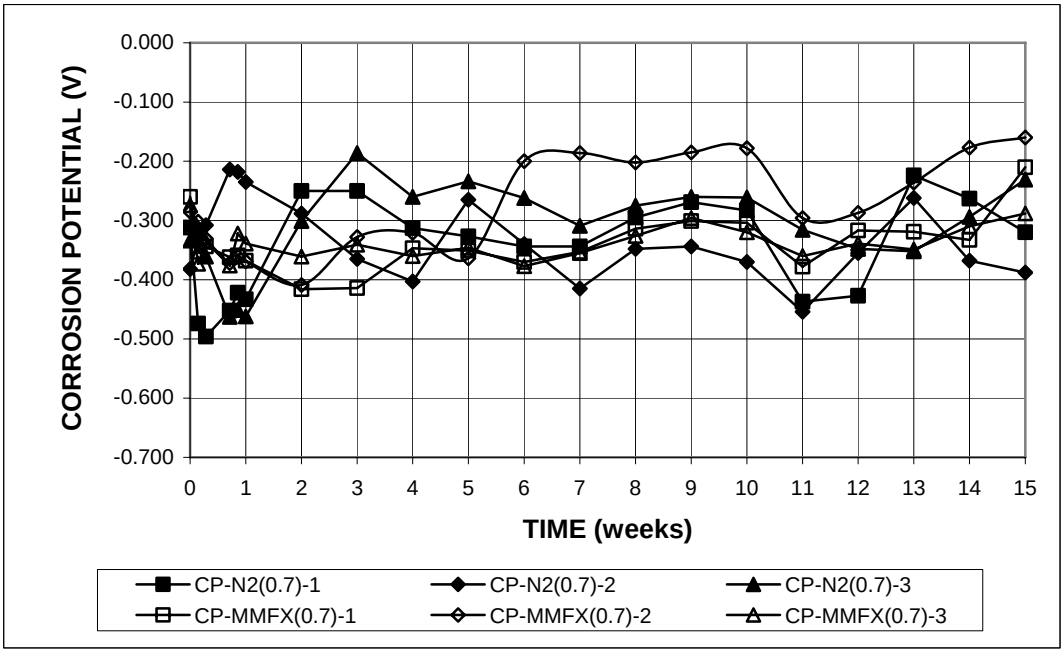

Figure D.13 -Corrosion potential test. Corrosion potentials with respect to saturated calomel electrode for conventional N2 and MMFX steels in simulated concrete pore solution with 0.7 molal ion NaCl. Solutions are replaced every 5 weeks.

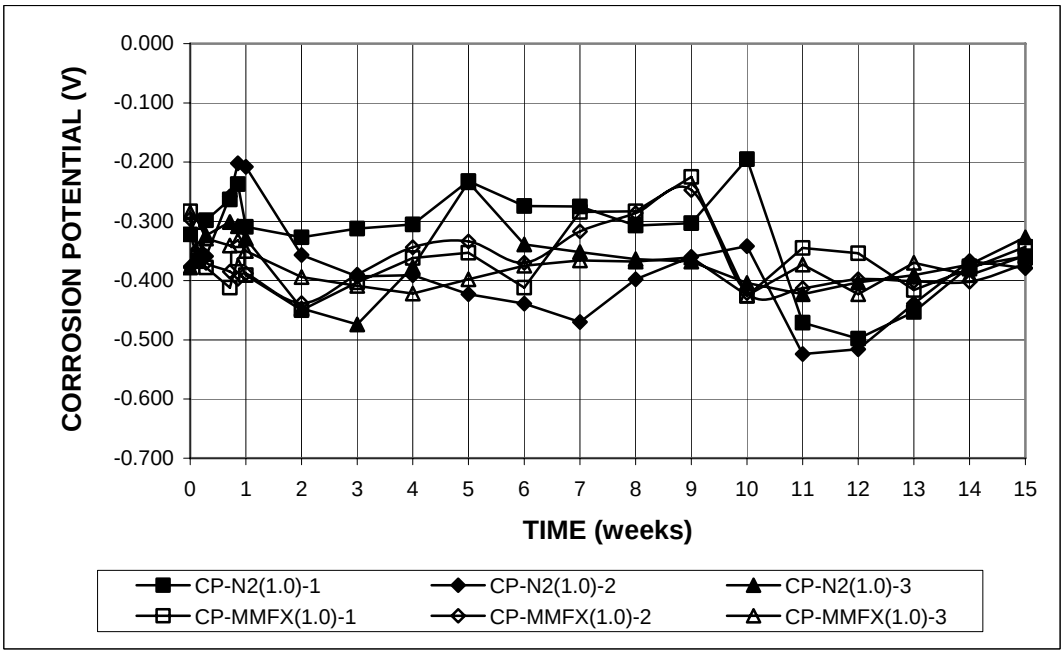

Figure D.14 -Corrosion potential test. Corrosion potentials with respect to saturated calomel electrode for conventional N2 and MMFX steels in simulated concrete pore solution with 1.0 molal ion NaCl. Solutions are replaced every 5 weeks.

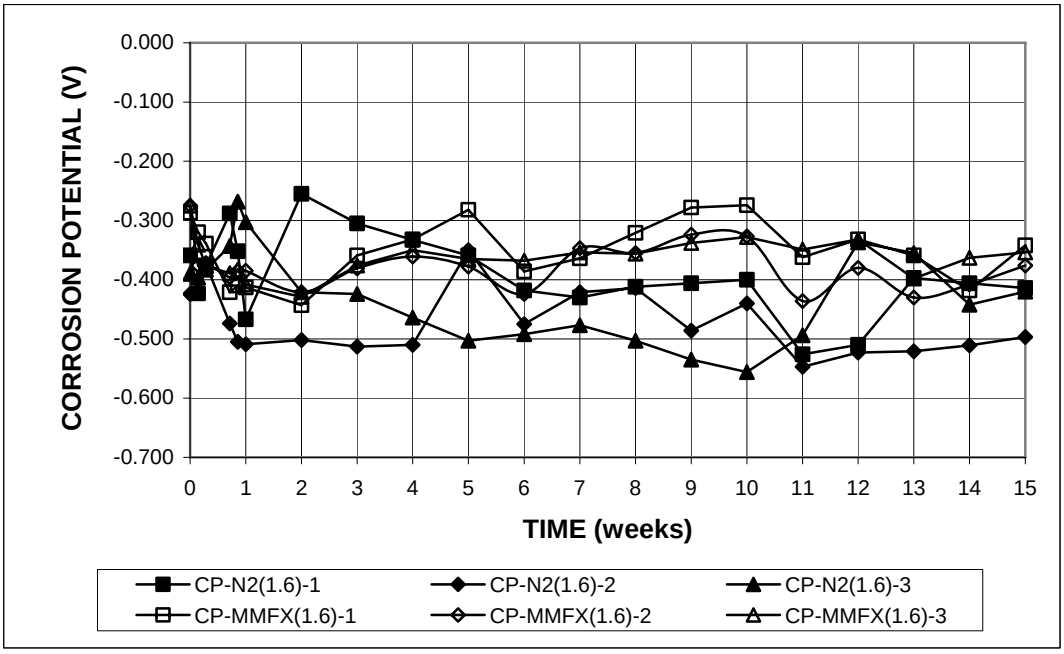

Figure D.15 -Corrosion potential test. Corrosion potentials with respect to saturated calomel electrode for conventional N2 and MMFX steels in simulated concrete pore solution with 1.6 molal ion NaCl. Solutions are replaced every 5 weeks.

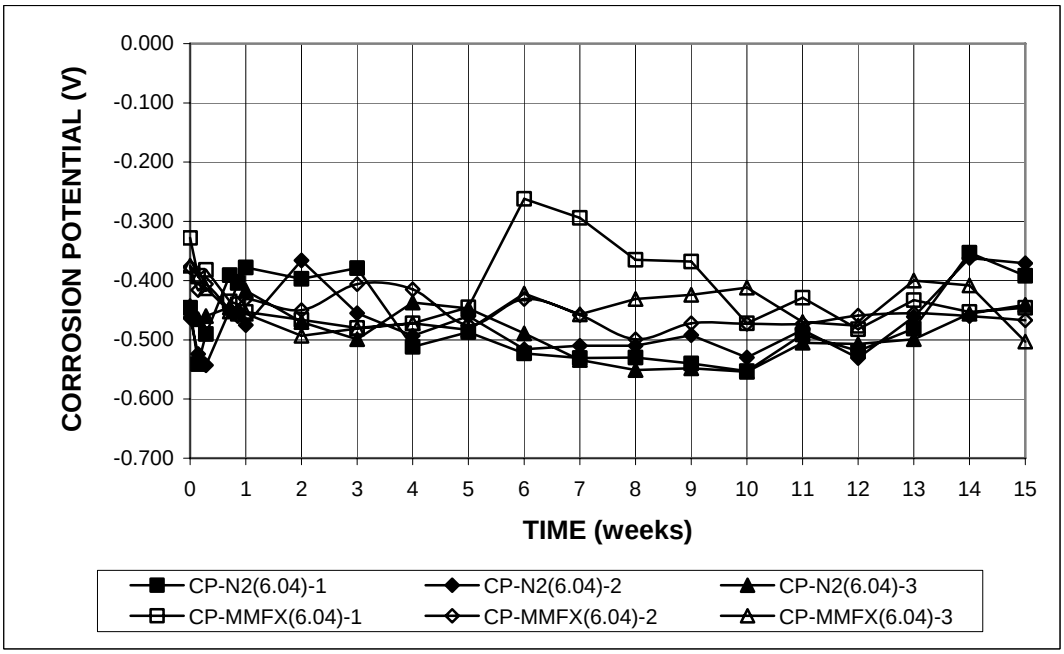

Figure D.16 -Corrosion potential test. Corrosion potentials with respect to saturated calomel electrode for conventional N2 and MMFX steels in simulated concrete pore solution with 6.04 molal ion NaCl. Solutions are replaced every 5 weeks.

APPENDIX E

CHLORIDE PROFILES, SURFACE CONCENTRATIONS, AND DIFFUSION COEFFICIENTS

Table E.1 - Total chloride profiles for dummy SE specimens in the first study (SE-D1**)

Time (weeks)	Total chloride concentrations at varing depths (kg/m^3)														
	Specimen SE-D1-1					Specimen SE-D1-2					Specimen SE-D1-3				
	13 mm	25 mm	38 mm	76 mm	140 mm	13 mm	25 mm	38 mm	76 mm	140 mm	13 mm	25 mm	38 mm	76 mm	140 mm
6	5.87	1.30	0.18	0.15	0.14	7.09	3.29	0.29	0.20	0.17	4.40	1.04	0.17	0.20	0.20
12	7.57	3.97	1.32	0.23	0.26	6.85	3.73	0.48	0.14	0.32	6.10	2.39	0.45	1.15	0.20
18	6.30	4.29	1.20	0.27	0.32	5.77	3.10	0.29	0.15	0.16	7.51	2.10	0.29	0.18	0.20
24	16.45	10.75	3.93	0.49	0.51	12.81	9.58	5.04	5.41	0.59	10.33	5.68	1.67	0.40	0.41
30	12.97	7.76	4.48	0.35	0.52	14.87	11.46	6.21	0.43	0.29	17.57	7.56	4.04	0.32	0.33
36	14.42	8.07	3.03	0.39	0.46	18.74	11.52	4.83	1.08	0.49	14.85	6.58	4.85	0.42	0.52
42	19.06	14.73	4.43	0.33	0.71	18.04	13.82	5.97	1.23	0.48	19.30	12.65	5.63	0.33	0.37
48	13.53	11.77	7.87	1.47	0.41	17.73	11.67	6.23	0.30	0.35	18.73	13.19	5.04	0.35	0.45
54	15.42	12.64	8.28	0.39	0.33	16.93	12.54	7.73	0.37	0.37	17.88	13.53	8.86	0.50	0.20
60	18.05	17.90	7.08	0.26	0.65	18.56	13.20	11.79	0.74	0.70	19.28	11.35	9.79	0.65	0.29
66	23.29	15.11	10.43	0.47	4.70*	23.98	13.32	11.21	0.38	0.29	25.98	15.30	9.12	0.57	0.28
72	18.11	15.12	8.40	6.12	9.66*	18.72	14.97	11.84	0.84	0.33	16.97	11.40	8.67	0.45	0.30
78	15.64	17.00	11.00	1.15	5.02*	18.55	17.25	12.46	1.27	4.05*	21.00	13.23	12.46	1.08	0.35
84	24.12	17.46	11.69	0.87	11.22*	26.26	20.85	17.67	8.24	8.70*	23.39	11.71	10.83	4.73	4.56*
90	20.78	14.75	12.17	1.11	4.10*	23.45	19.93	11.05	0.99	0.33	22.64	16.72	13.62	2.70	0.38
96	24.49	20.51	16.12	2.27	4.36*	21.12	17.84	16.74	1.28	2.39*	23.18	21.48	19.66	6.59	8.95*

***** These values are excluded for least squares analysis since they may not have occurred as the result of chloride diffusion from the upper surface.

** A-B

A: test method, SE = Southern Exposure test; B: test specimens, D1 = Dummy SE specimens in the first study.

Table E.2 - Total chloride profiles for dummy SE specimens in the second study (SE-D2**)

Time (weeks)	Total chloride concentrations at varing depths (kg/m^3)														
	13 mm	25 mm	38 mm	76 mm	140 mm	13 mm	25 mm	38 mm	76 mm	140 mm	13 mm	25 mm	38 mm	76 mm	140 mm
	Specimen SE-D2-1					Specimen SE-D2-2					Specimen SE-D2-3				
0		0.29			0.28		0.27			0.25		0.30			0.28
2	2.88	0.34	0.26	0.24	0.32	-	0.73	0.39	0.27	0.32	2.19	0.30	0.31	0.25	0.25
4	2.84	0.31	0.32	0.27	0.28	5.98	0.92	0.31	0.32	0.27	4.66	0.35	0.33	0.35	0.36
6	7.87	0.54	0.34	0.35	0.47	5.77	0.76	0.37	0.33	0.35	6.24	0.36	0.32	0.34	0.33
12	9.38	2.71	0.32	0.30	0.35	10.72	4.06	0.39	0.34	0.35	14.85	2.77	0.35	0.35	0.35
24	15.07	2.19	0.27	0.27	0.32	9.31	3.63	0.31	0.29	0.30	9.60	1.93	0.27	0.29	0.35
36	13.43	3.46	0.74	0.31	0.40	14.51	6.49	1.08	0.32	0.47	11.81	4.06	0.82	0.30	0.32
48	18.04	7.13	1.48	0.30	1.29*	12.13	9.38	1.84	0.34	2.52*	12.28	5.01	1.91	0.29	0.37
60	21.87	11.70	5.51	0.33	0.28	20.00	11.25	5.33	0.29	0.31	17.53	9.22	4.45	0.28	0.31
72	21.81	14.41	10.27	0.31	0.34	21.44	14.47	6.67	0.34	3.88*	16.64	9.52	4.19	0.34	0.33
84	25.44	19.30	8.83	0.58	0.41	22.74	18.57	11.64	0.48	0.46	20.63	10.28	6.34	0.27	2.08*
96	20.64	18.88	11.13	1.29	5.08*	21.49	13.92	9.86	0.26	3.57*	26.86	12.96	8.44	0.36	0.33
	Specimen SE-D2-4					Specimen SE-D2-5					Specimen SE-D2-6				
0		0.29			0.31		0.30			0.32		0.35			0.35
2	4.92	0.39	0.31	0.42	0.36	7.15	0.53	0.32	0.30	0.35	6.15	0.33	0.30	0.31	0.32
4	4.14	0.29	0.29	0.34	0.29	6.25	0.77	0.33	0.33	0.33	9.10	1.19	0.27	0.28	0.30
6	9.46	0.57	0.28	0.29	0.30	7.47	1.06	0.30	0.30	0.29	7.25	0.31	0.29	0.28	0.29
12	8.03	1.08	0.30	0.35	0.31	11.15	3.12	0.33	0.30	0.31	12.04	2.77	0.40	0.31	0.32
24	14.45	2.93	0.36	0.36	0.50	14.09	5.86	0.77	0.34	0.25	16.49	3.83	1.06	0.33	0.32
36	12.15	3.32	0.56	0.30	0.30	22.58	8.66	3.03	0.31	0.31	14.35	7.75	1.32	0.33	0.34
48	12.38	11.70	4.13	0.41	0.32	27.70	17.11	10.38	0.37	0.33	20.65	10.92	3.30	0.33	0.33
60	14.23	13.68	6.58	0.34	0.32	20.95	16.00	5.31	0.30	0.29	20.46	12.96	4.22	0.31	0.54
72	17.44	10.75	6.53	0.30	0.32	18.33	15.83	7.26	0.35	0.35	23.24	16.97	11.44	0.36	0.34
84	17.61	10.38	6.90	0.28	1.13*	32.53	21.96	9.83	1.12	0.78	21.40	14.65	7.35	0.20	0.27
96	21.49	15.09	13.08	0.40	3.30*	31.68	20.28	13.31	0.47	0.33	27.47	19.74	8.05	0.27	0.25

***** These values are excluded for least squares analysis since they may not have occurred as the result of chloride diffusion from the upper surface.

** A-B

A: test method, SE = Southern Exposure test; B: test specimens, D2 = Dummy SE specimens in the second study.

Table E.3 - Water-soluble chloride profiles for dummy SE specimens in the second study (SE-D2**)

Time (weeks)	Water-soluble chloride concentrations at varing depths (kg/m^3)														
	13 mm	25 mm	38 mm	76 mm	140 mm	13 mm	25 mm	38 mm	76 mm	140 mm	13 mm	25 mm	38 mm	76 mm	140 mm
	Specimen SE-D2-1					Specimen SE-D2-2					Specimen SE-D2-3				
0		0.16			0.16		0.05			0.16		0.05			0.14
2	3.09	0.25	0.19	0.16	0.22	1.48	0.70	0.29	0.22	0.29	2.00	0.19	0.14	0.16	0.13
4	2.90	0.13	0.25	0.16	0.16	6.24	1.05	0.29	0.19	0.13	5.01	0.22	0.14	0.14	0.25
6	7.92	0.37	0.16	0.14	0.20	5.96	0.71	0.23	0.14	0.20	6.71	0.24	0.19	0.18	0.24
12	8.72	2.98	0.08	0.11	0.16	10.14	4.12	0.27	0.18	0.18	14.20	3.19	0.19	0.17	0.13
24	7.44	2.02	0.11	0.28	0.25	9.39	3.90	0.31	0.18	0.22	10.33	2.30	0.22	0.19	0.69
36	14.13	3.60	0.52	0.41	0.46	14.47	7.18	1.05	0.18	0.48	11.59	3.55	0.75	0.18	0.23
48	11.29	8.14	1.54	0.32	1.27	13.20	10.48	1.98	0.25	2.96*	12.97	5.61	2.20	0.22	0.24
60	22.62	11.03	4.78	0.20	0.21	19.89	11.51	4.67	0.18	0.22	20.67	9.05	5.12	0.22	0.18
72	21.49	14.47	8.93	0.16	0.18	20.33	14.09	7.36	0.18	3.96*	15.78	8.77	3.66	0.20	0.14
84	21.01	17.10	8.63	0.21	0.17	19.40	16.60	11.40	0.21	1.68*	21.61	14.28	7.21	0.25	3.89*
96	16.67	14.80	8.78	1.31	4.67*	19.38	13.58	9.97	0.46	3.81*	23.70	13.79	9.74	0.30	0.34
	Specimen SE-D2-4					Specimen SE-D2-5					Specimen SE-D2-6				
0		0.24			0.31		0.19			0.25		0.25			0.25
2	5.23	0.29	0.23	0.36	0.32	6.84	0.51	0.25	0.21	0.36	5.79	0.28	0.19	0.26	0.34
4	4.57	0.20	0.30	0.35	0.33	6.15	0.86	0.37	0.34	0.30	8.91	1.30	0.23	0.28	0.53
6	9.40	0.77	0.23	0.21	0.22	7.87	1.21	0.29	0.25	0.25	7.99	0.40	0.26	0.37	0.35
12	8.53	0.67	0.30	0.29	0.22	11.17	3.28	0.25	0.24	0.30	12.40	3.19	0.84	0.34	0.47
24	13.70	4.13	0.34	0.33	0.54	13.10	5.77	0.83	0.33	0.43	14.87	3.80	0.32	0.30	0.31
36	10.95	3.48	0.22	0.40	0.22	20.67	9.38	2.62	0.14	0.18	13.91	6.43	0.78	0.22	0.18
48	10.99	10.47	3.78	0.22	0.18	18.88	15.81	9.46	1.04	1.00	18.65	10.50	2.99	1.00	1.00
60	18.95	12.17	5.86	0.23	0.14	18.88	12.56	5.16	0.19	0.11	18.80	12.56	4.25	0.19	0.43
72	16.04	10.39	6.78	0.22	0.22	21.57	15.06	5.94	0.18	0.18	19.74	14.35	10.62	0.18	0.18
84	17.42	10.02	7.14	0.14	1.04*	21.49	17.94	10.43	0.21	0.06	21.64	13.27	7.10	0.18	0.25
96	18.99	15.10	8.45	0.28	3.59*	26.58	15.36	12.67	0.32	0.32	18.88	15.70	6.62	0.32	0.32

***** These values are excluded for least squares analysis since they may not have occurred as the result of chloride diffusion from the upper surface.

** A-B

A: test method, SE = Southern Exposure test; B: test specimens, D2 = Dummy SE specimens in the second study.

Table E.4 – Diffusion coefficients (D_c) and surface concentrations (C_s) for individual dummy SE specimens, by the least square analysis, based on chloride profiles at all time periods using Eq. (4.3)

Specimens[a]	**Unique values**		**Sum of square errors**	**Cl^-**
	D_c (mm^2/day)	**C_s (kg/m^3)**	**$(kg/m^3)^2$**	
Dummy SE specimens in the first study				
SE-D1-1	1.73	25.85	379	total
SE-D1-2	1.85	26.67	449	
SE-D1-3	1.43	27.72	407	
Dummy SE specimens in the second study				
SE-D2-1	0.90	32.18	158	total
SE-D2-2	1.04	28.21	152	
SE-D2-3	0.74	28.55	185	
SE-D2-4	1.23	23.56	159	
SE-D2-5	1.06	37.49	291	
SE-D2-6	1.16	27.04	132	
SE-D2-1	0.98	27.24	204	water-soluble
SE-D2-2	1.19	26.04	109	
SE-D2-3	0.85	28.04	172	
SE-D2-4	1.18	23.06	130	
SE-D2-5	1.30	29.90	140	
SE-D2-6	1.18	27.08	133	

a: SE = Southern Exposure test, D1, D2 = dummy SE specimens in the first and second study, respectively

Table E.5 – Chloride concentrations at a depth of 29 mm (1.125 in.) versus time, based on the diffusion equations Eq. (4.4), (4.5), and (4.6)

Weeks	Chloride concentrations at a depth of 29 mm (kg/m^3)		
	Total chlorides[a]	Total chlorides[b]	Water-soluble chlorides[c]
1	0.17	0.30	0.19
2	0.18	0.30	0.19
3	0.19	0.30	0.19
4	0.26	0.30	0.19
5	0.39	0.32	0.22
6	0.59	0.35	0.27
7	0.85	0.42	0.35
8	1.14	0.51	0.46
9	1.47	0.63	0.61
10	1.81	0.77	0.77
11	2.16	0.94	0.96
12	2.51	1.13	1.16
13	2.86	1.33	1.38
14	3.21	1.54	1.60
15	3.55	1.76	1.83
16	3.88	1.99	2.07
17	4.21	2.23	2.30
18	4.52	2.47	2.54
19	4.83	2.70	2.77
20	5.13	2.94	3.01
21	5.42	3.18	3.24
22	5.70	3.42	3.47
23	5.97	3.66	3.69
24	6.23	3.89	3.92
25	6.48	4.12	4.14
26	6.73	4.35	4.35
27	6.97	4.57	4.56
28	7.20	4.79	4.77
29	7.42	5.01	4.97
30	7.64	5.22	5.17
31	7.85	5.43	5.36
32	8.06	5.64	5.55
33	8.25	5.84	5.74
34	8.45	6.04	5.92
35	8.63	6.23	6.10
36	8.82	6.43	6.28
37	8.99	6.61	6.45

Table E.5 (con't) – Chloride concentrations at a depth of 29 mm (1.125 in.) versus time, based on the diffusion equations Eq. (4.4), (4.5), and (4.6)

Weeks	Chloride concentrations at a depth of 29 mm (kg/m^3)		
	Total chlorides[a]	Total chlorides[b]	Water-soluble chlorides[c]
38	9.17	6.80	6.62
39	9.33	6.98	6.78
40	9.50	7.15	6.94
41	9.65	7.33	7.10
42	9.81	7.50	7.25
43	9.96	7.67	7.40
44	10.11	7.83	7.55
45	10.25	7.99	7.69
46	10.39	8.15	7.84
47	10.53	8.30	7.97
48	10.66	8.45	8.11
49	10.79	8.60	8.24
50	10.92	8.75	8.38
51	11.04	8.89	8.50
52	11.16	9.04	8.63
53	11.28	9.17	8.75
54	11.40	9.31	8.87
55	11.51	9.44	8.99
56	11.62	9.58	9.11
57	11.73	9.71	9.22
58	11.84	9.83	9.34
59	11.94	9.96	9.45
60	12.04	10.08	9.56
61	12.14	10.20	9.66
62	12.24	10.32	9.77
63	12.34	10.44	9.87
64	12.43	10.55	9.97
65	12.52	10.66	10.07
66	12.62	10.78	10.17
67	12.71	10.88	10.26
68	12.79	10.99	10.36
69	12.88	11.10	10.45
70	12.96	11.20	10.54
71	13.05	11.31	10.63
72	13.13	11.41	10.72
73	13.21	11.51	10.81
74	13.29	11.60	10.90

Table E.5 (con't) – Chloride concentrations at a depth of 29 mm (1.125 in.) versus time, based on the diffusion equations Eq. (4.4), (4.5), and (4.6)

Weeks	Chloride concentrations at a depth of 29 mm (kg/m^3)		
	Total chlorides[a]	Total chlorides[b]	Water-soluble chlorides[c]
76	13.44	11.80	11.06
77	13.52	11.89	11.15
78	13.59	11.98	11.23
79	13.66	12.07	11.31
80	13.73	12.16	11.39
81	13.80	12.25	11.46
82	13.87	12.34	11.54
83	13.94	12.43	11.61
84	14.01	12.51	11.69
85	14.07	12.60	11.76
86	14.14	12.68	11.83
87	14.20	12.76	11.90
88	14.27	12.84	11.97
89	14.33	12.92	12.04
90	14.39	13.00	12.11
91	14.45	13.08	12.18
92	14.51	13.15	12.25
93	14.57	13.23	12.31
94	14.62	13.30	12.38
95	14.68	13.38	12.44
96	14.74	13.45	12.50

a: the total chloride contents are based on Eq. (4.4)
b: the total chloride contents are based on Eq. (4.5)
c: the water-soluble chloride contents are based on Eq. (4.6).

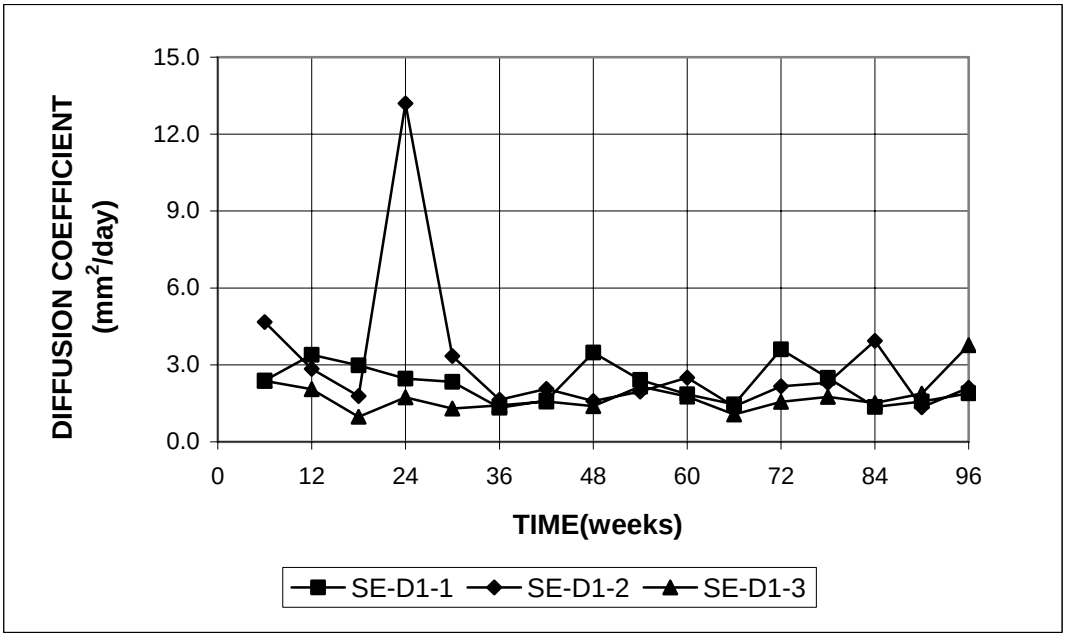

Figure E.1 - Effective diffusion coefficients vs. time, based on total chloride profiles for dummy SE specimens SE-D1, w/c = 0.45, ponded with 15% salt solution.

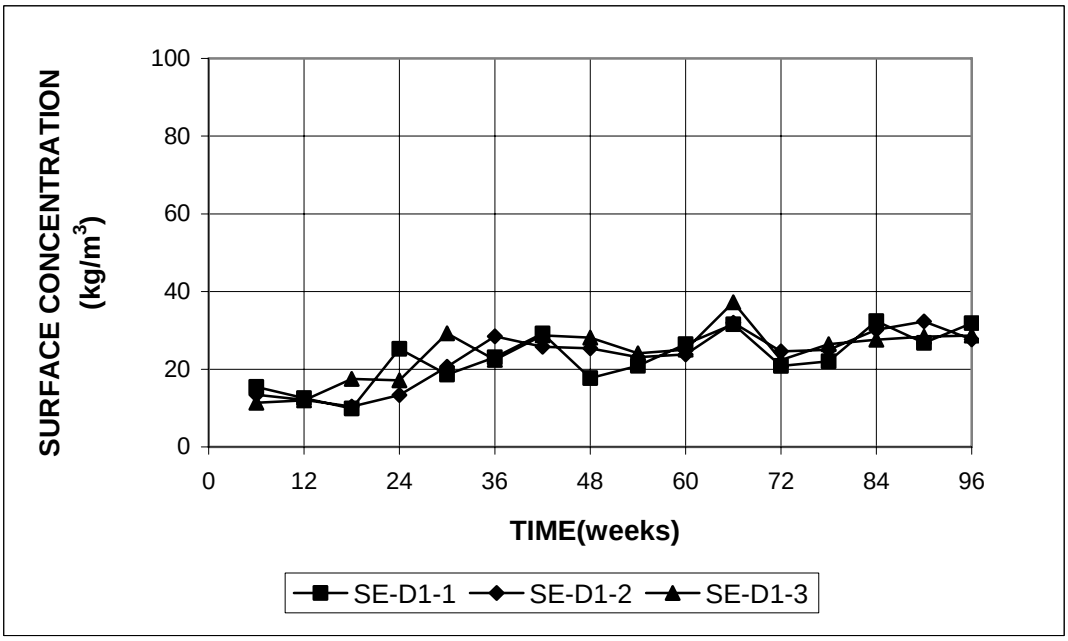

Figure E.2 - Surface concentrations vs. time, based on total chloride profiles for dummy SE specimens SE-D1, w/c = 0.45, ponded with 15% salt solution.

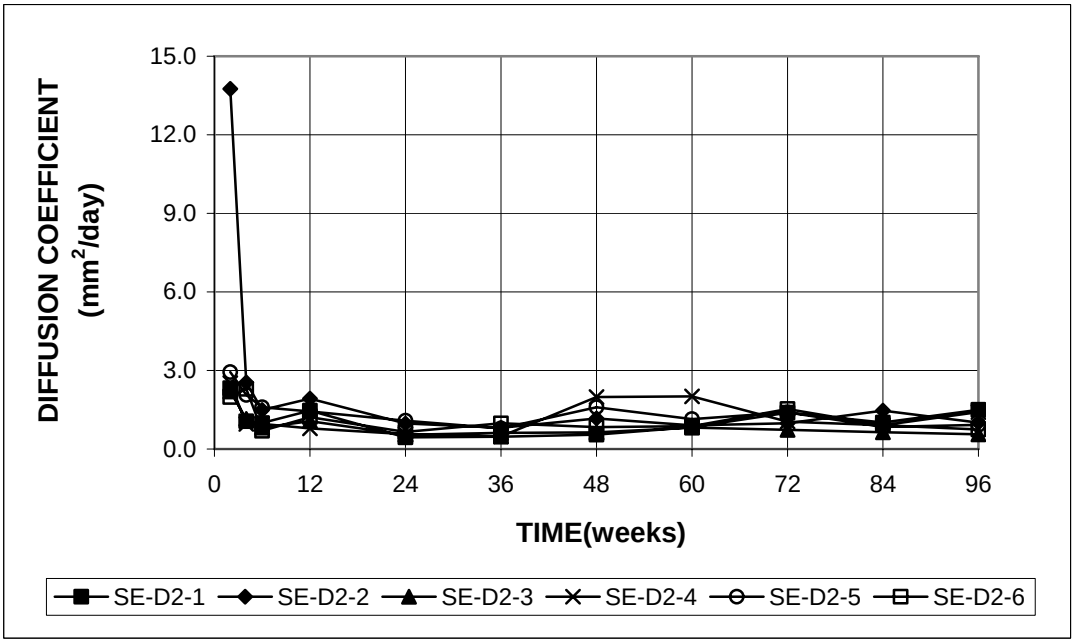

Figure E.3 - Effective diffusion coefficients vs. time, based on total chloride profiles for dummy SE specimens SE-D2, w/c = 0.45, ponded with 15% salt solution.

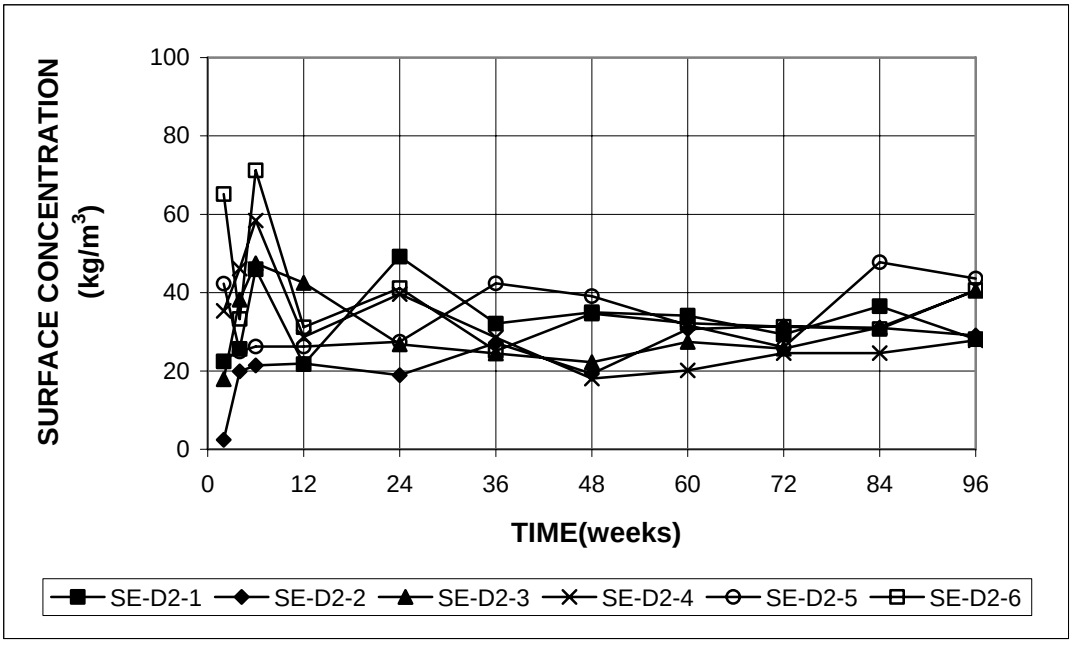

Figure E.4 - Surface concentrations vs. time, based on total chloride profiles for dummy SE specimens SE-D2, w/c = 0.45, ponded with 15% salt solution.

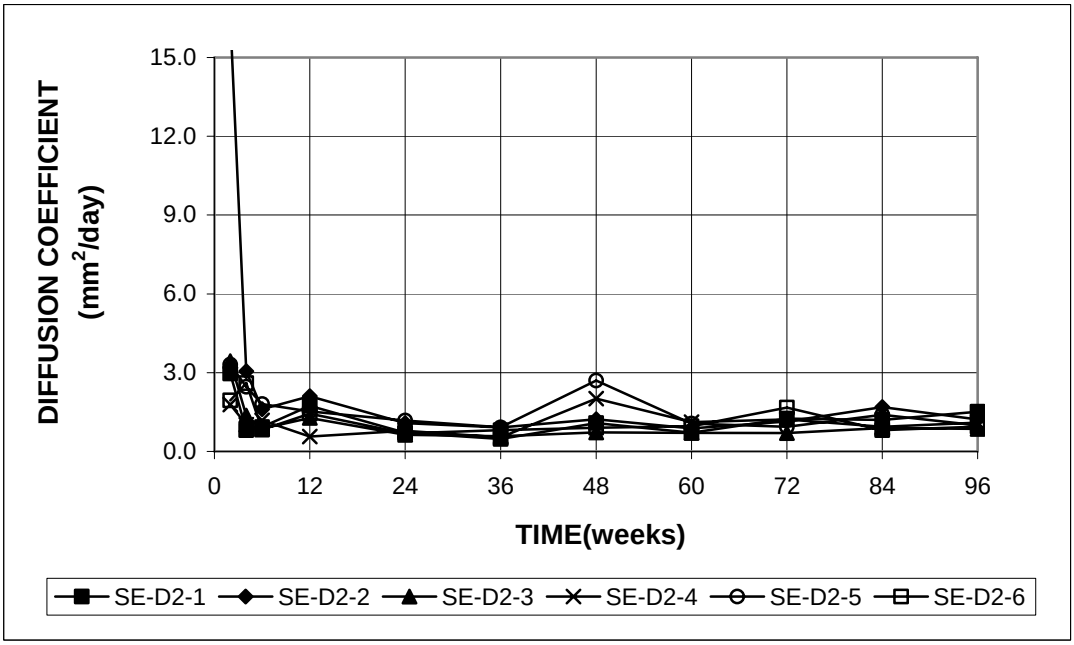

Figure E.5 -Effective diffusion coefficients vs. time, based on water-soluble chloride profiles for dummy SE specimens SE-D2, w/c = 0.45, ponded with 15% salt solution.

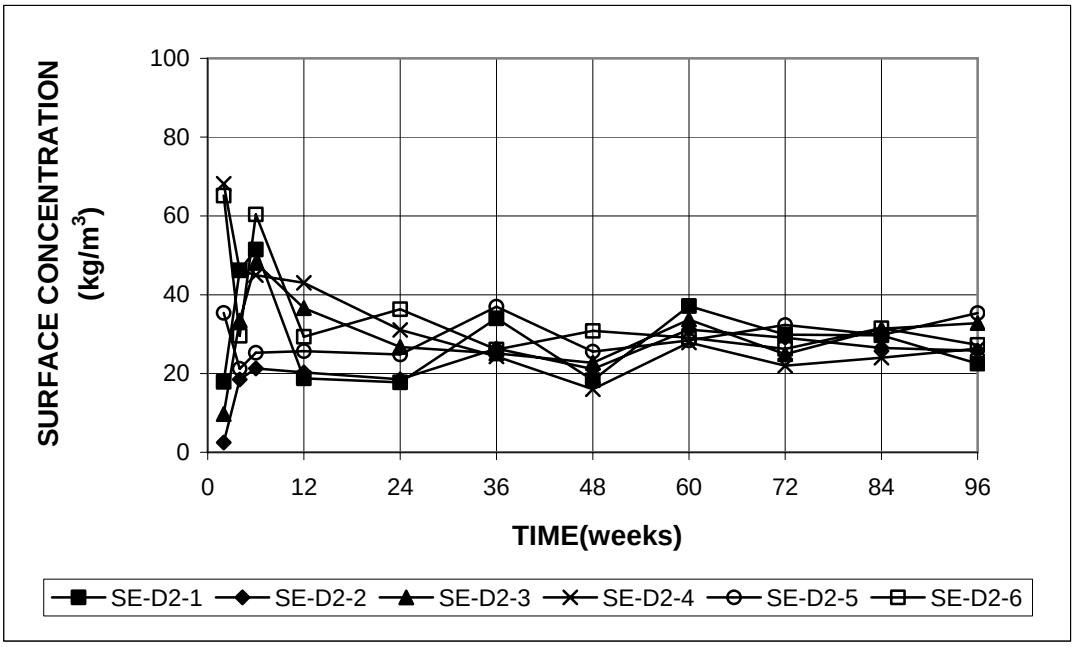

Figure E.6 - Surface concentrations vs. time, based on water-soluble chloride profiles for dummy SE specimens SE-D2, w/c = 0.45, ponded with 15% salt solution.